97-3958
Vol 1 of 3

364001

CRA EXPLORATION PTY. LIMITED
ACN 000 057 125

MINERAL RESOURCES
24 DEC 1996
TASMANIA

Eighth Annual Report
For The Period Ending 9 November 1996
EL 28/88 Zeehan 1, Tasmania

MINERAL RESOURCES
EL28/88
-2 JAN 1997
See folio 11

~~Volume I of III~~

MICROFILMED
FICHE No. 014213 -22

Author: S J Tear / S A J Russell

Date: November 1996

Licence Holder: CRA Exploration Pty. Limited
Allegiance Mining NL

Submitted to: Chief Geologist, South East District

Copies to: Mineral Resources Tasmania
CRAE - South East District
CRAE - Zeehan
CRAE - ETIG
Allegiance Mining NL

Submitted by:

Accepted by:

All rights in this report and its contents (including rights to confidential information and copyright in text, diagrams and photographs) remain with CRA Exploration and no use (including use of reproductions, storage or transmission) may be made of the report or its contents for any purpose without the prior written consent of CRA Exploration.
© CRA Exploration Pty. Limited 1996"

97-3958

ANNUAL REPORT ZEEHAN NO 1
EL 28/88 - P.E. NOV 1996 - CRA
S TEAR/R RUSSELL- **VOL 1 OF 3**

CRAE Report No. 22160

Abstract

Exploration continued on EL 28/88 (Zeehan 1) for carbonate hosted base-metal deposits within the Gordon Limestone of the Zeehan area, West Tasmania. Analogies with Irish style carbonate hosted Zn/Pb deposits are being used to guide exploration.

Work undertaken during the 12 month period 9 November 1995 to 9 November 1996 consisted of diamond drilling and wacker bedrock sampling, 3 holes totalling 600m and 22 holes (129m), respectively.

Myrtle and Pyramid prospect areas were selected for further investigation. In addition, results from the helimag survey became available during the renewal period although only minimal interpretation has been carried out over the Zeehan carbonate areas.

Diamond drilling failed to intersect economic base-metal mineralisation. The geology of Myrtle remains enigmatic and further processing of the helimag data is required.

Diamond drilling at Pyramid produced some surprises, including a 100m thick quartzite unit within the middle of the carbonate sequence. The wacker bedrock sampling on EL 28/88 covered only a small area in the west of the prospect. This work confirmed the existence of elevated zinc values associated with siderite at the basal sandstone/limestone contact.

A basin analysis study was completed using Geosea Consultants (Dr Clive Burrett). Three formations were recognised in the Gordon Limestone, corresponding to different carbonate depositional environments.

At the Stonehenge prospect the search for Late Proterozoic shale hosted base-metal mineralisation (Oonah Formation) has consisted of detailed structural mapping, the results of which are part of an honours project based at Monash University. Conclusions from the honours thesis by Mark Upton include the identification of fold interference and steeply plunging fold structures at Stonehenge. He has also identified two phases of sulphide mineralisation, the former is stratiform pyrite in block shales (pre-Cambrian), the latter is Heemskirk granite-related veins (+1-skarn) of Devonian age.

From the helimag data, a discrete magnetic anomaly was identified at the Avebury prospect. The source of the anomaly is believed to be in Gordon Limestone overlain by a thrust sheet of Cambrian sediments (Dundas Group). Modelling of the magnetic data has shown that the anomaly is a body <100m wide, 1 km long, buried between 30-100m and dipping steeply to the south.

Rehabilitation consisted of removal of rubbish and cuttings around drillsites.

Expenditure for the 12 month period was $263,515.

Total expenditure for this licence to 31st October 1996 is $1,301,273.

With the exception of the Avebury exclusion zone this licence is currently being offered for joint venture.

364003

Contents

		Page No.
Abstract		
List of Plans		
List of Appendices		
1.	Conclusions and Recommendations	1
2.	Introduction	1
3.	Review of Previous Work	2
4.	Exploration Completed in the 12 Month Period 9/11/95 to 9/11/96	2
	4.1 Myrtle	3
	4.1.1 Diamond Drilling	3
	4.2 Pyramid	4
	4.2.1 Diamond Drilling	4
	4.2.2 Wacker Bedrock Sampling	5
	4.2.3 Conodont Age Dating	5
	4.3 Detailed Helimag Survey	5
	4.4 Basin Analysis Study	6
	4.5 Stonehenge	6
5.	Discussion of Results	7
	5.1 Myrtle	7
	5.2 Pyramid	7
6.	Environment and Rehabilitation	8
7.	References	9
8.	Location	9
9.	Keywords	9
10.	DPO Register	9

List of Plans

Plan No.	Title	Scale
Tv 1021	EL 28/88 Zeehan 1 Location Plan	1:100,000
Tv 1022	Zeehan Project Target Plan	1:50,000
Tv 714	EL 28/88 Zeehan 1 Zeehan Carbonate, Myrtle Project Geology and Drill Hole Location Plan	1:2,500
Tv 1153	EL 28/88 Zeehan 1 Zeehan Carbonate, Myrtle Prospect, Section A - B	1:2,500
Tv 1154	EL 28/88 Zeehan 1 Zeehan Carbonate, Myrtle Prospect, Section C - D	1:1,000
Tv 1110	EL 28/88 Zeehan 1 Zeehan Carbonate, Myrtle Prospect Section E - F DD96ZM191	1:1,000
Tv 1018	EL 28/88 Zeehan 1 Zeehan Carbonate, Pyramid Prospect, Geology and Drillhole Location Plan	1:2,500
Tv 1113	EL 28/88 Zeehan 1, Zeehan Carbonate, Pyramid Prospect, DD96ZP64 and 65 Section: A - A'	1:1,000

Appendices

Appendix I	The Gordon Limestone Lithostratigraphy
Appendix II	Exploration by Major Mining Ltd (now Allegiance Mining) and CRAE prior to 9/11/95
Appendix III	Analytical Methods for Drillcore and Bedrock Wacker Sampling
Appendix IV	Myrtle - DD96ZM191 Drill Logs and Assay Results
Appendix V	Pyramid - DD96ZP64 - ZP65 - Drill Logs and Assay Results
Appendix VI	Pyramid Wacker Bedrock Sampling - Geology and Assay Data
Appendix VII	DD96ZP65 Conodont Age Dating Report
Appendix VIII	Detailed Helimag Data
Appendix IX	Basin Analysis Report
Appendix X	Mark Upton's Honours Thesis
Appendix XI	Additional Assays for DD95ZS31: Stonehenge
Appendix XII	Zinc Mineralisation in the Gordon Limestone

1. Conclusions and Recommendations

Diamond drilling of the Myrtle prospect failed to intersect base metal mineralisation within the sub-Siltstone Unit sequence. The Siltstone Unit itself was not intersected, and it is concluded that Myrtle is more structurally complex than previously thought. This complexity is confirmed by the helimag data, which may indicate tighter folding and/or thrust repetition of units.

Diamond drilling at Pyramid highlighted a 100m thick quartzite believed to be a correlative sequence of the Siltstone Unit. This siliciclastic package is juxtaposed with the Silurian Amber Slate, presumably with a faulted contact. The quartzite indicates nearby major syn-sedimentary faulting and with its elevated zinc values and dolomitisation demonstrates that there has been the pervasive passage of mineralising fluids through the unit.

Wacker bedrock sampling on EL28/88 and 45/92 has provided geological control for the central and southern part of the prospect. Elevated zinc values of up to 1780 ppm Zn are found in association with siderite alteration at the Moina Sandstone / Gordon Limestone contact on the western limb of the Pyramid syncline (EL 28/88).

The detailed helimag survey will provide major assistance with the geological mapping, in particular, the mapping of individual limestone units. No large scale siderite alteration zones have been inferred, although two small 100 - 200m long anomalies do occur on the western margin of the Pyramid limestone.

The basin analysis study concluded that at the Myrtle prospect, there is a much thicker carbonate sequence, with DD95ZM189 providing the benchmark stratigraphy for the Zeehan carbonate sub-basin.

Collection and compilation of data in the last two years has significantly increased the understanding of the geology of the Ordovician/Silurian sequence. Prior to further drilling or surface work, greater effort should be put into three-dimensional aspects of the geology and the unique pattern of carbonate sedimentation.

Recommendations for further work are:

- Infill the wacker bedrock sampling at Pyramid utilising multi-element analyses to map out lithological units. Assess results for diamond drill targets.
- Diamond drill test the siderite anomalies on the western carbonate margin of Pyramid prospect.
- More interpretation work eg. helimag data should be completed at Myrtle and Firewood Siding prospects prior to drilling.

2. Introduction

Zeehan 1, EL 28/88 covers 64 km^2 located near Zeehan on the Tasmanian W coast (Plan Tv 1021). EL 28/88 was granted to "His Grace, The Most Noble, The Duke of Avram" on 9th December, 1988, and transferred to Major Mining Ltd on the 23rd November 1989. CRA Exploration Pty. Limited entered into a joint venture agreement with Major Mining to explore EL 28/88, commencing on 23rd April 1991. Major Mining Ltd divested its interest in the joint venture to Allegiance Mining NL, with the exploration tenements transferred to CRAE (90%) and Allegiance (10%) as tenants in common on 22nd January 1994.

During the period under review, the eighth year of tenure, CRAE has a statutory obligation to spend $128,000 on exploration. This report details all exploration activities conducted within EL 28/88 by CRAE during 1996.

CRAE's principal focus in the Zeehan area is zinc (Plan Tv 1022), either as:

1) Irish-style carbonate hosted zinc mineralisation in the Ordovician Gordon Limestone Formation - at Myrtle, Pyramid, Sassafras and Firewood Siding prospects, or

2) Shale-hosted zinc mineralisation in the Late Proterozoic Oonah Formation - at Stonehenge

Secondary targets include nickel mineralisation in ultramafic bodies (Trial Harbour), and skarn-type Zn-Pb deposits peripheral to the Heemskirk Granite (Avebury).

Work undertaken on the licence during 1996 included diamond drilling at Myrtle and Pyramid, with wacker sampling also at Pyramid.

Sub-divisions of the Gordon Limestone have been made on a lithologic/lithostratigraphic basis for utilisation in drillhole logging. An explanation of the formation codes is in Appendix I.

See Parkinson (1992, 1993, 1994) and Tear (1995) for regional setting, prospect geology and mineralisation.

3. Review of Previous Work

See Appendix II.

4. Exploration Completed in the 12 Month Period 9/11/95 to 9/11/96

Diamond Drillhole Summary

DDH	Prospect	East AMG	North AMG	AMG Zone	Elev (m a.s.l.)	TD (m)	Azim (AMG)	Dip	Date Drilled	Details Appendix
DD96ZM191	Myrtle	364056	5352092	55	149	300	134	60	24/4/96	IV
DD96ZP64	Pyramid	364335	5356607	55	129	48	198	60	28/3/96	V
DD96ZP65	Pyramid	364329	5356591	55	129	252	200	69	3/4/96	V

For a description of the analytical method see Appendix III.

Wacker Sampling Summary

Prospect	No. of Samples	Depth		Zinc		Lead	
		Range (m)	Average (m)	Max. (ppm)	Mean (ppm)	Max. (ppm)	Mean (ppm)
Pyramid	22	0.8-17.7	5.85	1780	389	985	112

Pyramid is divided by the EL 28/88 - 45/92 boundary. For reporting circumstances the wacker sampling has been split up between the two licences.

For a description of the analytical method see Appendix III.

4.1 Myrtle

One 300m diamond drillhole (DD96ZM191) was completed at the Myrtle prospect.

A revised geology map was completed showing the location of all drill holes (Plan Tv 714). The geology of the area is more complex than previously presented.

Drill logs and results are shown in Plan Tv 1110 and in Appendix IV.

The target at Myrtle is zinc mineralisation developed in clean carbonate units immediately beneath the Siltstone Unit. This is a conceptual target based in part on experience of Irish-style mineralisation. A cap rock such as the Siltstone Unit is believed to have acted as a trap to mineralising fluids introduced into the system via a proximal major structure eg. the Professor Range Fault. The assumptions of this model are that the mineralising fluids are Ordovician, giving rise to very early replacement or even sedex-style deposits. The fluids are also associated with basement-tapping syn-sedimentary faults.

An additional two sections were drawn in an attempt to rationalise the geological information (Plans Tv1153 and Tv1154).

Myrtle is considered prospective due to :-

- elevated surface geochemistry including outcropping pyrite, sphalerite and barite mineralisation.
- being close to the Professor Range Fault
- a major processed bouguer gravity anomaly
- excessive stratigraphic limestone thicknesses relative to other prospects, probably indicating the presence of nearby syn-sedimentary faulting.

4.1.1 Diamond Drilling

DD96ZM191 60° to 134° (AMG) TD 300.0m Drillrig: Universal 250
(Diamond Drilling of Tasmania Pty Ltd)

Aim of Hole

Diamond drill test of the sub-Siltstone Unit sequence.

Results

The drill hole intersected 17m of ferruginous and dark grey clays passing into clean fine grained calcarenite and micrite. The dark grey clays from 9.5 to 17m contained elevated zinc values up to 0.62% Zn at their base. Elsewhere assays show minimally elevated zinc values and minor amounts of dolomitisation. No siltstone was intersected unless the sequence is flat dipping and the surficial clays represent the base of the Siltstone Unit. However, this is contradicted by a number of core orientations which show the beds to be steeply dipping. An alternative explanation is that the sequence is tightly folded with repetition of units, but erosional contacts indicate that all beds are the right way up.

4.2 Pyramid

A revised geology map was completed showing diamond drill sites and wacker bedrock sample locations (Plan Tv 1018).

Drill/wacker logs and results are shown in Appendices V and VI.

4.2.1 Diamond Drilling

DD96ZP64 60° to 198° (AMG) TD 48m Drillrig: Universal 250
(Diamond Drilling of Tasmania Pty. Ltd.)

Aim of Hole

Diamond drill test the same conceptual target as that at Myrtle. The Oceana Mine (approximately 2 km north west of the drill-sites) lies in the same stratigraphic position as this target.

Results

This hole collared in dark grey-green phyllite, now interpreted as the Amber Slate (Silurian). However, this unit passes into a mixed black shale and light grey sandstone unit with increasing bands of carbonate - more typical of the Siltstone Unit (Plan Tv 1113). Conodont age dating of the carbonate beds in this unit gives a Silurian - Devonian age, consistent with the age of the Amber Slate; however, there are no previously recorded instances of carbonate in this unit. The hole was stopped due to severe flooding of the site. The drill-rig was relocated 15m south and collared as DD96ZP65. No samples were assayed from DD96ZP64.

DD96ZP65 69° to 200° (AMG) TD 252m Drillrig: Universal 250
(Diamond Drilling of Tasmania Pty. Ltd)

Aim of Hole

Diamond drill test the same conceptual target as that at Myrtle. The Oceana Mine (approximately 2 km north west of the drill-sites) lies in the same stratigraphic position as this target.

Results

The hole was collared in a dark grey-green phyllite grading conformably into the Siltstone Unit followed by a 100m package of massive quartzite with intercalated conglomeratic bands. There is weak evidence for major faulting and/or thrusting at the contacts. This quartzite sequence resembles the Moina Sandstone, but contains up to 9.5% calcium within its matrix. Moina quartzite usually contains no detectable calcium. Small scale galena and sphalerite veins occur between 40.9m and 41.2m giving a maximum lead value of 1.4% and a maximum zinc value of 0.4%. Consistently elevated zinc values up to 1180 ppm are recorded throughout this quartzite (average of samples taken is 537 ppm Zn). The lower contact of the quartzite passes into heavily dolomitised and haematised carbonates. This 30m thick dolomite is underlain by unfaulted calcarenites and micrites with zinc values up to 0.18% in rotted argillaceous calcarenite. Pervasive but low grade dolomitisation has also occurred in the limestones. Conodont age dating has confirmed that the basal part of the hole intersected Ordovician limestones of the Myrtle Formation.

4.2.2 Wacker Bedrock Sampling

Because the central and southern parts of the Pyramid prospect have no surface geochemical coverage, two reconnaissance bedrock sampling lines were completed. One line was positioned across the middle of the prospect, over the thickest section of the limestone. The other line was positioned parallel to the southern margin, near to the Little Henty Fault. The majority of this area is located on EL 45/92 which is reported in CRAE report number 22159.

The 22 samples show elevated zinc values up to 1780 ppm associated with the Moina Sandstone/ Gordon Limestone contact. The presence of siderite alteration at this contact is implied by geological logging and the iron assays.

4.2.3 Conodont Age Dating

Dr Clive Burrett of Geosea Consultants was contracted to provide conodont age dating of DD96ZP64/DD96ZP65 drillcore. Sampling of the core involved taking 3-5 kg of half core. Argillaceous bioclastic calcarenites were preferentially selected as they usually provide the best samples for conodont dating.

Results imply an overturned sequence with likely fault disruption. A copy of the report is included in Appendix VII.

4.3 Detailed Helimag Survey

The Gordon Limestone of the Zeehan area was flown over as part of a detailed sub-regional helicopter magnetic survey. Line spacing was approximately 60m with an average flight height of 30m and sampling intervals were approximately every 3-4m. A feature of the survey was that the flight lines were aimed perpendicular to the strike of the limestone. This innovation resulted in time consuming and complex processing.

Relevant parts of an initial report (CRAE report 22222) are included in Appendix VIII. This report was written just after CRAE decided to joint venture the EL 28/88. No major interpretation has been transferred to the geological maps.

Prospects on EL 28/88 covered by the magnetic survey include:- Pyramid, Myrtle, Sassafras, Firewood Siding and Avebury.

4.4 Basin Analysis Study

Dr Clive Burrett of Geosea Consultants was contracted to provide a stratigraphic study of the Zeehan carbonates to establish:-

- a stratigraphic column for the Zeehan carbonate sub-basin, including identification of formational boundaries.
- a measure of the variability of carbonate depositional environments and the possible inference of syn-sedimentary faults.

The Myrtle hole DD95ZM189 intersected the most continuous unfaulted carbonate sequence recorded in the Zeehan area (total thickness 470m). Consequently, it provided the basis for a stratigraphic column for the Ordovician Limestone of the Zeehan sub-basin.

A copy of the Geosea report is included in Appendix IX.

Holes from EL 28/88 examined were DD95ZM189, DD95ZM190, DD95ZP63, DD95ZF37 and ZM1008 (Pasminco).

4.5 Stonehenge

The target at Stonehenge is a shale hosted base-metal deposit within the dolomite and black shale of the Oonah Formation (Late Proterozoic).

DD95ZS31 exhibited considerable structural complexity. Structural mapping of the area was undertaken by Mark Upton, a student from Monash University. A copy of the Honours Thesis is in Appendix X.

Early deformation fabrics are indicative of regional isoclinal folding. This deformation event is represented by the widespread development of a spaced cleavage at low angle to bedding, throughout the Proterozoic units. Although generally obscured by later folding, early structures are preserved as microlithons within pelite units of the Oonah Formation. Timing of this early deformation is thought to coincide with the Penguin Orogeny (700 to 750 Ma), a common cause of folding within Proterozoic succession of Tasmania.

Early structural development is followed by thrusting events which form an integral component of the Cambrian development of western Tasmania. During this event, the Precambrian Oonah Formation headed (detached from its basement sequence) a complex sheet of Cambrian sediments containing mafic-ultramafic sequences of arc-forarc signature. This allochthonous sheet was thrust from east to west into and onto early Cambrian stratigraphy. Evident compressional structures within the Oonah Formation include large scale folds striking along a north-south axis.

Deformation post dating this Cambrian thrusting event has produced the complex fold and fault structures seen throughout the Zeehan area. In conjunction with prior folds, near-contemporaneous folding along differing axes has produced fold a interference patterns containing simple dome and basin structures, and more intricate antiform/synform structures within the Oonah Formation. Faulting of east-northeast and north-northwest trend has dislocated the fold structures. Regional Siluro-Devonian sequences host the last dominant phase of fold/fault deformation, providing a timing estimate of Middle to Late Devonian. Intense veining and mineralisation is associated with granite intrusion during this period. Faulting of an intrusive body beneath Stonehenge indicates emplacement before the completion of deformation. Timing of this deformational event correlate with the 'Tabberabberan Orogeny'.

Oonah Formation shale and dolomite/dolomitic sediment horizons host pyrite, sphalerite and galena mineralisation at Stonehenge. Two styles of mineralisation are evident. The *first* contains massive disseminated pyrite as a stratiform deposit with black shale sequences. The *second* is the product of hydrothermal fluid activity related to the intrusion of granite bodies (Heemskirk Granite) during the Devonian. In this case, low to medium temperature veins deposits, and minor carbonate replacement mineralisation (skarn) has formed along the peripheral margins of a skarn environment.

Mineralised horizons at Stonehenge (and throughout the Zeehan area) have been fault interrupted, implying deposition prior to or during completion of tectonic activity. Veins hosting the mineralisation overprint at least one earlier vein set, and are the last to have occurred.

Features of Stonehenge include:

- the 1000 ppm zinc contour for the wacker bedrock sampling is over 600m long in an east-west direction, and is open to the west
- the dominant vein orientation for veins in the Zeehan area is NNW-SSE
- the Sylvester and Comstock replacive deposits have an approximate east-west strike
- an interpreted steep plunge for the folded Oonah Formation.

Additional assays for DD95ZS31 are included in Appendix XI. The new elements analysed for were Au, P and Sn.

Follow up drilling to DD95ZS31 did not proceed due to budgetary constraints.

5. Discussion of Results

5.1 Myrtle

The structural pattern at Myrtle remains enigmatic. Topography indicates open folding with gentle plunges, therefore, it is possible that large areas of the limestone are flat dipping. However, core orientations of some of the drill core indicate that the beds are steeply dipping. Detailed inspection of the helimag data and images will lead to a better delineation of the Siltstone Unit. Complexity of the magnetic patterns suggests tight folding and/or thrust repetition of units.

5.2 Pyramid

Drilling at Pyramid shows:

- The upper phyllitic sequence is part of the Silurian Amber Slate.
- There may be a subtle faulted contact between the Amber Slate and the Siltstone Unit of the Gordon Limestone.
- The calcareous silicic quartzite is part of the Siltstone Unit and signifies proximity to a major syn-sedimentary fault. This lithology is previously unrecorded in the Zeehan area.
- Conodont age dating implies complex thrusting within DD96ZP65. The carbonate beds may be overturned.

- Elevated zinc values and dolomite in the quartzite and the dolomitisation of its underlying limestone implies the passage of mineralising fluids; probably accessed by a syn-sedimentary fault. Mapping this quartzite will be important.
- The helimag and wacker data suggest a north plunging synclinal fold hinge in the centre of the prospect.
- Discrete subtle magnetic anomalies relating to siderite alteration occur on the western flank of the prospect.
- Modelling of the magnetic data indicates that these two anomalies dip to the west suggesting that the folding is tight with a slightly overturned western limb.

6. Environment and Rehabilitation

A number of activities conducted during 1996 have impacted on the environment. These include:-

- diamond drilling at Myrtle
- diamond drilling at Pyramid
- line cutting and wacker sampling at Pyramid.

Rehabilitation of surface disturbance included:-

- capping of diamond drill hole collars
- raking of drill sites
- removal of rubbish and cuttings

Drill sites and grid lines will naturally revegetate. No permanent new access tracks were created. Where possible, low-impact technologies were employed in exploration.

All exploration work is discussed on site with the Department of Industry, Safety and Mines personnel prior to it being undertaken. Their advice allows for environmental impact of the proposed work to be kept to a minimum.

One potential problem area may be the Myrtle prospect where gorse infestation along access tracks put in by previous explorers has got beyond control. This illustrates the importance of not removing the natural vegetation, and minimising the area of disturbance.

7. References

Parkinson, R.G.	1992b	Zeehan No. 1 EL 28/88, Tasmania. Report on exploration for the fourth year of tenure, 9/11/91 to 9/10/92. CRAE Report No. 18355.
Parkinson, R.G.	1993	Zeehan No. 1 EL 28/88, Tasmania. Report on exploration for the fifth year of tenure, 9/11/92 to 9/11/93. CRAE Report No. 19284.
Parkinson, R.G.	1994	Zeehan No. 1 EL 28/88, Tasmania. Report on Exploration for the Sixth Year of Tenure 9/11/93 - 9/11/94. CRAE Report No. 20424.
Summons, T.G.	1991	EL 28/88 Zeehan, Tasmania. Statutory Progress Report for the Period Ending 9th November 1991. CRAE Report No. 17636.
Tear, S J	1995	Zeehan No. 1 EL 28/88, Tasmania. Report on Exploration for the Seventh Year of Tenure 9/11/94 - 9/11/95. CRAE Report No. 21102.

8. Location

Queenstown	SK55-5	1:250,000
Pieman	7914	1:100,000
Zeehan	7914-S	1:50,000

9. Keywords

Tasmania, Late Proterozoic, Ordovician, Oonah Fm, Gordon Limestone, Wacker Bedrock, Sampling, Helicopter-borne Magnetics, Diamond Drilling, Zinc, syn-sedimentary faulting, Siderite, Dolomite.

10. DPO Register

CRA Exploration Pty Limited
DPO Register

EL 28/88 Zeehan 1

DPO Number	LAB Batch Number	Lab Name	DPO Location	Office Date	Geologist	Tenement Number	Tenement Name	Sample Type	Number of Samples	250,000 Map Sheet	100,000 Map Sheet
82156	11833	Analabs	Zeehan	18/4/96	S. Tear	28/88	Pyramid	Bedrock	63	SK55-5	7914
82159	11893	Analabs	Zeehan	5/5/96	S. Tear	28/88	Pyramid	$^1/_2$ DDHQ/NQ	58	SK55-5	7914
82162	??	Laola, (Perth)	Zeehan	13/5/96	S. Tear	28/88	Pyramid	Conodont Prep	6	SK55-5	7914
82167	11949	Analabs	Zeehan	28/5/96	S. Tear	28/88	Myrtle	$^1/_2$ DDHQ/NQ	36	SK55-5	7914

364014

145.2°
350000 mE
145.3°
360000 mE
145.4°
370000 mE
41.8°
5370000 mN
41.9°
5360000 mN
42°
5350000 mN

Lake Pieman
Renison Bell
Mt. Heemskirk
Parting Creek Lake
EL28/88
Dundas
Zeehan
Mt. Agnew
Comstock
Cumberland Lake
Austral
Mt. Zeehan
Remine
Trial Harbour
Henty Road
Southern Ocean
Foreshore Flats
Henty Dunes

N

0 2 4
Kilometers

Projection: AMG Zone 55
Grid: AMG Zone 55 & Lat/Long AGD66

5 cm

Burnie
Hobart

Location Diagram

Conical Rocks 7814	Pieman 7914	Sophia 8014
	Cape Sorell 7913	Franklin 8013

Mapsheet Reference

Legend

- Town
- Mountain
- EL Boundary
- Perennial Drainage
- Non-Perennial Drainage
- Highway
- Secondary Road
- Minor Road
- Track
- Railway
- Lake
- Swamp
- Urban

97-3958

ANNUAL REPORT ZEEHAN NO 1
EL 28/88 - P.E. NOV 1996 - CRA
S TEAR/R RUSSELL- **VOL 1 OF 3**

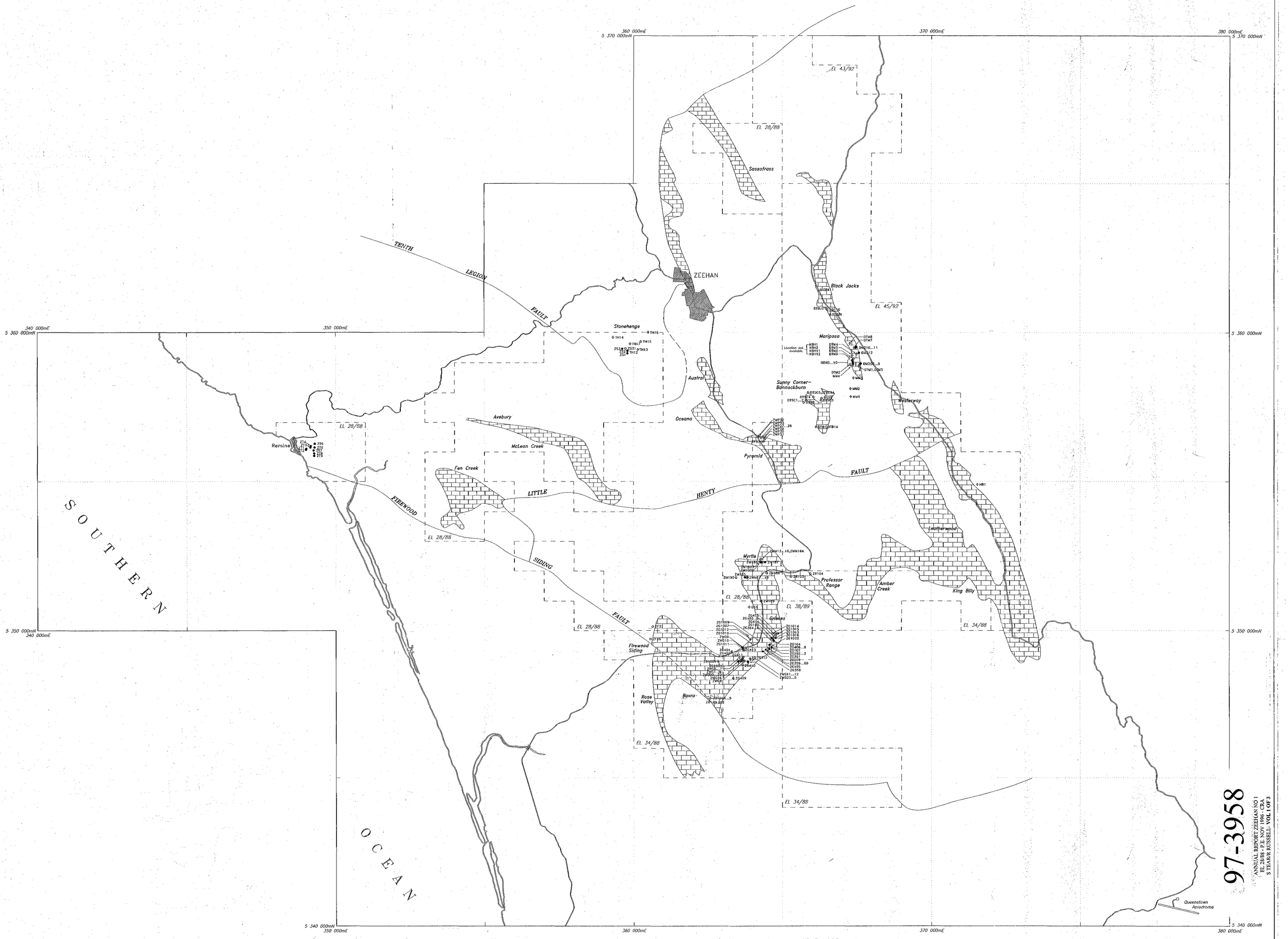
CRA EXPLORATION PTY. LIMITED

364015

EL28/88 Zeehan 1

Location Plan

Author: Simon Tear	Reference: SW Tasmania SK55-22
Drawn: Tony Sargeant	File Name: Tv1021.wor
Date: December 1996	Report No: 22160
Scale: 1:100,000	Plan No: Tv1021



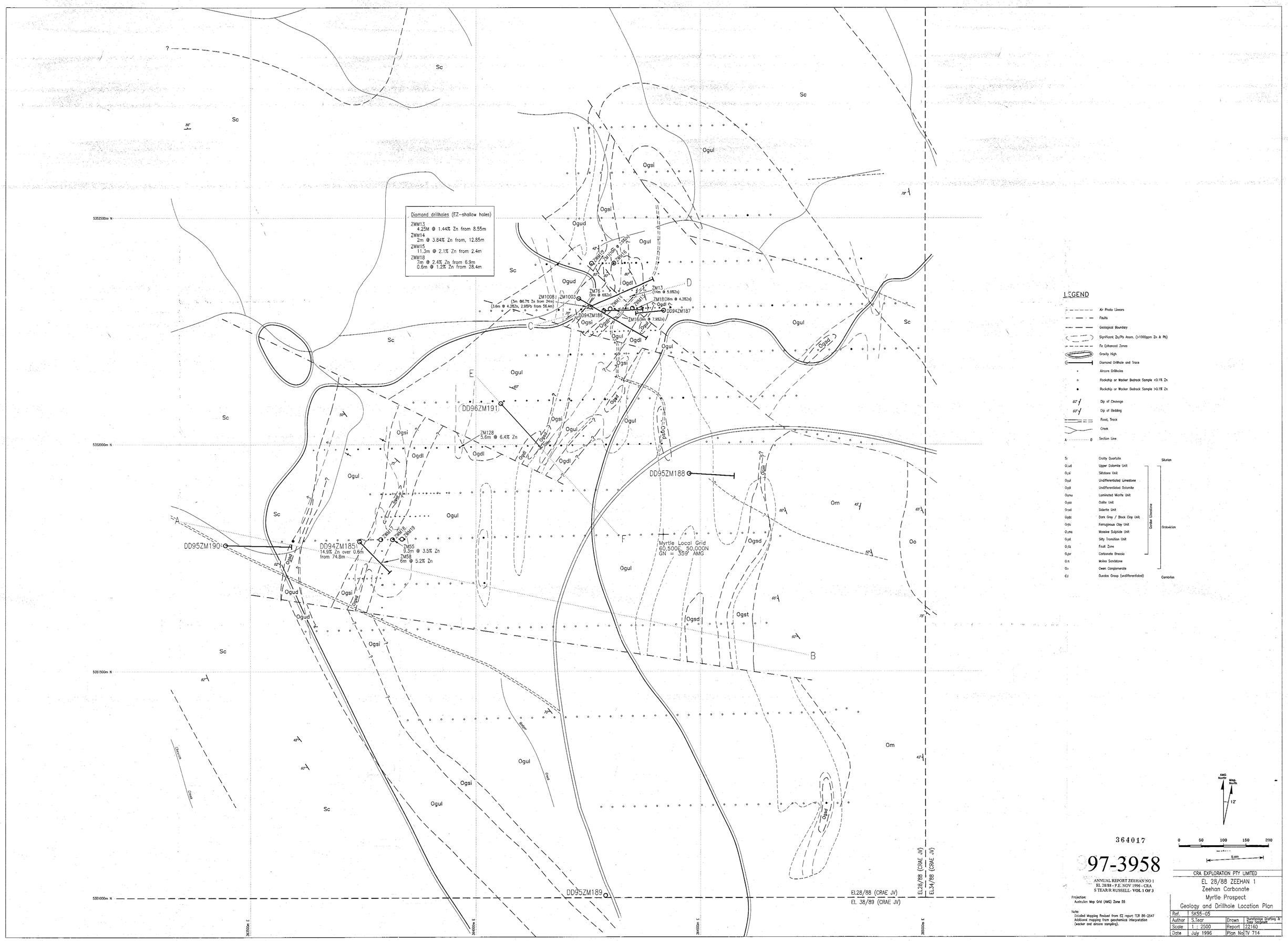
97-3958

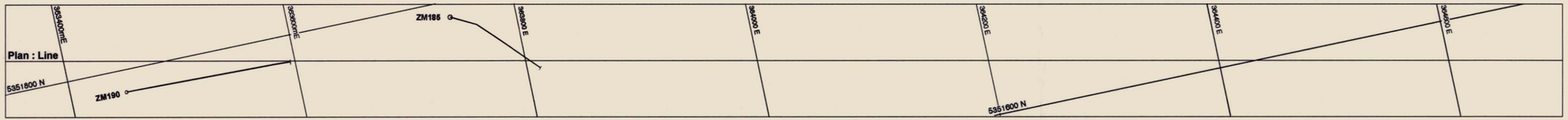
ANNUAL REPORT ZEEHAN NO 1
EL 28/88 - P.E. NOV 1996 - CRA
S TEAR/R RUSSELL- VOL 1 OF 3

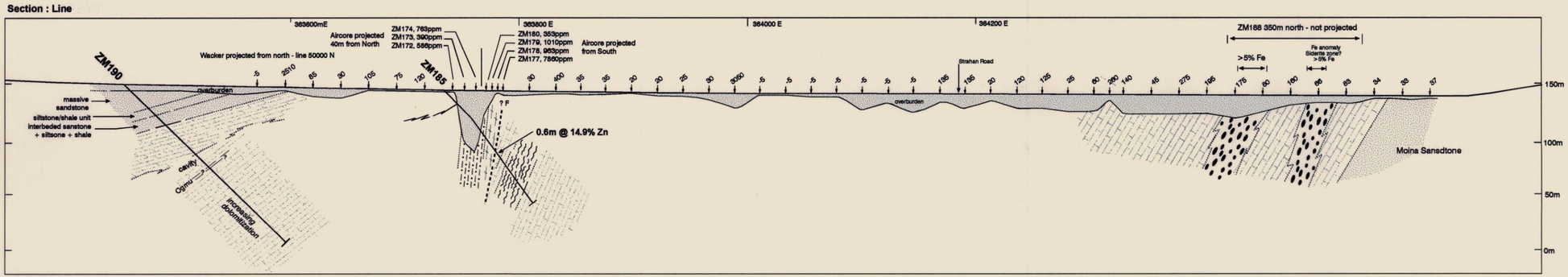
CRA EXPLORATION PTY. LIMITED

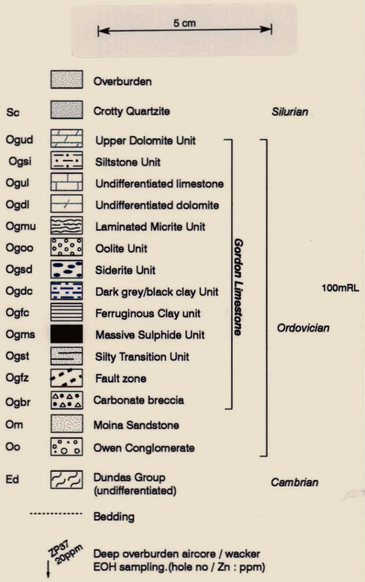
ZEEHAN PROJECT
Target Plan

Ref.:	SK55 – 5	File:	Tv1022.dwg
Scale:	1 : 50000	Date:	November 1995
Author:	Simon Teor	Report No.:	22160
Drawn:	T. Sargeant	Plan No.:	Tv 1022


Diamond drillholes (EZ-shallow holes)
ZWM13
4.25M @ 1.44% Zn from 8.55m
ZWM14
2m @ 3.84% Zn from, 12.85m
ZWM15
11.3m @ 2.1% Zn from 2.4m
ZWM18
7m @ 2.4% Zn from 6.9m
0.6m @ 1.2% Zn from 28.4m
5352500m N
5352000m N
5351500m N
5351000m N
364000m E
364500m E
365000m E
365500m E
Sc
Ogud
Ogsi
Ogul
Ogdl
Ogsd
Ogst
Om
Oo
ZM1008
ZM1003
(3m @6.7% Zn from 24m)
(3.6m @ 4.3%Zn, 2.5%Pb from 56.4m)
ZM76
(9m @ 6%Zn)
ZM13
(14m @ 5.9%Zn)
ZM18(38m @ 4.3%Zn)
ZM16(8m @ 7.9%Zn)
DD94ZM186
DD94ZM187
DD96ZM191
ZM128
5.6m @ 6.4% Zn
DD95ZM188
DD95ZM190
DD94ZM185
14.9% Zn over 0.6m
from 74.8m
ZM55
9.3m @ 3.5% Zn
ZM58
6m @ 5.2% Zn
Myrtle Local Grid
60,500E, 50,000N
GN = 359° AMG
DD95ZM189
EL28/88 (CRAE JV)
EL 38/89 (CRAE JV)
EL28/88 (CRAE JV)
EL34/88 (CRAE JV)
A
B
C
D
E
F
LEGEND
Air Photo Linears
Faults
Geological Boundary
Significant Zn/Pb Anom. (>1000ppm Zn & Pb)
Fe Enhanced Zones
Gravity High
Diamond Drillhole and Trace
Aircore Drillholes
Rockchip or Wacker Bedrock Sample <0.1% Zn
Rockchip or Wacker Bedrock Sample >0.1% Zn
Dip of Cleavage
Dip of Bedding
Road, Track
Creek
Section Line
Sr Crotty Quartzite
Oud Upper Dolomite Unit
Ogsl Siltstone Unit
Ogul Undifferentiated Limestone
Ogdl Undifferentiated Dolomite
Ogmu Laminated Micrite Unit
Ogoo Oolite Unit
Ogsd Siderite Unit
Ogdc Dark Grey / Black Clay Unit
Ogfc Ferruginous Clay Unit
Ogms Massive Sulphide Unit
Ogst Silty Transition Unit
Ogfz Fault Zone
Ogbr Carbonate Breccia
Om Molina Sandstone
Oo Owen Conglomerate
Cd Dundas Group (undifferentiated)
Garden Limestone
Silurian
Ordovician
Cambrian
AMG North
Mag. North
12°
0 50 100 150 200
5 cm
364017
97-3958
ANNUAL REPORT ZEEHAN NO 1
EL 28/88 - P.E. NOV 1996 - CRA
S TEAR/R RUSSELL- VOL 1 OF 3
Projection:
Australian Map Grid (AMG) Zone 55
Note:
Detailed Mapping Revised from EZ report TCR 86-2547
Additional mapping from geochemical interpretation
(wacker and aircore sampling).
CRA EXPLORATION PTY LIMITED
EL 28/88 ZEEHAN 1
Zeehan Carbonate
Myrtle Prospect
Geology and Drillhole Location Plan
Ref. SK55-05
Author S.Tear
Drawn Thurstanridge Drafting & Tear Sediment
Scale 1 : 2500
Report 22160
Date July 1996
Plan No. TV 714







ZP37 200ppm — Bedrock sampling (aircore EOH / wacker) Hole no / Zn : ppm

Strong siderite in aircore holes

Moderate siderite

Elevated Zn

20 40 60 80 100 200m

364018

CRA EXPLORATION PTY LIMITED

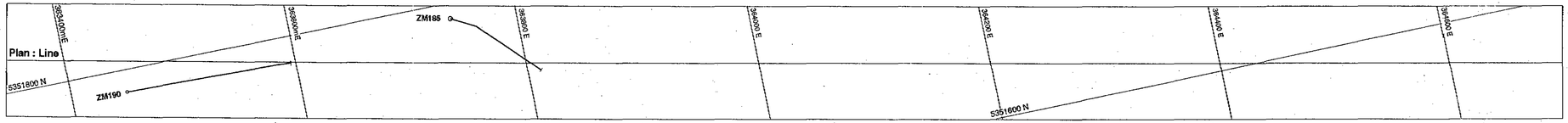
EL28/88 - Zeehan 1

Zeehan Carbonate

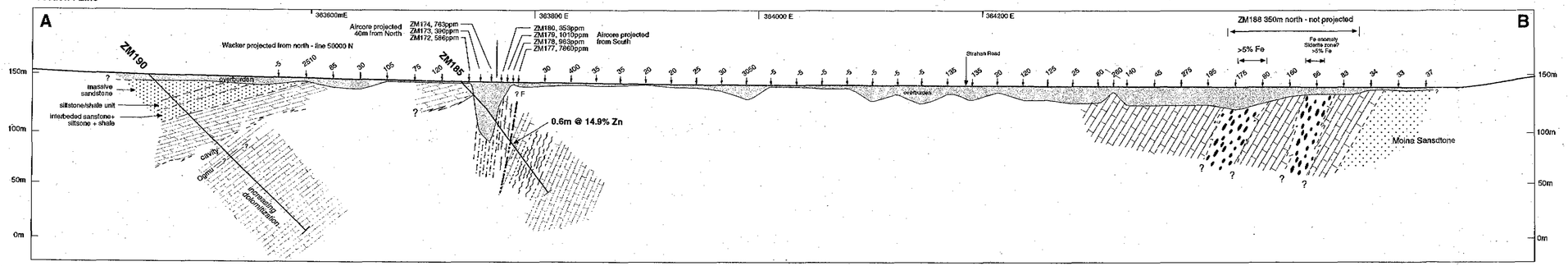
MYRTLE PROSPECT

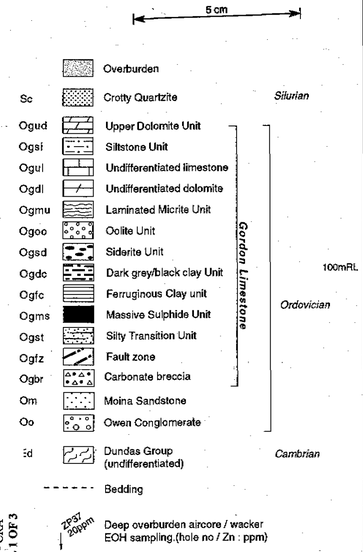
Cross Section : A - B

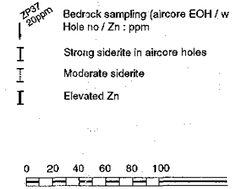
Author:	S J Teer	Reference:	SK5505 Queenstown
Drawn :	D Oliver	File Name :	Tv1035
Date :	February 1996	Report No:	22160
Scale :	1:2500	Plan No :	Tv1035



Section : Line







97-3958

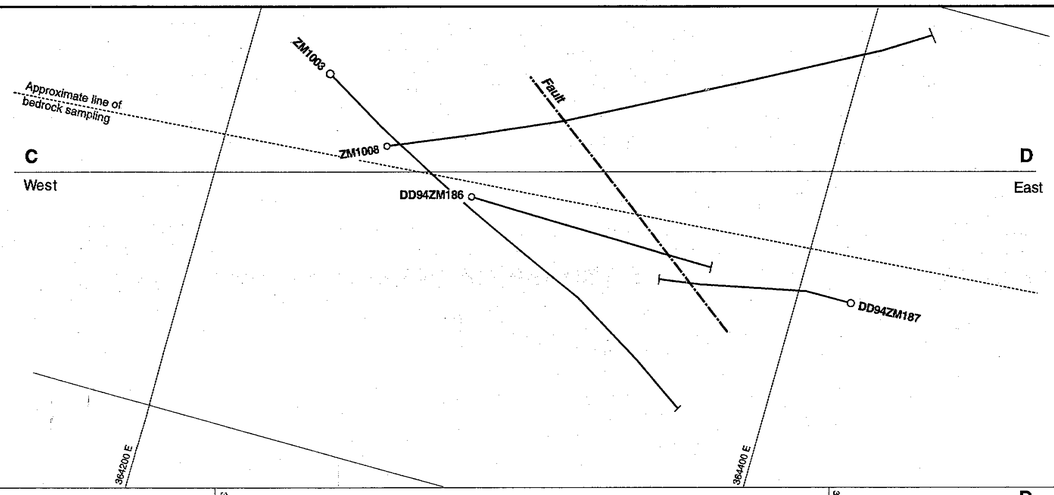
ANNUAL REPORT ZEEHAN NO 1
EL 28/88 - P.E. NOV 1996 - CRA
S TEAR/R RUSSELL- VOL 1 OF 3

364019

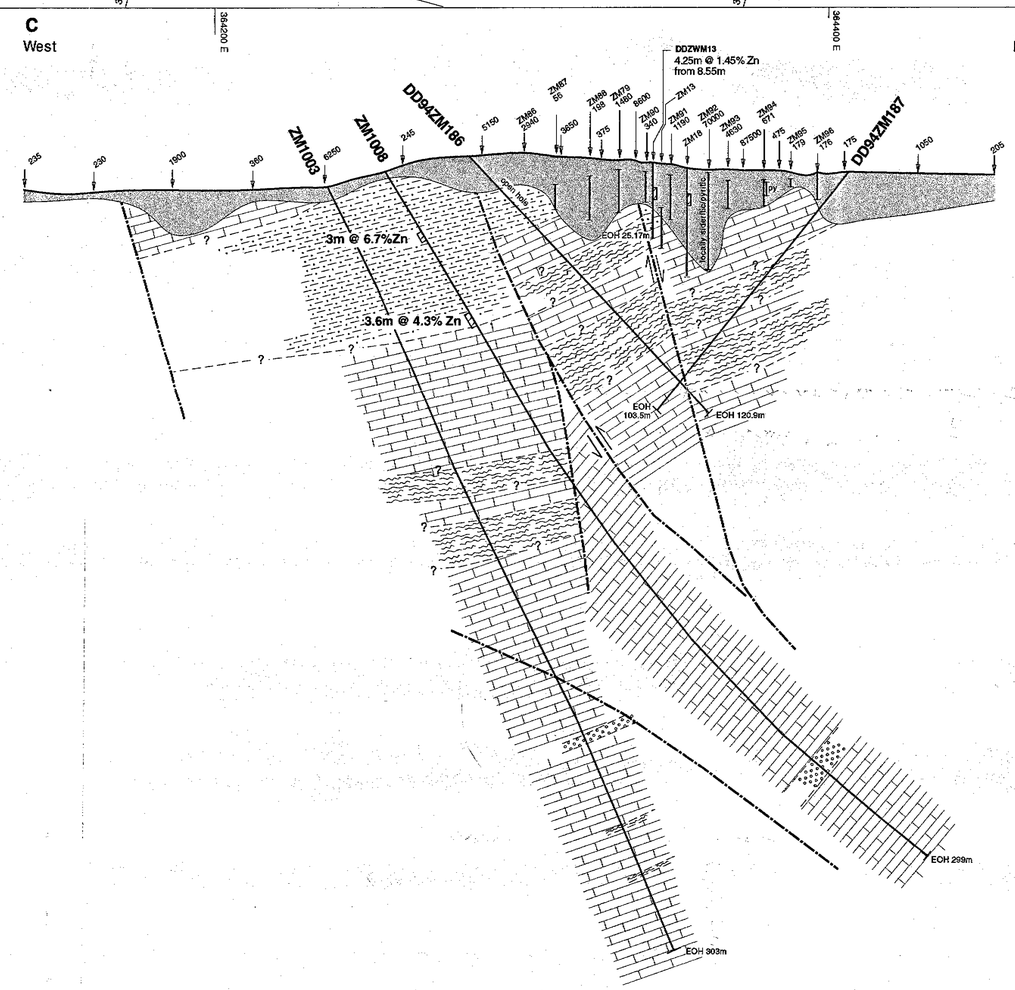
CRA EXPLORATION PTY LIMITED

EL28/88 - Zeehan 1
Zeehan Carbonate
MYRTLE PROSPECT
Cross Section : A - B

Author:	S J Tear	Reference:	SK5505 Queenstown
Drawn :	D Oliver	File Name :	Tv1153
Date :	February 1996	Report No:	22160
Scale :	1:2500	Plan No :	TV1153



200m RL



100m RL

0m

-100m RL

-200m RL

Aircore holes projected 0 - 35m from south.
Wacker bedrock samples projected 28m from north (western end) and 50m from south (eastern end).

ZM13	14m	@ 5.9%	Zn from 14m
ZM18	36m	@ 4.3%	Zn from 0m
ZM87	9m	@ 7.9%	Zn from 9m
ZM88	15m	@ 1.66%	Zn from 6m
ZM89	3m	@ 1.25%	Zn from 12m
ZM90	3m	@ 1.01%	Zn from 12m
ZM91	3m	@ 1.99%	Zn from 3m
ZM92	28m	@ 4.5%	Zn from 0m
ZM93	9m	@ 2.6%	Zn from 3m
ZM94	12m	@ 2.1%	Zn from 3m

Sc		Crotty Quartzite	*Silurian*
Ogud		Upper Dolomite Unit	
Ogsi		Siltstone Unit	
Ogul		Undifferentiated limestone	
Ogdl		Undifferentiated dolomite	
Ogmu		Laminated Micrite Unit	
Ogoo		Oolite Unit	
Ogsd		Siderite Unit	
Ogdc		Dark grey/black clay Unit	
Ogfo		Ferruginous Clay Unit	
Ogms	SMS	Massive Sulphide Unit	
Ogst		Silty Transition Unit	
Ogfz		Fault zone	
Ogbr		Carbonate breccia	
Om		Moina Sandstone	
Oo		Owen Conglomerate	
Ed		Dundas Group (undifferentiated)	*Cambrian*

Gordon Limestone — *Ordovician*

Drillhole Intercept Mineralisation Styles

- Zinc as Sphalerite
- Zinc as mixed sphalerite, zinc rich siderite and zinc silicates (+carbonates)
- Zinc as zinc rich siderite

ZM87 9m@7.9% — Bedrock sampling (aircore EOH / wacker) Hole no / Zn : ppm

- Strong siderite in aircore holes
- Moderate siderite in aircore holes
- Elevated Zn in aircore holes

97-3958

ANNUAL REPORT ZEEHAN NO 1
EL 28/88 - P.E. NOV 1996 - CRA
S TEAR/R RUSSELL- **VOL 1 OF 3**

Note : Section is partly schematic due to the boreholes *not* being on the section line and the section not perpendicular to strike.

5 cm

0 10 20 30 40 50 60m

364020

CRA EXPLORATION PTY LIMITED

EL28/88 Zeehan 1
Zeehan Carbonate
MYRTLE PROSPECT
Section : C - D

Author:	S J Tear	Reference:	SK5505 Queenstown
Drawn :	D Oliver	File Name :	Tv1039
Date :	Feb 1996	Report No:	22160
Scale :	1:1000	Plan No :	Tv1154

E

Bearing of section 138° (AMG)

F

NW

SE

Maximum range of wacker projection onto section is 60m from North-east or South-west

projected from NE

projected from SW

Projection from North-east

Projected from South-west

Projected from North-east

Projected from South-west

7350 390 390 75 90 625 855 5 5 6005 1055 5 85 30 385 30 30 30 20 35 135 115 105 455

DD96ZM191

60°

overburden

overburden

overburden

1.5m @ 0.62% Zn from 15.5m

?

?

?

?

synsedimentary breccia

EOH 300m

200m RL

100m RL

0m

-100m RL

-200m RL

0 10 20 30 40 50 60m

Sc		Crotty Quartzite	Silurian
Ogud		Upper Dolomite Unit	Gordon Limestone / Ordovician
Ogsi		Siltstone Unit	
Ogul		Undifferentiated limestone	
Ogdl		Undifferentiated dolomite	
Ogmu		Laminated Micrite Unit	
Ogoo		Oolite Unit	
Ogsd		Siderite Unit	
Ogdc		Dark grey/black clay Unit	
Ogfc		Ferruginous Clay Unit	
Ogms		Massive Sulphide Unit	
Ogst		Silty Transition Unit	
Ogfz		Fault zone	
Ogbr		Carbonate breccia	
Om		Molina Sandstone	
Oo		Owen Conglomerate	
Ed		Dundas Group (undifferentiated)	Cambrian

Drillhole Intercept Mineralisation Styles

Zinc as Sphalerite

Zinc as mixed sphalerite, zinc rich siderite and zinc silicates (+carbonates)

Zinc as zinc rich siderite

zn-pr 200ppm

Bedrock sampling (aircore EOH / wacker)
Hole no / Zn : ppm

Strong siderite in aircore holes

Moderate siderite in aircore holes

Elevated Zn in aircore holes

5 cm

97-3958

ANNUAL REPORT ZEEHAN NO 1
EL 28/88 - P.E. NOV 1996 - CRA
S TEAR/R RUSSELL- VOL 1 OF 3

364021

CRA EXPLORATION PTY LIMITED

EL28/88 Zeehan 1
ZEEHAN CARBONATE
MYRTLE PROSPECT
Section : E - F

Author:	S J Tear	Reference:	SK8505 Queenstown
Drawn :	D Oliver	File Name :	Tv1110
Date :	December 1996	Report No:	22160
Scale :	1:1000	Plan No :	Tv1110

EL28/88 CRAE JV
Pasminco (Oceana)

EL45/92 CRAE
EL28/88 CRAE JV

Costean
6m@7.2% Pb
2.1% Zn

DD96ZP64
DD96ZP65
DD95ZP63
ZWP27
1m @ 2.7% Zn from 9.1m
(inc. 0.4m @0.3% Zn, 4.8% Pb)
ZWP28
ZWP29
ZWP30
ZWP31
ZWP32
ZWP33

Section A
Wacker Line 'A'
Wacker Line 'B'
1400E Baseline
1000E
1100N
1200N
400N
Possible major siderific zone from helimag data
Major alteration zone of basal Gordon limestone
Fe-rich zone of sandy clays
Pyramid quartzite unit
Wolfe Quartzite
Strahan-Zeehan highway
Little Henty River

5356400m N
5356200m N
5356000m N
5355800m N
5355600m N
5355400m N
5355200m N
5355000m N
5354800m N
363800m E
364000m E
364200m E
364400m E
364600m E
364800m E
365000m E
365200m E

LEGEND

- Strahan–Zeehan highway
- Disused tramway
- Local Grid (EZ)
- Wacker Bedrock Sample Site
- Aircore Sample Site
- 5852423 Wacker Bedrock Sample Site (1996)
- ZP63 EZ Diamond Drillhole
- CRAE diamond drill hole collar & trace
- Field Survey Control Point
- Strike & Dip of Bedding
- Strike & Dip of Joint
- Inferred Lithological Boundary
- Thrust Fault
- Ground Magnetic Linear
- Significant Zn/Pb Anomaly (>1000 ppm Zn & Pb)
- Significant Iron Enhancements

Sc	Crotty Quartzite	Silurian
Ogud	Upper Dolomite Unit	Ordovician
Ogsl	Siltstone Unit	
Ogul	Undifferentiated Limestone	
Ogdl	Undifferentiated Dolomite	
Ogmu	Laminated Micrite Unit	
Ogoo	Oolite Unit	
Ogsd	Siderite Unit	
Ogdc	Dark Grey / Black Clay Unit	
Ogfc	Ferruginous Clay Unit	
Ogms	Massive Sulphide Unit	
Ogst	Silty Transition Unit	
Ogfz	Fault Zone	
Ogbr	Carbonate Breccia	
Om	Moina Sandstone	
Oo	Owen Conglomerate	
Cd	Dundas Group (undifferentiated)	Cambrian

5 cm

AMG North
Mag. North
11°

0 50 100 150 200
metres

997-3958

ANNUAL REPORT ZEEHAN NO 1
EL 28/88 - P.E. NOV 1996 - CRA
S TEAR/R RUSSELL- **VOL 1 OF 3**

364022

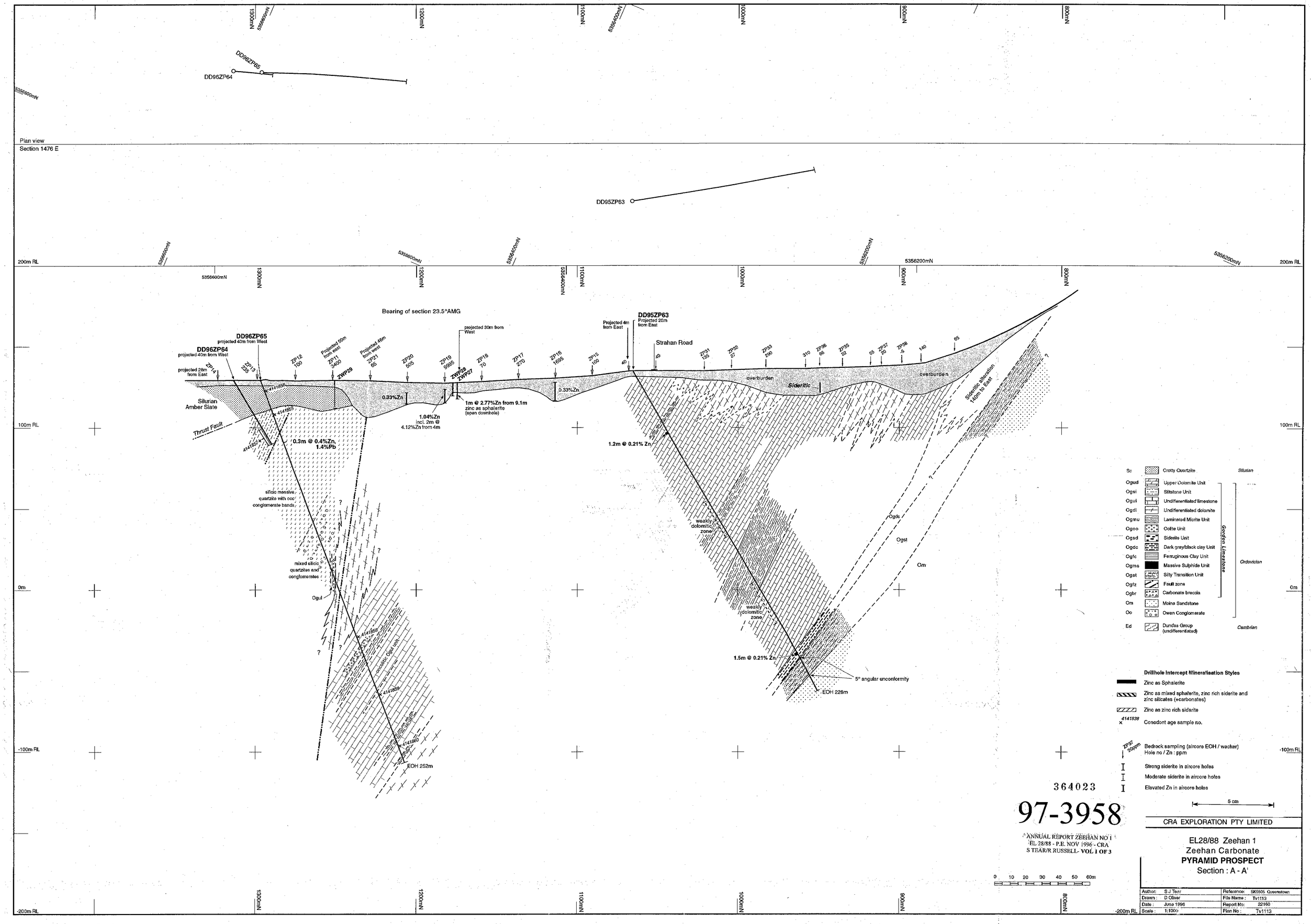
Projection:
Australian Map Grid (AMG) Zone 55

Note:
Approximate topographic error of up to 25m.

CRA EXPLORATION PTY LIMITED			
EL 28/88 ZEEHAN 1 Zeehan Carbonate Pyramid Prospect Geology & Drillhole Location Plan			
Ref.	SK55-05		
Author	S.Tear	Drawn	Hurstbridge Drafting P/L Data Digitised
Scale	1 : 2500	Report	22160
Date	14-11-95	Plan No.	TV 1018

Plan view

Section 1476 E



Sc	Crotty Quartzite	*Silurian*
Ogud	Upper Dolomite Unit	
Ogsi	Siltstone Unit	
Ogul	Undifferentiated limestone	
Ogdl	Undifferentiated dolomite	
Ogmu	Laminated Micrite Unit	
Ogoo	Oolite Unit	
Ogsd	Siderite Unit	
Ogdc	Dark grey/black clay Unit	
Ogfc	Ferruginous Clay Unit	
Ogms	Massive Sulphide Unit	
Ogst	Silty Transition Unit	
Ogfz	Fault zone	
Ogbr	Carbonate breccia	
Om	Moina Sandstone	*Ordovician*
Oo	Owen Conglomerate	
Ed	Dundas Group (undifferentiated)	*Cambrian*

Gordon Limestone

Drillhole Intercept Mineralisation Styles

- Zinc as Sphalerite
- Zinc as mixed sphalerite, zinc rich siderite and zinc silicates (+carbonates)
- Zinc as zinc rich siderite
- 4141838 Conodont age sample no.
- ZP37 200ppm Bedrock sampling (aircore EOH / wacker) Hole no / Zn : ppm
- Strong siderite in aircore holes
- Moderate siderite in aircore holes
- Elevated Zn in aircore holes

0 10 20 30 40 50 60m

5 cm

364023

97-3958

ANNUAL REPORT ZEEHAN NO 1
EL 28/88 - P.E. NOV 1996 - CRA
S TEAR/R RUSSELL- **VOL 1 OF 3**

CRA EXPLORATION PTY LIMITED

EL28/88 Zeehan 1
Zeehan Carbonate
PYRAMID PROSPECT
Section : A - A'

Author:	S J Tear	Reference:	SK5505 Queenstown
Drawn :	D Oliver	File Name :	Tv1113
Date :	June 1996	Report No:	22160
Scale :	1:1000	Plan No :	Tv1113

364024 96/3958 Vol. 2 of 3

CRA EXPLORATION PTY. LIMITED
ACN 000 057 125

MINERAL RESOURCES
24 DEC 1996
TASMANIA

Eighth Annual Report
For The Period Ending 9 November 1996
EL 28/88 Zeehan 1, Tasmania

EL 28/88
see folio 11

Volume II of III

MICROFILMED
FICHE No. 014213-22

Author: S J Tear / S A J Russell

Date: November 1996

Licence Holder: CRA Exploration Pty. Limited
Allegiance Mining NL

Submitted to: Chief Geologist, South East District

Copies to: Mineral Resources Tasmania
CRAE - South East District
CRAE - Zeehan
CRAE - ETIG
Allegiance Mining NL

97-3958

ANNUAL REPORT ZEEHAN NO 1
EL 28/88 - P.E. NOV 1996 - CRA
S TEAR/R RUSSELL- **VOL 2 OF 3**

"All rights in this report and its contents (including rights to confidential information and copyright in text, diagrams and photographs) remain with CRA Exploration and no use (including use of reproductions, storage or transmission) may be made of the report or its contents for any purpose without the prior written consent of CRA Exploration.
© CRA Exploration Pty. Limited 1996"

CRAE Report No. 22160

364025

Appendix I

The Gordon Limestone Lithostratigraphy

Zeehan Carbonate Project

In the Zeehan sub-basin the Gordon Limestone has a thickness of 500m (DDH ZB1007). Drilling by CRAE has subdivided this formation into lithologic and lithostratigraphic units. These subdivisions have been utilised in the drillhole logging and are displayed below.

Drill Hole Logging Formation / Lithology Codes

Sc	=	Crotty Quartzite		**SILURIAN**
Ogud	=	Upper Dolomite	**GORDON LIMESTONE**	**ORDOVICIAN**
Ogsi	=	Siltstone Unit		
Ogul	=	Undifferentiated limestone		
Ogdl	=	Undifferentiated dolomite		
Ogmu	=	Laminated Micrite Unit		
Ogoo	=	Oolite Unit		
Ogsd	=	Siderite Unit		
Ogdc	=	Dark Grey / Black Clay Unit		
Ogfc	=	Ferruginous Clay Unit		
Ogms	=	Massive Sulphide Unit		
Ogst	=	Silty Transition Unit		
Om	=	Moina Sandstone		
Oo	=	Owen Conglomerate		
Ed	=	Dundas Group (undifferentiated)		**CAMBRIAN**

An explanation for the sub-divisions is given below.

1) The Crotty Quartzite

This formation is a sequence of deltaic quartzites of Silurian age. However in drillcore there appears to be no consistency in lithologies at its base. The question of faulted contacts is brought to mind and the unit has not been subdivided. In DD95ZM190 the sequence passes from white massively bedded sandstone into interbedded/interlaminated sands, shales and silts before finally passing into dark shales (fissile) and clays (possible fault gouge). This is possibly matched in DD95DS98 but there are considerable thickness variations, as would be expected in the depositional environment.

2) The Upper Dolomite Unit (Ogud)

This is a dolomitised limestone unit that always occurs beneath the Crotty Quartzite contact. Its thickness is variable, up to 100m in DD95ZR104 and down to 25m in DD95ZM190. It is possible that the dolomitisation is fault related, the fault being the Crotty Quartzite/Gordon Limestone Contact.

3) The Siltstone Unit (Ogsi)

This is an argillaceous calcsiltite with bands of bioclastic calcarenite and nodular calcsiltite. Locally it is unreactive to dilute hydrochloric acid. It generally occurs at the base of the top third of the stratigraphic column and has an average thickness of 15m.

There are transitional upper and lower sequences to the main Siltstone Unit.

4) Undifferentiated Limestone (Ogul)

This is a bucket term to fit all limestones that do not separate out into any distinctive lithology subdivision

5) Undifferentiated Dolomite (Ogdl)

Localised zones of dolomitised limestone occur within various parts of the stratigraphic column. Unless it is part of the Upper Dolomite, it is referred to as undifferentiated dolomite. The dolomitisation is attributable to faults and/or due to mineralisation, often Ogdl units have elevated base metal values.

6) Laminated Micrite Unit (Ogmu)

This is a distinctive lithofacies comprising of banded and stylolitic fine grained calcarenites and micrites. Sometimes the laminae consist of argillaceous material. The individual laminated units have an upper thickness limit of generally <3m except in specific circumstances eg DD95ZP63. Birds eye micrite units are often associated with the laminated zones. The unit is not a marker horizon but occurs with sufficiently regularity in drillcore as to be able to assist stratigraphic correlations.

7) Oolite Unit (Ogoo)

This unit occurs in outcrop at the Grieves Prospect as a dolomitised equigranular calcarenite unit - thought to be an oolite. It is believed that the well sorted, clean medium grained bioclastic calcarenite unit, locally oolitic, is really part of a package of well sorted calcarenites seen towards the base of the limestone sequence, possibly representing a sand bar.

8) Siderite Unit (Ogsd)

The Siderite Unit is an alteration facies imposed on and replacing limestone (?dolomitised) at the base of the Gordon Limestone. It is regarded as being part of the alteration associated with the replacement Zn/Pb mineralisation.

Siderite alteration also occurs at Grieves in the middle of the limestone sequence. Siderite is also present at the upper sandstone/limestone contact at Blackjacks (DD95DB110) and Myrtle (DD95ZM190).

9) Dark Grey/Black Clay Unit (Ogdc)

These clays are encountered at surface and in drill core above 300m vertical depth. They generally are to be found at the base of the limestone, although they can occur at the top contact (DD95DB110). Dark clays can also be found in the top of drillholes where surficial weathering of the limestones has produced a black pug - depths of 45 vertical metres have been recorded (DD95ZR103). The exact nature of the clays at the basal part of the limestone is unclear. They always underlie the Oolite Unit, often can be intermixed with siderite zones of the Siderite Unit and can be part of the underlying Silty Transition Unit. Whether they are products of deep surface weathering, palaeo-weathering, fault zones or mineral-related alteration remains to be resolved.

10) Ferruginous Clay Unit.

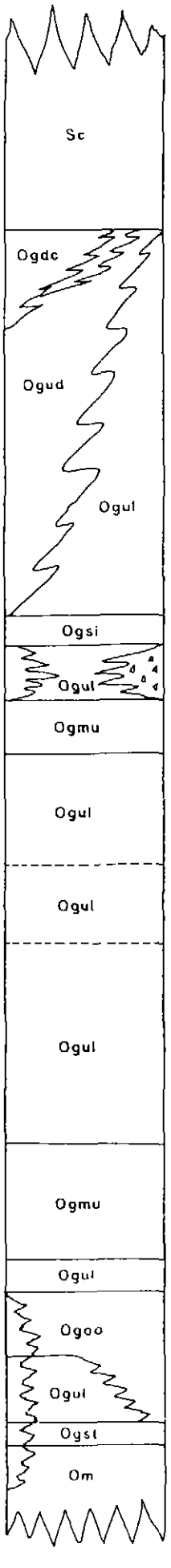
These are light grey, orange, yellow, brown and red coloured clays, often banded. They generally occur beneath the Dark Clay Unit, although at Grieves they can be intermixed with it. In some instances they are sericitic, in others they can be sandy (fine grained quartz grains). They are heavily limonitic and their exact nature is unsure. It is possible that the clays are part of the Silty Transition Unit or even the underlying Moina Sandstone. Alternatively they could be weathering products of mineralisation associated with the dark clay unit.

11) Silty Transition Unit

This is the basal unit of the Gordon Limestone. It comprises of a series of partly dolomitised limestones and fine grained arenaceous units with black siltstones. It appears to have a well defined thickness of between 12-16m and in some instances overlies the Moina Sandstone conformably. Mineralisation would appear to lie immediately above the top contact of the Silty Transition Unit.

12) Moina Sandstone

This sandstone formation is characterised by a silicic quartzite with localised conglomerate bands, often becoming a pink silicic quartzite.



CROTTY QUARTZITE

SIDERITE ALTERATION (Ogsd)

DARK GREY CLAYS

UPPER DOLOMITE

UNDIFFERENTIATED LIMESTONE

MINERALISATION (WEAK)

SILTSTONE UNIT

Ogdl) DOLOMITE (Coarse bioclastic unit)

DOLOMITIC BRECCIA (Ogbr)

MINERALISATION

MICRITE UNIT

?ARGILLACEOUS UNIT

UNDIFFERENTIATED LIMESTONE

MINERALISATION

SIDERITE ALTERATION (Ogsd)

DARK GREY CLAY ALTERATION (Ogdc)

FERRUGINOUS CLAY ALTERATION (Ogfc)

EQUIGRANULAR BIOCLASTIC UNIT → OOLITE UNIT → OFFSHORE BAR

ARGILLACEOUS BIOCLASTIC UNIT

SILTY TRANSITION UNIT

MOINA SANDSTONE

MINERALISATION

0 40 80 120 160 200m

CRA EXPLORATION PTY. LIMITED

SEMI-SCHEMATIC

GORDON LIMESTONE STRATIGRAPHY

Ref.:	Scale:
Author: S.J.TEAR	Report No.:
Drawn: A. IELEN	Plan No.

Appendix II

Exploration by Major Mining Ltd (now Allegiance Mining) and CRAE Prior to 9/11/95

Year 1, Year 2	Activities by Major Mining prior to CRAE's involvement are detailed in the relevant statutory reports. Field activities included a gradient array IP survey covering a small area between the South Comstock and Tasmanian workings.
Year 3	Exploration by CRAE on EL 28/88 prior to 9/11/91 focused on an extensive compilation and review of existing open-file data (Summons, 1991). Analysis of the structural controls to historical mineralisation suggested that the Devonian NNW-trending shear/fracture controlled mineralisation possibly overprints an earlier (Precambrian?) ENE-trending mineralised corridor. Statistical evaluation of Ag:Pb ratios indicated a decline in Ag:Pb from Proterozoic to Ordovician deposits. Considering the ratio as a vector, areas of high Ag:Pb could be close to a postulated Precambrian "Mother Lode". On this basis, the Spray, Montana No. 2 and Junction deposits are the "closest to source".
Year 4	CRAE's exploration strategy in 1992 aimed to test these two models (Parkinson, 1992). Dipole-dipole IP surveys at Stonehenge defined a chargeable conductor exceeding 1 km strike length, coincident with mapped black shale. Soil and wacker sampling indicated this horizon to be anomalous in Zn and Pb. Previous drilling by RGC (hole TH12) intersected several metres of percent-level Zn in the area of interest. Diamond drilling to test stratigraphic and structural targets within the envelope of anomalous geophysics and geochemistry were proposed for 1992/93. Soil sampling at the Avebury stream sediment anomaly detected Zn-Pb-Cu-As anomalism, in an area of poor outcrop within either Cambrian or Proterozoic lithologies. Infill soil sampling was proposed. Open-file literature review revealed the presence of significant surface enrichment of Zn within residual black clays developed over Ordovician Gordon Limestone. Air-core drilling traverses were recommended for Myrtle and Pyramid prospects. Systematical soil/rock sampling of dunite at Trial Harbour was recommended to determine whether the body was capable of hosting a bulk low-grade Ni sulphide resource.
Year 5	(Parkinson, 1993). Three diamond drill holes were drilled at Stonehenge testing stratigraphic and structural targets within the black shale package. Low grade Zn mineralisation was intersected in Devonian age structures, not considered to be economically significant. An air-core traverse across the shale is recommended as diamond drill recoveries were poor near surface. Infill soil sampling at the Avebury showed the central area to be characterised by high background Zn-Pb-Fe. High Fe is suggestive of skarn-related mineralisation. Further investigations are required. Air-core drilling of near-surface decomposed limestone at Myrtle intersected significant Zn mineralisation in several holes (best hole ZM18 - 36m @ 4.3% Zn). The Zn is present as clean

monominerallic grains of low Fe sphalerite, apparently easily liberated from the unconsolidated pug. Additional air-core and diamond drilling is warranted.

Air-core drilling of near-surface decomposed limestone at Pyramid showed patchy weak mineralisation was developed in several holes. Further air-core drilling is required closer to the Limestone-Moina Sandstone contact.

Wacker sampling of limestone at the N end of Firewood Siding prospect returned strongly elevated Zn values near the contact with the Crotty Quartzite. Air-core drilling is recommended.

Soil/rock sampling at Trial Harbour outlined a large area of elevated Ni. Nickel sulphides in olivine orthocumulates were observed in the adit, and a 50m wide unit of olivine orthocumulate was mapped within the body. Drilling beneath the adit intersected weak pyrrhotite mineralisation only, and the intercumulus phases within the main olivine orthocumulate were dominated by magnetite and chromite. Elevated Ni in soil/rock samples is due to a thin skin of secondary Ni-rich serpentinite. No further work is required.

Year 6

(Parkinson, 1994) Reconnaissance soil sampling and magnetometry was confined to a single line across the magnetic anomaly at Avebury.

At Myrtle a total of 121 reverse circulation air-core drillholes amounting to 1876m was completed; air-core bottom-of-hole sampling was also undertaken with assay results being merged with previous wacker sampling. Follow-up diamond drilling consisted of 3 holes totalling 361.4m using a LY38 rig (ZM185-187). The drilling failed to intersect significant mineralisation or relevant alteration of limestone. Some sampling of previously unsampled EZ drillcore was carried out with the best result being 2.4% Zn for 7.05m from 6.85.

Minor amounts of additional rock chip and wacker sampling were also completed.

At Pyramid air-core drilling amounted to 32 holes totalled 348m; end-of-hole samples were also collected with results merged into the wacker sampling database.

Year 7

(Tear 1996) Three diamond drill holes (totalling 1107.4m) were drilled at Myrtle. Two of these holes aimed to test the upper and lower sandstone/limestone contacts , following up elevated zinc values in wacker samples. Weakly elevated zinc mineralisation was intersected (maximum 0.28% Zn). The third hole was designed to test a major gravity high , which was inferred to be a down dip extrapolation of the Grieves mineralisation. No immediate explanation for the gravity feature was found although it is possible that it is in response to a greater than normal thickness of clean calcarenites. These calcarenites would be more calcareous and possess slightly higher than average densities.

One diamond drill hole was drilled at Pyramid, designed to test the lower sandstone/limestone contact close to where siderite alteration was recorded in AC94ZP43. Assay results for the dark clay unit at the lower contact were disappointing (0.21% Zn for 1.5m from 201m).

One diamond drill hole was drilled at Firewood Siding to test a geochemical anomaly associated with the upper sandstone/limestone contact identified during previous deep overburden sampling. Elevated zinc grades (0.38% Zn) were intersected for 10m from 59m across the Crotty Quartzite/Upper Dolomite contact, and also associated with brown dolomite zones for 3.2m @ 0.5% Zn from 87.8m.

Aircore drilling at Stonehenge (27 holes totalling 503m) designed to systematically test inferred shallow mineralisation produced significant zinc mineralisation in several holes. Drilling was conducted on two 0.3 km traverses at a 25m spacing. Best result was 17m @ 2.82% Zn, 2.06% Pb from 9m to EOH. Mineralisation consisted of galena and dark brown sphalerite, intergrown with fine grained pyrite in a black shale unit within the Oonah Formation. One follow-up diamond drill hole (DD95ZS31) was drilled in an attempt to get superior core recovery. Results included 10.15m @ 4.49% from 30.35m, inc. 6.5m @ 6.3% from 34m; and 3.25m @ 2.51% Zn from 152.95m.

A new Gordon Limestone prospect at Sassafras was explored. Reconnaissance wacker drilling (130 holes) confirmed relatively simple geology with an elongate base metal anomaly associated with the lower sandstone/limestone contact (+/- siderite alteration). Moina Sandstone, however, is absent in most instances with limestone overthrusted by Cambrian Dundas Group sediments. Results showed a peak zinc value of 2590 ppm (mean 164 ppm) with lead values up to 441 ppm (mean 31 ppm).

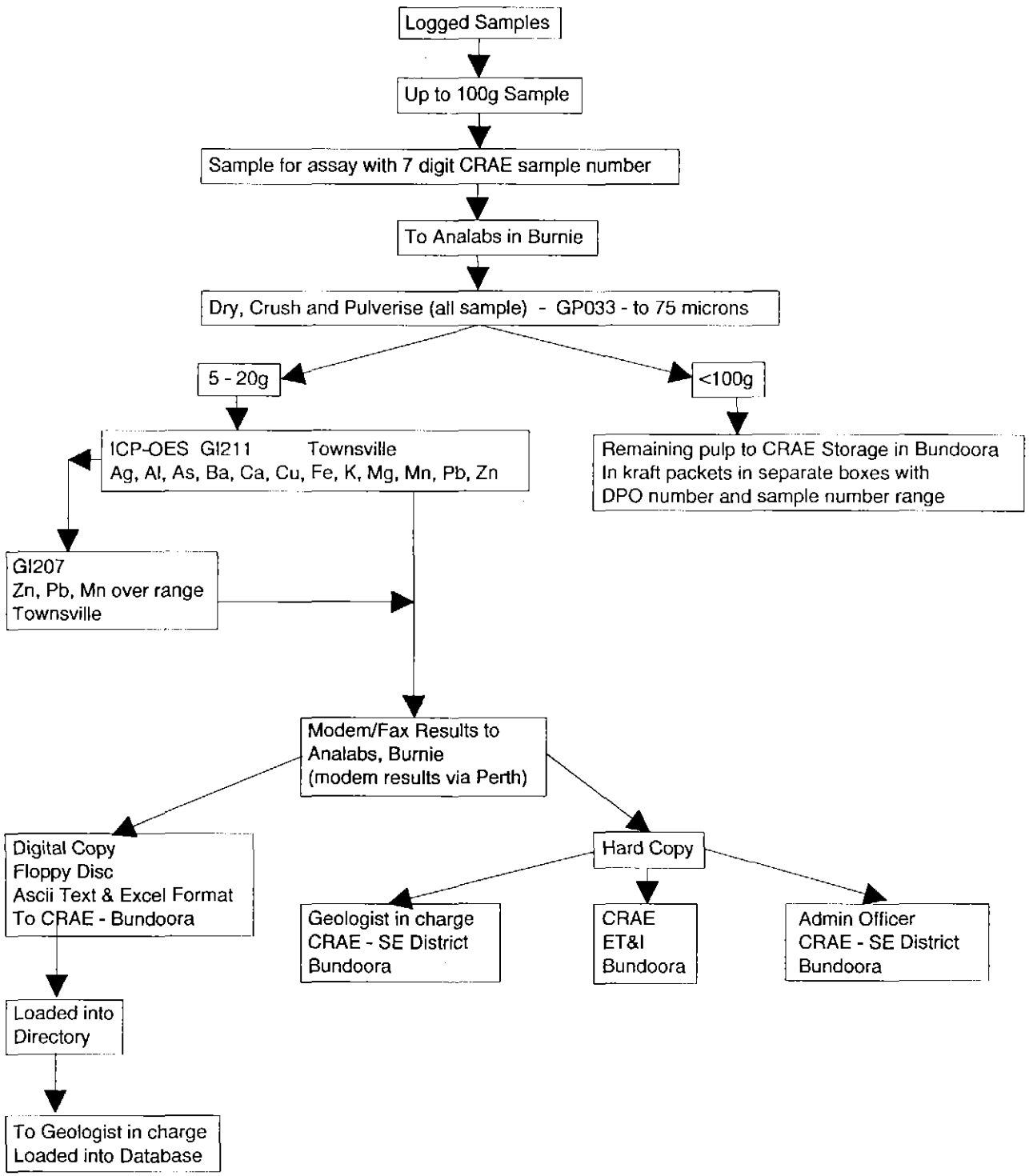
The Gordon Limestone in the Zeehan area was flown over as part of a sub-regional helicopter magnetic survey. Line spacing was approximately 60m with an average flight height of 30m. Sampling intervals were approximately every 3-4m. A feature of the survey was that the flight lines were aimed at being perpendicular to the strike of the limestone.

Appendix III

Analytical Methods for Drillcore and Bedrock Wacker Sampling

364035

Bedrock Wacker Sampling Flowsheet

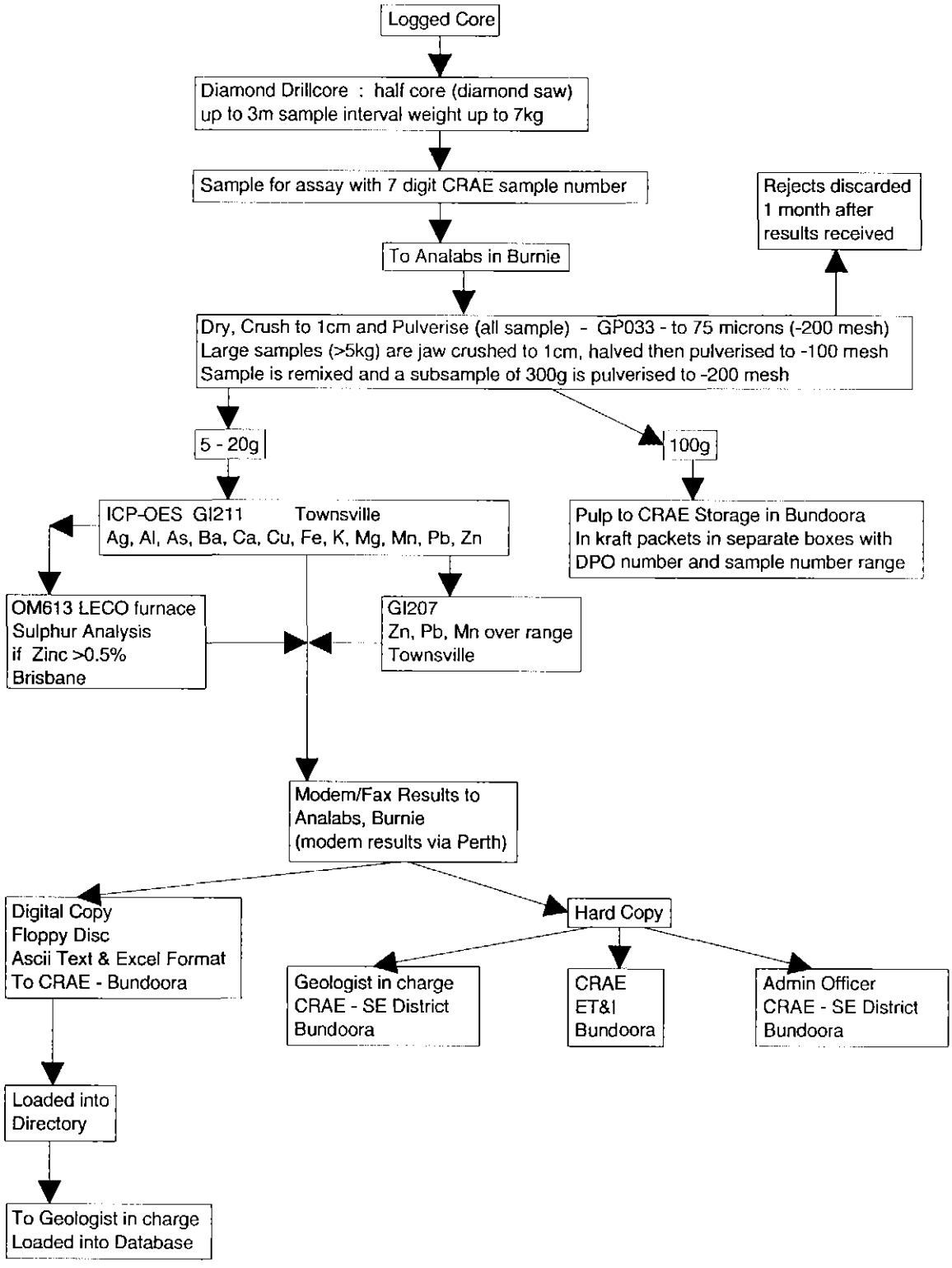


GI211 - Aqua Regia/Perchloric/hydrofluoric acid : acid digest
GI207 - Aqua Regia/Perchloric/hydrofluoric acid : acid digest

S.J.Tear August 1996

364036

Diamond Drillcore Sampling Flowsheet



GI211 - Aqua Regia/Perchloric/hydrofluoric acid : acid digest
GI207 - Aqua Regia/Perchloric/hydrofluoric acid : acid digest

S.J.Tear August 1996

364037

Appendix IV

Myrtle - DD96ZM191 Diamond Drill Logs and Assay Results

CRA EXPLORATION PTY. LIMITED

DRILL-HOLE SUMMARY LOG

364038

HOLE NAME: DD96ZM191 AMG EAST 364056 NORTH 5352092

PROSPECT: MYRTLE GRID EAST 60144E NORTH 50296N.

EL: ZEEHAN 1 EL28/88 RL 149m. DEPTH 300M

DATE DRILLED: 24/4/96

LOGGED BY: S.J.TEAR

DRILLING CO.: DD.TAS.

DRILL TYPE: DIAMOND

DRILL RIG: U.250

LOC DRILL CORE: ZEEHAN

SURVEYS:

DEPTH	AZIM (AMG)	DIP	DEPTH	AZIM (AMG)	DIP
0	134°	60°	251m	142°	59°
50m	137°	60°	299m	141°	59°
101m	139°	60°			
149m	138°	60°			
200m	140°	60°			

OBJECTIVES OF HOLE:

Diamond Drilltest of the Sub-Siltstone Unit sequence

LITHOGICAL SUMMARY:

FROM	TO	FORM CODE	COMMENTS
0	2	Qha	Overburden
2	11.7	Ogfc	Ferruginous clays
11.7	17.0	Ogdc	Dark grey clays
17.0	31.3	Ogul	Nodular calcarenite and bioclastic argillite.
31.3	68.5	Ogmu	Laminated micrite unit.
68.5	158.3	Ogul	Mixed sequence of shallow water/intertidal limestones
158.3	286.8	Ogul	Mixed sequence of argillites and calcarenites sub-tidal
286.8	300.0	Ogul	Shallow/subtidal mixed sequence of laminated micrite units, bioclastic units and argillaceous calcarenites.

MINERALISATION SUMMARY:

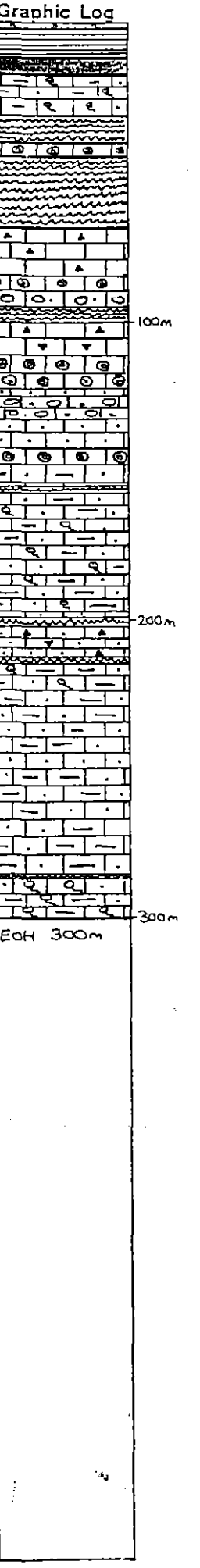
FROM	TO	COMMENTS
15.5	17.0	Sulphidic dark grey clays at base of unit. 0.62% Zn.

CONCLUSIONS:

The hole seemingly missed its target unless the top most dark clays represented the Siltstone Unit - the underlying slightly coarse bioclastic calcarenite and laminated micrite unit may be a clue.

Bedding @ 32.1m 60° to c/A. @ 101.3m 45° to c/A @ 156m 55° to c/A @ 200.8m 80° to c/A @ 286.8m 70° to c/A.

Graphic Log



C.R.A. EXPLORATION PTY. LIMITED

DRILL CORE LOG

SHEET No. 1 of 8

TENEMENT NAME MYRTLE. No. 28/88.

AMG E 364056 E.

CO-ORDINATES 5552092 N. AZIMUTH 134° DRILLERS DDTAS COMMENCED 24/4/1996. PLAN – MAP REFERENCE

RL COLLAR 149m INCLINATION 60° DRILL TYPE U250 Diamond COMPLETED 10/5/1996. DEPTH 300m HOLE No. DD96ZM19

CASING LEFT DPO No(s) 82167

DEPTH From (M)	DEPTH To(M)	Core Rec. %	RQD	Graphic Log	CORE DESCRIPTION	SPECIAL FEATURES Weath, Alteration, Fracturing, Veining, Mineralization	Sample No.	From (M)	To (M)	Depth	(CL = CORE LOSS) Magnetic susceptibility Value	Depth	Value	Depth	Value	REC (mm)	REC (m)	REC (m)	REC (%)
0	9.5	28	5x	Qha	Light grey/orange/white clays with sandstone material.		54710379	0	2.0	0	CL	15.5	0	31	4	0	2.0	0.5	25
							80	2.0	3.3	0.5	CL	16	5	31.5	5	2.0	3.5	0.75	50
							81	3.3	6.5	1	CL	16.5	CL	32	5	3.5	5.0	0.15	10
9.5	11.7		5x	Ogfc	Orange ferruginous clays		82	6.5	8.0	1.5	CL	17	5	32.5	2	5.0	6.5	0.1	7
							83	8.0	9.5	2	0	17.5	0	33	5	6.5	8.0	0.6	40
11.7	17.0		5x	Ogdc	Black/dark grey clay (locally light grey)		84	9.5	11.0	2.5	0	18	CL	33.5	9	8.0	9.5	0.6	40
							85	11.0	11.7	3	CL	18.5	CL	34	7	9.5	11.0	0.5	33
							86	11.7	12.5	3.5	1	19	CL	34.5	5	11.0	12.5	1.4	93
17.0	20.5		5	Ogwl	Rotted argillaceous limestone		87	12.5	14.0	4	0	19.5	CL	35	5	12.5	14.0	1.2	80
							88	14.0	15.5	4.5	CL	20	CL	35.5	5	14.0	15.5	0.8	53
20.5	31.3		1	Ogwl	Intermixed/nodular argillaceous bioclastic calcarenite; bioclasts in argillite; nodules have irregular margins - mottled appearance.		89	15.5	17.0	5	CL	20.5	CL	36	6	15.5	17.0	0.9	60
							90	17.0	18.5	5.5	0	21	5	36.5	0	17.0	18.5	0.75	50
							91	23.0	24.5	6	CL	21.5	4	37	8	18.5	20.0	–	0
										6.5	CL	22	2	37.5	4	20.0	20.7	0.3	43
										7	0	22.5	0	38	4	20.7	21.7	0.95	95
										7.5	0	23	6	38.5	2	21.7	23.0	1.3	100
31.3	40	100	1	Ogmw	Micrite unit – partially laminated; with birds eyes; locally massive micrite. Stylolitic with pyrite on seams.	Bedding @ 32.1m 60° to c/A. Shear vein zone calcite @ 39.8m 75° to c/A; breccia vein.	92	35.0	36.5	8	CL	23.5	10	39	0	23.0	26.0	3.0	100
										8.5	0	24	5	39.5	4	26.0	29.0	3.0	100
										9	0	24.5	5	40	0	29.0	32.0	3.0	100
										9.5	CL	25	5	40.5	5	32.0	33.5	1.5	100
										10	5	25.5	7	41	5	33.5	35.0	1.5	100
										10.5	CL	26	8	41.5	6	35.0	36.5	1.5	100
40	45.9	100	1	Ogwl	Oncolite unit up to 3cm oncolites in diameter. Fine grained calcarenite/micrite & minor argillite.	Calcite breccia vein 75° to c/A 25cm thick in middle of unit. Calcite breccia vein 15cm thick 70° to c/A @ 45.9m.	93	42.2	44.0	11	7	26.5	5	42	8	36.5	38.0	1.25	83
										11.5	9	27	8	42.5	5	38.0	41.0	3.0	100
										12	12	27.5	5	43	5	41.0	42.5	1.5	100
										12.5	0	28	6	43.5	9	42.5	44.0	1.5	100
										13	0	28.5	5	44	2	44.0	47.0	3.0	100
45.9	68.5	100	1	Ogmw	Micrite unit - weakly laminated in places, with birds eye micrites; with stylolites and argillaceous stylocumulates.	Cleavage 15° to c/A. - 35° to c/A Bedding 45° to c/A Calcite veining ? bedding parallel? 63m 1cm thick.	94	53.0	54.5	13.5	0	29	6	44.5	5	47.0	50.0	3.0	100
enter @ 57m							95	68.0	71.0	14	0	29.5	5	45	5	50.0	51.5	1.5m	100
										14.5	0	30	5	45.5	8	51.5	53.0	1.5	100
										15	0	30.5	5	46	0	53.0	56.0	3.0	100

39003

C.R.A. EXPLORATION PTY. LIMITED

DRILL CORE LOG

SHEET No. 2 of 8

TENEMENT NAME MYRTLE No 28/88

PLAN – MAP REFERENCE

AMG 3640560E

CO-ORDINATES 5352092N AZIMUTH 134° AMG DRILLERS DOTAS COMMENCED 24/4/96 DEPTH 300M HOLE No. DD96ZM191

RL COLLAR 149m INCLINATION 60° DRILL TYPE U250 COMPLETED 10/5/96 CASING LEFT DPO No(s) 82167

DEPTH From (M)	DEPTH To(M)	Core Rec. %	RQD	Graphic Log	CORE DESCRIPTION	SPECIAL FEATURES Weath, Alteration, Fracturing, Veining, Mineralization	Sample No.	From (M)	To (M)
					localised zone of fenestral micrite with both dark argillaceous calcarenite fill and calcite fill. Some light grey seemingly coarser beads maybe large ? coral <30cm @ 64.9m - INTERTIDAL FACIES	Calcite breccia vein with large zoned calcite veining. Bedding 45° to c/A @ 65m			
68.5	82.1	100	1	Ogul	Slightly deeper water intermixed argillite and light grey/grey calcarenite micrite - burrowed and bioturbated; occ coral bioclasts. Occ more micritic zones; possible syn-sedimentary breccia zones; possible oncolites				
82.1	83.4	100	1	Ogoo	light grey possibly bioclastic equigranular calcarenite.		5471096	83	85.8
83.4	94.4	100	1	Ogul	Intermixed argillite and bioclastic calcarenite with more equigranular calcarenite zones; possibly bioclasts and possible oncolites + possible syn-sedimentary breccias	This calcite veining <2mm 70° to c/A.			
94.4	96.3	100	2	Ogfz	Ag above with calcite veining + breccia veining Possible fault zone	lower contact 70° to c/A.	5471097	94	96.3

ASSAY VALUES (Analysed by Mag. SUS.) Depth	Value	Depth	Value	Depth	Value	REC (from)	REC (to)	REC (m)	REC (%)
46.5	10	62	10	77.5	10	56.0	57.0	1.0	100
47	10	62.5	10	78	9	57.0	59.0	2.0	100
47.5	6	63	2	78.5	8	59.0	62.0	3.0	100
48	5	63.5	0	79	6	62.0	65.0	3.0	100
48.5	5	64	0	79.5	9	65.0	68.0	3.0	100
49	5	64.5	9	80	9	68.0	71.0	3.0	100
49.5	5	65	2	80.5	0	71.0	74.0	3.0	100
50	5	65.5	8	81	10	74.0	77.0	3.0	100
50.5	5	66	8	81.5	6	77.0	80.0	3.0	100
51	5	66.5	6	82	5	80.0	83.0	3.0	100
51.5	5	67	10	82.5	5	83.0	85.8	2.8	100
52	5	67.5	10	83	0	86.8	89.0	3.2	100
52.5	6	68	9	83.5	6	89.0	92.0	3.0	100
53	4	68.5	5	84	5	92.0	95.0	3.0	100
53.5	5	69	10	84.5	6	95.0	98.0	3.0	100
54	2	69.5	10	85	7	98.0	101.0	3.0	100
54.5	6	70	5	85.5	10	101.0	104.0	3.0	100
55	5	70.5	6	86	5	104.0	107.0	3.0	100
55.5	5	71	8	86.5	0	107.0	110.0	3.0	100
56	5	71.5	4	87	3	110.0	113.0	3.0	100
56.5	8	72	6	87.5	2	113.0	116.0	3.0	100
57	5	72.5	5	88	5	116.0	119.0	3.0	100
57.5	8	73	5	88.5	5	119.0	122.0	3.0	100
58	6	73.5	8	89	6	122.0	125.0	3.0	100
58.5	2	74	9	89.5	5	125.0	128.0	3.0	100
59	5	74.5	9	90	0	1280	131.0	3.0	100
59.5	5	75	8	90.5	4	131.0	134.0	3.0	100
60	4	75.5	9	91.0	5	134.0	137.0	3.0	100
60.5	6	76	5	91.5	9	137.0	140.0	3.0	100
61	8	76.5	4	92	5	140.0	143.0	3.0	100
61.5	7	77	5	92.5	5	143.0	146.0	3.0	100

3640440

C.R.A. EXPLORATION PTY. LIMITED

DRILL CORE LOG

SHEET No. 3 of 8

TENEMENT NAME MYRTLE No. 28188

AMG 364056E

PLAN – MAP REFERENCE

CO-ORDINATES 5352092N AZIMUTH 134° AMG DRILLERS DDTAS COMMENCED 24/4/96 DEPTH 300M HOLE No. DD96ZM191

RL COLLAR 149m INCLINATION 60° DRILL TYPE U250 COMPLETED 10/5/96 CASING LEFT DPO No(s) 82167

DEPTH From (M)	DEPTH To(M)	Core Rec. %	RQD	Graphic Log	CORE DESCRIPTION	SPECIAL FEATURES Weath, Alteration, Fracturing, Veining, Mineralization	Sample No.	From (M)	To (M)
96·3	101·3	100	1	Ogmu	Micritic looking fine grained calcarenite, with birds eye micrite zones becoming more argillaceous (? stylo cumulates) after 100m. Stromatactis cavities 100·7–101·2 in ? Coral.	Minor calcite veining until 100m.			
101·3	111·7	100	1	Ogul	Shallow water possibly intertidal fine grained micritic calcarenites with birds eye micrites + fenestral micrite/calcarenite; possible burrowing texture @ 105·5m.	Bedding 45° to c/A. Calcite veining ⊥ or sub-parallel to c/A.	5471098	107·0	108·5
111·7	121·2	100	1	Ogul	Oncolite? zone with red grained calcarenites and bioclasts. Syn sedimentary breccias with large >20cm Coral fragments, increase in amount of argillite.		5471099	115	117
121·2	126·3	100	1	Ogio	Med grained equigranular grey bioclastic calcarenite with occ argillaceous stylolite; occ micrite clast		5471100	124	126
126·3	134·0	100	1	Ogul	Syn sedimentary breccia/heavily bioturbated argillaceous bioclastic calcarenite.				

ASSAY VALUES (Analysed by.....) Mag. Sus.									
Depth	value	Depth	value	Depth	value	Rec (from)	Rec (to)	Rec (m)	Rec (%)
93	3	108·5	11	124	0	146·0	149·0	3·0	100
93·5	5	109	10	124·5	5	149·0	152·0	3·0	100
94	5	109·5	8	125	4	152·0	153·5	1·5	100
94·5	0	110	5	125·5	2	153·5	155·0	1·5	100
95	5	110·5	10	126	6	155·0	158·0	3·0	100
95·5	0	111	9	126·5	6	158·0	161·0	3·0	100
96	0	111·5	4	127	5	161·0	164·0	3·0	100
96·5	5	112	5	127·5	6	164·0	167·0	3·0	100
97	4	112·5	5	128	6	167·0	170·0	3·0	100
97·5	8	113	8	128·5	9	170·0	173·0	3·0	100
98	4	113·5	5	129	5	173·0	176·0	3·0	100
98·5	0	114	0	129·5	4	176·0	179·0	3·0	100
99	5	114·5	6	130	4	179·0	182·0	3·0	100
99·5	9	115	5	130·5	5	182·0	185·0	3·0	100
100	5	115·5	5	131	5	185·0	188·0	3·0	100
100·5	6	116	2	131·5	5	188·0	191·0	3·0	100
101	0	116·5	6	132	4	191·0	194·0	3·0	100
101·5	6	117	5	132·5	5	194·0	197·0	3·0	100
102	10	117·5	6	133	4	197·0	200·0	3·0	100
102·5	5	118	5	133·5	5	200·0	203·0	3·0	100
103	5	118·5	6	134	6	203·0	206·0	3·0	100
103·5	6	119	4	134·5	4	206·0	209·0	3·0	100
104	5	119·5	6	135	2	209·0	212·0	3·0	100
104·5	5	120	5	135·5	8	212·0	215·0	3·0	100
105	9	120·5	5	136	8	215·0	218·0	3·0	100
105·5	5	121	5	136·5	5	218·0	221·0	3·0	100
106	6	121·5	2	137	6	221·0	224	3·0	100
106·5	9	122	5	137·5	9	224·0	227·0	3·0	100
107	8	122·5	5	138	10	227·0	230·0	3·0	100
107·5	10	123	2	138·5	10	230·0	233·0	3·0	100
108	11	123·5	5	139	9	233·0	236·0	3·0	100

3640411

C.R.A. EXPLORATION PTY. LIMITED

DRILL CORE LOG

SHEET No. 4 of 8

TENEMENT NAME MYRTLE No. 28188

PLAN – MAP REFERENCE

CO-ORDINATES 364056E 5352092N AZIMUTH 134° MMG DRILLERS ODTAS COMMENCED 24/4/96 DEPTH 300m HOLE No. DD96ZM191

RL COLLAR 149m INCLINATION 60° DRILL TYPE U250 COMPLETED 10/5/96 CASING LEFT DPO No(s) 82167

DEPTH From (M)	DEPTH To(M)	Core Rec. %	RQD	Graphic Log	CORE DESCRIPTION	SPECIAL FEATURES Weath, Alteration, Fracturing, Veining, Mineralization	Sample No.	From (M)	To (M)
					occ large coral fragment, numerous bioclasts in argillite interstitial and fine grained calcarenite; becoming more equigranular calcarenite at base				
134	134.8	100	1	Ogoo	Equigranular bioclastic calcarenite unit with calcite veining parallel to c/A				
134.8	138.4	100	1	Ogul	Sequence of interbedded dark grey argillaceous calcarenite and fine grained (?oncolitic) grey calcarenite; often gut bioclastic grey calcarenite bands, - particularly towards base - lam brachiopod shells	Bedding: slightly irregular contacts (70° t c/A) - due to disturbance by ?burrowing or dewatering. Minor vein of pyrite ? clasts @ 137.3m.			
138.4	143.4	100	1	Ogul	Burrowed fine grained grey calcarenite with argillite ~~from~~ cross laminae locally; occ argillite band. rare bioclasts until 141m coarse brachiopods:- possible oncolites towards base. Well cleaved cln planes	5cm calcite @ 143.4m - pyrite on lower contact. bedding parallel 60° t c/A with slickensides. V. minor diseam blebs of pyrite @ 142m, 142.2m. cleavage 45° t c/A - maybe 35° t c/A 1cm 2 phase calcite breccia vein @ 139.3m 50° t c/A ll t bedding locally?	S471271	140.0	141.5
143.4	144.3	100	1	Ogul	Oncolite Unit	Minor veining with pyrite blebs			

ASSAY VALUES (Analysed by.....) Mag Sus Depth	Value	Depth	Value	Depth	Value	Rec (from)	Rec (to)	Rec (m)	Rec (%)
131.5	9	155	6	170.5	7	234.0	239.0	3.0	100
140	9	155.5	10	171	9	239.0	242.0	3.0	100
140.5	10	156	10	171.5	2	242.0	245.0	3.0	100
141	10	156.5	8	172	9	245.0	248.0	3.0	100
141.5	10	157	10	172.5	9	248.0	251.0	3.0	100
142	9	157.5	6	173	10	251.0	254.0	3.0	100
142.5	10	158	5	173.5	8	254.0	257.0	3.0	100
143	9	158.5	9	174	5	257.0	260.0	3.0	100
143.5	10	159	10	174.5	6	260.0	263.0	3.0	100
144	2	159.5	0	175	5	263.0	266.0	3.0	100
144.5	4	160	9	175.5	9	266.0	269.0	3.0	100
145	10	160.5	10	176	7	269.0	272.0	3.0	100
145.5	6	161	8	176.5	10	272.0	274.6	3.0	100
146	7	161.5	10	177	10	274.6	277.6	3.0	100
146.5	10	162	10	177.5	5	277.6	280.8	3.0	100
147	10	162.5	10	178	6	280.8	284.0	3.0	100
147.5	10	163	8	178.5	9	284.0	287.0	3.0	100
148	10	163.5	9	179	6	287.0	290.0	3.0	100
148.5	8	164	10	179.5	8	290.0	293.0	3.0	100
149	10	164.5	6	180	6	293.0	296.0	3.0	100
149.5	10	165	9	180.5	6	296.0	299.0	3.0	100
150	10	165.5	10	181	4	299.0	300.0	3.0	100
150.5	12	166	5	181.5	8				
151	10	166.5	5	182	10				
151.5	11	167	5	182.5	6				
152	11	167.5	10	183	5				
152.5	10	168	9	183.5	6				
153	5	168.5	10	184	10				
153.5	9	169	9	184.5	5				
154	6	169.5	11	185	7				
154.5	5	170	9	185.5	10				

CRA 4063

C.R.A. EXPLORATION PTY. LIMITED

DRILL CORE LOG

SHEET No. 5 of 9

TENEMENT NAME MYRTLE No. 28188

364056E.

CO-ORDINATES 5352092N AZIMUTH 134° AMG DRILLERS DOSAS COMMENCED 24/4/96 DEPTH 300m HOLE No. DD96ZM191

PLAN – MAP REFERENCE

RL COLLAR 149m INCLINATION 60° DRILL TYPE LF250 COMPLETED 10/5/96 CASING LEFT DPO No(s) 82167

DEPTH From (M)	DEPTH To (M)	Core Rec. %	RQD	Graphic Log	CORE DESCRIPTION	SPECIAL FEATURES Weath, Alteration, Fracturing, Veining, Mineralization	Sample No.	From (M)	To (M)	Rec (M)
144.3	156.0	100	1	Ogul	Burrowed argillaceous calcarenite with equigranular unit at top; locally argillite dominant units. Occ bioclastic band	cleavage subparallel & c/a. + variable 35° to c/a. Minor blebs often with calcite veinlets eg 150.2 150mm. bedding 60° to c/a. some fg in crosser units	5471272	152.0	153.5	
156.0	156.8	100	1	Ogul	Possible oncolite band with coarse bioclasts passing into an interlaminated argillite/calcarenite unit – ? cleavage related	Bedding 55° to c/a.				
156.8	158.3	100	1	Ogmu	med/coarse equigranular bioclastic unit – calcite filled cavities – ?stromatactis. Non laminated micrite units. Brecciated bottom contact – syn sed.	Pyrite blebs at top contact. Minor blebs of pale sphalerite in top 20cm.				
DISTINCTIVE UNIT re Walsh et al Reef Ireland.										
158.3	165.7	100		Ogul	Intermixed and bedding disturbed light grey almost micritic calcarenite and argillaceous calcarenite; calcite vug infill. Occ bioclasts in argillite burrowed in places. 159–159.7 – recrystallised carbonate unit or large coral bioclasts <30cm. Becoming less argillaceous after 164m; more micritic with birds eyes + burrows.					

ASSAY VALUES (Analysed by .....)

Mag SUS.

Depth	Value	Depth	Value
186	11	201.5	4
186.5	6	202	4
187	9	202.5	5
187.5	5	203	2
188	6	203.5	4
188.5	6	204	3
189	7	204.5	4
189.5	6	205	0
190	6	205.5	5
190.5	6	206	0
191	9	206.5	0
191.5	10	207	0
192	10	207.5	0
192.5	5	208	2
193	5	208.5	2
193.5	4	209	2
194	5	209.5	5
194.5	9	210	4
195	9	210.5	4
195.5	10	211	5
196	5	211.5	5
196.5	5	212	2
197	5	212.5	0
197.5	9	213	0
198	6	213.5	0
198.5	0	214	0
199	9	214.5	0
199.5	4	215	4
200	5	215.5	0
200.5	6	216	5
201	5	216.5	8

364043

C.R.A. EXPLORATION PTY. LIMITED

DRILL CORE LOG

SHEET No. 6 of 8

TENEMENT NAME MYRTLE No. 28188

PLAN – MAP REFERENCE

CO-ORDINATES AMG 3640566 S352092N AZIMUTH 134° AMG DRILLERS DOTAS COMMENCED 24/4/96 DEPTH 300m HOLE No. DD96ZM191

RL COLLAR 149m INCLINATION 60° DRILL TYPE U250 COMPLETED 10/5/96 CASING LEFT DPO No(s) 82167

DEPTH From (M)	DEPTH To(M)	Core Rec. %	RQD	Graphic Log	CORE DESCRIPTION	SPECIAL FEATURES Weath, Alteration, Fracturing, Veining, Mineralization	Sample No.	From (M)	To (M)	Rec (M)	ASSAY VALUES (Analysed by Mag Sus) Depth	Value	Depth	Value
165.7	170.8	100	1	Ogwl	Intermixed argillaceous burrowed ?bioclastic calcarenite; with calcite filled vugs + recrystallisations Disturbed bedding (heavy) locally; argillaceous calcarenite bands 167–167.6 syn sed breccia.	Minor pyrite in calcite blebs.	5471273	165.5	167.0		217	3	232.5	5
											217.5	5	233	6
											218	5	233.5	7
											218.5	4	234	5
											219	6	234.5	5
											219.5	10	235	10
											220	6	235.5	5
											220.5	4	236	5
											221	5	236.5	6
170.8	173	100	1	Ogwl	Med/fine grained calcarenite almost micritic; fine grained abundant bioclasts; burrowed appearance. Increase in argillaceous calcarenite material after 169.3m	Well cleaved unit 50–40° to c/a. Calcite vn 3cm 60° to c/A @ 173.9m Bedding @ 169m 65° to c/A.					221.5	6	237	5
											222	5	237.5	6
											222.5	10	238	5
											223	9	238.5	5
											223.5	5	239	10
											224	11	239.5	5
											224.5	9	240	2
											225	6	240.5	4
173.0	192.2	100	1	Ogwl	Fine grained grey calcarenite and dark grey argillaceous calcarenite; with occ bioclastic bands. Beds of argillite orientated along cleavage occ burrowed zone. Calcite filled elongated burrows V. featureless limestone Often lath-like bioclasts in argillaceous patches after 188m	Bedding 70° to c/A. cleavage 25° to c/A. Small blebs of pyrite in small calcite vugs eg 182.4m	5471274	174.0	176.0		225.5	7	241	2
											226	5	241.5	2
							5471275	185.0	186.5		226.5	10	242	0
											227	10	242.5	4
											227.5	10	243	5
											228	0	243.5	0
											228.5	10	244	6
											229	5	244.5	6
											229.5	10	245	7
											230	5	245.5	5
											230.5	7	246	9
192.2	193.5	100	1,	Ogwl	Zone of small scale equigranular bioclastic calcarenites – channel samples.						231	5	246.5	8
											231.5	0	247	3
											232	0	247.8	2

3640444

C.R.A. EXPLORATION PTY. LIMITED

DRILL CORE LOG

SHEET No. 7 of 8

TENEMENT NAME MYRTLE No. 28188

PLAN – MAP REFERENCE

AMG 364056E
CO-ORDINATES 5352092N AZIMUTH 134° AMG DRILLERS DOTAS COMMENCED 24/4/96 DEPTH 300m HOLE No. DD96ZM191

RL COLLAR 149m INCLINATION 60° DRILL TYPE U250 COMPLETED 10/5/96 CASING LEFT DPO No(s) 82167

DEPTH From (M)	DEPTH To(M)	Core Rec. %	RQD	Graphic Log	CORE DESCRIPTION	SPECIAL FEATURES Weath, Alteration, Fracturing, Veining, Mineralization	Sample No.	From (M)	To (M)	Rec (M)
193.5	198.4	100	1	Ogwl	Fine grained grey calcarenite with calcite veins on base of more micritic units. Argillaceous beds/bands <5cm becoming more burrowed after 197.3m					
198.4	200.8	100	1	Ogwl	V. fine grained calcarenite / micrite with med grained argillaceous calcarenite as interstitial fill - ?cleavage affected. Calcite filled elongate burrows?					
200.8	203.7	100	1	Ogmu	Laminated micrite unit birds eye micrites.	bedding 80° to c/A.	5471276	200.6	203	
203.7	214.1	100	1	Ogwl	Fine grained calcarenite with bioclasts and birds eyes. Argillite bands and occ channel samples - shallow sub-tidal.		5471277	211.0	212.6	
214.1	216.7	100	1	Ogmu	Laminated micrite unit	bedding 70° to c/A. Core orientation @ 215m bedding closer to subvertical.				
216.7	221.0	100	1	Ogwl	V. fine grained bioclastic calcarenite with irregular argillite bands.					

ASSAY VALUES (Analysed by Mag Sus)

Depth	Value	Depth	Value
248	4	263.5	5
248.5	5	264	5
249	10	264.5	3
249.5	6	265	4
250	9	265.5	4
250.5	7	266	3
251	6	266.5	5
251.5	11	267	5
252	10	267.5	5
252.5	14	268	6
253	13	268.5	6
253.5	7	269	9
254	11	269.5	4
254.5	8	270	9
255	14	270.5	1
255.5	5	271	1
256	5	271.5	2
256.5	5	272	1
257	9	272.5	2
257.5	9	273	1
258	11	273.5	0
258.5	11	274	4
259	5	274.5	5
259.5	5	275	4
260	2	275.5	4
260.5	5	276	0
261	5	276.5	0
261.5	3	277	0
262	10	277.5	2
262.5	5	278	4
263	6	278.5	5

3640445

C.R.A. EXPLORATION PTY. LIMITED

DRILL CORE LOG

SHEET No. 8 of 8

TENEMENT NAME MYRTLE No. 2888

PLAN – MAP REFERENCE

AMG : 3640560E.

CO-ORDINATES 5352092N AZIMUTH 134° AMG DRILLERS DOTAS COMMENCED 24/4/96 DEPTH 300m HOLE No. DD96ZM191

RL COLLAR 149m INCLINATION 60° DRILL TYPE U250 COMPLETED 10/5/96 CASING LEFT DPO No(s) 82167

DEPTH From (M)	DEPTH To(M)	Core Rec. %	RQD	Graphic Log	CORE DESCRIPTION	SPECIAL FEATURES Weath, Alteration, Fracturing, Veining, Mineralization	Sample No.	From (M)	To (M)	Rec (M)
221.0	286.8	100	1	Ogd	Fine grained calcarenite locally micritic with irregular argillite bands acc burrowing zone. channel @ 227.5 – 228.2m. one other small channels. Less distinct argillite banding downhole. Possible mottled zones locally.	Calcite vein + veining zone @ 231.6m – 232.3m. Veining either as thin veinlets <3mm thick or 5–10cm masses. Calcite vein from 276.1 – 277m.	8471278	227.0	228.5	
							79	242.8	244.7	
							80	259.2	261.7	
							81	274.2	276.1	
							82	280.8	282.8	
286.8	287.4	100	1	Ogmu	Laminated micrite unit	Bedding 70° to c/A				
287.4	300.0	100	1	Ogd	V. fine grained locally coarsely bioclastic calcarenite with argillaceous bands Increased effect of cleavage – possible contorted bedding V. shallow subfidal – inc channel deposits + coarse bioclastic in micrites.	Calcite vein 5mm 15° to c/A with diffuse blebs of pyrite.	83	289.6	292.2	
							84	294.0	295.9	
						Bedding back to 55° to c/A @ 298.6m.				
					END OF HOLE –	300m.				

ASSAY VALUES (Analysed by NAG SUS.)

Depth	Value	Depth	Value
279	1	284.5	5
279.5	1	285	5
280	5	285.5	0
280.5	6	286	0
281	8	286.5	2
281.5	5	287	5
282	6	287.5	5
282.5	6	288	5
283	1	288.5	5
283.5	2	289	5
284	1	289.5	0
284.5	1	300	5
285	2	300 EOH	
285.5	2		
286	2		
286.5	5		
287	1		
287.5	0		
288	0		
288.5	1		
289	5		
289.5	9		
290	10		
290.5	4		
291	6		
291.5	2		
292	2		
292.5	1		
293	4		
293.5	4		
294	2		

3640416

bhole	fullddh	DPO	smpno	Prospect	EL	afrom	ato	aag	aal	aas	aba	aca	acu	afe	ak	amg	amn	apb	azn	as	MRTLith
bhole	fulldh	DPO	smpno	Prospect	EL	afrom	ato	aag	aal	aas	aba	aca	acu	afe	ak	amg	amn	apb	azn	as	MRTLith
ZM191	DD96ZM191	82167	5471079	Myrtle	28/88	0	2	-0.5	8.5	33	899	0.09	31	2.57	3.26	0.3	16	1580	108		Qha
ZM191	DD96ZM191	82167	5471080	Myrtle	28/88	2	3.3	-0.5	7.97	42	1080	-0.05	18	2.81	3.37	0.31	10	423	49		Ogfc
ZM191	DD96ZM191	82167	5471081	Myrtle	28/88	3.3	6.5	-0.5	8.48	-5	757	-0.05	15	1.4	3.38	0.31	-10	216	29		Ogfc
ZM191	DD96ZM191	82167	5471082	Myrtle	28/88	6.5	8	-0.5	8.38	14	1020	-0.05	14	1.67	3.63	0.41	12	192	67		Ogfc
ZM191	DD96ZM191	82167	5471083	Myrtle	28/88	8	9.5	-0.5	7.51	23	650	-0.05	15	1.25	3.49	0.34	-10	297	60		Ogfc
ZM191	DD96ZM191	82167	5471084	Myrtle	28/88	9.5	11	-0.5	5.78	133	311	0.09	64	10.2	2.07	0.23	127	974	2330		Ogfc
ZM191	DD96ZM191	82167	5471085	Myrtle	28/88	11	11.7	-0.5	6.81	100	400	0.08	45	10.88	2.55	0.29	100	631	2480		Ogfc
ZM191	DD96ZM191	82167	5471086	Myrtle	28/88	11.7	12.5	1.5	5.61	34	319	0.09	35	2.11	2.43	0.3	12	126	4960		Ogdc
ZM191	DD96ZM191	82167	5471087	Myrtle	28/88	12.5	14	-0.5	7.24	44	343	0.05	55	2.1	3.18	0.37	20	62	3150		Ogdc
ZM191	DD96ZM191	82167	5471088	Myrtle	28/88	14	15.5	-0.5	7.34	14	301	0.05	17	0.96	3.07	0.33	13	40	834		Ogdc
ZM191	DD96ZM191	82167	5471089	Myrtle	28/88	15.5	17	-0.5	5.45	187	241	1.37	26	7.18	2.44	0.6	30	247	6180	9.2	Ogdc
ZM191	DD96ZM191	82167	5471090	Myrtle	28/88	17	18.5	0.9	0.58	-5	22	31.62	-5	0.51	0.28	2.6	95	16	55		Ogul
ZM191	DD96ZM191			Myrtle	28/88	18.5	23														Ogul
ZM191	DD96ZM191	82167	5471091	Myrtle	28/88	23	24.5	-0.5	0.66	-5	28	32.5	-5	0.47	0.32	2.08	86	12	17		Ogul
ZM191	DD96ZM191			Myrtle	28/88	24.5	35														Ogul
ZM191	DD96ZM191	82167	5471092	Myrtle	28/88	35	36.5	0.5	0.57	-5	26	34.92	-5	0.17	0.26	0.29	70	11	15		Ogmu
ZM191	DD96ZM191			Myrtle	28/88	36.5	42.2														Ogmu
ZM191	DD96ZM191	82167	5471093	Myrtle	28/88	42.2	44	-0.5	0.13	-5	-5	35.28	-5	0.27	0.06	0.88	85	11	222		Ogmu
ZM191	DD96ZM191			Myrtle	28/88	44	53														Ogmu
ZM191	DD96ZM191	82167	5471094	Myrtle	28/88	53	54.5	0.8	0.52	-5	22	36.95	-5	0.22	0.24	0.47	60	10	15		Ogmu
ZM191	DD96ZM191			Myrtle	28/88	54.5	68														Ogmu/Ogu
ZM191	DD96ZM191	82167	5471095	Myrtle	28/88	68	71	-0.5	0.58	-5	27	33.65	-5	0.39	0.3	1.79	86	16	192		Ogul
ZM191	DD96ZM191			Myrtle	28/88	71	83														Ogul/Ogbr
ZM191	DD96ZM191	82167	5471096	Myrtle	28/88	83	85.8	-0.5	1.11	-5	58	30.02	-5	0.59	0.56	2.24	108	20	27		Ogul
ZM191	DD96ZM191			Myrtle	28/88	85.8	94														Ogul
ZM191	DD96ZM191	82167	5471097	Myrtle	28/88	94	96.3	-0.5	1.31	-5	70	31.32	-5	0.71	0.65	1.95	178	202	154		Ogul
ZM191	DD96ZM191			Myrtle	28/88	96.3	107														Ogul
ZM191	DD96ZM191	82167	5471098	Myrtle	28/88	107	108.5	0.7	0.34	-5	14	32.42	-5	0.32	0.18	2.11	70	11	16		Ogul
ZM191	DD96ZM191			Myrtle	28/88	108.5	112.5														Ogul
ZM191	DD96ZM191			Myrtle	28/88	112.5	115														Ogbr
ZM191	DD96ZM191	82167	5471099	Myrtle	28/88	115	117	-0.5	1.08	-5	50	29.23	-5	0.61	0.55	3.61	86	10	9		Ogbr
ZM191	DD96ZM191			Myrtle	28/88	117	121.3														Ogbr
ZM191	DD96ZM191			Myrtle	28/88	121.3	124														Ogoo
ZM191	DD96ZM191	82167	5471100	Myrtle	28/88	124	126	-0.5	0.39	-5	20	36.76	-5	0.37	0.21	0.74	109	12	18		Ogoo
ZM191	DD96ZM191			Myrtle	28/88	126	140														Ogul
ZM191	DD96ZM191	82167	5471271	Myrtle	28/88	140	141.5	-0.5	1.6	-5	74	26.91	-5	0.89	0.78	1.68	140	-10	8		Ogul
ZM191	DD96ZM191			Myrtle	28/88	141.5	152														Ogul
ZM191	DD96ZM191	82167	5471272	Myrtle	28/88	152	153.5	0.6	1.68	-5	79	25.3	-5	1.1	0.79	2.27	147	11	9		Ogul
ZM191	DD96ZM191			Myrtle	28/88	153.5	156.7														Ogul
ZM191	DD96ZM191			Myrtle	28/88	156.7	158.3														Ogmu
ZM191	DD96ZM191			Myrtle	28/88	158.3	165.5														Ogul
ZM191	DD96ZM191	82167	5471273	Myrtle	28/88	165.5	167	-0.5	1.14	-5	51	29.53	-5	0.61	0.55	1.77	78	-10	9		Ogul
ZM191	DD96ZM191			Myrtle	28/88	167	174														Ogul
ZM191	DD96ZM191	82167	5471274	Myrtle	28/88	174	176	-0.5	1.73	-5	82	30.11	-5	0.66	0.82	1.38	112	-10	11		Ogul
ZM191	DD96ZM191			Myrtle	28/88	176	185														Ogul
ZM191	DD96ZM191	82167	5471275	Myrtle	28/88	185	186.5	-0.5	0.86	-5	43	30.47	-5	0.58	0.42	2.25	89	11	12		Ogul
ZM191	DD96ZM191			Myrtle	28/88	186.5	200.6														Ogul
ZM191	DD96ZM191	82167	5471276	Myrtle	28/88	200.6	203	1	0.71	-5	36	30.52	-5	0.27	0.36	0.7	66	-10	9		Ogmu
ZM191	DD96ZM191			Myrtle	28/88	203	203.7														Ogmu
ZM191	DD96ZM191			Myrtle	28/88	203.7	211														Ogul
ZM191	DD96ZM191	82167	5471277	Myrtle	28/88	211	212.5	-0.5	0.66	-5	36	25.57	-5	0.48	0.34	1.88	71	-10	-5		Ogul
ZM191	DD96ZM191			Myrtle	28/88	212.5	214.2														Ogul
ZM191	DD96ZM191			Myrtle	28/88	215.2	216.7														Ogmu
ZM191	DD96ZM191			Myrtle	28/88	216.7	227														Ogul
ZM191	DD96ZM191	82167	5471278	Myrtle	28/88	227	228.5	0.6	0.75	-5	41	25.77	-5	0.5	0.37	1.86	68	10	18		Ogul
ZM191	DD96ZM191			Myrtle	28/88	228.5	242.8														Ogul
ZM191	DD96ZM191	82167	5471279	Myrtle	28/88	242.8	244.7	1.2	0.56	-5	18	31.93	-5	0.48	0.26	1.66	142	12	15		Ogul
ZM191	DD96ZM191			Myrtle	28/88	244.7	259.2														Ogul
ZM191	DD96ZM191	82167	5471280	Myrtle	28/88	259.2	261.7	-0.5	0.67	-5	22	30.13	-5	0.47	0.33	1.11	177	11	24		Ogul
ZM191	DD96ZM191			Myrtle	28/88	261.7	274.2														Ogul
ZM191	DD96ZM191	82167	5471281	Myrtle	28/88	274.2	276.1	-0.5	0.73	-5	22	32.01	-5	0.48	0.36	0.98	248	16	15		Ogul
ZM191	DD96ZM191			Myrtle	28/88	276.1	280.8														Ogul
ZM191	DD96ZM191	82167	5471282	Myrtle	28/88	280.8	282.8	-0.5	0.91	-5	30	28.48	-5	0.68	0.44	2	199	15	21		Ogul
ZM191	DD96ZM191			Myrtle	28/88	282.8	289.6														Ogul
ZM191	DD96ZM191	82167	5471283	Myrtle	28/88	289.6	292.2	-0.5	2.13	-5	76	23.55	-5	0.89	1	1.37	148	17	16		Ogul
ZM191	DD96ZM191			Myrtle	28/88	292.2	294														Ogul

See plan No TW115 3

3641047

bhole	lulfddh	DPO	smpno	Prospect	EL	afrom	ato	aag	aai	aas	aba	aca	acu	afe	ak	amg	amn	apb	azn	as	MRTLith
ZM191	DD96ZM191	82167	5471284	Myrtle	28/88	294	295.9	-0.5	1.36	-5	46	27.93	-5	0.97	0.65	1.28	128	13	18		Ogul
ZM191	DD96ZM191			Myrtle	28/88	295.9	300														Ogul

394048

Appendix V

Pyramid - DD96ZP64 - ZP65 - Diamond Drill Logs and Assay Results

CRA EXPLORATION PTY. LIMITED

DRILL-HOLE SUMMARY LOG

364050

HOLE NAME: DD96ZP64 AMG EAST 364335 NORTH 5356607

PROSPECT: PYRAMID GRID EAST 1736E NORTH 1073N

EL: ZEEHAN 1 EL28/88 RL 129m. DEPTH 48m.

DATE DRILLED: 28/03/96

LOGGED BY: S.J.TEAR

DRILLING CO.: DDTAS

DRILL TYPE: DIAMOND

DRILL RIG: U250

LOC DRILL CORE: ZEEHAN

SURVEYS:

DEPTH	AZIM (AMG)	DIP	DEPTH	AZIM (AMG)	DIP
0m	198°	60°			

no surveys.

OBJECTIVES OF HOLE:

DIAMOND DRILLTEST OF 'OCEANA HORIZON' - below Ogsi (Siltstone Unit)
Also subsurface test of ZWP27 mineralisation.

LITHOGICAL SUMMARY:

FROM	TO	FORM CODE	COMMENTS
0	3.2	Qha	Overburden.
3.2	13.5	Sa.	Dark grey green phyllite.
13.5	25.0	Ogsi	Dark grey shales with light grey sandstones bands.
25.0	48	Ogsi	Dark grey non-calcareous siltstone with bioclastic carbonate bands.

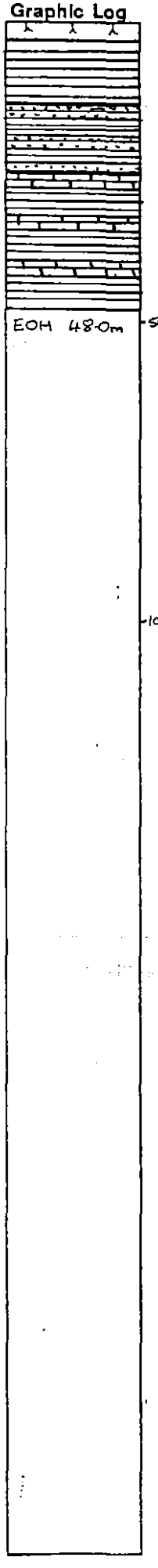
MINERALISATION SUMMARY:

FROM	TO	COMMENTS

CONCLUSIONS:

Hole abandoned due to flooding.
Hole collared in Amber Slate.
Conodont age dating gave a Silurian-Devonian age for bioclastic zone ⇒ ∴ not Siltstone Unit?
Bedding @ 13.5m 60° to c/A. @ 25.0m 55° to c/A.

Graphic Log



C.R.A. EXPLORATION PTY. LIMITED
DRILL CORE LOG

SHEET No. 1 of 2

TENEMENT NAME EL 28/88 ZEEHAN No.

PLAN – MAP REFERENCE PYRAMID

CO-ORDINATES 364335E 5356601N AZIMUTH 198° DRILLERS DD TAS COMMENCED 28/3/1996 DEPTH 48m HOLE No. DD96ZP64

RL COLLAR 129m INCLINATION 60° DRILL TYPE U250 COMPLETED 2/4/1996 CASING LEFT DPO No(s) —

DEPTH From (M)	DEPTH To (M)	Core Rec. %	RQD	Graphic Log	CORE DESCRIPTION	SPECIAL FEATURES Weath, Alteration, Fracturing, Veining, Mineralization	Sample No.	From (M)	To (M)	Rec (M)
0	3.2	45	5	Qha	Overburden : peat and gravels					
3.2	13.5	47	4x		Dark grey/green fine grained non calcareous siltstone zones of broken and fractured core.	Shearing ? sub parallel to c/a				
13.5	25.0	74	3x		Dark grey/green fine grained non calcareous siltstone now with fine grained light grey sandstone bands.	Bedding 60° to c/a (? 55°) some shearing + disturbed bedding locally.				
25.0	48.0	88	35		Dark grey/green fine grained non calcareous siltstone now with limestone bands <10cm thick +/- bioclasts limestone bands more frequent after 32.1 m (more competent core).	Sheared. some bedding parallel. Bedding 55° to c/a Irregular bedding @ 31.2m.				
					END OF HOLE (no Surveys)	48m.				
					Hole stopped due to flooding.					

ASSAY VALUES (Analysed by MAC SU3)

Depth	Value	Depth	Value	Rec (from)	Rec (to)	Rec (m)	Rec (%)
3.0	C.L	18.5	20	0	1.5	1.0	67
3.5	0	19.0	0	3.5	3.5	0.5	25
4.0	C.L	19.5	0	3.5	5.0	0.3	20
4.5	C.L	20.0	0	5.0	6.5	0.4	27
5.0	5	20.5	2	6.5	8.0	0.5	33
5.5	C.L	21.0	C.L	8.0	9.5	0.5	33
6.0	C.L	21.5	0	9.5	11.0	0.1	7
6.5	0	22.0	10	11.0	12.0	1.0	100
7.0	C.L	22.5	15	12.0	12.6	0.6	100
7.5	5	23.0	18	12.6	13.5	1.1	100
8.0	4	23.5	10	13.5	14.5	0.9	90
8.5	C.L	24.0	0	14.5	15.8	0.79	50
9.0	C.L	24.5	5	15.8	16.7	0.65	50
9.5	0	25.0	11	16.7	18.0	1.0	77
10.0	C.L	26.5	11	18.0	19.0	0.7	70
10.5	C.L	26.0	5	19.0	19.6	0.5	83
11.0	0	26.5	12	19.6	20.7	0.9	81
11.5	0	27.0	C.L	20.7	22.1	0.7	50
12.0	2	27.5	11	22.1	23.1	0.9	90
12.5	0	28.0	5	23.1	24.8	1.3	76
13.0	0	28.5	10	24.8	26.0	1.2	100
13.5	8	29.0	14	26.0	27.5	0.9	60
14.0	5	29.5	2	27.5	28.8	1.1	85
14.5	4	30.0	15	28.8	29.5	0.6	86
15.0	C.L	30.5	15	29.5	30.6	1.0	90
15.5	5	31.0	12	30.6	31.6	1.0	100
16.0	C.L	31.5	10	31.6	33.1	1.5	100
16.5	0	32.0	0	33.1	35.0	1.9	100
17.0	0	32.5	15	35.0	36.5	1.5	100
17.5	0	32.0	7	36.5	38.0	1.5	100
18.0	0	33.5	15	38.0	39.5	1.5	100

CRA 6407

C.R.A. EXPLORATION PTY. LIMITED

DRILL CORE LOG

SHEET No. 2 of 2

TENEMENT NAME Zephan 1 No. 28188

PLAN – MAP REFERENCE PYRAMID

CO-ORDINATES AMG 364335E 7358607N AZIMUTH 198° DRILLERS DDIAS COMMENCED 28/3/96

DEPTH 48M HOLE No. DD96ZP64

RL COLLAR 129M INCLINATION 60° DRILL TYPE U250 COMPLETED 2/4/96

CASING LEFT DPO No(s) –

DEPTH From (M)	DEPTH To (M)	Core Rec. (M)	Core Size	Graphic Log	CORE DESCRIPTION	SPECIAL FEATURES Weath, Alteration, Fracturing, Veining, Mineralization	Sample No.	From (M)	To (M)	Rec (M)

ASSAY VALUES (Analysed by MAG SUS)

DEPTH	VALUE	Rec (From)	Rec (To)	Rec (M)	Rec (%)
34.0	15	37.5	40.7	1.2	100
34.5	10	40.7	41.5	0.6	75
35.0	15	41.5	44.0	2.5	100
35.5	10	44.0	44.7	0.7	100
36.0	21	44.7	45.7	0.6	60
36.5	14	45.7	47.6	0.7	77
37.0	12	47.6	48.0	0.4	100
37.5	C.L				
38.0	5				
38.5	16				
39.0	5				
39.5	2				
40.0	5				
40.5	0				
41.0	5				
41.5	8				
42.0	15				
42.5	8				
43.0	5				
43.5	2				
44.0	5				
44.5	16				
45.0	C.L				
45.5	5				
46.0	5				
46.5	5				
47.0	0				
47.6	0				
48.0	5				

CRA 0003

CRA EXPLORATION PTY. LIMITED
DRILL-HOLE SUMMARY LOG

364053

HOLE NAME: DD96ZP65 AMG EAST 364329 NORTH 5356591

PROSPECT PYRAMID GRID EAST 1720E NORTH 1077N

EL: ZEEHAN 1 EL28/88 RL 129m. DEPTH 252m.

DATE DRILLED: 3/4/96

LOGGED BY: S.J.TEAR

DRILLING CO.: DD.TAS.

DRILL TYPE: DIAMOND

DRILL RIG: U250

LOC DRILL CORE: ZEEHAN

SURVEYS:

DEPTH	AZIM (AMG)	DIP	DEPTH	AZIM (AMG)	DIP
0m	200°	69°			
50m	202°	70°			
100.5m	200°	69°			
200m	198°	69°			
251m	198°	68°			

OBJECTIVES OF HOLE:

Diamond drilltest of near surface mineralisation in ZWP27 at or around the 'Oceana Horizon' - middle zone test

LITHOGICAL SUMMARY:

FROM	TO	FORM CODE	COMMENTS
0	3.2	Qha	Overbourden
3.2	18.7	Sa	Grey non-calcareous siltstone with grey sandstone bands.
18.7	35.4	Ogsi	Dark grey/black argillaceous calcsiltite with bioclastic micrite bands
35.4	38.0	Ogdl.	Dolomite – ? shear zone
38.0	123.3	Ogsi	Series of silicic sandstones, quartzites and conglomerates. Rotted limestone unit.
123.3	125.8	Ogul	Fine grained grey quartzite
125.8	132.3	Ogsi	Dolomite - hematitically altered – poss faulted zone.
132.3	137.5	Ogdl	Dolomite - hematitically altered
137.5	140.9	Ogdl	Sheared zone with dolomite and dolomite breccias.
140.9	144.0	Ogfz	sheared dolomite - calcarenite at base.
144.0	164.8	Ogdl	Argillaceous bioclastic calcarenite
164.8	180.9	Ogul.	Shallow subtidal & intertidal calcarenites (+/- argillite) with oncolites.
180.9	206.5	Ogul	Argillaceous calcarenites with bioclastic bands.
206.5	234.6	Ogul.	Fine grained slightly argillaceous calcarenite with laminated micrite units
234.6	252.0	Ogul	

MINERALISATION SUMMARY:

FROM	TO	COMMENTS
40.9	41.2	0.4% Zn, 1.4% Pb – Galena and sphalerite veins in silicic quartzite.
38.0	140.9	The Silicic quartzite contains up to 9% Ca and averages nearly 500 ppm zinc.

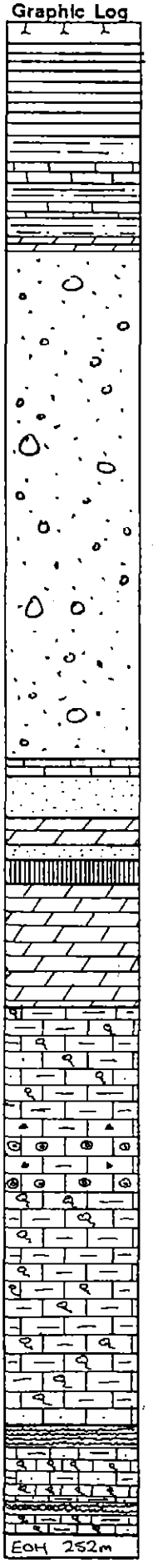
CONODONT AGE DATING. – Inconclusive for top of hole.

CONCLUSIONS:

The age dating suggests the top phyllite is Amber Slate. This seems to pass conformably into Siltstone Unit with an Amber Slate age!? The Quartzite is a local feature within the limestone signifying major syn-sed faulting + rapid sedimentological deposition - Anomalous in Zinc ∴ mineralising fluids have passed through.

Bedding @ 18.7m 60° to c/a. @ 108.5m 45° to c/a. @ 140.9m 60° to c/a. @ 164.8 50° to c/a @ 247.15m 55° to c/a.

Graphic Log



C.R.A. EXPLORATION PTY. LIMITED
DRILL CORE LOG

SHEET No. 1 of 8

ANG: 364329E 5356591N

TENEMENT NAME ZEEHAN 1 28/88 No.

PLAN – MAP REFERENCE PYRAMID

LOCAL CO-ORDINATES 1720E 1077N AZIMUTH 200° Ams. DRILLERS DDTAS COMMENCED 3/4/96

DEPTH 252m HOLE No. DD96ZP65

RL COLLAR 129m INCLINATION 69° DRILL TYPE U250-DIAMOND COMPLETED 22/4/96

CASING LEFT DPO No(s) 82159

DEPTH From (M)	DEPTH To(M)	Core Rec. %	RQD	Graphic Log	CORE DESCRIPTION	SPECIAL FEATURES Weath, Alteration, Fracturing, Veining, Mineralization	Sample No.	From (M)	To (M)	Mag Susceptibility Depth	Value	Depth	Value	Depth	Value	REC (mm)	REC (%)	REC (m)	REC (%)
0	3.2	25	5x	Qha	Overburden. - peat and gravel.					0	0	15.5	10	31	10	0	2	0.3	20
										0.5	CL	16	11	31.5	0	2	3.2	0.3	25
										1	CL	16.5	0	32	0	3.2	4.2	0.7	70
3.2	18.7	47	4x	Ogsi	Grey siltstone - non calcareous with occ fine grained	Plane 45° to c/A	547 1001	3.2	5.0	1.5	CL	17	CL	32.5	15	4.2	5.0	0.2	25
					clean bands of Sandstones.	? Bedding or cleavage.	2	9.4	11.0	2	0	17.5	CL	33	15	5.0	6.4	1.1	79
					Brittle core. Possible	Bedding @ 7.6m 50° to c/A.	3	15.9	18.7	2.5	CL	18	10	33.5	0	6.4	7.8	1.0	71
					Amber Slate - or Siltstone Unit					3	15	18.5	55	34	5	7.8	9.4	0.8	50
										3.5	CL	19	5	34.5	0	9.4	11.0	0.8	50
										4	5	19.5	CL	35	10	11.0	12.5	0.3	20
18.7	35.4	97	1	Ogsi	Dark grey/black argillaceous	Bedding 60° to c/A.	4	18.7	20.4	4.5	CL	20	14	35.5	CL	12.5	14.0	0.8	7
					calcisiltite with light grey	cleavage 15° to c/A.				5	12	20.5	15	36	CL	14.0	15.9	0.5	26
					often bedded/laminated calcarenite	Calcite veining 70° to c/A	5	24.5	26.0	5.5	10	21	35	36.5	CL	15.9	18.9	2.0	67
					bands Argillite dominant.	in argillite only < 3mm 5/10cm.				6	0	21.5	0	37	CL	18.9	20.0	0.9	81
					Occ bioclastic micrite band.	Small shear zone @ 31m	6	29.0	29.9	6.5	5	22	10	37.5	15	20.0	21.5	1.5	100
						45° to c/A.				7	CL	22.5	10	38	10	21.5	23.0	1.5	100
						Bedding @ 33.2 35° to c/A.				7.5	13	23	8	38.5	5	23.0	24.5	1.5	100
										8	10	23.5	5	39	0	24.5	26.0	1.5	100
35.4	38.0	83	2f	Ogsl	Sheared zone with calcite dolomite veining	Shearing? 70° to c/A.	7	35.4	38.0	8.5	CL	24	20	39.5	0	26.0	29.0	3.0	100
										9	CL	24.5	20	40	5	29.0	29.9	0.8	89
					Appearance of bioturbation at base.					9.5	10	25	11	40.5	0	29.9	32.0	2.1	100
										10	CL	25.5	20	41	0	32.0	33.4	1.4	100
										10.5	5	26	5	41.5	0	33.4	35.1	1.7	100
38.0	43.7	100	1		Silicic white, grey quartzite	Minor irregular calcite veining	8	38.0	39.5	11	5	26.5	9	42	0	35.1	36.8	0.7	100
					small vuggy appearance	semi-massive sphalerite/galena	9	39.5	40.9	11.5	CL	27	10	42.5	0	36.8	38.0	0.8	67
					with alloch +/- pyrite fill.	in calcite/dolomite vein @	10	40.9	41.2.	12	CL	27.5	10	43	2	39.0	39.5	1.5	100
					?Conformable upper contact.	41.05m for 2cm. 70° to c/A.	11	41.2	42.5	12.5	5	28	15	43.5	0	39.5	40.9	1.4	100
					Medium grained with fine		12	42.5	43.7.	13	CL	28.5	CL	44	0	40.9	42.5	1.6	100
					black ?shale specks					13.5	CL	29	15	44.5	0	42.5	44.0	1.5	100
										14	11	29.5	11	45	5	44.0	47.0	3.0	100
43.7	48.4	100	1		med/coarse grained white/grey	Minor calcite veining 75° to c/A	13	43.7	46.0	14.5	CL	30	10	45.5	0	47.0	48.5	1.5	100
					quartzite with alkali fspar clasts					15	CL	30.5	5	46	0	48.5	50.0	1.5	100

36405A

C.R.A. EXPLORATION PTY. LIMITED

DRILL CORE LOG

SHEET No. 2 of 8

TENEMENT NAME PYRAMID No. 28/88

PLAN – MAP REFERENCE

AMG 364329 E

CO-ORDINATES 5356591N AZIMUTH 200° AMG DRILLERS DDTAS COMMENCED 31/1/96 DEPTH 252m HOLE No. DD96ZP6

RL COLLAR 129m INCLINATION 69° DRILL TYPE U250 COMPLETED 22/1/96 CASING LEFT DPO No(s) 82159

DEPTH From (M)	DEPTH To (M)	Core Rec. %	RQD	Graphic Log	CORE DESCRIPTION	SPECIAL FEATURES Weath, Alteration, Fracturing, Veining, Mineralization	Sample No.	From (M)	To (M)
					vac black phyllite fragments, pink feldspar + jasper. locally coarser particularly at base.	minor disseminated pyrite. ?Bedding 40° to c/A @ 484 Calcite infill crystals. Calcareous		50	-
48.4	62.0	100	1		Fine grained silicic quartzite massive sandstone. v. minor calcite in matrix - Massive quartzite	Minor calcite veining; localised zones of brecciation. Quartz/calcite veining planar features possibly cleavage <45° to c/A.	5471014 15 16	50 51.5 53.0	51.5 53.0 54.5
62.0	65.0	100	1		White/grey massive quartzite with occ fine conglomerate bands vac black phyllite frags	Calcareous veining locally more thinner + intense	17	62.0	63.5
65.0	66.6	100	1		Fine grained conglomeratic quartzite with black phyllite clasts + a variety of others	Calcareous matrix locally (poss vug infill).			
66.6	92.6	100	1		Grey med/coarse grained silicic quartzite with black clasts out of qtz vein clasts; massive bedding Uniform looking; mixed angular + rounded clasts Occ finer zones.	Occ calcite veining generally 70° to c/A. More intense veining at basal metre.	18 19 20 21	67.8 78.3 88.8 90.3	69.3 79.8 90.3 92.6
92.6	93.3	100	1		Altered fine conglomerate. with calcite in matrix	Quartz/pink carbonate vein 12cm 45° to c/A with green (? fuchsite) mineral on margins + surrounding veinlets	22 23	92.6 93.3	93.3 94.8

Magnetic Susceptibility

Depth	Value	Depth	Value	Depth	Value
46.5	2	62	12	71.5	0
47	0	62.5	10	78	2
47.5	0	63	5	78.5	4
48	7	63.5	6	79	4
48.5	4	64	0	79.5	0
49	5	64.5	2	80	4
49.5	2	65	4	80.5	5
80	0	65.5	8	81	10
80.5	0	66	6	81.5	9
51	2	66.5	10	82	7
51.5	0	67	4	82.5	10
52	0	67.5	5	83	5
52.5	20	68	5	83.5	4
53	5	68.5	4	84	5
53.5	6	69	0	84.5	5
54	5	69.5	9	85	0
54.5	3	70	0	85.5	0
55	0	70.5	0	86	0
55.5	4	71	0	86.5	5
56	5	71.5	5	87	5
56.5	2	72	0	87.5	5
57	5	72.5	0	88	5
57.5	6	73	0	88.5	0
58	3	73.5	0	89	5
58.5	12	74	4	89.5	2
59	10	74.5	4	90	4
59.5	5	75	2	90.5	5
60	5	75.5	5	91	2
60.5	10	76	0	91.5	4
61	5	76.5	0	92	2
61.5	7	77	5	92.5	0

REC From (m)	REC To (m)	REC (m)	REC %
50	51.5	1.5	100
51.5	53.0	1.5	100
53.0	54.5	1.5	100
54.5	56.0	1.5	100
56.0	57.5	1.5	100
57.5	59.0	1.5	100
59.0	60.5	1.5	100
60.5	62.0	1.5	100
62.0	63.5	1.5	100
63.5	65.0	1.5	100
65.0	66.5	1.5	100
66.5	67.8	1.3	100
67.8	69.3	1.5	100
69.3	70.8	1.5	100
70.8	73.8	3.0	100
73.8	75.3	1.5	100
75.3	76.8	1.5	100
76.8	78.3	1.5	100
78.3	79.8	1.5	100
79.8	81.3	1.5	100
81.3	82.8	1.5	100
82.8	84.3	1.5	100
84.3	85.8	1.5	100
85.8	87.3	1.5	100
87.3	88.8	1.5	100
88.8	90.3	1.5	100
90.3	91.8	1.5	100
91.8	93.3	1.5	100
93.3	94.8	1.5	100
94.8	96.3	1.5	100
96.3	99.3	3.0	100

394052

C.R.A. EXPLORATION PTY. LIMITED

DRILL CORE LOG

SHEET No. 3 of 8

TENEMENT NAME PYRAMID No. 28/88

PLAN – MAP REFERENCE

CO-ORDINATES 364329E 5356591N AZIMUTH 200° MAG DRILLERS DOTAS COMMENCED 3/4/96 DEPTH 252m HOLE No. DD96ZP65

RL COLLAR 129m INCLINATION 69° DRILL TYPE U250 COMPLETED 22/4/96 CASING LEFT DPO No(s) 82159

DEPTH From (M)	DEPTH To(M)	Core Rec. %	RQD	Graphic Log	CORE DESCRIPTION	SPECIAL FEATURES Weath, Alteration, Fracturing, Veining, Mineralization	Sample No.	From (M)	To (M)
93.3	97.8	100	1		Med/coarse silicic quartzite locally conglomeratic, grey reduction in amount of black angular clasts. patches of pink/brown alteration; more variety of clasts.	Occ calcite veining			
97.8	98.9	100	1		Brown, buff, pink altered? silicic med/coarse quartzite		25	97.8	98.8
98.8	104.9	100	1		light grey fine grained conglomerate - silicic massive - possible unpaved alteration ?hydrothermal greater variety of generally rounded clasts.	occasional calcite veining localised brecciation light green veining @ 103.3-10 - chlorite or fuchsite.	26	98.8	100.8
104.8	106.9	100	1		Pink hue to ?feldspathic med/coarse grained q/zite with coarser ?alkali fspar clasts.	Pink feldspar - also pink calcite - calcareous.	27 28	103.3 104.8	104.8 106.8
106.9	113.7	100	1		Med grained grey silicic quartzite with coarser zones.	Thin calcite veining. occ green veining and pink carbonate zones in matrix Bedding contact @ 108.5m 40° to c/a. ?Buff dolomite in matrix			

Depth	Value	Depth	Value	Depth	Value	Recovery Rec (from)	Rec (to)	Rec (m)	Rec (%)
93	4	108.5	11	124	5	99.3	100.8	1.5	100
93.5	8	109	2	124.5	10	100.8	102.3	1.5	100
94	10	109.5	5	125	75	102.3	103.8	1.5	100
94.5	10	110	0	125.5	23	103.8	105.3	1.5	100
95	10	110.5	0	126	2	105.3	106.8	1.5	100
95.5	5	111	2	126.5	5	106.8	108.3	1.5	100
96	10	111.5	0	127	9	108.3	109.8	1.5	100
96.5	11	112	5	127.5	2	109.8	111.3	1.5	100
97	9	112.5	4	128	10	111.3	112.8	1.5	100
97.5	11	113	0	128.5	9	112.8	114.3	1.5	100
98	7	113.5	0	129	5	114.3	115.8	1.5	100
98.5	11	114	5	129.5	6	115.8	117.3	1.5	100
99	6	114.5	0	130	9	117.3	118.8	1.5	100
99.5	0	115	5	130.5	6	118.8	120.3	1.5	100
100	0	115.5	5	131	15	120.3	121.8	1.5	100
100.5	0	116	4	131.5	6	121.8	123.3	1.5	100
101	0	116.5	5	132	0	123.3	124.7	1.54	100
101.5	0	117	5	132.5	10	124.7	126.2	1.5	100
102	0	117.5	5	133	CL	126.2	127.8	1.6	100
102.5	0	118	8	133.5	25	127.8	129.3	1.5	100
103	0	118.5	6	134	12	129.3	130.8	1.5	100
103.5	0	119	8	134.5	15	130.8	132.3	1.3	87
104	0	119.5	11	135	0	132.3	133.2	0.45	50
104.5	0	120	9	135.5	14	133.2	134.6	1.4	100
105	5	120.5	0	136	12	134.6	136.1	1.5	100
105.5	0	121	20	136.5	5	136.1	136.8	0.7	100
106	5	121.5	5	137	16	136.8	138.3	1.6	100
106.5	5	122	5	137.5	12	138.3	139.8	1.5	100
107	5	122.5	2	138	0	139.8	141.3	1.5	100
107.5	3	123	22	138.5	11	141.3	142.8	1.5	100
108	8	123.5	21	139	14	142.8	144.3	1.5	100

364056

C.R.A. EXPLORATION PTY. LIMITED

DRILL CORE LOG

SHEET No. 4 of 8

TENEMENT NAME PYRAMID No. 28188

364329E

CO-ORDINATES 5385911N AZIMUTH 200° MAG DRILLERS ODTAS COMMENCED 2/4/96 DEPTH 252m HOLE No. DD96ZP65

PLAN – MAP REFERENCE

RL COLLAR 129m INCLINATION 69° DRILL TYPE U250 COMPLETED 22/4/96 CASING LEFT DPO No(s)

DEPTH From (M)	DEPTH To(M)	Core Rec. %	RQD	Graphic Log	CORE DESCRIPTION	SPECIAL FEATURES Weath, Alteration, Fracturing, Veining, Mineralization	Sample No.	From (M)	To (M)	Rec (M)
113.7	122.5	100	1		Medium grained dark grey silicic quartzite occ conglomeratic band. massive	rare veining becoming greater intensity d/hole.	347029	117.3	118.8	
121.5	123.3	100	2		Fine grained ? sandstone (non-calcareous) with bands of coarser calcareous material — ?limestone. Occ dolomite.		30	121.8	123.3	
123.3	125.8	100	2f		?Limestone band (argillaceous) ; matrix vuggy + calcareous	Top angle contact 10° c/A Bottom angle " 25° c/A.	31	123.3	125.8	
125.8	132.3	95	1		med/fine grained grey quartzite; occ blade shale bands with shearing.	Bedding sub parallel to c/A. Some cal/dol veining and minor brecciation.	32	125.8	127.8	
							33	130.8	132.3	
132.3	133.2	50	5x		Broken core + core loss Poss cavity		34	132.3	133.2	
133.2	137.5	100	3f	Qgdl	Brown/pink/buff ?dolomite massive looking (porrilly & weakly calcareous silicic quartzite) - soft. Zones of grey dolomite	Red hematitic alteration minor thin veinlets minor disseminated pyrite	35	133.2	134.6	
							36	134.6	136.8	
							37	136.8	137.5	
137.5	140.9	100	3f		Possible calcareous quartzite; light grey with pink hue	Shear zone @ 139.9m.	38	137.5	139.8	
							39	139.8	140.9	

ASSAY VALUES (Analysed by.....)

Mag Sus. Depth	Mag Sus. Value	Mag Sus. Depth	Mag Sus. Value	Rec (from)	Rec (to)	Rec (m)	Rec (%)
139.5	5	156	5	144.3	145.8	1.5	100
140	9	155.5	11	145.8	147.3	1.5	100
140.5	11	156	0	147.3	148.8	1.5	100
141	20	156.5	15	148.8	150.3	1.5	100
141.5	9	157	9	150.3	151.9	0.6	86
142	5	157.5	0	151.0	152.5	1.5	100
142.5	15	158	0	152.5	153.6	0.8	72
143	10	158.5	6	153.6	155.2	1.1	69
143.5	11	159	6	155.2	156.3	1.1	100
144	14	159.5	8	156.3	157.8	1.4	93
144.5	9	160	0	157.8 / 159.3	159.3 / 159.8	1.5 / 0.4	100 / 80
145	10	160.5	0	159.8	161.4	1.6	100
145.5	10	161	9	161.4	162.8	1.4	100
146	9	161.5	4	162.8	163.8	1.0	100
146.5	8	162	0	163.8	165.3	1.5	100
147	5	162.5	0	165.3	166.8	1.5	100
147.5	30	163	6	166.8	168.3	1.5	100
148	9	163.5	0	168.3	169.8	1.5	100
148.5	14	164	0	169.8	171.3	1.5	100
149	13	164.5	5	171.3	172.8	1.5	100
149.5	9	165	4	172.8	174.3	1.5	100
150	0	165.5	6	174.3	175.8	1.5	100
150.5	5	166	5	175.8	177.3	1.5	100
151	5	166.5	4	177.3	178.8	1.5	100
151.5	0	167	5	178.8	180.3	1.5	100
152	16	167.5	5	180.3	181.8	1.5	100
152.5	0	168	11	181.8	183.3	1.5	100
153	0	168.5	5	183.3	184.8	1.5	100
153.5	clc	169	5	184.8	186.3	1.5	100
154	5	169.5	2	186.3	187.8	1.5	100
154.5	clc	170	5	187.8	189.3	1.5	100

364057

C.R.A. EXPLORATION PTY. LIMITED

DRILL CORE LOG

SHEET No. 5 of 9

TENEMENT NAME PYRAMID No. 28/188

PLAN – MAP REFERENCE

CO-ORDINATES 364329E. 5356591N AZIMUTH 200° AMG DRILLERS DDTAS COMMENCED 31/4/96 DEPTH 252m HOLE No. DD96ZP65

RL COLLAR 129m INCLINATION 69° DRILL TYPE U25D COMPLETED 22/4/96 CASING LEFT DPO No(s) 82159

DEPTH From (M)	DEPTH To(M)	Core Rec. %	RQD	Graphic Log	CORE DESCRIPTION	SPECIAL FEATURES Weath, Alteration, Fracturing, Veining, Mineralization	Sample No.	From (M)	To (M)	Rec (M)
140·9	142·9	100	1	Ogdl	Dolomite - grey/dark grey well bedded locally; argillaceous zones and dolomitised fenestral micrite.	bedding 60° to c/A but locally faulted	5471040	140·9	142·9	
142·9	143·2	100	5X	Ogfz	Shear zone - brecciated dolomite clasts.	Upper contact 45° to c/A.	41	142·9	144·3	
143·2	143·45	100	1	Ogdl	Altered dolomite.					
143·45	144·0	100	1	Ogbr	Pink/buff/brown/fawn calcite - dolomite vein:- breccia vein with pink altered clasts.	Contacts 75° to c/A at base & Top.				
144·0	145·8	100	1	Ogmu	Grey dolomitised fine grained calcarenite. Locally bedded. Possibly a micrite (laminated) unit + birds eye micrite.	Bedding 50° to c/A cal/dol veining <1cm 70–80° to c/A. 40° to c/A	42	144·3	145·8	
145·8	152·8	95	1	Ogdl	Grey dolomitised fine grained calcarenite ? locally argillaceous. + locally Ogmu type.	Occ cal/dol filled vug. Bearing mm veined even brecciated.	43	148·8	150·3	
152·8	155·2	92	3F	Ogdl	Sheared zones in dolomite - possible cavities - dk grey clays.					
155·2	155·8	100	1	Ogdl	Varied dolomite.		44	153·6	155·8	

ASSAY VALUES (Analysed by .....)

Mag Sus. Depth	Mag Sus. Value	Mag Sus. Depth	Mag Sus. Value		Rec (from)	Rec (to)	Rec (M)	Rec %
170·5	4	186	6		189·3	190·8	1·5	100
171	4	186·5	5		190·8	192·3	1·5	100
171·5	2	187	9		192·3	193·8	1·5	100
172	0	187·5	6		193·8	195·3	1·5	100
172·5	5	188	9		195·3	196·8	1·5	100
173	0	188·5	10		196·8	198·3	1·5	100
173·5	5	189	15		198·3	199·8	1·5	100
174	2	189·5	16		199·8	201·3	1·5	100
174·5	0	190	16		201·3	202·8	1·5	100
175	0	190·5	13		202·8	204·3	1·5	100
175·5	0	191	10		204·3	205·8	1·5	100
176	2	191·5	10		205·8	207·3	1·2	80
176·5	2	192	10		207·3	208·8	1·5	100
177	0	192·5	10		208·8	210·3	1·5	100
177·5	0	193	10		210·3	211·8	1·5	100
178	5	193·5	12		211·8	213·3	1·5	100
178·5	0	194	11		213·3	214·8	1·5	100
179	2	194·5	14		214·8	216·3	1·5	100
179·5	8	195	10		216·3	217·8	1·5	100
180	5	195·5	9		217·8	219·3	1·5	100
180·5	4	196	6		219·3	220·8	1·5	100
181	6	196·5	10		220·8	222·3	1·5	100
181·5	5	197	20		222·3	223·8	1·5	100
182	5	197·5	12		223·8	225·3	1·5	100
182·5	10	198	20		225·3	226·8	1·5	100
183	9	198·5	6		226·8	228·3	1·5	100
183·5	5	199	14		228·3	229·8	1·5	100
184	10	199·5	10		229·8	231·3	1·5	100
184·5	10	200	10		231·3	232·8	1·5	100
185	5	200·5	10		232·8	234·3	1·5	100
185·5	5	201	9		234·3	236·8	1·5	100

364329E 5356591N

C.R.A. EXPLORATION PTY. LIMITED
DRILL CORE LOG

SHEET No. 6 of 8

TENEMENT NAME PYRAMID No. 28188

PLAN – MAP REFERENCE

CO-ORDINATES 3643296E 5356591N AZIMUTH 200° AMG DRILLERS DDTAS COMMENCED 3/4/96 DEPTH 252m HOLE No. DD96PYP65

RL COLLAR 129m INCLINATION 69° DRILL TYPE U250 COMPLETED 22/4/96 CASING LEFT DPO No(s) 82159

DEPTH From (M)	DEPTH To(M)	Core Rec. %	RQD	Graphic Log	CORE DESCRIPTION	SPECIAL FEATURES Weath, Alteration, Fracturing, Veining, Mineralization	Sample No.	From (M)	To (M)	Rec (M)	ASSAY VALUES (Analysed by Mag SUS - Mag SUS) Depth	Value	Depth	Value	REC (from)	REC (to)	REC (m)	REC (%)
155·8	157·5	100	3f	Ogfz	Sheared zone with lt grey pink altered and brecciated ?dolomite locally.	cal/dol veins 70° to c/A. dol breccia 157·3-157·5· two phases of veining	5471045	155·8	157·5		201·5	10	217	10	235·8	237·2	1·0	71
											202	10	217·5	7	237·2	238·8	1·6	100
											202·5	12	218	11	238·8	240·3	1·5	100
											203	10	218·5	15	240·3	241·8	1·5	100
157·5	160·6	95	3f	Ogdl	Veined dolomitised fine grained calcarenites occ small sheared zone	Veining cal/dol and often small and irregular locally brecciation.	46	157·5	159·8		203·5	8	219	10	241·8	244·8	3·0	100
											204	10	219·5	6	244·8	247·8	3·0	100
											204·5	9	220	5	247·8	250·8	3·0	100
											205	5	220·5	7	250·8	252·0	1·2	100
160·6	164·8	100	1	Ogdl	Partially dolomitised laminated calcarenite. - hints of syn sed breccias decrease in dolomitisation downhole.	occ calcite veining irregular Bedding @ 165·8 45° to c/A. Pyrite blebs + semi massive with calcite infilling part of matrix to a syn sed breccia @ 164·3 m. Minor pyrite with calcite veins	47	163·8	164·8		205·5	11	221	6				
											206	10	221·5	6				
											206·5	6	222	10				
											207	6	222·5	10				
											207·5	11	223	11				
											208	8	223·5	11				
											208·5	0	224	10				
											209	5	224·5	9				
											209·5	6	225	7				
164·8	171·8	100	1	Ogul	Fine grained grey calcarenite locally micritic interbedded with more argillaceous med grained (locally non calcareous) calcarenites. light grey calcarenites can be brecciated. occ bioclastic band ?subtidal facies.	Bedding 50° to c/A.					210	5	225·5	6				
											210·5	6	226	9				
											211	5	226·5	6				
											211·5	6	227	10				
											212	9	227·5	10				
											212·5	5	228	12				
											213	9	228·5	13				
											213·5	10	229	5				
											214	10	229·5	9				
171·8	174·8	100	1	Ogul	Argillaceous bioclastic Calcarenite with tetradium. locally light grey micrite bands.	some calcite veining 70° to c/A.					214·5	6	230	5				
											215	7	230·5	2				
											215·5	10	231	6				
											216	6	231·5	5				
174·8	178·5	100	1	Ogpo	Dominantly med grained equigranular calcarenite.	Calcite veining 1 per 10cm generally 70° to c/A.	48	176·8	177·3		216·6	8	232	2				

3640569

C.R.A. EXPLORATION PTY. LIMITED

DRILL CORE LOG

SHEET No. 7 of 8

TENEMENT NAME PYRAMID No. 28188

364329 E

CO-ORDINATES 5356591N AZIMUTH 200° AMG DRILLERS DDTAS COMMENCED 3/4/96

PLAN – MAP REFERENCE

DEPTH 252m HOLE No. DD96ZP65

RL COLLAR 129m INCLINATION 69° DRILL TYPE U250 COMPLETED 22/4/96

CASING LEFT DPO No(s). 82159

DEPTH From (M)	DEPTH To(M)	Core Rec. %	RQD	Graphic Log	CORE DESCRIPTION	SPECIAL FEATURES Weath, Alteration, Fracturing, Veining, Mineralization	Sample No.	From (M)	To (M)	Rec (M)	ASSAY VALUES (Analysed by.....) Mag Sus		Mag Sus	
											Depth	Value	Depth	Value
78.5	180.9	100	1	Ogul	Dominantly argillaceous bioclastic calcarenite with tetradium						232.5	5	248	0
											233	6	248.5	5
											233.5	5	249	7
											234	9	249.5	5
180.9	206.5	98	1	Ogul	Poss'ble start of Myrtle Fm. Interbedded fine grained, locally micritic + coarsely bioclastic calcarenite with argillaceous bands. ?PAC units - but no real laminated micrite units - Oncolites locally. Some birds eye micrite. Poss laminated micrite 182.3-183.3 more channel like towards base Disturbed bedding at base (v.c. variable bedding angles)	Bedding 50° to c/a. calcite veining increases in intensity towards base of units generally <1cm 70° to c/a	5141049	182.0	183.3		234.5	6	250	5
											235	5	250.5	6
							50	192.3	193.8		235.5	5	251	5
											236	4	251.5	0
							51	202.8	204.3		236.5	5	252	6
											237	C/L	2	
							52	205.8	206.5		237.5	5		
											238	5		
											238.5	5		
											239	9		
											239.5	9		
											240	5		
											240.5	5		
											241	2		
206.5	209.7	90	1	Ogul	Altered (?oolited) argillaceous limestone		53	206.5	207.7		241.5	5		
											242	10		
											242.5	5		
209.7	216.3	100	1	Ogul	Interbedded argillaceous calc arenite and burrowed fine grained calcarenite with bioclastic calcarenite bands - bands rather uniform 10cm thickness		54	207.7	208.8		243	0		
											243.5	2		
											244	10		
											244.5	7		
											245	6		
											245.5	6		
											246	8		
216.3	231.9	100	1	Ogul	Fine grained grey calcarenite with occasional argillaceous beds and zones; occ bioclastic scattered occ argillaceous bioclastic unit.	Bedding 50° to c/a.	55	219.3	220.8		246.5	2		
											247	5		
											247.5	2		

364060

C.R.A. EXPLORATION PTY. LIMITED

DRILL CORE LOG

SHEET No. 8 of 8

TENEMENT NAME PYRAMID No. 28/83

PLAN – MAP REFERENCE

364329E.

CO-ORDINATES 5356591N AZIMUTH 200° AMG DRILLERS DDTAS COMMENCED 3/4/96 DEPTH 252m HOLE No. DD962P65

RL COLLAR 129m INCLINATION 69° DRILL TYPE U250 COMPLETED 22/4/96 CASING LEFT DPO No(s) 82159

DEPTH From (M)	DEPTH To(M)	Core Rec. %	RQD	Graphic Log	CORE DESCRIPTION	SPECIAL FEATURES Weath, Alteration, Fracturing, Veining, Mineralization	Sample No.	From (M)	To (M)	Rec (M)	ASSAY VALUES (Analysed by.....)
					Core orientation @ 226.8m. bedding sub-vertical.						
231.9	232.2	100	5	Ogfz	Small shear zone	55° to c/A. ? bedding parallel.					
232.2	234.6	100	1	Ogul	Intermixed argillaceous calcarenite and light grey fine calcarenite.		547 056	232.8	234.3		
234.6	238.2	96	3f	Ogmu	Laminated micrite unit. with birds eye micrites.	Bedding 55° to c/A.					
238.2	247.16	100	1	Ogul	Intermixed argillaceous calcarenite and fine-grained nodular light grey calcarenite locally with discrete argillite bands and discrete bioclastic bands	?large coral @ 238.7-238.95m Core Orientation @ 238.8m sub-vertical bedding Minor calcite veining.	57	240.3	244.8		
247.15	249.4	100	1	Ogmu	Laminated micrite unit with abundant birds eye micrites	Bedding 55° to c/A.					
249.4	252.0	100	1	Ogul	Grey med/fine grained bioclastic calcarenite with large argillite masses – <6cm. Large coral bioclasts <5cm	Core Orientation @ 250.8m	58	249.4	250.8		
					END OF HOLE 252m.						

364061

bhole	fulldah	DPO	smpno	Prospect	EL	afrom	ato	aag	aal	aas	aba	aca	acu	afe	ak	amg	amn	apb	azn	as	MRTLith
bhole	fulldah	DPO	smpno	Prospect	EL	afrom	ato	aag	aal	aas	aba	aca	acu	afe	ak	amg	amn	apb	azn	as	MRTLith
ZP65	DD96ZP65			Pyramid	28/88	0	3.2														Qha
ZP65	DD96ZP65	82159	5471001	Pyramid	28/88	3.2	5	-0.5	7.84	18	2040	0.4	31	3.55	3.89	1.43	99	12	171		Sc
ZP65	DD96ZP65			Pyramid	28/88	5	9.4														Sc
ZP65	DD96ZP65	82159	5471002	Pyramid	28/88	9.4	11	-0.5	7.53	20	1560	0.35	20	3.38	3.7	1.4	89	21	149		Sc
ZP65	DD96ZP65			Pyramid	28/88	11	15.9														Sc
ZP65	DD96ZP65	82159	5471003	Pyramid	28/88	15.9	18.7	-0.5	8.61	10	1560	0.73	21	7.36	4.22	1.66	2310	14	104		Sc
ZP65	DD96ZP65	82159	5471004	Pyramid	28/88	18.7	20.4	-0.5	7.95	7	1290	2.82	24	4.94	3.92	1.7	987	12	109		Ogsi
ZP65	DD96ZP65			Pyramid	28/88	20.4	24.5														Ogsi
ZP65	DD96ZP65	82159	5471005	Pyramid	28/88	24.5	26	-0.5	5.88	-5	1040	10.05	26	3.31	2.81	1.33	626	13	89		Ogsi
ZP65	DD96ZP65			Pyramid	28/88	26	29														Ogsi
ZP65	DD96ZP65	82159	5471006	Pyramid	28/88	29	29.9	-0.5	3.28	-5	368	13.42	-5	2.55	1.6	1.28	785	31	60		Ogsi
ZP65	DD96ZP65			Pyramid	28/88	29.9	35.4														Ogsi
ZP65	DD96ZP65	82159	5471007	Pyramid	28/88	35.4	38	-0.5	4.56	9	558	7.17	12	3.04	2.42	1.51	720	110	527		Ogsi
ZP65	DD96ZP65	82159	5471008	Pyramid	28/88	38	39.5	1.2	0.83	11	98	2.4	9	1.24	0.45	0.72	411	941	348		Ogsi
ZP65	DD96ZP65	82159	5471009	Pyramid	28/88	39.5	40.9	0.8	0.49	21	87	1.71	10	1.03	0.21	0.49	444	597	372		Ogsi
ZP65	DD96ZP65	82159	5471010	Pyramid	28/88	40.9	41.2	5.8	0.4	11	48	2.27	81	1.2	0.2	0.59	743	14000	4020		Ogsi
ZP65	DD96ZP65	82159	5471011	Pyramid	28/88	41.2	42.5	-0.5	0.36	11	45	2.24	10	0.78	0.17	0.53	465	918	338		Ogsi
ZP65	DD96ZP65	82159	5471012	Pyramid	28/88	42.5	43.7	-0.5	0.5	-5	49	1.44	8	0.75	0.2	0.33	283	241	210		Ogsi
ZP65	DD96ZP65	82159	5471013	Pyramid	28/88	43.7	46	0.6	0.61	5	64	3.01	33	0.8	0.27	0.47	377	667	557		Ogsi
ZP65	DD96ZP65			Pyramid	28/88	46	50														Ogsi
ZP65	DD96ZP65	82159	5471014	Pyramid	28/88	50	51.5	0.8	0.61	8	52	2.23	5	0.82	0.32	0.5	449	250	419		Ogsi
ZP65	DD96ZP65	82159	5471015	Pyramid	28/88	51.5	53	1	0.52	-5	85	8.57	-5	1.06	0.27	0.77	1220	192	634		Ogsi
ZP65	DD96ZP65	82159	5471016	Pyramid	28/88	53	54.5	0.7	0.6	-5	48	1.72	7	0.72	0.31	0.23	221	66	287		Ogsi
ZP65	DD96ZP65			Pyramid	28/88	54.5	62														Ogsi
ZP65	DD96ZP65	82159	5471017	Pyramid	28/88	62	63.5	-0.5	0.58	5	48	1.71	7	0.78	0.3	0.43	288	43	193		Ogsi
ZP65	DD96ZP65			Pyramid	28/88	63.5	67.8														Ogsi
ZP65	DD96ZP65	82159	5471018	Pyramid	28/88	67.8	69.3	-0.5	0.66	14	50	4.14	7	1.81	0.35	0.89	822	27	176		Ogsi
ZP65	DD96ZP65			Pyramid	28/88	69.3	78.3														Ogsi
ZP65	DD96ZP65	82159	5471019	Pyramid	28/88	78.3	79.8	-0.5	1.39	10	79	4.41	9	1.02	0.73	0.53	564	22	76		Ogsi
ZP65	DD96ZP65			Pyramid	28/88	79.8	88.8														Ogsi
ZP65	DD96ZP65	82159	5471020	Pyramid	28/88	88.8	90.3	-0.5	1.56	-5	106	1.13	36	0.78	0.83	0.25	185	46	85		Ogsi
ZP65	DD96ZP65	82159	5471021	Pyramid	28/88	90.3	92.6	-0.5	1.35	6	121	2.64	56	0.72	0.72	0.3	323	70	174		Ogsi
ZP65	DD96ZP65	82159	5471022	Pyramid	28/88	92.6	93.3	-0.5	1.88	-5	135	5.71	69	1.14	0.99	0.74	700	155	1180		Ogsi
ZP65	DD96ZP65	82159	5471023	Pyramid	28/88	93.3	94.8	0.8	0.96	-5	85	7.04	38	2.01	0.52	1.71	1570	145	276		Ogsi
ZP65	DD96ZP65			Pyramid	28/88	94.8	96.3														Ogsi
ZP65	*DD96ZP65*	*82159*	*5471024*	*Pyramid*	*28/88*	*96.3*	*97.8*	*1.3*	*0.92*	*-5*	*105*	*9.48*	*49*	*1.99*	*0.5*	*1.78*	*1700*	*152*	*666*		*Ogsi*
ZP65	DD96ZP65	82159	5471025	Pyramid	28/88	97.8	98.8	0.6	0.94	-5	131	8.65	152	1.88	0.5	1.85	1820	151	849		Ogsi
ZP65	DD96ZP65	82159	5471026	Pyramid	28/88	98.8	100.8	-0.5	0.67	-5	69	4.65	23	0.88	0.36	0.49	519	41	330		Ogsi
ZP65	DD96ZP65			Pyramid	28/88	100.8	103.3														Ogsi
ZP65	DD96ZP65	82159	5471027	Pyramid	28/88	103.3	104.8	-0.5	1.23	-5	101	3.98	11	0.71	0.66	0.5	591	130	495		Ogsi
ZP65	DD96ZP65	82159	5471028	Pyramid	28/88	104.8	106.8	-0.5	1.35	-5	147	4.04	7	1.04	0.71	0.49	402	71	372		Ogsi
ZP65	DD96ZP65			Pyramid	28/88	106.8	117.3														Ogsi
ZP65	DD96ZP65	82159	5471029	Pyramid	28/88	117.3	118.8	-0.5	1.41	-5	104	2.35	8	1.48	0.75	0.59	400	32	202		Ogsi
ZP65	DD96ZP65			Pyramid	28/88	118.8	121.8														Ogsi
ZP65	DD96ZP65	82159	5471030	Pyramid	28/88	121.8	123.3	-0.5	1.69	-5	111	3.8	-5	1.87	0.94	0.78	734	49	359		Ogsi
ZP65	DD96ZP65	82159	5471031	Pyramid	28/88	123.3	125.8	-0.5	1.54	-5	94	7.32	6	3.22	0.83	1.33	1360	57	331		Ogul
ZP65	DD96ZP65	82159	5471032	Pyramid	28/88	125.8	127.8	-0.5	2.28	-5	153	2.32	6	1.76	1.26	0.57	708	58	442		Ogsi
ZP65	DD96ZP65			Pyramid	28/88	127.8	130.8														Ogsi
ZP65	DD96ZP65	82159	5471033	Pyramid	28/88	130.8	132.3	-0.5	3.43	6	218	3.29	10	2.21	1.91	0.99	699	41	315		Ogsi
ZP65	DD96ZP65	82159	5471034	Pyramid	28/88	132.3	133.2	-0.5	1.79	6	207	5.44	19	2.83	0.95	1.81	1190	34	623		Ogdl
ZP65	DD96ZP65	82159	5471035	Pyramid	28/88	133.2	134.6	0.9	0.51	-5	138	20.15	14	2.79	0.2	10.21	2190	78	1090		Ogdl
ZP65	DD96ZP65	82159	5471036	Pyramid	28/88	134.6	136.8	0.8	0.26	-5	107	18.03	11	1.76	0.14	9.13	1250	156	882		Ogdl
ZP65	DD96ZP65	82159	5471037	Pyramid	28/88	136.8	137.5	0.6	0.21	-5	86	18.28	8	1.98	0.08	9.12	1240	135	661		Ogdl
ZP65	DD96ZP65	82159	5471038	Pyramid	28/88	137.5	139.8	0.6	0.47	-5	102	20.65	10	1.09	0.26	11.15	736	94	536		Ogdl
ZP65	DD96ZP65	82159	5471039	Pyramid	28/88	139.8	140.9	-0.5	0.4	-5	62	19.47	9	0.96	0.22	10.51	633	145	380		Ogdl
ZP65	DD96ZP65	82159	5471040	Pyramid	28/88	140.9	142.9	0.9	1.12	12	96	18.29	16	2.33	0.65	8.88	908	344	461		Ogfz
ZP65	DD96ZP65	82159	5471041	Pyramid	28/88	142.9	144.3	0.9	0.56	-5	92	16.53	74	2.18	0.29	8.2	1130	659	760		Ogfz/Ogdl
ZP65	DD96ZP65	82159	5471042	Pyramid	28/88	144.3	145.8	0.7	1.02	-5	143	16.98	8	1.64	0.6	8.19	626	71	164		Ogdl
ZP65	DD96ZP65	82159	5471043	Pyramid	28/88	148.8	150.3	0.8	0.24	-5	290	20.32	11	1.07	0.13	10.28	718	66	547		Ogdl
ZP65	DD96ZP65			Pyramid	28/88	150.3	153.6														Ogdl
ZP65	DD96ZP65	82159	5471044	Pyramid	28/88	153.6	155.8	1.2	0.86	-5	65	20.02	7	1.39	0.51	8.09	847	78	500		Ogdl
ZP65	DD96ZP65	82159	5471045	Pyramid	28/88	155.8	157.5	0.6	1.15	-5	259	19.24	13	2.19	0.62	8.55	1120	210	888		Ogdl
ZP65	DD96ZP65	82159	5471046	Pyramid	28/88	157.5	159.8	0.8	0.6	-5	134	19.26	8	1.59	0.32	9.12	840	187	429		Ogdl
ZP65	DD96ZP65			Pyramid	28/88	159.8	163.8														Ogdl
ZP65	DD96ZP65	82159	5471047	Pyramid	28/88	163.8	164.8	0.8	1.03	-5	70	20.18	13	2.16	0.56	6.15	408	107	216		Ogdl
ZP65	DD96ZP65			Pyramid	28/88	164.8	175.8														Ogul/Ogoc

364062

bhole	fulldah	DPO	smpno	Prospect	EL	afrom	ato	aag	aal	aas	aba	aca	acu	afe	ak	amg	amn	apb	azn	as	MRTLith
ZP65	DD96ZP65	82159	5471048	Pyramid	28/88	175.8	177.3	1.2	0.69	-5	62	27.31	-5	0.66	0.39	2.26	196	21	32		Ogoo
ZP65	DD96ZP65			Pyramid	28/88	177.3	182														Ogoo/Ogu
ZP65	DD96ZP65	82159	5471049	Pyramid	28/88	182	183.3	0.6	1.56	-5	91	26.99	-5	0.6	0.89	1.12	140	13	45		Ogmu
ZP65	DD96ZP65			Pyramid	28/88	183.3	192.3														Ogmu/Ogu
ZP65	DD96ZP65	82159	5471050	Pyramid	28/88	192.3	193.8	0.6	0.98	-5	64	25.82	-5	0.56	0.56	2.61	127	15	31		Ogul
ZP65	DD96ZP65			Pyramid	28/88	193.8	202.8														Ogul
ZP65	DD96ZP65	82159	5471051	Pyramid	28/88	202.8	204.3	1.7	0.72	-5	79	29.29	-5	0.45	0.41	1.45	260	143	598		Ogul
ZP65	DD96ZP65			Pyramid	28/88	204.3	205.8														Ogul
ZP65	DD96ZP65	82159	5471052	Pyramid	28/88	205.8	206.5	1.7	0.92	-5	87	28.35	-5	0.57	0.5	2.42	635	209	1820		Ogul
ZP65	DD96ZP65	82159	5471053	Pyramid	28/88	206.5	207.7	2	1.08	-5	73	29.03	-5	1.43	0.61	0.68	661	146	378		Ogul
ZP65	DD96ZP65	82159	5471054	Pyramid	28/88	207.7	208.8	0.9	1.31	-5	76	28.04	-5	0.66	0.75	1.76	177	16	68		Ogul
ZP65	DD96ZP65			Pyramid	28/88	208.8	219.3														Ogul
ZP65	DD96ZP65	82159	5471055	Pyramid	28/88	219.3	220.8	-0.5	0.72	-5	60	29.17	-5	0.6	0.4	2.11	172	27	79		Ogul
ZP65	DD96ZP65			Pyramid	28/88	220.8	232.8														Ogul
ZP65	DD96ZP65	82159	5471056	Pyramid	28/88	232.8	234.3	1.2	1.03	-5	62	26.69	-5	0.5	0.58	1.96	106	15	39		Ogul
ZP65	DD96ZP65			Pyramid	28/88	234.3	240.3														Ogmu/Ogd
ZP65	DD96ZP65	82159	5471057	Pyramid	28/88	240.3	241.8	-0.5	1.22	-5	71	25.14	-5	0.8	0.68	3.81	224	91	195		Ogdl
ZP65	DD96ZP65			Pyramid	28/88	241.8	249.4														Ogdl/Ogmu
ZP65	DD96ZP65	82159	5471058	Pyramid	28/88	249.4	250.8	0.9	0.74	-5	52	26.55	-5	0.77	0.42	3.89	247	133	84		Ogdl
ZP65	DD96ZP65			Pyramid	28/88	250.8	252														Ogdl

364063

364064

Appendix VI

Pyramid Wacker Sampling Geology and Assay Data

Sampno	DPO	Prospect	EL	LocalE	LocalN	AMGE	AMGN	SampType	Depth	Bedrock?	MRTLith	FieldID	Texture	Alt/Min	Colour	Comments	82153	Ag	Al	As	Ba	Ca	Cu	Fe	K	Mg	Mn	Pb	Zn
5852439	82156	PYRAMID	28/88	25		364883	5355190	WACKER	1.8	Y	Sc	Sss	Sand	LI	WO	Sugary looking slightly ferruginous sandstone	5852439	5.6	1.85	29	244	0.05	46	3.08	0.51	0.18	4240	985	1240
5852440	82156	PYRAMID	28/88	0		364981	5355179	WACKER	5	Y	Sc	Sss	Sandy clay		DB	Fine sandy siltstone ?with shale	5852440	-0.5	5.44	55	167	-0.05	67	1.13	2.3	0.34	22	143	1780
5852441	82156	PYRAMID	28/88	0		364841	5355607	WACKER	1.2	Y	Om	Sss	Sand		K	Pink sugary sandstone	5852441	-0.5	0.06	-5	10	-0.05	-5	0.16	-0.05	-0.01	18	-10	10
5852442	82156	PYRAMID	28/88	25		364858	5355626	WACKER	2.5	Y	Qha	Cg	Sandy clay		DBLG	?Peaty gravels	5852442	-0.5	4.38	-5	257	-0.05	-5	0.65	1.77	0.3	35	36	23
5852468	82156	PYRAMID	28/88	525		364973	5355982	WACKER	4.1	Y	Ogul	Sls	Sand		G	Fine grained calcarenite	5852468	-0.5	1.54	-5	65	27.9	-5	0.92	0.83	3.49	114	20	46
5852469	82156	PYRAMID	28/88	500		364957	5355963	WACKER	7.4	Y	Ogul	Sls	Sandy clay		G	Fine grained calcarenite	5852469	-0.5	2.16	-5	111	25.1	-5	1.59	1.12	3.3	406	17	33
5852470	82156	PYRAMID	28/88	475		364940	5355944	WACKER	4.3	Y	Ogul	Sls	Sand		G	?Micritic limestone with argillite partings	5852470	-0.5	2.35	-5	94	28.8	-5	0.92	1.29	1.08	129	28	86
5852471	82156	PYRAMID	28/88	450		364924	5355926	WACKER	6.3	Y	Ogul	Sls	Sand		G	Fine grained bioclastic calcarenite	5852471	-0.5	2.76	-5	145	19.1	-5	1.52	1.56	3.37	295	-10	19
5852472	82156	PYRAMID	28/88	425		364907	5355907	WACKER	4.1	Y	Ogul	Sls	Sand		G	A couple of large odd dolomitic/sandstone fragments	5852472	-0.5	1.61	-5	58	24.3	8	1.06	0.68	1.66	304	30	59
5852473	82156	PYRAMID	28/88	375		364890	5355886	WACKER	6.6	Y	Ogdl	Sdl	Sand		G	Fine grained calcarenite/dolomitic	5852473	-0.5	0.91	-5	47	26	-5	3.46	0.48	5.99	1670	124	838
5852474	82156	PYRAMID	28/88	350		364874	5355869	WACKER	15.4	Y	Ogdl	Sdl	Sand		LGG	Bioclastic? micrite/dolomitic	5852474	0.7	1.46	-5	66	24.1	-5	0.82	0.77	4.63	185	48	176
5852475	82156	PYRAMID	28/88	325		364857	5355850	WACKER	17.7	Y	Qha	Cg	Clay		LGG	Mixed micaceous sst and limestone	5852475	-0.5	5.87	19	347	0.48	23	4.35	2.68	0.72	1030	264	582
5852476	82156	PYRAMID	28/88	300		364841	5355832	WACKER	11.5	Y	Ogul	Sls	Sandy clay		G	Fine grained calcarenite	5852476	1	0.83	-5	32	27	-5	0.57	0.35	2.54	162	35	177
5852477	82156	PYRAMID	28/88	275		364824	5355813	WACKER	9.3	Y	Ogul	Sls	Sand		G	Fine grained calcarenite and argillite	5852477	-0.5	2.02	-5	87	25.2	-5	1.83	1.05	0.83	580	40	160
5852478	82156	PYRAMID	28/88	225		364791	5355776	WACKER	10.7	Y	Ogdl	Sdl	Sand		GLG	Large non calcareous fragments in calcareous lime sand	5852478	1.4	2.33	-5	166	23.1	-5	1.43	1.12	2.29	535	245	1450
5852479	82156	PYRAMID	28/88	200		364774	5355757	WACKER	3	Y	Ogul	Sls	Sand		LG	Poss. dolomite or sst fragments	5852479	-0.5	2.89	7	152	4.13	-5	2.12	0.94	0.77	239	34	57
5852480	82156	PYRAMID	28/88	175		364758	5355739	WACKER	3.4	Y	Ogul	Sls	Sand		LG	Poss. dolomite or sst fragments	5852480	-0.5	1.85	-5	105	20.2	8	1.13	0.73	0.85	129	86	101
5852481	82158	PYRAMID	28/88	150		364741	5355720	WACKER	2.3	Y	Qha	Cg	Sand		LGGRB	Mixed fragments poss dol + some calcareous material	5852481	-0.5	2.02	-5	118	6.52	-5	0.55	0.91	0.25	156	11	8
5852482	82158	PYRAMID	28/88	125		364725	5355701	WACKER	3	Y	Ogdl	Sdl	Sand		DG	Probable dolomite	5852482	-0.5	4.89	-5	240	11.9	10	2.59	2.25	4.3	319	106	549
5852483	82158	PYRAMID	28/88	100		364708	5355682	WACKER	3.2	Y	Ogul	Sls	Sand		LGG	Fine slightly micritic calcarenite	5852483	0.6	2.61	-5	135	27	5	1.4	1.21	1.69	489	214	1180
5852484	82158	PYRAMID	28/88	75		364692	5355684	WACKER	0.8	N	Om	Cg	Sand		WK	??Bedrock	5852484	-0.5	1.15	-5	89	0.21	-5	0.41	0.51	0.09	33	-10	18
5852485	82158	PYRAMID	28/88	50		364675	5355645	WACKER	3.1	Y	Ogul	Sss	Sand		WKB	Moina sandstone	5852485	-0.5	1.4	-5	77	0.09	9	0.41	0.52	0.14	31	29	43

364065

Appendix VII

DD96ZP65 Conodont Age Dating Report

364067

CONODONTS FROM WESTERN TASMANIA

Clive Burrett
GEOSEA CONSULTANTS
22 Hinman Drive
Klngston
Tasmania
Australia 7050

Report to CRAE, 1-7-1996

364068

CONODONTS FROM LIMESTONE SAMPLES, W.TASMANIA

Clive Burrett
GEOSEA
22 Hinman Drive
Kingston
Tasmania
Australia 7050

20-6-1996

SUMMARY

Four out of six limestone core samples from western Tasmania submitted by CRAE yield fragmentary and generally identifiable conodonts. Sample 4141859 is certainly Blackriveran (equivalent to the Myrtle Fm.) and samples (in decreasing order of certainty) are Siluro-Devonian (4141857), earliest Ordovician (4141855) and Chazyan-Ugbrook Fm or older equivalent (4141858). Sample 4141860 is Middle Ordovician or younger.

INTRODUCTION

Six large limestone core samples were collected by Simon Tear of CRAE (Melbourne), processed through acetic acid and heavy liquids by LAOLA Pty Ltd (Perth) and sent to Clive Burrett at GEOSEA in Hobart in June 1996. These samples were picked and assessed by Burrett over a period of 10 days. Four out of six samples yield fragmented and cleaved conodont elements. One sample was barren and 4141860 yielded 3 broken elements. This success rate (4/6) is good for Tasmanian carbonates as are the average yields (see appendix). One large residue from sample 414858 is dominated by dolomite and took many hours to pick.

Because of the low numbers and fragmentary nature of the conodont elements, age assignments, except for 4141859, are not completely certain and no important decisions should be based on them unless more samples are collected and processed. These assessments are the best possible without more sampling plus a lengthy study utilizing a SEM and a thorough literature search.

CONODONT ALTERATION INDEX (CAI)

All conodonts are black and have a CAI of 5 indicating burial/low grade metamorphic temperatures of around 300^{0}C. This is consistent with other CAI values from western Tasmania (Burrett 1992).

AGE ASSIGNMENTS

The age assignments are shown in the attached figure from Burrett (1995, fig.1). Solid lines indicate the most likely biostratigraphic age range of each sample with dashed lines indicating the most likely uncertainty limits.

4141855

Contains simple cones with inflated bases referable to *Drepanoistodus suberectus* and a simple cone with a denticulated posterior margin *cf. Acanthodus* plus two simple cordylodiform elements. This looks like an earliest Ordovician assemblage.

4141857

Contains a species of *Oulodus* and fragments referable to *Peleksygnathus* and *Icriodella* and probable ichthyoliths (fish-bits). These suggest a Silurian to early Devonian age.

4141858

A dichognathiform element similar to that of *Phragmodus flexuosus* is present but this could be a broken and cleaved fragment of a younger species of *Phragmodus*. A trichondelliform element is similar to that of *Plectodina aculeata*. This assemblage is found in the Standard Hill Fm and lower Ugbrook Fm of Mole Creek (Burrett 1978, Burrett and Goede 1987, Burrett *et al.* 1989).

4141859

Contains a trichonodelliform element of *Tasmanognathus careyi* which ranges through the Lower Limestone Member of the Florentine Valley (Burrett 1979) and would be present presumably in the Myrtle Fm. of Zeehan (Burrett 1995).

4141860

Contains 3 fragments including a prioniodiniform element and one cusp fragment similar to that of *Tasmanognathus* elements (as 4141859). However, no firm date is possible.

CONCLUSIONS

Age ranges of the four productive samples are shown in Fig.1. They range from Early Ordovician to Late Silurian-Early Devonian. The early Ordovician age of 4141855 is unexpected as early Ordovician conodonts have not been recorded from western Tasmania before except from one deep core in the lower Gordon River. The 4141855 conodonts could be reworked into younger strata or there could be structural complications. A previous record (Burrett 1984) of reworking of Ordovician conodonts into Devonian limestones based on channel samples collected by Jim Conkin in the 1950's from Point Hibbs, west coast Tasmania turned out to be tectonic juxtaposition of Owen/Gordon/ 'Eldon' in thin thrust slices (Carey and Berry 1988). From the work of Keele (1991) there is no reason to suppose that similar, thin thrust slices could not be present in parts of the Zeehan area.

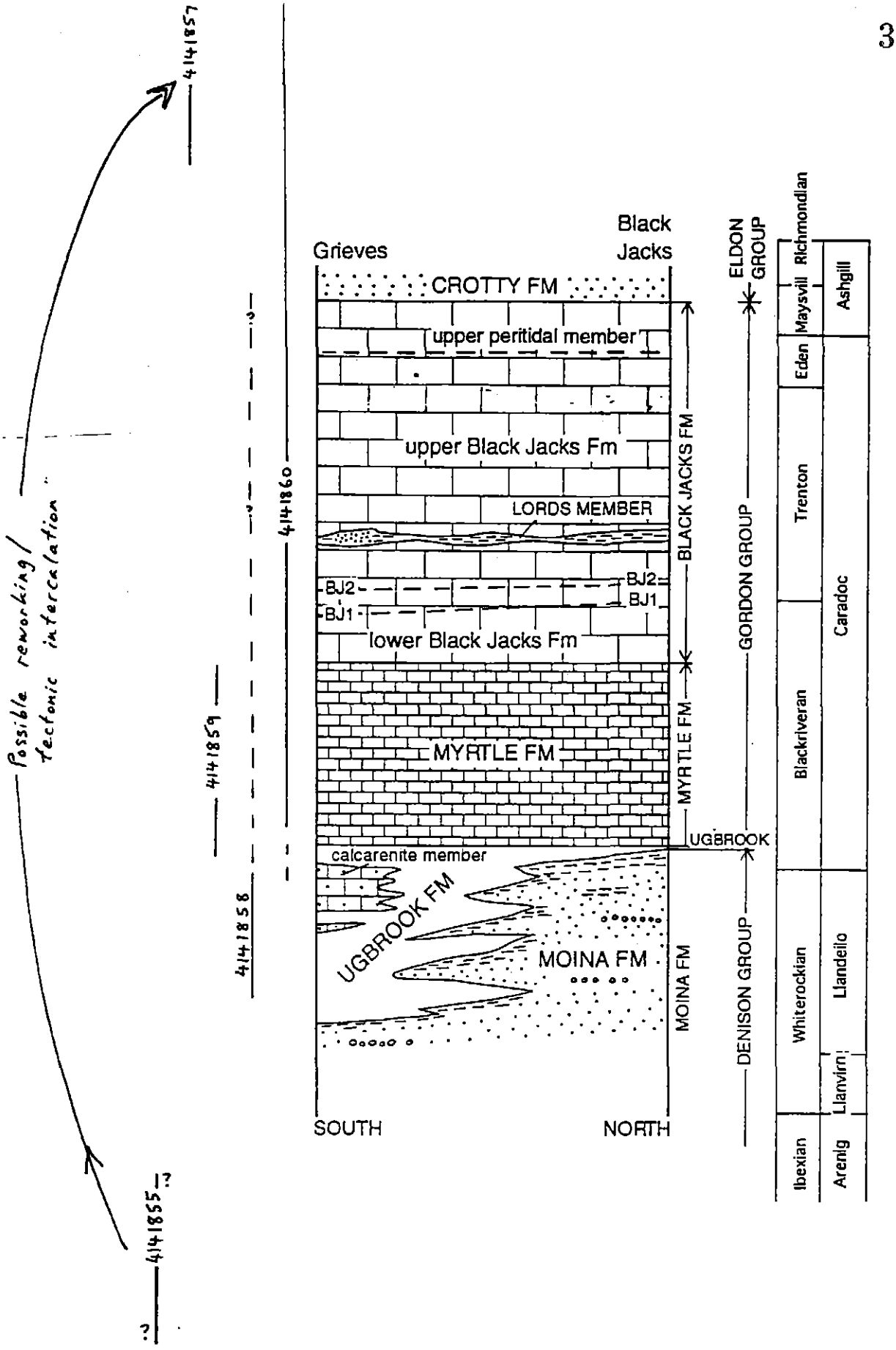


Fig.1 Summary of Ordovician lithostratigraphy in the Zeehan region.
Chronostratigraphic units are based on the standard North American scheme and the standard British scheme. Correlations are most easily made to the American scheme but the British scheme is used in the text because of its greater familiarity.

Conodonts are present in the majority of likely-looking core in the Zeehan region. If any future work is contemplated in the region then it is recommended that a study of the conodonts from one or two complete stratigraphic cores be financed in order to obtain a reliable local biostratigraphic framework and to establish exactly the relationship of the conodont succession to the local lithostratigraphy. This would enable short cores to be placed in lithostratigraphic context quickly and cheaply.

REFERENCES

Banks, M.R., and Burrett, C.F., 1971: Report on Ordovician limestone in the Olga river area. Unpublished report HEC Tasmania

Burrett, C. 1978: Middle-Upper Ordovician Conodonts and Stratigraphy of the Gordon Limestone, Tasmania, Unpublished PhD thesis, University of Tasmania, 342pp.

_____, 1979: Tasmanognathus a new Ordovician conodont genus from Tasmania. Geologica et Palaeontologica 13: 31-38.

_____,1984: Early Devonian deformation and metamorphism of conodonts in western Tasmania. In: Baillie, P., and Collins, P., Mineral exploration and Tectonic Processes in Tasmania, Geological Society of Australia, Hobart, pgs.14-17.

_____ ,1992: Conodont geothermometry in the Palaeozoic carbonate rocks of Tasmania and its economic implications. Australian Journal of Earth Science 39, 61-66.

_____,1995: Stratigraphy and Palaeoenvironments of the Ordovician Gordon Group, Zeehan Tasmania. Report to CRA Exploration Pty Ltd.

_____, Banks, M., Clota, G. and Seymour, D. 1989: Stratigraphy and structure of the Ordovician of Mole Creek Synclinorium, N.W. Tasmania. Records of the Queen Victoria Museum Launceston 96, 1-14.

_____ , and Goede, A., 1987: Mole Creek - A geological excursion guide. Geological Society of Australia. Tas. Div. Field Guide 1: 1-23.

Carey, S., and Berry, R., 1988: Thrust sheets at Point Hibbs, Tasmania, Australian Journal of Earth Science 35, 169-180.

Keele, R., 1991: Structure and Mineralisation of Western Tasmania. Unpublished AMIRA Project P291 Report, CODES University of Tasmania, pgs. 40-49.

APPENDIX

Sample no.	residue size	residue	other foss	element	age
4141855	small	pyrite grey rock fragments	inartic.	9	1-2 early Ord.
4141856	small	iron oxides		0	-
4141857	small	pyrite	chitinozoa gastropods ichthyoliths	32	Sil-early Dev.
4141858	large	dol+ pyrite		9	6?Chazyan
4141859	small	pyrite		6	7 Blackriveran
4141860	small	pyrite		3	M.Ord to Devonian

364073

Appendix VIII

Detailed Helimag Data

96-3958A
364074

CRA EXPLORATION PTY. LIMITED
ACN 000 057 125

96-3958A
app 8 & 9

Preliminary Notes and Observations of Helicopter-borne Magnetic Survey Zeehan, Tasmania

Author: SJ Tear
J Tesselaar

Date: July 1996

Submitted to: Chief Geologist, Vic/Tas

Copies to: Mineral Resources Tasmania
CRAE - SE District
CRAE - ETIG
CRAE - Zeehan
Allegiance Mining NL

Submitted by:

Accepted by:

"All rights in this report and its contents (including rights to confidential information and copyright in text, diagrams and photographs) remain with CRA Exploration and no use (including use of reproductions, storage or transmission) may be made of the report or its contents for any purpose without the prior written consent of CRA Exploration.
© CRA Exploration Pty. Limited 1995"

CRAE Report No. 22222

364075

List of Figures

Tv 1026	Zeehan Helimag Survey Total Magnetic Intensity Map	1:50,000
Tv 1027	Zeehan Helimag Survey Vertical Derivative Map	1:50,000
Tv 1141	EL 28/88 Zeehan 1 Zeehan Helimag Survey, Pyramid Prospect, Vertical Derivative Image, Flight Line Overlay and Modelled Anomalies	1:10,000
Tv 1142	EL 28/88 Zeehan 1 Zeehan Helimag Survey, Myrtle Prospect, Vertical Derivative Image, Flight Line Overlay and Modelled Anomalies	1:10,000
Tv 1147	EL 28/88 Zeehan 1 Zeehan Helimag Survey, Sassafras Prospect, Coloured Total Field on Shaded Relief Image	1:25,000
Tv 1148	EL 28/88 Zeehan 1 Zeehan Helimag Survey, Avebury Prospect, Contoured Total Magnetic Intensity Image	1:10,000

List of Appendices

Appendix I	Flight Line Maps

1. Introduction

Drillcore from the Gordon Limestone of the Zeehan area shows zinc mineralisation being related to weakly magnetic siderite alteration. This alteration predominantly occurs at the base of the Limestone just above its contact with the underlying Moina Sandstone. Siderite alteration can occur at the limestone's upper contact with the overlying Crotty Quartzite eg at Blackjacks and Myrtle whilst intense alteration is also associated with limestones in the middle of the Gordon Limestone eg the Oceana Mine and the Grieves South area. The magnetic response of the siderite is weak, in the range of 50-200 x 10-5 SI, but is deemed detectable by an airborne magnetic survey. Forward modelling indicated that the siderite would give weak aeromagnetic anomalies (1-5nT). Thus a helimag survey was commissioned to fly over all the Gordon limestone outcrops of the Zeehan under licence to CRAE.

The aim of the survey was to identify mineral-related siderite zones for follow-up diamond drilltesting. The target is a stratabound zinc/lead orebody hosted by the Ordovician Gordon Limestone with analogies to Irish-type Zn/Pb orebodies.

A separate survey was flown over the Gordon Limestone of McLean Creek. This area is known to have a large magnetic anomaly - attributed to a magnetite skarn - known as the Avebury target. In addition the nickel target areas at Melba Flats were also flown.

This report provides technical details of the survey and processing as well as some geological interpretations of the results. Locations of the prospects are shown in plan Tv1022.

The survey was flown in March 1995 by Universal Tracking Systems Pty. Ltd. with initial results received in December 1995. Data processing and some interpretation was undertaken by Tony Doe and John Tesselaar (CRAE - Orange).

Sub-divisions of the Gordon Limestone for drillhole logging purposes have been made on a lithostratigraphic and lithologic basis and is included elsewhere in this report.

2. Flight Survey and Data Processing Details

The flight line height was a nominal 30m with the line spacing approximately 60m with readings taken every 4-5m. A total of 2400 line km was completed covering the following prospects :- Sassafras, Blackjacks-Mariposa-Sunny Corner-Pyramid, Professor Range-Amber Creek-King Billy-Leatherwood, Myrtle-Grieves-Baura-Firewood Siding-Rose Valley. New areas between Leatherwood and Mariposa were also investigated and this included the Westerway and Tom Creek areas. Flight line maps are shown in Appendix I.

The data from the helimag survey was obtained as an XYZ file of easting, northing and total magnetic intensity. No terrain clearance data was provided with the original XYZ file.

Over each area of Gordon Limestone to be interpreted, a small (<3km2) data subset was selected. These areas were designed to include all of the Gordon Limestone but as little as possible of the surrounding rocks, particularly the Dundas Group which tended to 'swamp' the more subtle magnetic data variations of the limestone. This data was then imaged.

The vertical derivative of the magnetic data was produced along the flight line using TRAKPAK. This data was then imaged with the previously existing geology data superimposed. Some of the small linear anomalies coincided with mapped siderite. Other lithological units were also mapped eg the Moina Sandstone and the Crotty Quartzite.

Where applicable, magnetic inversion using MAGMOD was undertaken over the siderite-like anomalies. In most cases, anomalies over 1nT were able to be successfully inverted. These models should only be used as a guide as to the geometry of the source of the anomalies. This is due to :-

- There is no account of terrain clearance;
- The anomalies have small amplitudes;
- Not all lines were perpendicular to strike;
- The problem of "non-uniqueness" in magnetic inversion.

3. *Magnetic Interpretations*

Initial raster images failed to highlight major zones of inferred siderite alteration (plan Tv1026). Removal of regional gradients and the selective use of sub-area vertical derivative data greatly improved the resolution (plan Tv 1027). From the modelling it was impossible to distinguish between siderite zones and other stratabound weakly magnetic units.

As a result of this work a much better understanding was gained of the geology of the Ordovician-Silurian sequence in the Zeehan area.

The Gordon Limestone is relatively more magnetic than the surrounding clastic sequences whilst the Siltstone Unit of the limestone is less magnetic than the limestone. The high magnetic susceptibility of the surrounding Cambrian Dundas Group of sediments, volcaniclastics and basic intrusions caused imaging problems. Major units which appeared as magnetic highs included the Upper Dolomite Unit of the Gordon Limestone (possibly other dolomitic zones are relatively magnetic but lack of geochemical surface control could not confirm them) and the Amber Slate of the Silurian clastic sequence. Major structures are difficult to identify and follow. Interpreted linears deemed to represent faults show a lack of continuity eg the Firewood Siding Fault and the Little Henty Fault.

Comments on the interpretation of these sub-areas are :-

3.1 Pyramid (plan Tv 1141)

- The Gordon Limestone intersected in DD95ZP63 is part of a magnetic low, perhaps to be expected in the absence of any siderite. However, south of this is a significant magnetic anomaly at the lower sandstone/limestone contact; wacker bedrock sampling suggests that the anomaly is siderite alteration. Modelling of this anomaly points to a west dipping body, possibly implying tight, slightly overturned synclinal folding - as seen in proximal outcrops of Moina Sandstone (364650mE, 5355750mN).

- An identical anomaly occurs on the same contact 400m further south adjunct to the cross cutting E-W Little Henty Fault (364800mE, 5355250mN). Reconnaissance wacker bedrock sampling shows siderite alteration with elevated zinc values (up to 1050ppm).

- A distinctive unit, with an enhanced vertical derivative, occurs in the middle of the limestone in such a way as to indicate possible folding (hinge point at 364870mE, 5355950mN).

- The contacts of the Gordon Limestone with the underlying Moina Sandstone are well defined by the magnetic data.

- Cultural effects in the NW of the area are due to a bridge over the Pyramid Creek (364100mE, 5356600mN).

3.2 Myrtle (plan Tv 1142)

- The Professor Range Fault is visible in the vertical derivative image. Several magnetic anomalies are associated with the fault (364300mE, 5352300mN). This is in an area of high zinc surface geochemistry (aircore and bedrock wacker drilling)

- A possible siderite-related anomaly lies at the lower limestone contact within the horizontal projection of DD95ZM188 -<30cm of siderite occurs within this drillhole (364650mE, 5351250mN). This may be due to discrete plunging siderite bodies.

- There are numerous mappable units from the magnetic data including the Siltstone Unit (a magnetic low).

- Further modelling and interpretation is required.

3.3 Sassafras (plan Tv 1147)

- A series of discordant magnetic highs confirms the presence of Dundas Group rocks east of the Gordon Limestone valley.

- Minor but discrete, elongate strike parallel anomalies occur in the overlying Crotty Quartzite (363800mE,5364800mN).

- No significant siderite-related targets are observed but further magnetic interpretative work should be undertaken.

3.4 Avebury (plan Tv 1148)

- A strong dumbbell shaped anomaly, 1km by 0.3km, is underlain by overthrusted Cambrian sediments (355200mE, 5357400mN).

- The width of the source is <100m with burial depth between 30-100m.

- The anomaly is interpreted to be a possible magnetite skarn deposit hosted within tightly folded and shallowly plunging Gordon Limestone.

- Ground follow up is required.

4. General Geological Interpretation Summary

- The Amber Slate is a non-calcareous slate of Silurian age which is recognised in the dataset as a magnetic high.

- The Crotty Quartzite appears on the vertical derivative map as a magnetic low.

- The Gordon Limestone appears as a magnetic high except for the non-calcareous, argillaceous Siltstone Unit eg King Billy, Amber Creek, Grieves, Myrtle, Baura and Firewood Siding. The Siltstone Unit is not apparent in the magnetic data at Blackjacks, Mariposa, Sunny Corner Tom Creek and Pyramid.

- The Moina Sandstone is a magnetic low near the overlying Gordon Limestone. At Grieves this low unit is 200-300m thick before passing down sequence into a magnetic high. This high unit may be part of the Owen Conglomerate.

- The Owen Conglomerate is generally a magnetic high eg Professor Range and Pyramid.

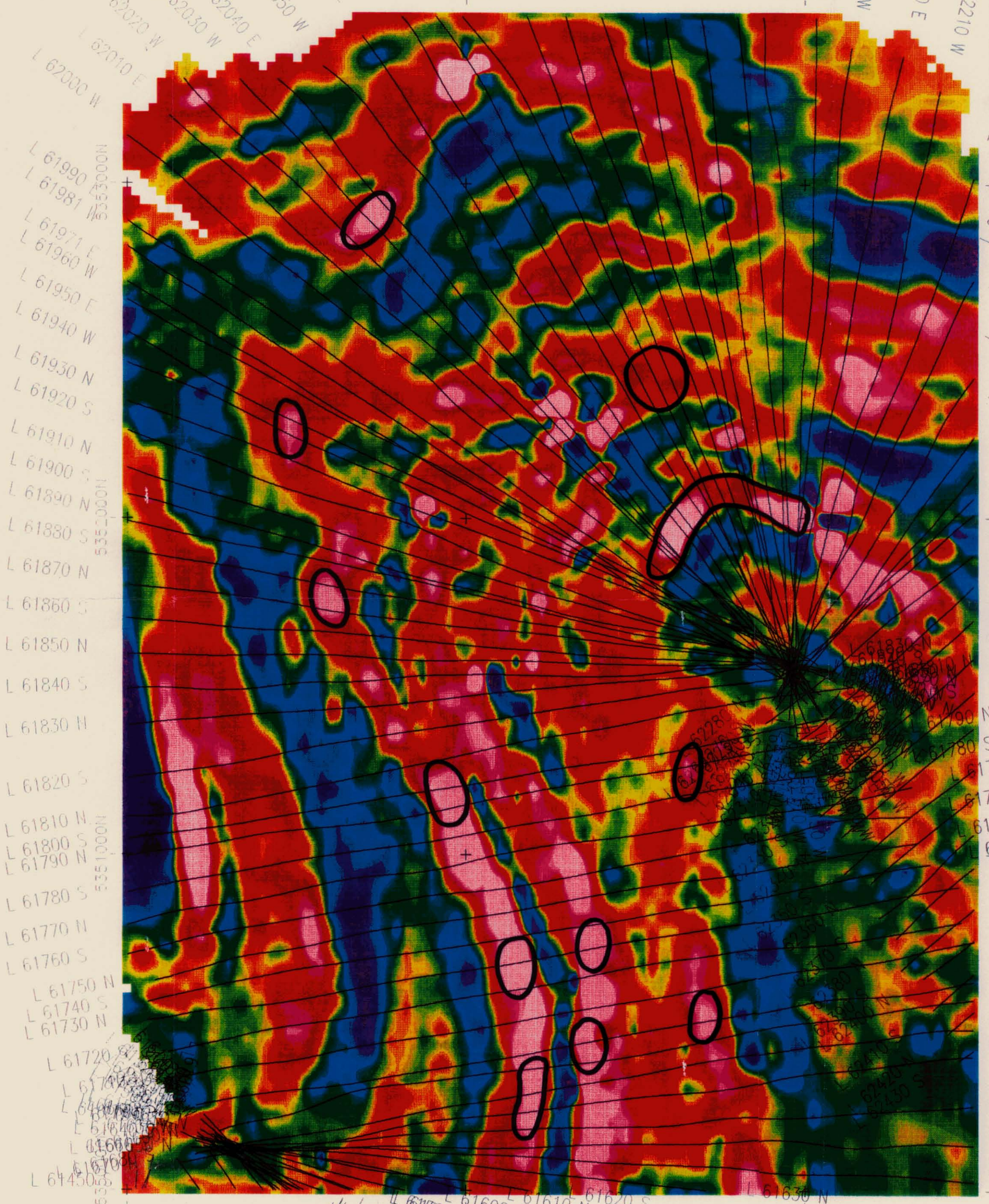
- Major, brittle faults are not readily identifiable, often disappearing along strike eg the Balstrup Fault in the Pyramid and Tom Creek areas.

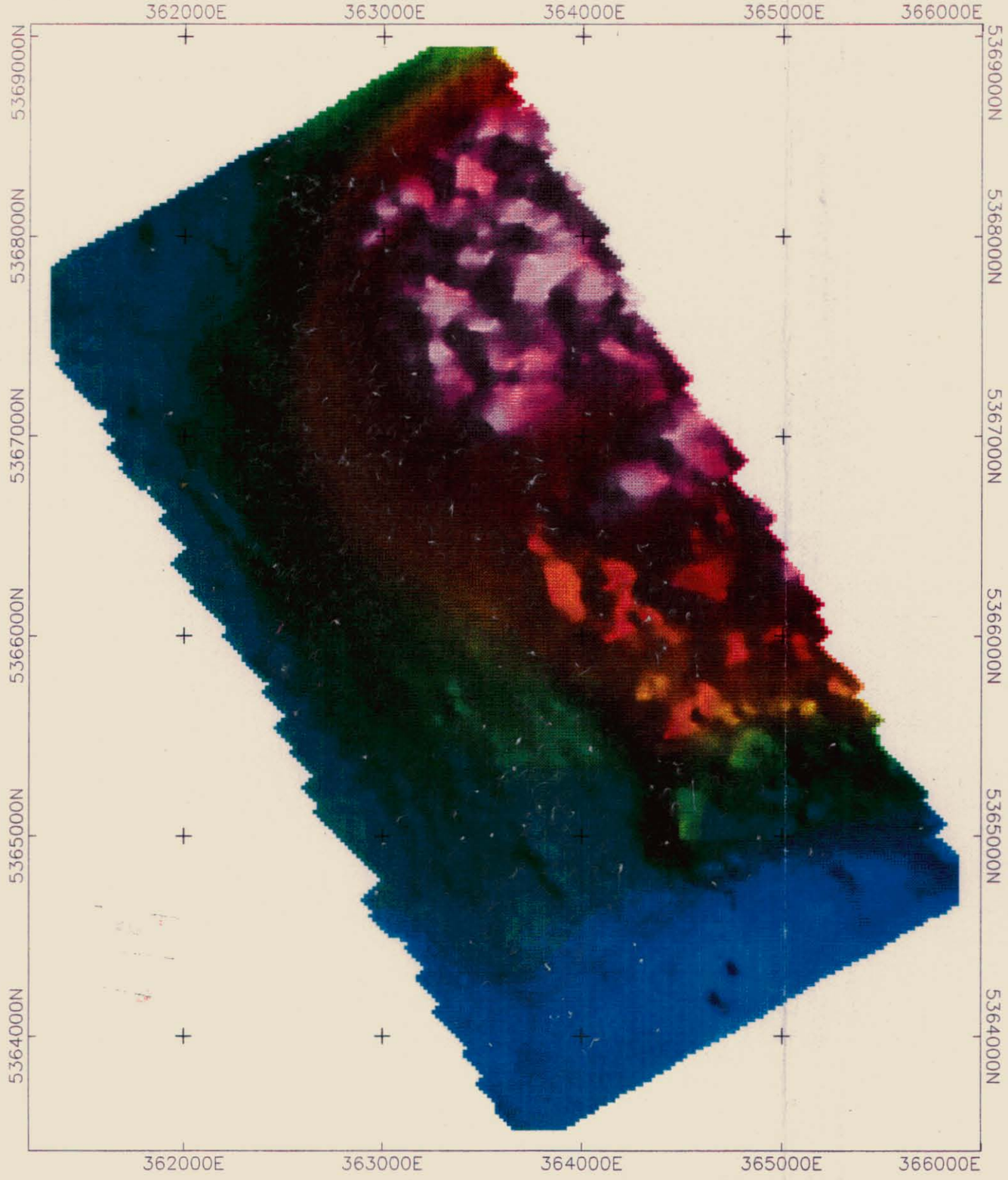
- Parts of the Gordon Limestone display more continuously intense magnetic zones eg at Grieves and Firewood Siding South. This may be a reflection on mineral fluids having altered the limestone particularly via dolomitisation. Alternatively these highs may be a reflection of powerful surface weathering producing surficial de-calcified clays. It is possible to say that the rotting of variably composed limestone may give rise to differential surface effects that have different magnetic susceptibilities.

- The diamond drilling identified siderite zones at Blackjacks, Mariposa and Grieves can be seen in the magnetic data. However numerous anomalies of a similar intensity occur elsewhere, generally in areas of the Gordon Limestone considered as non-prospective.

- There are several targets in the magnetic data that lie at the base of the Gordon Limestone which require drill testing.

Simon Tear
John Tesselaar


364000E
365000E
363000E
5352000N
5351000N
5350000N
L 62240 N
L 62250 S
L 62260 N
L 62270 S
L 62280 N
L 62290 S
L 62300 N
L 62310 S
L 62320 N
L 62330 S
L 62340 N
L 62350 S
L 62360 N
L 62370 S
L 62380 N
L 62390 S
L 62400 S
L 62410 N
L 62420 N
L 62430 S
L 61700 S
L 61690 N
L 61680 S
L 61670 N
L 61660 S
L 61650 N
L 61640 S
L 61630 N
L 61620 S
L 61610 N
L 61600 S
L 61590 N
L 61580 S
L 61570 E
L 61560 W
L 61550 E
L 61540 W
L 61530 E
L 61520 W
L 61510 E
L 61500 W
L 61490 E
L 61480 E
L 61470 W
L 61460 E
L 61450 S
L 61440 N
L 61430 S
L 61420 N
L 61410 S
L 61400 N
L 61390 S
L 61380 N
L 61370 S
L 61360 N
L 61350 S
L 61340 N
L





Plot Coordinate System: AMG
Grid Angle: 0.0 deg.
True North Angle: 358.8 deg.
Magnetic North Angle: 11.8 deg.

5 cm

250 0 250 500 750 1000 1250
(metres)

CRA EXPLORATION PTY. LIMITED

Zeehan Helimag Survey

EL28/88 Zeehan 1 - Sassafras Prospect

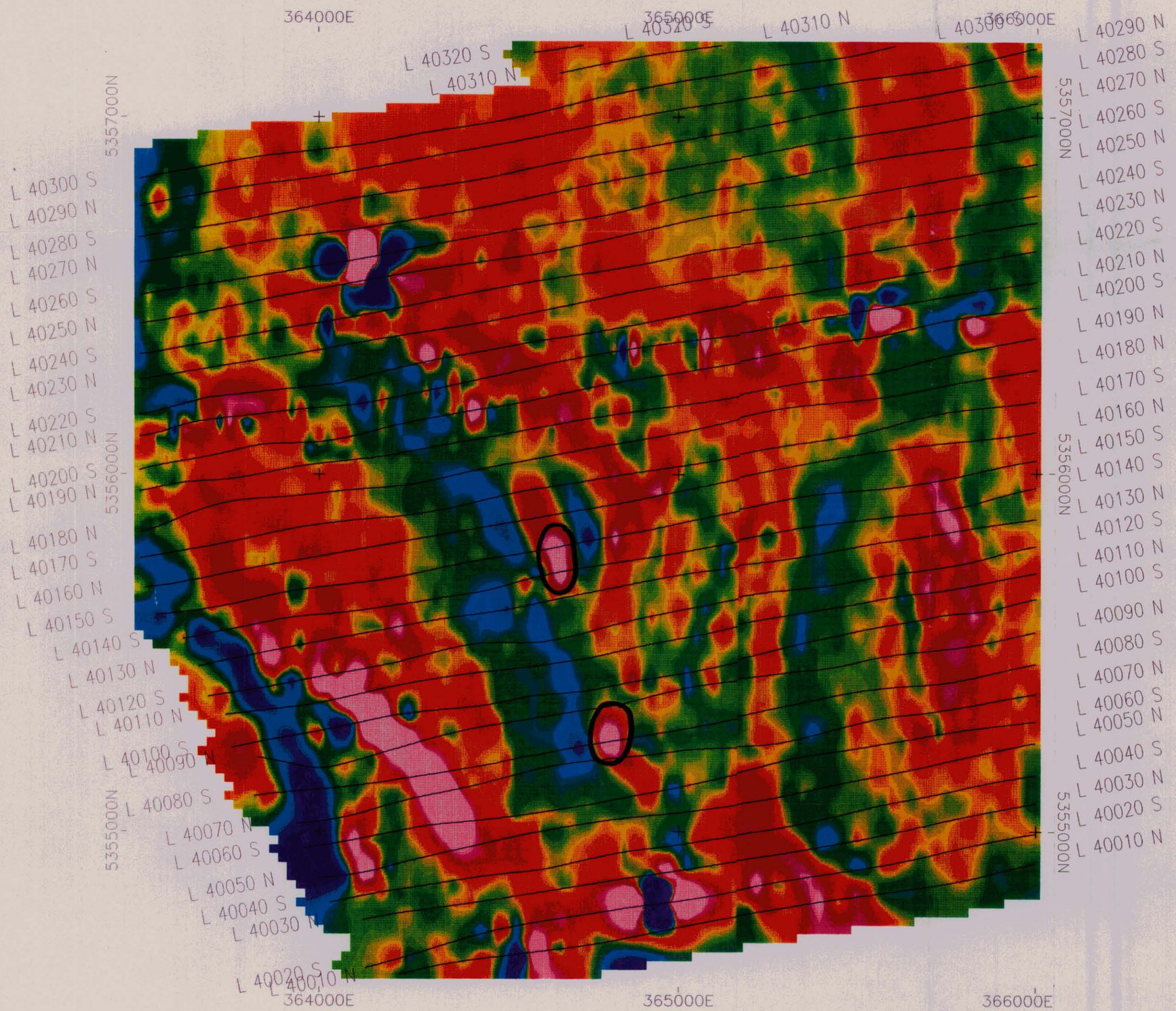
Coloured Total Field on Shaded Relief Image

Author: John Tesselaar	Reference: SK55-05
Drawn: John Tesselaar	File Name:
Date: July 1996	Report No: 22222
Scale: 1:25,000	Plan No: Tv1147

364082

97-3958

ANNUAL REPORT ZEEHAN NO 1
EL 28/88 - P.E. NOV 1996 - CRA
S TEAR/R RUSSELL- VOL 2 OF 3



3.7
3.3
3.0
2.7
2.4
2.2
2.0
1.8
1.6
1.5
1.3
1.1
1.0
0.8
0.7
0.6
0.4
0.3
0.2
0.0
-0.1
-0.3
-0.4
-0.5
-0.7
-0.8
-1.0
-1.1
-1.3
-1.4
-1.6
-1.8
-2.0
-2.4
-2.7
-3.0
-3.3
-3.7
-4.4

nT/m

Magnetic North

364083

100 0 100 200 300 400 500 600 700
(meters)

5 cm

97-3958

ANNUAL REPORT ZEEHAN NO 1
EL 28/88 - P.E. NOV 1996 - CRA
S TEAR/R RUSSELL- VOL 2 OF 3

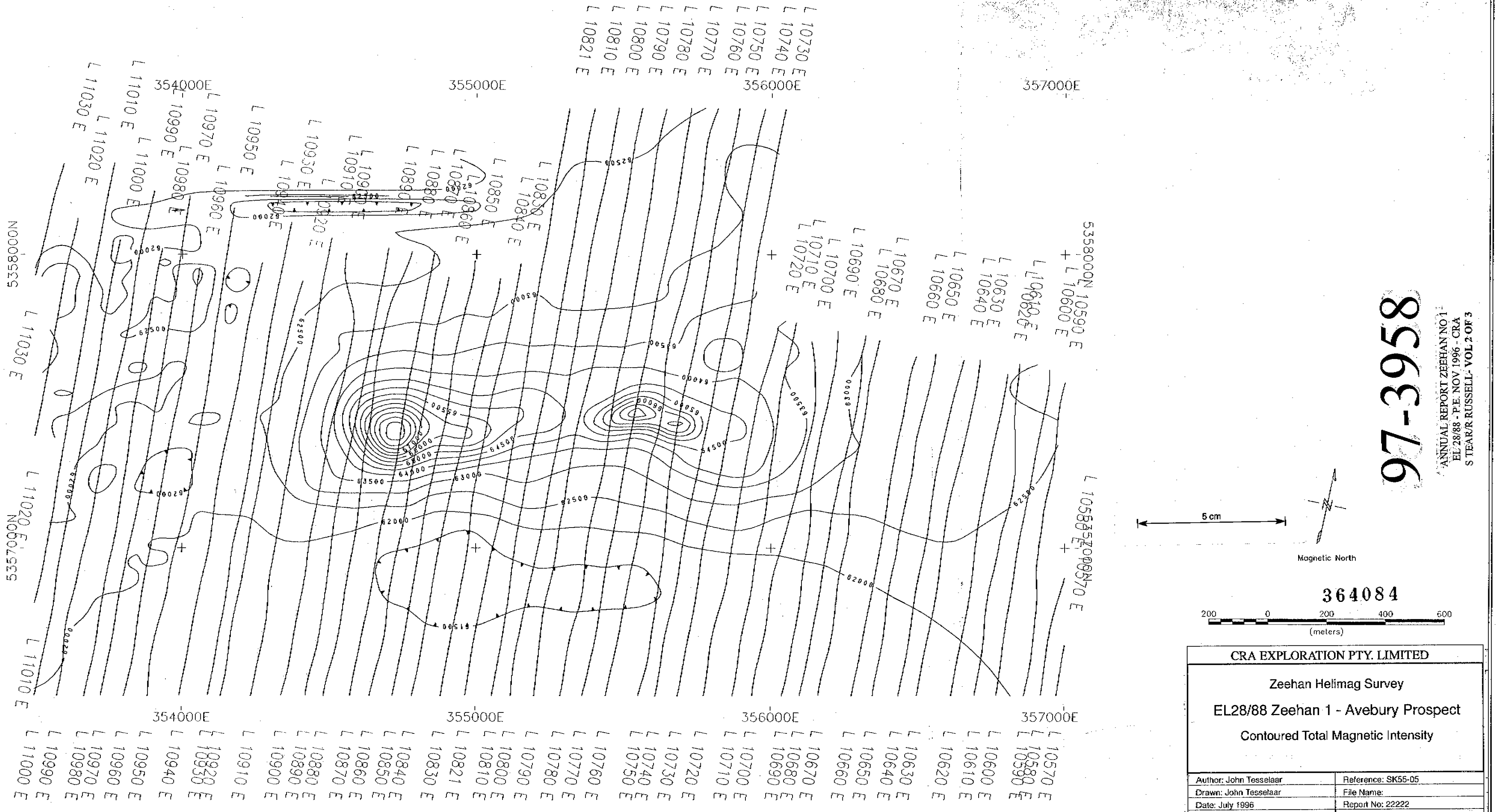
CRA EXPLORATION PTY. LIMITED

Zeehan Helimag Survey

EL28/88 Zeehan 1 - Pyramid Prospect

Vertical Derivative Image, Flight Line Overlay & Modelled Anomalies

Author: John Tesselaar	Reference: SK55-05
Drawn: John Tesselaar	File Name:
Date: July 1996	Report No: 22222
Scale: 1:10,000	Plan No: Tv1141



97-3958

ANNUAL REPORT ZEEHAN NO 1
EL 28/88 - P.E. NOV 1996 - CRA
S TEAR/R RUSSELL- **VOL 2 OF 3**

CRA EXPLORATION PTY. LIMITED

Zeehan Helimag Survey

EL28/88 Zeehan 1 - Avebury Prospect

Contoured Total Magnetic Intensity

Author: John Tesselaar	Reference: SK55-05
Drawn: John Tesselaar	File Name:
Date: July 1996	Report No: 22222
Scale: 1:10,000	Plan No: Tv1148



CRAE AIRBORNE MAGNETIC SURVEY, ZEEHAN AREA
TOTAL FIELD (GEOSOFT GRIDDING)
CRAE SURVEY NUMBER T27M AMG PROJECTION ZONE 55 DATUM AGD 66
CELL SIZE 20M RESAMPLED TO 10M PLOT NO QIP0496 1:50,000

© COPYRIGHT
CRA EXPLORATION
PTY LTD 1994

This image remains the property of CRA Exploration and may not be used in whole or in part without the written permission of the company

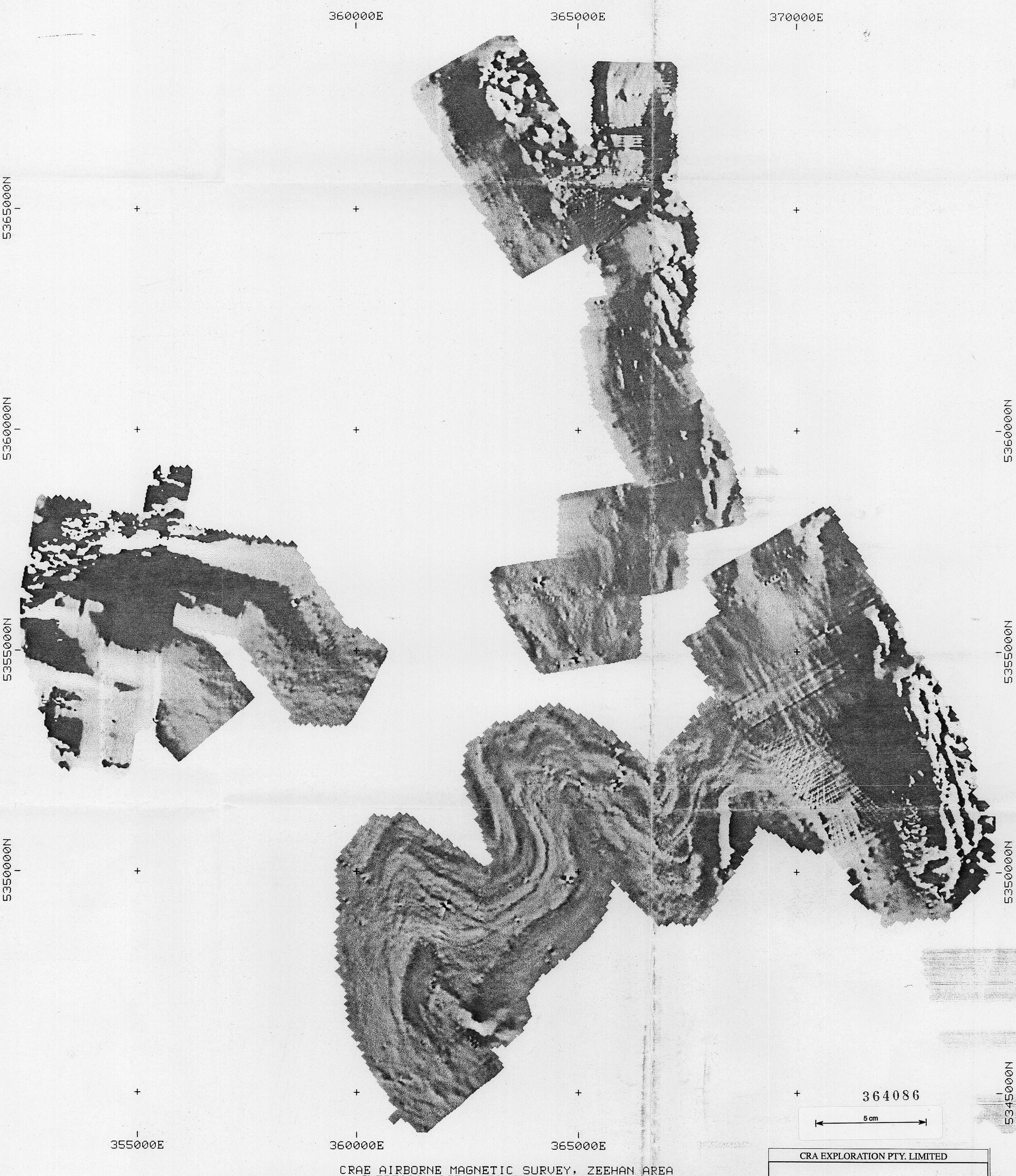
CRA EXPLORATION PTY. LIMITED

Zeehan Helimag Survey

Total Magnetic Intensity Map

Author: John Tesselaar	Reference: SK55-05
Drawn: John Tesselaar	File Name:
Date: July 1996	Report No: 22222
Scale: 1:50,000	Plan No: Tv1026

97-3958
ANNUAL REPORT ZEEHAN NO 1
EL 28/88 - P.E. NOV 1996 - CRA
S TEAR/R RUSSELL- VOL 2 OF 3



364086

5 cm

CRAE AIRBORNE MAGNETIC SURVEY, ZEEHAN AREA
VERTICAL DERIVATIVE (GEOSOFT GRID)
CRAE SURVEY NUMBER T27M AMG PROJECTION ZONE 55 DATUM AGD 66
CELL SIZE 20M RESAMPLED TO 10M PLOT NO QIP0497 1:50,000

© COPYRIGHT
CRA EXPLORATION
PTY LTD 1996

This image remains the property of CRA Exploration and may not be used in whole or in part without the written permission of the company

CRA EXPLORATION PTY. LIMITED

Zeehan Helimag Survey

Vertical Derivative Map

Author: John Tesselaar	Reference: SK55-05
Drawn: John Tesselaar	File Name:
Date: July 1996	Report No: 22222
Scale: 1:50,000	Plan No: Tv1027

97-3958

ANNUAL REPORT ZEEHAN NO 1
EL 28/88 - P.E. NOV 1996 - CRA
S TEAR/R RUSSELL- **VOL 2 OF 3**



AIRBORNE SURVEY EQUIPMENT

Aircraft:	AS350B Helicopter
Magnetometer:	Geometrics G-833 Helium
Resolution:	0.001 nT
Sensitivity:	0.001 nT
Recording Interval:	0.10 Hz
Compensation:	RMS AADC II Compensator

AIRBORNE SURVEY SPECIFICATIONS

Flight Line Direction:	CRA Digitised
Flight Line Separation:	CRA Digitised
Tie Line Direction:	CRA Digitised
Tie Line Separation:	CRA Digitised
Mean Terrain Clearance:	30 metres
Sample Interval:	3-4 metres
Navigation:	Differential GPS
Survey Flown:	March 1995

PROCESSING DETAILS

Diurnal Corrections Applied.
Tie Line Levelling Applied.

TRIAL BLOCK 364087

0 200 400 600 800 1000 1200 1400 1600
Scale 1: 10000

97-3958

ANNUAL REPORT ZEEHAN NO 1
EL 28/88 - P.E. NOV 1996 - CRA
S TEAR/R RUSSELL - VOL 2 OF 3

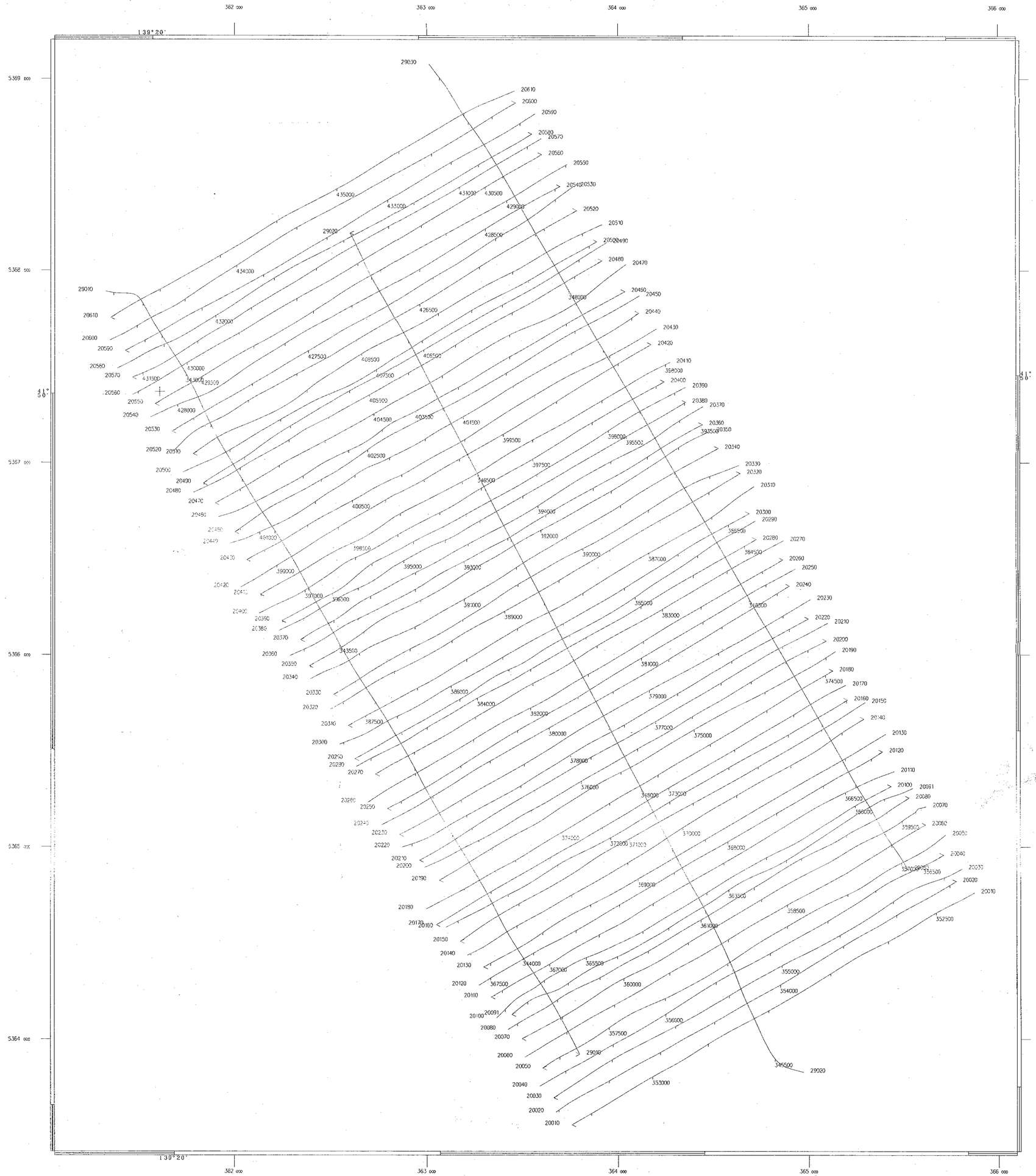
5 cm

TRIAL 364087

UTS GEOPHYSICS PTY LTD

CRA EXPLORATION PTY LTD
TASMANIA SURVEY - AREA 1
DETAILED HELI-MAG SURVEY
FLIGHT PATH MAP

DRAWN: UTS GEOPHYSICS	SCALE: 1: 10000
DATE: 1 MAY 1995	JOB: A95701



AIRBORNE SURVEY EQUIPMENT

Aircraft:	AS350B Helicopter
Magnetometer:	Geometrics G-833 Helium
Resolution:	0.001 nT
Sensitivity:	0.001 nT
Recording Interval:	0.10 Hz
Compensation:	RMS AADC II Compensator

AIRBORNE SURVEY SPECIFICATIONS

Flight Line Direction:	CRA Digitised
Flight Line Separation:	CRA Digitised
Tie Line Direction:	CRA Digitised
Tie Line Separation:	CRA Digitised
Mean Terrain Clearance:	30 metres
Sample Interval:	3-4 metres
Navigation:	Differential GPS
Survey Flown:	March 1995

PROCESSING DETAILS

Diurnal Corrections Applied.
Tie Line Levelling Applied.

1st contour interval	1nT
2nd contour interval	10nT
3rd contour interval	100nT
4th contour interval	1000nT

Grid North

0 200 400 600 800 1000 1200 1400 1600
Scale 1: 10000

5 cm

97-3958

ANNUAL REPORT ZEEHAN NO 1
EL 28/88 - P.E. NOV 1996 - CRA
S TEAR/R RUSSELL - **VOL 2 OF 3**

364088 SASSAFRAS

UTS GEOPHYSICS PTY LTD

CRA EXPLORATION PTY LTD

TASMANIA SURVEY

DETAILED HELI-MAG SURVEY

FLIGHT PATH MAP

DRAWN: UTS GEOPHYSICS	SCALE: 1: 10000
DATE: 25 APRIL 1995	JOB: A06702

364089

Appendix I

Flight Line Maps

364090

Appendix IX

Basin Analysis Report

See 96-3957A

364091

ORDOVICIAN GORDON GROUP CARBONATES, ZEEHAN REGION, TASMANIA, AUSTRALIA - STRATIGRAPHY AND PALAEOENVIRONMENTS

CLIVE BURRETT,
GEOSEA CONSULTANTS,
22 HINMAN DRIVE,
KINGSTON, TASMANIA,
AUSTRALIA, 7050

Final Report 15-11-1995

364092

CONTENTS

ABSTRACT	p.3
INTRODUCTION	p.4
LITHOSTRATIGRAPHY	p.4
PALAEOENVIRONMENTS	p. 8
CONCLUSIONS	p.12
RECOMMENDATIONS	p. 12
REFERENCES	p.13
APPENDICES	p.15

364093

ABSTRACT

The Gordon Group in the Zeehan area comprises 3 conformable formations; the Ugbrook, Myrtle (new) and Black Jacks (new). The Ugbrook Fm, first defined in the Mole Creek area, was deposited in protected shallow subtidal to low intertidal waters in an offshore bar to lagoonal to lagoonal-island environment during the Early Caradoc.

The basal Ugbrook interdigitates with the siliciclastic Moina Fm and suggests that the Early Caradoc shoreline was at or very close to Black Jacks. A transgression shifted these environments northwards and eastwards during the Caradoc and Ashgill.

The tidal flat complex of the Myrtle Fm developed throughout the area in the mid-Caradoc and consists of fifteen 1m to 4m thick Punctuated Aggradational Cycles (PACs) which can be correlated throughout the area. The Myrtle Fm is similar lithologically, environmentally and chronostratigraphically to the Lower Limestone Member of the Florentine Valley.

The Myrtle Fm is succeeded by mainly shallow to moderately deep subtidal alternating micrites and shales with minor PACs, belonging to the Black Jacks Fm which is similar to the Upper Limestone Member of the Florentine Valley. The lack of PACs in the Upper Black Jacks and the very common occurrence of coarse carbonates in the Myrtle stratigraphic drillcore suggests that the Myrtle area might have been in a slightly deeper and more rapidly subsiding region. The Lords Member of the Black Jacks Fm is present in several of the drillcores and, as is normal elsewhere in the state, varies in thickness and lithology from mudstones to coarse sandstones. Minor PACs and some faunal horizons help in the correlation of the Black Jacks.

INTRODUCTION

At the request of CRA, 8 full days in October 1995 were spent logging core through Ordovician sedimentary sequences from drillholes in the Zeehan area. An extra four days were allocated to plotting, drafting, report preparation and the examination of thin sections and fossils. Logging concentrated on the Gordon Group carbonates but short sections of the underlying Denison Group (Moina Fm) and overlying Eldon Group (Crotty Fm) siliciclastics were also examined.

The Gordon Group carbonates are deformed and the extent of stratigraphic loss or repetition is difficult to establish from the numerous veined and crushed intervals. In any sedimentary basin analysis it would be desirable to plot isopachs in order to define the basin shape and its evolution through time. Unfortunately, depending on the relation of bedding to the principal axis of the strain ellipsoid, bedding thickness may be increased or decreased substantially. Tectostylolites, which are pervasive in the Zeehan cores, will decrease stratigraphic thickness. They preferentially affect more argillaceous sections and the amount of section loss will (as with cleavage) depend on their angle of incidence with bedding. This problem is soluble but not within the confines of this study. A full palinspastic study would also need to remove, in map view, the Devonian folding and the thrust faulting.

LITHOSTRATIGRAPHY

Several major lithostratigraphic units are recognisable in the Zeehan cores. The Gordon Group comprises the Ugbrook Fm, the Myrtle Fm (new name) and the Black Jacks Fm (new name). The Black Jacks Fm includes the Lords Siltstone Member (Fig.1). The positions and suggested correlations of these units are shown in Fig. 5 (large diagram in pocket). All thicknesses are uncorrected downhole distances rather than dip-corrected stratigraphic thicknesses.

Denison Group, Moina Formation

The Moina Fm of the Denison Group underlies the Gordon Group in northern and western Tasmania (Fig. 2). The boundary between the Moina Fm and the Gordon Gp is everywhere marked by a siltstone-mudstone transitional zone that may be a metre thick or 30m thick. This transition is 200m thick in the Florentine Valley and is known as the Florentine Valley Fm. The separation between the Denison Gp and the Gordon Group is based on the dominance of siliciclastics (Denison Gp) and limestone (Gordon Gp). The siltstone-mudstone transition is therefore historically and pragmatically regarded as the topmost part of the Moina Fm and the base of the Gordon Gp is defined on the incoming of carbonates. However, where there is an interdigitation of siliciclastics and carbonates, as in DB111, or where the lowest limestones are replaced by siderite or are mineralised then the placement of the boundary may be arbitrary. In all sections, delineation of the boundary has to regarded as a matter of taste. In most sections I have taken the boundary to be the first obvious and definite limestone.

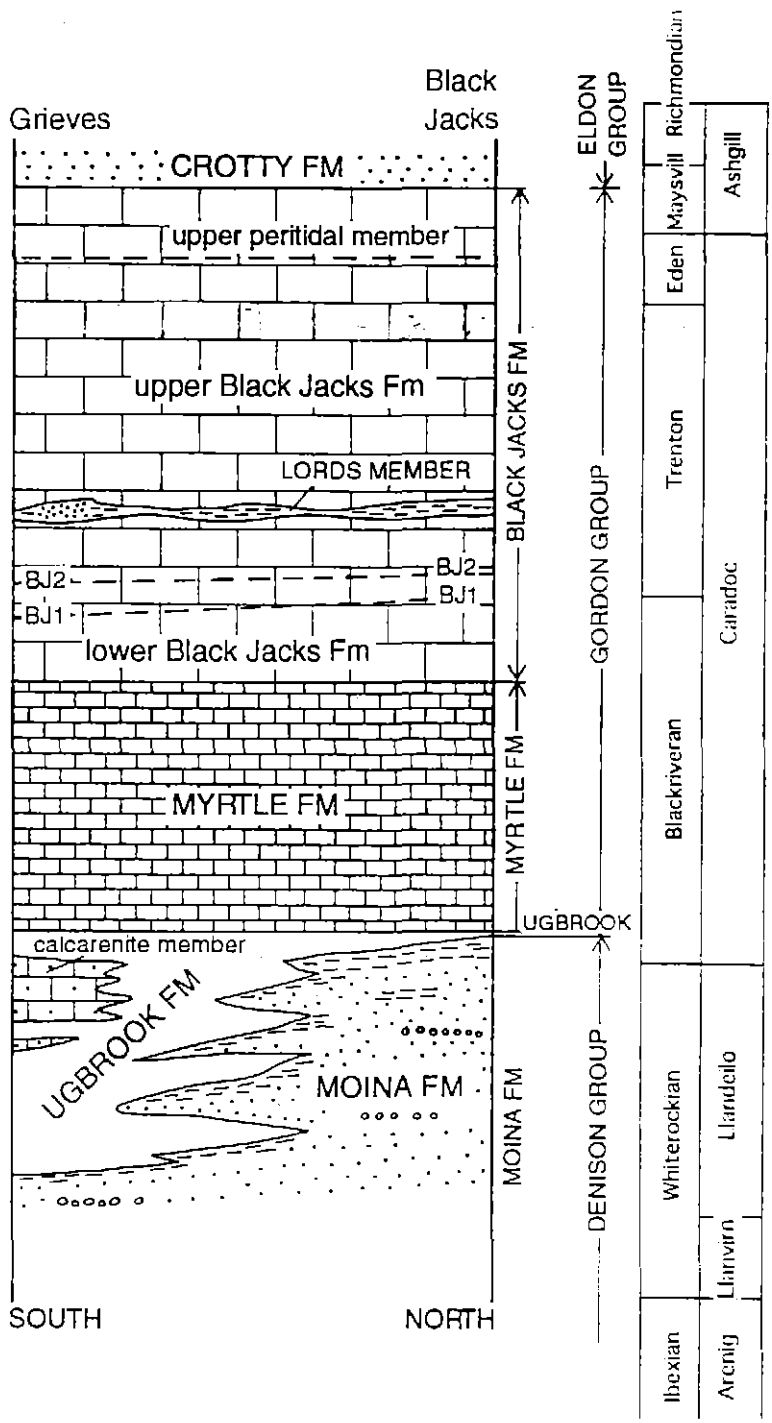


Fig.1 Summary of Ordovician lithostratigraphy in the Zeehan region.
Chronostratigraphic units are based on the standard North American scheme and the standard British scheme. Correlations are most easily made to the American scheme but the British scheme is used in the text because of its greater familiarity.

364096

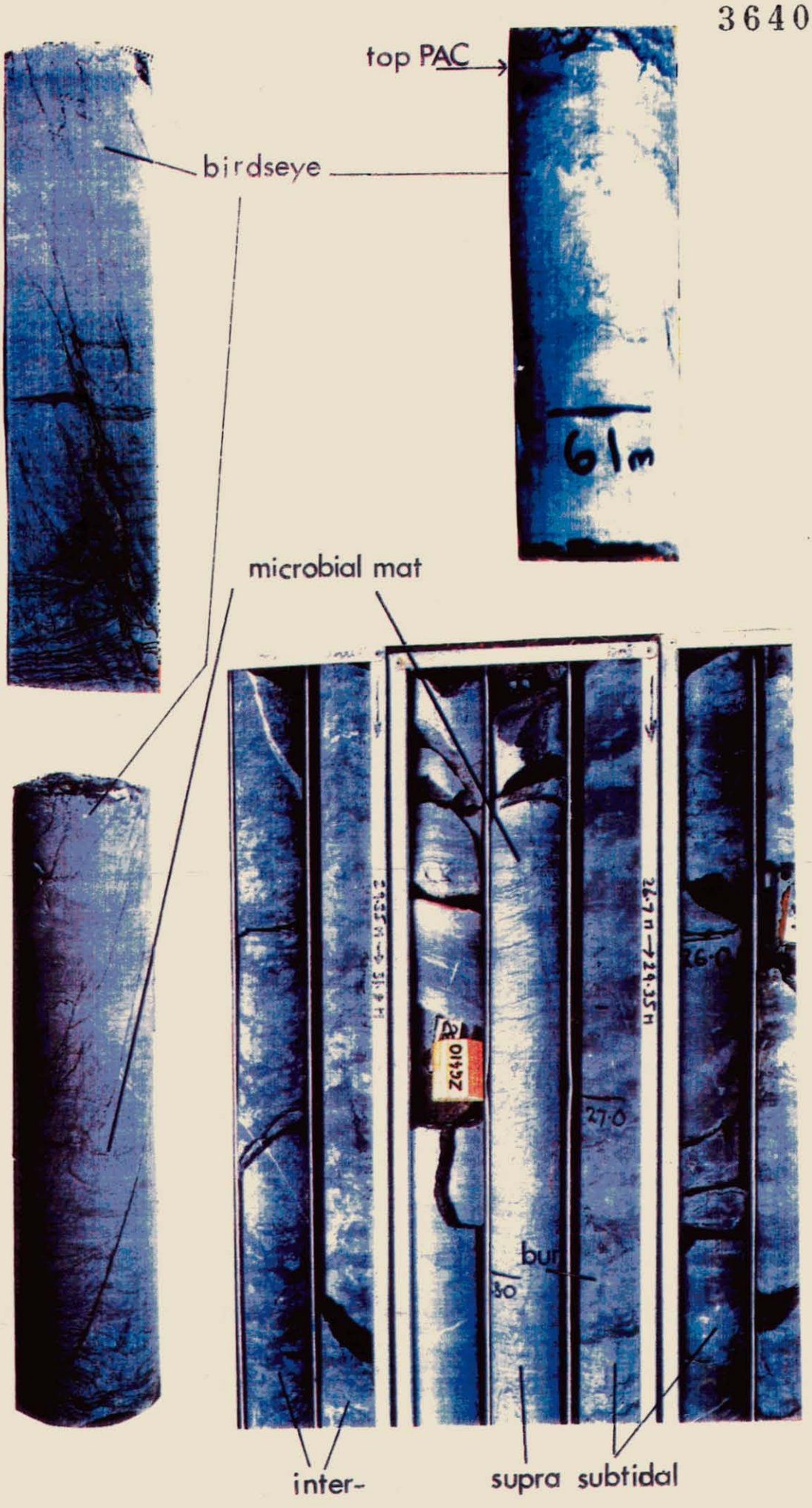


Plate 1 Typical PAC lithologies from ZG 410. Note darkening of limestone from shallow to deep.Core between 26.7m and 27m is typical subtidal alternation of argillaceous and micritic limestone and this lithology is typical of much of the Black Jacks Fm. but forms a small percentage of the Myrtle Fm. Boundary between Myrtle Fm and Black Jacks Fm is at 27.5m.

Ugbrook Formation (Burrett & Goede 1987, Burrett *et al.* 1989)

The siltstones of the upper part of the Moina Fm are succeeded by alternating thin micrites and shales with, in some cores, siltstones and sands (notably DB111). These centimetre-decimetre scale alternations are frequently bioturbated and often nodular (due to sedimentary boudinage). Pelloids and comminuted shells are very common. Asaphid trilobites are present but other identifiable fossils are rare. Several sections have developments of biocalcarenites and/or biosparites composed mainly of crinoidal debris. These sequences are very similar to the Ugbrook Fm in Mole Creek (Burrett *et al.* 1989; Appendix C) and, rather than erect a new name, I will use that term. This lithology is only a few metres thick in DB 110 (possibly 40m thick if a sideritised zone is included) and thickens towards Myrtle which also has a thick development of the crinoidal biospararenite member.

Myrtle Formation (new name)

The Myrtle Fm consists of between 40-170m of micrites, biomicrites, dolomitised micrites and minor calcarenites and shales deposited as upwardly shallowing tidal flat cycles known as Punctuated Aggradational Cycles (PACs). These were first recognised and used as a correlation tool by Calver (1977). Unfortunately, he did not publish and PACs have since been recognised worldwide as a useful correlation and palaeoenvironmental tool. The PAC concept is summarised in Appendix B and photographs of representative lithologies are shown on the attached photographs (Plate 1). Calver (1977) used PACs to correlate throughout the Florentine River Valley recognising 18 PACs in the Lower Limestone Member of the Benjamin Limestone. In the Florentine Valley, and in Zeehan, this correlateability is due to a basinwide or at least sub-basinwide response to changing sea level. PAC boundaries may therefore be regarded as essentially isochronous horizons. Fifteen PACs are recognised in the Myrtle Fm. and each section has most of them. The extent of faulting in ZG 403 is clear as only the first PAC is present.

Black Jacks Formation (new name)

The Myrtle Fm is succeeded by the Black Jacks Fm which consists of alternating micrites and shales with some biomicrites, calcarenites and calcisiltites. Two PACs occur in the Lower Black Jacks but are not present in every section. These are labelled BJ1 and BJ2 on Fig. 5. The Lords Member is a thin (1m-15m) siltstone-shale-sometime sandstone unit that is surprisingly variable on a kilometre scale for a unit that appears over most of western Tasmania from Precipitous Bluff on the south coast to the Florentine Valley to Zeehan to Mole Creek (Fig.2). The Lords Member equivalent at Mole Creek (the Mole Creek Fm) is discontinuous (see p.7 of Appendix C). A coarse, quartz sandstone occurs at the appropriate stratigraphic level in ZF 37 (Firewood Siding). The Lords Member is characterised, statewide, by a distinctive fauna consisting of abundant *Pliomerina* trilobites, strophomenid brachiopods (*Sowerbyites*) and the Tasmanian endemic ostracod *Dominina*.. The Lords Member lithology/fauna does not appear suddenly but is preceded by a gradual deepening of both biofacies and lithofacies.

The Upper Black Jacks Fm is completely dolomitised in some holes (ZR 104) and partially in others (DTM 84-6, DTB 84-1). Complete dolomitisation is unusual in the Gordon Group and increased porosity, including vuggy porosity, is evident in ZR 104 due to the 12% volume loss when calcite is replaced by dolomite. As dolomitised limestones are important petroleum reservoirs (and therefore porous for ore forming fluids) it might be useful to plot the distribution of dolomitisation within the Gordon Group at Zeehan (see Appendix A).

Where undolomitised, there is an abundant coral-stromatoporoid fauna, some of which is correlated to the widespread 'Den fauna'. A diverse trilobite-brachiopod-bryozoan fauna, which in previous studies has been called the 'Smelters fauna' (Zeehan Smelters fauna described by Pitt (1961) and mentioned by Banks and Burrett (1980), occurs below an 'upper peritidal member '. This 'upper peritidal member' occurs in ZF 37, DS 98, DTM 84-6 and DB 110 but is not obvious in ZM190.

PALAEOENVIRONMENTS

Most sections of the Gordon Group were deposited in predominantly very shallow subtidal to peritidal conditions on a mini-platform. due to a marine transgression from the south, west and east towards the Precambrian/Cambrian islands of the Tyennan and Rocky Cape regions (Fig. 3). Thick siliciclastic sandstone sequences, followed

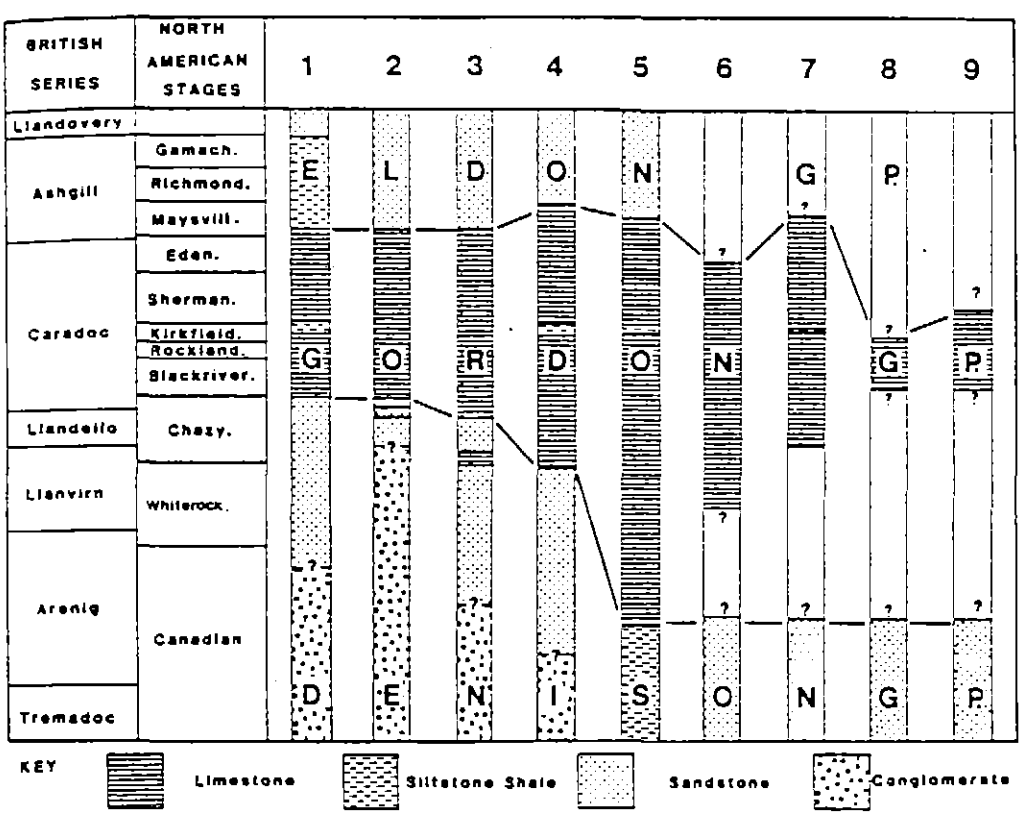


Fig.2. Simplified stratigraphic columns showing diachronous base of the Gordon Gp and of the Moina Fm. 1=Queenstown, 2=Vale of Belvoir, 3=Lower Gordon River,4=Mole Creek, 5=Florentine Valley, 6=Ida Bay, 7=Precipitous Bluff, 8=Point Cecil, 9=Surprise Bay. (Burrett *et al.* 1984).

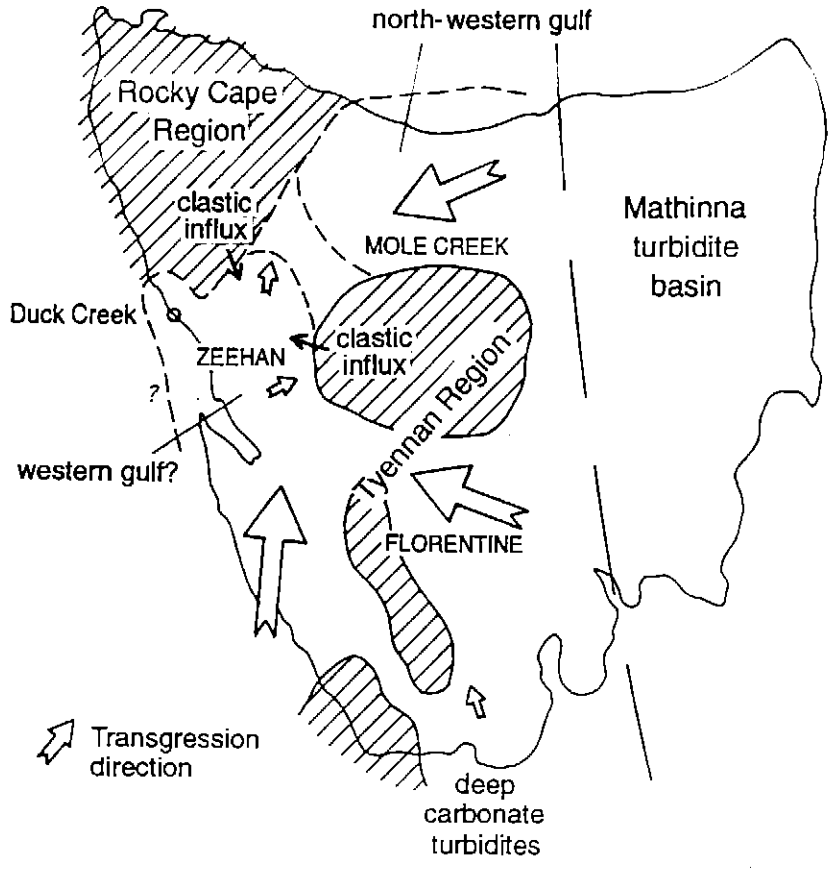


Fig.3. Generalised palaeogeography of the Tasmanian miniplatform in the Caradoc showing inferred directions of transgression. Dotted link between Tyennan and Rocky Cape regions may be an isthmus transgressed during Late Caradoc times.

by thick carbonate successions were gradually built up. This transgression started in the Tremadoc (in the Florentine Valley) and continued up to the Late Caradoc or even Early Ashgill (Figs.2-3). Probably much of the Tyennan and Rocky Cape regions were still emergent in the Late Ordovician (Ashgill). The timing of the transgression is mainly determined from conodont dates on the lowest Gordon Group carbonates with supplementary information from macrofossils in the underlying Denison Group siliciclastics (Fig.2). In the north of the state, the transgression moved towards the Tyennan and Rocky Cape regions from the north and east possibly forming an east-west aligned gulf (Burrett 1978). In the west, the transgression was from the south towards the west and north. Very thin sequences of the Gordon Group are found at Duck Creek (just to the north of the Heemskirk Granite) and at Heazlewood River. It is possible that a similar gulf to the one in the northwest existed in the west of the state. The siliciclastic sands at the Lords level in the Firewood Siding hole (ZF 37) also suggest proximity to land. A solution to this palaeogeographic problem depends on studies on the Ordovician around Queenstown, outcrops south of Grieves and the poor limestone outcrops between Zeehan and the Vale of Belvoir and south of Firewood Siding.

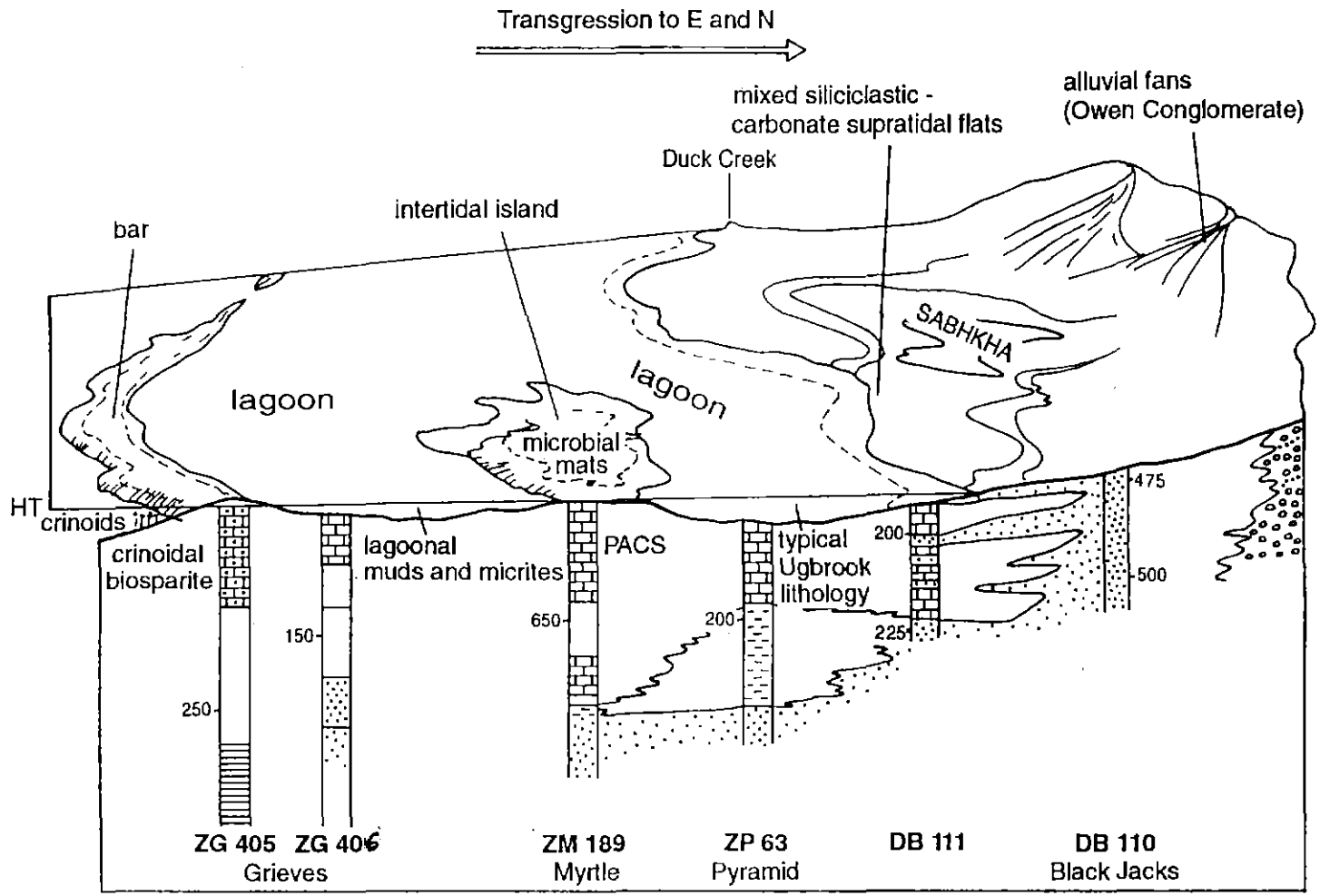


Fig. 4 Environmental reconstruction of the Zeehan area for early Ugbrook Fm times (about Early Caradoc) from the south of the area at Grieves to Black Jacks in the north. Shoreline is to the north (right) and east (behind the viewer). Not to scale. HT = normal high tide level. Numbers refer to down hole depth in m not stratigraphic thickness.

364100

The Ugbrook Fm thins dramatically from DB111 to DB 110 and there is no suggestion that this is due to Devonian faulting. Unlike the other cores examined, the Ugbrook in DB 111 has several coarse siliciclastic interbeds as well as reddened tops to PACs in its basal part. The simplest explanation for this is that the (irregular) shoreline was between DB111 and DB 110 in early Ugbrook time (approximately mid-Caradoc or Blackriveran time) as shown in Fig.4, with clastic debris being derived from the Tyennan region to the east. This date, or a slightly younger one, also applies to the basal carbonates at Duck Creek and Heazlewood River. The typical Ugbrook micrites and pelloidal bioturbated shales were deposited in a lagoon formed behind (north of) a northerly or northeasterly migrating offshore carbonate bar with the minor PAC carbonates formed on intertidal islands within the lagoon (Fig.4). As the transgression continued, the carbonate bar moved from Grieves towards Myrtle during late Ugbrook time. Stabilisation occurred during Myrtle times (Upper Blackiveran) with the whole Zeehan area covered with waxing and waning PACs. Probably by that time, the shoreline (i.e. high supratidal limit) had moved north to Duck Creek and east onto the Tyennan region.

Deepening occurred after Myrtle Fm times, probably due either to the incapacity of the carbonate factory to keep-up with rising sea level or to an increased rate of basinal subsidence. Open subtidal sediments were deposited over the whole area with brief peritidal flat deposition (BJ 1 and BJ2) at Grieves, Myrtle (ZM189) and at Black Jacks (DB110).

The Myrtle core, ZM189, is unusual in that coarse grained carbonates including sparites, spararenites, calcarenites, biosparites are common through the section. This is presumably the consequence of the production of large bioclasts due to deposition further from the micrite producing tidal flats and due to the preponderance of a good subtidal fauna such as crinoids.

The Lords event appears to be isochronous across the whole Tasmanian miniplatform. It was a time of uplift in the Tyennan region leading to coarse quartzite conglomerates being deposited within the middle of the Benjamin Limestone Fm to the west of the Florentine Valley (in the Vale of Rasselas), a deepening in most sections but a shallowing in the deepwater Surprise Bay sequence (Burrett *et al.* 1984). The Lords event was clearly a significant but short lived epeirogenic episode during the mid-Trentonian (Late Caradoc). Normal shallow subtidal conditions resumed during the remainder of Black Jacks time except for a widespread peritidal interlude in late Black Jacks time (Late Trentonian/Early Ashgill). This upper peritidal interval is not found in the Upper Black Jacks Fm at Myrtle (ZM190) which again may suggest that Myrtle may have been in slightly deeper water. The upper peritidal member may correlate to a similar shallowing interlude recognised in the Overflow Creek Fm at Mole Creek.

CONCLUSIONS

The Gordon Group sequence at Zeehan, although starting later during the earliest Blackriveran rather than in the Chazyan, is similar to that at Mole Creek and dissimilar to that in the Florentine Valley. It lacks the oncolitic Standard Hill Fm but the fauna, lithofacies and interdigitation of the Ugbrook with the Moina is very similar. The Myrtle Fm has similarities with both the thicker Lower Limestone Member in the Florentine Valley and the Sassafras Creek Fm at Mole Creek. The generally subtidal Black Jacks Fm is, though, closer to that of the Upper Limestone Member of the Florentine Valley than to the dominantly peritidal Dogs Head and Overflow Creek Fms at Mole Creek.

Interdigitation of the Moina with the Ugbrook and a greatly thinned Ugbrook sequence at Black Jacks suggests that the Blackriveran (Early Caradoc) shoreline was at about the position of DB 110, moving eastwards onto the Tyennan region and northwards towards Duck Creek by the Late Blackriveran.

Identification of PACs or shallowing-upward sequences in the Myrtle Fm and in the Upper Black Jacks Fm allows correlation across the region.

There are several argillaceous horizons present in some sections and the identification of the Lords Member is helped by the identification of its characteristic fauna and by the lithofacies deepening prior to its deposition.

RECOMMENDATIONS

Chronostratigraphic correlations in the Zeehan area could be improved substantially by employing conodonts. Conodonts are rare in peritidal sections but this study has shown that there are sufficient subtidal intervals that would yield sufficient useable conodont elements per kilogram of core. If this was coupled with an intensive study of the macrofossils then very reliable chronostratigraphic correlations are possible. Conodonts also record the maximum temperature that they have experienced and, more importantly, are pitted in a characteristic manner by hydrothermal fluids. Such a study could define flowpaths of hydrothermal fluids.

There are sufficient drillholes to define the extent of any basin or basins by the use of isopachs. However, a complete palinspastic study is recommended that takes into account extension due to cleavage and stratigraphic loss due to tectostylolites as well as removing the effects of Devonian folding and thrusting.

The extent of pervasive dolomitisation in the Black Jacks Fm should be plotted. This might reveal a zone of enhanced porosity/ permeability within the Gordon Group into which hydrothermal fluids might have flowed (see Appendix A).

REFERENCES

Baillie, P., & Burrett, C., 1990. Conodonts as indicators of mineral prospectivity. Tasmanian Department of Mines Report 1990/4; 1-4.

Banks, C.F., Baillie, P., Calver, C. and Burrett, C.F., 1989. Upper Cambrian-Devonian. In Burrett, C. and Martin, E. (Eds.) Geology and Mineral Resources of Tasmania, Geological Society of Australia Special Publication 15. Hobart, 600pp .

Banks, M.R. and Burrett, C.F., 1980: A preliminary Ordovician biostratigraphy of Tasmania. Journal of the Geological Society of Australia 26:363-376.

Banks, M.R. and Burrett, C.F., 1986: Some Ordovician and Silurian rocks and fossils from the Huskisson River area, W. Tasmania 151-162 in Brown, A.V., Geology of the Mt. Lindsay-Youngbuck area, W. Tasmania. Dept. Mines Geol. Survey, Tasmanian Bulletin 62.

Bendall, M., Volkman,J., Leaman, D. & Burrett, C., 1991: Recent developments in oil exploration in Tasmania. Australian Petroleum Exploration Association Journal, 1991, 74-84.

Burrett, C.F., !978: Stratigraphy and conodonts of the Ordovician Gordon Group, Tasmania. Unpublished Ph.D. thesis, University of Tasmania.

Burrett C.F., 1979: Tasmanognathus a new Ordovician conodont genus from Tasmania. Geologica et Palaeontologica 13: 31-38.

Burrett, C., 1984: Early Devonian deformation and metamorphism of conodonts in western Tasmania - economic, theoretical and nomenclatural implications, p. 14-17 in Baillie, P. and Collins, P. (eds.) Mineral Exploration and tectonic processes in Tasmania. Geological Society Australia, Hobart.

Burrett, C., Sharples, C., Stait, B. and Laurie, J., 1984: A Middle-Upper Ordovician tropical carbonate platform to basin transition, southern Tasmania, Australia. In: Bruton, D. (ed.) Aspects of the Ordovician system. Universitetsforlaget, Oslo, 149-157.

Burrett, C.F. & Martin, E., (Eds.) 1989. Geology and Mineral Resources of Tasmania, Geological Society of Australia, Special Publication 15, Sydney, 603 pp.

Burrett, C.F. 1992. Conodont geothermometry in the Palaeozoic carbonate rocks of Tasmania and its economic implications. Australian Journal of Earth Science 39, 61-66.

Burrett, C.F., Banks, M., Clota, G. and Seymour, D. 1989. Stratigraphy and structure of the Ordovician of Mole Creek Synclinorium, N.W. Tasmania. Records of the Queen Victoria Museum Launceston 96, 1-14.

Burrett, C.F., Laurie, J. and Stait, B., 1981: Gordon Subgroup (Ordovician) carbonates at Precipitous Bluff and Pt. Cecil, South West Tasmania, Australia. Pap. Proc. Roy. Soc. Tasm. 115: 93-99.

Burrett, C.F., Stait, B. and Laurie, J., 1983: Trilobites and microfossils from the Middle Ordovician of Surprise Bay, southern Tasmania, Australia. Memoirs Australian Association of Palaeontologists, 1: 177-193.

Calver, C., 1977: Palaeoecology of the Lower Limestone member, Florentine Valley, Unpublished thesis, University of Tasmania.

Ellis, A.,1984: Mineralization and palaeoenvironments in Gordon Group sediments, south of Zeehan, western Tasmania. Unpublished thsis, University of Tasmania.

North, F.K., 1985: Petroleum Geology. Allen and Unwin. 607pp.

Pitt, R.P.B., 1961: The Geology of the Zeehan Area. Unpublished Thesis, University of Tasmania.

Webby, B.D., VandenBerg, A., Burrett, C., Laurie, J. and Stait, B., 1981: The Ordovician System in Australia, New Zealand and Antarctica. Correlation Chart and Explanatory Notes. IUGS, Canada.

Webby,B., Stait,B., Laurie, J., Cooper,I., Burrett,C.F. & Shergold, J., 1991: Subdivisions of the Ordovician System in Australia. In: Advances in Ordovician geology. Geological Survey Of Canada Paper 90-9, 47-58.

Appendix A

Dolomitization and its control on porosity and reservoirs in the Trenton Limestone
(from North, 1985 p.198-199).

Appendix B

Peritidal Carbonates from Walker and James Eds 1992. Facies Models. Geological Association of Canada.

Appendix C

Lithostratigraphy at Mole Creek , Burrett et al. 1989.

Appendix A

364106

recrystallization, and most commonly of *dolomitization*. About 80 percent of all hydrocarbon reserves contained in carbonate reservoirs in North America are in essentially pure dolomites. This percentage is by no means representative of other regions of the world, and unquestionably reflects the number of North American carbonate reservoirs that are Paleozoic in age. In the Persian Gulf Basin, with the most prolific carbonate reservoirs in the world, the proportion of dolomite reservoirs is no more than 20 percent.

The replacement of $CaCO_3$ by dolomite involves a loss of volume of about 12.3 percent, and a consequent increase in porosity by that amount, if the replacement is molecule for molecule. It may not always be so, because volume for volume replacement is also possible. Yet it remains the case that in many fields having partially dolomitized carbonate reservoirs the oil is restricted entirely to the dolomitized portion. This portion is favorable because of *partial* dolomitization, preferentially of the finer-grained components of the limestone, and later leaching of the remaining calcitic parts which are more soluble. The most-quoted example of this phenomenon is the sprawling Lima–Indiana field south of the Great Lakes (Fig. 13.52). The oil is confined to porous dolomitic zones in the Ordovician Trenton Group where it passes over the axis of the broad, bifurcating Cincinnati Arch. Updip, porosity disappears in the unaltered limestone and only gas is recovered. Among the fields providing case histories for this book is the Jay field in Florida (Ch. 26), another example of restriction of oil to the dolomitized part of a carbonate formation. Up the dip, the undolomitized micritic limestone lacks porosity and is barren of oil. Most carbonate producing basins afford comparable examples.

An intriguing small example is provided by the Dover field, at the southwestern extremity of Ontario in Canada, like Lima–Indiana in the Ordovician Trenton Group. During the 1920s, articles on oil-bearing structures quoted Dover as an example of the rare synclinal trap. The syncline is controlled by an elongate fracture zone (Fig. 13.53) along which migrating waters have been able to dolomitize a considerable thickness of strata; the oil is restricted to the porous dolomite and therefore to the "syncline." The Albion–Scipio "trend", in Michigan's part of the same basin, is very similar and produces from the same formation (Fig. 13.52). From outside the normal concern of petroleum geologists comes the parallel case of Mississippi Valley-type lead–zinc deposits, in some of which it is established that the brines, derived from evaporite deposits, that deliver the metals also bring about dolomitization.

The selective nature of dolomitization extends to its

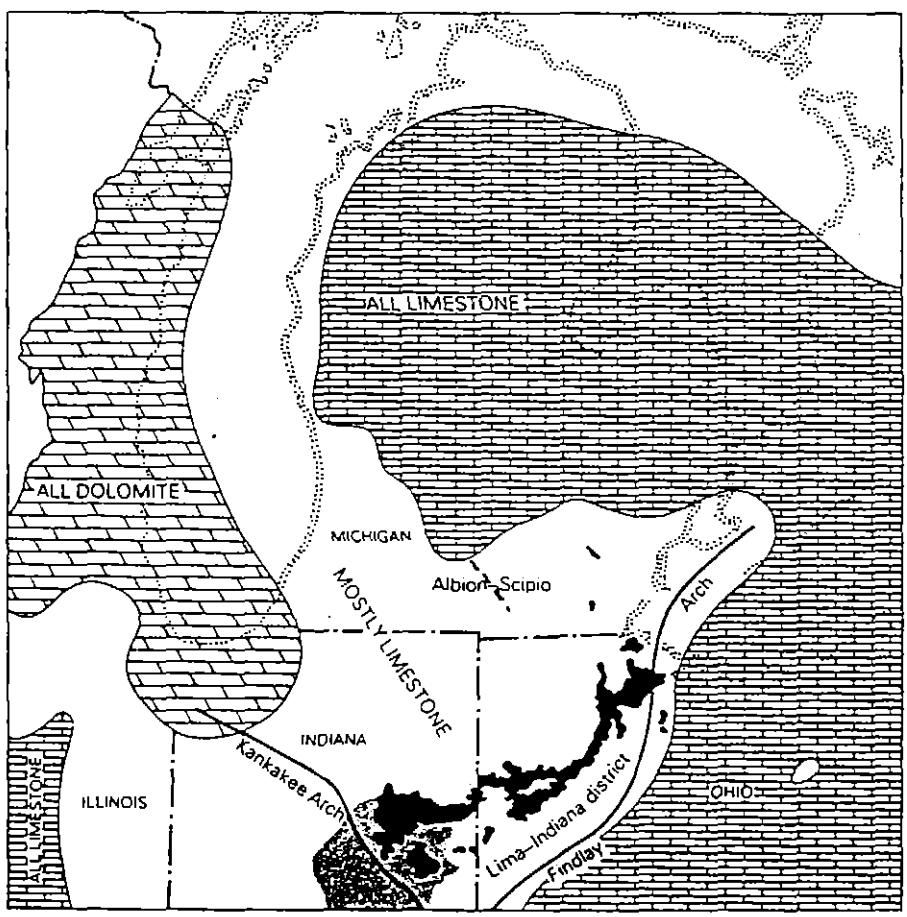


Figure 13.52 Michigan Basin in Middle Ordovician time, showing the Cincinnati Arch bifurcating into two arches as it crosses the basin from the south. The Trenton Group carbonates are dolomitized over the arches and along linear fracture zones; oil accumulations are restricted to the dolomitized portions. Dotted outlines on map delineate present Lakes Michigan and Huron. (After K. K. Landes, *Petroleum geology of the United States*, New York: Wiley–Interscience, 1970; and G. V. Cohee, US Geol. Survey Preliminary Chart no. 9, 1945.)

364107

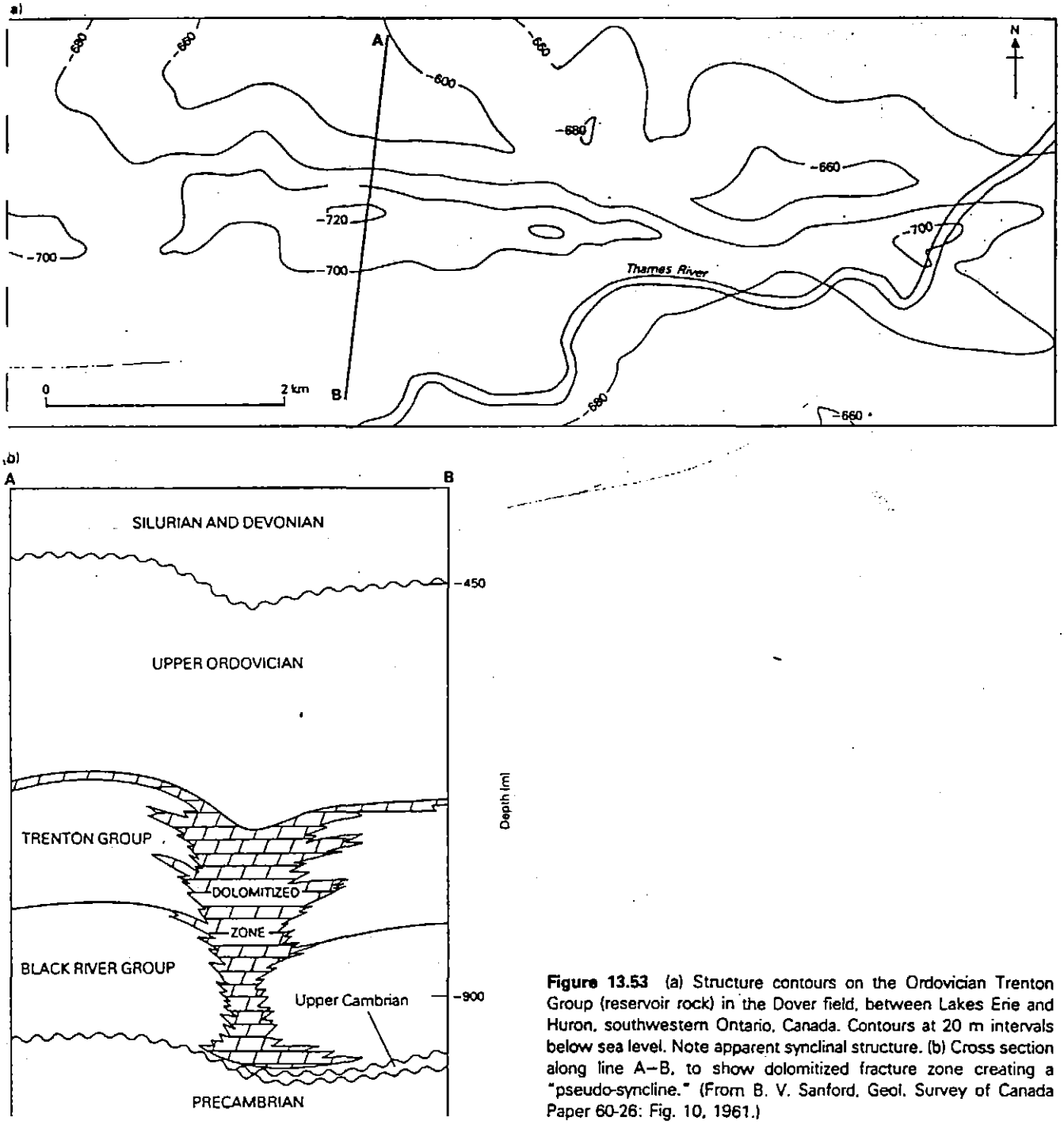
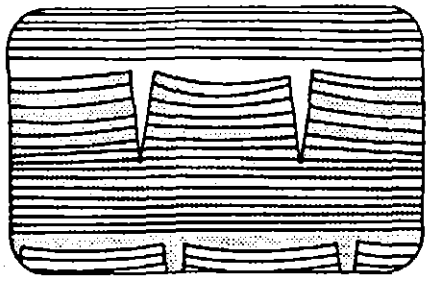


Figure 13.53 (a) Structure contours on the Ordovician Trenton Group (reservoir rock) in the Dover field, between Lakes Erie and Huron, southwestern Ontario, Canada. Contours at 20 m intervals below sea level. Note apparent synclinal structure. (b) Cross section along line A–B, to show dolomitized fracture zone creating a "pseudo-syncline." (From B. V. Sanford, Geol. Survey of Canada Paper 60-26: Fig. 10, 1961.)

effects on skeletal remains. Aragonite is much more easily dolomitized than is calcite, so shells of gastropods, cephalopods, and corals are dolomitized earlier than those of brachiopods, ostracodes, or echinoids. Well sorted crinoidal or shelly limestones are less dolomitized than surrounding rocks which contain less coarse material and more cement. Calcareous algae are easily dolomitized because high-magnesium calcite is deposited on them during their lives, and the algae themselves reduce sulfate which would otherwise inhibit dolomitization (especially of calcite). The vast mats of algae in the shallow epicontinental seas of the great Paleozoic transgressions are undoubtedly a factor in the prevalence of Paleozoic dolomites. There is very little dolomite in the stratigraphic record since the early Cretaceous, especially in the Northern Hemisphere. This may be because the present oceans, originating at that time, have a distribution and orientation different from those of earlier oceans, and epicontinental seas in low latitudes are highly restricted.

Appendix B

364108



16. Peritidal Carbonates

Brian R. Pratt, Department of Geological Sciences, University of Saskatchewan, Saskatoon, Saskatchewan S7N 0W0

Noel P. James and Clinton A. Cowan, Department of Geological Sciences, Queen's University, Kingston, Ontario K7L 3N6

INTRODUCTION

Limestones and dolostones composed of calcareous sediment deposited in very shallow seawater and on muddy tidal flats are probably the most conspicuous carbonate facies in the rock record (Fig. 1). The term *peritidal* (from the Greek *peri*, meaning around or near, and tidal, relating to tides) was coined in passing by Folk (1973) and has proven a useful general name for the spectrum of nearshore and shoreline depositional environments and facies.

What distinguishes these rocks is their wide variety of features that can be compared directly with modern analogues, making them both easy to recognize in the field and important paleobathymetric indicators. The facies are generally arranged vertically in a *shallowing-upward sequence* (James, 1984), now referred to as a *shallowing-upward succession*, in which marine sediments are overlain successively by muddy carbonates deposited in paleoenvironments subject to varying periods of exposure. This vertical stacking of peritidal and related facies is a valuable record of the dynamics of carbonate platform development, on both large and small scales. It hints at extrinsic factors such as relative sea level change and climate, and records the effect on periodically exposed sediment of biotic evolution through geologic time. Peritidal carbonates are also economically important because they host Pb and Zn deposits and frequently form hydrocarbon reservoirs.

In this chapter, we first summarize the tidal flat environment from a Recent standpoint. We then discuss how the record of carbonate tidal flats may have changed through time in response to biological evolution and provide ancient examples of commonly encountered peritidal facies, with evidence for their interpretation. Finally, we outline how peritidal facies are preserved in the stratigraphic record, describe current hypotheses used to explain stratigraphic repetition and suggest how these facies can best be used in sequence stratigraphic analysis.



Figure 1 Panorama of Cambrian shallow water limestones and dolostones, Dezaiko Range, east-central British Columbia. Distinctive "stripy" bedding of lower unit, to the right of the small ice field, is from peritidal facies of the Snake Indian Formation. The unit in the middle of the photograph is the Eldon Formation, consisting of locally dolomitized subtidal limestones, and the left side comprises peritidal limestones of the Lynx Group.

THE PERITIDAL ENVIRONMENT

The understanding of tidal flat carbonate rocks underwent a dramatic boost with the largely petroleum company-funded research on Holocene tidal flats during the 1950s and 1960s. This produced comprehensive studies on shallow water sedimentation of south Florida (Ginsburg, 1956; Gebelein, 1977; Enos and Perkins, 1979), Andros Island of the northern Bahamas (Hardie, 1977), Belize (Wantland and Pusey, 1975), the Arabian (Persian) Gulf (Purser, 1973), and Shark Bay, Western Australia (Logan *et al.*, 1970, 1974). Observations from these areas were quickly applied to ancient examples (e.g., Beales, 1958; Roehl, 1967; Matter, 1967; Laporte, 1967; Ginsburg, 1975; Schwarz, 1975), which ushered in the modern era of carbonate sedimentological thinking. These Holocene examples, together with more recently studied flats in the Caicos Islands (Wanless *et al.*, 1988) and southern Australia (Burne and Colwell, 1982; Belperio *et al.*, 1988) are fundamental reference points for the interpretation of carbonate rocks and illustrate the wide variety of potentially preservable peritidal environments. The carbonate tidal flat is an easily accessible area and students are encouraged to explore for themselves a modern example.

Three bathymetric zones are recognized in the nearshore setting: subtidal, intertidal and supratidal (Fig. 2).

364109

The subtidal zone is permanently submerged and ranges from low-energy, lagoonal environments to higher energy shoals. Semimonthly neap tides may briefly expose the shallowest portions. The intertidal, or littoral, zone lies between normal low- and high-tide levels and is therefore submerged on a diurnal or semidiurnal basis. It is generally dissected by subtidal creeks and dotted with brackish or saline ponds. The supratidal zone is above normal high tide, and is flooded only during storms and semimonthly spring tides. It may become evaporitic in semiarid and arid climates, and for these supratidal flats the Arabic word *sabkha* has been adopted by sedimentologists (Chapter 19).

The three-fold environmental subdivision is only an approximation, however, since tidal flats are often geographically complex, and tidal range can be modified by winds. While the environments are due to the variable submergence and emergence brought about by lunar tides, little sediment is transported onto the flats by the daily rise and fall in sea level. It is storms, which stir up the adjacent offshore sediments and drive sediment-laden waters up the tidal creeks and onto the flats, that result in sediment deposition. Even so, it is still the depositional environments, which are generated by daily lunar tides, that contain the distinctive sedimentary features that allow us to pinpoint facies so precisely. One approach to the analysis of environmental subdivision is to assign a specific, quantitative "exposure index" to lithologic features based on Holocene examples (see Hardie, 1977), but few ancient deposits have been described in this way (Smosna and Warshauer, 1981).

Marine coastlines can be separated into microtidal (<2 m), mesotidal (2-4 m) and macrotidal (>4 m) settings. Tidal range depends on basin shape and water depth. Strong tidal currents are generated when water is forced through relatively narrow straits or mouths of bays or over shallow shoals. Modern peritidal carbonate environments are exclusively microtidal. There is as yet no satisfactory way of judging ancient tidal range, but the scarcity of sedimentary structures formed by strong tidal currents suggests that most ancient carbonate peritidal settings were also microtidal.

Where do they form?

Carbonate sediment, generated mostly in the subtidal zone (the *carbonate factory*), can be subsequently transported and molded into tidal flats by physical processes. In this sense, tidal flats are repositories of allochthonous sediment, and accrete as wedges along shorelines (e.g., Qatar, Shark Bay, Spencer Gulf), in the lee of rocky islands (e.g., northern Bahamas, Caicos, Belize), spits (e.g., Florida) and reefs and shoals (e.g., Trucial Coast), and as discrete islands and banks in shallow seas (Fig. 3). This last setting is inferred from ancient examples because modern shelves are comparatively narrow and not directly analogous to the broad epeiric seas that were common in the past.

For muddy tidal flats to form they must be protected from open ocean swells and such protection can be provided by a platform rim or in the case of a ramp or unrimmed platform, by nearshore carbonate sand shoals (Fig. 4). Muddy tidal flats do not, therefore, generally occur in the facies spectrum of high-energy, unrimmed platforms, except behind nearshore shoals or islands.

Holocene carbonate tidal flat environments

Shallow subtidal and lower intertidal

The shallow seafloor oceanward of modern tidal flats is generally a bio-

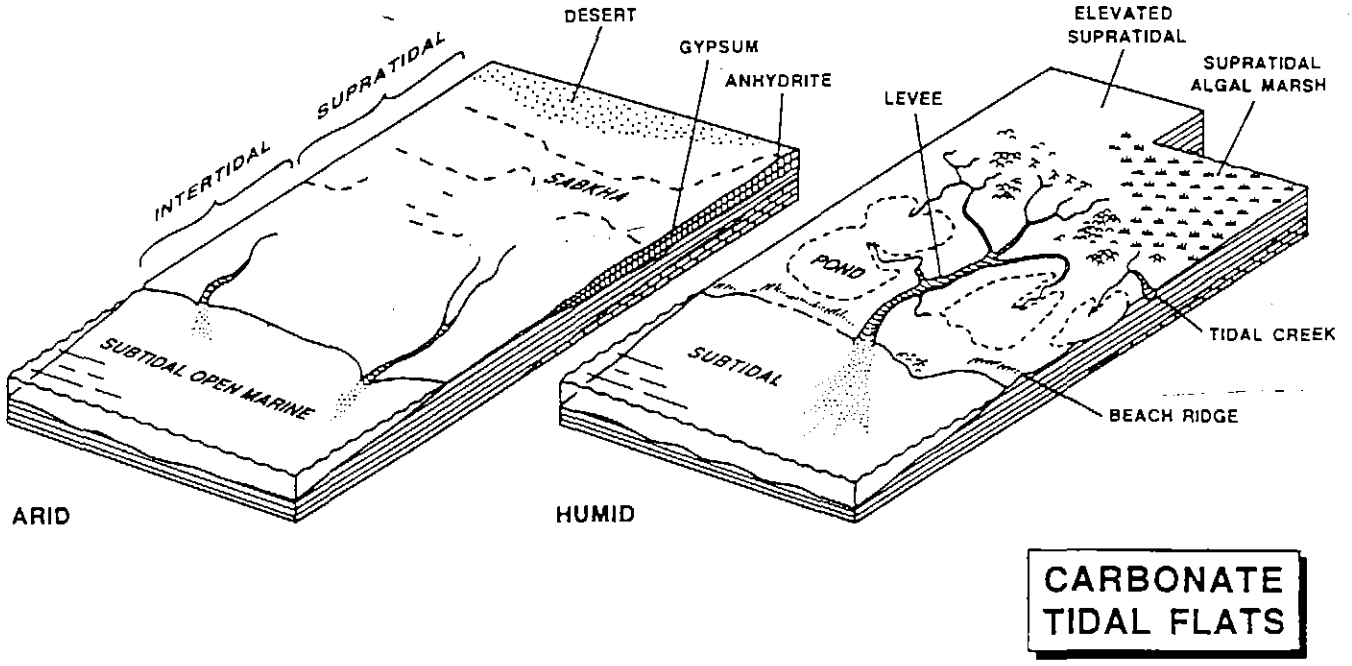


Figure 2 Block diagram showing the main morphological elements of a carbonate tidal flat. Left: a hypersaline tidal flat with few channels bordering a desert and developing evaporite deposits (based on modern Persian [Arabian] Gulf). Right: normal-marine tidal flat with many creeks, or channels, and ponds in a humid to sub-humid setting (based on modern Bahamas).

364110

turbated and pelleted lime mud variably rich in shelly material from benthic oganisms, and commonly supports a cover of sediment-stabilizing sea grasses (Chapter 15). Protective low-relief banks of cross-stratified oolitic or bioclastic sand are present in some higher-energy nearshore areas where wave agitation is frequent.

In tranquil settings of normal salinity, the lowermost intertidal zone tends also to be a thoroughly bioturbated mixture of lime mud, pellets and bioclasts. This sediment is usually covered during low tide with an ephemeral microbial ("algal") slick that is the source of food for grazing organisms such as gastropods and worms. Crabs, shrimps, worms and fish are responsible for the bioturbation in the underlying sediment. Many low-energy flats are fronted by beaches of bioclastic sand winnowed from creeks and ponds or the adjacent seafloor during storms. Beach sands can be partially lithified by synsedimentary cement composed of aragonite fibres or bladed and micritic high-Mg calcite, forming gently seaward-dipping layers of beachrock. Beachrock tends to be crumbly and easily eroded, and supports a hard-substrate biota of encrusting and boring invertebrates, plants and microbes.

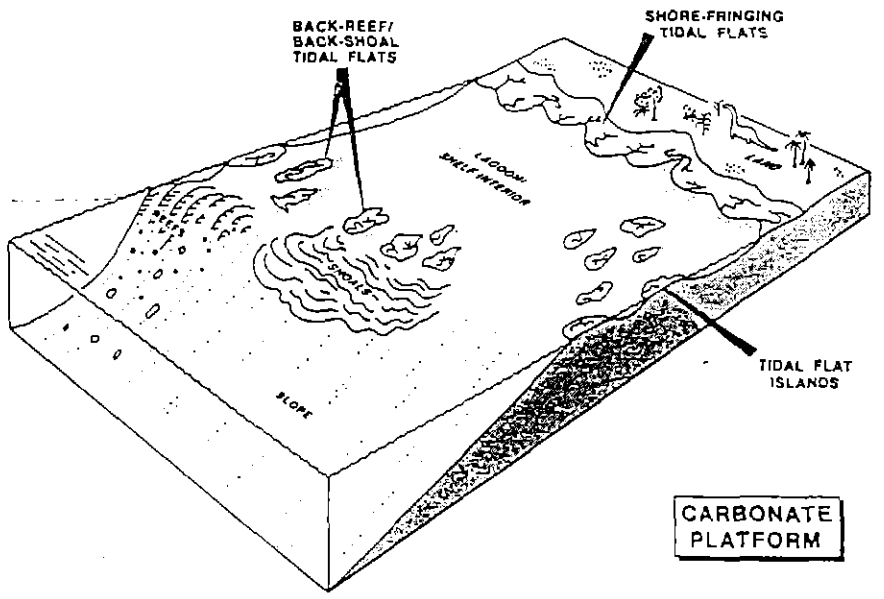


Figure 3 Block diagram of a carbonate platform, with basinward to left and landward to right, showing possible locations of tidal flats: in the lee of reefs and carbonate sand shoals, as islands, and as shoreline deposits.

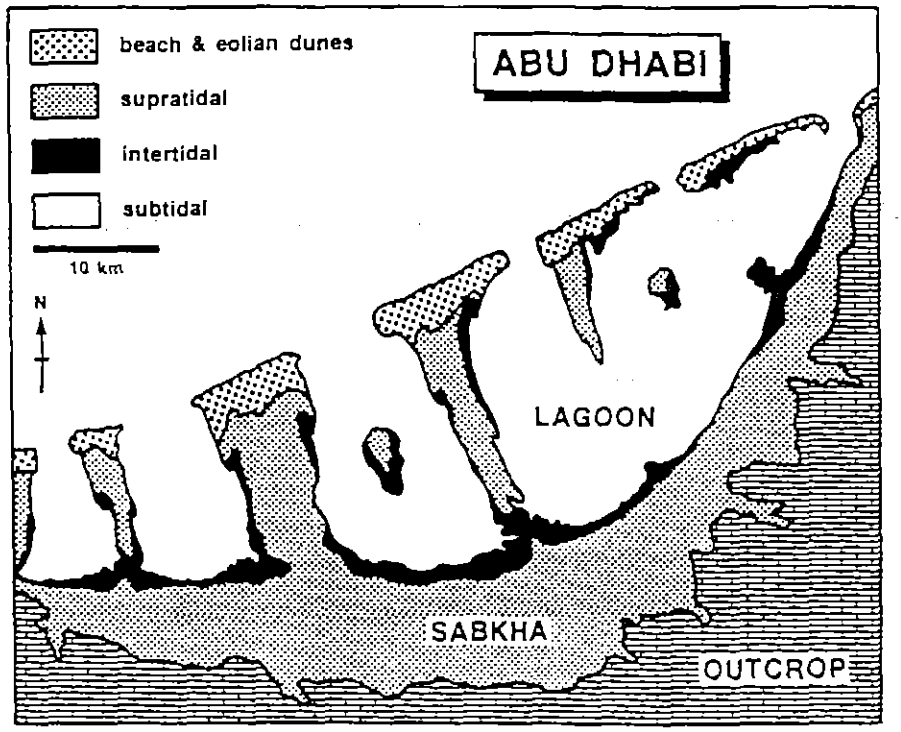


Figure 4 Simplified map of modern tidal flat areas near Abu Dhabi, Persian (Arabian) Gulf; based on Purser (1973).

Intertidal flats

Higher in the intertidal zone, microbial mat cover is more permanent, and forms thick, leathery carpets that can be locally shrunken, torn and folded over (Fig. 5). These exhibit various surface features such as pustules, blisters, wrinkles, crenulations or small, domical stromatolites. These mats are composed of a variety of filamentous and coccoid cyanobacteria ("blue-green algae") and bacteria, and are responsible for the millimetre-scale lamination exhibited by most of the sediment beneath them. The taxonomic makeup and surface appearance of such mats varies with degree of subaerial exposure and can be reflected in the microscopic nature of the underlying lamination. This type of lamination was called "algal" or "cryptalgal" before geologists became familiar with the detailed biological nature of the mats; "microbial" seems now to be the preferred adjective.

Ponds and creeks

Ponds containing brackish or hypersaline water are a common feature of the intertidal zone (Fig. 6), especially in more humid climates. These contain a restricted biota of microbial mats, foraminifera, gastropods, small bivalves, shrimps, ostracodes, and nematode and polychaete worms that is adapted to fluctuating salinity. This assemblage, living in a stressed environment, is typically one of high numbers of individuals but low species diversity, different from the immediate offshore

364111

biota. Copses of mangroves are usually present, except in the most arid areas. Also characteristic of the intertidal zone are permanently submerged tidal creeks or channels that are the conduits for tidal flooding and draining (Fig. 6). Such tidal creeks (least common in arid settings) are up to several metres deep and tens of metres wide, and contain a basal lag of semilithified intraclasts eroded from the surrounding flats and flanking levees, and bars of bioclastic sand winnowed from the ponds. Supratidal levees protrude above high-tide level and are microbially laminated. Creeks migrate laterally, as they do in siliciclastic tidal flats, and leave behind a vertical succession of cross-stratified, intraclastic and bioclastic sand overlain in turn by bioturbated bioclastic and peloidal lime mud and microbially laminated sediment. The amount of lateral migration of creeks and the proportion of the internal facies mosaic of intertidal flats that is generated by such migration are not well understood, but studies of modern flats suggest that it may be considerable (Hardie, 1977).

Supratidal flats

Most of the sediment surface in the upper intertidal and supratidal zones is covered by microbial mats that are typically shrunken into desiccation polygons and commonly dislodged into chips or intraclasts. The laminated sediment beneath these mats is generally fine grained with occasional coarser intercalations that reflect deposition by exceptional storms and, in some regions, by winds blowing off the neighbouring land surface. Beds and nodules of anhydrite precipitate in these sediments in arid settings (Chapter 19). In many areas, the supratidal zone is the locus of widespread synsedimentary cementation by microcrystalline aragonite, high-Mg calcite, or dolomite. This forms lithified pavements a few centimetres thick that are usually broken into intraclasts by forces exerted during crystal growth, groundwater pore pressure, or the roots of halophytic (salt-tolerant) plants such as grasses and mangroves. Evaporating sea spray can be responsible in some arid areas for fans and isopachous layers of fibrous aragonite that encrust stable substrates such as beachrock and shells, forming objects termed coniatolites.

Landward parts of the supratidal zone grade into eolian deposits, soils or freshwater marshes and lakes, or onlap bedrock surfaces, depending on the region's geography and climate. Marshes and lakes, which exist in the more humid areas and have fluctuating water chemistry, are characterized by microbial mats and stromatolites; these are partially lithified by high-Mg calcite cement and calcification of organic substrates, and are interbedded with thin-bedded, locally bioturbated lime mud and bioclastic and peloidal carbonate sand deposited during storms. Much of the microbially laminated sediment shows fenestral fabric, i.e., the presence of millimetre-



Figure 5 Upper intertidal microbial mat mainly composed of filamentous cyanobacteria *(Microcoleus)* that has shrunken into desiccation polygons. Boca Jewfish, Bonaire; trowel is about 25 cm long.



Figure 6 Oblique aerial photograph of the tidal flats on the northeast coast of Andros Island, Bahamas, looking north. Offshore subtidal is to the left. The white areas along the channel edges are supratidal levees. The dark patches are intertidal microbial flats between the levees and around the periphery of the mainly subtidal ponds. The field of view is about 3 km across

364112

to centimetre-sized subhorizontal, sheet-like pores formed as voids bridged by microbial mats or as molds of degraded mats. Decimetre-scale tepee structures (Fig. 7), consisting of disrupted and overthrust crusts of lithified, tufa-like fenestral sediment giving an inverted V-shaped cross section, form in areas of groundwater discharge (Kendall and Warren, 1987). These also contain complex generations of internal sediment and aragonite and high-Mg calcite cements.

Geological evolution of peritidal facies

Biological and environmental developments through geologic time have exerted an important influence on the nature of carbonate tidal flats. This is manifest in several ways, via 1) the increase in diversity of carbonate-secreting organisms and consequent change in sediment type, 2) the evolution of bioturbating and herbivorous invertebrates, and 3) the evolution of angiosperms.

The subtidal carbonate factory was in its infancy during Precambrian time, when $CaCO_3$ was extracted from seawater by inorganic and microbial processes only. Peritidal strata during this phase in Earth's history are composed of ooids, intraclasts, stromatolites, supratidal tufas, and variable amounts of lime mud. Some subtidal units are entirely siliciclastic, and large-scale cyclicity of alternating calcareous and noncalcareous facies (e.g., Grotzinger, 1986; Bertrand-Sarfati and Moussine-Pouchkine, 1988) may have involved basin-wide, or greater, changes in carbonate saturation of seawater. The dramatic increase in skeleton-secreting and sediment-ingesting invertebrates beginning in Cambrian time meant that the carbonate factory changed in character and increased its output manyfold. New types of sedimentary particles appeared, in the form of abundant shells, fecal pellets, and carbonate mud from the breakdown of fragile skeletons and other biologically influenced precipitates. This no doubt changed the nature of tidal flats by causing increased mobility of the substrate, making it less and less likely to be cemented quickly or encrusted by stromatolite-forming microbial mats except in hypersaline areas (Pratt, 1982). It has been commonly held (Garrett, 1970) that grazing invertebrates such as gastropods caused intertidal stromatolites to become scarce after the Proterozoic, but the above sedimentary reasons rather than ecologic pressure seem likely to have been responsible for this decline.

Proterozoic tidal flat carbonates are distinctive too because, in comparison with other Precambrian carbonate facies and younger sediments, they were the preferred sites of diagenetic silica precipitation and formation of chert nodules (Maliva *et al.*, 1989). These cherts are important because they host the bulk of the Precambrian fossil record (Knoll *et al.*, 1991).

Bioturbation became a sediment-

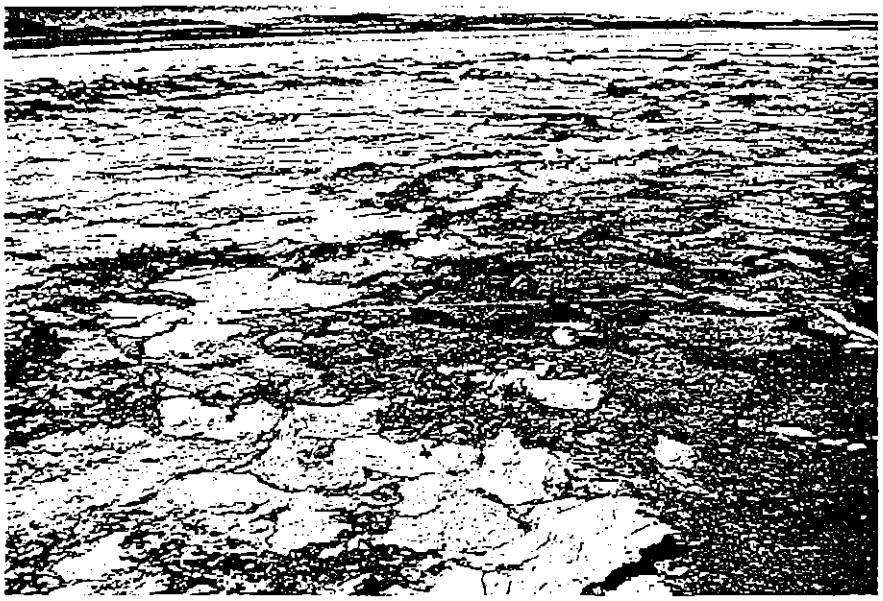


Figure 7 The supratidal flat at Fisherman Bay, Spencer Gulf, southern Australia. The polygonal crusts are lithified and have been thrust into teepees by episodic groundwater resurgence. Crusts in the foreground are roughly 30 cm across.

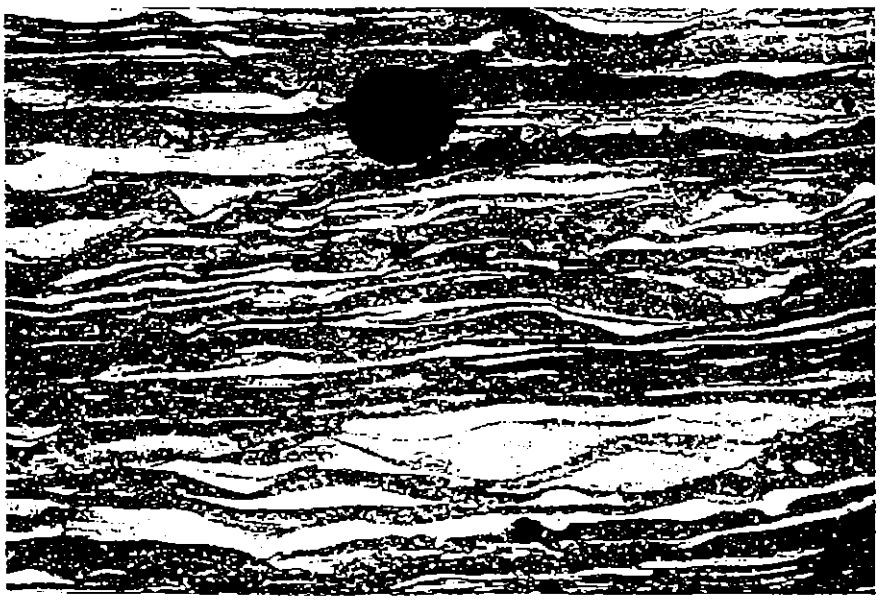


Figure 8 Outcrop of lenticular and wavy beds of wave-rippled peloidal grainstone (light coloured) in argillaceous dolostone (dark coloured), probably deposited in the lower intertidal zone. Petit Jardin Formation (Upper Cambrian), Port-au-Port Peninsula, western Newfoundland; lens cap is 6 cm across.

364113

modifying process in Late Proterozoic time. Diversification of microbes, especially those involved in the breakdown of organic material, must have occurred in tandem with invertebrate diversification and the resulting appearance of new organic substances. The organic content and therefore the geotechnical properties of tidal flat sediments surely changed in the early Paleozoic. The effect of bioturbation seems to have increased dramatically after the late Paleozoic or earliest Mesozoic (Thayer, 1983; Bottjer and Ausich, 1986; Pratt, 1991). This was heralded by the evolution of a more diverse fauna including animals, such as certain shrimps and crabs, capable of burrowing as deeply as 1 m. Consequently, tidal bedding that would have been preserved in the Precambrian and early Paleozoic was commonly destroyed by infaunal activity, except in the upper intertidal and supratidal zones. Furthermore, intertidal to supratidal sedimentary and organosedimentary structures that escaped destruction were often subsequently bioturbated when buried by subtidal or lower intertidal sediments with an active deeply burrowing infauna.

Evolution of angiosperms since Cretaceous time has meant that the disruption of tidal flat sediments by halophytic plants has become a characteristic of Cenozoic deposits. In addition, shallow subtidal sea bottoms are especially well stabilized by the rhizomes (roots) of angiosperm sea grasses *(Thalassia, Posidonia, Cymodocea)*. Such grasses also support a prolific encrusting biota that supplies fine-grained carbonate sediment to the factory. These carpets of sea grasses, however, are disrupted only by intense storms, causing "blowouts" (Wanless, 1981), and we suggest that pre-Cenozoic subtidal sediments, especially silt- and sand-sized particles, might have been more readily moved onto tidal flats than they are now, because they were not bound by these grasses. This is analogous to the suggestion that the post-Devonian presence of widespread terrestrial plant cover, with its stabilizing, soil-forming and weathering attributes, affected the subaerial sedimentary system of the Earth. It may partly explain why some early Paleozoic intertidal carbonates look so much like siliciclastic counterparts from settings that lack significant seagrass communities.

Ancient peritidal carbonate facies

Environmental interpretation of peritidal limestones and dolostones is easily achieved in the broad sense, especially when they contain features unequivocally of subaerial origin. However, some facies cannot be assigned confidently to a bathymetric position, and for these Walther's Law must be invoked. Furthermore, tidal processes involve such a variety of energy regimes, sediment sizes and climates that there may be a limit as to

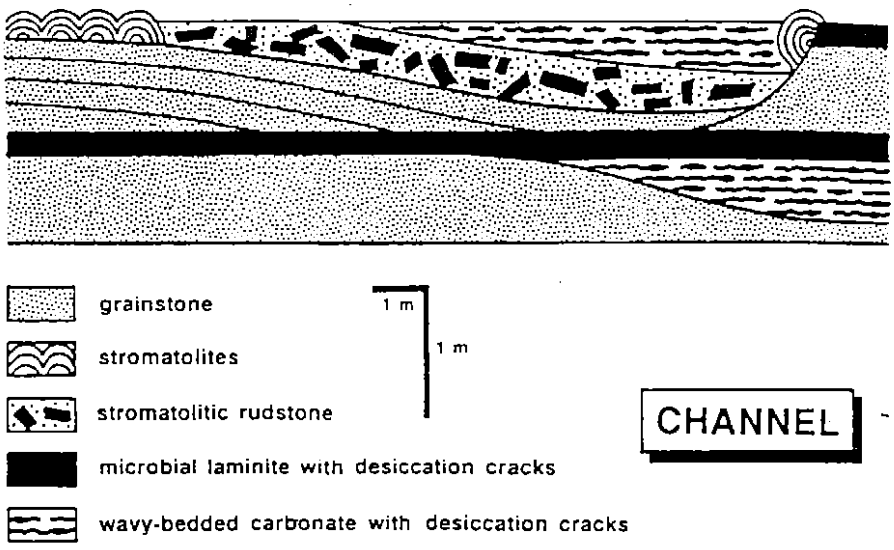


Figure 9 Simplified outcrop sketch of hypothetical channel or creek deposits cut into tidal flat facies, based on examples from the Waterfowl Formation (Upper Cambrian, Rocky Mountains, Alberta; Waters *et al.*, 1989) and Elbrook-Conococheague Formations (Middle and Upper Cambrian, Virginia; Koerschner and Read, 1989).

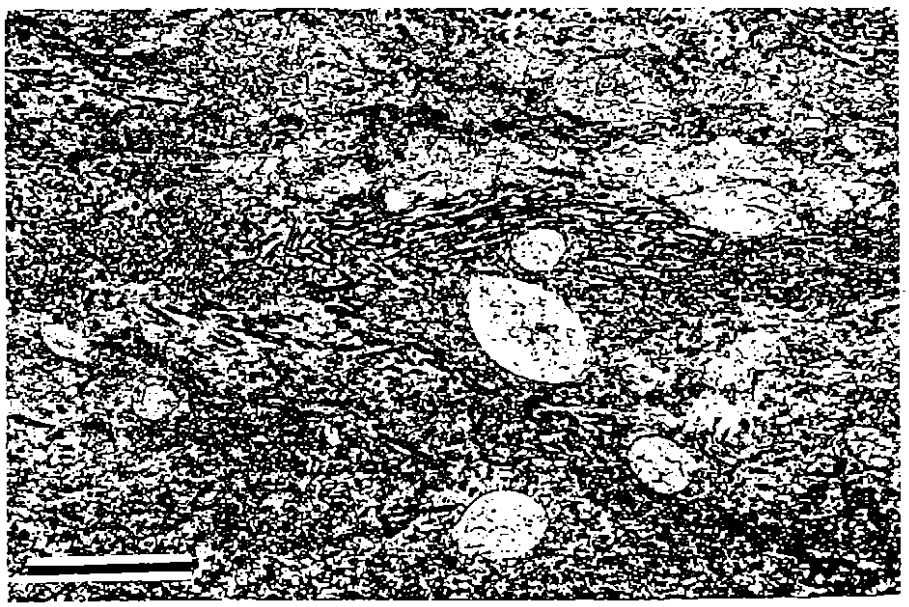


Figure 10 Thin section photomicrograph of limestone composed of loosely packed micrite, micrite peloids, articulated ostracode valves, and calcimicrobe *(Girvanella)* filaments with organic-rich walls. This sediment is interpreted to have been deposited in a tidal flat pond because of the low-diversity biota and the calcification of filamentous cyanobacterial thalli. Table Point Formation (Middle Ordovician), Port-au-Port Peninsula, western Newfoundland; scale bar is 1 mm.

364114

how precise an interpretation one can make. The present level of detail is generally at the scale of units decametres to metres in thickness; few studies have gone down to the scale of individual beds and laminae.

Shallow subtidal and lowermost intertidal facies

Precambrian subtidal rocks are the most difficult to recognize, because the carbonate was produced by inorganic or microbially mediated precipitation, and there were no distinctive skeleton-secreting organisms. Such subtidal facies tend to be variably siliciclastic, or frequently dolomitized lime mudstone with local oolitic, peloidal or intraclastic beds. Nearshore limestones of Phanerozoic age are fossiliferous, commonly bioturbated to some degree, and may exhibit patch reefs and oolites. Units of thinly interbedded bioturbated lime mudstone and wackestone and ripple or dune cross-laminated grainstone that are overlain by rocks exhibiting clearly supratidal facies are typical. Subtidal and lower intertidal carbonates of Mesozoic and Cenozoic age are commonly thick bedded and totally bioturbated, reflecting the post-Paleozoic increase in the diversity and effect of the bioturbating fauna.

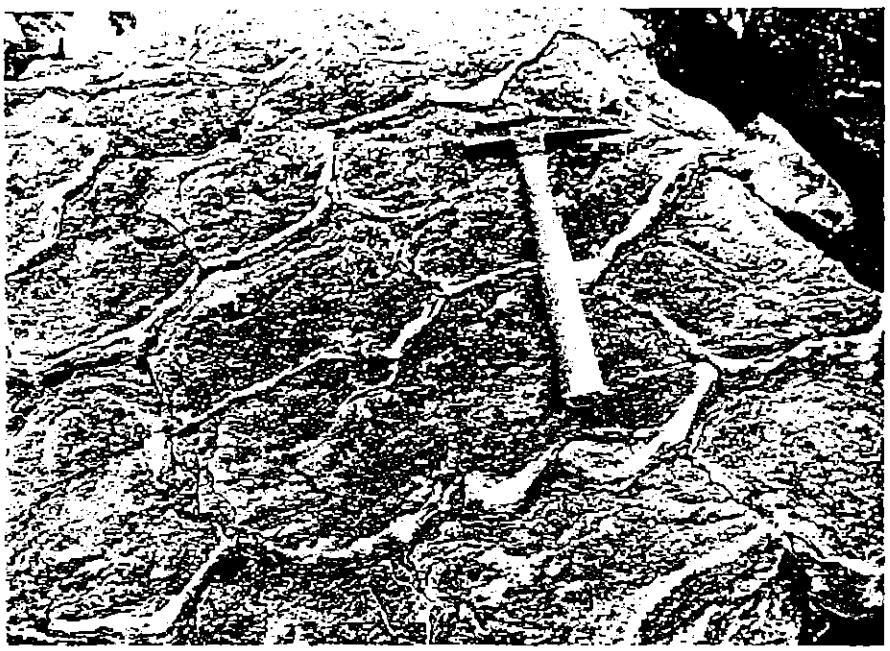


Figure 11 A bedding plane of desiccation-cracked polygons in which the edges of each polygon are curled up, probably because the original microbial mats shrivelled upon exposure. East Arm Formation, Upper Cambrian, Bonne Bay, western Newfoundland; hammer is 30 cm long.

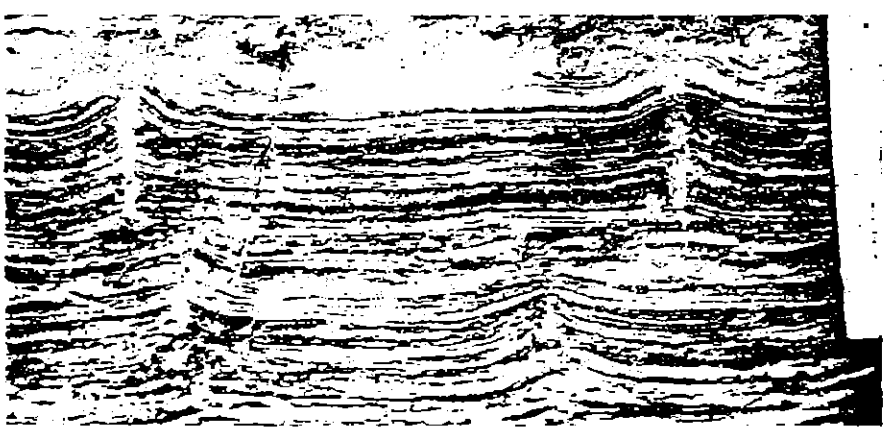


Figure 12 A cross section of desiccation cracks in microbially laminated peritidal dolostones; Providence Island Dolomite, Middle Ordovician, Lake Champlain, New York State.

Intertidal flat facies

Wavy-, lenticular- and flaser-bedded peloidal lime mudstone or grainstone (calcisiltite) and dolomitized argillaceous lime mudstone (sometimes interbedded with small hemispheroidal stromatolites), arising from the alternation between slack water and sediment transport by both unidirectional currents and waves under lower flow regime, are particularly distinctive of Precambrian and lower Paleozoic sequences (Fig. 8). This facies is directly comparable to the tidal bedding in siliciclastic peritidal deposits, including those forming in many modern settings (see Reineck and Singh, 1980). The carbonate strata, however, commonly contain intraclastic horizons which are absent in siliciclastic counterparts. Phanerozoic intertidal facies frequently have bioclastic layers. Well-sorted coquinas were likely washed in from the subtidal zone by storms, whereas poorly sorted shelly deposits containing a low-diversity assemblage of gastropods or bivalves probably represent the in situ intertidal fauna. Laminae that appear laterally continuous, undulating and uniform in thickness, are typically intercalated in this facies, and record periods of stabilization or binding of the substrate by a microbial mat. This tidal bedding can be burrowed in Phanerozoic sequences, and in the lower Paleozoic the trace fossil fauna is dominated by a low-diversity assemblage of horizontal burrows and U-shaped forms like *Arenicolites* and *Diplocraterion*. As with subtidal deposits, post-Paleozoic intertidal sediments are likely to be thoroughly churned: bioturbated, poorly fossiliferous lime mudstone units may be interpreted as intertidal if other criteria, such as vertically juxtaposed beds with desiccation cracks, are evident.

Tidal creek facies

Rocks specifically interpreted as having accumulated in tidal creeks or channels piercing intertidal flats are relatively uncommon. The reasons for this are mainly 1) the rarity of laterally

364115

extensive exposures that intersect the possible margins of channels once they stop migrating laterally, 2) the difficulty in distinguishing creek fills from regressive packages with a basal, higher-energy component that resulted from tidal flat progradation, 3) the similarity between bedforms and lateral-accretion bedding from bar migration in channels and inclined and tabular cross stratification from migrating offshore carbonate sand shoals, and 4) the difficulty in separating creeks in tidal flats from channels between adjacent offshore islands or shoals. The presence of flat-pebble and blocky intraclasts derived from the surrounding flats and levees, respectively, along with bipolar (herringbone) cross stratification typically exhibiting reactivation surfaces and *tidal bundles* (couplets of sandy and muddy laminae), seem to be diagnostic of creek or channel deposits (e.g., Pratt and James, 1986). Grainstone beds with erosional bases and containing stromatolite or thrombolite mounds in some Proterozoic and Cambrian sequences are reasonably interpreted as channel deposits, (Koerschner and Read, 1989; Wright *et al.*, 1990). Waters *et al.* (1989) and Cloyd *et al.* (1990) have mapped Cambrian channels at least 10 m wide and 1 m deep with erosional bases, filled with lateral-accretion beds of individually graded, locally bipolar cross-laminated grainstone containing desiccation-cracked lime mud drapes and reactivation surfaces (Fig. 9). Care must be taken in late Proterozoic and early Paleozoic carbonates, however, to differentiate subaerial (desiccation) cracks and other cracks of submarine origin (Knoll and Swett, 1990; Cowan and James, 1992).

Beach facies

Beaches, which also have not been reported frequently from ancient tidal flat sequences, are characterized by seaward-dipping, low-angle laminae and thin beds of grainstone, often with hardgrounds exhibiting bored surfaces. This facies passes laterally to subtidal deposits in the seaward direction and tidal-bedded strata in the landward direction (e.g., Inden and Moore, 1983; Waters *et al.*, 1989). Steeper shorelines, such as Tertiary and Quaternary examples from the Mediterranean and Red seas, are often onlapped by gravelly beds of well-rounded pebbles and large shells.

Pond facies

Recognition of schizohaline pond deposits on humid intertidal flats may be impossible in most rock sequences unless the ponds were particularly long-lived. In one example (Pratt, 1979), burrowed wackestone containing ostracodes and horizontal meshes of *Girvanella* filaments with organic-rich walls (Fig. 10) are intercalated within burrowed and microbially laminated lime mudstone and tidal-bedded dolostone and lime mudstone. The restricted biota of this deposit, the well-preserved microbial remains, and its lenticular geometry within a peritidal sequence argue against a normal-marine subtidal environment.

Supratidal facies

Microbially laminated limestone or dolostone, usually with desiccation cracks and coarser rippled layers, is a common peritidal rock type (Figs. 11, 12); such rocks, however, may be



Figure 13 Polished slab of clotted and peloidal lime mudstone showing microbial lamination and fenestral fabric of laminoid, millimetre- to centimetre-sized, cement-filled pores. This distinctive fabric probably formed in the upper intertidal or lower supratidal zone. Eldon Formation (Middle Cambrian), Exshaw, Alberta; scale bar is 1 cm.



Figure 14 Thin section photomicrograph of peloidal and clotted micrite containing bioclasts (mainly ostracodes and gastropods) and exhibiting fenestral fabric. Upper parts of the laminoid fenestral pores have pendant fringes of fibrous calcite cement (grey coloured) suggesting that this sediment was deposited in the upper intertidal zone and that the fibrous calcite precipitated as marine or mixed waters percolated through the pores during low tides. Table Point Formation (Middle Ordovician), western Newfoundland; scale bar is 1 mm.

364116

upper intertidal or supratidal in origin. In older Phanerozoic sequences, a supratidal setting might be inferred if bioturbation is rare or absent, or there is evidence for prolonged subaerial exposure such as evaporites, karst horizons or paleosols. Intercalated within many microbially laminated rocks are intraclastic horizons, which are analogous to pavements of microbial mat chips or fragments of cemented crusts in modern supratidal environments. Fenestral lime mudstone and peloidal grainstone (Fig. 13) are common (Shinn, 1983b) and, by analogy with tidal flats of Florida and the Bahamas, were probably deposited in moist supratidal "algal marshes" or around ponds. This facies sometimes exhibits features, such as pendant fibrous cement (Fig. 14), brecciated crusts and tepees, pisolites and pores with geopetal sediment floors, suggestive of flushing by downward-percolating seawater and rainwater and upward-flushing by groundwaters in a subaerial environment. Precambrian supratidal deposits often contain digitate stromatolites, millimetres to centimetres in diameter, which have been interpreted as supratidal, tufa-like aragonite precipitates (e.g., Grotzinger, 1986). Post-depositional leaching of evaporites causes collapse brecciation in supratidal facies.

THE PERITIDAL SHALLOWING-UPWARD SUCCESSION

Ancient peritidal carbonate lithofacies are characteristically organized stratigraphically into metre- to decametre-thick, shallowing-upward successions (Fig. 15) each with a basal subtidal unit, intermediate intertidal facies, and an upper supratidal unit with or without a terrestrial horizon on the top (James, 1984; Wright, 1984; Tucker and Wright, 1990). Contacts between the members are gradational or sharp and may show evidence of local synsedimentary scour. Walther's Law tells us that, if there are no major depositional breaks, we can reconstruct the ancient environmental mosaic by dealing out each facies like a deck of cards. There are departures from this ideal pattern, however, and it is not unusual to find the supratidal member overlain by intertidal facies, or components missing because of nondeposition or erosion.

Characteristics

The lithologic nature of the subtidal → intertidal → supratidal succession is variable, reflecting the broad spectrum of intertidal and supratidal depositional environments, the dictates of biotic evolution and past changes in ocean chemistry. Such peritidal shallowing-upward successions can be subdivided into two types, low energy (Figs. 16, 17) and high energy (beach; Fig. 18) , and both may show the effects of climate, such as thin beds of evaporites, especially anhydrite (Chapter 19).

In the simplest case, and referring only to the Phanerozoic, low-energy shallowing-upward successions have a burrow-mottled, variably argillaceous lime mudstone to wackestone or packstone lowest member, often with a basal bioclastic and intraclastic grainstone or rudstone as a transgressive lag on top of the pre-existing succession (Fig. 16). Patch reefs may be present in the subtidal member. The intertidal member exhibits thin-, lenticular- and wavy-bedded, variably bioturbated lime mudstone and bioclastic, peloidal and sometimes oolitic grainstone, locally with small domical stromatolites. This grades upward to an upper intertidal and supratidal member that is usually a microbially laminated, locally desiccation-cracked, slightly argillaceous lime mudstone frequently exhibiting fenestral fabric, with thin interbeds of intraclastic horizons and laminae of peloidal or bioclastic grainstone. If the sediments were laid down in an arid climate, nodular to wavy beds of anhydrite may displace and replace sediment of the intertidal and supratidal members (Fig.16). Higher-energy cycles (Fig. 18) also have a bioturbated subtidal bioclastic basal member, but the intertidal component is made up of bioclastic and/or locally oolitic grainstones representing beach deposits. These may exhibit inclined- and cross-stratification and hardgrounds. The upper intertidal and supratidal units are generally desiccation-cracked microbial laminites.

Both kinds of shallowing-upward successions can have a capping horizon of marsh sediments, paleosol or calcrete. Successions may be separated from overlying units by a karst surface caused by subaerial weathering, or an erosion surface formed during the environmental shift responsible for the next succession. Supratidal sediments may show the diagenetic effects of groundwater dis-



Figure 15 A shallow pit excavated on the Holocene sabkha: Abu Dhabi, United Arab Emirates. The roughly 1 m of section is composed of light-hued subtidal sediment at the base, overlain in turn by conspicuous black intertidal microbial mats with desiccation cracks and light-coloured supratidal sediment and capped by eolian quartz-rich sands. Photo courtesy P. Scholle.

364117

charge, such as tepees, cements and leaching of evaporites.

A warning! Tidal creek or channel fills can look suspiciously like shallowing-upward successions produced by tidal flat progradation (Fig. 18). Predictably, they should be composed of a basal intraclastic, peloidal and bioclastic grainstone lag or bar facies, overlain by thin-bedded and bioturbated lime mudstone and wackestone, and capped by microbially laminated lime mudstone, recording waning energy conditions as the creek is abandoned (e.g., Waters *et al.*, 1989; Cloyd *et al.*, 1990). Unless a channel margin or lateral-accretion bedding is exposed, or blocky intraclasts from margin collapse are present, these deposits could easily be misunderstood.

Geometry

To interpret how any particular peritidal shallowing-upward succession may have developed there must be firm local and regional lateral control on the distribution of units; bed or event correlation must be demonstrable. Besides walking or tracing out individual beds, the lithologic features that may be widely correlatable in peritidal successions are subaerial exposure horizons (karst surfaces, collapse breccias and paleosols), evaporite beds and siliciclastic horizons resulting from sea level fall. We recognize two geometries. *Laterally continuous* metre-scale successions are widespread, possibly platform-wide, and correlatable. *Laterally discontinuous* metre-scale successions are local in extent and noncorrelatable and supratidal facies can be traced laterally into intertidal and/or subtidal facies over kilometre-scale distances.

Origin

An aspect of carbonate sedimentology that has become a maxim over the last decade, for Phanerozoic rocks at least, is that healthy carbonate platforms, i.e., those not stressed by environmental conditions like cold water, hypersalinity, turbidity or nutrient poisoning that hinder organism growth, can produce enough carbonate sediment to aggrade, and commonly a surplus, causing progradation, while relative sea level rises (Schlager, 1981). Shallow water sediments thus overlie deeper water facies. Each shallowing-upward peritidal succession records the vertical and lateral accretion of a single tidal flat to a level just exceeding high-tide mark; if there was no subsidence or sea level change, the thickness of the intertidal-supratidal component might approximate the tidal range, but if there was any relative sea level change, the thickness is no indication of this at all.

There are currently three models used to explain how a shallowing-upward succession forms 1) as a prograding wedge, 2) as a simultaneously

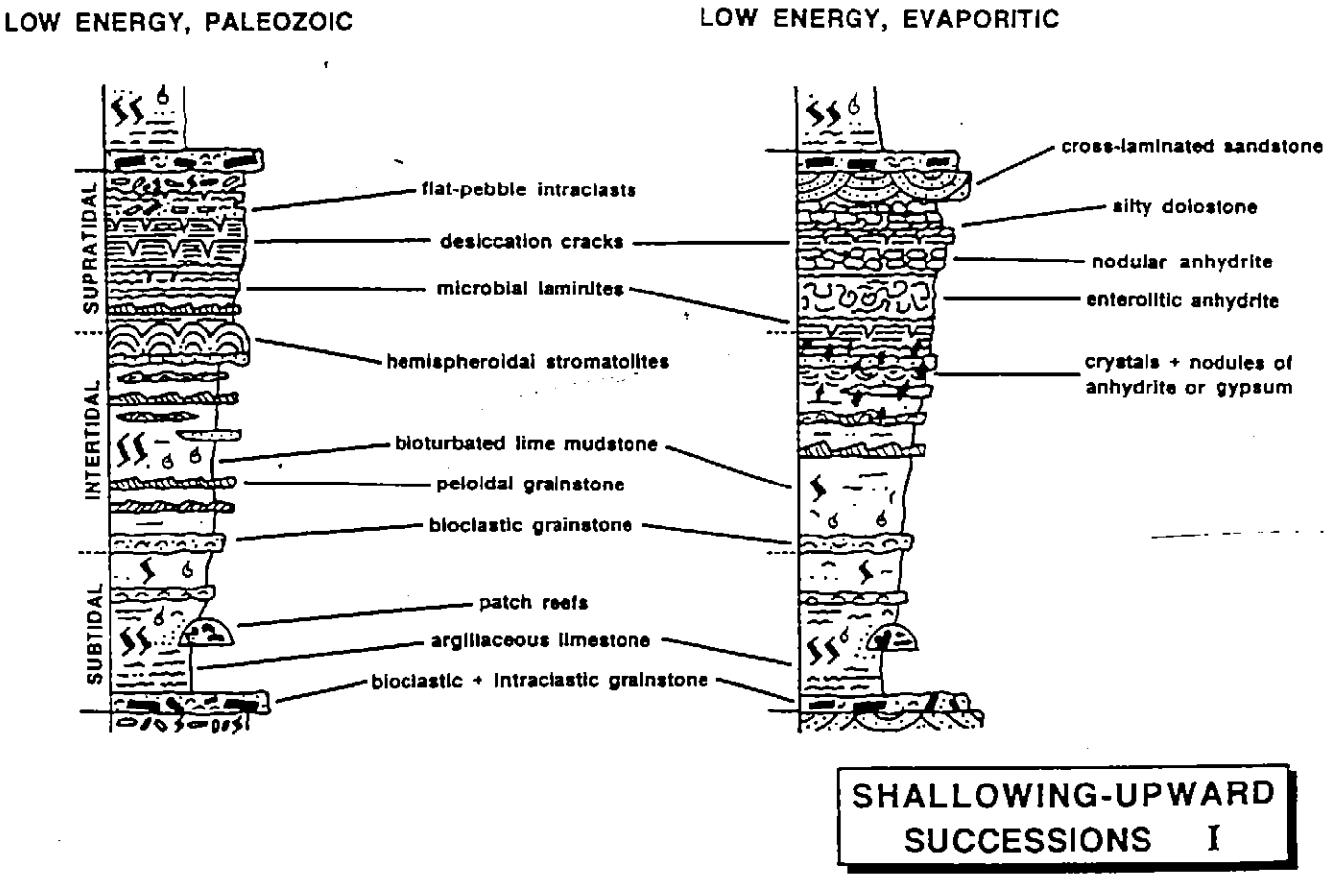


Figure 16 Hypothetical vertical profiles of individual low-energy, metre-scale, peritidal shallowing-upward successions. Left: from the lower Paleozoic; upper Paleozoic examples might exhibit calcretes at the top. Right: an evaporitic example (Chapter 19). No scale is implied, but each succession is typically 1-10 m thick.

364118

aggrading sheet or, 3) as a mosaic of tidal flat islands (Fig. 19).

The prograding wedge

Holocene shallow-marine and peritidal environments are dynamic in that they shift geographically over geologically short periods of time in response to both local and regional changes in climate, prevailing wind direction, current pattern, and sediment supply. A single coastline, for example, may possess tidal flats that are accumulating and prograding, and tidal flats that are dormant or are eroding (e.g., Shinn *et al.*, 1969; Strasser and Davaud, 1986). Regardless, to generate a single, laterally extensive wedge that has peritidal, shallowing-upward attributes throughout, the tidal flat must prograde laterally from a nucleus. Such accretion can develop seaward from land, outward from islands, or shelfward from platform margin buildups and/or shoals. It must be stressed that deposition on the tidal flat is a physical process. Sediment generated on the platform is swept onto the flats by storms producing the gradually prograding tidal flat wedge. As such, the size and dynamics of the peritidal wedge are primarily a function of the health and nature of the source area (the subtidal carbonate factory) and the way in which sediment is redistributed on the platform (i.e., how much is transported to the flats, how much stays in place, how much is transported offshore into deep water).

The Holocene record of sea level change is one of rapid rise between 11 ka and 6 ka, followed by decelerated rise from 6 ka to the present. There are, unfortunately, few tidal flats that have been cored in enough detail to provide a good three-dimensional stratigraphic picture of deposition during this period. As a result of this small data base it is difficult to make generalizations. Nevertheless, at present there appear to be two styles of progradation (Fig. 20), *simple offlap* and *staggered offlap* (Hardie and Shinn, 1986). Simple offlap is typified by the gradually prograding wedge along the southern coast of the Persian (Arabian) Gulf. Staggered offlap is characterized by the northern Bahamas tidal flats. In the latter case the tidal flat does not seem to have prograded but instead aggraded behind a protecting beach ridge. The vertical succession is mainly burrowed sediment, reflecting deposition in a variety of pond, channel and intertidal flat environments, capped by laminated upper intertidal to supratidal sediments. It is thought that tidal flat sedimentation began only when the offshore carbonate sand bar emerged to become a barrier. Once the flat aggraded to sea level, progradation took place by a series of jumps followed by back filling (Hardie, 1986). Such successions in the rock record should

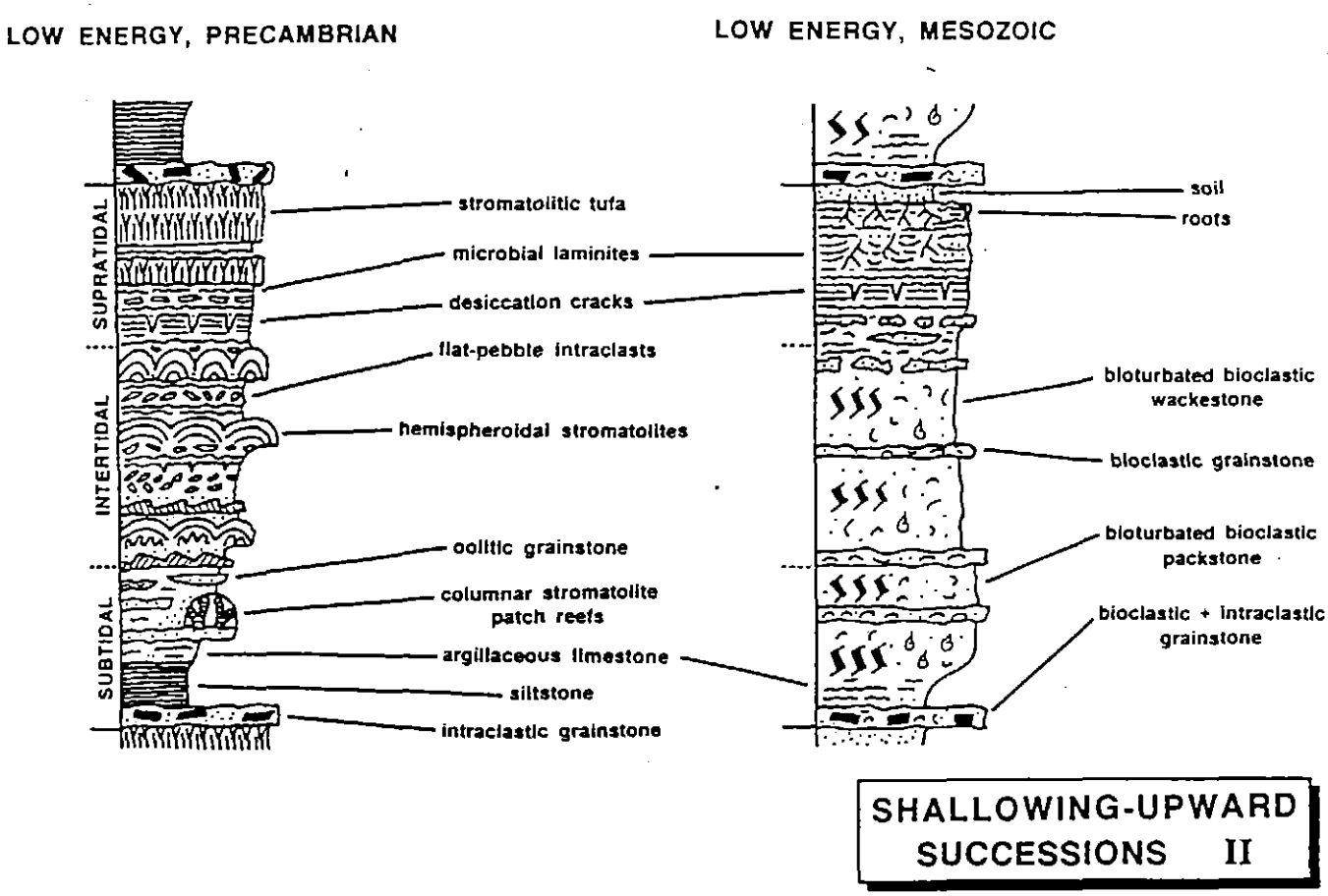


Figure 17 Hypothetical vertical profiles of individual low-energy, metre-scale, peritidal shallowing-upward successions from the Precambrian (left) and Mesozoic (right). A comparison of these with the Paleozoic example in Figure 16 shows some of the lithologic changes exerted by biotic evolution through geologic time.

364119

contain remnants of these barriers. The Abu Dhabi sabkha is reported to have buried barriers (Warren and Kendall, 1985) and may have also developed, in part, through staggered offlap.

For a wedge of tidal flat sediment to prograde from the strandline across an entire platform, accumulation of sediment must occur under relatively stable hydrographic conditions (i.e., sea level and climate) for the length of time represented by progradation. A rapid rise in sea level would flood the broad supratidal flat and halt progradation, whereas any fall in sea level would strand the tidal flat before transplatform progradation was complete.

This style of accumulation has been proposed to explain the extensive Cambro-Ordovician peritidal strata of the southern Appalachians (Hardie, 1986). Metre-scale peritidal shallowing-upward successions of this epeiric platform have been correlated (but not traced) for distances greater than 100 km parallel and perpendicular to depositional strike. Progradation at this scale, however, would produce vast areas of abandoned supratidal flats behind the prograding shoreline, far distant from the subtidal source of sediment and exposed to protracted subaerial diagenetic effects. Since constant and uniform subsidence would inundate this supratidal surface, progradation must have taken place while relative sea level was stationary or gradually falling. If progradation was simple offlap, then successions will be laterally continuous. If progradation was staggered offlap, successions will be discontinuous and separated by lenticular beach deposits.

Simultaneously aggrading sheet

In this situation, continuous in situ carbonate sediment production results in aggradation of the seafloor steadily to sea level. The entire platform becomes intertidal and then supratidal, and can be completely exposed before flooding and deposition of the next overlying succession (Fig. 19). There are no Holocene analogues for this process; it is derived entirely from interpretation of the rock record, and therefore is poorly constrained. Platform-wide peritidal exposure under these circumstances cannot be *intertidal* per se, because it is unlikely that tides could operate across such a vast horizontal distance all at once. Instead, alternating flooding and exposure would have to be induced through the movement of the sea surface by periodic storm surges or persistent winds. Such a style of *occasional* exposure and submergence may be difficult to distinguish in the rock record from true *intertidal* conditions. This hypothesis demands that at least some sediment be produced on the flats when the whole platform is in the intertidal-supratidal environment. Such accretion could predictably produce platform-wide, laterally continuous, metre-thick shallowing-upward successions, such

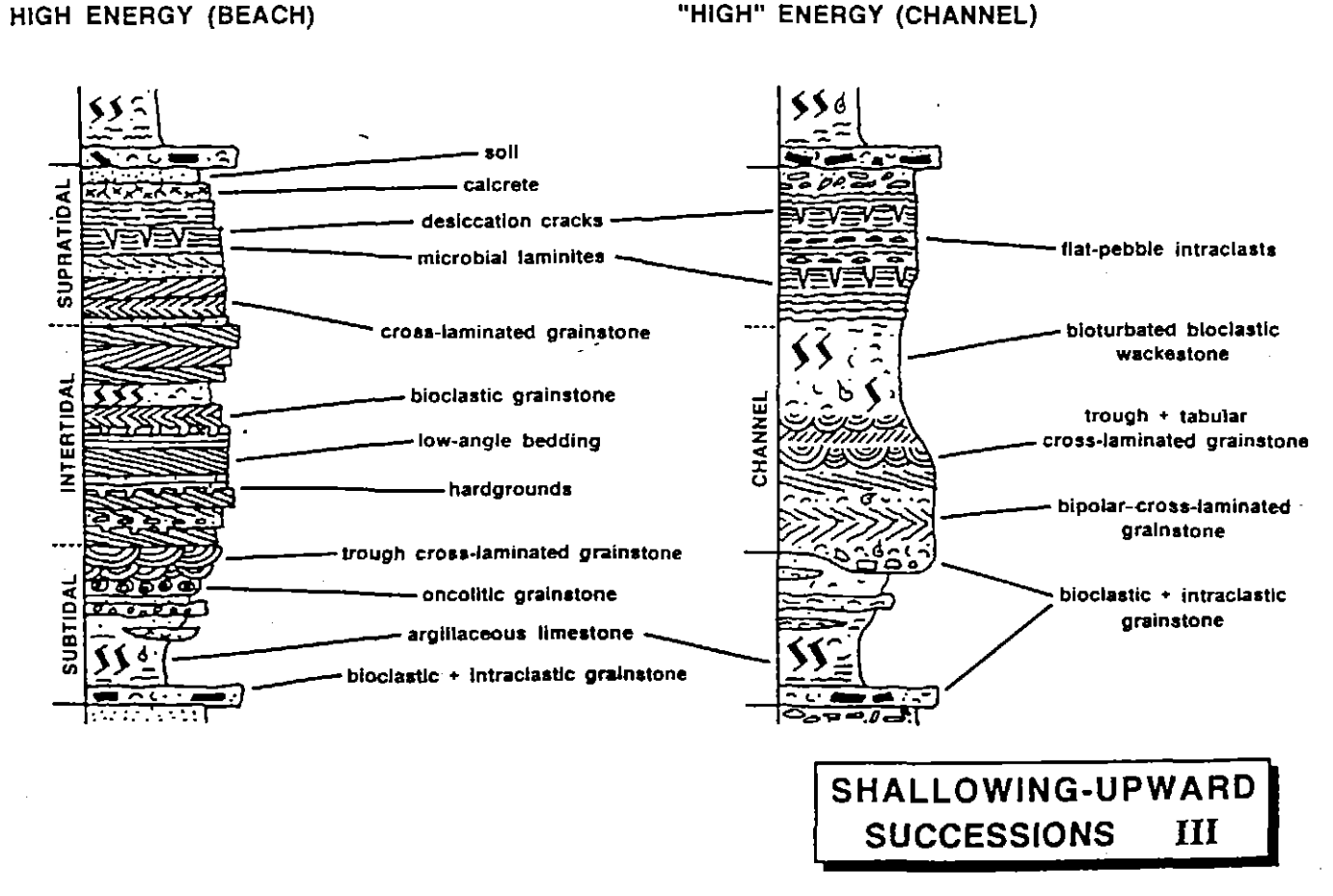


Figure 18 Hypothetical vertical profiles of individual high-energy, metre-scale, peritidal shallowing-upward successions, from a setting characterized by beach development (left) and a tidal flat penetrated by channels or creeks (right).

as those inferred from Cambrian strata by Koerschner and Read (1989).

Tidal flat-islands

An alternative model has been postulated to explain shallowing-upward peritidal successions that are demonstrably laterally discontinuous (Pratt and James, 1986). In this *tidal flat island* model deposition is envisioned as taking place on a platform dotted by a mosaic of exposed low-relief islands and intertidal banks separated by subtidal source areas (Fig. 19), with the whole complex shifting laterally and vertically through time in response to a range of local and regional hydrographic conditions. Such islands are developed today in Florida Bay and illustrate two modes of Holocene accumulation, 1) physically deposited mud banks capped by prograding intertidal and supratidal sediments, and 2) entirely supratidal deposition of a coastal mud flat, later dissected by erosion (Enos and Perkins, 1979; Wanless and Tagett, 1989). These islands, however, have not migrated much during the relatively short period of Holocene flooding. If viable, this tidal flat island model severely limits the architectural predictability of ancient platforms, as the constituent facies, particularly the supratidal caps, are of inherently limited regional extent.

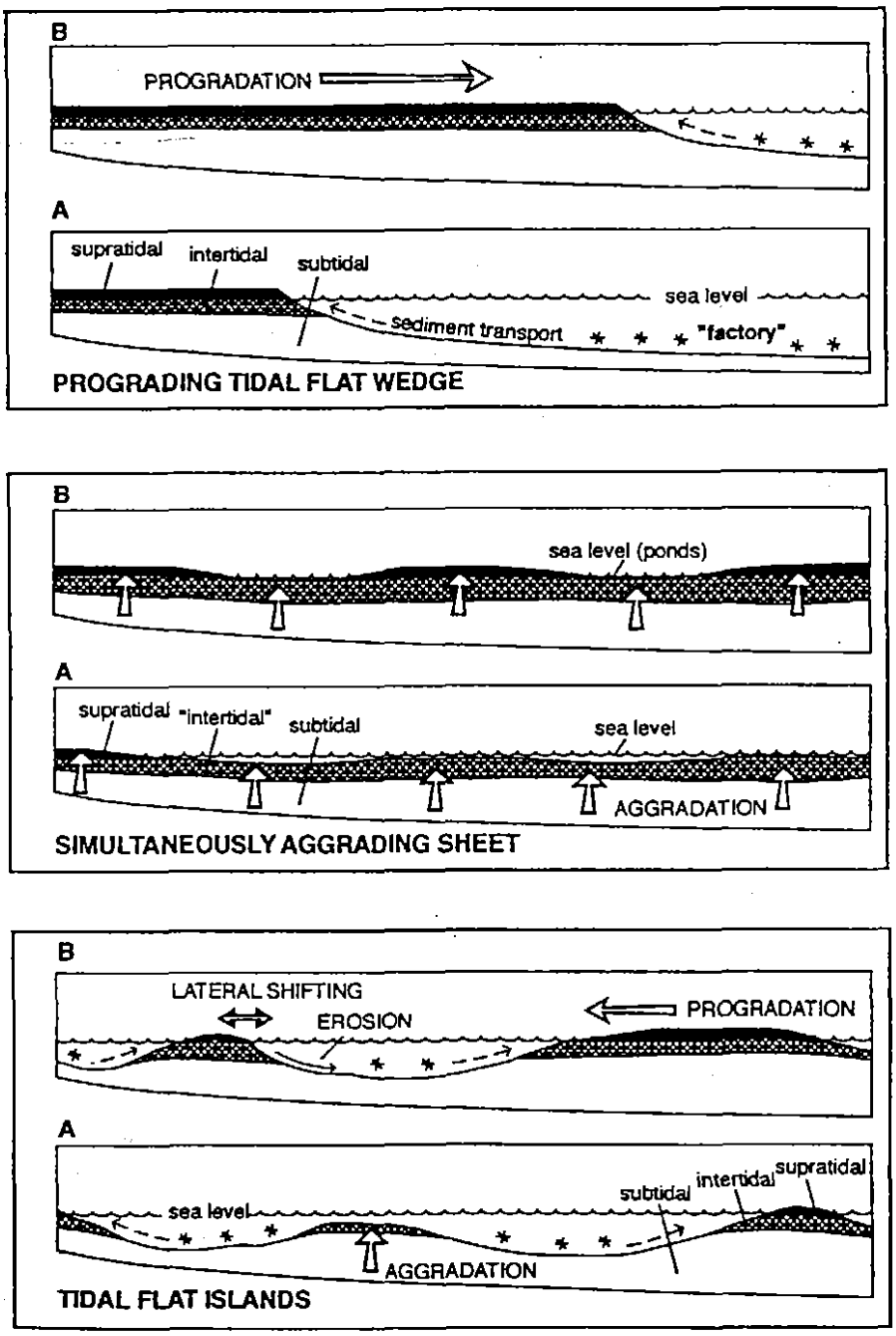


Figure 19 Diagrams illustrating various ways in which a metre-scale, peritidal, shallowing-upward succession can form. A prograding wedge is generated by sediment transported onto the tidal flat from the offshore carbonate factory. A simultaneously aggrading sheet accretes vertically to sea level and the whole platform becomes sequentially intertidal and then supratidal. Tidal flat islands nucleate and accrete by aggradation and progradation and shift in response to hydrographic forces.

Asymmetry

Why is a metre-scale, peritidal shallowing-upward succession asymmetric? The characteristic asymmetry of a typical shallowing-upward succession, i.e., subtidal (A), intertidal (B) and supratidal (C) stacked in ABC → ABC *hemicycles* (Figs. 16, 17, 18), as opposed to full CBABC cycles, is generally attributed to problems with the source area during platform inundation. If the flooding which begins a succession were gradual, then the seafloor during initial submergence is thought to have been too wave swept and/or too shallow or restricted to produce much carbonate sediment. Thus there is a "lag time" or "lag depth" (Hardie, 1986) before the seafloor becomes deep enough to actively produce sediment that is subsequently moved onto the tidal flats. In some successions this time interval is represented by a coarse-grained "transgressive" facies at the base, whereas in others there is no obvious record of this hiatus in deposition. Alternatively, if flooding was rapid, then supratidal facies (C) would be rapidly drowned and intertidal facies (B) would not have time to accumulate.

PERITIDAL CYCLOSTRATIGRAPHY

The stratigraphic record of ancient peritidal carbonates tends to be one of persistent repetition of the basic metre-scale, shallowing-upward succession, imparting a characteristic *cyclic* or, more appropriately, *rhythmic* appearance to the strata. While Holocene tidal flats sometimes provide an analogue for the generation of one

364121

shallowing-upward succession, the cause of stratigraphic repetition must be derived from the rock record. The Pleistocene history of climate and sea level change, although the most detailed and best understood of past epochs, has left a stratigraphic record of limited usefulness because sea level fluctuations were so large that they did not result in stacked metre-scale shallowing-upward successions. Consequently, there is currently much discussion as to what causes the rhythmic stacking into thick stratigraphic packages of ancient shallowing-upward successions. Debate has centred around the question of whether the new space made available for each successive shallowing-upward succession is the result of 1) recurring sea level changes (perhaps eustatic) at the same scale and temporal rhythm as the lithologic packaging; or 2) a high-frequency packaging mechanism *intrinsic* to processes of carbonate sedimentation which are superimposed on a low-frequency or irregular sea level rise. These are the *allocyclic* and *autocyclic* mechanisms, respectively, (see also Wilkinson, 1982). The two stacking mechanisms are not necessarily mutually exclusive, and it is uncertain at the moment whether or not evidence for either mechanism can be isolated in the rock record (Hardie *et al.*, 1991; Read *et al.*, 1991).

There is good evidence that a typical shallowing-upward succession was deposited within a time span of 10-100 k.y. (Algeo and Wilkinson, 1988). This is a scale of resolution beyond that provided by biostratigraphic methods. Much of the time represented by stacked shallowing-upward successions, however, is accounted for by hiatuses. Thus the time of deposition for a given tidal flat succession may be only a small fraction of the total apparent stratigraphic time; Wilkinson *et al.* (1991) have suggested as little as 3-30 per cent for some successions.

Autocyclicity

The driving force behind autocyclicity is the dynamics of sedimentation on the platform. Assuming optimum conditions, production rates for shallow-marine carbonate detritus could potentially provide enough sediment over a period of 10-100 k.y. to account for tidal flat aggradation to sea level or progradation of many tens to perhaps hundreds of kilometres under essentially static sea level conditions on a gradient which experienced typical passive-margin rates of subsidence (see also Hardie and Shinn, 1986).

Progradation is inherently limited by the sediment budget of the carbonate platform. For example, in a model first proposed by Ginsburg (1971; see Bosellini and Hardie, 1973; Mossop, 1979), a tidal flat wedge is envisioned as prograding across a gently inclined, gradually subsiding platform under static or slowly changing sea level (Fig. 19). As progradation covers the platform, the subtidal source area for tidal flat sediments becomes increasingly smaller (and deeper). Eventually the source area is too small or too deep to provide sediment for the tidal flat, so sedimentation stops. If relative sea level continues to rise, however, soon the whole platform will once again be subtidal and, after a lag period, the carbonate factory will be robust enough for sediment production, and the cycle will begin again.

The meagre areal coverage of present-day tidal flats makes it difficult to envision a platform literally choking itself off through hundreds of kilometres worth of tidal flat progradation under steady-state sea level and subsidence conditions. Furthermore, it should be emphasized that interpretations of platform-wide progradation in ancient examples are usually based on correlation of strata assumed to be diachronous, not on continuous stratigraphic exposure.

Under conditions of platform-wide *aggradation* it is thought that, once flooded, a shallow platform could generate enough sediment in situ that the whole seafloor would inexorably build to sea level (Fig. 19). Fundamental to this hypothesis is the ability of the "intertidal" and "supratidal" environments to produce sediment. The next cycle would accrete once relative sea level rise had submerged the platform in water deep enough for subtidal sedimentation to begin again. Critics of this hypothesis argue that, in order for the sediment surface to intersect the air/water interface on a platform-wide scale, there must be a sea level fall (albeit minor — a metre or less?), because it is unlikely that the seafloor would everywhere build right up to sea level of its own accord. This model is based on examples where shallowing-upward successions are correlated on a regional scale and assumed to be synchronous deposits.

Tidal flat islands are in part aggradational and in part progradational and their location is thought to shift through time in response to changing hydrographic conditions (Fig. 19). During intervals of prolonged static sea level, or slow sea level rise, they would, like the

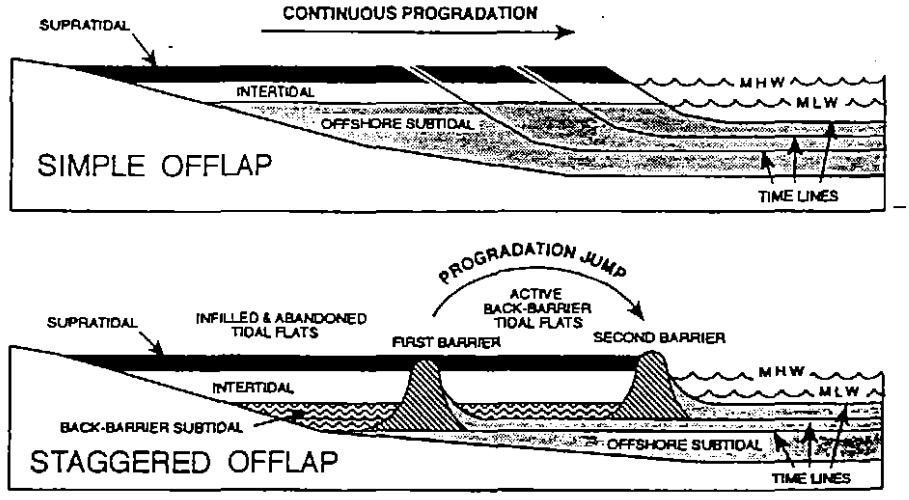


Figure 20 A diagram depicting two styles of tidal flat progradation envisioned from Holocene tidal flats. Simple offlap takes place by continuous progradation. Staggered offlap takes place by formation of an offshore bar which creates a leeward, protected setting in which tidal flat aggradation occurs. Once the flat builds to sea level it becomes dormant until another bar forms seaward and the process of backfilling begins again. Adapted from Hardie (1986).

364122

prograding wedge, gradually choke off local source areas, eventually becoming dormant. For sedimentation to begin again after a period of local stasis and probably protracted exposure of supratidal flats, there must be creation of new accumulation space. Under conditions of more rapid long-term sea level rise, and continually renewed accumulation space, the islands would form a series of laterally discontinuous peritidal units.

These autocyclic models express a basic premise that pervades current thinking about peritidal carbonates. Persistent and ubiquitous stratigraphic repetition of the basic shallowing-upward succession seems to indicate that these systems are, *at least in part*, intrinsically self-governing.

Allocyclicity

The extrinsic factors of subsidence and eustacy, which cause relative sea level change, have long been assumed to exert strong control on *large-scale* peritidal stratal patterns. High-frequency, low-amplitude sea level changes, the fourth- and fifth-order fluctuations of sequence stratigraphy (Chapter 2), are commonly invoked to drive the packaging of metre-scale, shallowing-upward peritidal successions (Grotzinger, 1986; Koerschner and Read, 1989; Read *et al.*, 1991). In this situation, a metre-scale rise in relative sea level provides a *window of opportunity*, in the sense of both time and accumulation space, for the generation of a single shallowing-upward succession (Fig. 21). Deposition occurs while sea level is rising and at its apex, and is arrested by sea level fall.

Formation of the shallowing-upward succession in this window is envisioned in different ways by different workers. All three styles of accretion presented above are viable within this scheme (prograding wedge, Grotzinger, 1986; aggradation, Koerschner and Read, 1989; and tidal flat islands, Strasser, 1988). Extrinsically controlled metre-scale successions of many kinds, including peritidal, have also been called *punctuated aggradational cycles* (PACs; Goodwin *et al.*, 1986) or more recently *metre-scale allocycles* (Anderson and Goodwin, 1990). Such cycles are metre-scale units, bounded by surfaces of abrupt change to deeper or disjunct facies and comprising a suite of contemporaneous facies, all of which shallow upward. The peritidal portions of such cycles are thought to be aggradational, but there is no reason why they could not be progradational (either wedges or islands).

The most commonly postulated external controls to drive, or at least reset, the system at the end of each shallowing-upward succession are rhythmic eustatic change or jerky subsidence. While spasmodic subsidence with the required short frequency has been documented from seismically active areas and for passive margins where listric faulting is common (e.g., Cisne, 1986; Hardie *et al.*, 1991), the importance of subsidence rate changes as a control on stratigraphic rhythmicity in peritidal shallowing-upward successions is unclear. Sudden base level drops have not been observed in modern passive margin platforms, and ancient epeiric settings, where much of the peritidal record is found, seem unlikely to have experienced metre-scale, high-frequency spasms of subsidence. Because there is currently no known frequency to such tectonism, it is difficult to use, and as yet impossible to model this mechanism as a universal control of stratigraphic rhythmicity. Nevertheless, the mechanism should not be dismissed as a potential control, especially in tectonically active regimes (e.g., Fischer, 1964; Knight *et al.*, 1991).

In the early to mid-1970s studies of DSDP sediment cores and relict coral reef terraces demonstrated that the Pleistocene record of eustatic change is one of superimposed orders of sea level variation (orders, in the sense of both magnitude and frequency; Chapter 2). Deep sea sediments were analyzed for oxygen isotopes (as proxy to glacial ice volume) and revealed a long-term (100 k.y.), 100 m-scale, asymmetric sea level oscillation. Pleistocene fossil reef data suggested that a shorter term (20 k.y.) sea level oscillation was superimposed on the longer term fluctuation. These various orders of eustatic change have been correlated to those predicted for icehouse glaciation driven by celestial mechanics, i.e., the Milankovitch rhythm (e.g., Fischer, 1986). It has been postulated that the stratigraphic rhythmicity apparent in ancient peritidal carbonates reflects a similar *composite eustasy* (Goldhammer *et al.*, 1987), both icehouse and greenhouse, of celestial origin. If astronomically forced composite eustasy is indeed the primary driver in the packaging of shallowing-upward successions, then presumably modulation of various orders of superimposed eustatic cycles could have provided potentially limitless rhythms to the stratigraphic record (Bova and Read, 1987; Koerschner and Read, 1989; Read *et al.*, 1991).

The common challenge to allocyclicity is that extrinsic controls on peritidal sedimentation are neither demonstrable in, nor theoretically re-

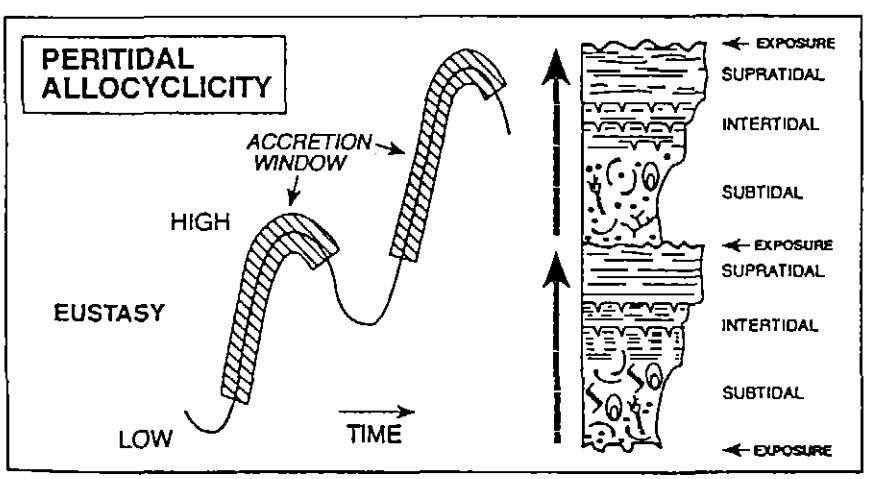


Figure 21 A diagram illustrating the relationship between fluctuating sea level and stacked metre-scale, peritidal, shallowing-upward successions. Sea level rise provides a window of opportunity for the succession to accrete as a prograding wedge, as a simultaneously aggrading sheet or as tidal flat islands. Sea level fall terminates accretion and results in subaerial exposure.

364123

quired to generate metre-scale shallowing-upward successions. It is hard, however, to imagine sea level remaining static for a long period of time, and therefore difficult, if not impossible, to dismiss some extrinsic control on succession development. Allocyclic, platform-wide event stratigraphy should not be underestimated, but its deterministic role in peritidal cyclostratigraphy is still uncertain.

The search for controls and rhythms

Significant effort has recently been devoted to unravelling the meaning of possible stratigraphic rhythms in stacked shallowing-upward successions by numerical analysis. Because peritidal carbonates are so sensitive to changes in climate and sea level, it was widely suspected (hoped?) that this rhythmicity might retain a causative signal of ancient climate and sea level fluctuations. If allocyclic eustatic control on stratal packaging is assumed, then reconstruction of the strata-generating sea level curve can be used as a tool to correlate and explain temporally correlative strata (Read and Goldhammer, 1988).

At the current level of understanding and data base, it is not possible to isolate unequivocal evidence in the rock record for either allocyclic or autocyclic control on most peritidal stratal patterns. Reasonable-looking, synthetic, one-dimensional stratigraphic sections can, however, be generated by varying the critical input parameters of cycle amplitude, duration and asymmetry, bathymetry for each facies, lag time (depth), type of sediment, sedimentation rate, regional and local subsidence, isostatic compensation, wave damping, tidal range, and platform slope and dimension (Grotzinger, 1986; Read *et al.*, 1986; Goldhammer *et al.*, 1987; Spencer and Demicco, 1989). These sections can then be compared to actual examples and eventually a match may be achieved. When similar modelling techniques are used to simulate two-dimensional (multisection) architecture it is often found that the time needed for a peritidal wedge to prograde across the platform is longer than that predicted by Milankovitch rhythms, and the wedges become *stranded*.

Techniques, such as relative time series analysis and *Fischer plotting*, which made a good case for allocyclic forcing of some examples of platform carbonate rhythmicity, i.e., stratigraphic patterns attributable to rhythmic Milankovitch composite eustasy (Goldhammer *et al.*, 1987, 1990), cannot be used for the analysis of metre-scale *peritidal* shallowing-upward successions. Relative time series analysis to reveal the rhythms of sedimentation are invalid for progradational wedges, either local or platform-wide in extent, because such deposits are by nature diachronous, and thicknesses of resultant shallowing-upward successions vary with position on the regional gradient and/or platform topography. Fischer (1964) presented a graphic means of plotting time versus cumulative thickness for laterally continuous, stacked, peritidal shallowing-upward successions. Fischer plots have often been used in recent studies of cyclic strata because they are designed to reveal changes in accumulation space which deviate from that space generated solely by subsidence; these deviations are postulated to result from changes in sea level. However, interpretations of Fischer plots are essentially model driven. For them to be viable two assumptions must be satisfied: 1) each peritidal succession must have been deposited in the same amount of time as every other succession in the chain, and 2) there must be few, if any, missing tidal flat successions. The use of Fischer plots is therefore dubious for any peritidal successions which formed as prograding wedge-shaped tidal flats. It is likely that variations in both the tempo and magnitude of changes in accumulation space, however they are caused, account for stacks of shallowing-upward successions which vary in thickness. Whereas demonstration of allo- or autocyclic control of stratal patterns in stacked shallowing-upward successions appears out of reach at this time, more sophisticated models, particularly those which integrate peritidal rhythms with coeval subtidal and perhaps offplatform stratal patterns, hold promise.

PERITIDAL SEQUENCE STRATIGRAPHY

The concepts of sequence stratigraphy were developed in terrigenous clastic successions and carbonates have only recently been analyzed in this fashion (Chapter 14). *Systematic* packaging of the basic metre-scale shallowing-upward succession is less common and seems less straightforward, or less well developed in carbonates compared to siliciclastics. This difference likely reflects the fundamental differences between carbonate and siliciclastic sediments generally. We have, therefore, avoided the term *parasequence* in this treatment of carbonate tidal flat deposits.

Peritidal deposits are not indicative of any particular systems tract because the controls on tidal flat development, such as climate, platform circulation, wind patterns and tidal range, vary with each platform's unique history and configuration. Nevertheless, tidal flat deposits are potentially useful in delineating sequences and their component systems tracts in two ways, 1) geographic position of the tidal flat on the platform may track long-term changes in sea level, and 2) changes in large-scale accumulation space, and thus sequences, can be recognized through analysis of stacking patterns (packaging) of shallowing-upward successions.

Tracking sea level

Tidal flats can be the first facies overlying a sequence boundary, deposited as the rate of relative sea level fall decreases and the sea slowly floods back across the platform. As third-order sea level fluctuates in response to long-term, large-amplitude driving forces, the location of the strandline on the platform will change. If conditions are favourable for their development, land-fringing tidal flat deposits will mark the position of coastal onlap through the third-order eustatic cycle (i.e., the "onlap-offlap" geometry of Hardie, 1986; Fig. 22). Sarg (1988) documented the utility of tidal flats at the outcrop scale in a sequence stratigraphic context for the Permian of New Mexico, where a sequence boundary and shelf-margin wedge systems tract were recognized in part by the downdip, basinward position of onlapping tidal flat deposits.

Stacking

The stratigraphic patterns of *laterally continuous*, metre-scale, shallowing-upward successions generated by pro-

grading tidal flat wedges, can be envisaged in the framework of long-term changes in relative sea level. Third-order sea level changes are thought to "modulate" the higher-frequency, fourth- and fifth-order sea level cycles represented by the tidal flat successions. This has two consequences.

Long-term, third-order fluctuations in sea level should carry the window of opportunity in which each individual metre-scale succession is formed back and forth across the platform. Depending upon the balance between different rates of subsidence, eustasy and sedimentation, the window will be geographically repositioned during each consecutive fourth or fifth-order change in relative sea level to result in backstepping, offlapping or stacking of peritidal shallowing-upward successions. Figure 22 illustrates, in a conceptual way, how this might work on an inclined shelf. If the rate of change of long-term relative sea level is *low*, the geographic position of successive windows should remain roughly the same. Thus, peritidal successions in lowstand (position 1) and early highstand (position 3) systems tracts will probably be stacked in one place and will be relatively thin because the rate of addition of new accumulation space is low. If the rate of change is *high*, the window should be forced backward and forward across the shelf. This will likely result in either relatively thick, backstepped tidal flat successions (position 2 – transgressive systems tract) or relatively thin successions which offlap in a shingled fashion (position 4 – late highstand or early lowstand systems tracts). It must be stressed that the distance of progradation in each case will be specific to each peritidal package on each shelf.

Long-term sea level rise should accentuate short-term rises and suppress short-term falls; long-term falls in sea level will have the opposite effect. The relative proportions of subtidal, intertidal and supratidal facies in successive shallowing-upward successions may change systematically in response to this long-term modulation of short-term changes in accumulation space. This relationship is as yet hypothetical, and interpretations of such controls in ancient strata are necessarily model driven.

SUMMARY

Peritidal limestones and dolostones exhibit a large number of easily recognized sedimentary and biosedimentary structures. While some of these are individually equivocal bathymetric indicators (stromatolites or wave-rippled beds, for example, can form in subtidal areas), in most cases the features can be used collectively to make a firm environmental conclusion. A boon to interpreting ancient peritidal facies is the wealth of knowledge gained from modern settings. Very often a one-to-one lithologic comparison can be made, leading to a refined understanding of paleoenvironments and paleoclimates in individual cases. A *hierarchy of models* has been formulated that deals with successive levels of interpretation of peritidal carbonate strata.

These kinds of rocks fall into two main depositional systems, low-energy tidal flats and higher-energy beaches. The facies associations are fairly distinctive for each setting: this is the first tier of models to guide basic interpretations.

The vertical record of peritidal facies commonly shows a trend from subtidal limestone through intertidal sediments to supratidal deposits, at a metre scale, as tidal flats aggrade to sea level and prograde laterally. Peritidal models are therefore shown as shallowing-upward successions as a reminder of these dynamic processes.

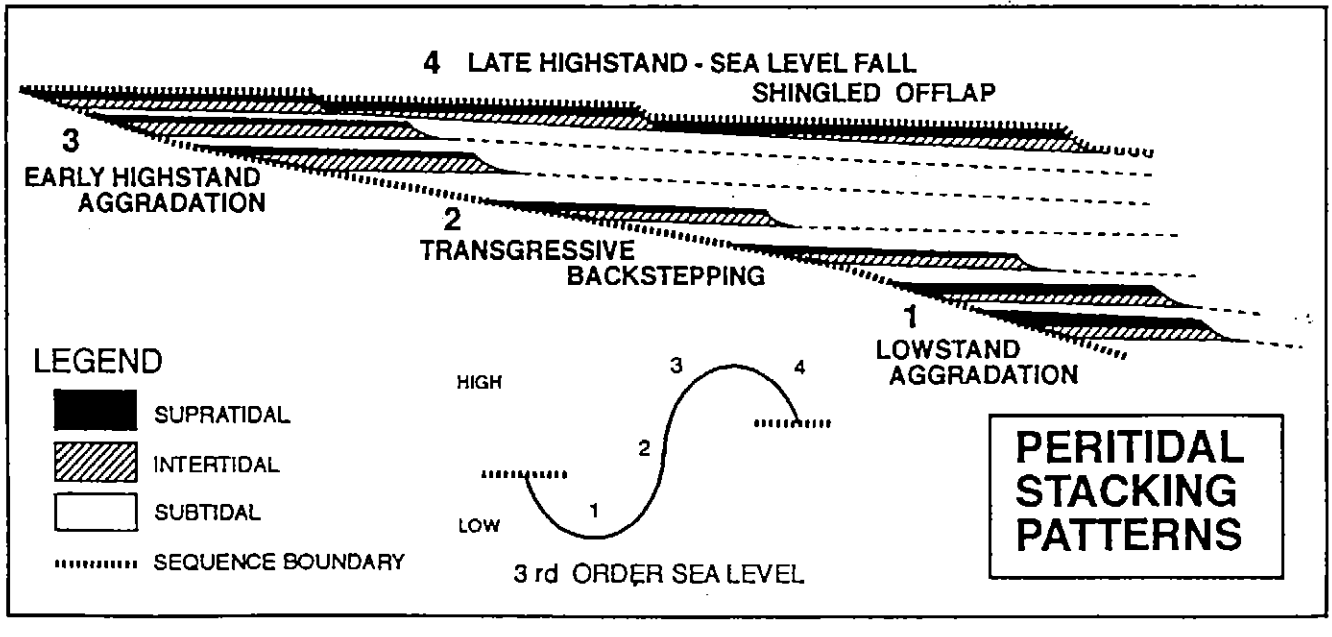


Figure 22 A diagram illustrating the hypothetical stratigraphy of metre-scale, peritidal, successions between two sequence boundaries. Each succession formed by progradation which took place in the window of opportunity produced by short-term fourth- and fifth-order fluctuations in relative sea level during a long-term, third-order rise and fall of sea level. Slow, third-order, sea level-controlled movement of the strandline will dictate where tidal flats develop on the shelf. The balance between sea level changes, sedimentation, and subsidence will dictate how successive tidal flats will stack, backstep or offlap.

364125

These models, as predictors, point to departures from the norm and other irregularities that might have important implications regarding intrinsic or extrinsic controls on deposition. They also provide a framework within which the diagenesis of the sediment can be tracked.

Peritidal carbonates occur repetitively in stratigraphic sequences, often in a seemingly regular, or cyclic, fashion. There is much debate about whether these metre-scale, shallowing-upward successions are platform-wide responses to allogenic forces such as spasmodic subsidence or episodic eustasy, or whether they represent localized tidal flat shorelines and islands shaped by autogenic, i.e., hydrographic, controls. Sedimentologists have their work cut out for them by these models; we are now charged with the job of deciding, if possible, which one best explains our own successions, or if a new approach is necessary. It is an exciting field of research, one that weds careful and precise field observations with increasingly sophisticated numerical modelling.

ACKNOWLEDGEMENTS

This article is an outgrowth of several research projects funded by the Natural Sciences and Engineering Research Council of Canada. An early draft of the text was critically read by E.C. Turner.

REFERENCES

Basic sources of information

Bathurst, R.G.C., 1975, Carbonate sediments and their diagenesis: Amsterdam, Elsevier, 658 p.
Still a good summary of several modern examples.

Ginsburg, R.N., ed., 1975, Tidal deposits: a casebook of Recent examples and fossil counterparts: New York, Springer-Verlag, 428 p.
Many examples of both siliciclastic and carbonate tidal deposits.

Goldhammer, R.K., Dunn, P.A. and Hardie, L.A., 1990, Depositional cycles, composite sea-level changes, cycle stacking patterns, and the hierarchy of stratigraphic forcing: Examples from Alpine Triassic platform carbonates: Geological Society of America, Bulletin, v. 102, p. 535-562.
Manipulation of sedimentological data for computer models to show eustatic effects on a shallow platform.

Hardie, L.A., ed., 1977, Sedimentation on the modern carbonate tidal flats of northwest Andros Island, Bahamas: Johns Hopkins University, Studies in Geology 22, 202 p.
Carbonate tidal flat sediments and biology in a humid setting.

Hardie, L.A. and Shinn, E.A., 1986, Carbonate depositional environments, modern and ancient. Part 3: tidal flats: Colorado School of Mines, Quarterly, v. 81, 74 p.
The place to start, a thorough discussion of peritidal carbonate sediments, facies and depositional models.

Koerschner, W.F. and Read, J.F., 1989, Field and modelling studies of Cambrian carbonate cycles, Virginia Appalachians: Journal of Sedimentary Petrology, v. 59, p. 654-687
Lower Paleozoic peritidal facies and manipulation for computer models trying to show controls by eustasy.

Logan, B.W., Hoffman, P. and Gebelein, C.D., 1974, Evolution and diagenesis of Quaternary carbonate sequences, Shark Bay, Western Australia: American Association of Petroleum Geologists, Memoir 22, 358 p.
Carbonate tidal flat sediments, including stromatolites, in a hypersaline setting.

Pratt, B.R. and James, N.P., 1986, The St George Group (Lower Ordovician) of western Newfoundland: tidal flat island model for carbonate sedimentation in shallow epeiric seas: Sedimentology, v. 33, p. 313-343.
Lower Paleozoic facies and outline of autocyclic island model.

Purser, B.H., ed., 1973, The Persian Gulf: Holocene carbonate sedimentation and diagenesis in a shallow epicontinental sea: Heidelberg, Springer-Verlag, 47 p.
Description of carbonate peritidal sediments in an arid setting.

Shinn, E.A., 1983a, Tidal flats, *in* Scholle, P.A., Bebout, D.G. and Moore, C.H., eds., Carbonate depositional environments: American Association of Petroleum Geologists, Memoir 33, p. 171-210.
Read in conjunction with this article; a colour-illustrated, review of carbonate tidal flat sediments and facies.

Tucker, M.E. and Wright, V.P., 1990, Carbonate sedimentology: Oxford, Blackwell, 482 p.
Succinct review of peritidal carbonate sediments, facies and models.

Wilgus, C.K., Hastings, B.S., Posamentier, H.W., Ross, C.A. and Kendall, C.G.St.C., eds., 1988, Sea level changes: an integrated approach: Society of Economic Paleontologists and Mineralogists, Special Publication 42, 407 p.
Collection of papers emphasizing conceptual basis of sequence stratigraphy plus nimerous case studies of sea level change from the geological record.

Other references

Algeo, T.J. and Wilkinson, B.W., 1988, Periodicity of mesoscale Phanerozoic sedimentary cycles and the role of Milankovitch orbital modulation: Journal of Geology, v. 96, p. 313-322.

Anderson, E.J. and Goodwin, P.W., 1990, The significance of metre-scale allocycles in the quest for a fundamental stratigraphic unit: Journal of the Geological Society of London, v. 147, p. 507-518.

Beales, F.W., 1958, Ancient sediments of Bahaman type: American Association of Petroleum Geologists, Bulletin, v. 42, p. 1845-1880.

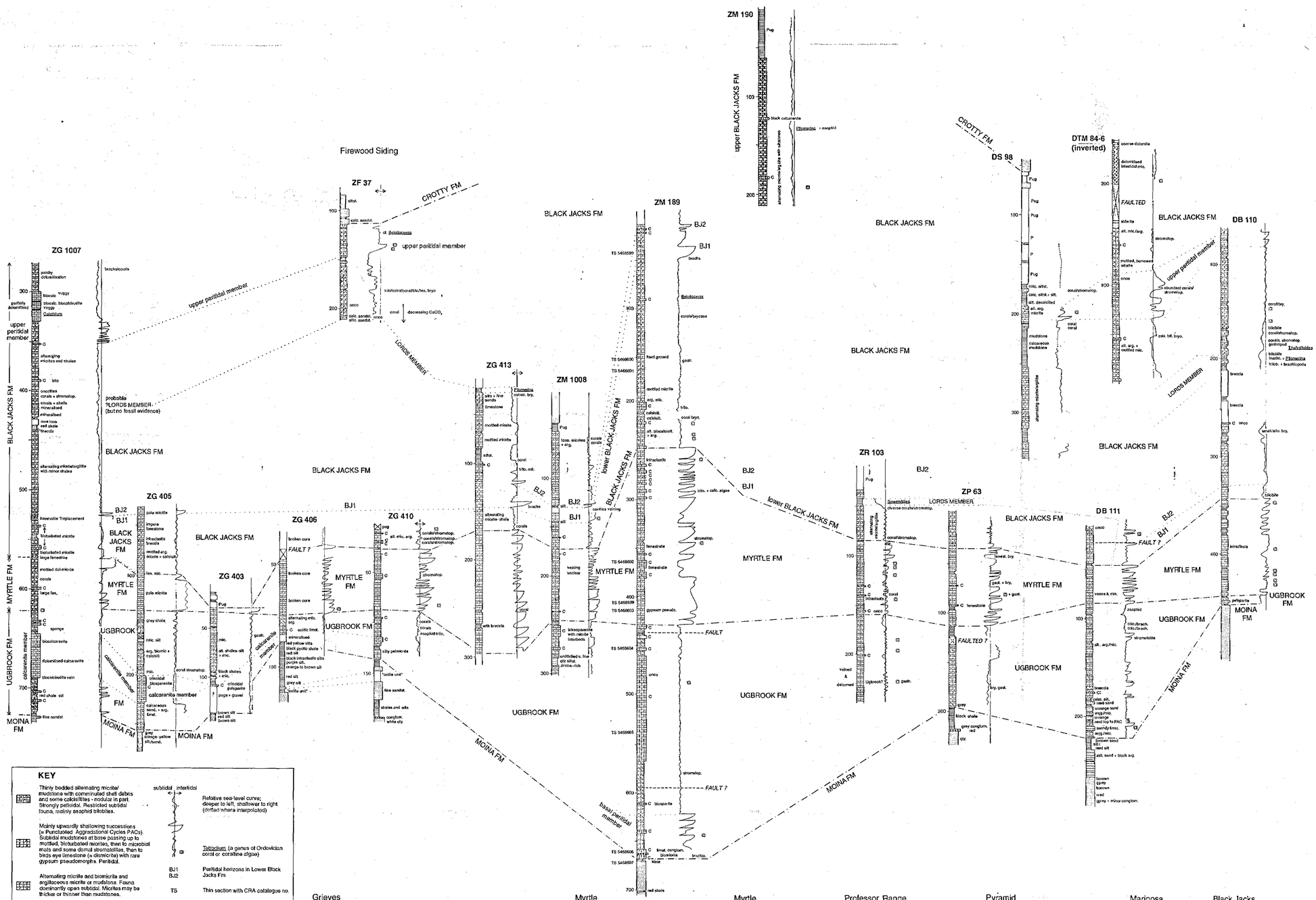
Belperio, A.P., Gostin, V.A., Cann, J.H. and Murray-Wallace, C.V., 1988, Sediment-organism zonation and the evolution of Holocene tidal sequences in southern Australia, *in* de Boer, P.L., van Gelder, A. and Nio, S. D., eds., Tide-influenced sedimentary environments and facies: Dordrecht, Reidel Publishing Company, p.475-497.

Bertrand-Sarfati, J. and Moussine-Pouchkine, A., 1988, Is cratonic sedimentation consistent with available models? An example from the Upper Proterozoic of the West African craton: Sedimentary Geology, v. 58, p. 255-276.

Bosellini, A. and Hardie, L.A., 1973, Depositional theme of a marginal marine evaporite: Sedimentology, v. 20, p. 5-27.

Bottjer, D.J. and Ausich, W.I., 1986, Phanerozoic development of tiering in soft substrata suspension-feeding communities: Paleobiology, v. 12, p. 400-420.

Bova, J.A. and Read, J.F., 1987, Incipiently drowned facies within a cyclic peritidal ramp sequence, Early Ordovician Chepultepec interval, Virginia Appalachians: Geological Society of America, Bulletin, v. 98, p. 714-727.



KEY

- Thinly bedded alternating micrite/ limestone with comminuted shell debris and some calcisiltites - nodular in part. Strongly peloidal. Restricted subtidal fauna, mainly anaphiod trilobites.
- Mainly upwardly shallowing successions (= Punctuated Aggradational Cycles PACs). Subtidal mudstones at base passing up to mottled, bioturbated micrites, then to microbial mats and some domal stromatolites, then to birds eye limestone (= dismicrite) with rare gypsum pseudomorphs. Peritidal.
- Alternating micrite and biomicrite and argillaceous micrite or mudstone. Fauna dominantly open subtidal. Micrites may be thicker or thinner than mudstones.
- Calcarenites, sparites, biosparenites etc. (i.e. calcite sandstones)
- Strongly dolomitised carbonate

subtidal ← → intertidal

- Relative sea-level curve; deeper to left, shallower to right (dotted where interpolated)
- Tetradium (a genus of Ordovician coral or coralline algae)
- BJ1 / BJ2 — Peritidal horizons in Lower Black Jacks Fm
- TS — Thin section with CRA catalogue no.
- Mudstone, siltstone (slates where cleaved).
- Siliciclastic sandstone
- Siliciclastic conglomerate
- Member correlation
- Formation boundary correlation

97-3958

364126

ANNUAL REPORT ZEEHAN NO 1
EL 28/88 - P.E. NOV 1996 - CRA
S TEAR/R RUSSELL- VOL 2 OF 3

364127 96-3958 Vol. 3 of 3

CRA EXPLORATION PTY. LIMITED
ACN 000 057 125

MINERAL RESOURCES
24 DEC 1996
TASMANIA

Eighth Annual Report
For The Period Ending 9 November 1996
EL 28/88 Zeehan 1, Tasmania

EL28/88
See folio 11

Volume III of III

MICROFILMED
FICHE No.014213 -22

Author: S J Tear / S A J Russell

Date: November 1996

Licence Holder: CRA Exploration Pty. Limited
Allegiance Mining NL

Submitted to: Chief Geologist, South East District

Copies to: Mineral Resources Tasmania
CRAE - South East District
CRAE - Zeehan
CRAE - ETIG
Allegiance Mining NL

"All rights in this report and its contents (including rights to confidential information and copyright in text, diagrams and photographs) remain with CRA Exploration and no use (including use of reproductions, storage or transmission) may be made of the report or its contents for any purpose without the prior written consent of CRA Exploration.
© CRA Exploration Pty. Limited 1996"

97-3958B

CRAE Report No. 22160

ANNUAL REPORT ZEEHAN NO 1
EL 28/88 - P.E. NOV 1996 - CRA
S TEAR/R RUSSELL- VOL 3 OF 3

97-3958B.

364128

97-3958B
Appx 10 of TCR 97-3958

Appendix X

Mark Upton's Honours Thesis

364129

THE GEOLOGY AND MINERALISATION OF THE STONEHENGE PROSPECT, ZEEHAN, TASMANIA

BY

MARK A. UPTON

NOVEMBER, 1996

This thesis is submitted in part fulfilment of the Bachelor of Science (Honours) Degree,
Department of Earth Sciences, Monash University, 1996.

364130

DECLARATION

This thesis contains no material which has been accepted for the reward of any other degree or diploma in any university and, to the best of the author's knowledge and belief contains no material previously published or written by another person, except where due reference is made in the text.



Mark Upton

November, 1996

364131

ACKNOWLEDEGMENTS

Many of people have supported me throughout the year, and assisted with preparation of this thesis.

Firstly, gratitude is forwarded to several people at CRA Exploration for providing a project, accommodation and continued support throughout the year. Thanks to Ian Clementson and Ross Andrew for advising me towards honours, and to Tim McConachy for providing such an interesting project. To the Tassie guys, thankyou Simon, Sandy, Sarah's, Roger, Andrew and Mark for making the often arduous work encountered in Tasmania one of the most enjoyable times of my life. Thanks to TVS for letting me steal his time on a number of occasions during the year, and far from least, thankyou to 'Col where's my brew Pike' and 'Miss Wendy' for providing me with the use of computing equipment, drafting advise and a fantastic work environment during the last two years.

Thankyou to Dave Gray for supervising my project, and for sharing knowledge of structural geology. Your willingness to see me at any time, and ability provide words of encouragement and motivation certainly helped during the year.

I would like to express my appreciation to all the students and staff members at Monash University for your friendly approach to a newcomer this year. Although only an occasional visitor throughout the year, you have always made feel welcome.

'KBH' - thanks Kev for helping to keep me on track throughout the year. Your patience has been greatly appreciated. See you out on the course!

Thankyou to all my family, Mum, Dad, Sue (and the gang) and Leanne, for your continued love and encouragement during year.

Finally, to 'Fieldy Randall', thanks mate for your help in the bush, for *finally* realising your niche, and for the good times during the year - RRRRR!

ABSTRACT

Precambrian Oonah Formation sedimentary sequences of siltstones, sandstones, shales and dolomites form the oldest rock units surrounding Zeehan, and dominate the geology of the Stonehenge prospect area. Poorly exposed, these rocks have been disrupted during multiple phases of folding and faulting, producing a complex pattern of fold structures. Thrust emplacement of the sequence has positioned the Oonah Formation upon younger Cambrian sediments of the Dundas Group and Crimson Creek Formations. Regional Devonian intrusives and localised granitoid bodies account for much of the geology of western Tasmania. Mineralisation at Stonehenge is dominated by fluids emanating from the intrusion of the Heemskirk Granite.

Early deformation fabrics are indicative of regional isoclinal folding. This deformation event is represented by the widespread development of a spaced cleavage at low angle to bedding throughout the Proterozoic units. Although generally obscured by later folding, early structures are preserved as microlithons within pelite units of the Oonah Formation. Timing of this early deformation is thought to coincide with the Penguin Orogeny (700 to 750 Ma), a common cause of folding within Proterozoic succession of Tasmania.

Early structural development is followed by thrusting events which form an integral component of the Cambrian development of western Tasmania. During this event, the Precambrian Oonah Formation headed (detached from its basement sequence) a complex sheet of Cambrian sediments containing mafic-ultramafic sequences of arc-forarc signature. This allochthonous sheet was thrust from east to west into and onto early Cambrian stratigraphy. Evident compessional structures within the Oonah Formation include large scale folds striking along a north-south axis.

Deformation post dating this Cambrian thrusting event has produced the complex fold and fault structures seen throughout the Zeehan area. In conjunction with prior folds, near-contemporaneous folding along differing axes has produced fold a interference patterns containing simple dome and basin structures, and more intricate antiform/synform structures within the Oonah Formation. Faulting of east-northeast and north-northwest trend has dislocated the fold structures. Regional Siluro-Devonian sequences host the last dominant phase of fold/fault deformation, providing a timing estimate of Middle to Late Devonian. Intense veining and mineralisation is associated with granite intrusion during this period. Faulting of an intrusive body beneath Stonehenge indicates emplacement before the completion of deformation. Timing of this deformational event correlate with the 'Tabberabberan Orogeny'.

Oonah Formation shale and dolomite/dolomitic sediment horizons host pyrite, sphalerite and galena mineralisation at Stonehenge. Two styles of mineralisation are evident. The *first* contains massive disseminated pyrite as a stratiform deposit with black shale sequences. The *second* is the product of hydrothermal fluid activity related to the intrusion of granite bodies (Heemskirk Granite) during the Devonian. In this case, low to medium temperature veins deposits, and minor carbonate replacement mineralisation (skarn) has formed along the peripheral margins of a skarn environment.

Mineralised horizons at Stonehenge (and throughout the Zeehan area) have been fault interrupted, implying deposition prior to or during completion of tectonic activity. Veins hosting the mineralisation overprint at least one earlier vein set, and are the last to have occurred.

364134

CONTENTS

1. INTRODUCTION 1

1.1. Forward. 1
1.2. Project Aims 2
1.3. Physiology 2
1.4. Investigation Techniques 5
1.5. Previous Work 5

2. GEOLOGY 6

2.1. Introduction 6
2.2 Regional Geology (W Tasmania) 8
2.2.1 Precambrian 8
2.2.2 Eo-Cambrian - Cambrian 10
2.2.3 Cambrian Mount Read Volcanics . . . 12
2.2.4 Late Cambrian to Devonian . . . 15
2.2.5 Late Carboniferous - Triassic . . . 15
2.2.6 Jurassic - Cainozoic 15
2.2.7 Quaternary 18
2.3 Local Geology (Zeehan) 18
2.3 Stonehenge Mapsheet 21

3. STRUCTURAL HISTORY OF WESTERN TASMANIA 27

3.1 Introduction 27
3.2 Geology 28
3.3 Structure 32
3.3.1 Early Palaeozoic Deformation . . . 32
3.3.2 Mid to Late Palaeozoic Deformation . . 34

4. STRUCTURAL GEOLOGY OF THE STONEHENGE AREA 43

4.1 Introduction 43
4.2 Fold Structures 43
4.3 Map Fold Pattern 45
4.4 Minor Folds 56
4.5 Foliation Development 64
4.6 Major Faults 68
4.7 Vein Generation and Deformation 71

364135

5. MINERALISATION OF THE STONEHENGE AREA 75

5.1 Introduction 75
5.2 Occurrence 75
5.2.1 West Coast Mineralisation . . . 76
5.2.2 Mineralisation of the Zeehan Area . . . 81
5.2.3 Mineralisation of the Stonehenge Area . . 81
5.3 Controls of Mineralisation 84
5.4.1 Stratigraphic Controls 84
5.4.2 Structural Controls 85
5.2.2 Spatial Controls 88
5.4 Style of Mineralisation 92

6. DISCUSSION 98

6.1 Structural Overview 98
6.2 'D1 Deformation' 99
6.3 'D2 Deformation' 99
6.4 'Post D2 Deformation' 100
6.5 Local and Regional Development 101
6.6 Evaluation of the Genesis and Timing of Mineralisation . 108
6.7 Interpretative Structure of the Mineralised Horizons . . 109

7. CONCLUSIONS 111

REFERENCES 113

APPENDICES AND MAPSHEETS

Appendix 1. Database of field mapping
Appendix 2. Stereonet plots
Appendix 3. Drillhole data
Appendix 4. Skarn-type lead-zinc deposits
Appendix 5. Previous workings of the Stonehenge area
Appendix 6. Thin section locations
Appendix 7. Profile lines

Mapsheet A. Geology
Mapsheet B. Stonehenge Structure
Mapsheet C. Field Stations
Mapsheet D. Drillhole Locations

364136

LIST OF FIGURES

Chapter 1. INTRODUCTION

Figure 1.1	*Geology surrounding the Stonehenge area from the ZEEHAN 1:50 000 map sheet (7914S (50)).*	Page 3
Figure 1.2	*Location of the Stonehenge area.*	Page 4
Figure 1.3	*Typical vegetation encountered along creeks and within valley depressions throughout the Stonehenge area.*	Page 4

Chapter 2. GEOLOGY

Figure 2.1	*Simplified stratigraphy showing the major events of the Lower Palaeozoic in Eastern and Western Terrains. (Solomon and Groves, 1994)*	Page 7
Figure 2.2	*Generalised geology map of Tasmania. (after Corbett and Turner, 1989)*	Page 8
Figure 2.3	*Distribution of rocks post-dating the Penguin Orogeny. (Turner, 1989)*	Page 9
Figure 2.4	*Geology of western Tasmania showing the Mount Read Volcanics between Hellyer and Mount Darwin and associated Dundas Trough sequences. (Corbett and Lees, 1987)*	Page 13
Figure 2.5	*Southern margin of Australia showing the major structural features of the passive margin.. (Wilcox, 1990)*	Page 16
Figure 2.6	*Bouger anomalies onshore and free-air anomalies offshore (Gravity Map of Australia, BMR 1976) of southern Australia.. (Wilcox, 1990)*	Page 17
Figure 2.7	*Stratigraphic column of the Zeehan area geology. (after Blissett, 1962)*	Page 20
Figure 2.8	*Geology map of the Henty River-Zeehan-Pieman River area. (after Blissett and Gulline, 1962; Baillie et al., 1977; Brown, 1986; Corbett and McNeill, 1986; Corbett, 1986a)*	Page 21
Figure 2.9	*Stonehenge area showing 'station' of data collection.*	Page 22
Figure 2.10	*Photograph of the Stonehenge area taken from Mount Zeehan, looking north.*	Page 23
Figure 2.11	*Simplified geology of the Stonehenge mapping area.*	Page 24
Figure 2.12	*Bedding traces within Oonah Formation quartzite.*	Page 25
Figure 2.13	*Geology interpretation from wacker and EM surveying.*	Page 26

364137

Chapter 3. STRUCTURAL HISTORY

Figure 3.1	*Generalised geology map of Tasmania showing major Precambrian and Cambrian suites. (after Solomon and Griffiths, 1974)*	Page 28
Figure 3.2	*Regional magnetic map of Tasmania showing major geological and structural features. (Muir, 1990)*	Page 31
Figure 3.3	*Regional gravity map of Tasmania showing dominant structural trends. (Muir, 1990)*	Page 32
Figure 3.4	*Diagrammatic longitudinal section through the Henty Fault System showing stratigraphic relationships. Corbett and Lees, 1987)*	Page 33
Figure 3.5	*Hinge traces of major Devonian folds and faults. (Williams, 1989)*	Page 36
Figure 3.6	*Shaded magnetic images of western Tasmania identifying major structural trends.*	Page 37
Figure 3.7	*Dominant structure of the Zeehan area. (after Blissett, 1962)*	Page 39
Figure 3.8	*Simplified Devonian structure of the Henty Fault System area. (Corbett and Lees, 1987)*	Page 40

CHAPTER 4. STRUCTURAL GEOLOGY OF THE STONEHENGE AREA

Figure 4.1	*Regional geological map of the Zeehan area showing the dominant NW-SE fold trend within Siluro-Devonian sequences.*	Page 44
Figure 4.2	*Fold interference patterns (dome and basin) with the Oonah Formation quartzite unit (Poq).*	Page 46
Figure 4.3	*Section along lines 359500E, 360000E and 360500E showing structural form from surface mapping, and major fault trends.*	Page 47
Figure 4.4	*NW-SE and NE-SW sections showing structural form from surface mapping, and major fault trends.*	Page 48
Figure 4.5	*Section along lines 5360000N, 5359000N and 5358500N showing structural form from surface mapping, and major fault trends.*	Page 49
Figure 4.6	*Contoured scatter plots of Stonehenge bedding showing a complete diversity of plot rather than clear trends.*	Page 50
Figure 4.7	*Scatter and contoured scatter plot of Stonehenge determined fold axis from poles to bedding.*	Page 52
Figure 4.8	*Scatter and contoured scatter plot of Stonehenge measured fold axis.*	Page 52
Figure 4.9	*Contoured scatter plots of Stonehenge measured cleavages showing 3 orientation: N-S, E-W and NW-SE.*	Page 53

Figure 4.10	*Fold interference patters. A. Type 1 interference folds, showing simple dome and basin interference patterns; B. Type 2 interference folds, showing arrowhead- or mushroom- shaped patterns; C. Type 3 interference folds showing wavy outcrop pattern of the S_1 axial surface. (from Twiss and Moores, 1992)*	Page 55
Figure 4.11	*Synclinal structures reflecting the occurrence of type 1 and type 3 fold interference patterns.*	Page 56
Figure 4.12	*Stereonet plots of bedding and fold axes for domain 25.*	Page 56
Figure 4.13	*Fold interference patters.*	Page 57
Figure 4.14	*F_1 fold hinge from field station MU96-169. So is folded about F_1, and S_1 is axial planar to the fold surface.*	Page 57
Figure 4.15	*Fold structure from station MU96-143. Plan: shows chevron-like folds with variable plunge, and cut by two sets of crenulation cleavages. Profile: shows chevron fold-form of varied plunge direction.*	Page 58
Figure 4.16	*Fold development within shales from station MU96-2. F_1 isoclinal folding in the limb of a later fold (F_2?).*	Page 59
Figure 4.17	*Folding from station MU96-35. Microlithon isoclinal folding within S_1.*	Page 59
Figure 4.18	*Box folding of a sandstone/shale sequence from ZS31, 162.1m. The fold has formed from differing layer competence. Microlithons represent first generation isoclinal folds along S_1. Quartz veins appear perpendicular to the core axis.*	Page 60
Figure 4.19	*A. Diagrammatic representation of axial surfaces developed within box-type folds. Dilation quartz veins exist within the centre confine of the box fold. The So/S1 fabric has been crenulated parallel to the axial plane. B. Photomicrograph from MU96-27 showing box folds within a sandstone. Both So and S1 have been folded by a later deformational event.*	Page 61
Figure 4.20	*Spaced cleavage development (S_1) within phyllite units. A. ZS31, 167.5m showing S1 sub-parallel to So; B. ZS31, 203m, showing S1 formation at low angle to So; C. Photomicrograph from station MU96-25..*	Page 63
Figure 4.21	*Possible sequence in the development of transposition layering (foliation). S_1 is the enveloping surface to the folds in bedding. S_2 is the transposition foliation. (from Twiss and Moores, 1992)*	Page 64
Figure 4.22	*Showing fold structures within shale/arenaceous sequences of ZS31.*	Page 65
Figure 4.23	*Transposition layering from ZS31, 90m. Isoclinal folding is seen parallel to both S_o/S_1.*	Page 66
Figure 4.24	*Crenulation cleavage development within Oonah Formation sequences.*	Page 67
Figure 4.25	*Styolite relationship to the direction of principal stress. (after McClay, 1987)*	Page 68
Figure 4.26	*Stylolite formation along bedding within shales from ZS31.*	Page 68

364139

Figure 4.27	*Representation of Reidel shearing associate with the Tenth Legion Fault.*	Page 69
Figure 4.28	*Proposed development models for the Tenth Legion and Balstrup Faults. A. Simultaneous (near) formation of each fault; B. Formation of each fault during separate thrusting events.*	Page 70
Figure 4.29	*Faults of the Stonehenge area.*	Page 71
Figure 4.30	*Quartz veining in quartzite outcrop from location MU96-213. As seen, the veins are often planar, intersecting at high angles, and are up to 4 cm in width. Vein orientations are: 139/65W and 070/80N.*	Page 72
Figure 4.31	*Veining within shales from ZS31, 92.5m As in outcrop, veins are planar, often forming thin fibres.*	Page 72
Figure 4.32	*First and second generation veins. The latter later folds are intersected by fault movement and stylolite formation sub-parallel to the core axis.*	Page 72
Figure 4.33	*En Echelon vein development and infilling of tension gashes developed within brittle sequences during folding.*	Page 73
Figure 4.34	*Implosion or phreatomagmatic breccia from ZS1, 86.9m. Wall rock fragments have been emplaced into magmatic fluids following significant changes in fluid pressure..*	Page 74
Figure 4.35	*Tectonic breccia zone from ZS31, 203m..*	Page 74

CHAPTER 5. MINERALISATION OF THE STONEHENGE AREA

Figure 5.1	*Discovery dates and production periods for the major ore deposits of Tasmania. (after Large, 1989)*	Page 75
Figure 5.2	*Mount read Volcanic belt of Tasmania.*	Page 76
Figure 5.3	*Resource estimates, occurrence and granite association of principal mid-Palaeozoic ore deposits. (Collins, Brown, Dronseika and Morland, 1989)*	Page 79
Figure 5.4	*Geology and mineralisation from wacker sampling.*	Page 82
Figure 5.5	*Graphs of zinc assays and stratigraphic logs for drillhole ZS1, ZS2, ZS3 and ZS31 show a stratigraphic control upon mineralisation.*	Page 85
Figure 5.6	*Veining orientations and estimated occurrence for drillhole ZS31.*	Page 86
Figure 5.7	*Pyrite mineralisation within black shale from ZS31, 124m*	Page 87
Figure 5.8	*Mineralisation of sphalerite, pyrite and minor galena within quartz-carbonate veining. The dolomite sample is from ZS1, 155.8m.*	Page 87
Figure 5.9	*Sphalerite, pyrite and minor galena mineralisation within brecciated zone of black shale from ZS1, 74.5 metres.*	Page 88

364140

Figure 5.10	*Dolomite from ZS1, 161 metres, showing post mineralisation fault dislocation. Movement parallel to the core axis has offset to pyrite zone by approximately 30mm.*	Page 88
Figure 5.11	*Groundmagnetic image of the Stonehenge area.*	Page 90
Figure 5.12	*Contour map depth to granite body between the Heemskirk and Pine Hill areas. (after Leaman, 1986a; Bramford and Green, 1986)*	Page 91
Figure 5.13	*General model for zinc skarn zonation (after Meinert, 1987).*	Page 92
Figure 5.14	*Massive pyrite mineralisation found within dolomite and shale horizons of ZS31.*	Page 94
Figure 5.15	*The photomicrographs clearly demonstrates the variation in Fe-content reflecting in zonation of the sphalerite grains.*	Page 95
Figure 5.16	*A. Sphalerite from ZS1, 120 metres showing iron zonation similar to Grubb's Workings. Later fracturing (cleavage development?) is evident at the bottom of the photomicrograph; B. Sphalerite and pyrite from ZS2, 101 metres within quartz veins; C. Cubic galena and cubic to sub-octahedral pyrite grains generally within quartz veins, but also present as fine disseminations within the country rock.*	Page 96
Figure 5.17	*Siderite alteration of quartz-carbonate veins producing a fawn colouring.*	Page 97
Figure 5.18	*Photomicrograph of quartzite from station MU96-100. Siderite alteration.*	Page 97

Chapter 6. DISCUSSION

Figure 6.1	*Thrust emplacement of the Oonah Formation during the Middle Cambrian to late Devonian.*	Page 100
Figure 6.2	*Simplified geology of western Tasmania showing the distribution of MUC and location of Tyennan and Rocky Cape Regions. (Berry and Crawford, 1988; after Brown, 1986 and Williams, 1976)*	Page 102
Figure 6.3	*Tectonic models proposed for the development of Cambrian geology in Tasmania. (Corbett, 1989)*	Page 104
Figure 6.4	*Schematic section (E-W) showing the evolution of Tasmania from Cambrian to the present. (Crawford and Berry, 1988)*	Page 105
Figure 6.5	*Comparison between structure of the Semail Ophiolite, Oman and the Middle Cambrian structure of Tasmania as proposed by Crawford and Berry. (Crawford and Berry, 1988; Hopson et al., 1981; Manghnani and Coleman, 1981)*	Page 106
Figure 6.6	*Interpretative model of black shale horizons surrounding mineralised horizons at Stonehenge.*	Page 110

364141

CHAPTER 1.

Introduction

364142

1. INTRODUCTION

1.1 FORWARD

This thesis evaluates the results of detailed study of the structure and mineralisation of the Stonehenge prospect area near Zeehan in Tasmania. The dominant lithology includes deformed Proterozoic Oonah Formation sequences of siltstone, shale, sandstone, dolomite/dolomitic sediment and quartzite. Cambrian Dundas Group sediments to the south, and Crimson Creek Formation units to the north form fault contacts with the older stratigraphy. The Proterozoic sequence continues north of Zeehan, to form the oldest geologic successions of Tasmania. Zeehan lies along the western margin of the Dundas Trough, one of the most important structural features of Tasmania's geology, and host to several world class mineral deposits.

The complex structure surrounding Zeehan reflects several phases of deformation. The earliest event within the local Proterozoic sequences is the polyphase Penguin Orogeny (700-750Ma) (Turner, 1989). Cambrian development of western Tasmania has involved postulation of many theories including formation models for the Dundas Trough of: a rift environment (Campana and King, 1963; Corbett, 1972), plate subduction (Corbett and Lees, 1987; Green, 1983), and the allochthon emplacement of Cambrian sequences (Berry and Crawford, 1989). Additional study by Woodward, Gray and Elliott (1993) in the northwest of Tasmania supports allochthon movement. With continued folding and faulting during the Devonian ('Tabberabberan Orogeny') dislocated dome and basin-type structures, and thrust fault contacts within the Oonah Formation have formed.

Extensive mineral exploration throughout the area has been conducted since the turn of the century. Activity throughout the Zeehan area during the late 1800's to early 1900's saw the extraction of significant amounts to tin, silver, lead and zinc from numerous small lode workings and larger scale shaft operations. Current exploration at Stonehenge is focussed upon zinc mineralisation seemingly restricted to shale and dolomitic horizons of the Oonah Formation. Fluids Cambrian volcanism (VHMS) and Devonian granite intrusions have been identified as the primary agents for mineralisation throughout the west coast. In close proximity to Stonehenge, the Heemskirk Granite is the largest intrusive body, situated 3-4 kilometres northwest of Zeehan.

364143

1.2 PROJECT AIMS

The aims of this project are:

- To produce a detailed geological and structural map of the Stonehenge area.
- To identify and interpret the major structural elements at mesoscopic and microscopic scale.
- To investigate the style and extent of mineralisation throughout the Stonehenge area.
- To evaluate the relationship between structure and local mineralisation.
- To develop a model for the structural evolution of the Stonehenge area.
- To relate the structure present at Stonehenge to that of the recorded regional geology

1.3 PHYSIOLOGY

The Stonehenge prospect area is located approximately 2 kilometres southwest of Zeehan on the west coast of Tasmania. Zeehan is easily accessed from Burnie to the north via the Murchison Highway. Access to Stonehenge requires 4 wheel drive transport along the historical tramways which form the basis of many roads throughout the region. Mapping is concentrated on Proterozoic Oonah Formation sequences within bounding coordinates of 357000mE 5360500mN, 361000mE 5360500mN, 357000mE 5357600mN and 361000mE 5357600mN.

Rock outcrop throughout the west coast of Tasmania is generally minimal. At Stonehenge, sharply undulating quartzite hills across the southeastern margin host maximum exposure. Following the north boundary and along creek valleys, native vegetation forms thick barrier through which movement is near-impossible (figure 1.3), however the general low-relief grass coverage enable near-complete coverage of the prospect by foot.

The McClean creek is a perennial water body flowing from east to west through the southern Stonehenge area. This is intersected by a tributary flowing from the north through the centre of the quartzite unit.

364144

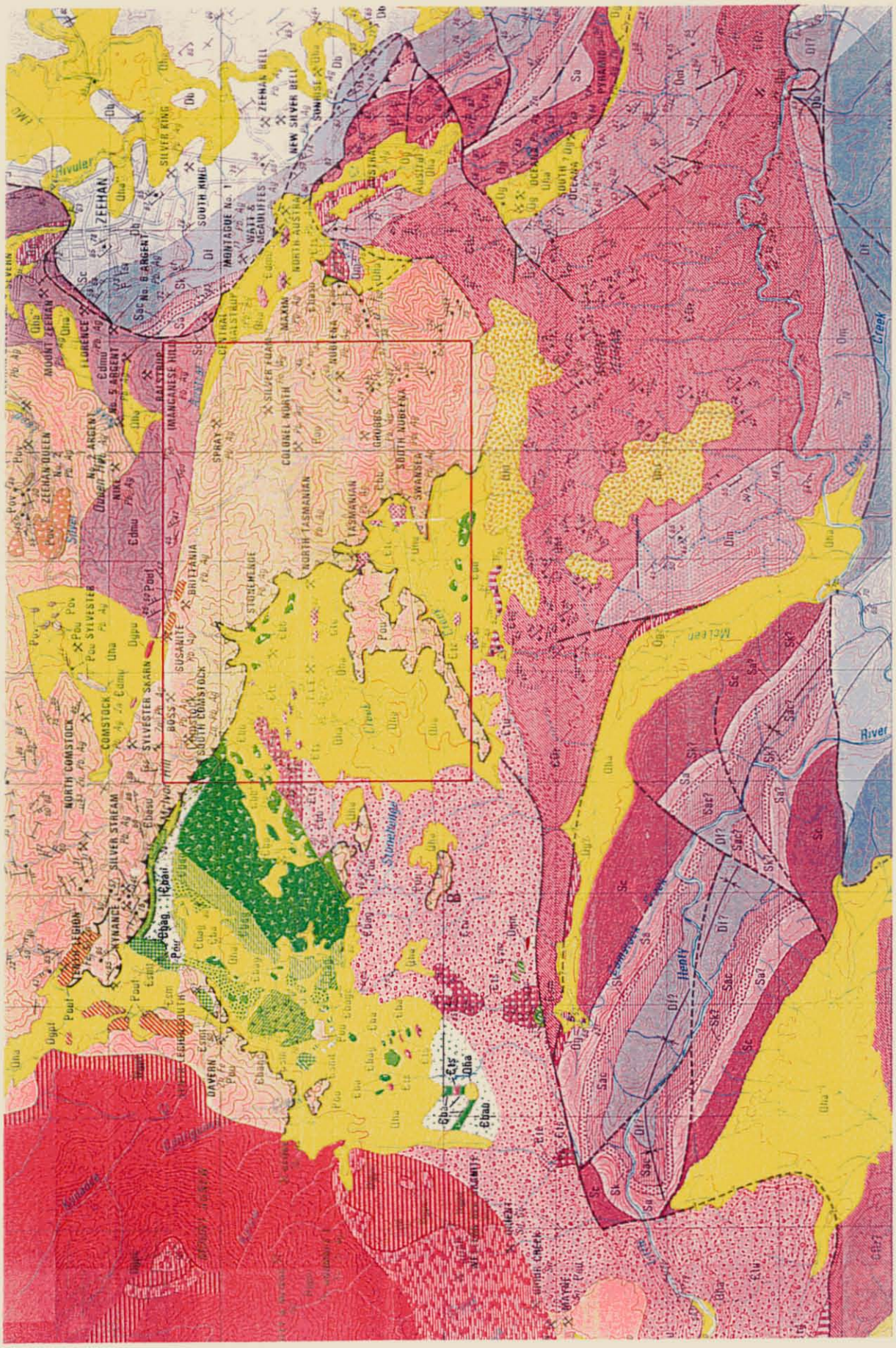


FIGURE 1.1 *Geology surrounding the Stonehenge area from the ZEEHAN 1:50 000 map sheet (7914S (50))*

364145

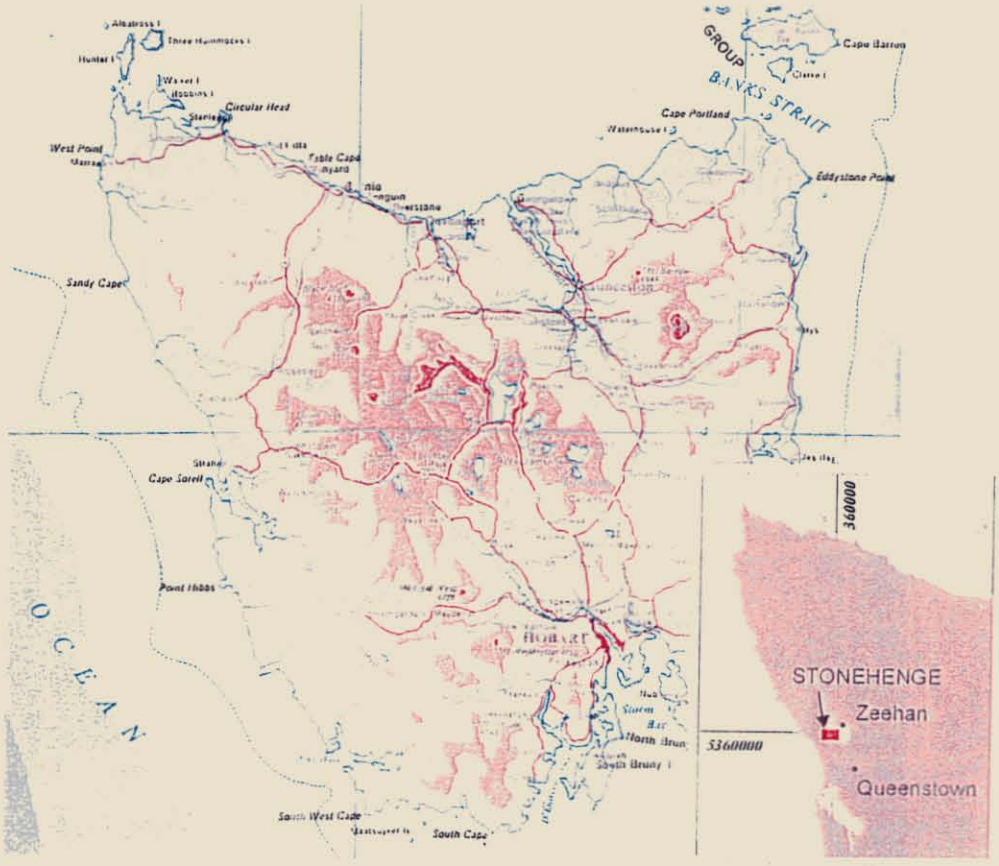


FIGURE 1.2 *Location of the Stonehenge area.*

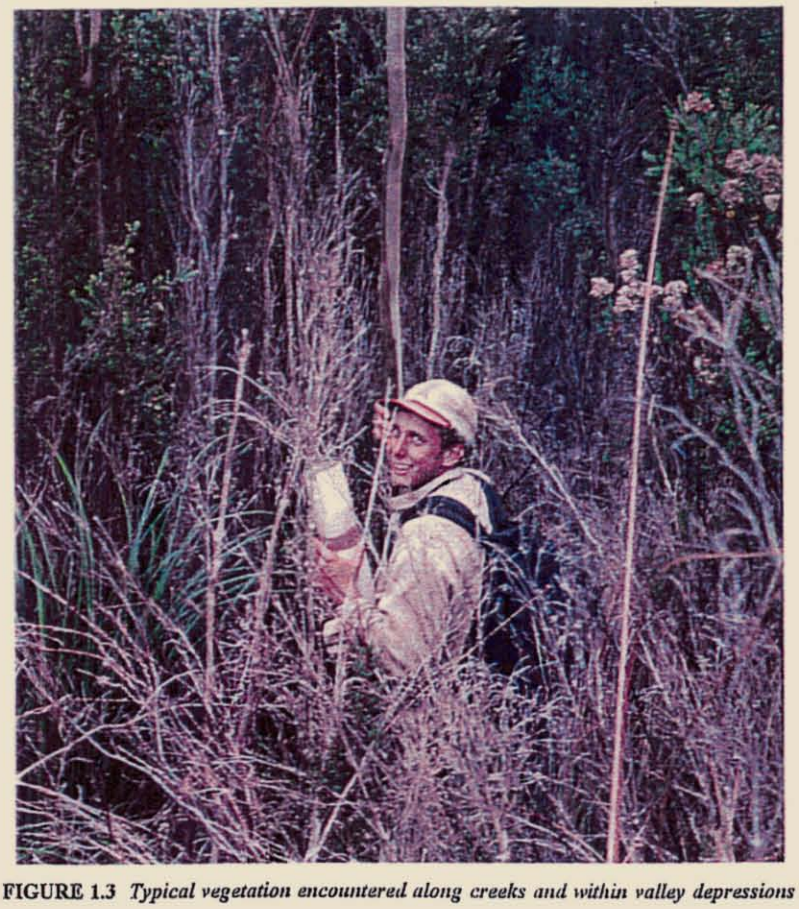


FIGURE 1.3 *Typical vegetation encountered along creeks and within valley depressions throughout the Stonehenge area.*

1.4 INVESTIGATION TECHNIQUES

364146

The primary investigative technique has involved field mapping. This was conducted over a four week period during February-March 1996. During this time, field operating condition are at a peak throughout the west coast of Tasmania, enabling maximum benefit to gained. Road cuttings, tramways and historical workings provided valuable outcrop through the generally vegetated area. Mapping within the field was recorded onto an aerial photograph base (approximately 1:10000 scale) and later transferred to drafted 1:5000 scale maps. Also during this period, four CRA Exploration drillholes (ZS1, ZS2, ZS3 and ZS31), and 27 aircore samples were logged. Stratigraphic and structural information has been obtained from the core, although none of the holes were orientated during drilling. Field records and drillhole logs have been tabulated in Appendices 1 and 3 respectively. A number of techniques have been sought to expand upon field data, and gain a wider understanding of the complex geological environment of Stonehenge. These include:

- Stereonet analysis
- Mineralogical and microstructural analysis
- Geophysical interpretation (regional and local)
- Aerial photo interpretation
- Literature research

1.5 PREVIOUS WORK

Little detailed structural analysis has been conducted over the Stonehenge area. Blissett's (1962) Geological Survey Report (One Mile Map Series, K'55-5-50) investigation of the Zeehan area incorporated the geology and nature of historical workings at Stonehenge. He identified the Proterozoic Oonah Quartzite and Slate (Oonah Formation), and recorded fault contact with Cambrian sequences to the north and to the south via the Balstrup and Tenth Legion Faults respectively. His study of mine activities concluded that lead, zinc and silver ore deposits at Stonehenge were generally extracted from galena, pyrite and sphalerite within a quartz-siderite gangue. Blissett also identified major structural fold trends throughout the Zeehan area along northwest-southeast axes as products of Devonian 'Tabberabberan' folding. More recent evaluations of geology, deformation and mineralisation throughout Tasmania are recorded in the *Geology and Mineral Resources of Tasmania*, edited by C.F. Burrett and E.L. Martin, 1989.

In recent years, exploration by Gold Fields Exploration and later CRA Exploration enabled breakdown of the Oonah Formation stratigraphy into specific horizons. A Gold Field Exploration drillhole intersecting mylonite supported theories that the Tenth Legion Fault was flat lying, and that the Oonah Formations stratigraphic overriding of Cambrian sequences was the likely product of thrust emplacement. To date, these investigation have been primarily focussed of geological mapping, and subsequently no detailed structural investigation of the area has been conducted.

364147

CHAPTER 2.

Geology

364148

2. GEOLOGY

2.1 INTRODUCTION

Geographically, Tasmania is relatively small in area, but it is host to a variety of geology and an exceptional array of mineral deposits. A distinct juxtaposition appears between the geology from west to east (figure 2.1). Pre-Carboniferous folded rocks and middle Palaeozoic granitoids in western Tasmania (Western Tasmania Terrain) and eastern Tasmania (Eastern Tasmania Terrain) are separated by the Tamar Fracture System (figure 2.2). This NNW trending dislocation formed during a period of post-Devonian granitoid to pre-Pareemer Supergroup emplacement.

Pre-Tamar Fracture System

Throughout the Western Terrain, Eo-Cambrian and Cambrian sediments and volcanics have accumulated within a number of 'troughs' overlying Precambrian basement rocks. Precambrian regions and inliers separating the 'troughs' include sedimentary successions, of generally low metamorphism to greenschist and higher facies. It is generally considered that the metamorphic rocks formed during orogenic activity prior to deposition of the comparatively unmetamorphosed sedimentary sequences, although they may been of the same orogenic pile. Eo-Cambrian and Cambrian 'troughs' developed during rifting of a Precambrian crust. The largest depositional basins consist of the meridional Dundas and Dial Range Troughs. Shallow water 'trough' deposits have been followed by deeper water turbiditic successions. Ultramafic-mafic suites of an island arc affinity present within Cambrian sediments are likely to have emplaced during westward thrusting events. The Mount Read Volcanic belt exists along the eastern margin of the Dundas Trough. This is one of the most mineralised provinces of its kind, containing VHMS deposits formed upon the sea floor during volcanism. Late Cambrian uplifting of Precambrian rocks and overlying sediments signifies completion of subduction resulting from continent/continent collision at the site of the future Tamar Fracture System (Williams, 1989). Subsequent deformation of older sequences and deposition of siliclastic alluvial fan and shallow marine units (including dolomites) resulted. Economically important carbonate sequences display rapid facies change and minimal emplacement deformation. Lower Silurian to Lower Devonian siltstone and quartz sandstone deposits overlying the carbonates accumulated in a shallow marine environment. Lower Devonian and older rocks have been extensively deformed during movements of the 'Tabberabberan Orogeny' of eastern Australia or correlate tectonic event. The Cambrian uplifts of Precambrian rocks have behaved as relatively competent blocks during two phases to Devonian deformation (Williams, 1989). The first phase produced folds within zones of closure between converging blocks, the second developing northwest and north trending folds. Middle Palaeozoic granitoids intruding much of the Western Tasmania Terrain are associated with middle Palaeozoic ore deposits of scheelite-bearing skarn, cassiterite-stannite-pyrrhotite carbonate replacement bodies, argentiferous lead-zinc veins and possibly some gold occurrences.

364149

The oldest rocks of the Eastern Tasmania Terrain are Ordovician and Devonian quartzwacke turbidite successions of lutite and lutite/arenite association derived from a source to the southwest. The timing of these sedimentary rocks correlates with the platform carbonates and clastic deposits of the Western Terrain. Folding events are also equivalent to those of the Western Terrain, although here they have resulted from transportation from the southwest. Middle Palaeozoic granitoids post-date plutons of the Western Terrain, and have been emplaced at a high level into the folded rocks. Tin-greissen and tin-tungsten vein deposits are important associations.

Post-Tamar Fracture System

Following sinistral lateral movement of the Tamar Fracture System, Tasmania formed part of a craton. Erosion and subsidence initiated formation of the Tasmania Basin and subsequent accumulation of Parmeener Supergroup sediments of Carboniferous to Triassic age. Continued subsidence along the fracture system enabled deposition of Carboniferous to Permian glacigene and glacimarine sequences, indicating marine transgression from the southeast. Extensively dolerites of Jurassic age have formed from small feeders within the Parmeener Supergroup. Sea-floor spreading between Australia, Antarctica and New Zealand commenced in Cretaceous times. Rifting associated with the dispersal of Gondwana produced early Cretaceous basin within the continental crust. Containing fresh water and shallow marine sequences, these basins have a high hydrocarbon potential. The crustal detachment between Australia and Antarctica opened eastward, and preceded marine transgression reaching offshore basins along the west Coast of Tasmania by late early Cretaceous, and the Bass Basin by late Palaeocene.

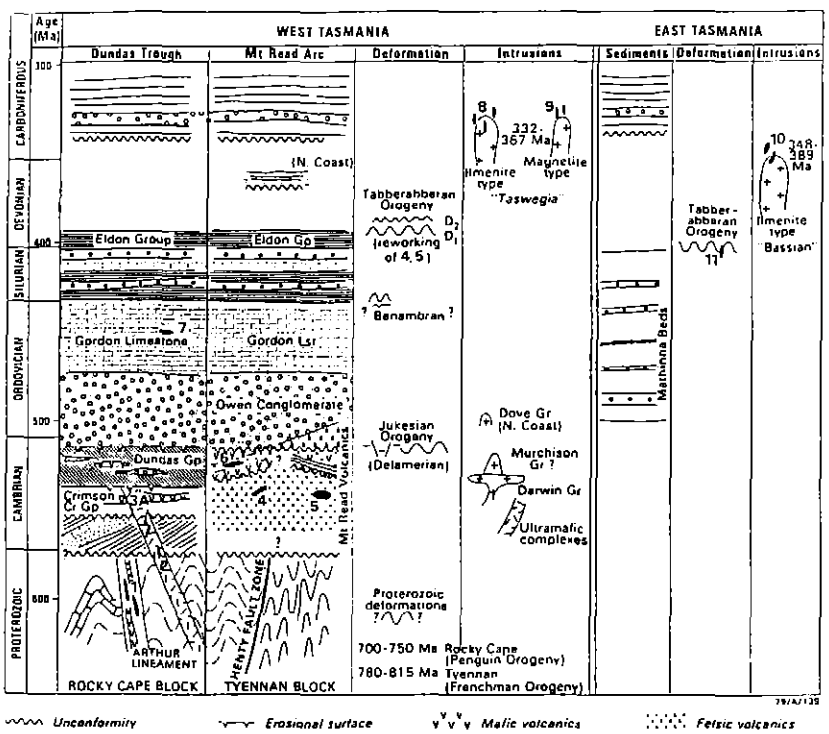


FIGURE 2.1 ***Simplified stratigraphy showing the major events of the Lower Palaeozoic in Eastern and Western Terrains. (Solomon and Groves, 1994)***

364150

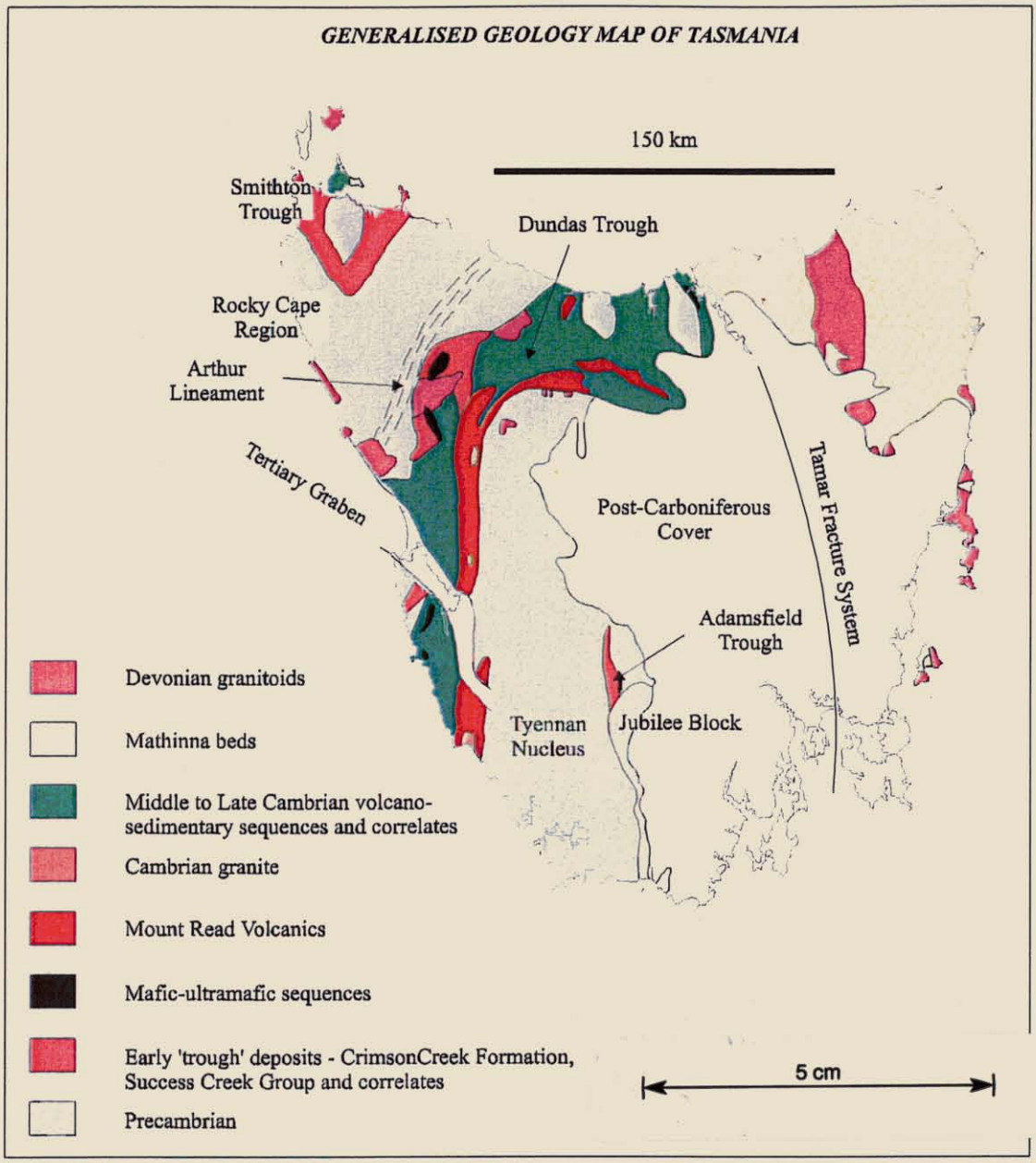


FIGURE 2.2 *Generalised geology map of Tasmania. (after Corbett and Turner, 1989)*

2.2 REGIONAL GEOLOGY

2.2.1 Precambrian

Tasmania's Precambrian rocks form the basement of much of Tasmania's geology, in particular throughout the west coast. The later Precambrian rocks are commonly at angular unconformity to the older units. Deformation is associated with the Penguin Orogeny (Williams *et al.*, 1976; Williams, 1976), a polyphase deformation period thought to have commenced 700-750Ma (Adams *et al.*, 1985). Rocks predating the Penguin Orogeny underlie around one fifth of Tasmania (figure 2.3), primarily throughout the western margins.

364151

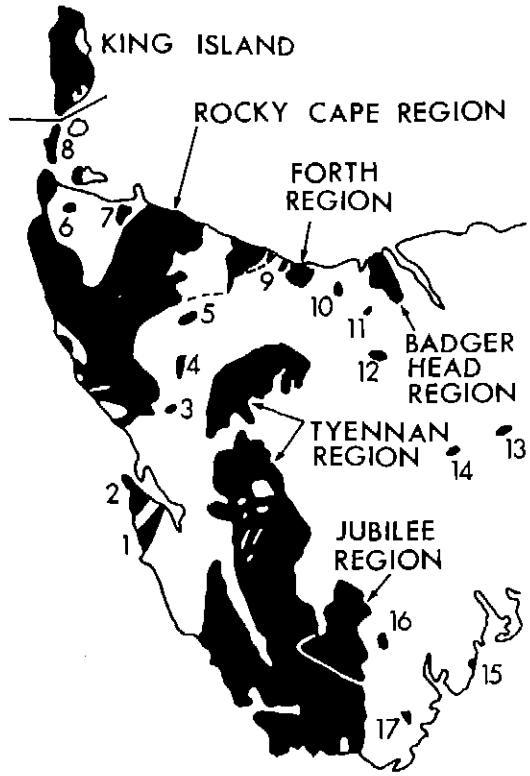


FIGURE 2.3 *Distribution of rocks post-dating the Penguin Orogeny. Inliers included are: Moddar River (1), Cape Sorell (2), Dundas (3), Ramsay River (4), Mount Bischoff (5), Welcome-Montagu (6), Briant Hill and Lake Mikany (7), Goat Island (9), Great Bend (10), The Avenue Road (11), Native Hop Hill (12), Glovers Bluff (16) and Hastings (17). Precambrian rocks also exist on several islands of the Hunter group (8), and have been found in drillholes at Ross (13), Interlaken (14) and Woodbridge (15). (Turner, 1989)*

Predominantly of sedimentary origin, rock of all Precambrian inliers vary from relatively unmetamorphosed sub-greenschist facies sequences containing slaty pelite, through greenschist and amphibolite sequences of phyllitic and schistose pelite to sequences of kyanite- and sillimanite-bearing gneisses and eclogite (Turner, 1989).

Different Precambrian inliers through northwest Tasmania combine to form the Rocky Cape region. Often overlain by unconformities, the region is host to a variety of lithological associations. Shallow marine, relatively unmetamorphosed, quartzarenite, siltstone, mudstone and subordinate dolomite present in the west have been stratigraphically sub-divided into the Rocky Cape Group (north coast) and the Interview Siltstone (near the Pieman River). To the east are younger, deeper water, turbiditic quartzose sandstone, slate and minor mafic lava (alkali basalt). Towards the north coast of Tasmania is the Burnie Formation. This unit is stratigraphically equivalent to the Oonah Formation present throughout the west coast region. The eastern and western associations are separated by the Arthur Lineament, a tectonic feature produced during the Penguin Orogeny. This high strain greenschist to amphibolite facies metamorphic belt exhibits structurally and metamorphically transitional boundaries with lithological associations to either side (east and west). A third association of mafic intrusives (tholeiitic) containing sediments of pelitic, dolomitic and quartzose compositions generally influence the metamorphic complex. Tectonic over-riding from the west is evident in the Rocky Cape, Tyennan, Jubilee and Badger Head regions, suggestive of syndeformational metamorphic ages close to or within the Penguin Orogeny (Turner, 1989).

Depositional event correlations have identified lithological associations similar to that of the Western Rocky Cape, to form much of the unmetamorphosed Tyennan and Cape Sorell regions, and the relatively unmetamorphosed Jubilee region. Lithological associations similar to the Burnie Formation underlie the Badger Head region and smaller inliers such as at Dundas and Mt. Bischoff. Metamorphic rocks of the Tyennan and Forth regions are divided into: lower greenschist facies quartzite-chloritic pelite assemblages, and upper greenschist to eclogite facies garnetiferous schist-quartzite assemblages, producing a juxtaposition between thrusted orogenic pile and rocks drawn from depths exceeding 30 kilometres.

2.2.2 Eo-Cambrian-Cambrian

Eo-Cambrian-Cambrian rocks of Tasmania comprise two associations. The older unconformably overlies Penguin Orogeny deformed rocks, and contains basal units of the Dundas Trough and Smithton basin succession. Incorporated are the Success Creek Group (Taylor, 1954) of shallow water terrigenous sequences and the Crimson Creek Formation (Taylor, 1954) grading into turbiditic, volcaniclastic, sedimentary rocks with interbedded basic volcanic lava flows. Contact between associations in the Dundas Trough appear faulted, with a carbonate sequence conformably separating the association within the Smithton basin.

Rocks of the Dundas Trough indicate deformation by Devonian fold phases and associated cleavages. Brown (1986) has identified emplaced, layered, orthopyroxene-rich ultramafic rocks and volcanic sequences within the Dundas Trough, evident of middle to late Cambrian tectonic activity. Success Creek Group rocks exist within an elongated area between the Mt. Lindsay and Renison Bell. Devonian faults dominate along the southwest margin, and faulted or conformable contact with the Crimson Creek Formation along the northeastern margin. Throughout the Pieman River, Success Creek Group basal rocks unconformably overlie rock sequences of the Oonah Formation. The base of the Success Creek Group is a combination of poorly sorted, immature, polymict conglomerate with sandstone lenses (Taylor, 1954; Brown, 1986). Greatest exposure along the Pieman River shows a primary composition of locally derived Oonah Formation material, mixed with minor, well-rounded quartzite and chert cobbles. Lenses of silt and coarse sand-grade material appear subparallel to bedding in the overlying sandstone sequence. Taylor (1954) identified a succession of compact mudstone with volcaniclastic and lava horizons, and defined it as the Crimson Creek Argillite. Brown (1986) also located a volcaniclastic lithic greywacke sequence within the Crimson Creek Formation.

The eo-Cambrian-Cambrian period has hosted three or more phases of basaltic-andesitic (mafic) volcanism, and several phases of andesitic-rhyolitic (felsic) volcanic rocks of the Mt. Read Volcanics throughout western Tasmania (Turner, 1989). The earliest mafic volcanic phases produced sub-alkaline to tholeiitic basal suites within the Crimson Creek Formation, with correlates found in the Smithton Basin. Petrographically similar rocks occur within the Cleveland-Waratah area.

364153

Associated suites of high magnesium andesite (HMA) lavas and low titanium, tholeiitic, basalt-andesite (LOTI) lavas, representing a second and third volcanic phase respectively.

The Mt. Read volcanics occur extensively throughout the west coast of Tasmania. This belt of felsic, intermediate and minor mafic volcanics overlap Tyennan Precambrian rocks to the east, mix with Cambrian sedimentary sequences to the west, and are overlain by Cambrian-lower Ordovician siliclastic Owen Conglomerates. The sequence primarily contains rhyolites, dacites and andesites, with occasional basalts. The Mt. Read Volcanics tend to be high-K to medium-K calc-alkaline volcanics, not unlike Andean-type continental margin oceanic suites (Corbett and Solomon, 1989). The volcanics tend to be altered, folded and cleaved to varying degrees. Hydrothermal alteration zones adjacent to major faults contain highly schistose and altered rocks. Ultramafic rocks of Tasmania are representative of three different magmatic phases. Prevalent throughout western Tasmania, eo-Cambrian-Cambrian ultramafic rocks are orthopyroxene rich. This is a distinguishing feature from dominantly clinopyroxene-rich sequences generally associated with mid-oceanic ridge and back-arc environments (Brown, 1989). The three recognised ultramafic-mafic rock associations are: a Layered Pyroxenite-Dunite (LPD) succession; a Layered Dunite-Hedenbergite (LDH) succession; and a Layered Pyroxenite-Peridotite and associated Gabbro (LPG) succession (Brown, 1986).

Fossiliferous units of mid to upper Cambrian age are present in the Dundas, Fossey Mountain, Dial Range, Beaconsfield and Adamsfield Troughs, the Smithton basin, the Rocky Boat Inlet-Surprise Bay area of the south coast and within sedimentary rocks associated with the Mt. Read Volcanics (Jago and Brown, 1989). The Dundas Group is host to the best known successions of Cambrian Faunas; present within an environment of two distinct fault juxtaposed (now) successions, possibly originally separated by hiatus or a period of shallow water deposition. Basal margins of the Dundas Group are ambiguous. Although the known boundaries between the Dundas Group and the Crimson Creek Formation are faulted, Brown (1986) proposes that the lower margins off the Dundas Group Succession were deposited upon tectonically emplaced ultramafic bodies, in an area of active low titanium tholeiitic volcanism. Brown has incorporated five formations after Elliston (1954) for the 'lower' Dundas Group succession: the Judith Formation of interbedded siltstone, sandstone and granule conglomerate with minor lithic wacke and turbiditic cobble conglomerate; the Red Lead Conglomerate consisting of poorly sorted, volcaniclastic, polymict conglomerate units of mass flow origin, interbedded with lenticular siltstone and sandstone horizons and rare pillow lavas; the Hodge Formation consisting of dark-grey to black indurated siltstone and minor lithic sandstone horizons occasionally graded; the Razorback Conglomerate conformably overlying the Hodge Formation is a well-rounded sequence of grey, green and greyish-white, turbiditic, chert-clast conglomerate with interbedded siliceous siltstone and sandstone; 'lower' Brewery Junction Formation gradationally overlying the Razorback Formation consists of unfossiliferous, thinly bedded and laminated grey and grey-green siltstone and sandstone with occasional granule conglomerate lenses.

364154

Brown (1986) considers the 'upper' Brewery Junction Formation as the start of a continuous succession of formations overlying the Brewery junction Formation: The 'upper' Brewery Junction Formation of interbedded purple, arenaceous siltstone with minor sandstone lenses; Fernfields Formation (Elliston, 1954) of irregularly alternating coarse and fine pebble conglomerate grading into granule conglomerate and sandstone with interbedded siltstone laminae; Comet Slate consists of thinly interbedding siltstone, mudstone and sandstone; Fernflow Formation of pebble to boulder conglomerate with interbedded purple siltstones; Climie Formation (Elliston, 1954) consists of purple and green laminated siltstone with thin interbeds of grey and grey-green lithic wacke and occasional conglomerates; Misery Conglomerate (Elliston, 1954; Williams, 1975) consists of thick-bedded red pebble to boulder conglomerate interbedded with graded sandstone, siltstone and mudstone units.

2.2.3 Cambrian Mount Read Volcanics

The Mt. Read volcanic belt (figure 2.4) is regarded as one of the most intensely mineralised zones of its type. Between Mt. Darwin and Hellyer mine, the complex stratigraphic and structural controls host base and precious metal orebodies of the Hellyer, Que River, Rosebery, Hercules and Mt. Lyell mines (Corbett and Solomon, 1989). The NNE trending Henty Fault is the major structure, longitudinally bisecting the volcanic belt. Three volcanic sequences are associated with the Mt. Read volcanic belt. Northwest of the Henty Fault, the Central Volcanic Complex (CVC) contains an early sequence of feldspar-phyric lavas and ignimbrites. This is overlain by mid to late Cambrian tuff, greywacke, siltstone and shale. A latter sequence includes andesitic and basaltic volcanics host to the Que River and Hellyer orebodies. East and south of the Henty Fault, feldspar-phyric lavas and pyroclasts dominate the CVC. The western margin contains volcano-sedimentary tuff, shale and greywacke with intercalated felsic to mafic lavas and intrusions. A third volcanic sequence, the Tyndall Group, overlies the CVC and western margin southeast of the Henty Fault. The group contains quartz-feldspar-pyric-lavas and pyroclasts with local volcaniclastic conglomerates.

Cambrian calc-alkaline rhyolitic to andesitic Mt Read Volcanics are critical in understanding the Lower Palaeozoic history of Tasmania. Interpretation of the unique geology is hampered by Devonian deformation overprinting pre-existing structures, obscuring stratigraphic and structural relationships. Recognition through mapping and confirmation by drilling of a major thrust fault at the margin of the volcanics is a significant development. Mapping has provided evidence for deformation of some of the sequences in the Cambrian - suggesting former subduction zone in the Rosebery Area (Corbett and Lees, 1987; also in agreement with work by Green, 1983).

364155

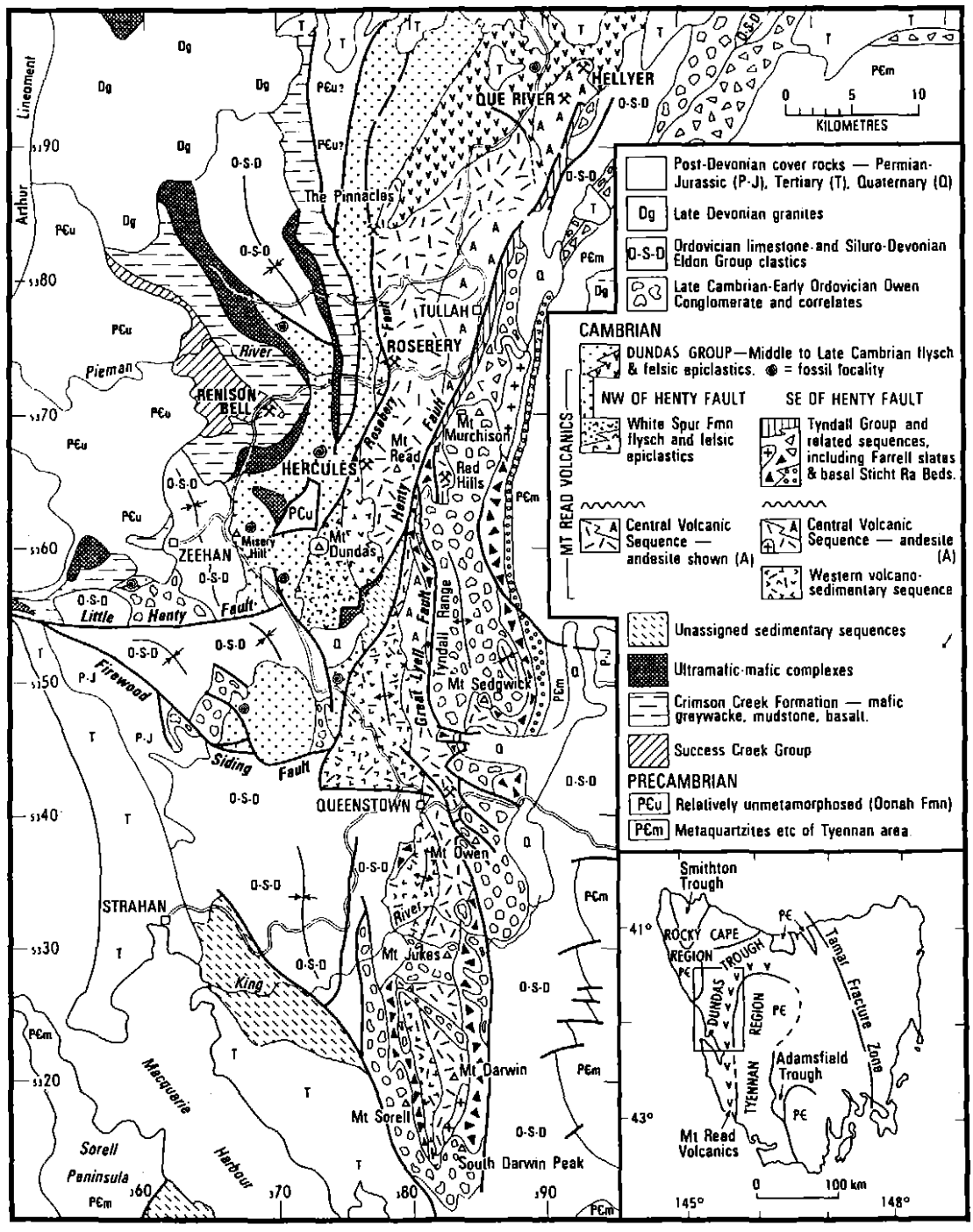


FIGURE 2.4 *Geology of western Tasmania showing the Mount Read Volcanics between Hellyer and Mount Darwin, and associated Dundas Trough sequences. (Corbett and Lees, 1987)*

5 cm

General settings for Mount Read Volcanics

Cambrian sequences occupy irregular areas or 'troughs' between, around and occasionally above Late Precambrian basement rocks. The largest such area is the Dundas Trough, between the Tyennan Region (generally of quartzites and schists to garnet-amphibolite grade) to the east, and the Rocky Cape Region (multiply folded relatively metamorphosed sediments) to the northwest.

364156

Mount Read Volcanics are present along the eastern margin of the trough. The Dundas Trough sequence is divided by Corbett and Lees as:

1. area lacking felsic volcanics and tied depositionally to the Rocky Cape region, and
2. area containing Mount Read Volcanics and associated volcano-sedimentary sequences (including Dundas Group) and attached to the Tyennan Region.

The basal unit of the western succession, the Success Creek Group, is a shallow marine sequence of sandstone, mudstone and dolomite of likely Vendian age, and is considered to rest unconformably on Rocky Cape basement rocks (Brown, 1980). Thick sequences of mafic greywacke, mudstone, tholeiitic basalt (including pillow lavas) and chert forming the Crimson Creek Formation conformably overlie. Various gabbroic and ultramafic-mafic complexes (containing high-MgO andesites and low-TiO_2 basalts; Brown, 1980) appear within this unit and the adjacent Dundas Group.

The Dundas Group of sediments contains felsic volcanic detritus derived from Mount Read Volcanic sequences. Middle Middle Cambrian to middle Late Cambrian fossils have been identified by Jago (1979). East of Mount Dundas, the sequence rests unconformably upon the Mount Read Volcanics, whilst to the north, contact is marked by the east-dipping Rosebery Thrust Fault (Corbett and Lees, 1987).

The north-northeast trending Henty Fault System has divided the volcanic belt into two regions. Significant variations in stratigraphy and composition exist across the fault system. The volcanics have undergone lower greenschist facies metamorphism, producing quartz-sericite-cholite-pumpellyite-epdote-actinolite assemblages. South and east of the Henty Fault, much of the volcanic belt is overlain by Owen Conglomerates. A derivative of Tyennan Precambrian rocks, this thick sequence of siliclastic shallow marine to fluvial conglomerate and sandstone ranges in age from middle Late Cambrian to Early Ordovician. Overlying (conformably) is an Ordovician limestone sequence (Gordon Limestone); transgressive across the Dundas Trough and surrounding basement areas. The Eldon Group of shallow marine clastic sequences conformably overlies in most areas, and is of Silurian to Early Devonian age.

A major period of folding, faulting and cleavage development in the late Early Devonian to Middle Devonian produced folds of north-south and northwest trends in western Tasmania (Williams, 1978). Widespread intrusion of granitoid bodies followed in Late Devonian, occasionally with associated economic tin-tungsten mineralisation.

364157

2.2.4 Late Cambrian to Devonian

A distinct contrast exists between Tasmania's eastern and western terrains dominated during a period of late Cambrian to Devonian. Middle Cambrian and older volcanic, sedimentary and metamorphic rocks of the western margins are overlain by slope deposits. Widespread uplift of Precambrian rocks has produced alluvial-fans and/or local scree breccias, occasionally overlapped by shallow-water marine sands (Banks, 1989). Movement associated with Cambrian uplift produced folding and cleavage locally; remnant of the Jukesian Orogeny.

The Eastern Terrain contains an early Ordovician lutite sequence. Now cleaved and folded, this distal turbidite succession is likely to have formed upon a continental slope. Early Devonian lutite and arenite sequences have been folded and eroded, often producing surface breccias. Middle Devonian rhyolitic flows may overlie, and late Devonian granitic margins have occasionally intruded the complete sequence.

2.2.5 Late Carboniferous-Triassic

Parmeener Supergroup rocks of this age generally lie unconformably upon late Devonian granites and older folded sequences. In contrast to the metamorphosed Precambrian rocks of the Tyennan region and folded Devonian rocks of northeast Tasmania, Arthur Lineament and Tamar Fracture System rocks were eroded by glaciers during this period, producing regions of low relief (Banks, 1989).

Marine beds deposited throughout the Tamar Fracture System suggest minor downwarping through this area. Widespread paraconformity supports slight uplift thought to have occurred during formation of the Mersey Coal Measures. Eastern Tasmania experienced minor uplift in the early Lymingtonian, although generally receiving a lesser amount of sediment in late Permian and Triassic than the western counterparts. During this period, the Tamar Fracture System sank at comparatively greater rates than others within Tasmania. Cuspate shards and abundant feldspars in southeastern Tasmanian rocks of this age suggest some nearby volcanism.

Rocks of the Lower Parmeener Supergroup are primarily siltstone with coarser-grained rocks forming marginal facies or occasional widespread incursions. Marked change in grainsize occurred during late Permian uplift within source areas around the basin, whilst intermittent phases of late Permian and Triassic uplift enabled successive phases of sand deposition.

2.2.6 Jurassic-Cainozoic

Tholeiitic dolerites dominate mid-Jurassic rock units across Tasmania. The crustal-type magmas were silica-saturated upon emplacement, unlikely to have been derived by partial-melting of typical upper mantle. During late Mesozoic and Cainozoic, several extensional sedimentary basins formed. Both events are thought to have been associated with the breaking of the Gondwana supercontinent. Basins in the west margins of Tasmania and in the South Tasmanian Rise have possible formed through a complex association of extensional and wrench-related phases of movement (Wilcox, 1986).

For example, the Strahan sub-basin of the Sorell Basin is bound to the east by a steep linear north-northwesterly-trending fault, and is floored by one or two half-graben with shallow normal faults of easterly trend. Wilcox (1989) considers the sub-basin to be of slip-strike origin, and the basin-forming faults are Cretaceous or Pre-Cretaceous in age (figures 2.5 and 2.6 show NE/SW trends through Tasmania). Australia's southern margin basin traditionally classified as components of a widespread Early Cretaceous rift-valley developing east along the entire southern margin. Cande and Mutter (1982) propose that the rift is a precursor to north-south orientated sea floor spreading of Cenomanian age.

East of 140°E, the Gippsland Basin contains west-northwest and north-northeast-trending gravity lineations related to basin boundaries and are representative of the direction of the normal and transfer faulting. Similar trends appear along the western margin of Tasmania (Sorell Basin) and in the southeast margin of Tasmania adjacent to the East Tasman Plateau. The constant orientation of lineations may be interpreted as transfer faults displacing basinal compartments (Wilcox, 1990). Formation of the southern margin has involved two discrete extensional events: pre-Late Jurassic (Oxfordian) northwest to southeast extension west of the Otway Basin area, becoming strike-slip along the Otway-west Tasmania margin, and Early Cretaceous north-northeast to south-southwest extension in the Gippsland/Tasmania region. The near orthogonal orientation of the two stress fields must have resulted in some proportion of structural 'overprinting', evident in the western Tasmanian margin (Thomas and Wilcox, unpubl. Data).

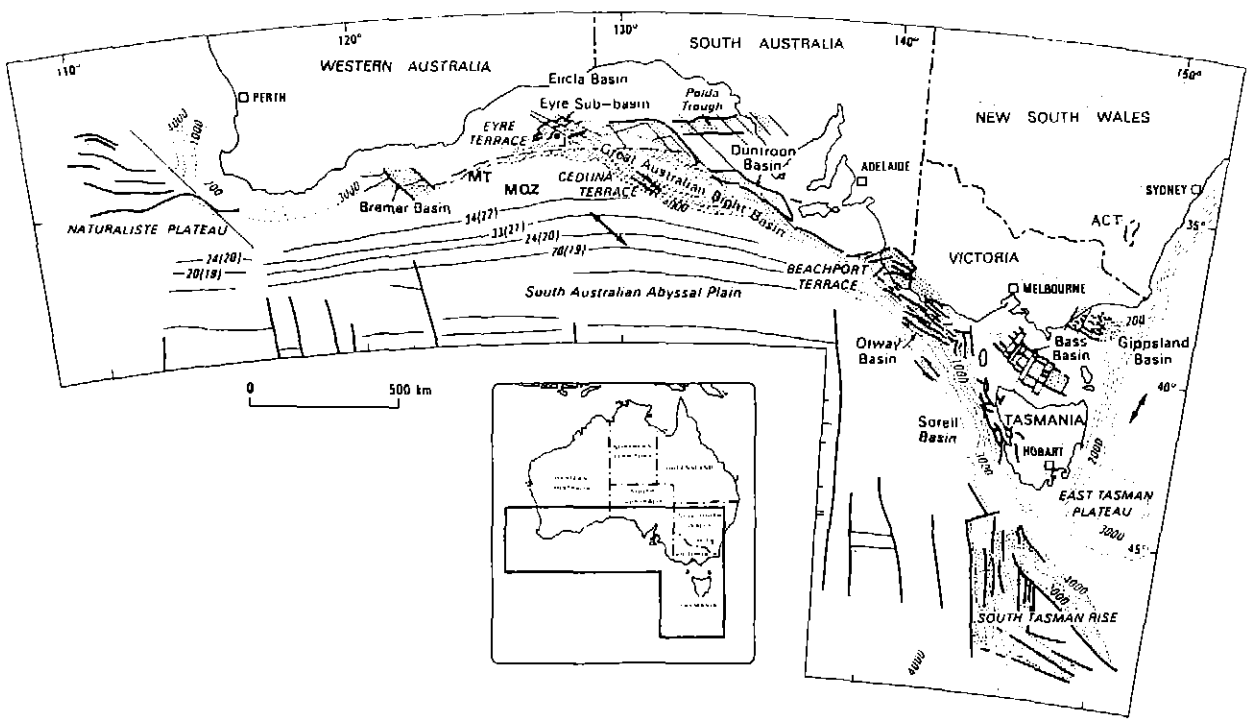


FIGURE 2.5 ***Southern margin of Australia showing the major structural features of the passive margin. Arrows show the sense of lithospheric extension based on seismic and gravity data (figure 2). Paired arrows show predicted strike-slip 'transpressional' or 'transtensional' zones during pre-Late Jurassic extension. (Wilcox, 1990)***

364159

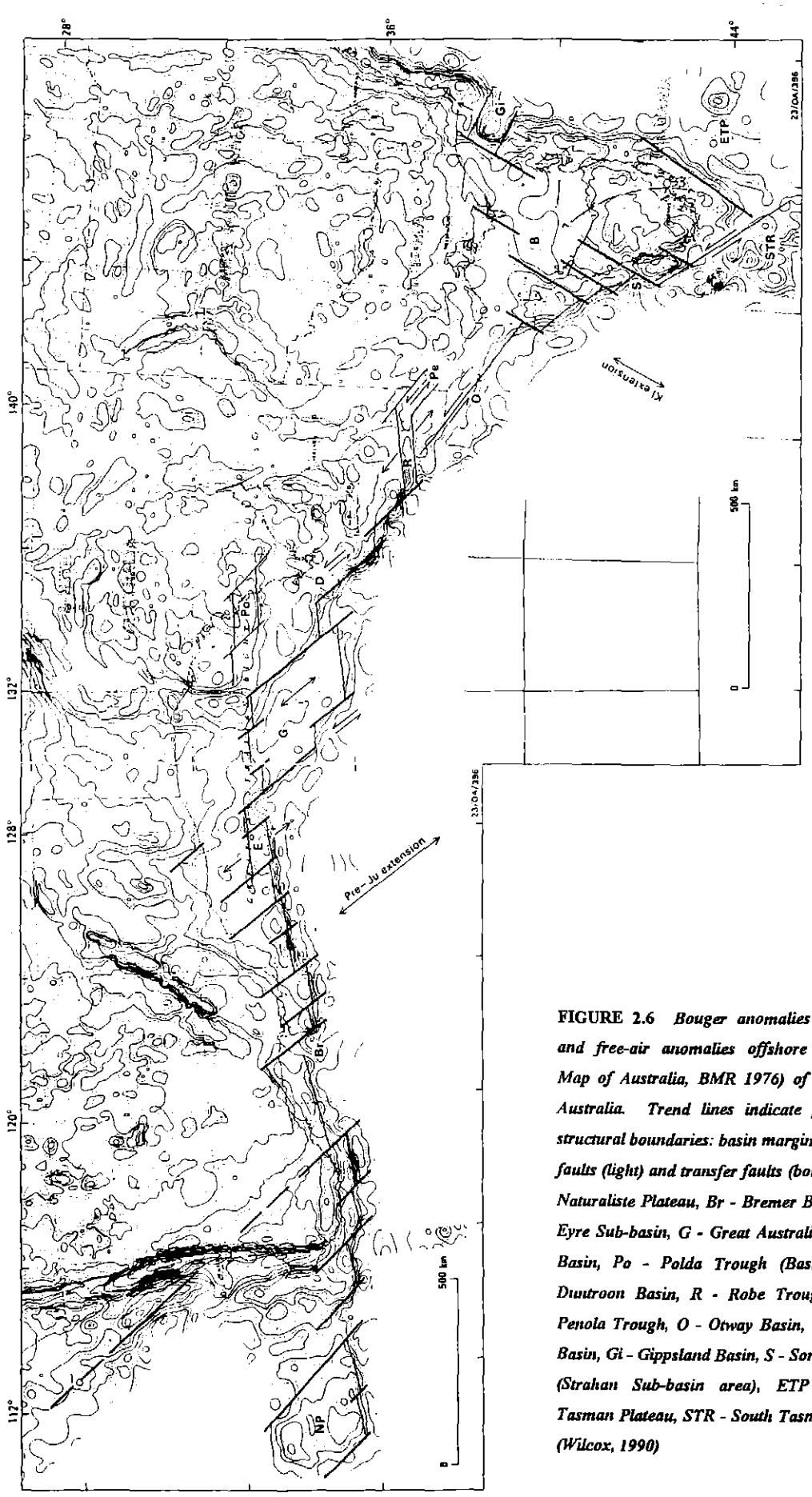


FIGURE 2.6 *Bouger anomalies onshore and free-air anomalies offshore (Gravity Map of Australia, BMR 1976) of southern Australia. Trend lines indicate predicted structural boundaries: basin margins/normal faults (light) and transfer faults (bold). NP - Naturaliste Plateau, Br - Bremer Basin, E - Eyre Sub-basin, G - Great Australian Bight Basin, Po - Polda Trough (Basin), D - Duntroon Basin, R - Robe Trough, Pe - Penola Trough, O - Otway Basin, B - Bass Basin, Gi - Gippsland Basin, S - Sorell Basin (Strahan Sub-basin area), ETP - East Tasman Plateau, STR - South Tasman Rise. (Wilcox, 1990)*

364160

The east-southeast to southeast linear strike of the gravity gradient in west Tasmanian margins suggests formation within a left-lateral strike-slip zone in pre-Late Jurassic. North-northeast to south-southwest gravity trends of western Tasmania correlate with similar extensional trends within the Gippsland Basin. This Early Cretaceous deformation has produced sequences of en echelon in the Mesozoic (Jurassic) as a strike-slip basin, with structure modification by extension during the Early Cretaceous (Thomas and Wilcox, unpubl. Data).

Onshore and offshore basins of late Jurassic to early Cretaceous formation occasionally contain economic/sub-economic petroleum accumulations, bounded by both stratigraphic and structural controls. Offshore, the Sorell, Otway, Bass and Gippsland rift basins filled with thick units of alluvial-fan and fluviatile sediments and occasional volcanics and pyroclastics. Continued fill from mid-Cretaceous includes varied successions of marine, marginal-marine fluviatile and volcanic rocks. Onshore the Tamar, Macquarie Harbour, Derwent, Coal River and Oyster Bay grabens, and basins of Devonport-Port Sorell and Scottsdale comprise non-marine and volcanic successions (Baillie, 1989).

Distributed across northern and eastern Tasmania are Tertiary basalts ranging in age from 59-8Ma. Including subaerial and subaqueous volcanics, these rocks may vary in composition from highly-unsaturated to oversaturated.

2.2.7 Quaternary

Landform suites of the Quaternary period have been greatly influenced by dramatic climatic variations. Glaciation, the development of bogs and swamps, frost weathering, and in the more humid areas of western, central and northeastern Tasmania, development of cave fill deposits, has directly influenced physical terrains. Subsequent changes in vegetation have effected the geomorphic processes of aeolian and fluvial erosion and deposition, whilst sea level fluctuations have influenced coastal margin landforms (Colhoun, 1989).

Additional Quaternary age developments include unconsolidated rock formations of glacigenic, slope, coastal, aeolian, fluvial and cave deposits, occasionally of economic significance.

2.3 LOCAL GEOLOGY

The geology surrounding the Zeehan area contains much of that seen throughout the west coast of Tasmania (figures 2.7 and 2.8). It is dominated by sedimentary rocks, with occasional intrusives. The oldest rocks throughout the Zeehan area comprise the Proterozoic Oonah Quartzite and Slate formation. This sequence consists of alternating white-weathering pale grey saccharoidal quartzitic sandstone or quartzite, thinly-bedded micaceous quartzite and siltstone, and laminated hard greenish, grey or black shale (Blissett, 1962). Golden-weathered muscovite is in bedding of the finer quartzite, and as flakes throughout black and dark grey siltstone. Coarser sandstone sequences often contain fragments of koalinised feldspar and subgreywacke grit.

364161

Locally, dark grey limestone and dolomitic limestone sequences have developed. High within the stratigraphic of Zeehan, spilitic lava flows and pyroclastics may occur. The Oonah Quartzite and Slate appears to have suffered little dynamic metamorphism. Formations are commonly cleaved, and shale or siltstone converted to slate of phyllite (bedding still visible). Blissett (1962) describes the Proterozoic unit as been 4 kilometres in thickness. Exposure is within a complex faulted anticlinorium north and west of Zeehan. Anticlinal folds plunge southeast below Zeehan and Renison Bell. Hills and Carey (1949) identified an upper sequence group as the 'Montana Melaphyre Volcanics'. This group included dark grey and black shale or slate, grey micaceous siltstone and fine quartzite with a subordinate occurrence of massive pale quartzite and subgreywacke.

Cambrian rocks at Zeehan fall into two categories. The Crimson Creek Formation in this area contains mudstones, siltstones, greywacke, greywacke conglomerate. Chert and gabbro were first identified southeast of the Heemskirk Granite by R.P.B. Pitt around the turn of the century. Green-greywacke conglomerate with chert pebbles, purple and grey laminated chert and hard siltstone also in close proximity to the granite are thought to have experienced mild contact metamorphism (A.B. Gulline, 1916?). The Dundas Group contains green and purple greywacke, slate, siltstone and mudstone (Blissett, 1962). Outcrop of these sediments is found approximately three kilometres southwest of Zeehan.

Ordovician rocks around Zeehan are widespread and easily identifiable. South of Zeehan, the Mount Zeehan conglomerate forms a warped and faulted anticline plunging to the southeast. Moina sandstone sequences form some 1200 feet of generally pale grey , thin-bedded, quartzose, pebbly grit along the flanks of the Mount Zeehan Anticline. Although rarely exposed, the Gordon Limestone covers much of the low relief areas surrounding Zeehan. Thought to be several hundred metres thick, the sequence is often decomposed to black, dark grey and blue-grey clay or soft shale.

Siluro-Devonian sediments of the Zeehan area form the Eldon Group. Incorporated therein are several units of sedimentary origin, including the Bell Shale, Florence Quartzite, Austral Creek Siltstone, Keel Quartzite, Amber Slate and the Crotty Quartzite. The Heemskirk Granite is a dominate feature of western Tasmanian geology, and is located approximately 5 kilometres west of Zeehan. Of Devonian age, this intrusive has maintained historical importance in mineralisation of the area.

Surrounding Zeehan, several small tillite outcrops are of Permian age. This forms a stiff, yellowish-weathering blue-grey or green-grey clay containing unsorted fragments of quartz, quartzite and sandstone (Blissett, 1862). The youngest rocks around Zeehan are Cainozoic sedimentary deposits (Tertiary and Pleistocene). These contain variable assemblages of gravels, sands and silts.

364162

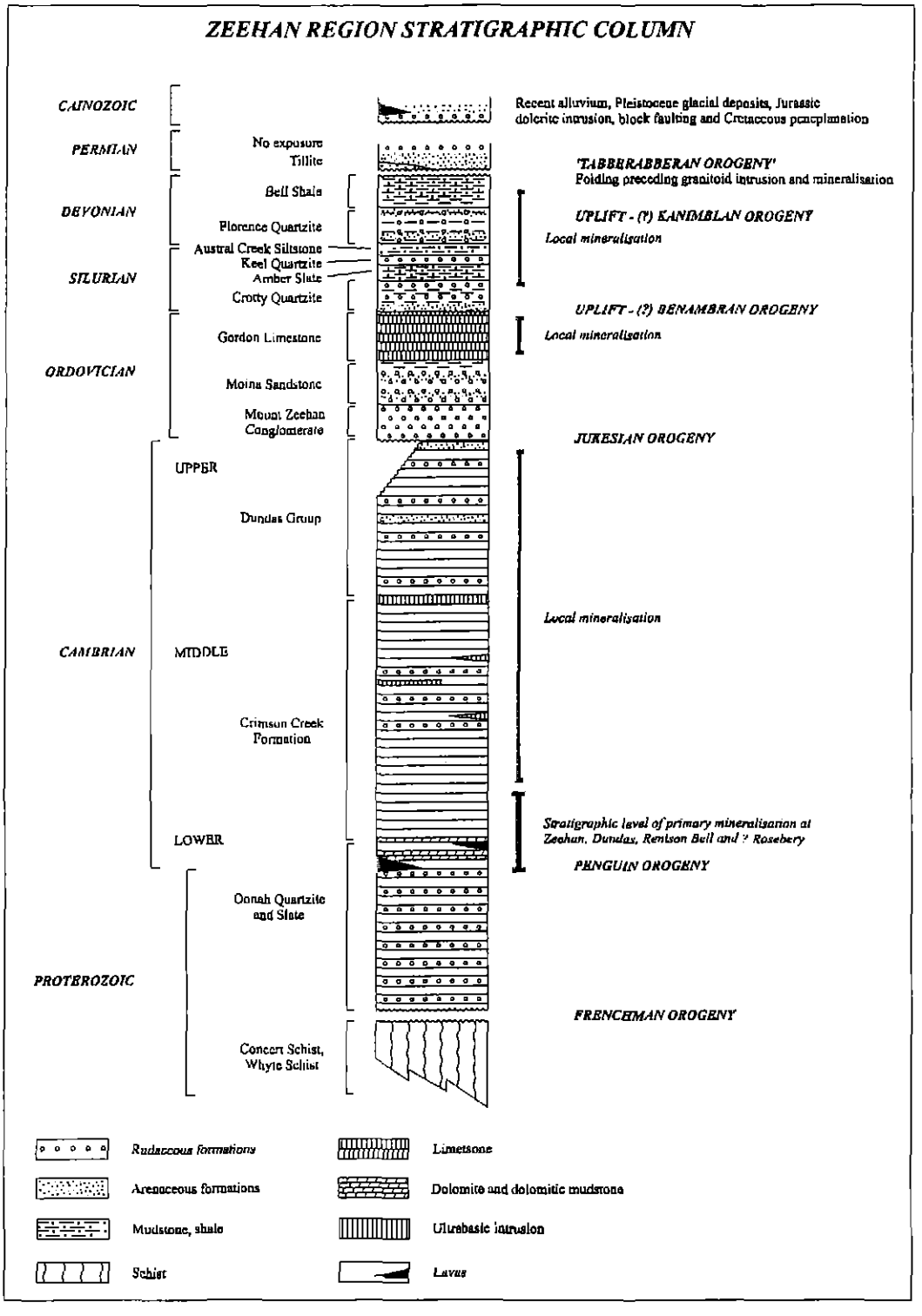


FIGURE 2.7 *Stratigraphic column of the Zeehan area geology. (after Blissett, 1962)*

364163

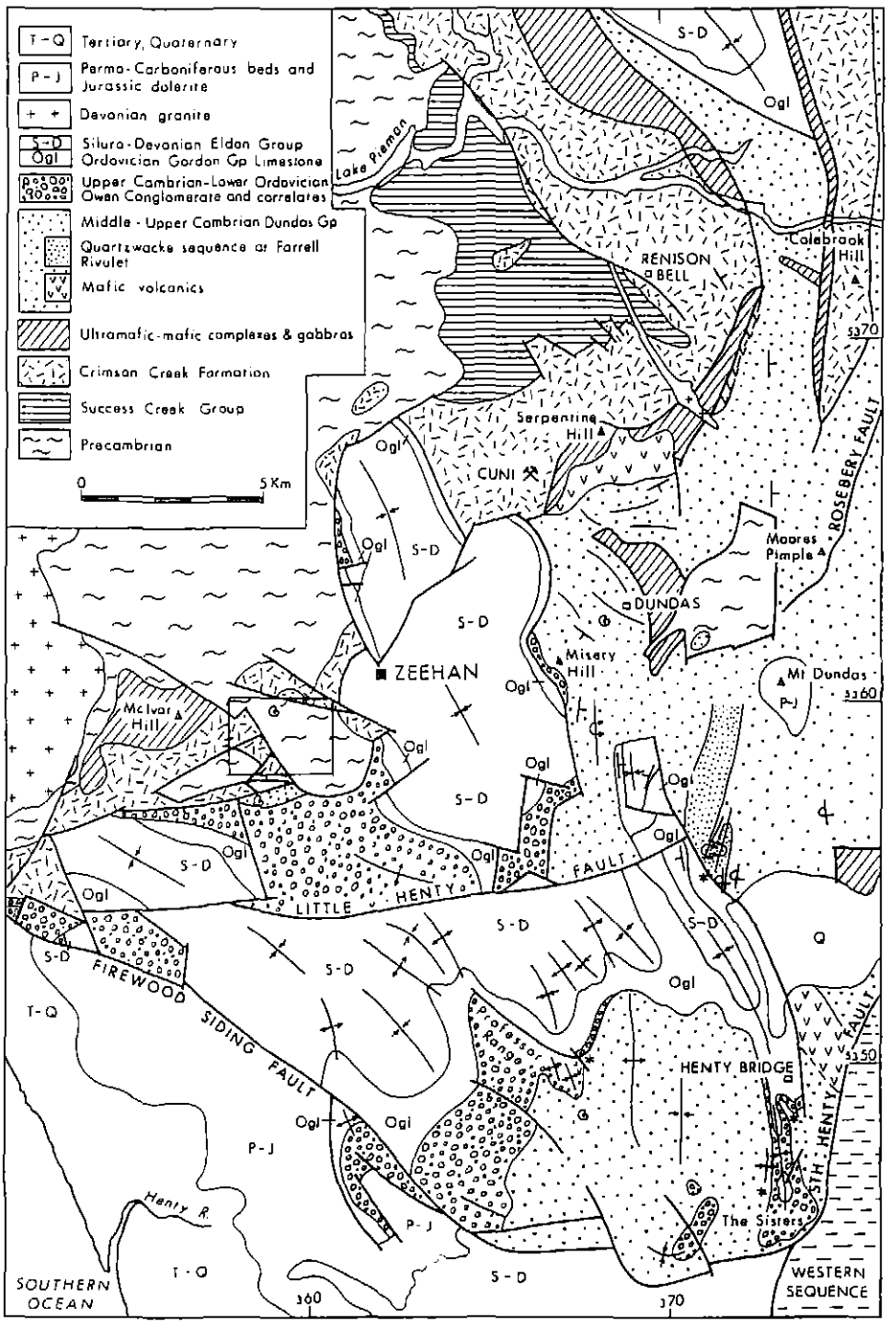


FIGURE 2.8 *Geology map of the Henty River-Zeehan-Pieman River area showing the approximate position of the Stonehenge map area. (after Blissett and Gulline, 1962; Baillie et al., 1977; Brown, 1986; Corbett and McNeill, 1986; Corbett, 1986a)*

2.4 STONEHENGE MAPSHEET

5 cm

Situated some 2 kilometres southwest of the township of Zeehan, the Stonehenge prospect covers the area of 357000mE to 361000mE and 5357600mN to 5360500mN (geology map, appendix 1). Precambrian sediments of the Oonah Formation are focus of the map sheet area.

364164

Comprehensive field mapping has been conducted over the Stonehenge study area. Figure 2.9 shows the extent of mapping, with stratigraphic and/or structural data and occasional rock samples gathered from each of the marked localities. A summary of field data collected throughout the mapping exercise is shown in appendix X. Some areas, such as the southwest corner of the mapping sheet have minimal if any outcrop, and subsequently interpretation may primarily be based upon additional techniques such as air photo interpretation. Mapping in the northwest was restricted due to ongoing exploration by competitors (drilling), limiting access to the area. The best exposure was found within the Proterozoic quartzite unit covering the southeast area of the mapping sheet. Far from extravagant, outcropping over this area was consistently in small portions, providing enough structural information to be gained for interpretative work. By nature, this quartzite sequence has formed undulating hills often with bedrock exposure along ridges and in valley waterways (figure 2.10). In addition, well cleared tracks, tramways and creeks (where accessible) have provided the most infrequent but continuous rock exposures. Fortunately, the extent to which the area has been worked this century has produced several sites which often provide exposure where no other outcrop is present. Although the majority of old mine workings consist of shafts, numerous shallow trenches often several metres in length are easily accessible and have provided important geological information. The Stonehenge area is somewhat unique to the west coast of Tasmania given its lack of extensive thick timber coverage. Although of varied relief, most areas (with the possible exception of the northern margin of the mapping area) are accessible. Vegetation around creeks and within valley lows may include thick coverage of native eucalypt, but is not extensive in occurrence.

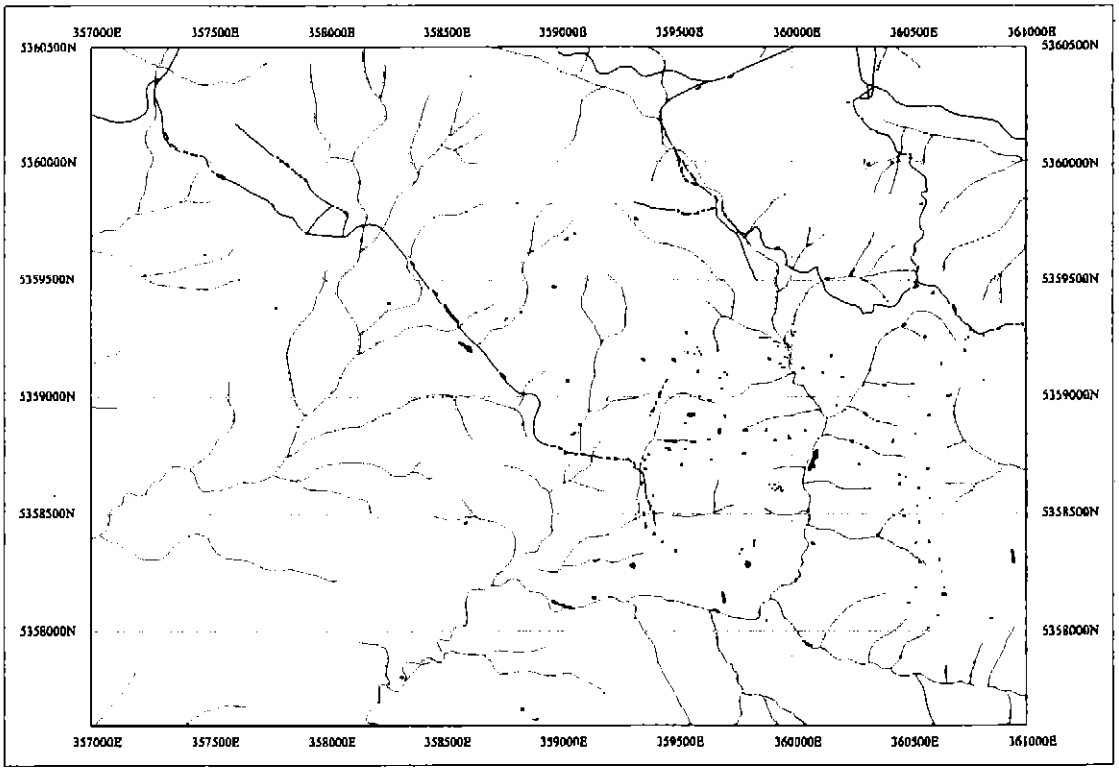


FIGURE 2.9 *Stonehenge area showing 'stations' of data collection.*

364165

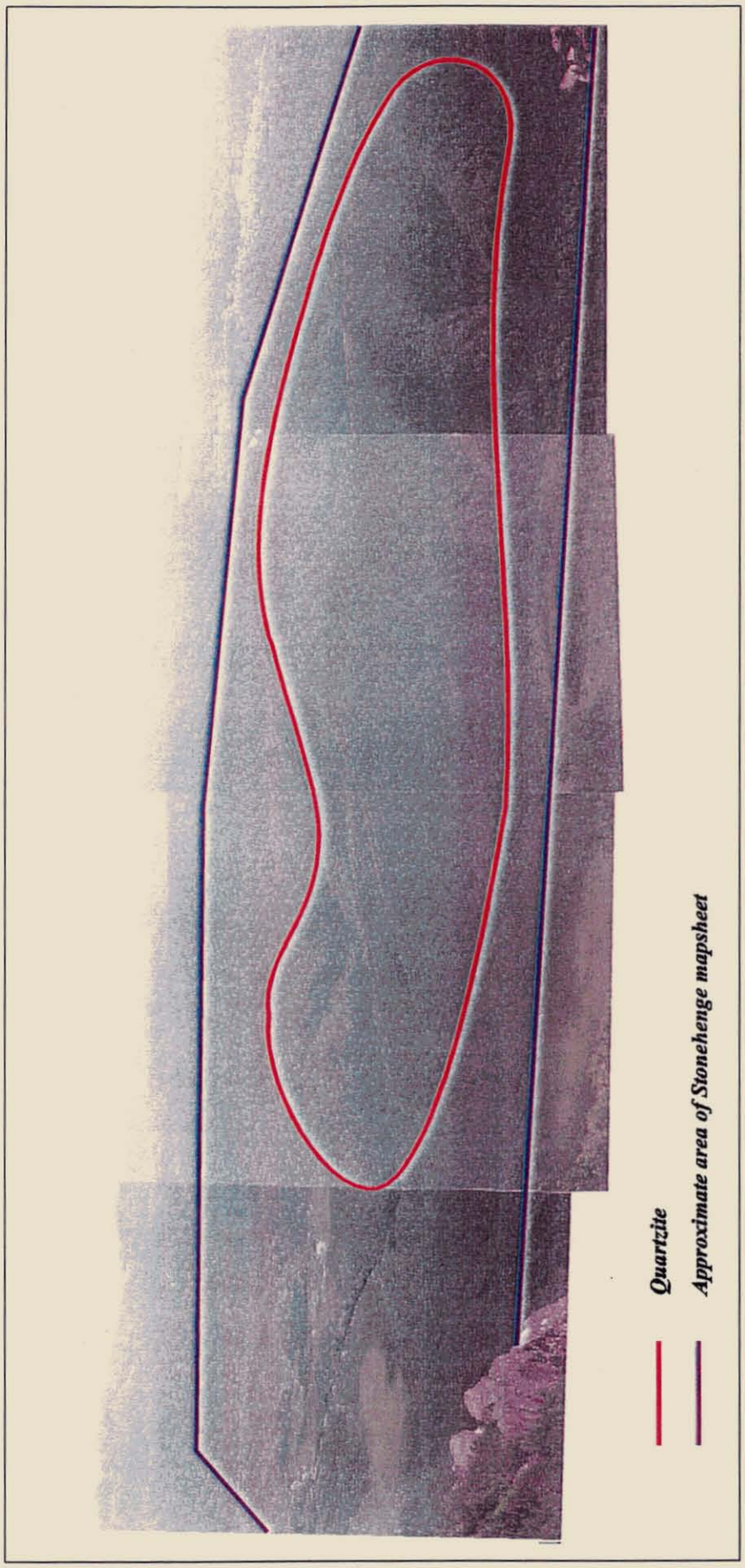
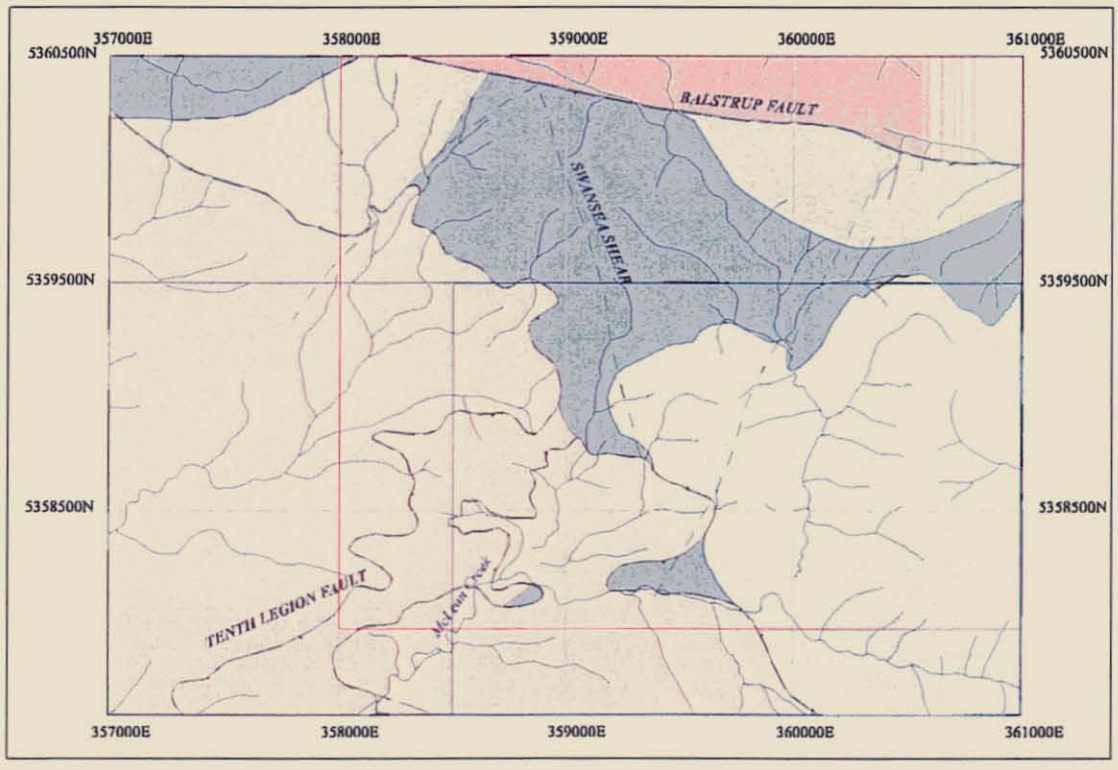


FIGURE 2.10 *Photograph of the Stonehenge area taken from Mount Zeehan, looking north.*

364166

Field mapping has identified the primarily outcropping sequence of Precambrian Oonah Formation sediments (figure 2.11) dominating the eastern mapping area. Quartzites are most common with phyllites, siltstones and shales found to be present in many of the lower relief areas. To the south, the Dundas Group of Middle to Late Cambrian sandstone, siltstone, chert conglomerate and basaltic sediments are thought faulted against the Oonah Formation via the Tenth Legion Fault. This sequence is generally overlain by Quaternary sediments. To the north, the Balstrup Thrust Fault separates the Oonah Formation from the Lower to Middle Cambrian Crimson Creek Formation sequence of mudstone, shale and volcaniclastic sediments.



CAMBRIAN

Cd — **Dundas Group:** *Undifferentiated chert conglomerates, gritty sandstone, siltstone and light green basalt.*

Cc — **Crimson Creek Formation:** *Interbedded dark green bassalt, reddish-orange volcaniclastics, khaki mudstone and dark grey shale.*

PROTEROZOIC

Oonah Formation: *Undifferentiated.*

Pom — *Micaceous sandstone, siltstone and minor shale.*

Pos — *Siltsone, shale and dolomite (undifferentiated).*

Posb — *Graphitic black shale.*

Poq — *Massive quartzite.*

Geological boundary possibly including faults

Thrust fault with teeth on upper plate

Undifferentiated fault

Creeks

Detailed area for wacker/EM/mapping coverage

Detailed investigation of quartzite (Poq)

Detailed geology shown Map Sheet A

FIGURE 2.11 *Simplified geology of the Stonehenge mapping area.*

The Oonah Formation is dominated to the southeast by a quartzite (rudaceous sediment) sequence. Structure therein is quite complex, and thought representative early deformation from the Penguin Orogeny of Late Proterozoic/Early Cambrian age, and later folding and/or thrust interference produced through Tabberabberan orogenic events. S_1 cleavages sub-parallel to bedding are common within the sequence, however latter cleavages are less prevalent. Shale, sandstone, dolomite and calcareous sediment comprise the remainder of the Proterozoic formation.

364167

The quartzite sequence forms dome and basin structures within an overall anticline formation trending northwest-southeast (figure 2.12). Less common in outcrop, graphitic black shales are the best illustrator of deformational phases, often exhibiting up to three cleavages. Rarely outcropping, EM surveys and wacker drilling have defined shale horizons (figure 2.13). The low relief southwestern margin of the map sheet is covered by recent alluvium, eluvium and marsh deposits.

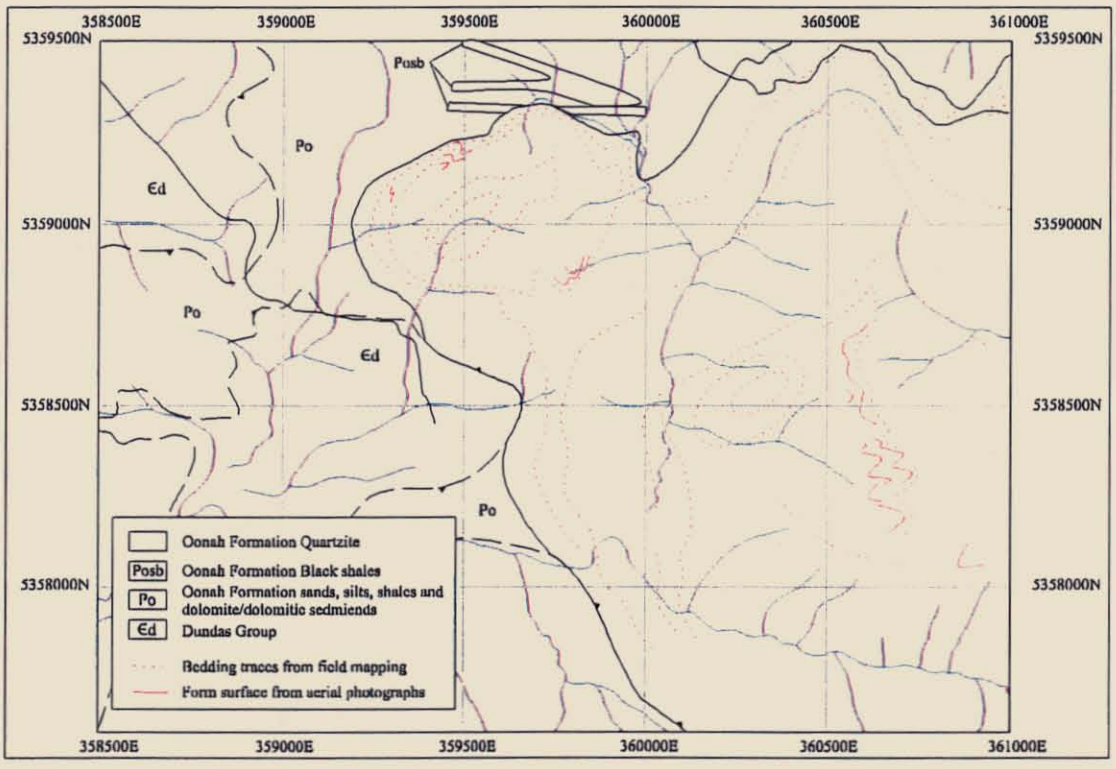


FIGURE 2.12 *Bedding traces within Oonah Formation quartzite.*

The northern region is faulted against the Crimson Creek Formation along the Balstrup Fault. Of Cambrian age, this sequence reputedly contains volcaniclastic, mudstone and shale units, however throughout only weathered green to dark grey shale sediments have been identified within the Stonehenge map sheet area. The fault contact is of a distinct discordant nature, likely to of thrust form as suggested by Blissett (1962). Dundas Group of chert conglomerates, sandstones, siltstones and basaltic sediments are separated from the Oonah Formation by the Tenth Legion Fault. This thrust fault extends beneath the Oonah Formation at low angle.

364168

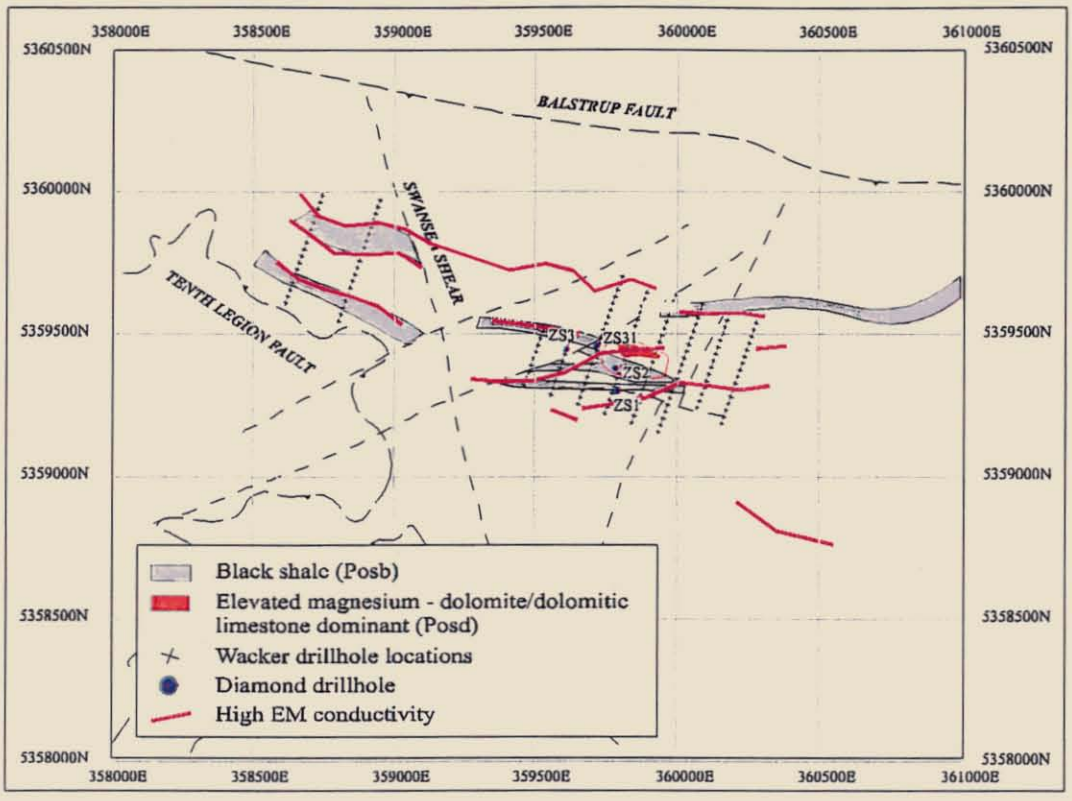


FIGURE 2.13 *Geology interpretation from wacker and EM surveying. Both techniques have enabled the identification of black shale horizons in an area of no exposure.*

364169

CHAPTER 3.

Structural history of western Tasmania

364170

3. STRUCTURAL HISTORY OF TASMANIA

3.1 INTRODUCTION

Tasmania's Precambrian inliers appear to have been subjected to a number of prominent Precambrian tectonometamorphic events, obscuring continuity between stratigraphic, structural and metamorphic relationship. Rocks in all Precambrian inliers are of sedimentary origin, and have been subjected to folding and regional metamorphism of greenschist and amphibolite facies to higher grade kyanite- and sillimanite-bearing gneiss and eclogite sequences (Turner, 1989). The most influential period of deformation has been the late Precambrian Penguin Orogeny (Spry, 1967). Folding during this phase effected areas possibly underlain by younger rocks such as the Rocky Cape region, the Jubilee region and several smaller inliers. Older, more intensely deformed and metamorphosed rocks have been tentatively interpreted by Spry (1962b) as belonging to a stratigraphic unit exposed to the Frenchman Orogeny prior to deposition of relatively unmetamorphosed rocks. This included the Whyte Schist of southern Rocky Cape region, rocks of the Tyennan and Forth regions and several small inliers.

All western and central Tasmania is underlain by multiply deformed metamorphic rocks of Precambrian age. These sequences are overlain by Late Precambrian-Middle Cambrian continental shelf sequences (figure 3.1). During the Middle Cambrian, a mafic-ultramafic complex is thought to have thrust over the majority of western Tasmania (Berry and Crawford, 1988). A phase of late Middle and Late Cambrian tectonic extension produced the Dundas Trough. Subsequent 'trough' filling included the deposition of generally acidic sequences of volcanic rocks and related sediments, including the Farrell Slates, Murchison Volcanics, Murchison Granite and Central Volcanics. Volcanism ceased during Late Cambrian, and the Owen Conglomerate prograded from the east prior to the onset of platform sedimentation in the Early Ordovician. During Owen Conglomerate deposition, significant faulting produced at least 1 kilometre of displacement along the Great Lyell Fault by Early Ordovician (Arnold and Fitzgerald, 1986). Substantial folding and greenschist facies metamorphism of the Early Palaeozoic sedimentary sequence occurred during the Devonian. Williams (1978) suggests an association of north-trending Devonian folds with the westward transport of the Henty Fault Zone. Granitic intrusions appear common towards the end of this orogeny. Tectonic activity post-Devonian has been restricted to minor faulting (Berry, 1989).

Brooks' (1962) mapped the Henty Fault Zone area in great detail, and has identified two cleavages: a widely distributed north-northwest striking cleavage associated with regional folding and a north-northeast striking cleavage restricted to a zone near the Henty Fault. The latter cleavage contains a strong down-dip lineation body referred to as a stretching lineation (Berry, 1989). Brooks' also identified zones of steeply plunging non-cylindrical folds in bedding, within both the Henty Fault Zone and the meta-sedimentary rocks of the Farrell Range. Gentle east-west folds appear to overprint the north-northeast striking cleavage along the base of the Farrell Range.

364171

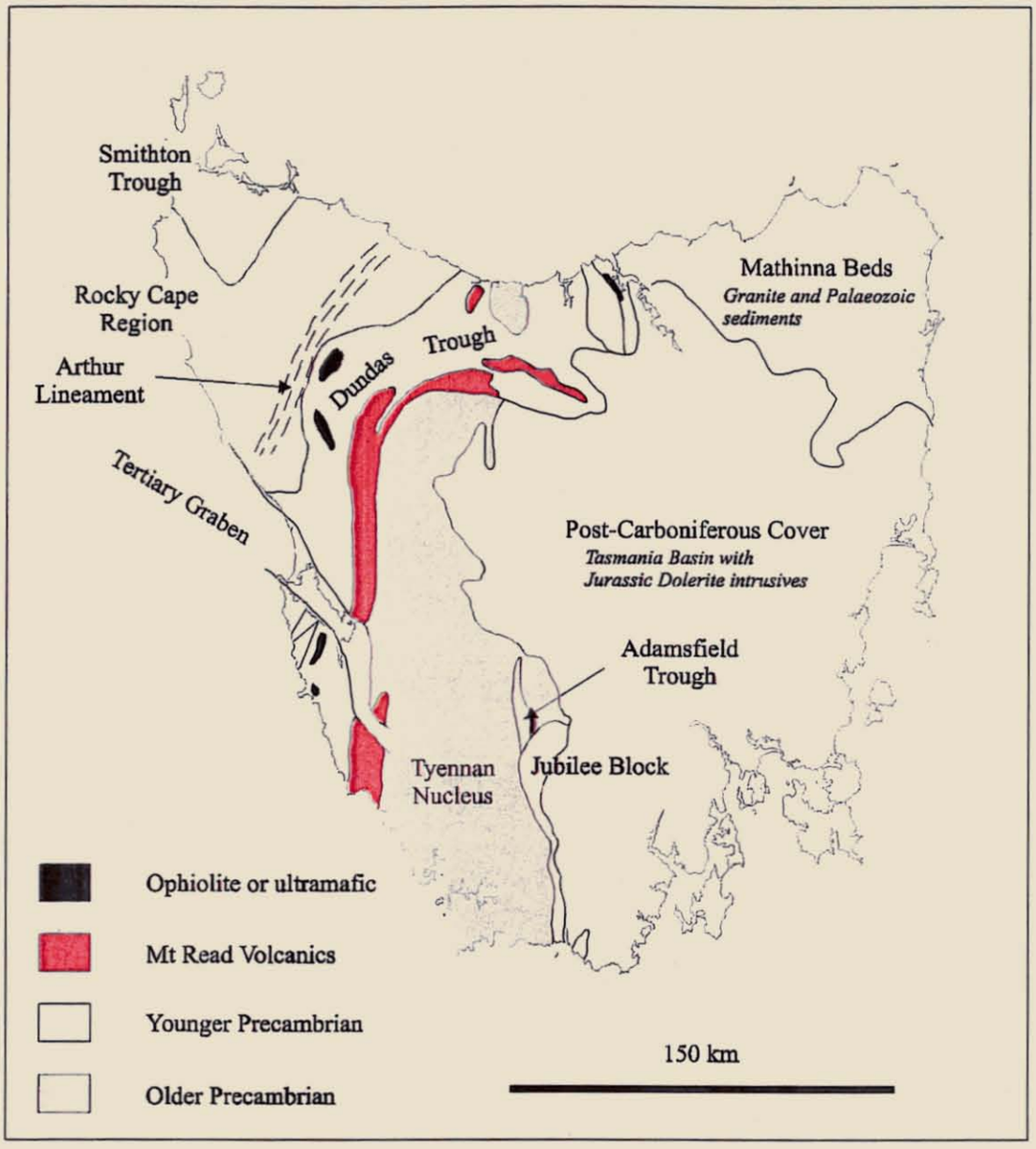


FIGURE 3.1 *Generalised geology map of Tasmania showing major Precambrian and Cambrian suites. (after Solomon and Griffiths, 1974)*

5 cm

3.2 GEOLOGY

The three prominent zones of Cambrian rocks (Smithton, Dundas-Fossey and Adamsfield) are generally referred to as 'troughs' or basins, although their origin is not known with absolute certainty. The Dundas-Fossey Trough is the largest continuous belt of Cambrian rocks, extending around the northern and western margins of the Tyennan region from south of Sorell Peninsula, through Queenstown, Zeehan, Deloraine and Beaconsfield to the north. The Mount Read Volcanics form the eastern margin, flanking against the Tyennan region.

364172

Within the Rocky Cape Region, the Smithton Trough remains unbound to the north, and may connect with a similar formation in the southeast crest of King Island. Prominent exposure of the Adamsfield Trough exists between the eastern margin of the Tyennan Region and the adjacent Jubilee region. A basic two-fold stratigraphy appears common to each 'trough' (Corbett, 1989):

i. early 'trough' sequences of shallow marine dolomite, sandstone, siltstone and mixtite conglomerate (Success Creek Group correlates) followed by deeper-water greywacke-mudstone-chert sequences with tholeiitic basalts (Dundas Group and correlates), and
ii. fossiliferous middle to late Cambrian units, generally rich in conglomeritic flysch deposits (Dundas Group and correlates)

Ultramafic-mafic complexes are present in both the Dundas-Fossey Trough and the Adamsfield-New River area. Felsic volcanic rocks appear restricted to the Dundas-Fossey Trough where they form the Mount Read Volcanics belt. Late Cambrian to early Ordovician siliclastic sediments of the Denison Group overlap most Precambrian elements and Cambrian 'trough's. Also covering major Precambrian and Cambrian elements are Ordovician limestone (Gordon Group) and Siluro-Devonian (Eldon Group) sequences, primarily within Devonian synclines (Corbett, 1989).

Cambrian 'trough' development is generally thought to be post-Penguin Orogeny (Corbett, 1989). Late Precambrian units (Success Creek Group and Crimson Creek Formation) lying unconformably upon Proterozoic rocks are likely to have experienced folding during this event. The Mount Read Volcanic belt contains an early arc sequence overlain (occasionally unconformably) by younger Tyndall Group volcanics. The early arc complex consists of a central volcanic sequence of lavas, pyroclastics and intrusives, and a flanking volcano-sedimentary sequence an the western side. Mafic rocks in the Corina district of similar or identical geochemical composition to those of the Crimson Creek Formation have seemingly been deformed and metamorphosed at the same time as the Arthur Lineament - suggesting pre-Penguin Orogeny formation of the Success Creek and Crimson Creek units (Corbett, after Turner, 1989).

The major north-northeast trending fault system (Henty Fault) obliquely transects the Mount Read Volcanics. In the southern area, the north and south Henty Faults converge near Mount Read, and intersect the Great Lyell Fault, to form a single broad fault zone which continues north beyond Tullah. Vein-type Pb-Zn-Ag mineralisation is common within Farrel Slates along the fault margin. Between the North and South Henty Faults, greywacke turbidites, siltstone, slate and minor conglomerate sediments contain felsic tuffs, a minor unit of andesitic volcanics, basalts, pillow lavas and intrusive gabbros. The basalts are of tholeiitic character, contrasting the general calc-alkaline nature of most of the Mount Read Volcanics (McClenaghan and Corbett, 1985).

The Henty Fault zone contains zones of intensely schistose material interfingering with lesser deformed material. The schistosity is generally sub-vertical, ranging from parallel to the fault trend to 30° divergent from it. Kinking and crenulation of the main schistosity along cross-cutting trends is common, with many sharp, steeply plunging minor folds of northeast to north trending axial surfaces.

364173

Away from the fault zone, the dominant cleavage in Tyndall Group rocks is sub-vertical with a north-northwest trend. Both the North and South Henty Faults contain zones of sub-vertical shearing and schistosity development. Schistosity in the former varies to steeply southeast dipping. Local gabbroic and basaltic dykes along the North Henty Fault and South Henty Fault (Corbett, 1975) suggests activity of this part of the system during the Cambrian. Dating of shales by Adams (1985) has provided Devonian and Carboniferous aging, indicating additional movement in the Devonian.

Between the North Henty Fault and Williamsford, the White Spur Formation of felsic tuff, siltstone, greywacke and slate, overlies the central volcanic sequence. The White Spur Formation is conformably overlain by a continuous sequence of conglomerate-quartzwacke-mudstone-lithicwacke in type localities. The Rosebery Fault forms the contact between the Dundas Group and central volcanics between Williamsford and The Pinnacles. To the north and northeast, a sedimentary contact exists at the base of a generally west-facing Dundas Group sequence. An upper part of the Dundas Group overlying the quartzwacke-conglomerate sequence contains interbedded siltstone, lithicwacke, mudstone and conglomerate with minor felsic tuffs. The uppermost exposed unit of the Dundas Group is a thick-bedded proximal flysch conglomerate (Misery Conglomerate). This is overlain by a unit of cross-bedded fossiliferous sandstone and siltstone from a relatively shallow water environment. Discordance between the Dundas Group sediments and the overlying Gordon Limestone group suggests that the Dundas Group was folded, uplifted and eroded prior to deposition of the limestone (Corbett and Lees, 1987).

Corbett and Lee (1987) have termed the major east-dipping thrust fault extending beyond 30 kilometres between Moores Pimple and Silver Falls as the Rosebery Fault. Analysis of the drill core has established an average dip for the fault of 40°. In this area, the fault passes through the Dundas Group of sediments, and follows the boundary of the central volcanics through an arcuate bend at Rosebery (exposing the White Spur Formation) and into The Pinnacles where it again enters the Dundas Group (Corbett and Lees, 1987). Intersection at depth with quartz-feldspar-phyric tuffs of the White Spur Formation indicates a minimum thrust displacement of 1.5 kilometres. The Rosebery Fault has been the focus for post-cleavage mineralisation in the Rosebery-Chamberlain area. Here the zone is host to large quartz vein deposits impregnated with black tourmaline. Accessory minerals within the veins include fluorite, pyrite, galena, chalcopyrite, jamesonite, bismuthinite and calcite, with significant assays of gold and silver. Structural interpretation is difficult given:

1. structures produced during Devonian orogeny are marked by widespread folding and cleavage development, and
2. structures from Cambrian to Early Ordovician movement are possibly fault dominated and marked by local or weak cleavage development along similar trends as the Devonian.

364174

Dominant regional structural trends and geological features are recognised from magnetic and gravity images of Tasmania (figures 3.2 and 3.3). Magnetically high zones through eastern Tasmania are of a general northwest trend. Paralleled by gravity highs, these lineation represent tholeiitic dolerite lenses and associated feeder dykes, emplaced into Tasmania during the mid-Jurassic. Wilcox (chapter 2) identified similar trends, supporting northeast-southwest extension during this time. Magnetic highs along western margins of Tasmania outline the extent of magmatic intrusion/extrusion sequences. These granite and basaltic rocks are generally of mid-Palaeozoic age. Granitoid intrusion are also identified by magnetic highs within the Tyennan Nucleus (Cambrian) and in northeastern Tasmania (Devonian). North-northeast trends (gravity and magnetic) of northwest Tasmania are representative of thrusting during the Cambrian development of Tasmania. Cutting northern Tasmania, the Young Fault cuts the Arthur Lineament and the Tasmania Basin. Trending parallel to basin-bounding faults of the Bass and Gippsland Basin's, the faults may be related to their development.

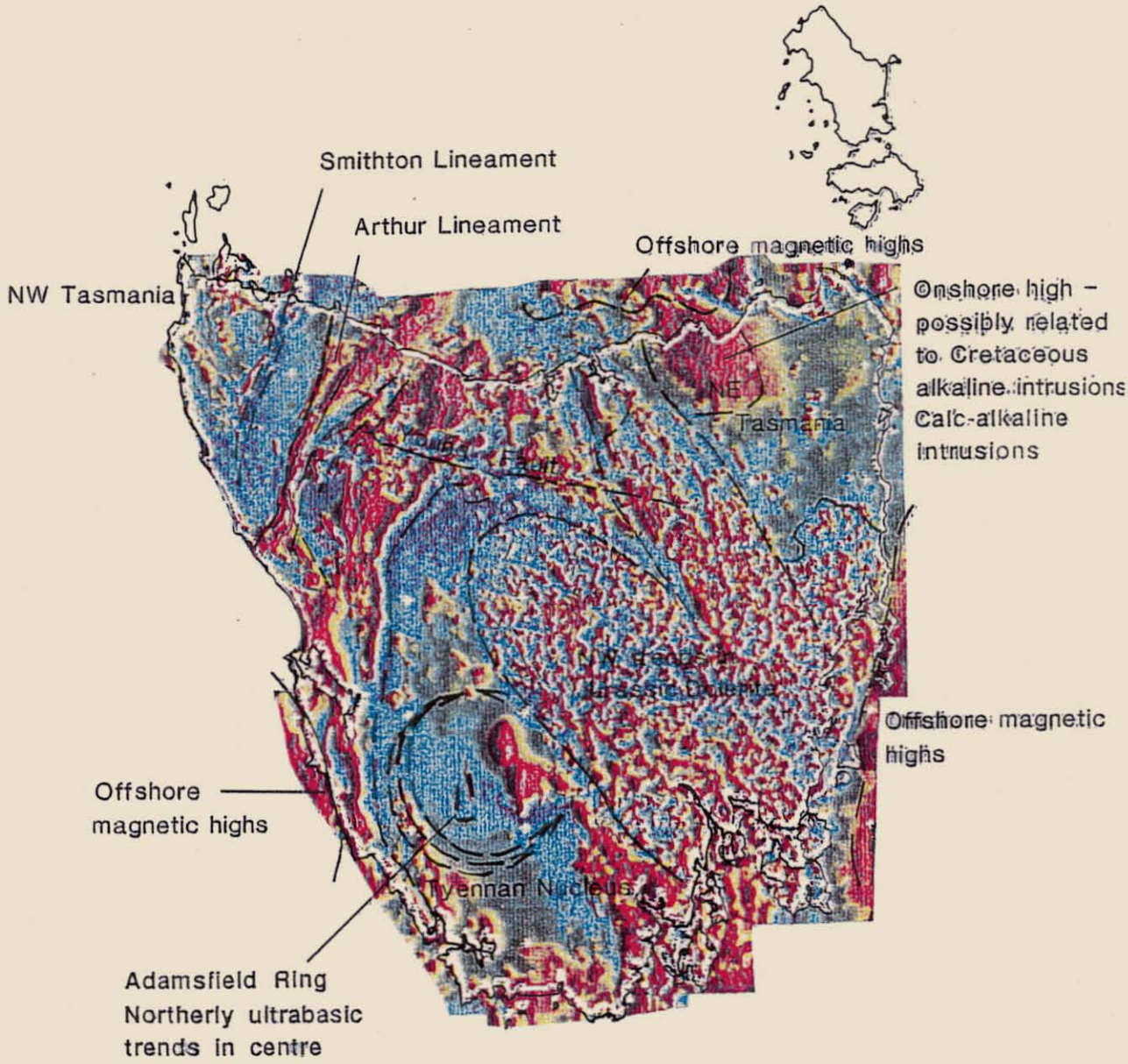


FIGURE 3.2 *Regional magnetic map of Tasmania showing major geological and structural features. (Contoured total field on first east derivative relief) (Muir, 1990)*

364175

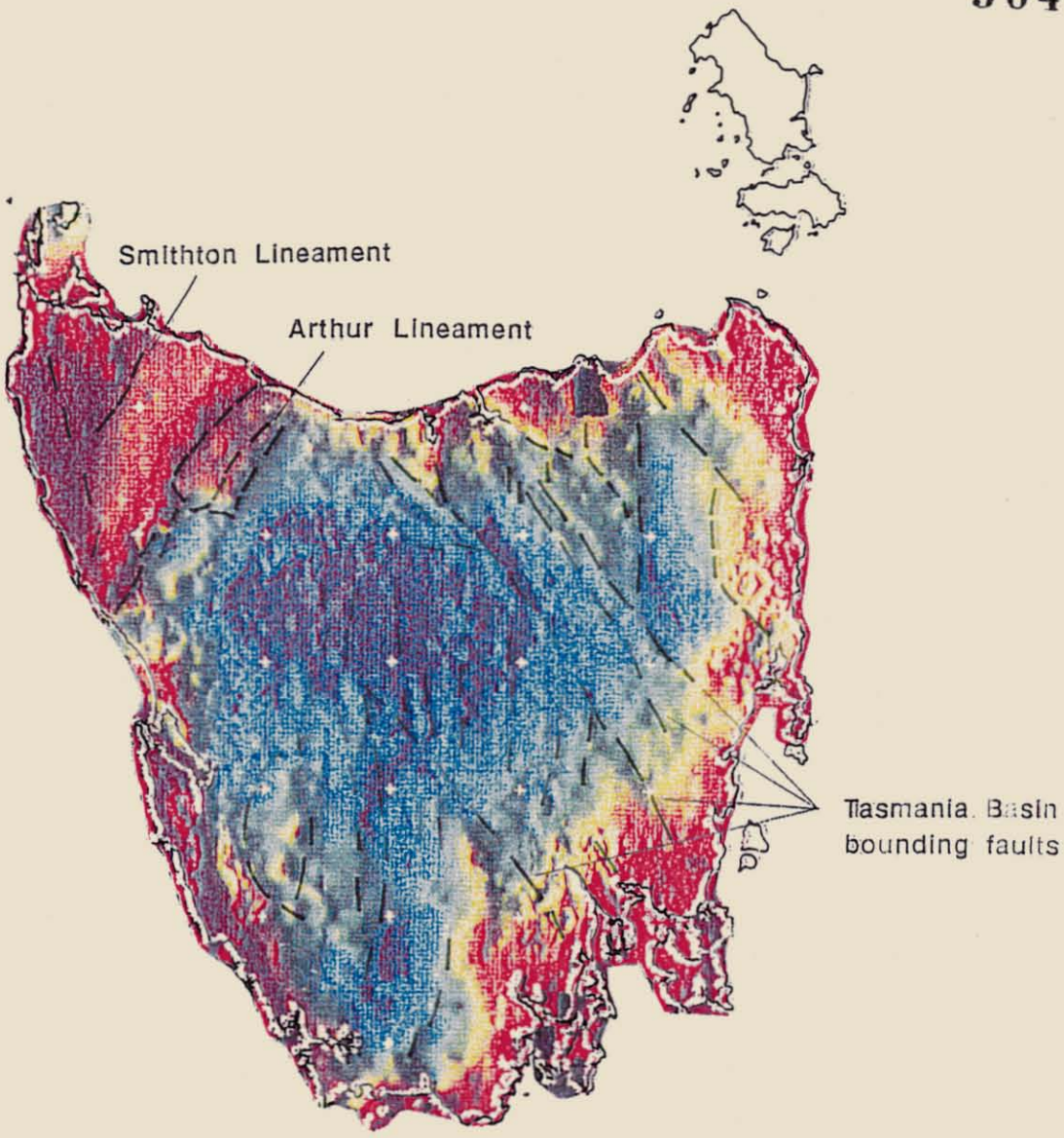


FIGURE 3.3 *Regional gravity map of Tasmania showing dominant structural trends. (Contoured Bouger gravity on first NE + NW derivative; relief enhanced) (Muir, 1990)*

3.3 STRUCTURE

3.3.1 Early Palaeozoic Deformation

The Dundas-Fossey 'Trough' and Associated Elements

This single structure wraps the northern and western margins of the Tyennan region, containing a concentric arrangement of stratabound elements (Corbett, 1988) such as the Mount Read Volcanic belt. The sedimentary and volcano-sedimentary sequences of the Dundas Group and correlates dominate the 'trough's axial regions. Early 'trough' units containing ultramafic-mafic bodies, Dundas Group sediments and Precambrian rocks are indicative of the western 'outer' margins. Stratigraphic 'trough' units are illustrated in figure 3.4.

364176

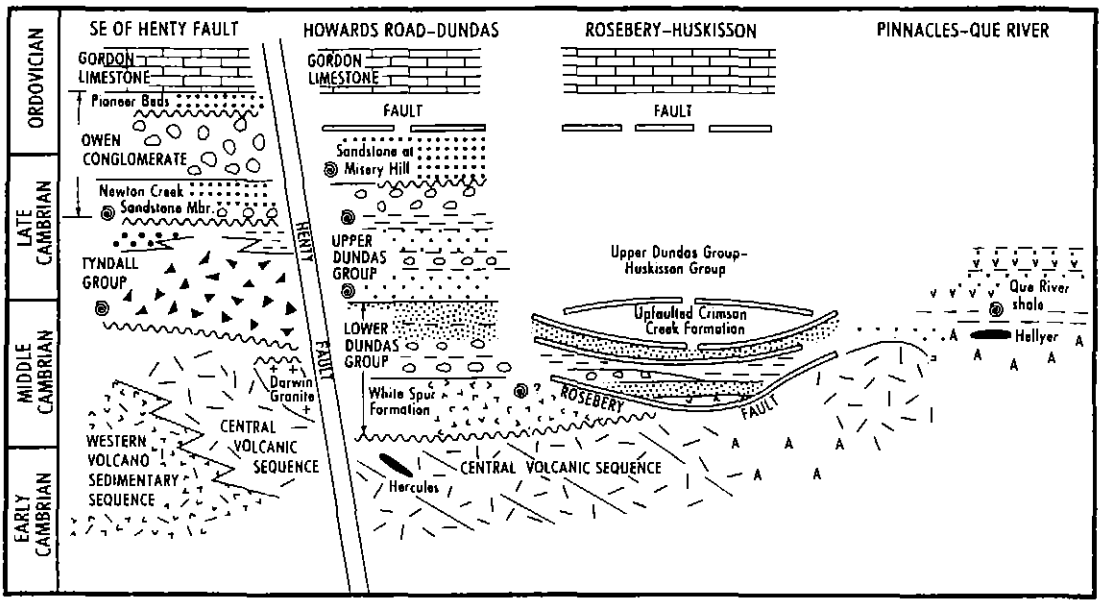


FIGURE 3.4 ***Diagrammatic longitudinal section through the Henty Fault System showing stratigraphic relationships. Corbett and Lees, 1987)***

The Success Creek Group and Crimson Creek Formation are thought to represent the earliest deposits within the Dundas-Fossey Trough. The former has evolved from a shallow marine environment of unstable shelf, containing late Proterozoic stromatolites. Overlying, the Crimson Creek Formation contains a thick (<5km) marine turbidite-mudstone sequence with varied tholeiitic basalt flows and associated breccias and hyaloclastites. Vidal (in Cooper and Grindley, 1982) has provided an age of early Cambrian for the sequence (identified from dating of a single spiny acritarch). Small Precambrian blocks about the outer of the Dundas-Fossey Trough margins between Sorell Peninsula and Beaconsfield appear faulted against adjacent Precambrian rocks. McClenaghan (1988) identifies the Cape Sorell block as a low angle thrust sheet.

Ultramafic-mafic complexes appear essential in gaining an understanding of the Palaeozoic evolution of western Tasmania. High Mg-andesites of boninite type, and low-Ti basalts have been identified and studied by Brown (1986). Known to be representative of oceanic forearc environments, these rocks suggest greater complexity in the formation of the Dundas Trough than a simple intra-cratonic rift setting. The most significant occurrence of ultramafic rocks is an S-shaped belt between Zeehan and Waratah (figure 3.1), and a zone across Sorell Peninsula. These complexes are generally fault bounded, and evidently have been tectonically dismembered and re-emplaced (Corbett, 1989). Occasional ultramafic detritus indicates some emplacement high into, or above the Crimson Creek Formation, and subjection to middle Cambrian erosion. Additional tectonic mobilisation during the Devonian orogeny resulted in ultramafic emplacement into the Dundas Trough.

364177

3.3.2 Mid- to Late-Palaeozoic Deformation

Early reverse faulting

Reverse faults show typical features of brittle-ductile shear zones as noted by Ramsay (1980). The faults commonly show ductile deformation of the walls with production of slaty cleavage and a stretching lineation. The cleavage does not have a strong rotational fabric of mylonitic foliation (Berry, 1989). Within the Henty Fault Zone, a strong slaty cleavage is determined by white mica and chlorite dipping steeply to the west. A prominent stretching lineation is identified by elongate pressure shadows around quartz and feldspar grains. Increased cleavage and lineation development to the south has been correlated to the likely intrusion of Devonian granites (Solomon, 1977; Large, 1986; Polya, 1987). The orientation of the cleavage and stretching lineation indicates the direction of maximum shortening to trend east-west and maximum extension direction plunging steeply west. The presence of steeply plunging folds is the likely product of interference with earlier north-northwest striking folds. Fault-bound folds were produced during an early phase of reverse faulting.

En echelon quartz-dominated extension veins are common throughout the Henty Fault Zone. The veins contain quartz, chlorite and pyrite with lesser amounts of galena and arsenopyrite. Veins within the Murchison Volcanics generally contain K-feldspars. Vein orientation is generally north-south, but of variable dip. Many of the veins pre-date cleavage development and are folded, whilst other cross cut the cleavage.

Berry (1989) has conducted a detailed study of the Henty Fault Zone region, focussing his investigation an brittle-type structures. Fault striations present in freshly exposed outcrop have enabled effective stress analysis. His analysis of fault striations suggests the last reverse fault movement of the Henty Fault Zone was Devonian. Strong cleavage development through southern fault zone margins is related to reverse faulting, with K/Ar dating by Adams (1985) supporting Devonian age. Brooks (1962) recognised cleavage (S_1) striking at 340° in the southeastern part of the fault zone; correlating with regional folds of Devonian age (Williams, 1978). This cleavage is overprinted by a north-south striking cleavage (S_2) of the Henty Fault Zone.

McKibben (1968) first identified that the Farrell orebodies filled north-northwest to north-northeast striking fractures of the Devonian Tabberabberan Orogeny. Striations within these fractures indicate oblique slip (dextral-reverse) (Berry, 1989). Correlation has been made by Rivers (1975) between this reverse movement in the Henty Fault Zone and that of the Great Lyell Fault. Furthermore, he has suggested that east-west dextral faults are related to the gentle east-west crossfaults. Sinistral displacement in the Henty Fault zone is likely to be less than 5 kilometres (Berry, 1989). A second set of striations demonstrate late wrench fault movement (Berry, 1989). Fine grooves (<1mm) exist without associated fibre growth. They cut earlier wrench striations, and plunge mainly to the south, or more shallowly to the north. Wrench faults strike at between 300° to 020°.

364178

Vein style mineralisation across the Henty Fault is primarily the product of a granite ridge intrusion during the Devonian (Large, 1986). These deposits appear synchronous with early reverse movement of the Henty Fault and predates the wrench faulting.

The Henty Fault Zone has a complex movement history. The earliest recognisable movement is east-directed thrusting (as identified from fold relicts in the Farrell Range and the west facing nature of the Farrell Slate), and may correlate with Early Ordovician movement of the Great Lyell Fault. A Second phase of reverse movement in the Henty Fault Zone uplifted the Central Volcanic Complex against the Farrell Slate and Owen Conglomerate on a steep west-dipping reverse fault. This produced S_2, a strong cleavage within the fault zone and footwall. It is thought by Berry that this cleavage post-dates northwest trending Devonian folds. The last Devonian movement involved sinistral wrench development (<5 kilometres) with near uniaxial compression from the north-northwest to the north (determined by Berry from stress solution and striations). This stress direction suggests correlation with late thrusting north of the Tyennan Block (Jennings, 1958) and in the Linda Fault Zone (Williams, 1978). Following periods of folding included sinistral wrench movement and normal faulting, most likely associated with post-Triassic faulting found throughout Tasmania (Berry and Banks, 1985).

Western Tasmania

Western Tasmanian rocks of lower Devonian age and older are deformed by parallel folds and associated structures. This deformation generally pre-dates granitoid emplacement also of mid-Palaeozoic age. There appears to be some correlation between the pre-granitoid deformation seen throughout western Tasmania and Tabberabberan Orogeny formations of eastern Australia. Cambrian uplifts have resulted in Precambrian rocks behaving as relatively competent blocks during periods Devonian deformation (Williams, 1976a,b, 1978). Earlier folds and associated structures developed in zones of closure as blocks converged to form prominent trend axis as seen in figure 3.5. The Tyennan Block, consisting of the Cradle Mountain and Prince of Wales Blocks, behaved as a competent unit, determining fold patterns of the Loongana/Wilmont trend, and the northerly West Coast Range/Valentines Peak trend.

Later folds and associated structures dominating northern Tasmania are of the northwesterly and northerly Deloraine/Railton trend, the product of movement from the northeast. A narrow zone of folding and faulting separating the Cradle Mountain and Prince of Wales Blocks was produced during this later period of deformation. Forming the Zeehan/Gormanston trend, this narrow northwesterly deformation zone extends north into the Rocky Cape Block (Williams and Seymour, 1989).

364179

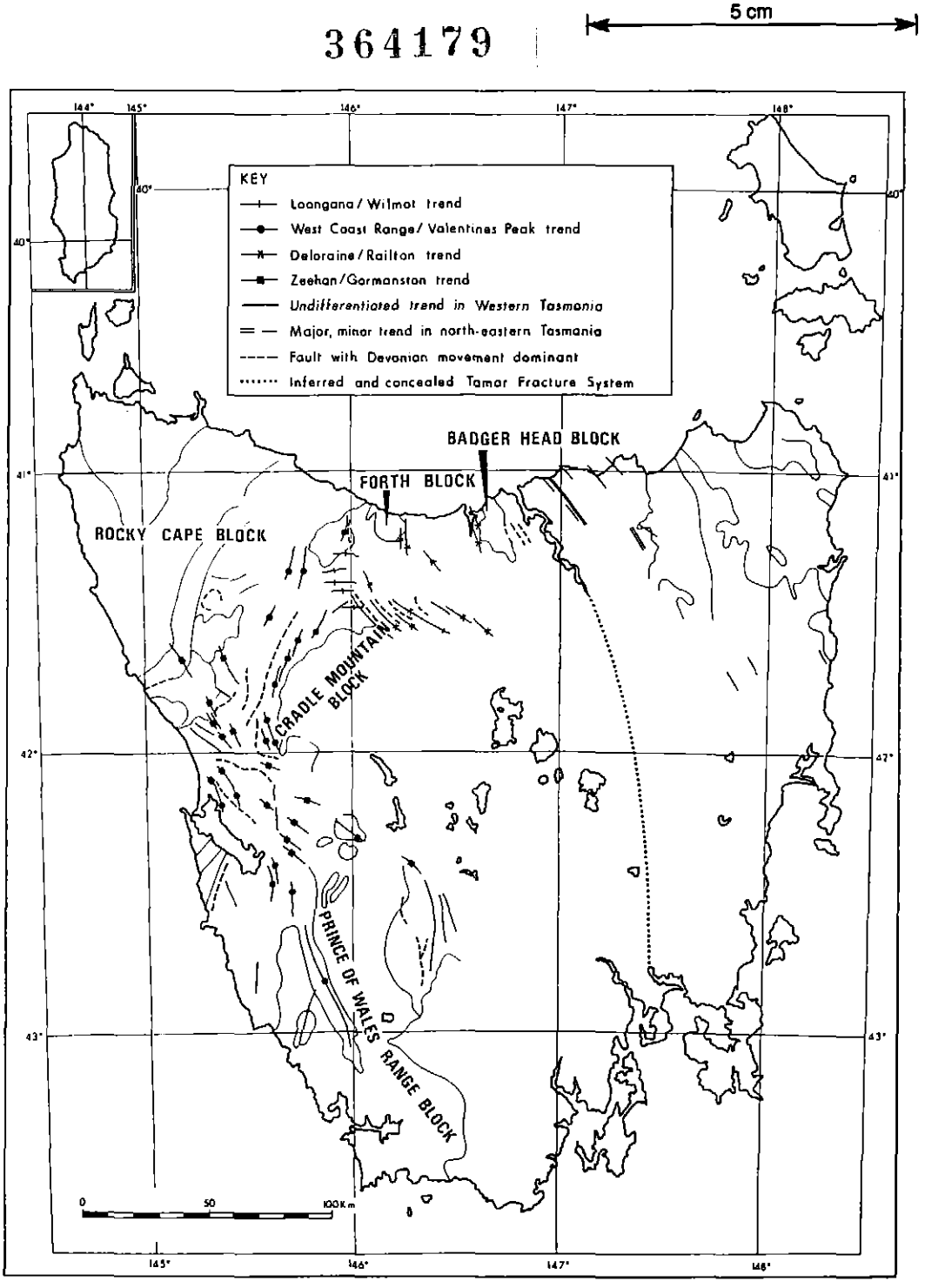


FIGURE 3.5 *Hinge traces of major Devonian folds and faults. (Williams, 1989)*

Folds of all major structural trends intersect in the Black Bluff-St. Valentines Peak area. Mapping by Seymour (1980) has identified general upright to steeply inclined fold trends, with horizontal to moderately plunging hingelines. Axial plane cleavage has developed. Interference of differing fold trends has developed dome and basin structures. The emplacement of mid-Palaeozoic granitoids is described by Williams, McClenaghan and Collins (1989) as post-kinematic given that they truncate the folded structures of surrounding country rocks. Structures present within some granitoids and country rock suggest deformation periods post-dating that of emplacement.

southeast axis. Allochthonous sheet movement containing mafic-ultramafic suites from an area southeast of Tasmania is thought to have been along such orientation.

364180

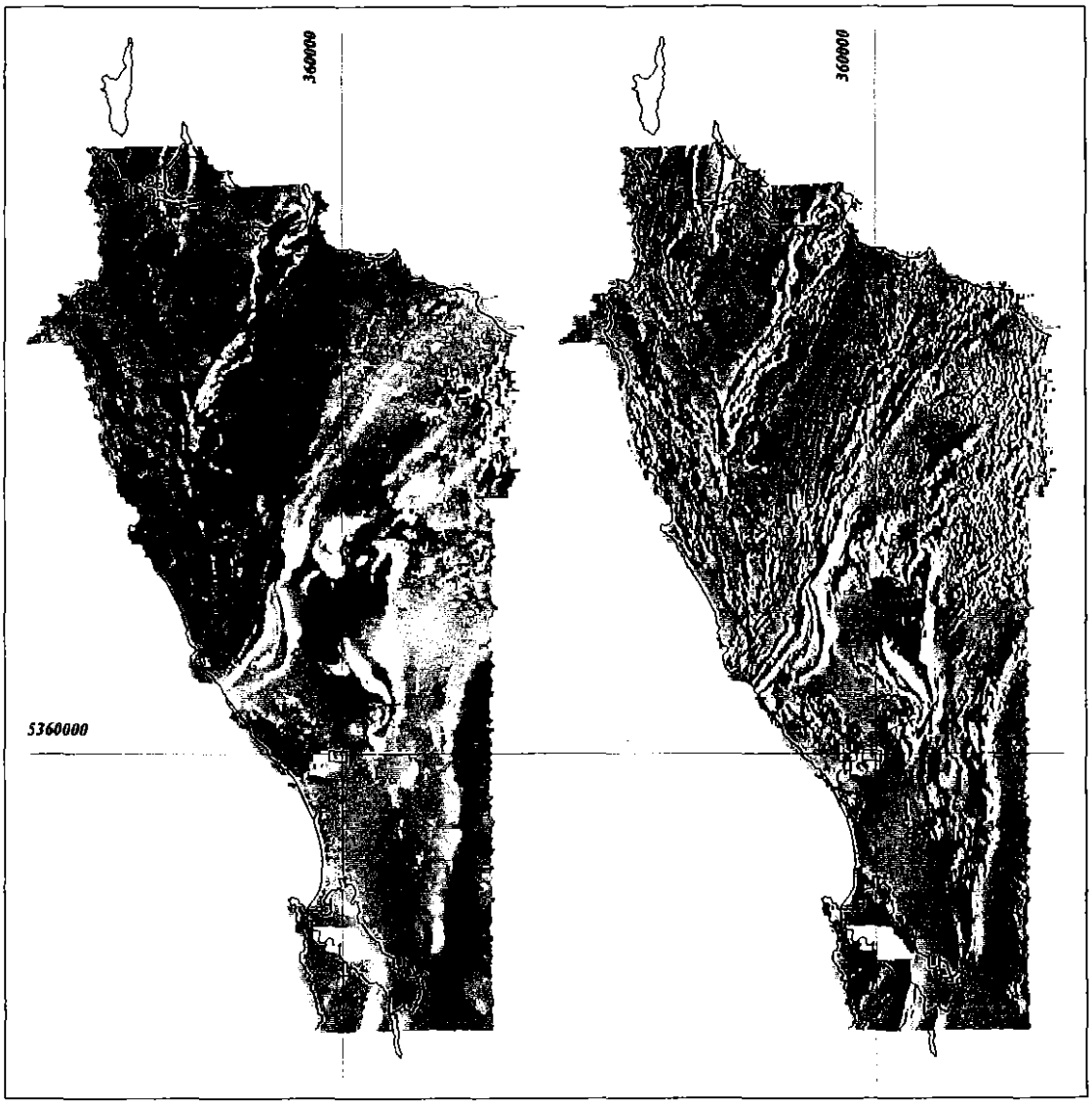


FIGURE 3.6 *Shaded magnetic images of western Tasmania identifying major structural trends.*

Zeehan/Gormanston Trend

An area separating the Cradle Mountain and Prince of Wales Blocks is host to the Zeehan/Gormanston trend of deformed Precambrian metamorphic rocks. Siliceous clastic beds (Denison Group correlates) unconformably overlie Precambrian metasedimentary rocks, and are conformable overlain by Ordovician to Devonian sedimentary sequences. Precambrian schists and quartzite's and overlying sediments are folded into a series of northwest trending anticlines and synclines. These large open folds and associated east trending faults are continuous through both Precambrian and Palaeozoic successions (Williams, 1989).

Prior to Devonian folding and sediment deposition, bedding and foliation of Precambrian metasedimentary rocks were flat-lying and isoclinal folds (often recumbent). Structures within the Zeehan area are dominated by faulted folds of the northwesterly Zeehan/Gormanston trend (Blissett,

364181

Prior to Devonian folding and sediment deposition, bedding and foliation of Precambrian metasedimentary rocks were flat-lying and isoclinal folds (often recumbent). Structures within the Zeehan area are dominated by faulted folds of the northwesterly Zeehan/Gormanston trend (Blissett, 1962). A steep dipping axial surface cleavage is generally found associated. The largest of such folds have a half-wavelength of approximately 4.5 kilometres. Smaller folds with a half-wavelength of up to 1 kilometre are often associated. Folding has been of elongated basins and portions of domes, plunging at up to 40° towards the end of structures (Williams and McClenaghan, 1989). Early Devonian sedimentary rocks may be found preserved within the synclinal 'trough's'.

Throughout the Zeehan area, fault movement along this northwesterly trend is common. Such movement, particularly those accompanied by shear zones, are the likely product of Devonian deformation, although post-Permian movement may mask their significance. West trending, the Little Henty Fault appears associated with similarly trending cross folds of Devonian age (Blissett, 1962), but show no offsets of the northwest trending regional fold hinges (Carey, 1953). Blissett (1962) conducted detailed investigation of the structure of the Zeehan area, and recorded the following structural elements as produced during Devonian tectonic activity (figure 3.7):

- Heemskirk Anticlinorium
- Little Henty Syncline
- Mount Zeehan-Professor Anticlinal Zone
- Zeehan Syncline
- Huskisson Syncline
- Duck Creek-Healy Creek Synclinal Zone
- Dundas Anticlinal Zone
- Westerway-Ewart Syncline

Regional strike through the Heemskirk Anticlinorium is to the northwest with warping to an easterly alignment near Trial Harbour. Alternating plunges of minor fold axis indicates northeast cross-folding. Ordovician formations at Mount Zeehan have been folded into a southeast plunging anticline, which has been warped to the north by east-west trend (Blissett, 1962).

The Zeehan Syncline forms a complex northwest trending folded basin. To the north, the syncline is faulted against Proterozoic beds, and plunges south-southeast. Southeast of Zeehan and north of the Balstrup Fault, the plunge changes to the northwest. South of the Balstrup Fault, upthrown beds plunge north-northwest at 25°, rising the Florence Quartzite and older formations. Bell Shales downthrown south of the Little Henty Fault are heavily cleaved along a northwest axis with steep easterly dips. Variations in plunge of the Zeehan Syncline are the likely product of east-west or north-east cross folding, and the subsequent downwarping from faulting. The apparent eastward shift of the southeast end of the Mount Zeehan Anticline north of the Little Henty Fault is explained by Blissett (1962, supporting Carey, 1953) as erosion of the upper part of an aymmetrical structure.

364182

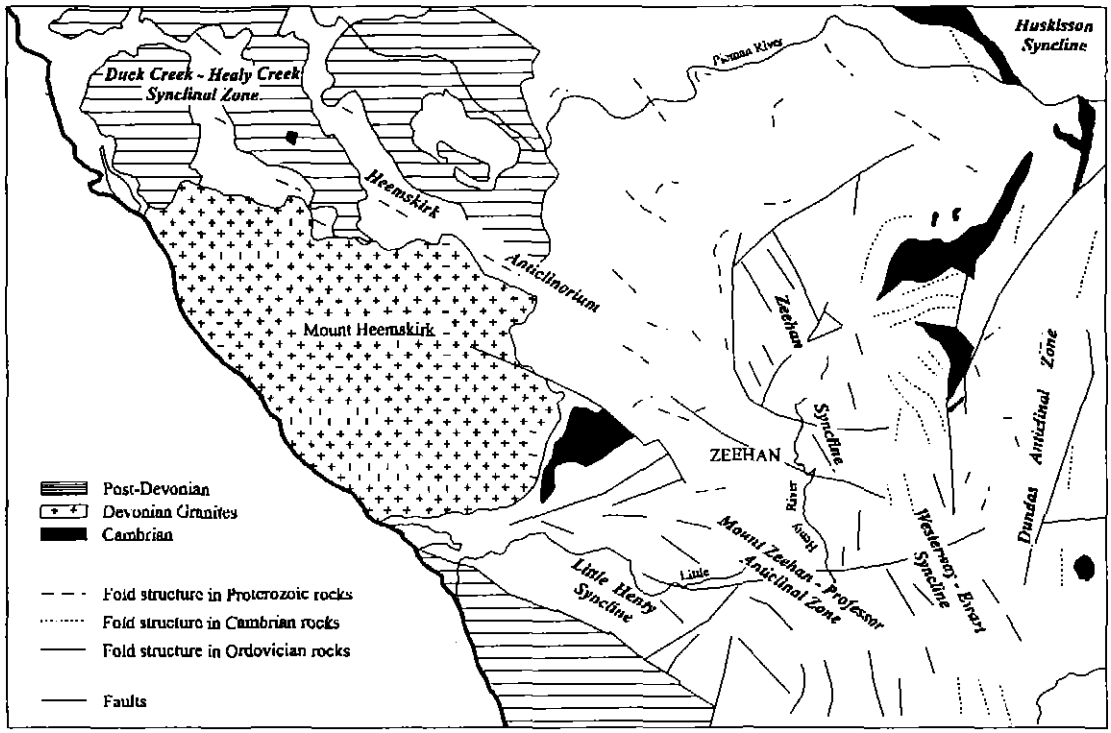


FIGURE 3.7 *Dominant structure of the Zeehan area. (after Blissett, 1962)*

Blissett (1962, supporting Carey, 1953) analysed 'Tabberabberan Orogeny' structures as:

- major northwest folding warped to ta north-northeast-south-southwest or north-south trend towards the east is due to compression from the southwest
- east-west or north-east cross-folding possible contemporaneous although it is not clearly demonstrated
- north-northeast, east-west and northeast faulting probably developed at a later stage

In the Zeehan district, major faults are often associated with warping due to cross-folding. West of Dundas latitude, major folds strike northwest. To the east the trend is distorted to north-south or north-northeast-south-southwest and close folding so that warping may by due to compression against the Tyennan ridge (as suggested by Solomon, 1962).

Devonian structures in post-Cambrian Rocks

Most prominent in the Ordovician-Silurian-Devonian sequences are two phases of folding. The first, early phase, recognised by Williams (1978) was produced by east-west shortening of the Dundas Trough. This deformation is represented by broad open folds of roughly meridional trend. The second phase is represented by folds and faults on northwest and west-northwest trends; most prominent in the area between Zeehan and Queenstown. Tectonic transport from the southwest is thought indicated by fold asymmetry and fault movement in the Queenstown area. The Firewood Fault and most folds in the Ordo-Devonian sequence around Zeehan is considered to be related to this phase.

364183

A northwest-trending syncline of Ordovician-Silurian rocks (2nd phase) transgresses the underlying Dundas Group sequence along the Zeehan Highway. Bedding in younger rocks dips at 30° to 65° and is the right-way-up, whilst in the underlying Cambrian sequence in overturned and dips southeast at 50 to 70°.

East and northeast of Zeehan, Ordo-Devonian sequences transgress the Dundas Group-Crimson Creek Formation boundary and entire width of the Crimson Creek Formation to rest upon Rocky Cape Basement. The Gordon Limestone sequence is likely to have been deposited upon an already folded and probably fault disrupted Cambrian sequence.

Structures in the Dundas Group and the Rosebery Tectonic Zone

Mapping by Blissett and Gulline (1962) of the Dundas Group in the Dundas-Mount Misery area has identified a complex array of fault blocks and major changes in strike and facing direction between some adjacent blocks (figure 3.8). The most prominent structure in the Dundas Group to the south is the north-northeast-trending overturned fold couple. A north-northeast-trending cleavage dipping east at 60° is associated with the folds. There appears no expression of this folding within overlying Ordovician-Devonian rocks to the west; implying that the folding pre-dates the Ordovician. K/Ar age data from slates of the Upper Dundas Group gave 515 ± 6Ma suggesting fold and cleavage development could have occurred in the Late Cambrian, soon after deposition.

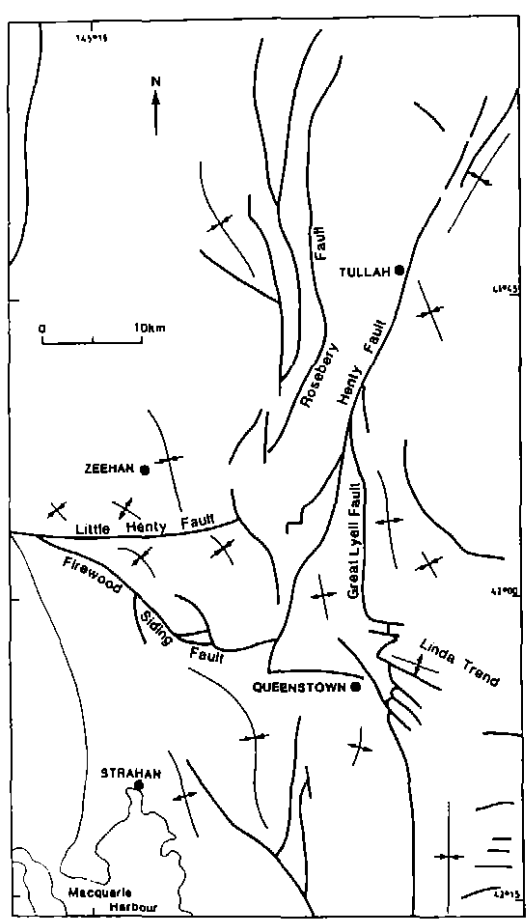


FIGURE 3.8 ***Simplified Devonian structure of the Henty Fault System area. (Corbett and Lees, 1987)***

364184

Complex faulting, disruption, overturning and folding is evident through the sedimentary sequence. An arcuate belt through Moores Pimple, Rosebery and the Pieman River has been termed by Corbett and Lees as the Rosebery tectonic zone. This zone is bound to the east by the east-dipping Rosebery Thrust Fault against the Mount Read Volcanics. Greater intensity of deformation within the fault footwall infers that the lower plate was relatively more active than the upper during tectonic transport; that is, the structure may be an underthrust from the west rather than overthrust from the east (Corbett and Lees, 1987). The variety of fault distribution dominating the internal structure of the Rosebery tectonic zone implies an anastomosing fault system. These faults vary from sub-vertical to moderate easterly dip. Fault pockets or slices extending along strike for up to 10 kilometres generally contain a myriad of close-spaced faulting and shearing. Disrupted zones up to 30 metres contain mélange with near total destruction of bedding. Irregular folding within fault pockets has produced isoclinal to box-like folds. The dominant cleavage within the Rosebery tectonic zone has a meridional trend, generally dipping steeply west to steeply east. The cleavage within more massive volcanic rocks east of the Rosebery Fault dip at 45° to 50° to the east, becoming steeper with movement away from the fault.

The complex fault patterns present in the Rosebery tectonic zone are indicative of extreme mechanical disruption. The development of mélange-type structures is atypical of the Devonian deformation present in similar post-Cambrian sequences within the Dundas trough. Dating of slates of the Stitt Quartzite 1.5 kilometres west-northwest of the Rosebery Mine has provided concordant ages of around 475 to 485 Ma, suggesting cleavages within these rocks to be Cambro-Ordovician (Adams, 1985). Fuchsite (hydrothermal mineral) present within many of the fault zones supports some faulting to be associated with Cambrian hydrothermal activity (Green, 1984). East of the Rosebery Fault, the White Spur Formation is locally tightly folded, however the intense deformation seen within the Rosebery tectonic zone is absent. Folds are generally of north-south trend, of steep axial surface, and of variable but generally low angle plunge with eastern or axial plane cleavage.

Folding east of the Rosebery Fault is along a north-northwest trending axis with a steep axial surface. Shale horizons in the Rosebery and Hercules mines dip to the east at 20° to 50°, although at the Dallwitz prospect and Howards Road, the beds are near vertical. Sulphide orebodies at Hercules have been remobilised and intruded along steep east-dipping cleavages. Within the volcanics, cleavage developed generally trends north-northwest to north, with steep easterly to sub-vertical dips. The dominant cleavage becomes shallow with approach to the Rosebery Fault, with an average dip of 45° adjacent o the fault. Dipping eat, this cleavage is axial planar to folds present within the Rosebery orebody (Brathwaite, 1972). The arcuate bend in the Rosebery Fault at Rosebery is reflected in cleavage immediately to the east - trending from north-northwest to north-northeast around the structure.

364185

Angular discordance the Dundas Group and overlying Ordovician limestones indicates disruption and folding of the Dundas Group in the Late Cambrian-Early Ordovician. Cambrian folding prominent in the Rosebery Tectonic Zone trend north-northeast, and are occasionally overturned from the east. The east-dipping Rosebery Fault bounds the eastern margin. The massive volcanic arc of the Mount Read Volcanics is thought to have acted as a barrier against which the sedimentary sequences of the tectonic zones were compressed and underthrust (Corbett and Lees, 1987). Williams (1978) has recognised that the style of disruption and deformation throughout the Rosebery zone differs from the general broad folding produced the north-south phase of Devonian deformation.

A significant fault slice of the Crimson Creek Formation exists in the western part of the Rosebery tectonic zone. To the east, Dundas Group quartzwacke flank the formation, and to the west, a serpentinised ultramafic body and Dundas Group sediments. Internal disruption and intense shearing adjacent to the faulted margins represent the involvement of the fault slice in the deformation producing the broader tectonic zone (Corbett and Lees). Corbett and Lees (1987) have postulated that the abundance of basaltic greywacke in the Crimson Creek Formation to the representative of deposition adjacent to a basaltic arc or edifice.

364186

CHAPTER 4.

Structural geology of the Stonehenge area

364187

4. STRUCTURAL GEOLOGY OF THE STONEHENGE AREA

4.1 INTRODUCTION

In unison with other western Tasmanian geology, the structure at Stonehenge shows a considerable degree of complexity. The lack of outcrop duly adds to the difficulty of interpretation. A number of deformational events are recognised to have occurred throughout the Zeehan area, the most significant of which are associated with the Frenchman Orogeny (separating early and late Proterozoic sequences), the Penguin Orogeny (Late Proterozoic), the Jukesian Orogeny (upper Ordovician/early Cambrian), the Benambran Orogeny (uplift during late Ordovician/early Silurian and the 'Tabberabberan Orogeny' or correlate event (late Devonian). The variety of structural styles and trends suggests that the Oonah Formation sediments have undergone multiple phases of deformation.

4.2 FOLD STRUCTURE

The geology surrounding the Stonehenge area is dominated by northwest-southeast trending folds. Most obvious south, southeast and east of Stonehenge, this folding is evident within Siluro-Devonian sediments of the Eldon Group (figure 4.1). The anticline-syncline structure forms an isoclinal fold pattern that has been disjointed by a latter period of faulting. The folds have wavelengths varying from 1 kilometre to 3 kilometres, and amplitudes of between 0.5 and 2 kilometres. The occurrence of folding within these sequences enables the estimate of time of folding of atleast Devonian. This is likely to coincide with 'Tabberabberan Orogeny' deformation during the Late Devonian.

Fold structures within Proterozoic units at Stonehenge and to the north thereof, and in Cambrian Rosebery Group Correlates to the east are not obvious. They are, however, likely to have been influenced by the northwest folds evident within the Siluro-Devonian sediments. The Cambrian Mount Zeehan conglomerate body immediately south of Stonehenge, forms an anticline structure which is also orientated along a general northwest-southeast trend.

The most dominant faults throughout this area (dissecting Devonian folds) are orientated along north-northeast and east-west to north-northwest trends. Displacement from the faulting is in the order of 100 to 300 metres. The most dominant fault structure at Stonehenge is the Tenth Legion Fault which is seen to cross through the western to central margins of the prospect area. This thrust fault trends along a northwest axis, separating the Precambrian rocks from underlying Cambrian sequences. It extends northwest beyond the Stonehenge area to meet the Heemskirk Granite

364188

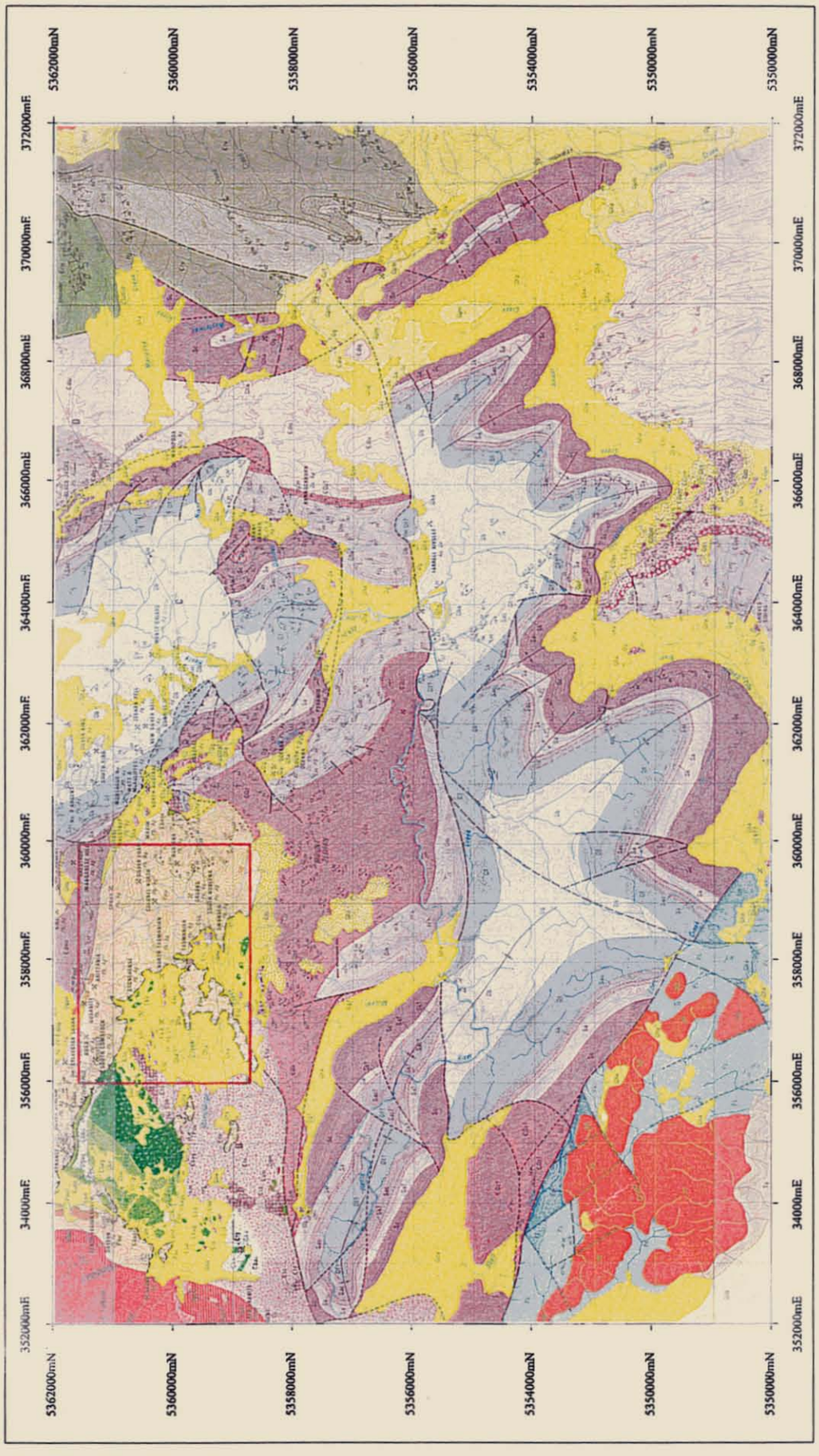


FIGURE 4.1 ***Regional geological map of the Zeehan area showing the dominant NW-SE fold trend within Siluro-Devonian sequences.***

364189

4.3 STONEHENGE FOLD PATTERN

One of the most prominent structural features of the Stonehenge area occurs within the massive quartzite unit outcropping over the central to southwestern margins of the mapsheet. This quartzite sequence provides the overwhelming majority of exposure found, and subsequently is the focus of mapping. Given the competent nature of the quartzite unit, greater deformation is apparent within surrounding pelite units, but they unfortunately are rarely exposed. Throughout the area, bedding is distinguished by a visible grain alignment identifiable in hand specimen. Cleavage development sub-parallel to parallel to bedding is generally well exposed throughout the quartzites. This spaced cleavage is likely to have developed during an event of regional isoclinal folding. Additional cleavages developed within surrounding pelite units are not evident within these less competent rocks.

Fold patterns evident across the Stonehenge area are suggestive of several phases of folding and interference. As shown in figure 4.2, structural traces within the quartzite unit reveal a number of fold sets contributing to the complex fold structure of an interference pattern. This map has been constructed from field data with the addition of surface traces from aerial photos. Up to five fold sets are identified:

1. Early isoclinal folds wrapping around the quartzite unit
2. Northeast-southwest folds
3. North-south folds
4. East-west folds
5. Northwest-southeast folds

Generation of folds sets is difficult to identify. The northwest-southeast fold set provides the best estimate of genesis. Its given orientation matches that of the dominant fold patterns evident within the Siluro-Devonian sediments seen in figure 4.1 to the south, southwest and west of the Stonehenge area. Likely to be produced during 'Tabberabberan' folding, this event is the last to have taken place throughout this area. The wavelength of this final phase fold within the Oonah Formation is around 2 kilometres. This scale of fold matches those of similar trend within the Siluro-Devonian sequences.

An early set is isoclinal folds are thought to exist given the occurrence of an S_1 spaced cleavage parallel to near parallel to bedding. In reference to the map pattern, this sequence is represented by the form shape of the quartzite unit. Its original orientation has been completely obliterated by the subsequent folding events. The remaining fold sets in combination contribute to the fold interference pattern. North-south and northeast-southwest sets appear to form large scale parallel folds with wavelengths of around 500 metres and 1 kilometre respectively. The east west set of folds have been identified from aerial photograph traces. Their shape indicates chevron to parallel folding with wavelengths around 60 metres.

364190

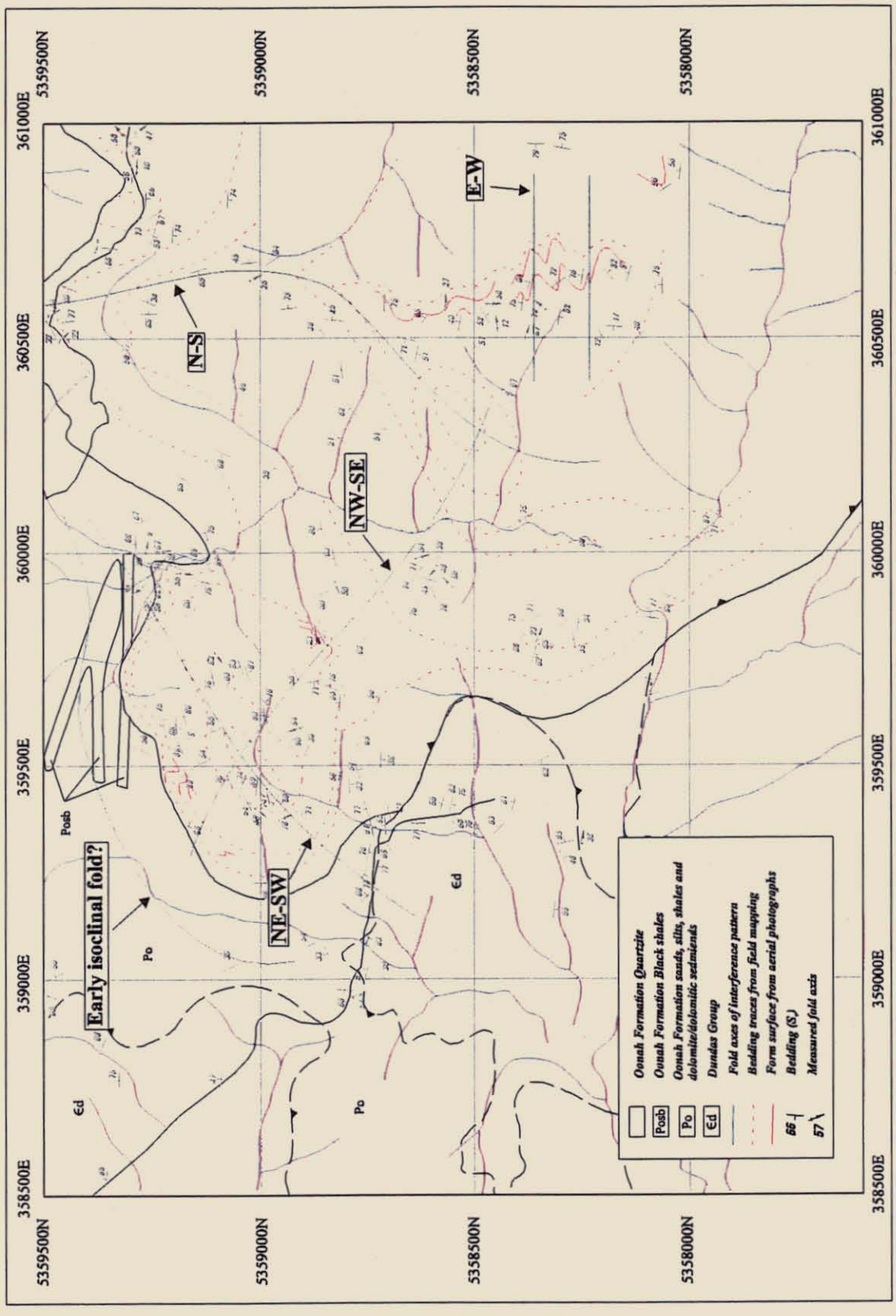


FIGURE 4.2 *Fold interference patterns (dome and basin) with the Oonah Formation quartzite unit (Poq).*

364191

The fold structures identified at surface are reflected by similar structures in section through the mapping area (figures 4.3, 4.4 and 4.5). It is of interest to note that there is apparent variation in the intensity of deformation along differing profile orientations. Cross sections along north-south gridlines (figure 4.3) reveals folded east-west structures. Bedding measurements are generally steep throughout the quartzite sequence. Chevron folds are common with wavelengths varying from 10's metres to 100-200 metres. Less exposure within Oonah Formation pelite units hinders interpretation of the structures within, however it appears to be continuous with the deformation seen in the quartzite unit.

Section along northwest and northeast profile lines (figure 4.4) reveal a similar style of deformation to that seen along north-south lines. Given the lesser amount of information relevant for these profiles, the structures have been interpreted as larger scale than those of figure 4.3, although they in fact be of similar magnitude. Chevron-type folds vary in wavelength up to 500 metres.

North-south trending fold structures are identified in figure 4.5 where the profiles are along east-west lines. There is marked change in the intensity of fold structures along this orientation in comparison with those previously mentioned. These folds form large open hinges with wavelengths exceeding 2 kilometres. The clear lack information gathered across the Dundas Group (representative of the outcrop present) requires considerable estimate of the structure, however the flat lying nature therein is supported by that identified within the Oonah Formation quartzite.

364192

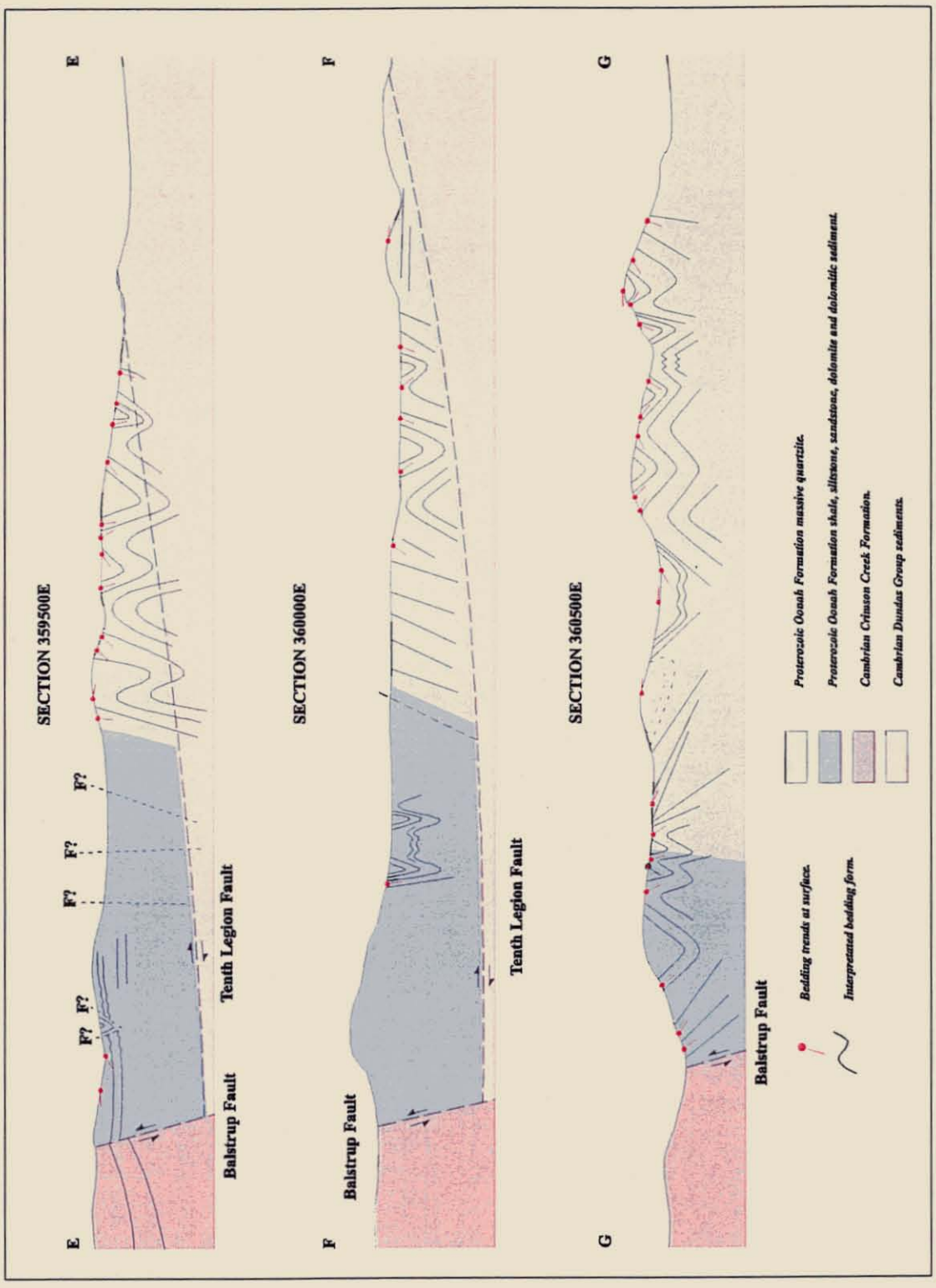


FIGURE 4.3 *Section along lines 359500E, 360000E and 360500E showing structural form from surface mapping, and major fault trends. (Location of section lines is shown in Appendix 7)*

364193

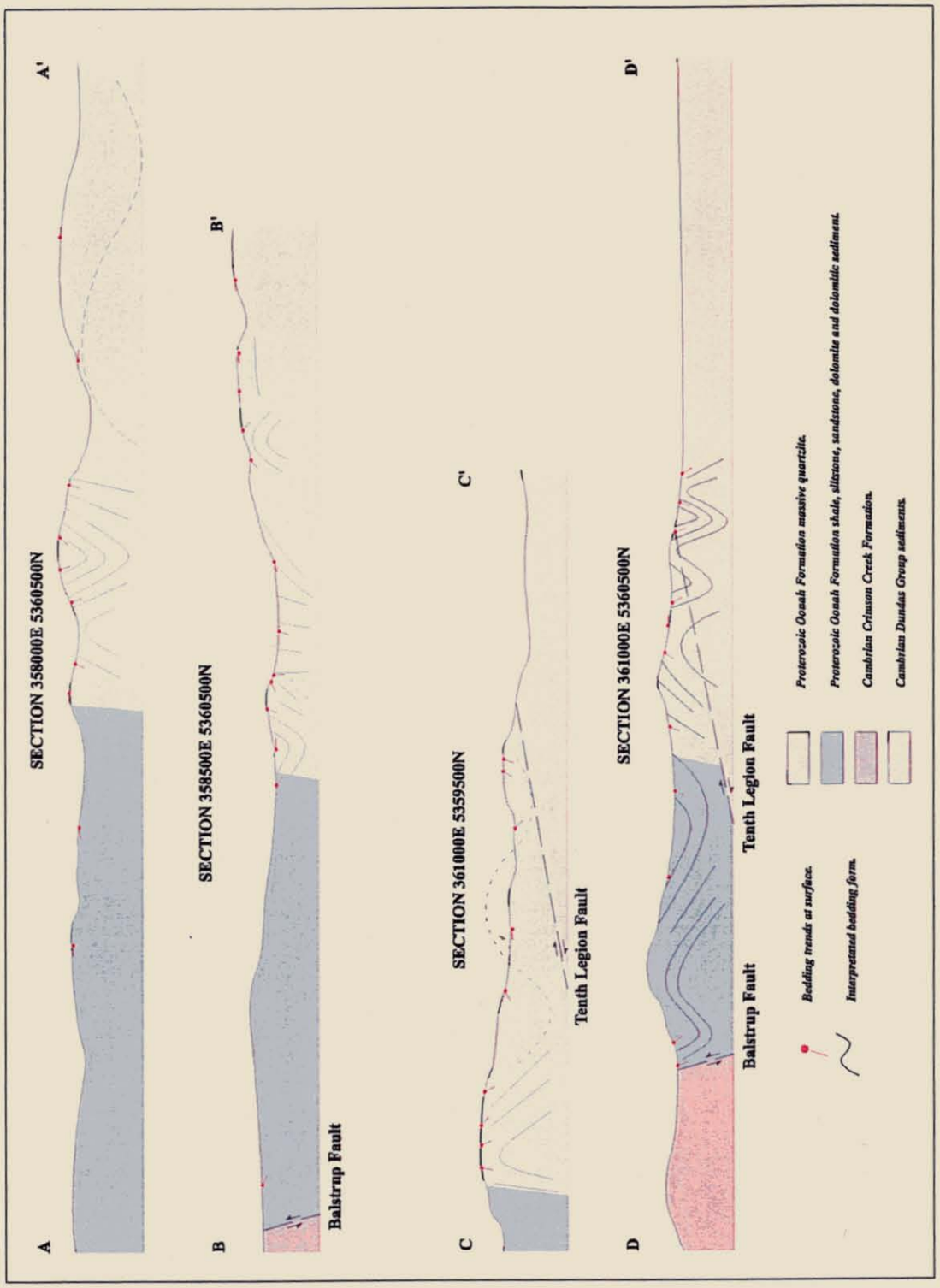


FIGURE 4.4 *NW-SE and NE-SW sections showing structural form from surface mapping, and major fault trends. (Location of section lines is shown in Appendix 7)*

364194

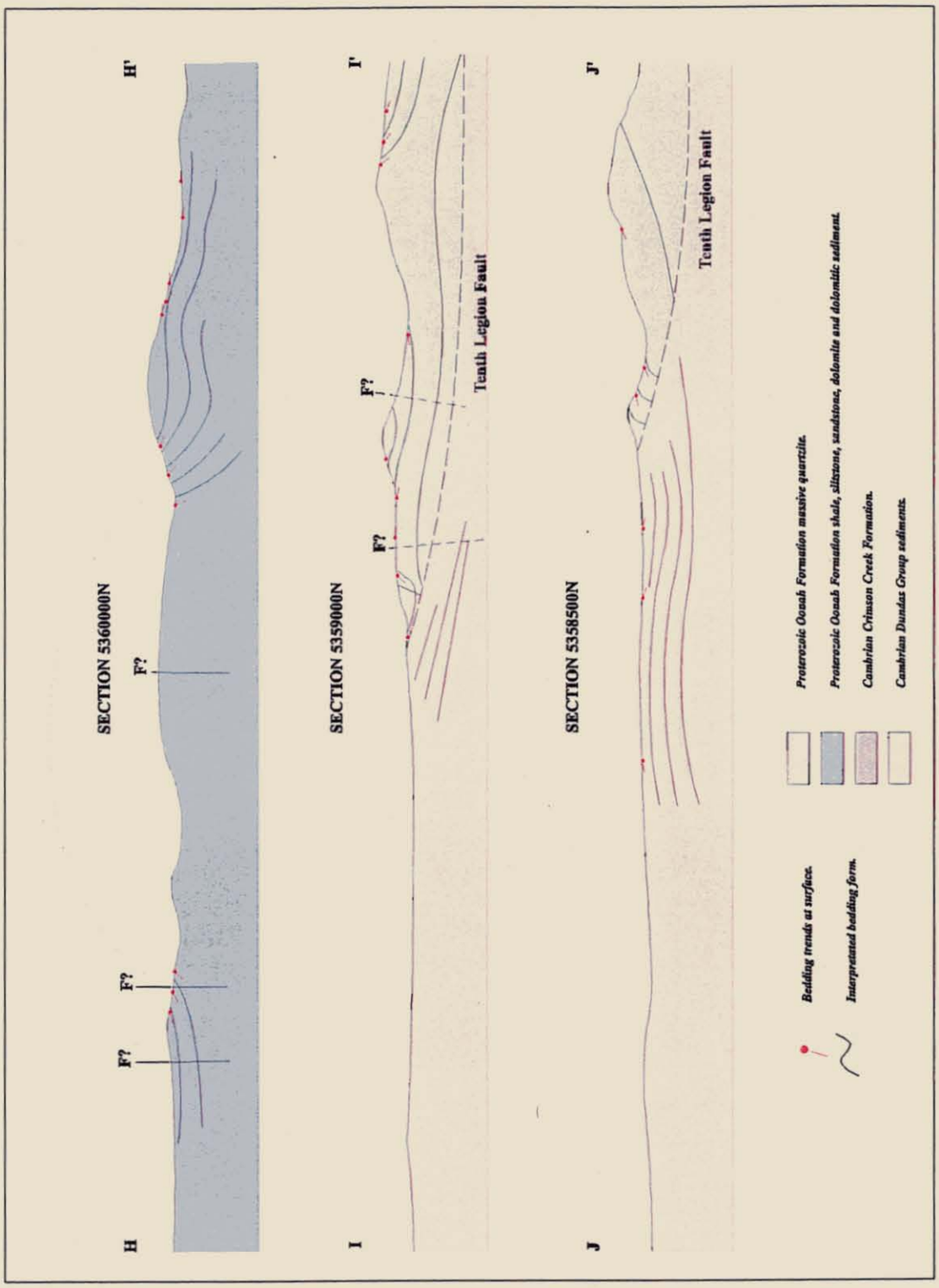


FIGURE 4.5 *Section along lines 5360000N, 5359000N and 5358500N showing structural form from surface mapping, and major fault trends. (Location of section lines is shown in Appendix 7)*

364195

Stereonets

Folding of the Proterozoic Oonah Formation rocks is vast and intense. Wavelengths vary from 10's millimetres to several metres. The spectrum of trend and plunge of fold axis (Fa) and axial surface (As) is diverse, with no outstanding trend orientations evident. To build on the information gathered during field mapping, and stereonet analysis has been sought to provide a greater understanding of the fold geometry at Stonehenge.

To assist in gaining an understanding of the extent, and more importantly trends, of deformation, the Stonehenge area has been divided into 38 structural domains for stereonet interpretation (Appendix 2). '*STEREONET*' Version 3.6 (Richard W. Allmendinger) has been used in the processing of structural field data. This program enables three dimension data to be plotted onto a lower hemisphere projection plane. Bedding and subsequent fold trends obtained via this process, provide an indication of general trends, but little of definitive nature. *STEREONET* plots of cleavage measurements have been conducted in an attempt to identify associated orientations.

The complex nature of the structure evident at Stonehenge is illustrated by the plotting of bedding poles (figure 4.6) From this, it is evident that no definitive bedding trends exist. Rather, the diverse nature of the plot is suggestive of fold interference between two or more fold generations, obscuring early formed structures. Contouring shows a slight dominance of bedding to the west (in particular to the northwest) and to the south.

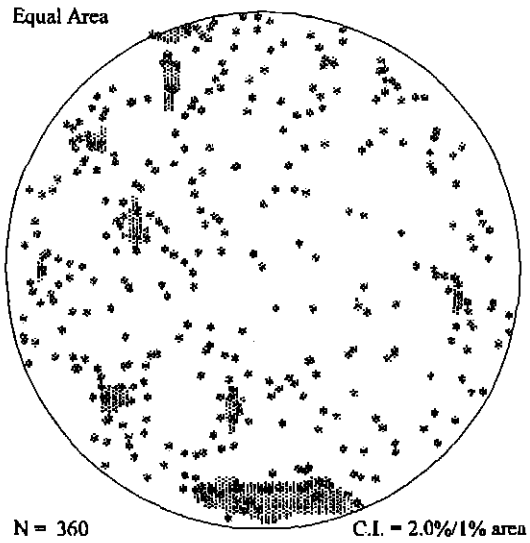


FIGURE 4.6 ***Contoured scatter plots of Stonehenge bedding showing a complete diversity of plot rather than clear trends.***

Two sets of fold axes have been plotted. The first, *determined fold axes*, has been produced from the plotting of great circles to poles to bedding. As seen in figure 4.7, plotting of all determined fold axes identifies no distinctive fold patterns. Rather, the fold axes produced are of a diverse range of trends and plunges, again suggesting the occurrence of fold interference patterns. Many of the domains recognised for stereonet interpretation contain limited data, hence it should be recognised that plotting of great circles may be often be open to error. Contouring has identified a cluster of steeply plunging folds of varied orientation.

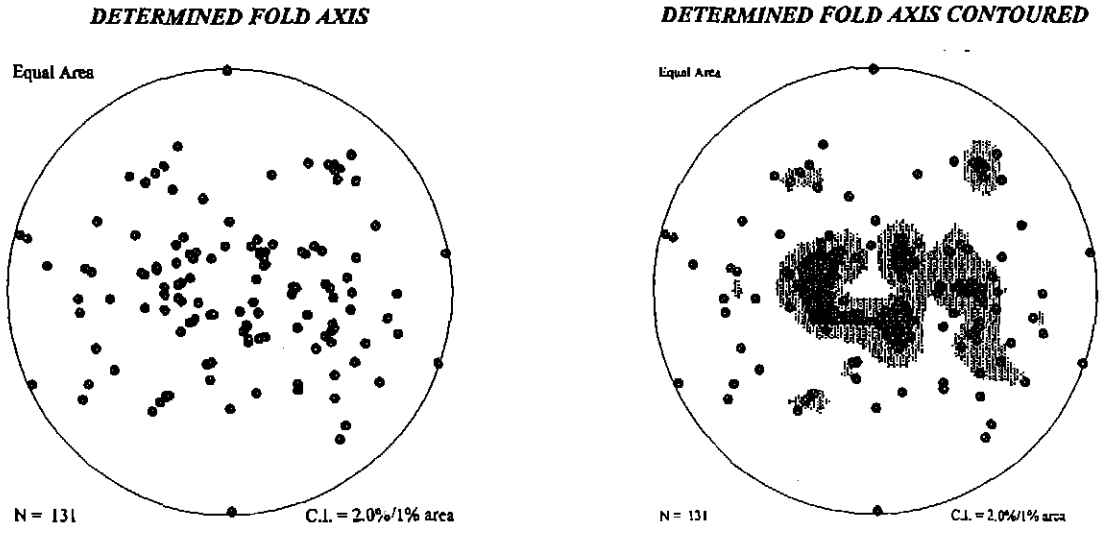


FIGURE 4.7 *Scatter and contoured scatter plot of Stonehenge determined fold axis from poles to bedding.*

The plotting of *measured fold axes* (measured in the field) shows a similar diversity of folding, however some general trends have been identified by contouring the plots (figure 4.8). Two main groupings of axes appear:

- The first is a near vertical grouping along an east-west axis. Differing fold orientations and variation in plunges of folds across the east-west axis is likely to be representative of fold interference pattern. Within, there appears to be a shallow plunging 'sub-group' to the east, and a steep plunging 'sub-group' to the southeast.
- The second forms a group steeply dipping west along a north-south trending plane. Along the plane, folds are seen to vary from shallow to steep plunge. A shallow plunge to the south is apparent, with a 'sub-group' of folds plunging steeply to the southwest. Contouring clearly illustrates additional fold sets, one steeply plunging east and south, the second gently plunging east.

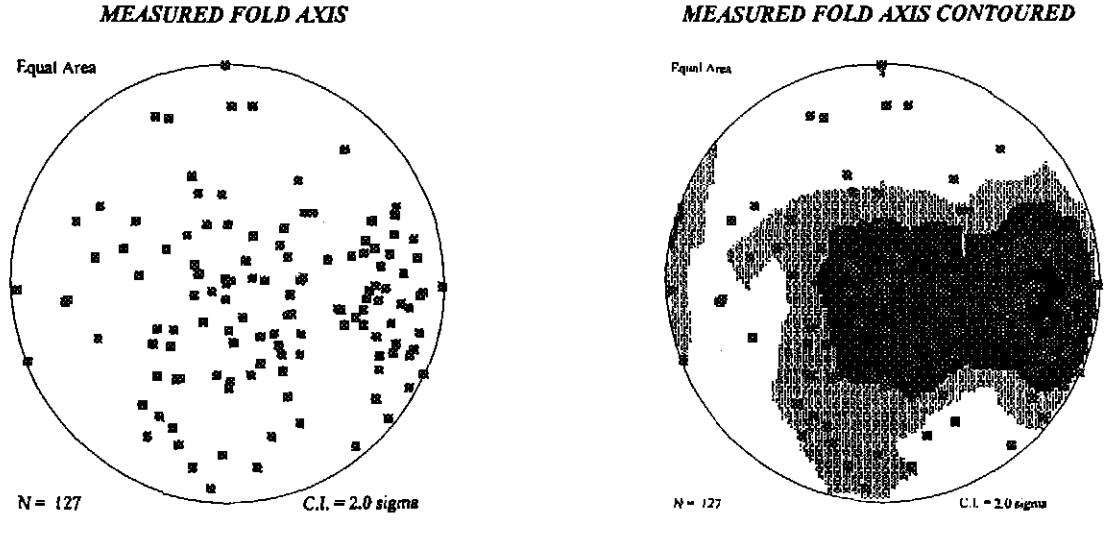


FIGURE 4.8 *Scatter and contoured scatter plot of Stonehenge measured fold axis.*

364197

In general, the plotted folds show steeply plunging dips along axes planes trending east-west, north south and seemingly less obvious. northwest-southeast. In each instance there is rotation of the plunge direction along the fold axes. As with the varied bedding plot, the scope of fold axes plots indicates the occurrence of fold interference patters.

Cleavage plots have been sought to define orientations for the three sets measured in the field and seen under microscope. Again plotting of the cleavage data shows distribution of dips, however three sets are distinguishable. Contouring of the sets has identified orientations of N-S, E-W and NE-SW (figure 4.9).

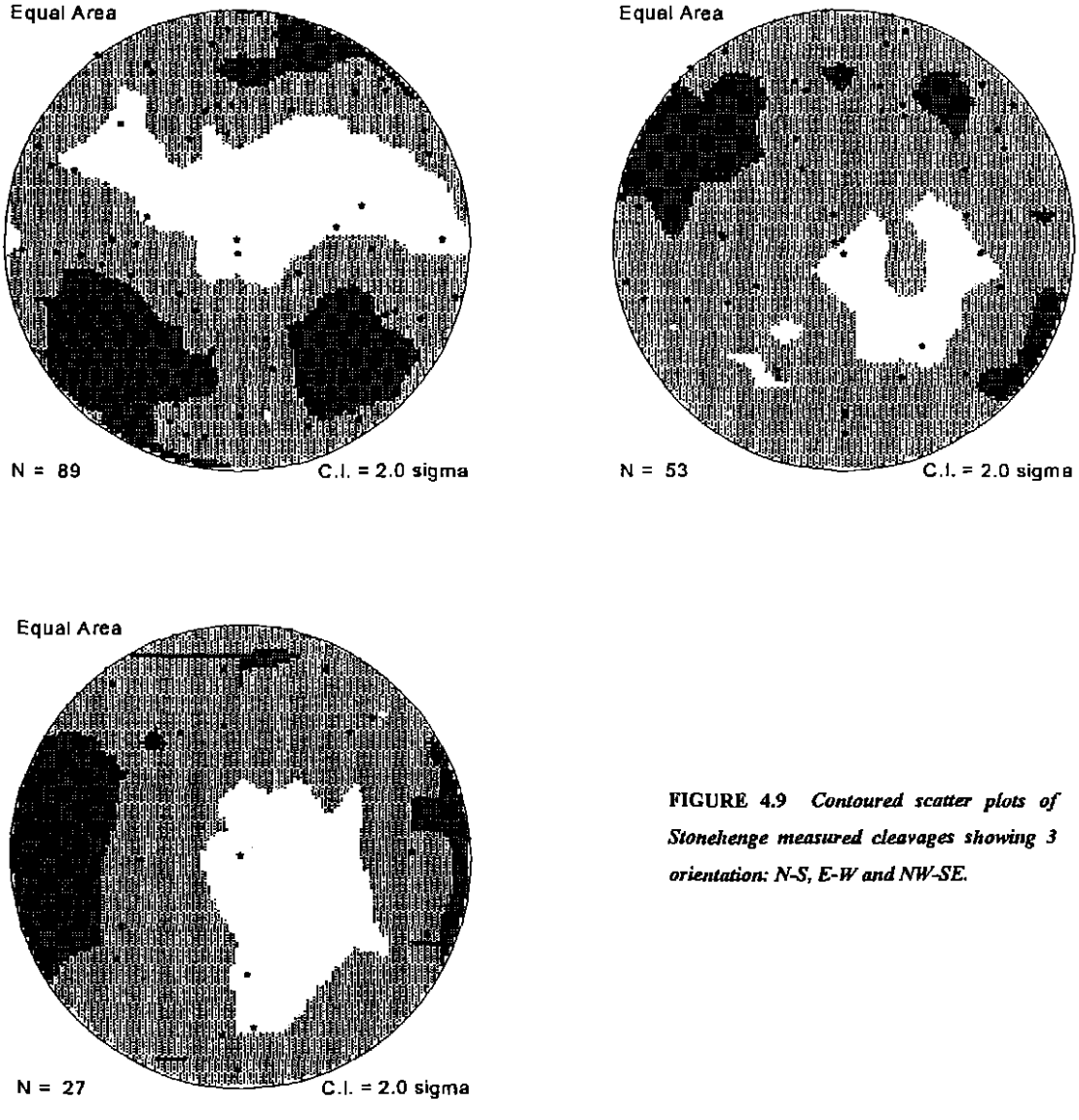


FIGURE 4.9 *Contoured scatter plots of Stonehenge measured cleavages showing 3 orientation: N-S, E-W and NW-SE.*

364198

No distinct fold trends and plunges have been exposed using stereonets, rather, the complex nature evident supports the mapped fold pattern seen in figure 4.2. The identification a of northwest-southeast fold set matches that evident within Siluro-Devonian sequences surrounding the Stonehenge area. These folds are recognised as the last set forming during the 'Tabberabberan Orogeny'. East-west and north-south trending fold sets identified by stereonet also match similar trends within fold pattern. In each of these stereonet plots, dips are seen to vary in plunge, indicative of beds rotation during interference folding.

Fold interference pattern

The mapped fold pattern appears to represent two types of interference as illustrated by Twiss and Moores (1992). The primary fold pattern evident within the quartzite unit is that of simple dome and basin structures (type 1, figure 4.10). Two dome regions (topographically high) covering the northwest and southeast margins of the Oonah Formation quartzite unit, are separated by a trough region (topographically low). Early isoclinal folding evident from near-bedding parallel cleavage development has been folded by subsequent fold sets of steep axial surfaces. These later sets of folds identified in the form map have orientations of north-south, east-west, northeast-southwest and northwest-southeast.

The primary type 1 fold interference pattern may involve additional type 3 patterns. Variation in the attitude of the S_1 spaced cleavage from flat to steep indicated the early fold to be isoclinal, as seen in type three interference patterns (figure 4.10). The type 3 fold pattern is seen produce plunging antiform/synform structures of wavy outcrop pattern such as those evident immediately north of the quartzite unit (figure 4.11). Although not exposed, a synform structure has been identified through interpretation of wacker sampling. This structure trends along an east-west axis, and plunges to the west. Half wavelength width for the fold is around 100 metres. Another fold structure along similar trend within pelite units north of the quartzite sequence also represents the interference of simple dome and basin structures (type 1) with more complex type 3 structures.

Stereonet domains 25 covers the majority of dome and basin structures within the central to northwestern margin of the quartzite unit (see stereonet domain map, Appendix 2). The bedding plot seen in figure 4.12A reflects the scattered nature of plot for the entire Stonehenge area. Steep beddings are of a complete scope of strike direction, with a dominance along the north-south trend. Along this orientation, dips are steep in both directions (north and south). The stereonet plot of fold axes over the same area (figure 4.12B) indicates the likely occurrence of fold sets along north-south, northwest-southeast and east-west orientations, all of which are steeply plunging. The extensive coverage that domain 25 maintains over the dome and basin structure suggests that subsequent stereonet plot should be representative of the structure present. Both bedding and fold axes plots in figure 4.12 support interpretation from the map pattern within the quartzite unit figure 4.2, and additional stereonet plots.

364199

Unfortunately the lack of exposed pelite and dolomitic sediments surrounding the quartzite unit hides the fold sets identified within the quartzite unit. It is, however, expected that the same structure would be evident given adequate outcrop.

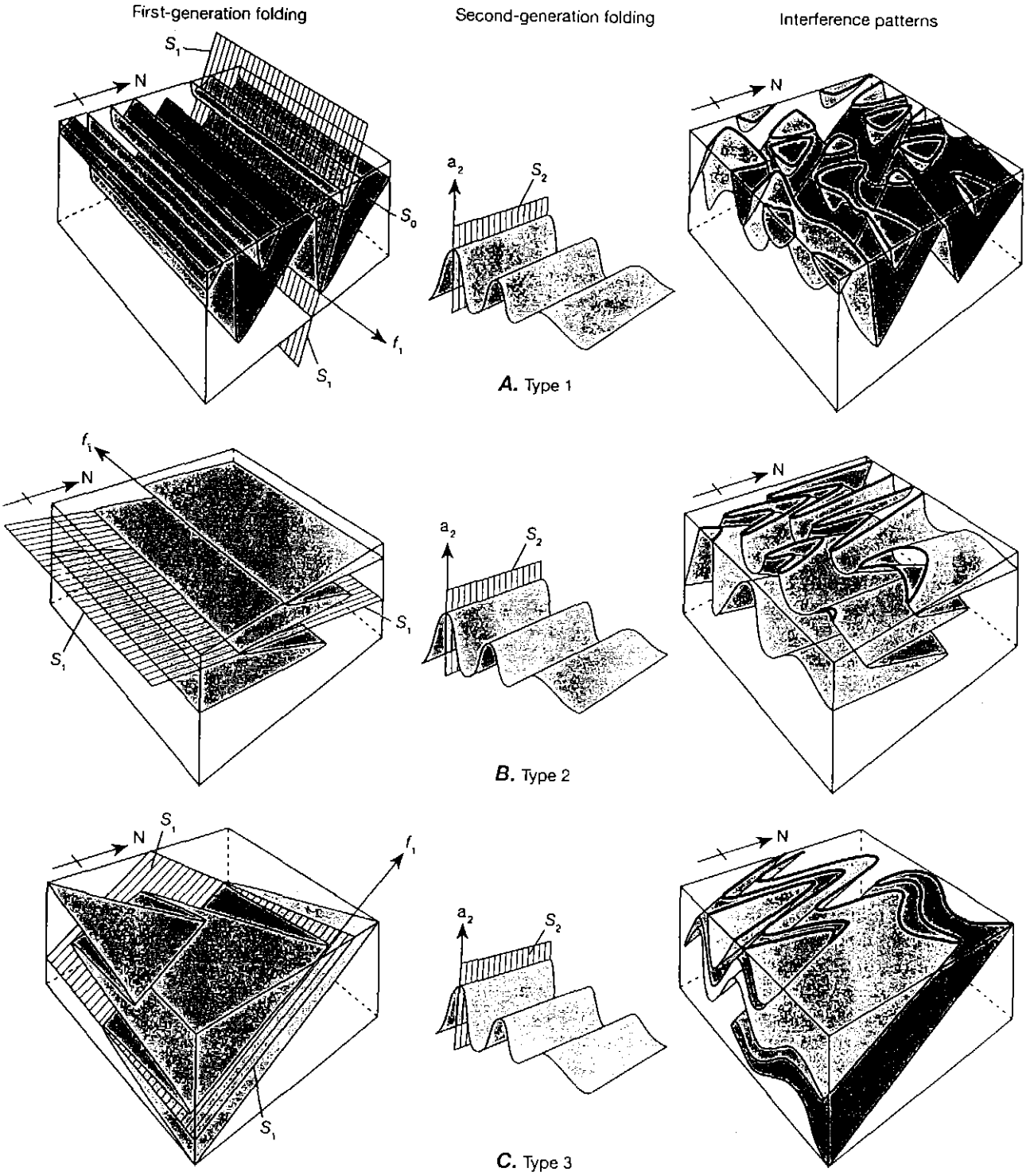


FIGURE 4.10 ***Fold interference patters. A. Type 1 interference folds, showing simple dome and basin interference patterns; B. Type 2 interference folds, showing arrowhead- or mushroom- shaped patterns; C. Type 3 interference folds showing wavy outcrop pattern of the S_1 axial surface. (from Twiss and Moores, 1992)***

364200

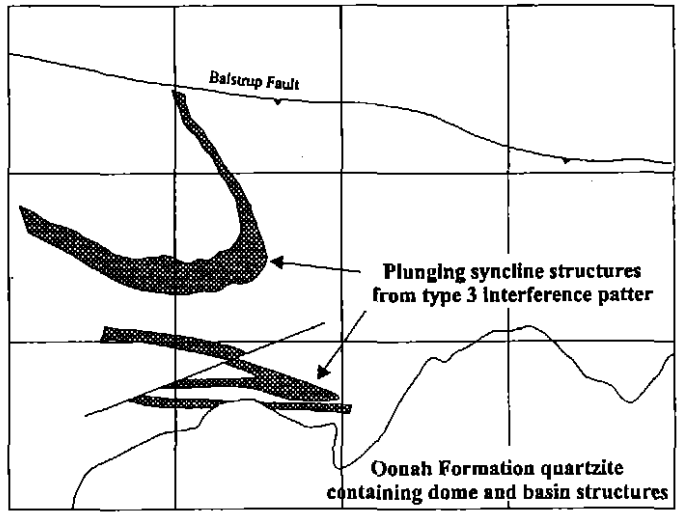


FIGURE 4.11 *Synclinal structures reflecting the occurrence of type 1 and type 3 fold interference patterns.*

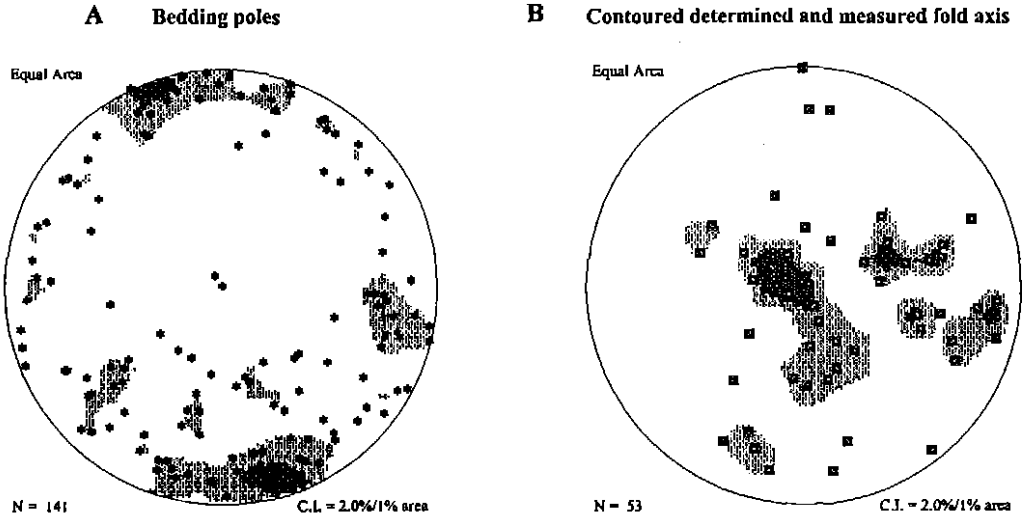


FIGURE 4.12 *Stereonet plots of bedding and fold axes for domain 25.*

4.4 MINOR FOLDS

Fold relationship have occasionally been identified in outcrop. Most common, early isoclinal folds (F_1) are seen to have been folded by latter events (F_2 and later). The size a folds vary from centimetre scale to several metres. Figure 4.13 (from station MU96-168) is a typical example of F_1/F_2 relationship. Figure 4.14 (from station MU96-169) shows a F_1 folding S_o with S_1 axial planar to the hinge. This fold forms the limb of an isoclinal fold structure. The fold hinge plunges at 23° to 103E, and the axial surface, 80/074S. The orientations of this F_1 fold suggests formation along an east-west fold axis, however interference from later folding events obscures any recognition of true fold axes.

364201

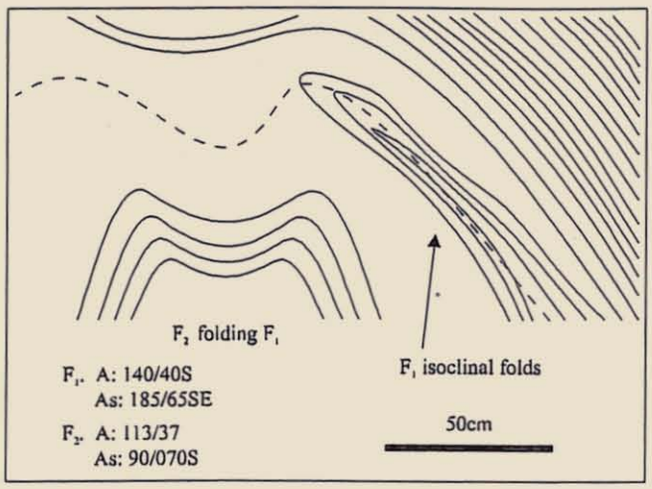


FIGURE 4.13 *Diagrammatic representation from MU96-168 showing common relationship between F_1 isoclinal folds and F_2 folds.*

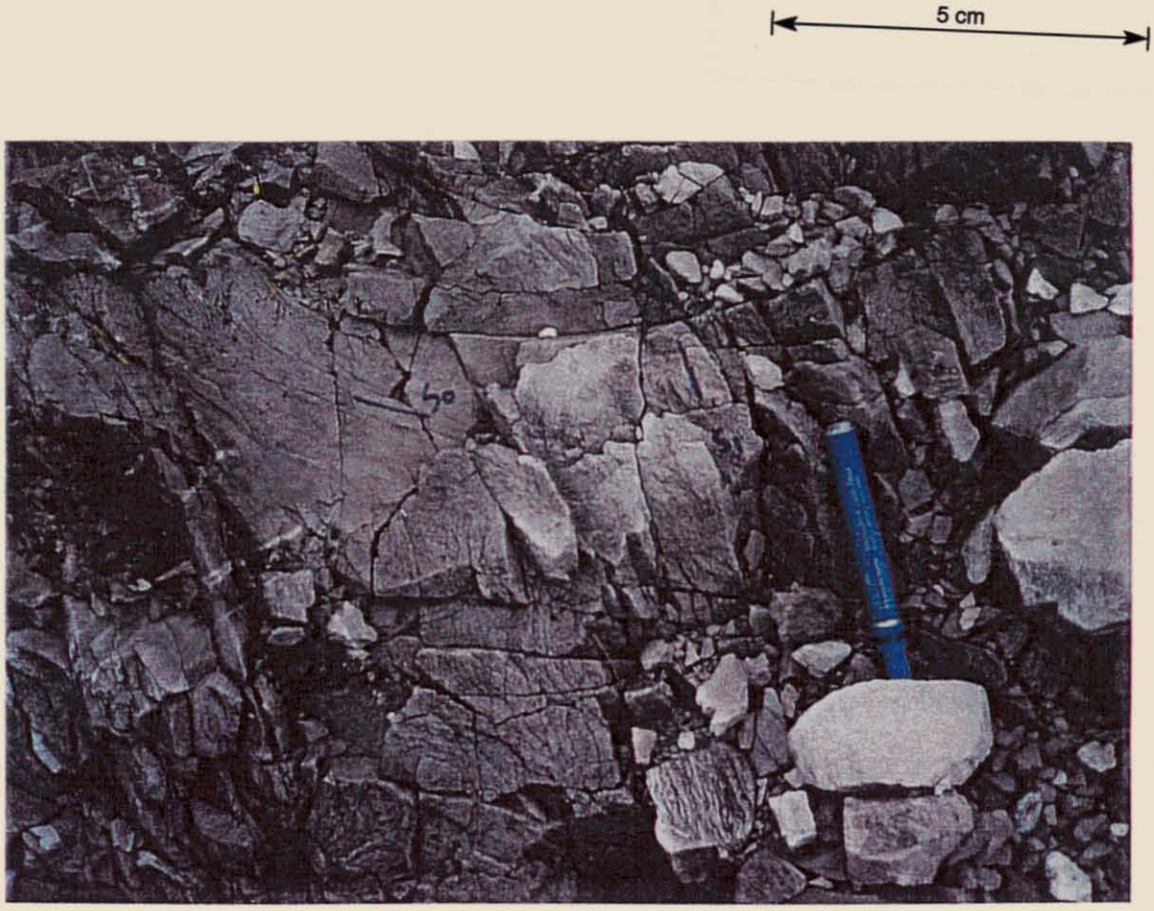


FIGURE 4.14 *F_1 fold hinge from field station MU96-169. So is folded about F_1, and S_1 has developed axial planar to the fold surface.*

364202

Chevron fold structures found in outcrop support similar folds in profile through the Stonehenge area. Figure 4.15 shows fold patterns from station MU96-143. The folds are moderate steeply plunging along an east-west axis. S_1 is sub-parallel to S_0 , and has been folded by S_2. This F_2 fold has S_2 developed axial planar to the fold hinge. A third cleavage (crenulation) dipping east along a north-south trend indicated a later F_3 folding.

Folds evident in figures 4.16 and 4.17 show later folding of early isoclinal folding. The latter shows microlithon development of So within S_1. The line of fault movement has been folded by a later period of deformation. Early folds in the upper left of the diagram have been folded by an F_2 'box-like- fold. Bedding trends are along a general north-south line, dipping steeply to the west, with fold hinges along similar orientation.

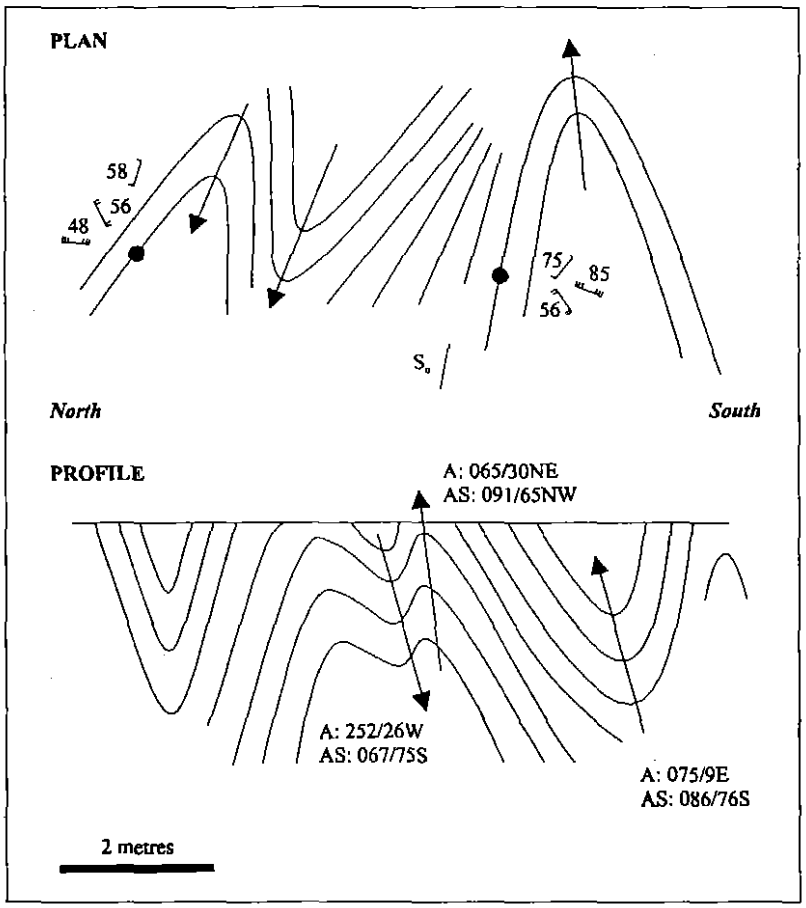


FIGURE 4.15 *Fold structure from station MU96-143. Plan: shows chevron-like folds with variable plunge, and cut by two sets of crenulation cleavages. Profile: shows chevron fold-form of varied plunge direction.*

5 cm

364203

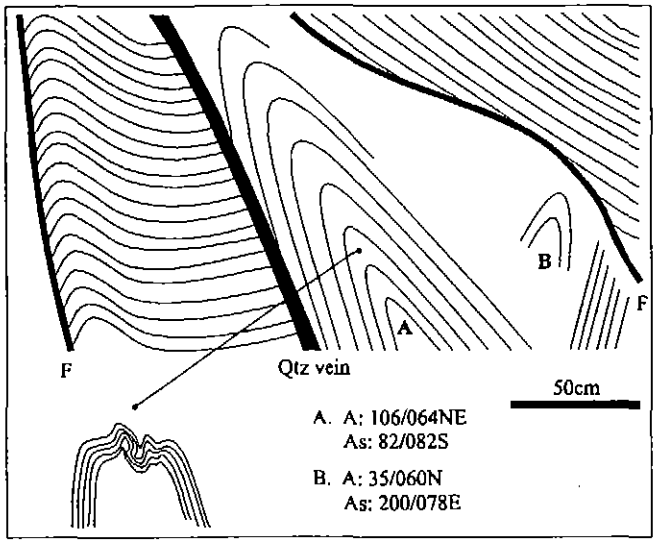


FIGURE 4.16 ***Fold development with shales from station MU96-2. F_1 isoclinal folding in the limb of a later fold (F_2?).***

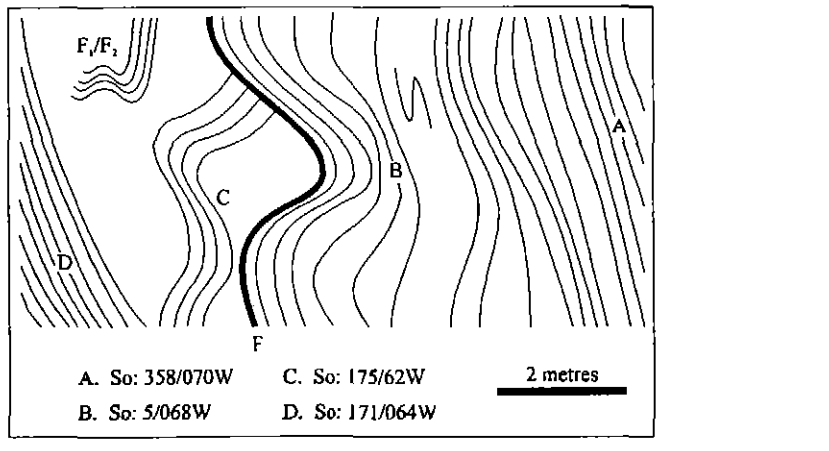
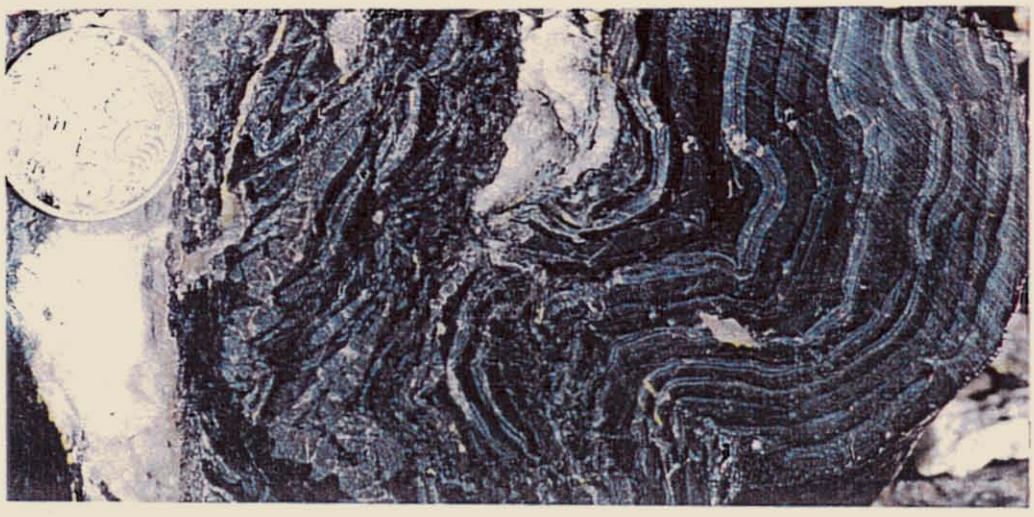


FIGURE 4.17 ***Folding from station MU96-35. Microlithon isoclinal folding within S_1. Faulting along S_1 has been folded by later fold events.***

Box folds (disharmonic or polyclinal folds) associated with weak cleavage development have been identified at both hand specimen and microscope scale. In figure 4.18, the box folds occur within a laminated siltstone/mudstone sequence. The folds have formed disharmonically with respect to the cleavage dominated segment apparent in the left margin of the photograph. The cleavage microlithons are seen to form along S_1 at approximately 45° to the core axis. Quartz filled tension gashes. Some slip must have occurred on the surfaces fold surfaces, now defined as quartz filled tension gashes.

364204

Dilation vein



Dilation vein

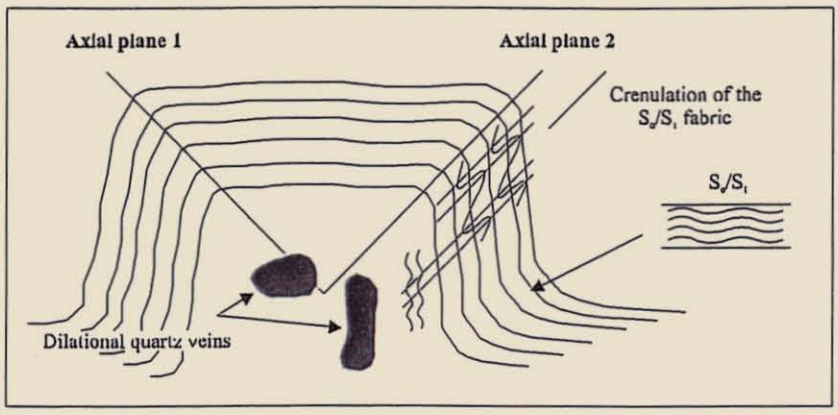
FIGURE ***4.18 Box folding of a sandstone/shale sequence from ZS31, 162.1m. The fold has formed from differing layer competence. Microlithons represent first generation isoclinal folds along S_1. Quartz veins appear perpendicular to the core axis.***

The photomicrograph (figure 4.19) of a sandstone from station MU96-27 shows folding of both bedding and an S_o/S_1 fabric identified by mica orientation, grain alignment and crenulation cleavage, and the formation of two axial planes (a common feature of box-type folds).

Bedding and S_1 cleavage are folded by a later second generation folding event. The quartz vein present in the centre of the box fold represents dilation during the box folding event. During slip movement between layers, crack growth begins whereby the volume of opening cracks begins to offset the normal volumetric decrease associated with increased stress. Eventually the volume decrease from increasing compression has been exceeded by the crack forming volume increase, producing a dilation along which shear fracturing may continue, and fluids may be included/trapped (Twiss and Moores, 1992). In this instance the resultant void has filled with quartz to produce the dilation vein. Box folding in figure 4.19B (photomicrograph from station MU96-27) shows the typical of axial plane formation intersecting each of the fold hinges. An S_1 fabric exists parallel to bedding. Both fabrics have been crenulated by later development parallel to axial plane 2. Mica's have formed along the So/S_1 fabric, and along each of the axial plane orientations. Again, quartz veins within the centre of the box fold appear to have formed within dilation voids produced during folding.

364205

A



B



FIGURE 4.19 *A. Diagrammatic representation of axial surfaces developed within box-type folds. Dilation quartz veins exist within the centre confine of the box fold. The S_2/S_1 fabric has been crenulated parallel to the axial plane. B. Photomicrograph from MU96-27 showing box folds within a sandstone. Both So and S_1 have been folded by a later deformational event.*

364206

4.5 FOLIATION DEVELOPMENT

Disjunctive foliation's ("disjoined or dislocated") are evident throughout the Stonehenge area. Styolitic, anastomosing and moderately rough foliation's are present within quartzite and phyllitic units of the Oonah Formation.

The first fabric to have formed through the Stonehenge area is that of a spaced moderate to rough foliation developed near parallel to bedding (figure 4.20A, 4.20B and 4.20C). This fabric is evident through all rock units and is clearly identified in field specimen. The anastomosing-like cleavage has foliation development often continuous for greater than 5 centimetres. Figure 4.20C is a photomicrograph of a phyllite sample from outcrop, clearly showing the spaced cleavage development at low angle to layer detrital micas which define the bedding. Minor grain alignment distinguishes foliation development along a similar orientation. The variation in angle to S_o is a function of the competency of the rock type. Within the quartzite/sandstone, this spaced cleavage ranges from parallel to S_o, to 25° to S_o, whilst in pelitic units, the cleavage is predominantly sub-parallel to S_o. The development of cleavage development along bedding signifies early isoclinal folding.

Microfoliations are evident in drill core samples. In figure 4.22B, such remnant structures developed between cleavage include isoclinal folds with relict hinges. Here, foliation development has been parallel to an S_1 cleavage fabric, and folded by a latter event. As demonstrated by Twiss and Moore's (1992) development model of transposition foliation (figure 4.21), folds enveloped within the S_1 fabric are deformed into the transposition foliation (S_2 or later). Relict hinges preserved within the S_1 foliation indicate early isoclinal folding. Figure 4.23 also contains microlithon structures within pelite sequences. Micro-fold and hinge structures in this example are parallel to bedding. The isoclinal fold structures produced are of centimetre scale, and have a 'wavy' texture representing the intensity at which deformation has occurred. The occurrence of transposed zones reflects very strong to intense deformation, and may represent high strain zones (shear zones?) associated with the early 'isoclinal' folding event.

364207

A



B





C

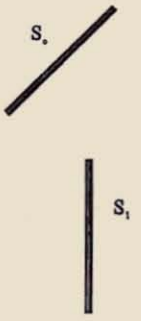


FIGURE 4.20 *Spaced cleavage development (S_1) within phyllite units. A. ZS31, 167.5m showing S_1 sub-parallel to So; B. ZS31, 203m, showing S_1 formation at low angle to S_o; C. Photomicrograph from station MU96-25. Note the mica growth along So representing the near-parallel nature of S_1/S_o. Some detrital micas within the cleavage zone are thought to have been introduced by passive rotation during pressure solution.*

364208

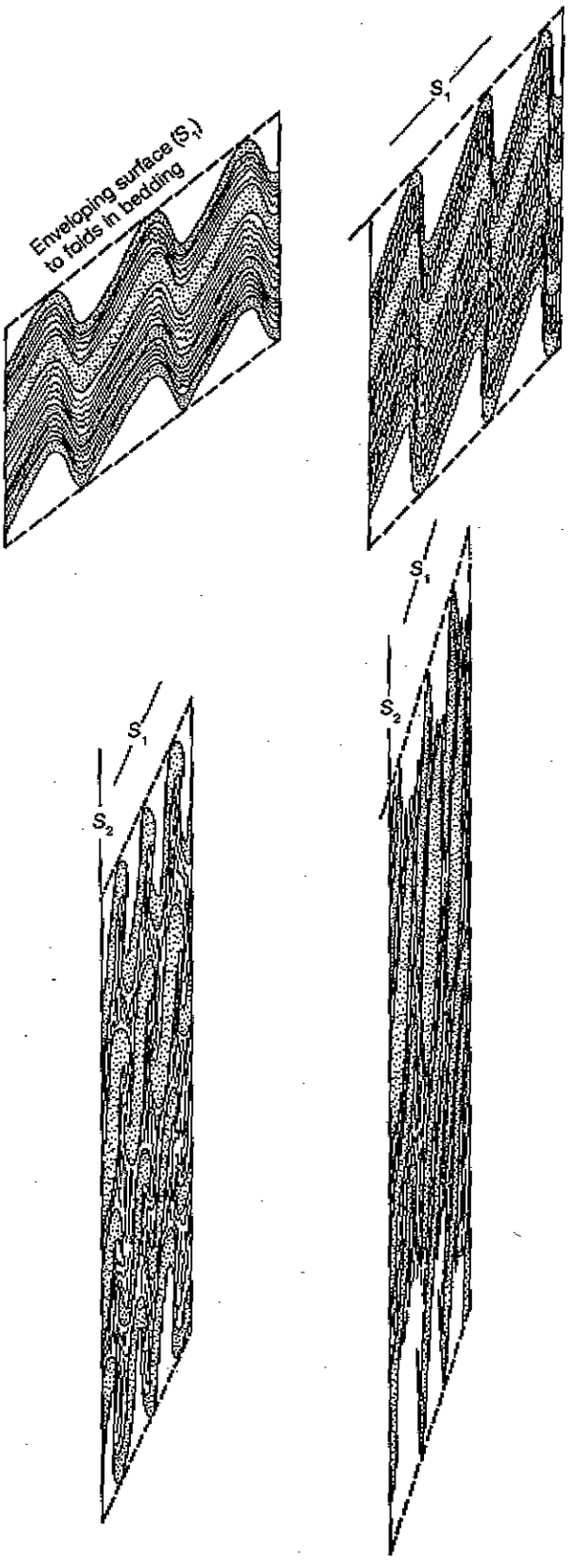
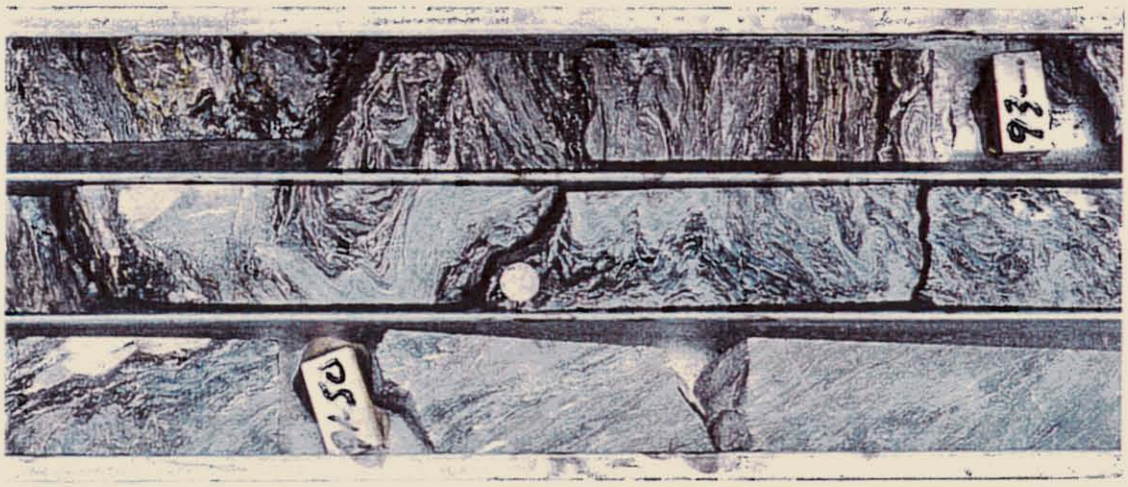


FIGURE 4.21 *Possible sequence in the development of transposition layering (foliation). S_1 is the enveloping surface to the folds in bedding. S_2 is the transposition foliation. (from Twiss and Moores, 1992)*

364209



A

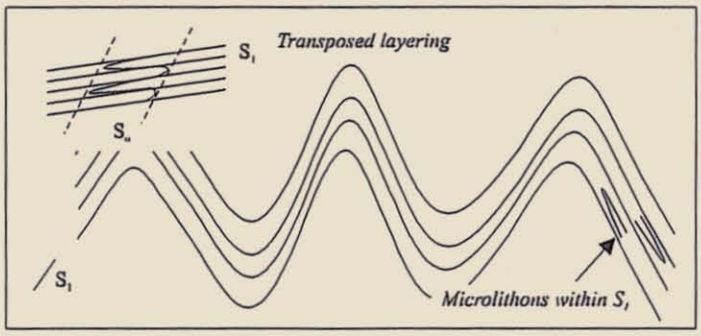


FIGURE 4.22 *Showing fold structures within shale/arenaceous sequences of ZS31. A. ZS31 90.9 to 93.7 showing continuous exposure of isoclinal fold sequences. B. ZS31 83.5m. Similar deformation with transposed layering producing relict fold hinges within S_1 microlithons. The earlier S_1 fabric has been folded by a latter deformation event. S_1 is parallel to isoclinal folds within the layering.*



B

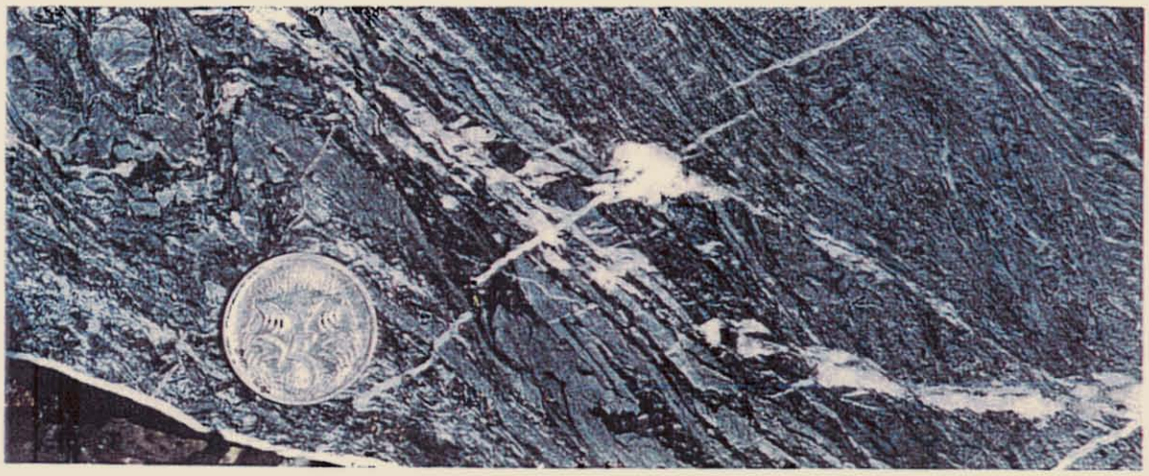


C

364210



FIGURE 4.23 *Transposition layering from ZS31, 90m. Isoclinal folding is seen parallel to both S_o/S_1.*

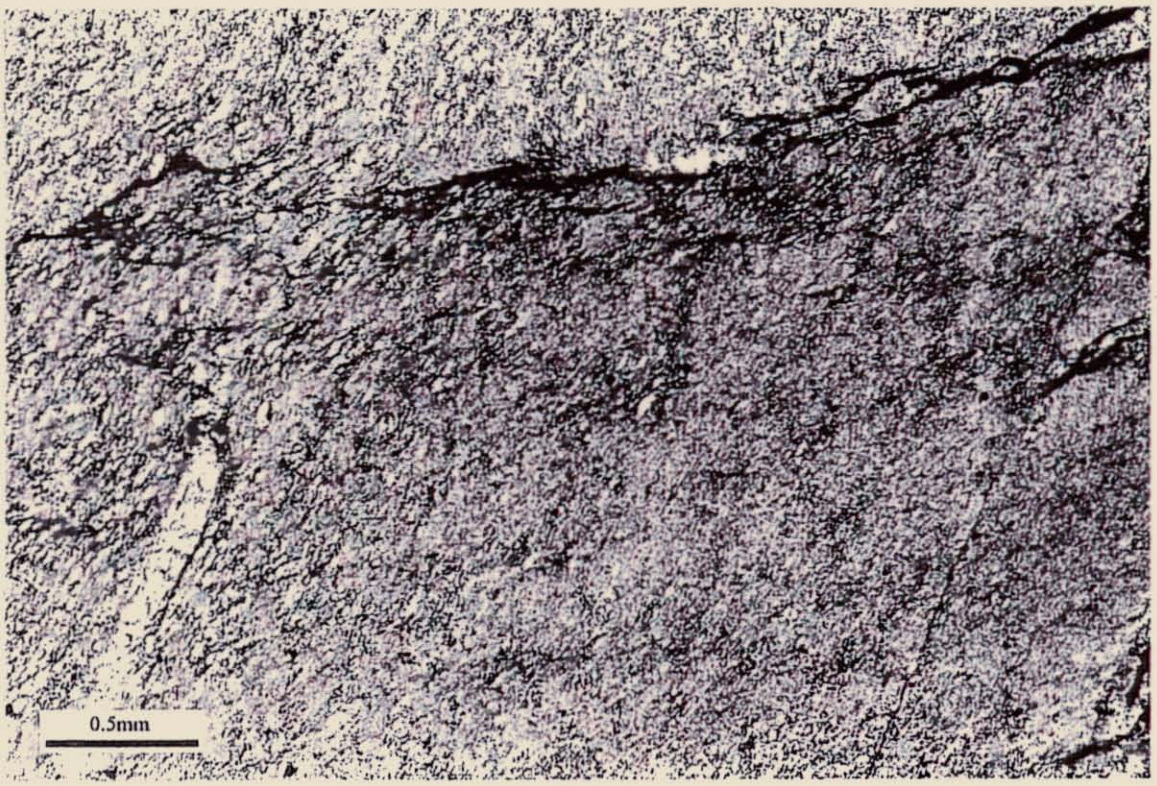


Transposed zone

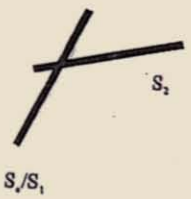
Most prevalent within the Oonah Formation shale sequences, the spaced S_1 cleavage has been overprinted by up to 2 crenulation cleavages. The S_2 cleavage is typically at high angle to S_1, and varies in nature from zonal crenulation foliation to discrete crenulation foliation. An S_3 cleavage is occasionally found to have formed at low angle to S_2, and is generally more discrete. Sample photomicrographs of figure 4.24 show the development of crenulation cleavages in pelitic units. The shale of figure 4.24B show formation of S_1 along S_o, and its subsequent folding by S_2. The angle between S_1/S_2 is close to 90°. Overprinting S_2 is a third crenulation orientate at approximately 65° to bedding.

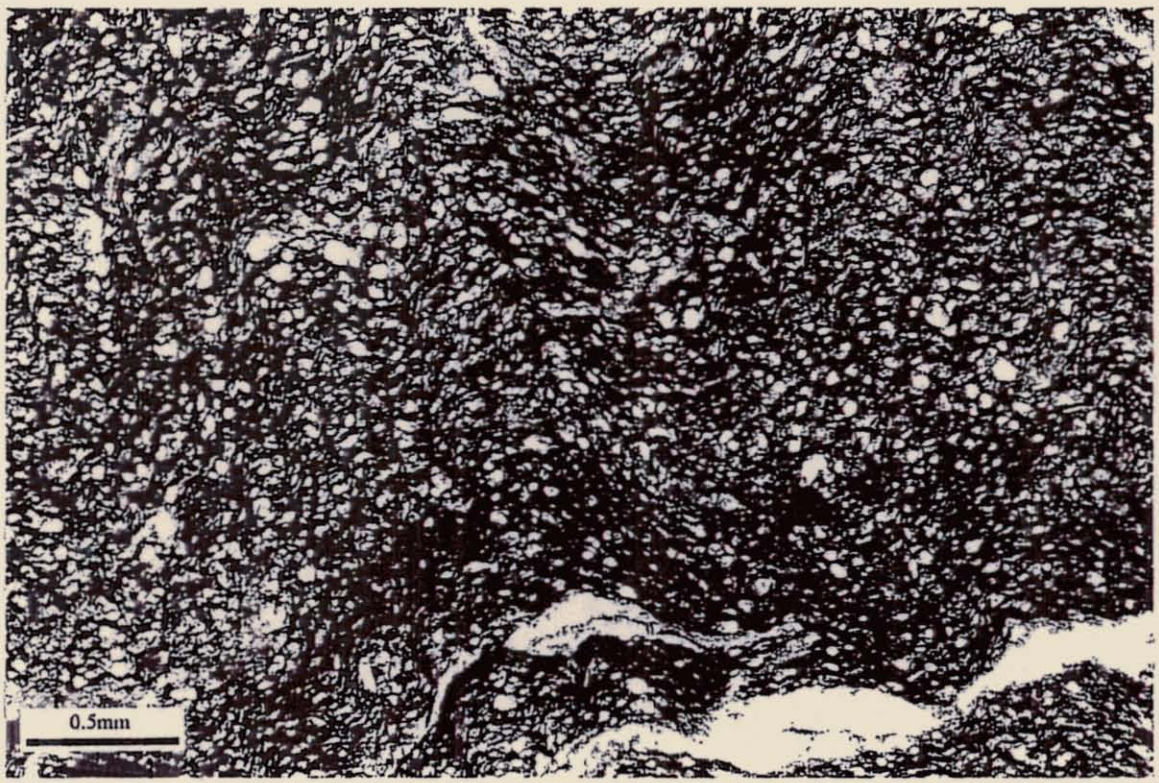
Across Stonehenge, the S_1 cleavage varies orientation with bedding as would be anticipated. There is a general roll from a north-south orientation in the pelites of the northern map area to an east-west orientation throughout the quartzite sequence further south. The S_2 cleavage appears to follow a similar rotation pattern to the S_1, however at a discordant angle (S_2 orientation tend to be perpendicular to S_1). Although rotating throughout the area, S_3 cleavages maintain a *general* north-south trend.

364211



A





B

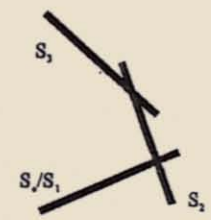


FIGURE 4.24 *Crenulation cleavage development within Oonah Formation sequences. A. Shale from station MU96-162 showing strong S_1 development sub-parallel to bedding, and S_2 at high angle; B. Shale from station MU96-25 showing S_0/S_1 crenulated by S_2 at high angle and S_3 at low angle to S_2.*

364212

Styolite foliation exists primarily within limestone/dolomite sequences (figure 4.26) where black irregular clay seams define the cleavage plane. Generally they appear parallel to sub-parallel to bedding. Such styolites are generally likely representative of volume-loss during burial (compactional strain), however the intense veining truncated by the styolites indicates reactivation during deformation. Styolites at high angle to bedding indicate a related tectonic event emplacement with layer-parallel shortening. The nature of styolite form is irregular, with the principal stress component σ_1 normal to the foliation (figure 4.25).

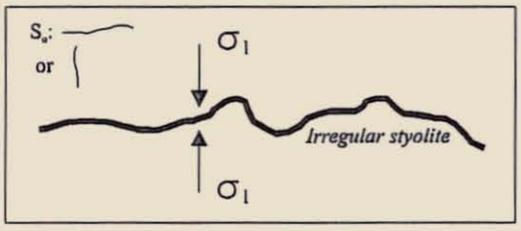


FIGURE 4.25 *Styolite relationship to the direction of principal stress. (after McClay, 1987)*



FIGURE *4.26 Stylolite formation along bedding within shales from Zs31.*

4.6 MAJOR FAULTS

Faulting is a prominent feature of the Stonehenge geology. To the north and south, major thrust faults trend around a west-northwest axis. To the south, the Tenth Legion Fault separates the Proterozoic Oonah Formation from the Cambrian Dundas Group of sediments. The fault intersects the centre mapping area from the northwest corner to the central southern boundary. The surface nature of this fault in unison with outcrop exposure near the South Comstock mine indicate thrusting to be near horizontal. The exposed fault zone contains brecciation of Dundas Group meta-sediment overlain by Oonah Formation silts and shales. Slikenslide striations are particularly evident with phyllitic sequences. Their northeast-southwest trend indicates thrust movement along this axis. In addition, Reidel shears (figure 4.27) indicate thrust movement of the Cambrian sequence to the east, lifting the Oonah Formation.

364213

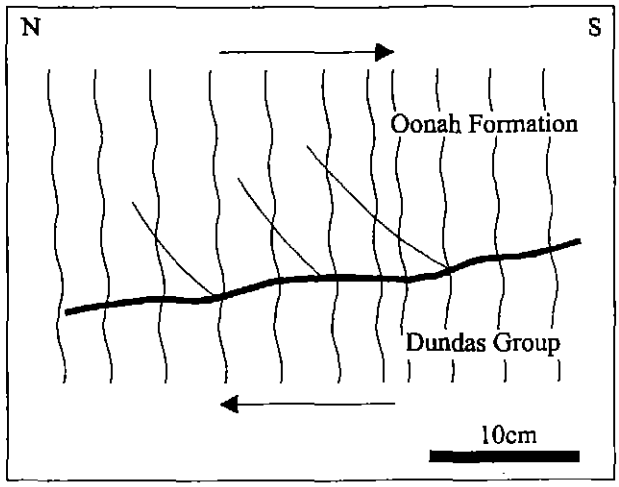
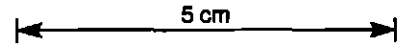


FIGURE 4.27 *Representation of Reidel shearing associate with the Tenth Legion Fault.*



Logs of a Gold Fields Exploration drillhole (TH12) record the intersection of brecciated and mylonitised mafic rock, possibly representing the thrust contact with Dundas Group sediments. The depth of TH12 is unknown to the author, however additional holes such as TH15 extend to a vertical depth of approximately 517 metres, without record of such intersection. Given the horizontal nature of the Tenth Legion Fault, it is anticipated that TH12 would have been to slightly greater depth.

The Balstrup Fault flanks the northern margin of the Stonehenge area, separating the Oonah Formation (to the south) from the Crimson Creek Formation (northern sequence). Although not mapped extensively by the author, form of the west-northwest thrust suggests a steeper dip than that of the Tenth Legion Fault. Dipping to the south confirms uplift of the Oonah Formation. Blissett (1962) interpreted this fault to be the product of 'Tabberabberan' uplift.

The relationship between the Tenth Legion Fault and the Balstrup Fault in uncertain. The steep southwest dip of the latter suggests an intersection between the two faults. The timing relationship of each fault may involve either a contemporaneous or a discrete episode event; that is they may both be the product of a similar event, or they may have formed during independent faulting periods (figure 4.28).

The Tenth Legion Fault forms the detachment of the Precambrian Oonah Formation from its basement. Cambrian thrusting is a recognised occurrence in the tectonic development of western Tasmania, responsible for the emplacement of mafic-ultramafic complexes into and surrounding the Dundas Trough (Chapter 2). Although the allochthonous late Cambrian sheet does not extend to the Zeehan area, thrusting events such as the Tenth Legion Fault may form the preceding boundary of movement. Crawford and Berry (1988) suggest sheet movement from the east, supporting the identified thrust direction of the Tenth Legion Fault (overthrust from the east or underthrust from the west). In a similar environment, major fault structures within the Henty Fault Zone have formed from westbound thrusting during the early Ordovician, and a later phase of reverse fault movement. Applying this scenario to the Stonehenge environment lends support towards the second thrust occurrence of separate episode formation for the Tenth Legion and Balstrup Faults.

364214

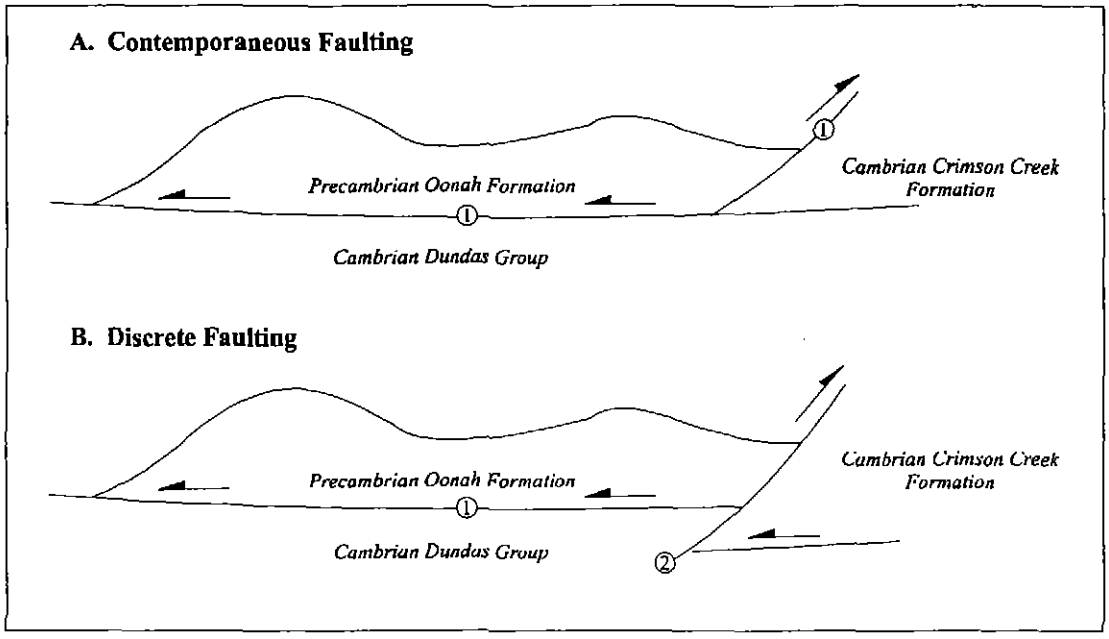


FIGURE 4.28 ***Proposed development models for the Tenth Legion and Balstrup Faults. A. Simultaneous (near) formation of each fault; B. Formation of each fault during separate thrusting events.***

The Stonehenge area is host to several additional faults which have been identified via aerial photograph interpretation (figure 4.29). Generally these faults are of east-northeast and (to a lesser degree) northeast trend, and show considerable amounts of displacement. Given the expanse of vegetation covering the area, the faults are not outcropping at surface. Again drill core has provided evidence of sub-surface faulting such as at the contact between Oonah Formation quartzites and surrounding pelites in ZS31. Dislocation of stratigraphic units seen in aerial photographs extends throughout the Proterozoic and Cambrian units, indicating an age of post-Cambrian. Trends within the intrusive body identified beneath Stonehenge are interpreted as representing faults therein. This enable a further limitation of the age to be Devonian or younger (assuming that the intrusive is a continuation of the Devonian Heemskirk Granite). Therefor, the later faulting events are likely to be apart of 'Tabberabberan Orogeny' deformation, as widely reported throughout the Zeehan area (Blissett, 1962)

364215

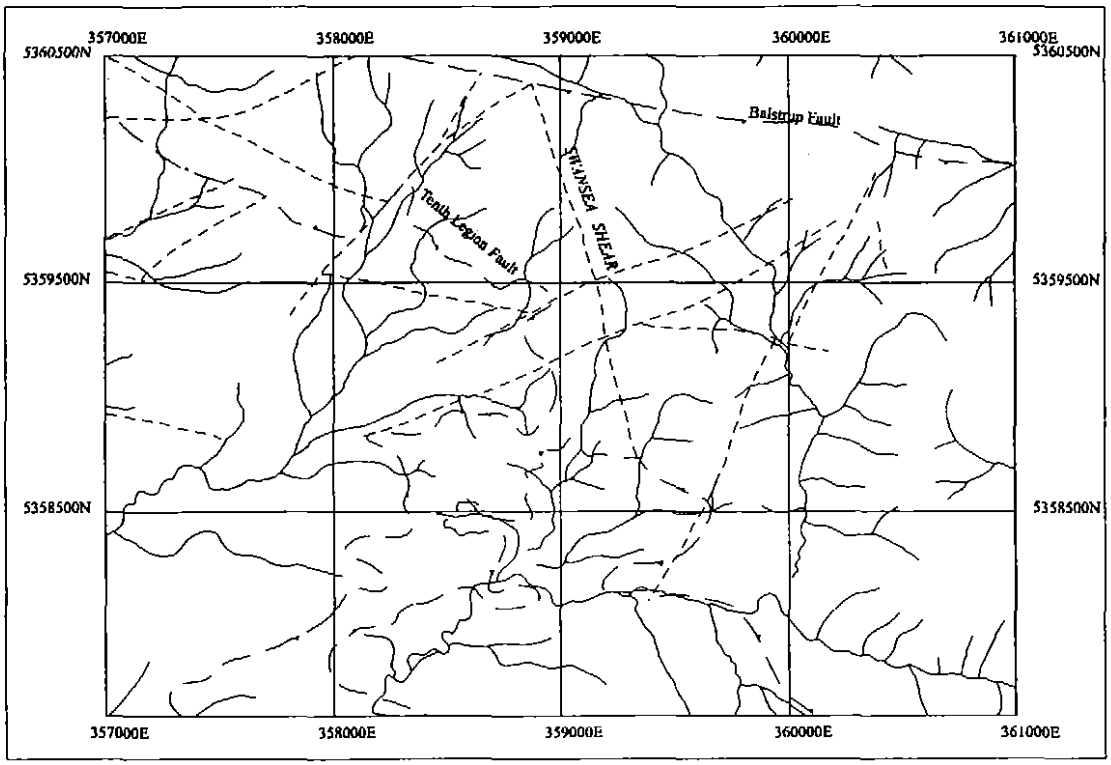


FIGURE 4.29 *Faults of the Stonehenge area.*

4.7 VEIN GENERATION AND DEFORMATION

Quartz veining is common throughout the Stonehenge area. All Oonah Formation rocks from the outcropping quartzites (figure 4.30) to shales and calcareous sediments found in drillcore (figure 4.31 and 4.32) contain veins of two or more generations. Veins present are important associates of mineralisation at Stonehenge, and reflect structure deformation events such as folding, shearing and faulting. An extensional phase of deformation has produced tensional gash vein fractures. This is related to shearing sense as seen in the figure 4.33. Here, thin quartz filled fractures have developed within more brittle layers of a folded sequence. Also evident in figure a is the occurrence of tensional gashes within a pre-existing quartz vein. Early emplaced veins are generally thin quartz (occasional calcite) veinlets concordant and discordant to bedding. Folding and faulting are common features. Fine veins of figure 4.31 are faulted by shearing along bedding plane movement during folding (faulted veins perpendicular to So) or are folded/sheared during the same event (veins sub-parallel to So). En echelon development seen in figure 4.33 indicates shearing, with fracture development perpendicular to the minimum compressive stress σ_3. A second generation of vein development overprints the first, and is thought related to mineralisation of the Stonehenge area. Generally of greater magnitude (10's mm to 10's cm), these veins often host sphalerite, pyrite and occasional galena ore minerals. Deformation is less extensive than the earlier formed vein set, and appears related near exclusively to fault movement (figures 4.32).

364216

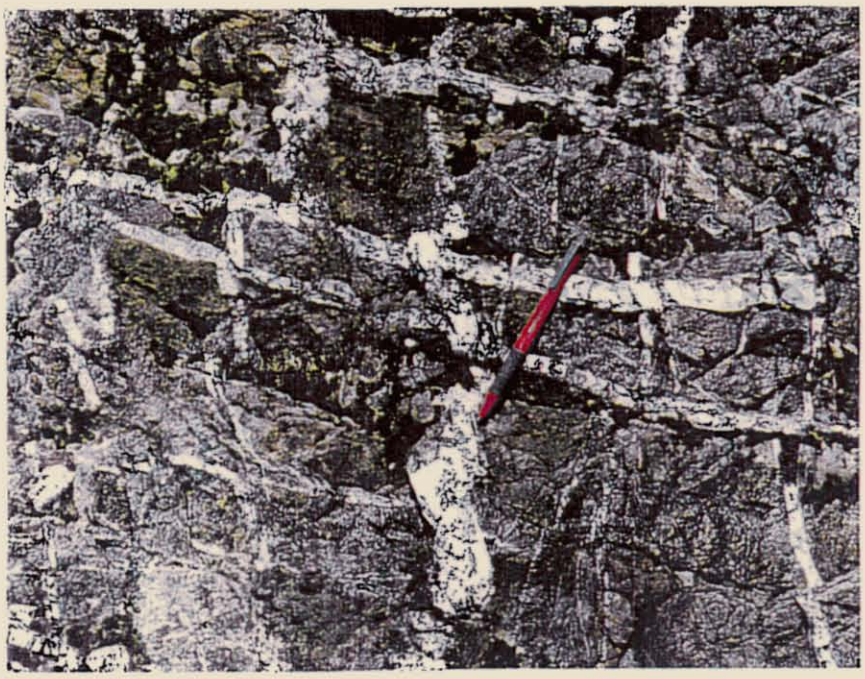


FIGURE 4.30 *Quartz veining in quartzite outcrop from location MU96-213. As seen, the veins are often planar, intersecting at high angles, and are up to 4 cm in width. Vein orientations are: 139/65W and 070/80N.*



FIGURE 4.31 *Veining within shales from ZS31, 142m As in outcrop, veins are planar, often forming thin fibres.*



FIGURE 4.32 *First and second generation veins from ZS31, 145.2m. The latter later folds are intersected by fault movement and stylolite formation sub-parallel to the core axis.*

364217

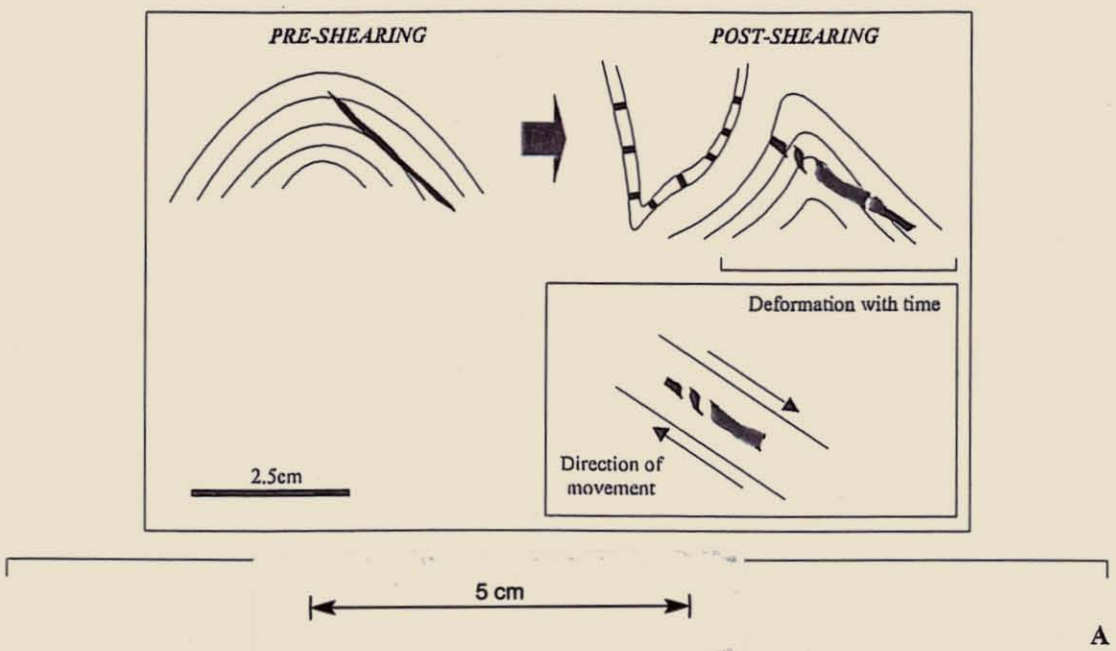


FIGURE 4.33 *En echelon vein development and infilling of tension gashes developed within brittle sequences during folding. A. ZS1102.1m; B. ZS1, 86.9m.*

364218

Brecciation evident in drillcore is the product of both hydraulic movement and tectonic pressure. Figure 4.34 (ZS1, 86.9m) shows emplacement of country rock fragments suspended in magmatic fluids, forming an implosion or phreatomagmatic breccia. Relatively sudden changes in fluid pressure have produced the collapse of rock fragments into magmatic fluids. Larger scale brecciation at the base of ZS31 is indicative of fault movement (figure 4.35). Brecciation in this quartzite unit supports mapping of fault movement at surface, separating the quartzite and surrounding pelite/carbonaceous sediments at this location.



FIGURE 4.34 *Implosion or phreatomagmatic breccia from ZS1, 86.9m. Wall rock fragments have been emplaced into magmatic fluids following significant changes in fluid pressure. Note the veining within rock fragments indicating a prior veining event.*



FIGURE 4.35 *Tectonic breccia zone from ZS31, 203m..*

CHAPTER 5.

Mineralisation of the Stonehenge area

364220

5. MINERALISTION OF THE STONEHENGE AREA

5.1. INTRODUCTION

For in excess of 100 years, Tasmania has hosted countless mining operations, including at least 20 major ore deposits (figure 5.1). The complex geology contains a diverse concentration of ore types, making it one of the most economically important mineralised areas in the world. The Mount Read Volcanic belt of western Tasmania is the greatest producer, with historical and currently operating deposits (often world class) of tin, silver, lead, zinc, copper and gold. Large deposits of scheelite (King Island), gold and iron may be found through the north and northeast of Tasmania.

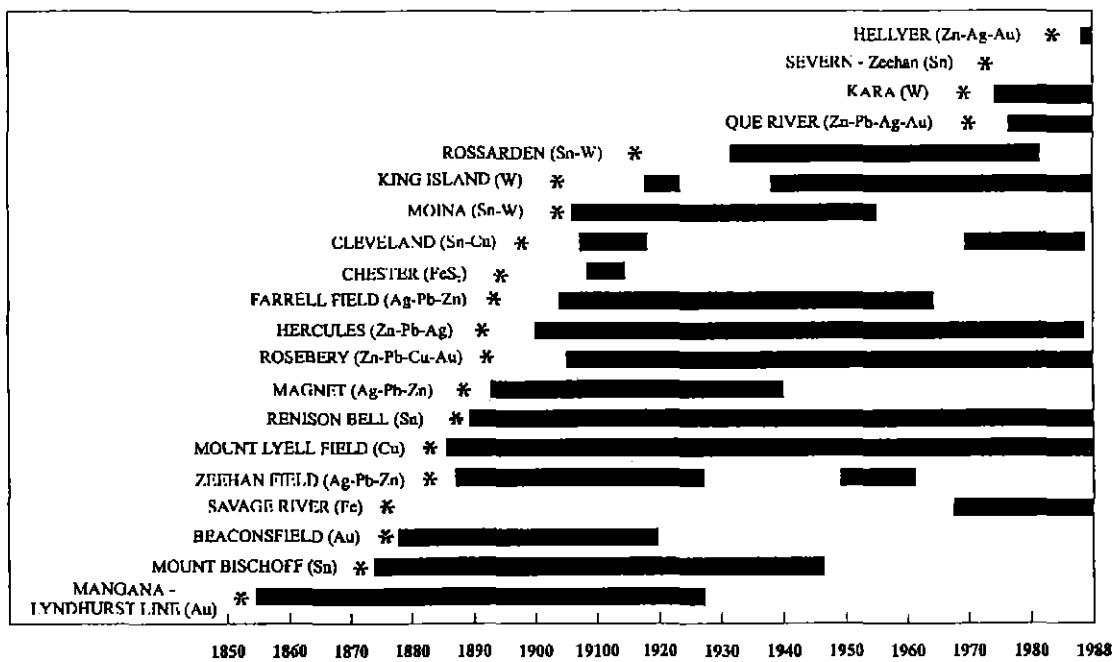


FIGURE 5.1 ***Discovery dates (*) and production periods for the major ore deposits of Tasmania. (after Large, 1989)***

5.2. OCCURRENCE

Mineralisation occurs within a wide range spectrum of geological sequences throughout Tasmania. Two major magmatic phases appear responsible for the introduction and movement of mineralised fluids. The first involved fluids associated with the Mount Read Volcanic belt, producing several large scale volcanic-hosted massive sulphide deposits during the Cambrian period. The second stage of mineralisation is related to the widespread introduction of granite bodies, emplaced (eg. the Heemskirk Granite) during the Devonian.

364221

5.2.1 West Coast Mineralisation

Cambrian Mount Read Volcanic Belt Mineralisation

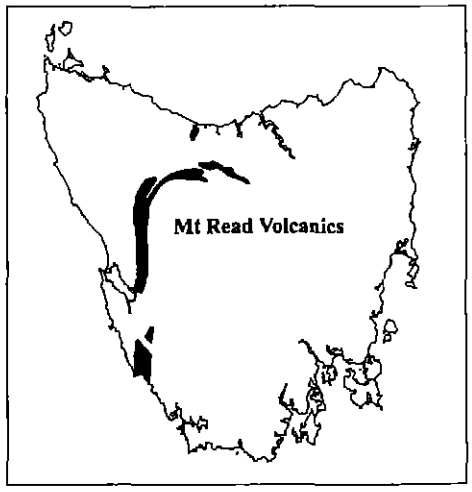


FIGURE 5.2 *Mount read Volcanic belt of Tasmania.*

The Mount Read mineral province is host to several large and small scale mining operations (figure 5.2). In this region, the grade of the ore, rather than pure volume, makes it one of the richest provinces in the world; comparable with Iberian pyrititic belt (Strauss and Madel, 1974) and the Scandinavian Caledonides (Stephens, 1986). Theories of ore genesis relate to two major magmatic events throughout the area: Mount Read Volcanism and Devonian granitoid intrusions.

Volcanic-hosted sulphide deposits (VHMS) host the major Cambrian ore deposits of the Mount Read belt (Mount Lyell, Hercules, Rosebery, Chester and Hellyer). The deposits form stratiform, pyritic, sphalerite-galena-chalcopyrite lenses of syngenetic origin within varying marine volcanic sequences (Solomon, 1989). The Hellyer Rosebery, Que River and Chester deposits contain massive stratiform, polymetallic lenses, whilst Cambrian ores at Mount Lyell contain disseminated pyrite and chalcopyrite within altered volcanics, making it unique in a world context. Seemingly a VHMS type variation, various chemical parameters and the presence of massive pyrite (eg the Mount Lyell orebody) and polymetallic sulphide lenses, enables genetic correlation of Mount Lyell with other VHMS style deposits. The polymetallic orebodies are of high grade, have high Zn/(Zn + Pb) ratios and contains significant gold and silver (2-4g/t Au and 100-170g/t Ag). The occurrence of zoning from copper-rich at the base, through Pb-Zn rich to barite-rich at the top is characteristic of these VMHS type deposits. Gold is found in greatest abundance near hanging walls of stratiform barite lenses, and in various intra-ore environments. At Rosebery, gold also exists in barite lenses and pyrite-chalcopyrite zones (Huston and Large, 1986; McArthur, 1989). The identification of distinctive characteristics has enabled Solomon (1981) to define the Rosebery and Hercules deposits as a subgroup (Rosebery type) of world VHMS deposits. They are large (Rosebery contained 20 million tonnes at 28% lead and zinc), have high zinc/copper ratios, are of a sheet-like form, and show prominent fine layering.

Campana *et al.* (1958) identified the change in mineralisation from copper-rich replacement deposits in the southern Central Volcanic Complex (CVC) of the Mount Read belt, and zinc-lead stratiform deposits in the northern CVC and Que-Hellyer Volcanics. These differing mineralisation styles may be the partial product of relative erosion depths, but are primarily due to variations in temperature, salinity, mass flux, depth of water and the nature of source rocks. Rocks underlying the orebodies often contain feeder dykes through which ore solutions have reached the seafloor.

364222

The main deposits are altered to quartz + sericite + chlorite ± carbonate ± apatite ± mylonite assemblages. Eastoe *et al.* (1987) identified that regionally, pre-ore volcanics are typically non-sodic and non-calcic, with sericite and local K-feldspars. Alteration is thought to be the result of seawater circulation related to ore development. Post ore volcanics contain abundant albite and epidote. Southern CVC pre-ore volcanics contain haematite, magnetite and a wide range of Na/K. At Mount Lyell, quartz-sericite-chlorite-pyrite alteration overprints the haematite-magnetite alteration. Alteration of footwall and hangingwall rocks at Rosebery has produced enrichment's of SiO_2, K, Rb, Mn, Mg, Fe, S and H_2O, and depletion in Al, Na, Ti, Ca, Sr, Zr, Y and Nb (Green *et al.*, 1981; Naschwitz, 1985). Fuschite developed above and below the Hellyer ore most likely reflects the basaltic composition of the wall rocks (McArthur, 1989). Fault zones provide a focus for fluid flow of many of the sulphide deposits. Ore zones at Mount Lyell occur at the intersection of two complex fault zones, one north-south (the Great Lyell Fault), the other east-west (the Linda Fault Zone).

Late Cambrian to Devonian Mineralisation

Mineralisation during the period of Late Cambrian to Devonian is extensive throughout the Gordon Group of Early Ordovician to Early Silurian platform carbonates. The Gordon Group contains a sequence of carbonaceous rocks and minor siliclastics that are widely distributed throughout the west coast of Tasmania. The deposits are generally from a shallow water environment, with the exception of deeper water sediments at Surprise Bay in southern Tasmania (Burrett *et al.*, 1984) and Beaconsfield in the north.

Gould (1862) first discovered galena in Gordon Group limestone outcropping along the Gordon and Franklin Rivers. Although common in small quantities, significant Pb-Zn-Ag mineralisation within the limestone appears restricted to an area of northwest Tasmania from Railton to Bubs Hill. Host to the high concentrations and volumes of such deposits, the Zeehan Mineral Field has supported exploits of many Pb-Ag workings during the 1890's (Taylor, 1989). The most economically significant working was the Oceana mine deposit (Jack, 1961; Blissett, 1962b). Recent evaluations of the Oceana workings dispel the original theories of a genetic model involving deposition within structurally controlled fissure veins from fluid emanating from the Heemskirk Granite towards completion of the Devonian 'Tabberabberan Orogeny' viz. Jack (1961). Rather, the deposit is a deviation of the sedimentary exhalative class (Taylor, 1989). The northern discordant, stratabound, epigenetic ore zone and silicified/dolomitised zones adjacent to the Oceana Fault represent a channel for mineralised fluids trapped at depth by the fault. Southern stratiform mineralised horizons are interpreted as syndiagenetic replacements of sub-seafloor shallow-water carbonate mud's prior to lithification. Previously interpreted as tectonic breccias, distinctive brecciation within the limestone is now thought to be the product of sub-marine debris-flow from gravity slides instigated by Oceana Fault movement during deposition Gordon Group sediments (Taylor, 1989).

364223

The Oceana deposit appears to resemble mineralisation, tectonic settings and host lithology's similar to Irish Carboniferous sedimentary exhalative deposits at Silvermines (Taylor, 1984) and Navon (Andrew and Ashton, 1985). Lead-isotope determinations from Oceana galena samples have shown that the leads are less radiogenic than those of Devonian granite related mineralisation. Subsequently, Oceana mineralisation is likely to be of Ordovician age (Gulson (CSIRO) pers. comm. with Taylor, 1984).

Mid Palaeozoic Mineralisation

Middle Palaeozoic ore deposits exist throughout northeast and west Tasmania in rocks of late Proterozoic to early Carboniferous age. Mineralisation is generally controlled both spatially and genetically by Devonian to early Carboniferous granitoid intrusions (figure 5.3). In northeastern Tasmania, tin, tungsten and gold mineralisation dominates with disseminated cassiterite in greisenised granite (eg Blue Tier district), dilatational quartz-wolframite-cassiterite veins (eg Aberfoyle, Storys Creek) and gold-quartz reefs (eg Mathinna, Lefroy). Throughout western Tasmania, the higher occurrence of carbonate rocks reflects in the amount of tin and tungsten carbonate replacement (eg Renison, Mount Bischoff, Cleveland, Zeehan King Island). Western Tasmania often contains exogranitic tin-tungsten deposits with outer haloes of argentiferous galena and sphalerite vein mineralisation (eg Zeehan, Moina), and large Ag-Pb-Zn vein deposits (eg Zeehan Field, Magnet, Mount Farrell).

The vast distribution of middle Palaeozoic ore deposits reflects the expanse of subsurface granitoids. Gravity interpretations by Leaman (1980) indicates that outcropping granitoids merely form roof projections of larger underlying 'batholiths. As seen in figure x, a large 'batholith' body trends along a north-northeast axis through northeast Tasmania, whereas western Tasmania is host to four (atleast)'batholiths' aligned along a north-northwest trend line. Palaeozoic ore deposits occur exclusively within a 1 kilometre subsurface encounter of the batholith bodies (Collins, Brown, Dronseika and Morland, 1989).

364224

Mine/deposit[1]	Type	Resource[2] Mt	Grade	Production Mt	Grade	Host Rock	Granite Association	Ore Minerals[3]	Mine/adjacent	Type	Measured Mt	Grade	Production Mt	Grade	Host Rock	Granite Association	Ore Minerals
TIN/TUNGSTEN DEPOSITS									SILVER-LEAD-ZINC DEPOSITS								
Upper Proterozoic Heazlett									Zeehan Western	Vein			0.3	8.75%Pb 480g/t Ag	Dundas Formation	Hercynian Granite(?)	Ga, Sp
Mt Bischoff	Carb-rep.[4] Alt. porph.	10.33	1.13%Sn	3.59	1.36%Sn	Mt Bischoff sequence (Dundas Fm con.)	Porphyry dykes assoc.(?) with Meredith Granite	Cs	Dundas (Zeehan)	Vein			0.2	5.34%Pb 0.49%Cu 0.05%Sn 384g/t Ag	Dundas Formation	Hercynian Granite(?)	Ga, Sp, Cp, Cs, Sl
Si Dieci	Skarn	5	0.5%Sn	-	-	Dundas Formation	Hercynian Granite	Sn-Bi-Cu-Sb-Ag									
Oakleigh Creek	Vein	0.12	1.1%WO_3	0.02	0.4%WO_3	Tyrrean region	Bobsleigh Granite	Wo	Zeehan Queen	Vein			0.2	7.5%Pb 0.1%Cu 0.1%Sn 273g/t Ag	Dundas Formation	Hercynian Granite(?)	Ga, Sp, Cp, Sl
Pre-Cambrian-Lower Cambrian Host																	
*Renison	Carb-rep. Fault fissure, Fracture filling	42.3	1.08%Sn	8.78	1.23%Sn	Crimson Creek Fm Success Creek Gp	Porphyry dykes and granite associated with Pine Hill pluton	Cs									
Cleveland	Carb-rep.	10.3	0.78%Sn 0.13%Cu	5.51	0.79%Sn 0.13%Cu	Hall Formation (Crimson Ck Fm.cont.)	Porphyry dykes and Meredith Granite(?)	Cs, Sl, Cp	Mamara (Zeehan)	Vein			0.33	5.5%Pb 1.03%Zn 143g/t Ag	Dundas Formation	Hercynian Granite(?)	Ga, Sp
Foley Zone	Stockwork Alt. porph.	3.0	0.29%WO_3 0.05%Sn 0.02%MoS_2	-	-	Crescent Spur Sandstone (Crimson Ck Fm.cont.) and porphyry dyke	Meredith Granite(?)	Wo, Cs, Mo, Bi, Sl, Cp	Zeehan Montana	Vein			0.3	9.78%Pb 430g/t Ag	Crimson Ck Fm and Dundas Fm	Hercynian Granite(?)	Ga, Sp
Zeehan	Carb-rep. Fault fissure, Stockwork	7.3	0.75%Sn	-	-	Crimson Creek Fm	Hercynian Granite(?) and porphyry dykes	Cs, Sl	Spray (Zeehan)	Vein			0.4	10.16%Pb 435g/t Ag	Dundas Fm and pan Crimson Ck Fm.	Hercynian Granite(?)	Ga, Sp
									Queensberry[5]	Vein	0.83	11.5%Pb 8.8%Zn 0.32%Cu 52g/t Ag				Hercynian Granite(?)	Ga, Sp, Cp
*King Island	Skarn	16.91	0.78%WO_3	9.77	0.61%WO_3	Grassy Group (Crimson Ck Fm.cont.)	Grassy Granodiorite Field Head Adamellite	Sch									
Hazelbank	Carb-rep. Fault fissure	0.39	0.65%Sn	0.14	0.9%Sn	Dundas Ultramafic Complex	Pine Hill pluton(?)	Cs	North Mt Farrell	Vein			0.38	14.9%Pb 506g/t Ag	Farrell Slate	?	Ga, Sp
									New North Mt Farrell	Vein	0.50	11.5%Pb 4.8%Zn 0.33%Cu 371g/t Ag	0.43	11.4%Pb 4.8%Zn 0.22%Cu 370g/t Ag	Farrell Slate	?	Ga, Sp, Cp
Ordovician-Lower Devonian Host																	
Melba	Skarn	26	0.11%Sn 0.15%WO_3 180g/t CuF_2	-	-	Gordon Gp limestone	Dalcoath Granite	Cs, Sch, Fl	Magnet	Vein			0.63	3.35%Pb 1.35%Zn 427g/t Ag	Mingan Ultramafic Complex	Meredith Granite	Ga, Sp
Shepherd & Murphy	Veins	0.28	0.23%Sn 0.11%WO_3	0.2	0.23%Sn 0.11%WO_3	Skarn (after Gordon Gp limestone) and Moina Sandstone	Dalcoath Granite	Cs, Wo, Bi, Mo	Howard Hill	Vein			0.06	8.1%Pb 186g/t Ag 0.3g/t Au	Moina Sandstone	Dalcoath Granite	Ga
*Ikara	Skarn	2.2	0.8%WO_3	0.6	0.8%WO_3	Gordon Gp limestone	Housetop Granite	Sch									
Aberfoyle	Veins			2.1	0.91%Sn 0.38%WO_3	Mathinna beds	Ben Lomond Granite	Cs, Wo	GOLD DEPOSITS Tasmania	Vein	3.99	24g/t Au 45g/t Ag 1%Cu	1.09	21g/t Au	Cabbage Tree Fm (Mount Stanley conc.)	Mt associated granites	As,Cp
Storys Creek	Veins			1.1	1.09%WO_3 0.18%Sn	Mathinna beds	Ben Lomond Granite	Cs, Wo	*Lefroy (3 mines)*	Vein			0.08	31g/t Au	Mathinna beds	Mt associated granites	Au
Great Pyramid	Veins	3	0.31%Sn	-	-	Mathinna beds	Mt Pierrot pluton(?)	Cs	*Mt Goodwin Gair*	Vein			0.30	29g/t Au	Mathinna beds	Blue Tier and Scottsdale batholiths	Au
Middle-Late Devonian Host									*Tas. Consols*	Vein			0.02	14g/t Au	Mathinna beds		Au
Sweeneys	Greisen	?	0.45%Sn 1.92%Zn 31g/t Ag	-	-	Hercynian Granite ('tin' granite)	Hercynian Granite ('tin' granite)	Cs, Sp									

* - operating mine. (1) Mine/deposits in northeastern Tasmania in italics. (2) Resource - estimated pre-mining size of deposit based on total production plus total reserves. Where no resource data are given, the size is equivalent to total production as there are no additional published reserves. (3) Ore minerals: Au - native gold, Bi - native bismuth, Bis - bismuthinite, Cp - chalcopyrite, Cs - cassiterite, Fl - fluorite, Ga - galena/sphalerite, Gn - argentiferous galena, Mo - molybdenite, Sch - scheelite, Sl - sphalerite, Sn - tin minerals, Sp - sphalerite, Wo - wolframite. (4) Carb-rep. - carbonate replacement, Alt. porph. - alteration of porphyry. (5) Silver-lead-zinc resource data from Cox & Doherty (1986).

Cleveland and Foley Zone resource data from Cox & Williams (1986, table 21).

FIGURE 5.3 ***Resource estimates, occurrence and granite association of principal mid-Palaeozoic ore deposits. (Collins, Brown, Dronseika and Morland, 1989)***

364225

Endogranitic Greisen-Vein Tin Deposits

Endogranitic tin deposits occur in small domal bodies of alkali-feldspar granite in the Blue Tier Batholith in the northeast of Tasmania, or locally along the southern margin of the Heemskirk granite of western Tasmania (Collins, Brown, Dronseika and Morland, 1989). These deposits tend to be of low grade (<0.5%Sn) and of small to moderate tonnage (figure 5.3)

Tin-Tungsten Skarn and Carbonate Replacement Deposits

Large primary tin deposits of Tasmania have formed in a distinct model environment. They are stratabound, massive sulphide cassiterite ores formed by replacement of carbonate bodies in Proterozoic to lower Cambrian sedimentary sequences (eg Renison, Mount Bischoff, Cleveland and Zeehan deposits; figure 5.3). In addition, significant Sn (and W) resources are associated as fracture fillings, vein stockworks and altered porphyry dykes. Important tungsten producers such as the King Island deposit are scheelite-bearing endoskarns. Tin and tungsten bearing skarns have often formed adjacent to Devonian granitoids throughout western Tasmania. Grades are generally low (<0.2% Sn or W) with associations of stanniferous magnetite-pyrrhotite-garnet (eg Stanley Reward within the Success Creek Group), magnetite-scheelite (eg Mount Youngbuck deposit of the Crimson creek Formation) and tin-tungsten-bismuth (eg Mt Ramsay within Crimson Creek Formation).

Tin-Tungsten Vein Deposits

Generally of small scale, quartz-wolframite-cassiterite vein deposits containing minor sulphides occur within Precambrian to Late Devonian rocks throughout Tasmania. Deposits of this type generally form discrete veins or sheeted vein systems penetrating country rocks above an altered granitic cupola (eg Aberfoyle, Storys Creek, Shepherd and Murphy, Oakleigh Creek). An exception to this is the Foley Zinc stockwork (at Cleveland), which is centred on an altered porphyry dyke.

Silver-Lead-Zinc Vein Deposits

Most of the argentiferous lead-zinc sulphide vein deposits of Tasmania (generally west coast) form at the outer haloes of zoned mineral fields which are centred upon exogranitic tin-tungsten deposits (Collins, Brown, Dronseika and Morland, 1989). The Zeehan field has yielded the greatest production (figure 5.3), although zoning has also been identified at Mount Bischoff (Groves et al., 1973), Cleveland (Collins, 1983b) and Moina-Round Hill (Jennings, 1965) in western Tasmania, and Scamander (groves, 1973; Ruxton and Plummer, 1984) in the states east.

364226

5.2.2 Mineralisation of the Zeehan Area

Mineralisation throughout the Zeehan area occurs within a complex system of faults and fractures related to middle Devonian deformation. Argentiferous galena, sphalerite, pyrite, siderite and quartz, with minor sulphide, arsenide and sulphosalt phases form steeply dipping ore shoots trending between north-northeast and north-northwest. Deposits are generally found within host rocks of the Proterozoic Oonah Formation and Cambrian Crimson Creek Formation. The average width of the irregular ore shoots is around 0.25 metres (maximum of 5 metres). Strike lengths rarely exceed 100 metres, and depths 100 to 150 metres (Collins, Brown, Dronseika and Morland, 1989).

Following much discussion, Solomon (1981) suggests that zoning of ore veins throughout the Zeehan mineral field is genetically associated with, and centred upon, the Queen Hill-Severn massive sulphide-cassiterite deposits. Originally attributed to solution flow away from the Heemskirk Granite. The west to east zoning of pyritic to sideritic gangue is most likely representative of local host rock composition (Collins, Brown, Dronseika and Morland, 1989). Dissolution of underlying Ordovician limestones in the east of the field may account for the subsequent siderite occurrence in this area.

5.2.3 Mineralisation of the Stonehenge area

Historical workings of the Stonehenge area

As with the majority of western Tasmania, the Zeehan area has been extensively explored and worked during the latter 1800's and early 1900's. The Stonehenge area has been host to a variety of such mining activities, primarily leading to the extraction of lead, zinc and silver. Deposits historically tend to be of pyrite, galena and sphalerite fissure veins within the Proterozoic Oonah Formation of quartzites, phyllites, slates and shales. Historical workings of the Stonehenge area are detailed in Appendix 5.

Recent Exploration of the Stonehenge Prospect

Recent and current exploration conducted over the Stonehenge area has identified an interest area of zinc mineralisation. Investigations by Gold Fields Exploration and RTZ-CRA Exploration have involved the use of geophysical techniques and diamond-aircore-wacker drilling. The most recent exploration has been conducted by RTZ-CRA Exploration. Four diamond drillholes (ZS1, ZS2, ZS3 and ZS31), aircore rock chips, and wacker assay results have been evaluated and exposed in the following interpretation of mineralisation at Stonehenge. In addition, existing logs of Gold Field Exploration diamond drillholes (TH13, TH14, TH15, TH16, TH17) have been used to expand the stratigraphic continuity below surface. Ground magnetics conducted over the majority of the Stonehenge area has been interpreted to evaluate possible connection between mineralisation and intrusive bodies within the area.

364227

encountered, and provides a small rock sample from the interface of overburden and bedrock. Drilling has been conducted at 25 metre spacings along traverse gridlines of 100 metres interval (as seen in figure 5.4). Sample assaying has provided an excellent basis for stratigraphic identification over an area of no exposure, and recognition of an elevated anomaly. The major anomaly body trends east-west, and appears to coincide with the identified black shale horizons. The stratigraphy surrounding includes silts, sands, shales, dolomite and dolomitic sediments of the Oonah Formation. An elevated magnesium occurrence north of ZS2 is a feature reflecting the presence of dolomitic units, and may be indicative of the style of mineralisation.

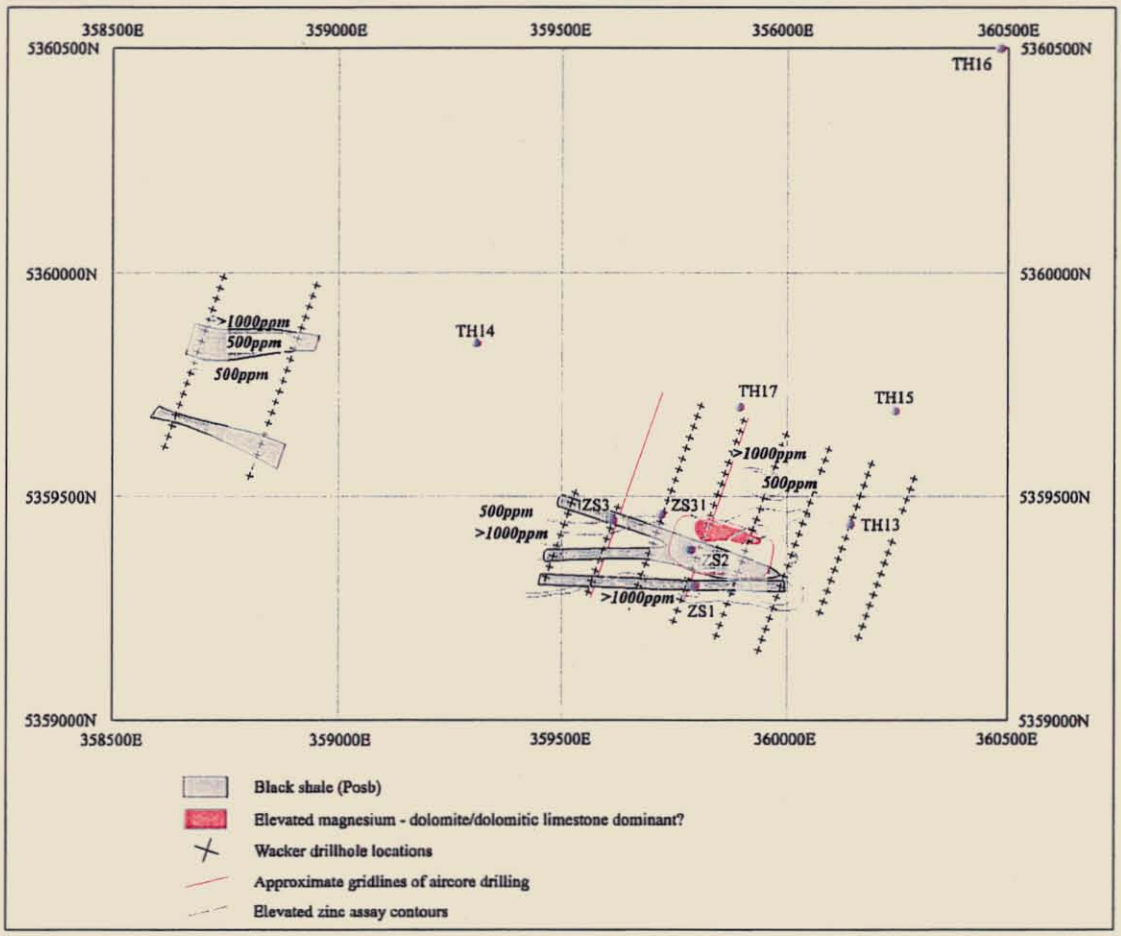


FIGURE 5.4 *Geology and mineralisation from wacker sampling.*

As seen above, wacker sampling of the Stonehenge grid has identified significant zinc occurrences. Contouring of assay results at 1000ppm or greater Zn and 500ppm Zn has identified two anomalous areas. The first, most prominent, covers an area extending beyond 500 metres in length (approximately between 359500mE and 360000mE) and 250 metres in width (5359250mN and 5359500mN). The east-west orientated body appears to correlate with similar trending black shales.

A second small group of two anomalous zones further west contains zinc of 500pmm plus between 358700mE to 238750mE and 5359750mN to 5359800mN. Again, black shales appear to the host lithology (atleast at surface level).

A second small group of two anomalous zones further west contains zinc of 500pmm plus between 358700mE to 238750mE and 5359750mN to 5359800mN. Again, black shales appear to the host lithology (atleast at surface level).

Aircore drilling conducted by RTZ-CRA Exploration over a restricted area has added to the information gained from wacker, to build a more accurate picture of stratigraphy and mineralisation. Aircore drilling is able to provide rock samples from constant intervals (3 metres) until solid bedrock is reached. To date, 27 vertical holes (shown in Mapsheet 4) have been drilled along two gridlines (figure 5.4) to an average depth of around 20 metres (ranging from 3 to 68 metres). In this investigation, the author has found logging the samples to be valuable in identifying stratigraphic horizons rather than mineralisation. In general the results concur with those of the wacker sampling.

Diamond drillholes are essential in establishing the extent of mineralisation with depth. The RTZ-CRA Exploration drillholes have made several intersections into mineralised horizons, the most significant of which are found within ZS31. Between 30.35 and 40.5 metres, 6% Zn was returned. At greater depth, 2.51% Zn was intersected over 3.25 metres. Other significant intersection of zinc mineralisation include (drillhole logs and additional intersections are noted in Appendix 3):

- 2.15 metres of 7.78% from ZS1, 119.2 metres
- 19.35 metres of 1.52% from ZS1, 143.5 metres
- 35.5 metres of 2.13% from ZS2, 100.5 metres
- 0.75 metres of 7.12% from ZS2, 190.25 metres
- 3 metres of 0.9% from ZS3, 130 metres.

ZS1 extends to a depth of 251 metres, and is the deepest of the RTZ-CRA Exploration holes Of the five Gold Fields Exploration drillholes, mineralised intersection were generally close to, or less than, 0.5% zinc. The close proximity and associated zinc intersections within the CRA-RTZ hole indicates confinement of high grade mineralisation. Gold Field Exploration holes TH14, TH15, TH17 are marginally north of the identified anomaly, whilst TH16 is located at the northeastern corner of the Stonehenge area (figure 5.4). Their lack of grade intersection suggests confinement of the mineralisation, possibly to specific stratigraphic horizons. Sections of each drillhole showing associated zinc intersections are located in Appendix 3.

364229

5.3 CONTOLS OF MINERALISATION

5.3.1 Stratigraphic controls

The extent of mineralisation throughout the Stonehenge area appears to be controlled by stratigraphic horizons within the Oonah Formation. As previously identified via wacker interpretation (figure 5.4), there is correlation between mineral anomaly and black shale horizons. This occurrence maybe representative of a syn-depositional stratiform pyrite deposit within the shales. More extensive mineralisation is essentially restricted to shale and dolomite/dolomitic horizons. Although likely to be the product of a differing mineralisation event, the diversity of this phase of sphalerite, pyrite and galena mineralisation is also controlled by stratigraphic horizons.

The logging to drill core provides the most conclusive evidence of features influencing mineralisation. Of the four RTZ-CRA Exploration drillholes (detailed logs in Appendix 3), common horizons are found to host the mineralisation. To detail the stratigraphy at Stonehenge, the Oonah Formation has been divided into the individual sequences of:

- Pom - micaceous sandstone, siltstone and minor shale
- Pos - siltstone, shale (minor undifferentiated dolomite)
- Posb - graphitic black shale
- Posd - dolomite/dolomitic sediment dominant
- Poq - massive quartzite

The black shale (Posb) sequences contain fine pyrite disseminations that appear unique to the horizons. Often the shales form sheared zones where the sediment is broken and rotted (eg. ZS31, 14.7-40.5 metres and 152.95-158.3 metres; ZS2, 103-130 metres). Recovery from these horizons is generally poor. Disseminated pyrite within black shale outcrops at stations MU96-19 to MU96-27 (see Mapsheet 3). Forming creek beds, the shales here a tightly folded, and form continuous exposure for approximately 75 metres. Finely disseminated pyrite therein is easily identified in hand specimen. The extensive nature of mineralisation within the black shales is indicative of stratiform deposition.

A second relationship between stratigraphy and mineralisation includes to occurrence of sphalerite, pyrite and galena within shale (Pos, Pom) and dolomitic sequences (Posd). In this instance, mineralisation occurs fine dissemination within the rocks, but is primarily confined to veins found in these horizons. Mineralisation within the rock sequences is generally restricted to dolomitic sediments, and is thought to be the product of replacement mineralisation, representing a second phase/style mineralisation.

364230

Zinc assays matched with stratigraphic logs of the drillholes shows the relationship between elevated mineralisation and specific horizons. It is evident from figure 5.5 that mineralisation in each of the RTZ-CRA Exploration drillholes correlates with shale or dolomitic horizons.

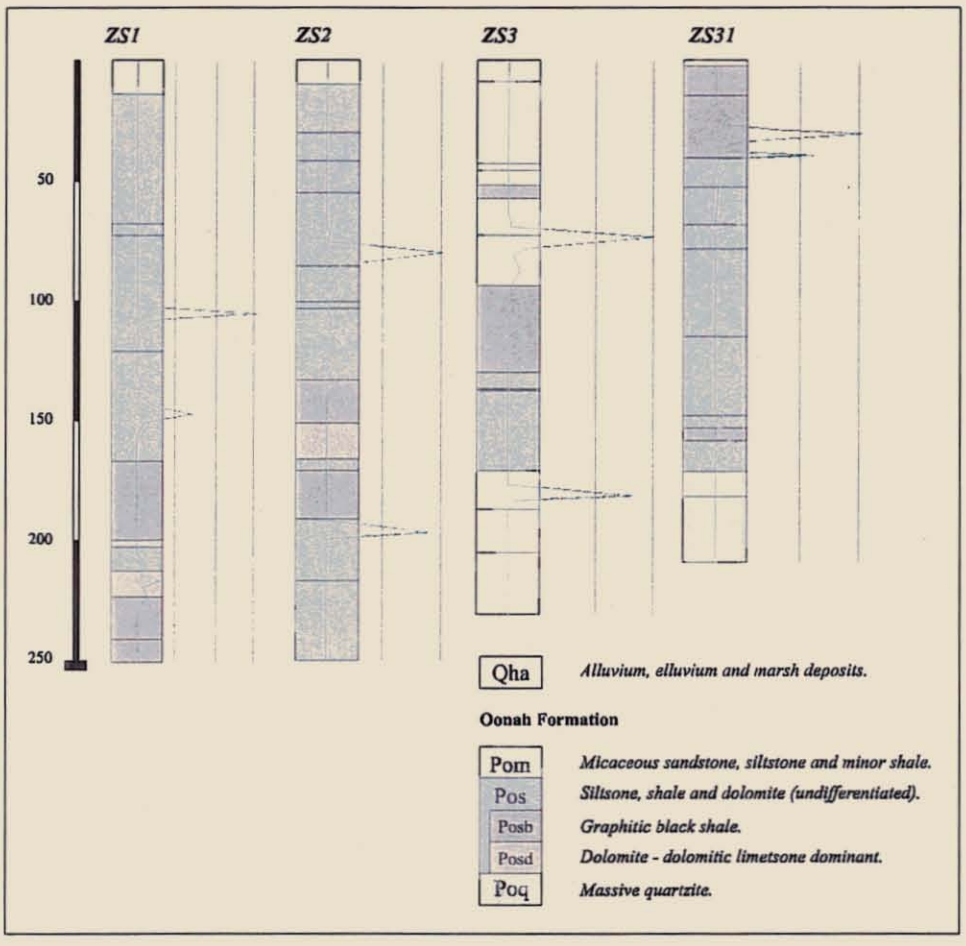


FIGURE 5.5 *Graphs of zinc assays and stratigraphic logs for drillhole ZS1, ZS2, ZS3 and ZS31 show a relationship between stratigraphy and mineralisation.*

5.4.2 Structural controls

Orebodies throughout the Zeehan area tend to strike between North-northwest and north-northeast, and occur as fissure veins formed along zones of faulting, shearing and fracturing of the Tabberabberan Orogeny. Mineralisation in the Gordon Limestone is fissure replacement type. At Zeehan, Dundas and Renison Bell, the mineralisation appears widespread in structural highs of the Oonah Quartzite and Slate, and the Overlying Crimson Creek Formation.

364231

The orebodies have been dislocated by post-Permian faulting and thrusts. Investigations by Blissett (1962) has found that several orebodies (such as near the Montana Silver-Lead Mine) were exposed during pre-Permian erosion, and blanketed by Permian Tillite, possible once covering the whole Zeehan district. The formation of erosion surfaces during the Cainozoic oxidised the orebodies to gossan, with leaching of the more soluble minerals and likely secondary enrichment at depth (Blissett, 1962).

Sphalerite-pyrite-galena mineralisation throughout Stonehenge often appears to be vein hosted. Quartz veining is often a significant feature, present in varying degrees at all depths within the drillholes. Figure s provides an estimate of veining occurrence and shows the dominant vein orientations to the core axis (additional drillhole vein logs shown in Appendix 3). The largest veins (generally <0.2 metre) tend to be near perpendicular to the core axis, whereas smaller veinlets are of varied orientations. Siderite alteration is a common feature of the veins, producing an orange/brown discolouration. A general historical feature of mineralisation throughout the Stonehenge area is the occurrence of ore deposits within a quartz-siderite gangue (Blissett, 1962).

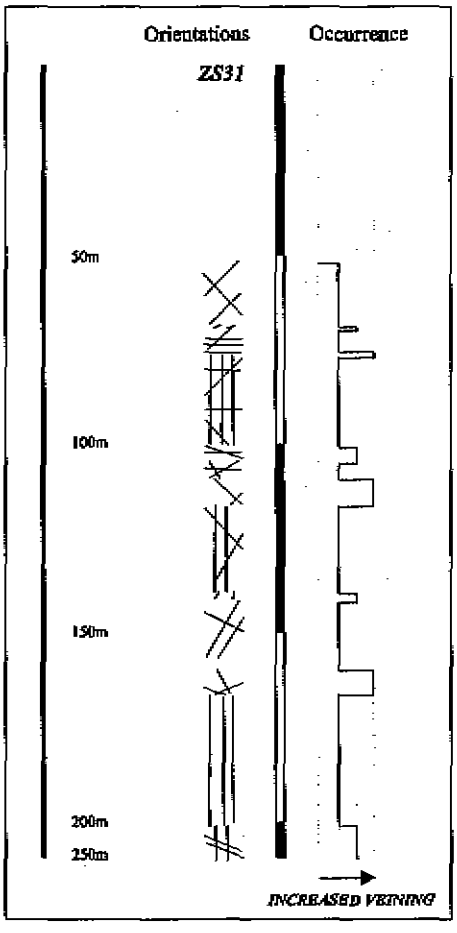


FIGURE 5.6 *Veining orientations and estimate occurrence for drillhole ZS31.*

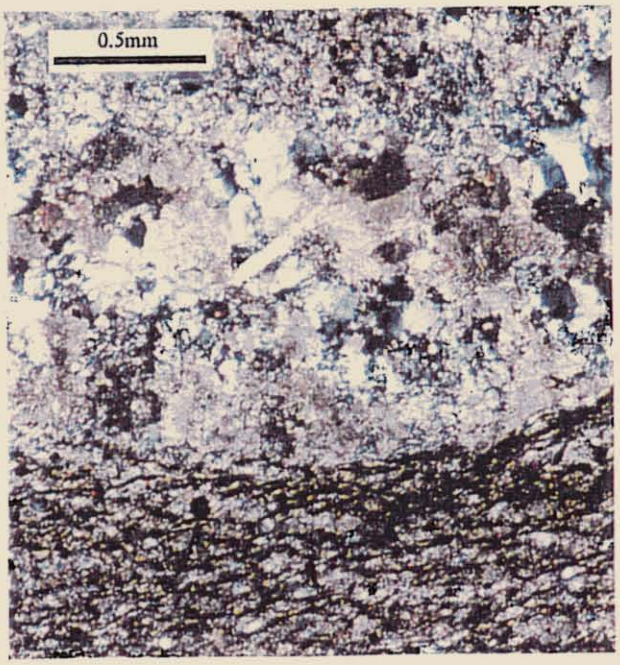
Figures 5.7 and 5.8 from ZS31 illustrate the occurrence of mineralisation within veins. Pyrite forms extensive disseminations throughout the quartz-carbonate veins of figure 5.7A, and is occasionally present within the host rock. The photomicrograph (figure 5.7B) reiterates mineralisation of the hand specimen whereby fine pyrite grains are scattered throughout the rock mass. Figure 5.8 shows sphalerite and pyrite forming 'blobs' along the margins quartz-carbonate veins.

Fault dislocation of mineralised systems indicates emplacement prior to the final phase of deformation. Blissett (1962) has identified that the major orebodies throughout the Zeehan area have all been faulted. Figures 5.9 and 5.10 support his findings. These samples from ZS1, 74.5 metres and 161 metres respectively have been offset by faulting near parallel to the core axis by up to 30mm. Mineralisation of figure 5.9 is within a brecciated zone, indicating an association between the movement of ore fluids and tectonic activity.

364232



A



B

FIGURE 5.7 *Pyrite mineralisation within black shale from ZS31, 124 metres. A. Pyrite locally massive disseminations within quartz-carbonate veining, and as occasional dissemination throughout the shale; B. Photomicrograph showing the sub-octahedral pyrite grains within the veins and the rock mass.*

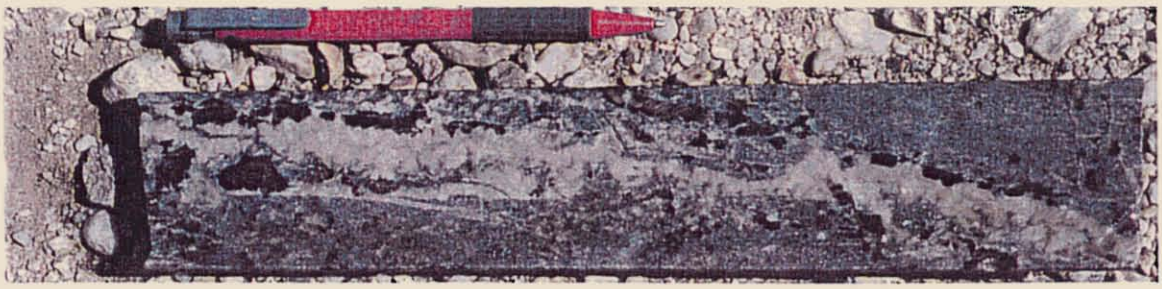


FIGURE 5.8 *Mineralisation of sphalerite, pyrite and minor galena within quartz-carbonate veining. The dolomite sample is from ZS1, 155.8 metres.*

364233

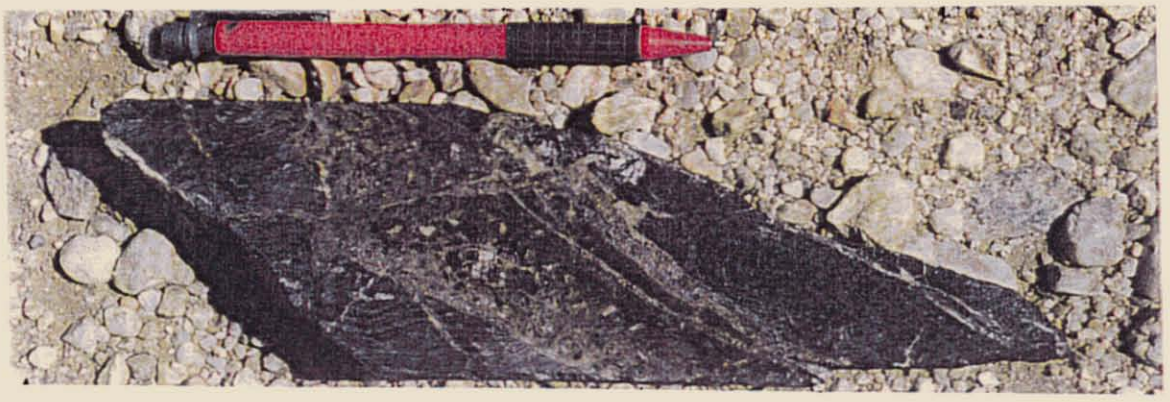


FIGURE 5.9 *Sphalerite, pyrite and minor galena mineralisation within brecciated zone of black shale from ZS1, 74.5 metres.*



FIGURE 5.10 *Dolomite from ZS1, 161 metres, showing post mineralisation fault dislocation. Movement parallel to the core axis has offset to pyrite zone by approximately 30mm.*

5.4.3 Spatial controls

Mineralisation of the Zeehan area is controlled by its proximity to Devonian granite intrusive bodies. The most significant such body ids the Heemskirk Granite located approximately 3 kilometres west of the Stonehenge area. Blissett (1962) states that the most important mineralisation of the Zeehan region is related to the intrusion of Devonian granites. All sequences up to late Devonian have been mineralised throughout the Zeehan area. Twelvetrees and Ward (1910) identified four mineral assemblages between Zeehan and outcropping of the Heemskirk Granite to the west:

364234

1. Within the granite: cassiterite is associated with tourmaline, pyrite, chalcopyrite and lesser amounts of tetrahedrite, siderite and fluorite. Bismuthinite, wolfram and molybdenite are rare.
2. Granite margins: cassiterite extends into the contact metamorphic zone. Between Comstock and Queen Hill, orebodies of galena, siderite and other sulphide occur in a pyritic gangue with subordinate siderite. Siderite zones exist east of Zeehan and throughout the Dundas area.
3. Quartz-porphyry dykes and sills: cassiterite lodes at Renison Bell, Pine Hill Exe River and near Mount Razorback are possible apophyses of a granite intrusion at depth.
4. Fine-grained cassiterite: axinite-sulphide deposits at Colebrook Hill and complex chalcopyrite, galena and arsenopyrite ores at North Dundas with fine-grained cassiterite locally are also Devonian.

Ground magnetics investigation conducted by RTZ-CRA Exploration across the Stonehenge prospect has identified a high anomaly zone indicative of a near-surface intrusive body (figure X). Magnetic data has been collected over the majority of the study area, with comprehensive coverage of the Proterozoic Oonah Formation along gridlines of 100 metre spacing. Contouring of this magnetic data (figure z) has produced a seemingly well defined body. Explanations for the existence of such a feature include the intrusion of a Devonian granitoid body (occasional throughout western Tasmania), extension of the Heemskirk granite (showing peripheral skarn type mineralisation) or an extremely large pyrrhotite-rich body. The latter seems least likely given the confinement of anomaly at surface to relatively smaller that expected areas for such a scenario. The magnetic anomaly extends from east to west across the Stonehenge grid. The body exceeds 2 kilometres in length, and generally decreases intensity (increases depth) from west to east. Three 'higher magnetic' zones appear within the anomaly. The greatest (centred about 358500mE, 5359500mN) covers an area of approximately 1 square kilometre, an is likely to be quite close to the surface.

364235

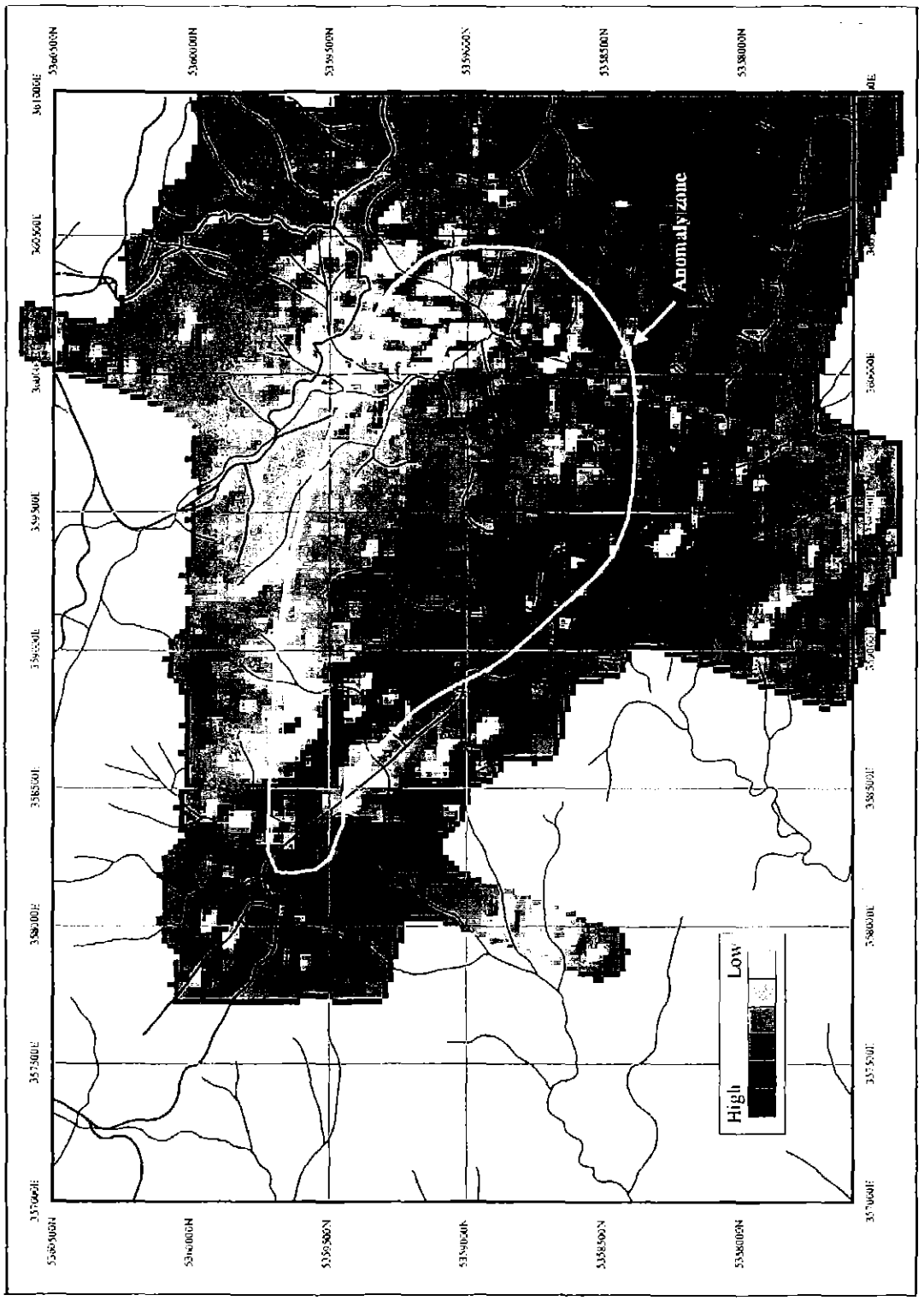


FIGURE 5.11 *Groundmagnetic image of the Stonehenge area.*

Again, the likelihood of this being a pyrrhotite-rich body is unlikely given the failure to detect the anticipated high mineral occurrence at surface. Along with a second (marking the eastern limit of the anomaly at 359750mE, 5358750mN) and third (southern margin of the anomaly/investigation at 359250mE, 5357600mN) area, these heightened magnetic zones may represent nearer surface caps of an intrusive body. Scattered small but high magnetic occurrences found over the prospect area geographically coincide with old mine workings, and are subsequently recorded as local magnetic variants. Structural lineations identified within the body indicates emplacement prior to final phases of deformation throughout the area. Mid to Late Devonian 'Tabberabberan Orogeny' is recorded across Tasmania's west coast, and is the likely proponent of late tectonic disruption of such a body. Blissett (1962) noted the likely relationship between mineralisation of the Zeehan area and intrusion of Devonian granites. These orebodies tend to occur along north-northwest and north-northeast strike lines as fissure veins formed during faulting shearing and fracturing of the Tabberabberan Orogeny. Trends present within the Stonehenge intrusive body lend to support to such deformation.

Modelling by Leaman (1986a) and Bramford and Green (1986) of the Heemskirk and Pine Hill area granites (figure s below) indicates a depth of between 1 and 2 kilometres a continued Heemskirk Granite for the Stonehenge area. The depth to granite increases to the east, as indicated by contouring of the Stonehenge groundmagnetic data.

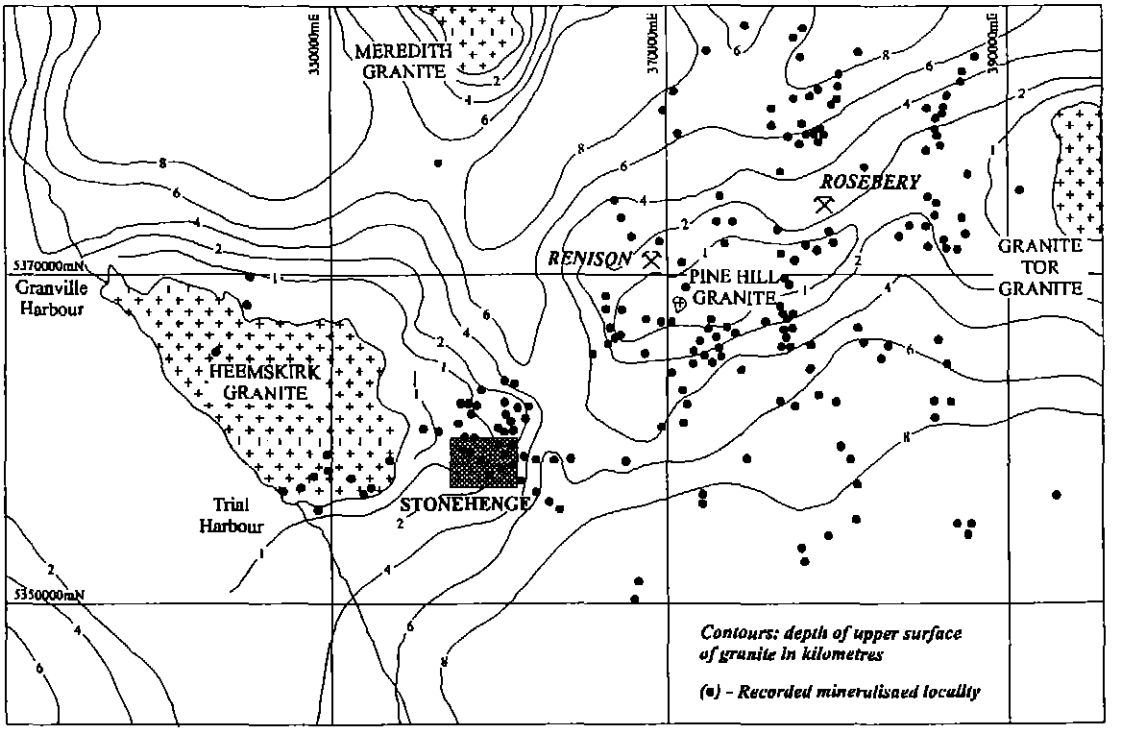


FIGURE 5.12 *Contour map depth to granite body between the Heemskirk and Pine Hill areas. (after Leaman, 1986a; Bramford and Green, 1986)*

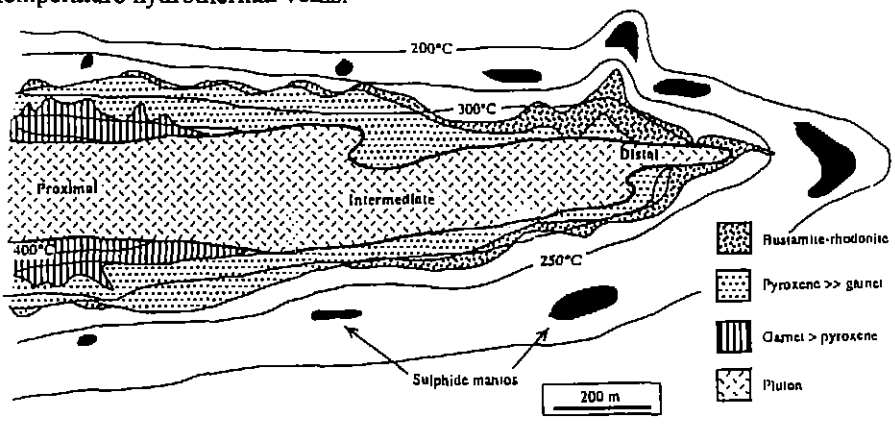
364237

5.4 STYLE OF MINERALISATION

At Stonehenge, mineralisation is thought to the related to two phases/styles of deposition. The first involves stratiform development within the black shale horizons, the second as vein formation throughout shale and dolomitic sequences. Blissett (1962) first recognised the importance of mid-Palaeozoic granite intrusion in relationship to mineralisation throughout the Zeehan area.

The majority of black shale sequences intersected by the diamond drillholes, and within aircore samples contain finely disseminated pyrite. The stratiform nature indicates a syndepositional environment. Often these zones have been sheared (such as in ZS31) by later deformation events. Later mineralisation appears related to the fluid activity noted by Blissett to have formed from granite intrusives. This mineralisation event forms vein deposits, massive disseminations and minor carbonate replacements within shale and dolomitic units of the Oonah Formation. Primary ore minerals hosting, or associated with, zinc mineralisation at Stonehenge include sphalerite, galena and pyrite.

Mineral associations and the physical environment are indicative of low- to medium-temperature hydrothermal Pb-Zn-Ag vein deposits often found along the peripheral boundary of a skarn environment, within the distal margins of hydrothermal systems. Meinert (1993) has identified that most zinc skarns are generally distal from a magmatic source, form veins and massive sulphide bodies, and may grade outwards from skarn-rich mineralisation to skarn-poor ores containing few, if any, skarn minerals. Figure 5.13 is a typical environment as theorised by Meinert (1987) for zinc skarn mineralisation. It is important to note that the sulphides form at distal margins of an intrusive body, at temperatures less than 250°C. Pyrite, sphalerite and galena form the ore hosting minerals throughout Stonehenge. These minerals are common associates, and are often found within low to medium temperature hydrothermal veins.



Feature	Proximal	Intermediate	Distal
Garnet:pyroxene	> 1:1	1:20	No garnet
Max Jo in pyroxene	< 25%	25-50%	> 50%
Fe oxides	mt > hm	hm ~ mt	hm > mt
Ore sulphides	sl > gl ~ cp	sl > gl > cp	sl ~ gl > cp
Skarnmanto ore	> 10	1-10	< 1
Temperature	> 400°C	320° - 400°C	< 320°C
Salinity (NaCl eq. wt.%)	> 15 %	7.5-15%	< 7.5%
Zn/Cu	< 10	10-20	> 20
Zn/Pb	> 5	2-5	< 2
Pb/Cu	< 5	5-10	> 10

FIGURE 5.13 *General model of zinc skarn zonation. (after Meinert, 1987)*

364238

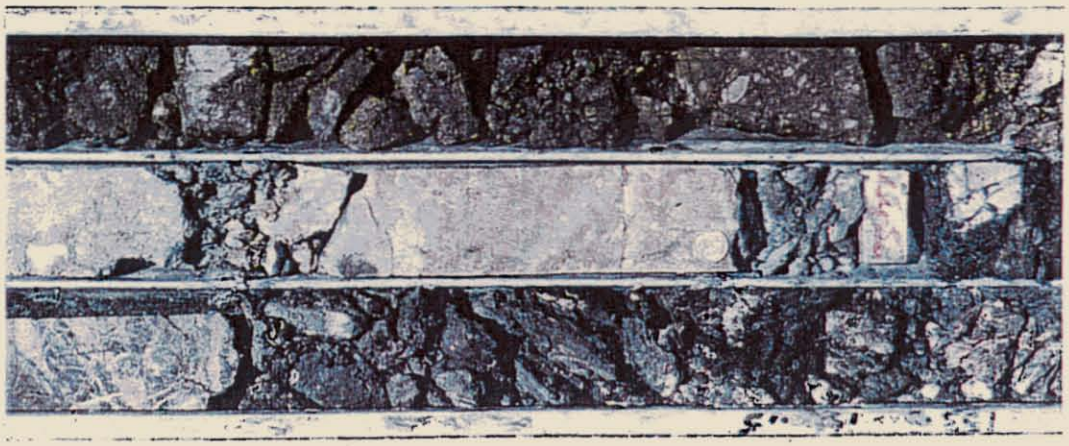
The photomicrograph of figure 5.14 metres shows the wide dispersion of pyrite through the rock mass. Pyrite is a common occurrence in plutonic, volcanic, sedimentary and metamorphic rocks, and is often associated with galena and sphalerite in hydrothermal veins. Sphalerite specimens from the Stonehenge area form two differing styles representing variations in the abundance of iron. The photomicrograph from Grubb's workings (figure 5.15A) shows zonation produced from a high-Fe content within the sphalerite grains. In contrast, the minimal Fe content of a Comstock sample (figure 5.15B) is evident from the consistency of colour and texture throughout. Samples from ZS1 and ZS2 (figure 5.16A and 5.16B) also exhibit similar characteristics. The sphalerite from ZS1, 120 metres has a distinctive semi-hexagonal shape, and obvious red-brown Fe zonation. Zonation is considered to represent the activity of FeS from associated minerals rather than purely the iron content of sphalerite (Prinz, Harlow and Peters, 1991). Pyrite and galena are common associates of sphalerite in calcareous nodules or veinlets of digenetic origin. Figures 5.16C (ZS31, 129.9m) shows cubic galena and cubic-octahedral pyrite grains. The quartz vein here is seen to host the majority of ore mineral, however there is some dissemination throughout the surrounding shale.

High magnesium values identified from wacker and drillhole assay is likely to be of two sources. In the stratigraphy of ZS31, magnesium generally exceeds 6% (often at >10%) (?), coinciding with dolomitic sediments throughout this zone. Wacker sampling has however identified a highly Mg-rich zone at surface level, which does not appear to correlate with distinctive dolomite beds as might be expected. The importance of magnesium within Pb-Zn skarn mineralisation has lead Yiming (1990) to establish the manganoan classification (unique to Pb-Zn skarns). In this instance, Yiming states that Pb-Zn manganoan skarns occur along some structural or lithological contact or carbonaceous rocks distal to intrusive bodies. These deposits are in the form of metasomatic veins, lenses or pipes, and have a temperature range of 200°C to 450°C. Magnesium, along with barite (at consistent 400ppm throughout ZS31), is often an indicator of low to medium temperature hydrothermal veins, diagenetically replacing calcite and dolomite.

Siderite within quartz-carbonate veining (figure 5.8?) is a common associate of barite, galena and sphalerite (Prinz, Harlow and Peters). Siderite within veins of the phyllite sequences at Stonehenge is altered to give a distinctive brown colouring (goethite coating). Siderite is another indicator of medium to low temperature hydrothermal vein activity, and is generally found in association with clay and carbonaceous material. Many veins of the Oonah Formation dolomitic sequences (figure 5.8?) contain such alteration of siderite.

Another feature of low to medium temperature hydrothermal activity is alteration to sericite. This fine aggregation of muscovite crystals often forms in low grade metamorphic pelite rocks, such as samples from MU96-100 (figure 5.9?). This photomicrograph of a quartzite specimen shows the fine grained sericite formed within the quartz grin matrix.

364239



A



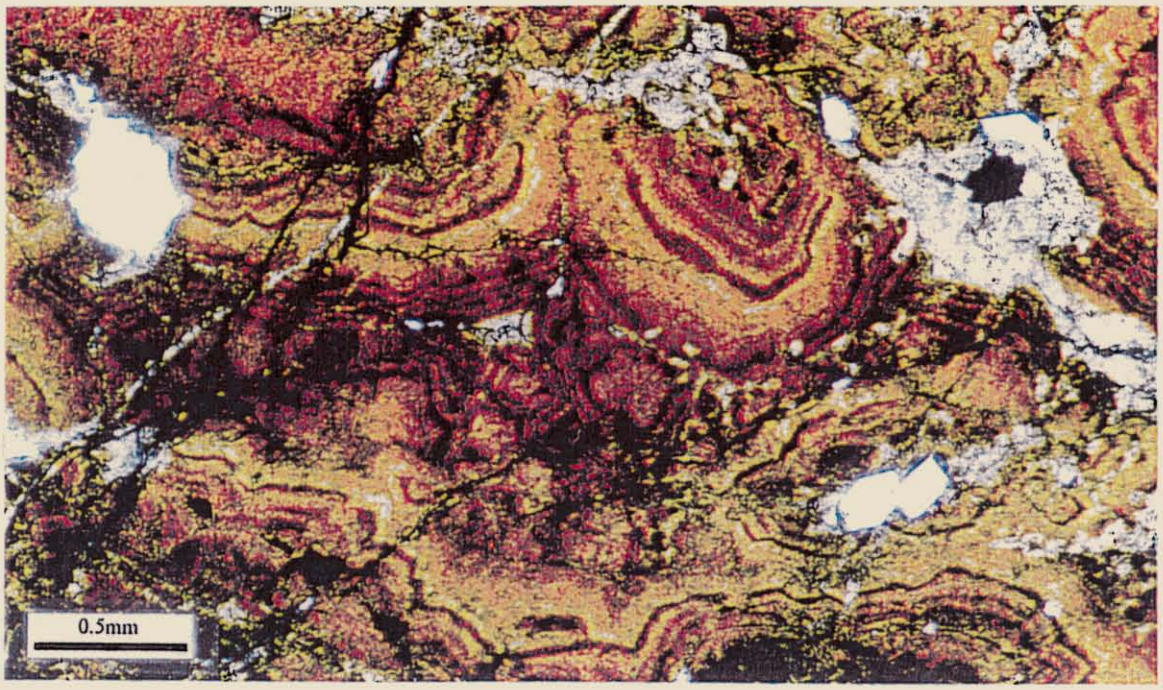
B



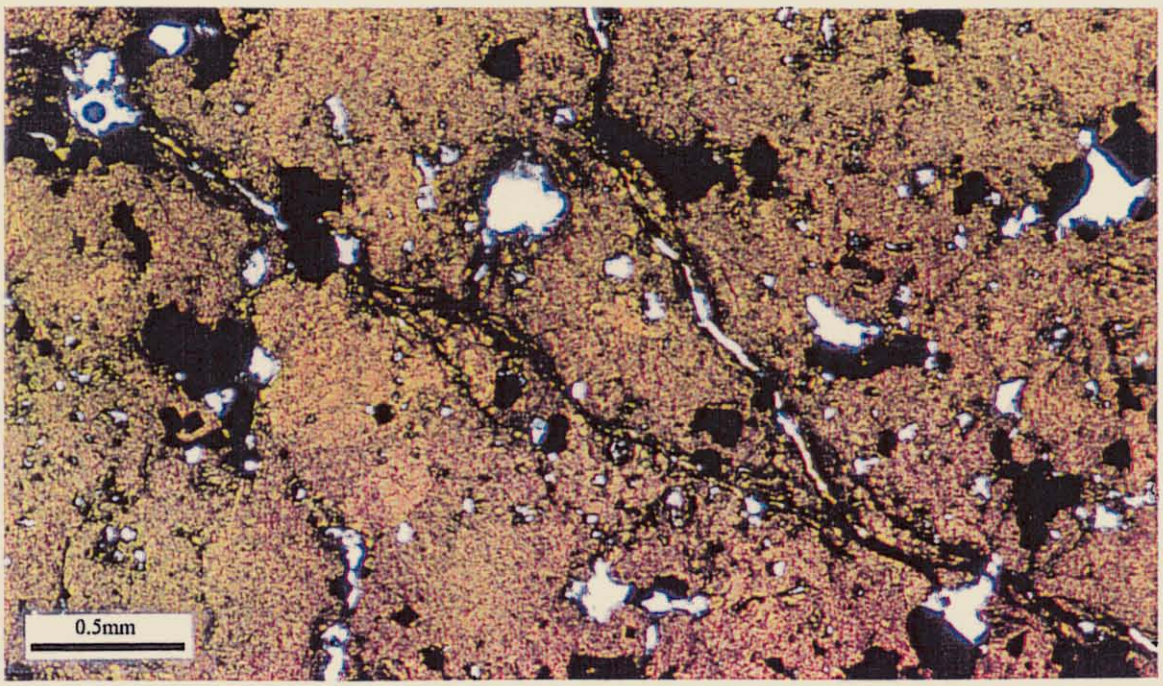
C

FIGURE 5.14 *Massive pyrite mineralisation found within dolomite and shale horizons of ZS31. A. Pyrite zone from ZS31, 153.5 to 156.15 metres. Note the common 'decomposition' of the mineralised sediment type, and the intensity of planar veins within the solid rock mass; B. Pyritic dolomite from ZS31, 154.6 metres showing the extent of mineralisation; C. This photomicrograph of ZS31, 154.6 metres also shows the dominance of pyrite throughout the matrix of the rock (black zones).*

364240



A

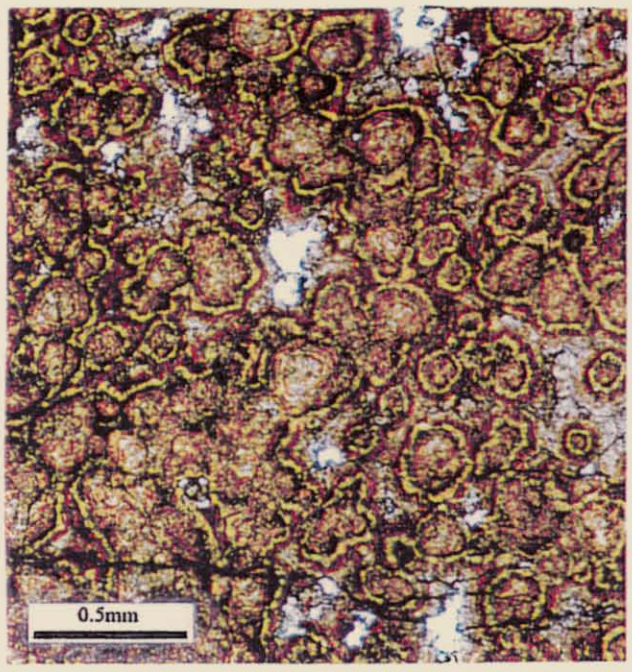


B

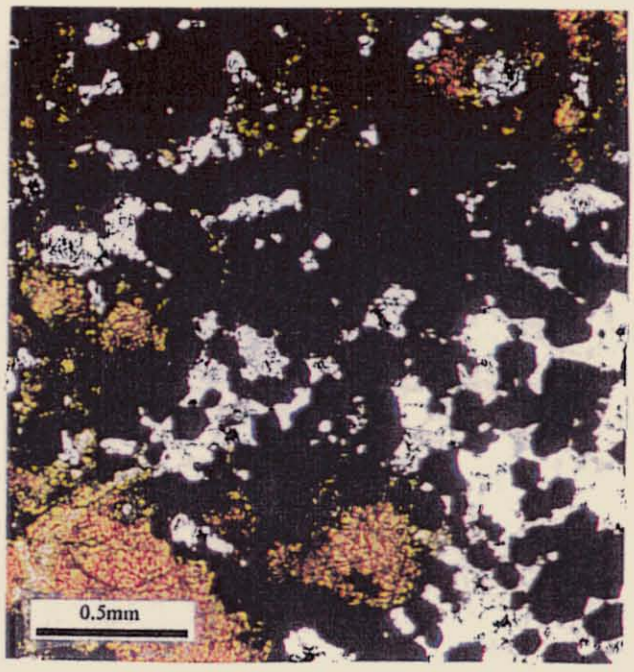
FIGURE 5.15 *The photomicrographs clearly demonstrates the variation in Fe-content reflecting in zonation of the sphalerite grains. A. This sample from Grubb's Workings (south of ZS2, see Appendix 6) Fe zonation of sphalerite. Post-mineralisation fractures and infilling are also evident; B. Sphalerite from Comstock (northwestern margin of Stonehenge area, see appendix 6) with uniform/low Fe-composition. Again fracturing of the mineral grains is evident. Small cubic to semi-octahedral pyrite grains fill voids within the sphalerite.*

364241

A



B



C

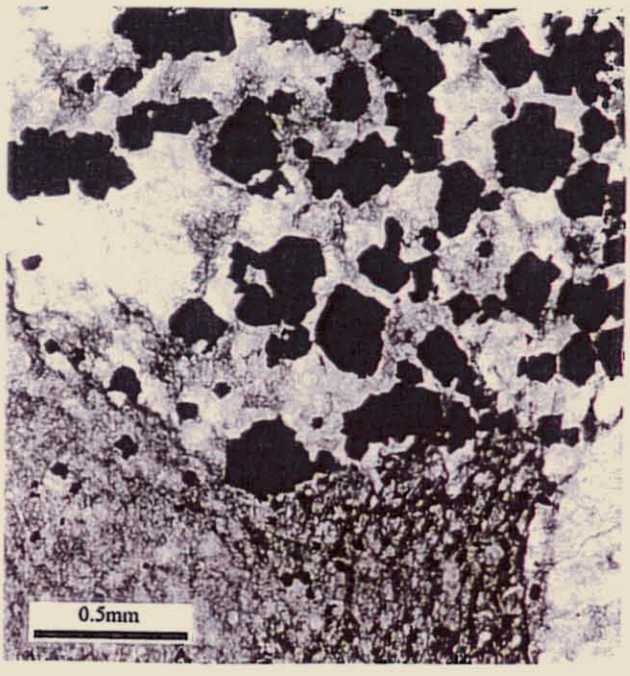


FIGURE 5.16 *A. Sphalerite from ZS!, 120 metres showing iron zonation similar to Grubb's Workings. Later fracturing (cleavage development?) is evident at the bottom of the photomicrograph; B. Sphalerite and pyrite from ZS2, 101 metres within quartz veins; C. Cubic galena and cubic to sub-octahedral pyrite grains generally within quartz veins, but also present as fine disseminations within the country rock;*

364242

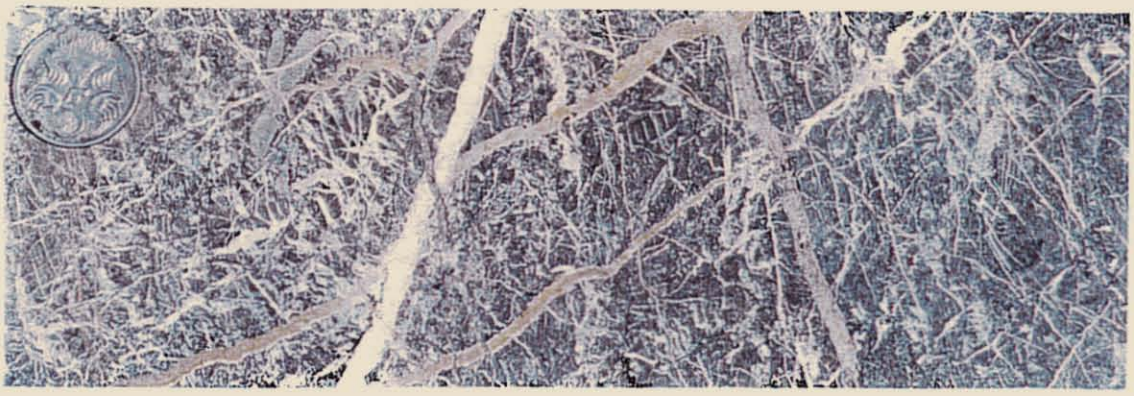


FIGURE 5.17 *Siderite alteration of quartz-carbonate veins producing a fawn colouring.*



FIGURE 5.18 *Photomicrograph of quartzite from station MU96-100. Siderite alteration*

CHAPTER 6.

Discussion

364244

6. DISCUSSION

6.1 STRUCTURAL OVERVIEW

The identification of several fold axes within the Oonah Formation reflects the deformed nature of the Stonehenge structure. A number of folding events (possibly of close timing relationship) have occurred to produce the following fold sets:

- Wrapping isoclinal folds
- North-south
- East-west
- Northeast-southwest
- Northwest-southeast

In combination, the folds have produced a complex structure containing simple dome and basin features which have been interfered with to form plunging antiform/synform folds. Local structures of varied intensity and degree of deformation are indicative deformation at Stonehenge. Differing competence of rock between phyllite and pelite sequences has produced box fold structures commonly identified in drill core. Chevron folding at outcrop scale varies from 10's centimetres to 10's metres. In profile, these structures are clearly exposed along north-south, northwest and southeast lines. Along east-west profiles (north-south structures) there is a notable absence of structure (partially reflecting the lack of exposure) concluding folding along this line to be minor. These structures are open parallel folds with wavelengths of 1 to 2 kilometres.

An interesting feature of the Stonehenge area is that to both the north and south of the Oonah Formation, Cambrian sediments are thrust beneath the older rock units. The flat lying Tenth Legion Fault separates Precambrian and Cambrian sequences. The occurrence of the older Oonah Formation rocks upon the Cambrian Dundas Group sediments required much stratigraphic juggling prior to identification of the Tenth Legion as a thrust event. Timing of is thrusting event is uncertain, however it is thought here that it may be related to major thrusting events of Cambrian age. During this time, Berry and Crawford (1988) propose that mafic-ultramafic suites formed within allochthonous sheets that were thrust onto the west coast of Tasmania. Prominent thrust lineations have been identified via aeromagnetic and gravity interpretations (Chapter 2) along north-northeast trends, indicating northwest-southeast thrust movement. Berry and Crawford have noted that the mafic-ultramafic sequences are likely to have formed from some source to the east. Their model supposes that early 'shelf' deposits such as the Crimson Creek Formation and Success Creek Croup were deposited prior to thrusting. Analysis of Precambrian basement units in northern Tasmania by Woodward, Gray and Elliott (1993) have also indicated allochthonous emplacement.

364245

6.2 'D1 DEFORMATION'

Forming the oldest rocks of Tasmania, Precambrian units have experienced several orogenic phases of deformation. The first event deforming the Oonah Formation has been noted by Blissett (1962), Spry (1962), Crook, 1979) and Turner, (1989) as the Penguin Orogeny. A polyphase deformation event, the Penguin Orogeny is estimated to have commenced 700-750 Ma (Adams, 1985), and regionally is responsible for folding and only minor metamorphism. At Stonehenge, this deformation has produced a spaced cleavage that is common throughout all Precambrian Oonah Formation units. Development of the cleavage at low angle to bedding implies isoclinal folding as the D_1 event. S_1 'roll over' to the south with movement in that direction across the quartzite provides some indication of trend and isoclinal fold type, however additional folding has obscured early fold structures.

Bedding and the subsequent near-parallel S_1 cleavage is recognised by the occurrence of grain alignment and orientated mica growth. Microlithon structures preserved within pelite sequences include tight isoclinal folds along S_1 that reflect the D_1 deformation.

6.3 'D2 DEFORMATION'

The placement of Precambrian Oonah Formation sequences upon Cambrian units reflects the second phase of deformation of the Stonehenge geology. The most prominent fault feature of the area is the Tenth Legion Thrust Fault which separates the Precambrian and Cambrian sequences (figure 6.1). It is thought that the Oonah Formation has been emplaced upon the younger rocks via this fault. By nature of the fault line, and analysis of shearing strains (eg. Reidel Shears) along the fault contact, indicate movements of the Tenth Legion Fault as either underthrust from the west or overriding from the east. A number of features lend evidence towards thrusting events during the Cambrian evolution of western Tasmania. Regional trends in northwestern Tasmania identified by aeromagnetic and gravity interpretations suggest thrust fault lineation along east-northeast trends - thrusting from the east or the west. Investigation by Berry and Crawford (1988), Berry (1989) and Woodward, Gray and Elliott (1993) have all identified thrusting events and allochthonous emplacement of Precambrian basement units into northern Tasmania and surrounding Dundas Trough areas. Furthermore, Berry and Crawford (1989) ideally propose thrusting from the east.

The detachment of the Oonah Formation from its base and thrusting into the Stonehenge geology has occurred within a time frame Middle Cambrian and mid to late Devonian. The sequence has been placed upon Dundas Group and Crimson Creek Formation sediments which have been dated as early Cambrian (Blissett, 1962). Devonian structural features and intrusive bodies influencing the Oonah Formation require emplacement prior to this time.

364246

This D2 event has produced folding within the Oonah Formation striking along a north-south axis. The broad gentle folds identified along east-west profile lines are attributed to compression of similar trend during thrust movement from east to west. It is unknown if these fold structures are continuous within the underlying Cambrian sequences, however the mapping conducted indicates there may be some discontinuity between fold structures. This implies that folding (striking north-south) within the Oonah Formation was produced prior to or during emplacement.

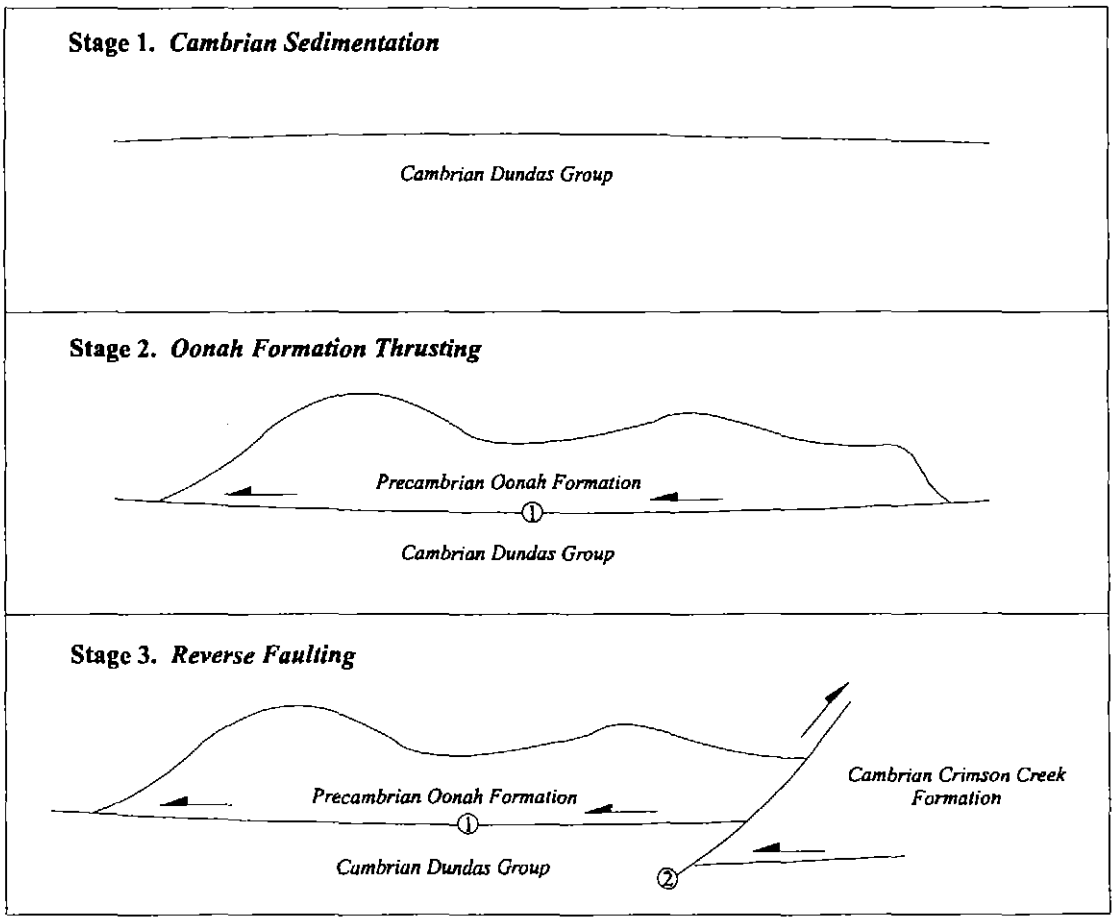


FIGURE 6.1 *Thrust emplacement of the Oonah Formation during the Middle Cambrian to late Devonian.*

6.4 'POST D2 DEFORMATION'

The complexity of deformation is evident from fold traces within the quartzite unit of the Oonah Formation, however identifying relationships is difficult. Deformation during this time incorporates the formation of folds and faults most likely produced during 'Tabberabberan' deformation. Fold sets along northwest-southeast, northeast-southwest and east-west axes are thought to have been produced during a relatively short time span. Their interference relationship has produced complex patterns within the Oonah Formation.

364247

The northwest-southeast fold set is correlated with structures of the surrounding geology to provide an accurate estimate of deformation. Similar trending folds within Siluro-Devonian sediments indicates folding to be no earlier than the Devonian. Widespread throughout the west coast of Tasmania, the 'Tabberabberan Orogeny' is thought responsible for this folding. Folds of younger age than the late Cambrian (?) D2 deformation event are all attributed deformation correlating to the Tabberabberan event, however it is unknown whether they formed during near-simultaneous or individual deformation events.

All of the Devonian folds have been faulted to varying degrees implying the continuation of deformation during this time after completion of folding. Faulting throughout the area represents the final phase of deformation. The folded Siluro-Devonian sequences southeast of Stonehenge are offset by lateral fault movement thought to mark the completion of the 'Tabberabberan Orogeny'. An intrusive body underlying the Stonehenge area marks the eastward continuation of the Heemskirk Granite. This Devonian body contains structural trends, further implying fault movement during the late Devonian.

6.4 LOCAL AND REGIONAL DEVELOPMENT

Traditional interpretation of the Late Proterozoic-Early Palaeozoic Tasmania has implied the basis of a volcano-sedimentary trough, the Dundas-Mount Read Volcanic Belt (Cambrian), wedged between two multiply deformed Precambrian highs: the Tyennan region and the rocky Cape Region (Berry and Crawford, 1988). North of the Tyennan Region, smaller Precambrian rocks of the Forth Metamorphic Complex and the Badger Head Metamorphic Complex separate northeastern continuation of the Dundas Trough into the Dial Range and Fossey Mountains Trough (figure 6.2).

Mafic-ultramafic complexes (MUC) scattered along the western margin of the Dundas Trough and wrapping the Tyennan region seemingly provide the key to development of tectonic models for Cambrian evolution in Tasmania. High-Mg andesites and low-Ti basalts forming the MUC complexes are generally restricted to arc-forearc settings (Corbett, 1989), raising questions as to their position within the Dundas Trough. Several authors are in agreement of tectonic emplacement of these complexes into and onto the Crimson Creek Formation, a Late Precambrian-Early Cambrian rift sequence, during Early or Middle Cambrian (Solomon and Griffiths, 1972; Williams, 1978; Brown, 1986; Corbett and Lees, 1987), however the nature of this Cambrian tectonism is uncertain.

364248

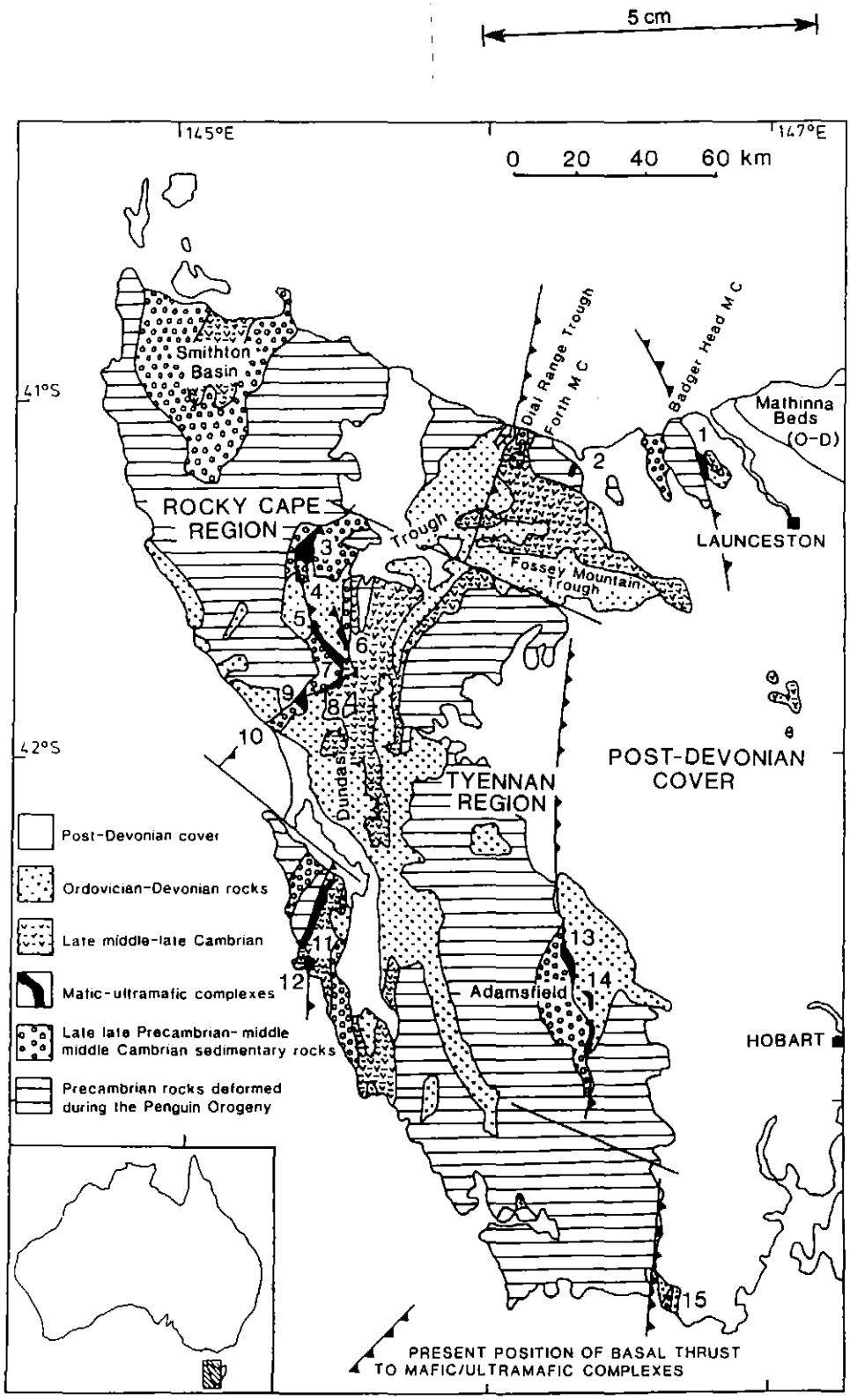


FIGURE X ***Simplified geology western Tasmania showing the distribution of MUC and location of Tyennan and Rocky Cape Regions. (Berry and Crawford, 1988; after Brown, 1986 and Williams, 1976)***

364249

The advent of plate tectonic hypothesis in the late 1960's has initiated numerous tectonic models as proposals for the early Palaeozoic development of western Tasmania. An inability thus far to produce a definitive conceptual model reflects the varied and complex geology involved. Most models to date may be categorised as either (sections of the relative model types are shown in figure 6.3):

- (Campana and King, 1963; Williams, 1978; Verne and Foden, 1987) consider that the Dundas Trough to represent a narrow rift formed by extension and thinning of continental crust with minimal generation of ocean crust.
- (Solomon and Griffiths, 1972, 1974; Crook, 1980; Green, 1983; Corbett and Lees, 1987) suggest that the Dundas Trough represents a wide basin zone which closed during Cambrian subduction, producing collision of the Rocky Cape Region and the Tyennan Region.
- (Berry and Crawford, 1988) propose that during the middle Middle Cambrian, Cambrian sediments containing the MUC were emplaced into western Tasmanian geology via allochthonous sheet movement from a forearc region outside western Tasmania (thought to be a passive continental block exposed to a subduction-type collision with an exotic island arc (Corbett, 1989)). Berry and Crawford state that this model has implications for much of the Lachlan Fold Belt.

Additional models relate the development of western Tasmania to movements along major fault systems such as the Tamar Fracture System (Varne and Foden, 1987; Bailie, 1985).

Most recent investigations (including Berry and Crawford 1988; Berry, 1988; Crawford and Berry, 1988) into allochthonous emplacement of MUC into western Tasmania account for several of the problems associated with both rift and plate tectonic models for western Tasmania. The allochthon model suggests that western Tasmania is part of a single continental block underlain by Precambrian rocks folded during the Penguin Orogeny. Overlying are 'shallow shelf' units containing large volumes of rift tholeiites (within the Success Creek Group and Crimson Creek Formation). A source outside present distribution of MUC, possibly to the east or north is preferred' (Berry and Crawford, 1988) as place for MUC origin. The significant composition component is within the MUC, implying a forearc origin. The allochthon sheet is thought to be a very shallow dipping sheet (<3° during emplacement; assuming maximum original thickness of continental shelf sediments of 5 kilometres) given its occasional position upon sediments overlying the basement, implying that the underlying sediments acted as a decollement for the sheet (figure 6.4). The complex nature of exposure of the allochthon is attributed to extensive erosion post-emplacement and intense folding and faulting during Tabberabberan orogenic events. Stretched and rotated, this passive continental margin moved towards an eastwards-directed subduction zone above which an oceanic island arc and forearc had formed. Middle Cambrian collision with the island arc initiated the emplacement of forearc ultramafics and boninites onto the underthrusting western Tasmanian block. These allochthonous sheets extent across the Tyennan region and Dundas Trough (Corbett, 1989).

364250

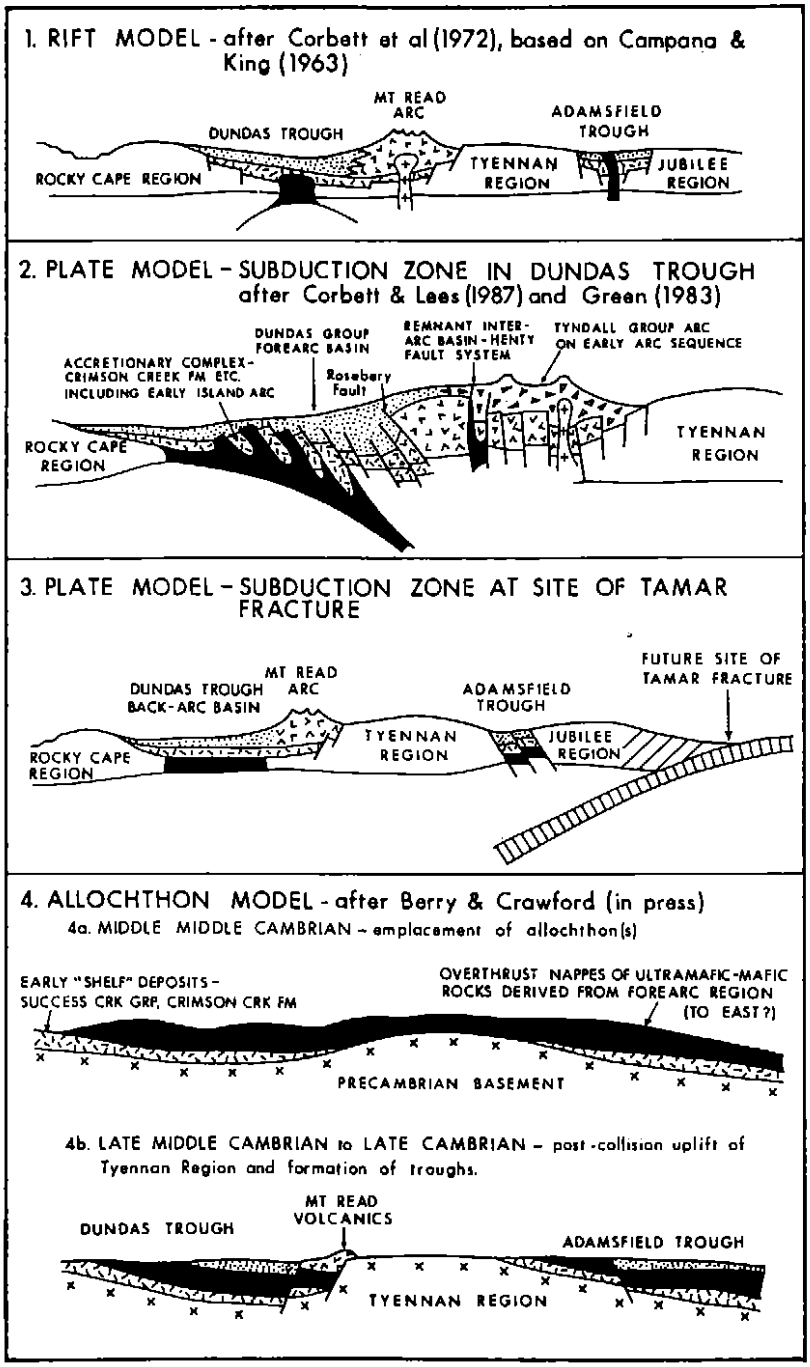


FIGURE 6.3 *Tectonic models proposed for the development of Cambrian geology in Tasmania. (Corbett, 1989)*

364251

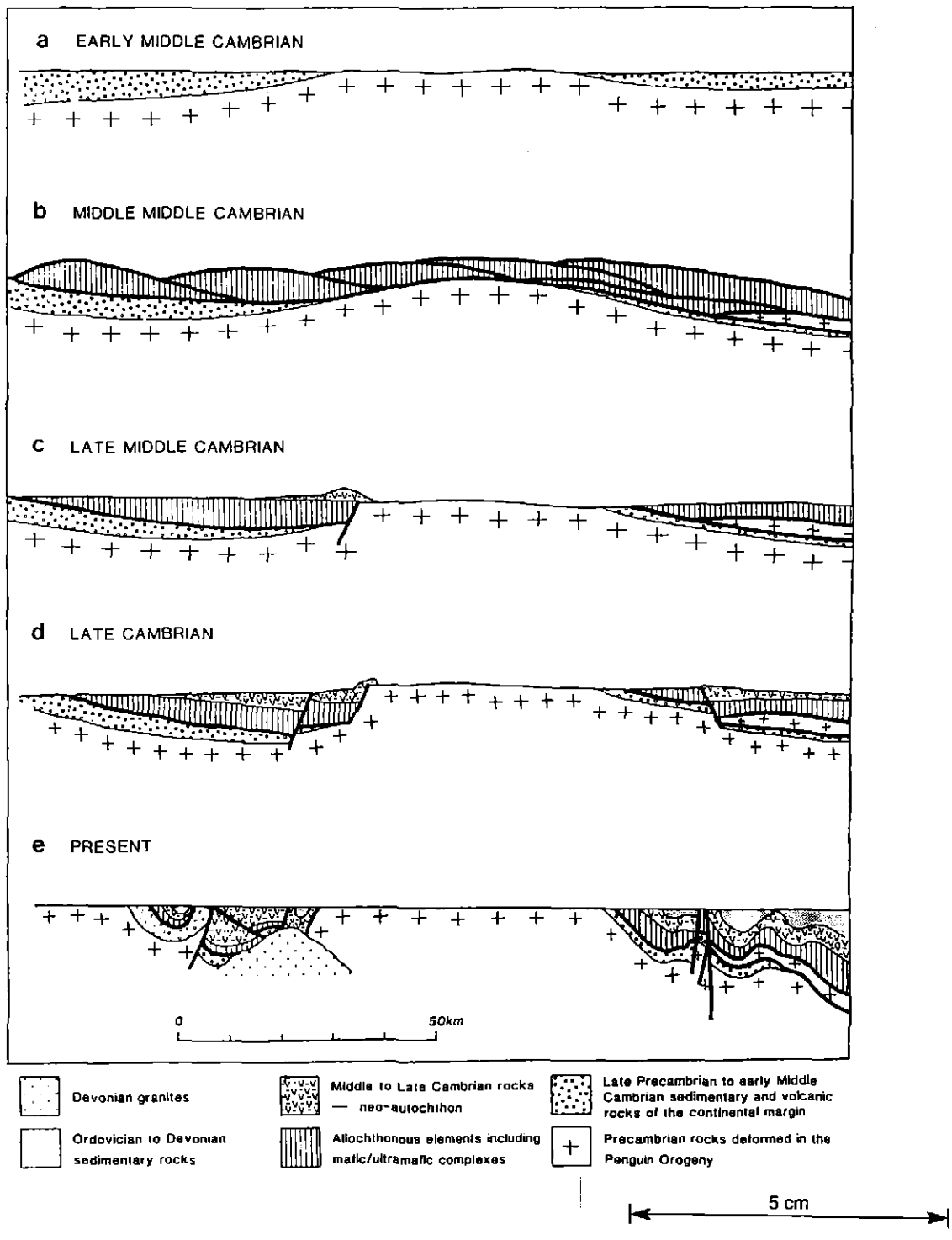


FIGURE 6.4 *Schematic sections (E-W) showing the evolution of Tasmania from Cambrian to the present. a. Late Precambrian to early Middle Cambrian shelf sedimentation upon folded basement; b. emplacement of allochthonous sheet containing forearc rocks; c. Tyennan Region uplift and erosion of allochthon sediments, and onset of volcanism and sedimentation within the Dundas Trough; d. full Dundas Trough development; e. current configuration complicated by Devonian folding and granite intrusion. (Crawford and Berry, 1988)*

364252

Crawford and Berry propose tat later extension produced graben-like troughs in which Dundas Group deposition was possible. The simultaneous eruption of the Mount Read Volcanics was generated by delayed partial melt of subduction modified subcontinental margin, or short-lived reversal of the subduction zone. Rebounding uplift of the Tyennan region resulted in stripping of the allochthonous cover rocks and much Precambrian material. Deposition of this coarse siliclastic detritus into trough resulted in the formation of the Denison Group. Representative of a middle to late Cambrian orogeny, arc-continent collision of this nature correlates with similar events on mainland Australia and Antarctica. Latest Cambrian to Early Ordovician thrusting (the Haulage Movement) terminated the Early Palaeozoic Orogenic stage of fold development. Platform conditions prevailed throughout the Ordovician. Allochthonous associated faults were generally reactivated and strongly folded during Devonian Tabberabberan deformation, so that most MUC-bounding fault contacts are steep. The original shallow dipping nature is recognised by comparison with nearby bedding in Ordovician and Devonian sedimentary rocks.

The geometry of Middle Cambrian evolution within Tasmania appears similar to that of the Semail Ophiolite sequence of Oman (figure 6.5). As with Berry and Crawford's proposal for Tasmania, the MUC of Oman were emplaced as a sheet across Late Proterozoic continental margin sediments around middle Middle Cambrian. Emplacement had ceased by the end of Middle Cambrian, from where tensional tectonism and related post-collision volcanism (of lesser volume than in Tasmania) commenced.

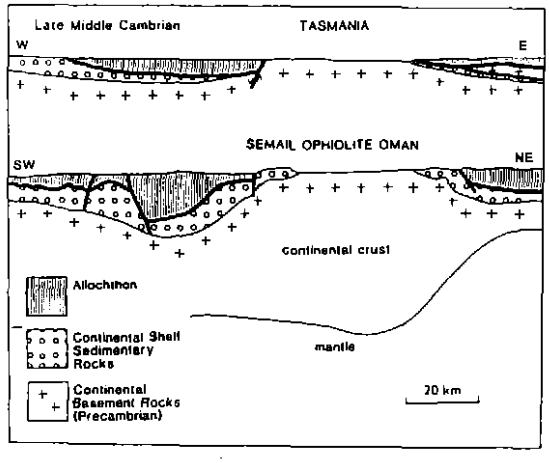


FIGURE 6.5 ***Comparison between structure of the Semail Ophiolite, Oman and the Middle Cambrian structure of Tasmania as proposed by Crawford and Berry. (Crawford and Berry, 1988; Hopson et al., 1981; Manghnani and Coleman, 1981)***

364253

The allochthon model fails to explain ever facet existing geology. Problems of the model include:

- Low-Ti basalts at Serpentine Hill are thought part of the allochthon, however Brown (1986) has identified these basaltic sequences within basal sediments of the Dundas Group (non-allochthonous).
- Absence of supporting evidence for the existence of a sheet of ultramafic-mafic rocks covering the Tyennan region.
- Postulation for Mount Read Volcanics formation does not account for the subsequent restriction of the belt to the western-northern margin of the Tyennan region.

364254

6.5 EVALUATION OF THE GENESIS AND TIMING OF MINERALISATION

The Stonehenge area has historically hosted several workings, primarily of silver, lead and zinc. Blissett (1962) noted the likely influence of the Heemskirk Granite intrusion (3-4 kilometres to the northwest) upon mineralisation. Although this is likely to be most dominant, this investigation has found that there appears to have been two phases of mineralisation within the stratigraphy:

1. Stratiform syn-depositional pyrite in black shale horizons.
2. Zinc mineralisation (sphalerite, pyrite and galena) as hydrothermal veins deposits and minor carbonate replacement.

Stratiform mineralisation is recognised by the extensive occurrence of fine pyrite disseminations throughout the black shale horizons. This is common for shales in each of the drillholes (RTZ-CRA Exploration diamond drillholes (ZS1, ZS2, ZS3 and ZS31).

Elsewhere in the stratigraphy, mineralisation is restricted to small disseminations of sphalerite, pyrite and galena in veins or as local replacements. This second mineralisation event is related to intrusion of the Heemskirk Granite 3-4 kilometres northwest of Stonehenge. Meinert's investigations of skarn mineralisation styles have identified that zinc deposits often form within the outer margins of intrusive bodies (along the periphery of a skarn environment). Groundmagnetic data collected over the Stonehenge area has identified an anomaly which is interpreted to represent the continuation of the Heemskirk Granite. This body has been modelled to a subsurface depth of 1-2 kilometres (Leaman, 1986a; Bramford and Green, 1986), placing Stonehenge within the distal intrusion margin. Several mineralogical features support mineralisation from low to medium temperature hydrothermal fluids emanating from a granite intrusive body and as replacement deposits (skarn):

- The hosting ore minerals of sphalerite, pyrite and galena are common associates within low to medium temperature hydrothermal solutions. Their occurrence is generally within thin vein systems, and often in close proximity to fracture systems.
- Sericitic alteration within host rocks and siderite in quartz-carbonate veins are common within an environment of medium to low temperature hydrothermal veins.

364255

6.6 STRUCTURE OF THE MINERALISED HORIZONS

Establishing the structural geology of the area currently sought for zinc mineralisation has been hindered by the:

- absence of outcrop across and surrounding the mineralised horizons
- *non*-orientated nature of diamond drill core

Two principles have been applied in order to overcome these problems. The *first* involves applying the nature of structure evident throughout Stonehenge to this specific area. Detailed mapping to the south (across the quartzite sequence) has established a structural picture which is believed to be applicable throughout the Oonah Formation at Stonehenge. Structural data collected from the drillholes has proved valuable in establishing the degree of, and features produced from, deformation. This information has been incorporated with surface stratigraphy as identified via acker sampling, to produce profiles for each of the drillholes (Appendix 3). The *second* process in establishing structural geology of the mineralised area involves correlation between drillholes - diamond holes at depth, and wacker stratigraphy horizons at surface level. This has been done in unison with the established structure to ensure continuity between interpretative processes.

Figure 6.6 shows the interpreted model of the area surround the four RTZ-CRA Exploration drillholes. The black shale horizons in each of the drillholes have been used as 'marker' beds since they appear in each of the holes, and are identified at surface. Surrounding stratigraphy comprises (minor) sands, silts, shales and dolomite/dolomitic sediments. Although dolomite beds have been logged as part of the drillholes stratigraphy, a lack of continuity between holes, and general absence at surface has led to their inclusion into the grouping of silts, shales and dolomitic sediment (Pos).

364256

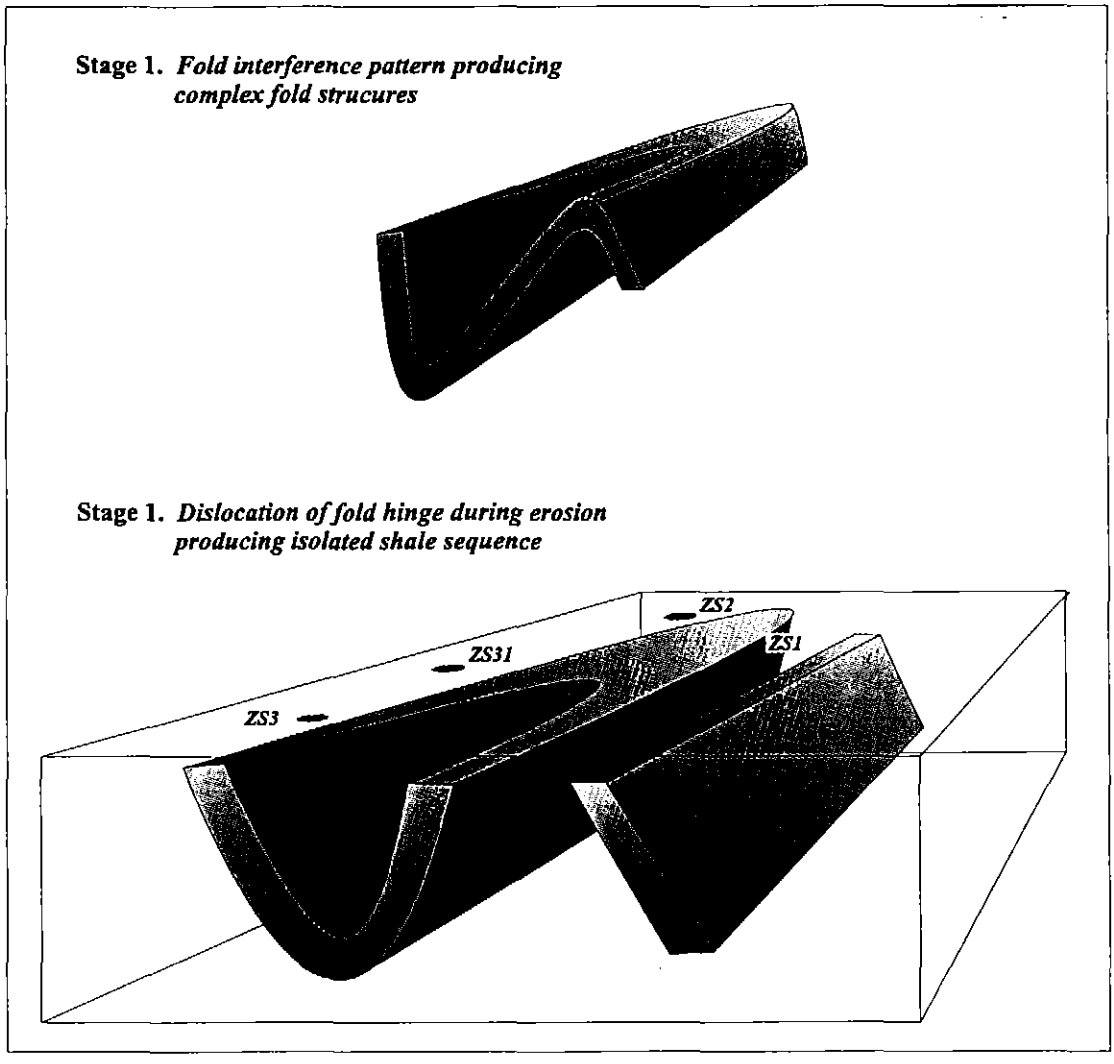


FIGURE 6.6 *Interpretative model of black shale horizons surrounding the mineralised horizons at Stonehenge.*

364257

CHAPTER 7.

Conclusions

364258

7. CONCLUSIONS

This detailed investigation of the Stonehenge prospect area has helped to unravel the complex structure, and identify elements of mineralisation. To date, investigations by RTZ-CRA Exploration, and previously by Gold Fields Exploration have focussed efforts on stratigraphy and mineralisation rather than structure. Blissett's coverage of the Zeehan area (1962) identified major 'Tabberabberan' folding within the Oonah Formation, however his study lacked the detail to identify to complex variation of dome and basin structures. Deformation of the Stonehenge area has involved several stages of folding and faulting between Late Proterozoic and Late Devonian. The stratigraphic position of Precambrian Oonah Formation above Cambrian sequences is the product of thrust faulting thought to have occurred during the Cambrian. This event correlates with thrusting recorded in the Dundas Trough region (Crawford and Berry, 1988) and throughout northwest Tasmania (Woodward, Gray and Elliott, 1993). Investigations of the mineralisation support Blissett's (1962) claim that the majority of mineralisation throughout the Zeehan area is influenced by the Heemskirk Granite intrusion. Mineral associations, and structural and spatial controls provide evidence for mineral deposition from low to medium temperature hydrothermal veins within the peripheral margins of a skarn environment.

- The development of foliation throughout the Stonehenge area is representative of the stratigraphy. Dominating quartzites of the Oonah Formation are less conducive to deformation than surrounding pelite sequences.

- Early deformation has produced a spaced cleavage at low angle to bedding. This fabric is found in all horizons of the Oonah Formation, and is thought representative of isoclinal folding.

- Isoclinal folds preserved as microlithons supports this fold type as the first phase of deformation

- The identified early low angle deformation within the Oonah Formation has formed during polyphase deformation of the Penguin Orogeny (700-750 Ma). This period of folding has been widely identified throughout Proterozoic sequences of western Tasmania.

- Oonah Formation sequences at Stonehenge have been emplaced above Cambrian sediments via the Tenth Legion Thrust Fault. This low angle fault forms a detachment between the Oonah Formation and its basement sequence. Mylonite intersected in drillcore represents the fault sequence, and has provided estimates of 500 to 600 metes for the thickness of the Oonah Formation.

- The thrust events at Stonehenge may correlate with allochthonous movement identified by Crawford and Berry (1988) to have taken place during the Cambrian.

- Fold interference patterns within the Oonah Formation have formed during Devonian folding. A complex set of dome and basin structures have been further deformed to produced plunging antiform/synform structures throughout the pattern.

- A dominant northwest-southeast fold set at Stonehenge correlates with folds of similar trend and magnitude in surrounding Siluro-Devonian sequences. Deemed to represent the final phase of folding, timing estimate from the hosting lithology shows equivalence with Devonian 'Tabberabberan Orogeny' deformation.

- All Stonehenge geology has been subjected to faulting, marking the final phase of deformation during completion of the 'Tabberabberan Orogeny (?)' during Late Devonian. Fault trends are generally west-northwest and north-northwest to north-northeast.

- Pyrite, sphalerite and galena are the host ore minerals, and have deposited during two phases of deformation. The first has produced stratiform deposits of extensive disseminated pyrite throughout black shale horizons. The second represents low to medium temperature hydrothermal vein solution emplaced via fracture/fault lines into shale and carbonaceous/dolomitic sequences. Minor replacement (skarn) has occurred.

- An intrusive body identified subsurface (1-2 kilometres) at Stonehenge marks continuation of the *Heemskirk Granite* body to the northwest. It is proposed that this Devonian body has sourced the hydrothermal fluids hosting the ore mineralisation.

REFERENCES.

REFERENCES

Anovitz, L.M. and Essene, E.J., 1990, Thermo-barometry and temperature-pressure paths in the Grenville Province of Ontario: Journal of Petrology, v. 31, p. 197-241.

Ashley, P.M., 1980, Geology of the Ban Ban zinc deposit, a sulphide bearing skarn, southeast Queensland, Australia: Economic Geology, v. 75, p. 15-29.

Baillie, P.W., 1989, Jurassic-Cainozoic *in* Burrett, C.F. and Martin, E.L., ed., *in* Geology and mineral resources of Tasmania: Geological Society of Australia, Special Publication 15, 1989.

Banks, M.R., and Baillie, P.W., 1989, Late Cambrian to Devonian *in* Burrett, C.F. and Martin, E.L., ed., *in* Geology and mineral resources of Tasmania: Geological Society of Australia, Special Publication 15, 1989.

Berry, R.F., 1989, The history of movement on the Henty Fault Zone, western Tasmania: an analysis of fault striations: Australian Journal of Earth Sciences (1989) 36, p 189-205.

Berry, R.F., and Crawford, A.J., 1988, The tectonic significance of Cambrian allochthonous mafic-ultra-mafic complexes in Tasmania: Australian Journal of Earth Sciences (1988) 35, p 523-533.

Blissett, A.H., 1962, Geological Survey Report, one mile geological map series K'55-5-50, Zeehan: Tasmania Department of Mines.

Bowers, J.R., Kerrick, D.M., and Furlong, K.P., 1990, Conduction model for the thermal evolution of the Cupsuptic aureole, Maine: American Journal of Science, v. 290, p. 644-665.

Bramford., and Green., 1986, *in* RGC Company Report.

Brown, A.V., Jago, J.B., Williams, P.R, Calver, C.R., and Turner, N.J., 1989, Eo-Cambrian-Cambrian *in* Burrett, C.F. and Martin, E.L., ed., Geology and mineral resources of Tasmania: Geological Society of Australia, Special Publication 15, 1989.

Burt, D.B., 1972, Mineralogy and geochemistry of Ca-Fe-Si skarn deposits: Unpublished Ph.D. thesis, Harvard University, 256p.

Burt, D.M., 1982, Skarn deposits - Historical bibliography through 1970: Economic Geology, v 77, p. 755-763.

364262

Clarke, M.J., and Forsyth, S.M., 1989, Late Carboniferous-Triassic *in* Burrett, C.F. and Martin, E.L., ed., *in* Geology and mineral resources of Tasmania: Geological Society of Australia, Special Publication 15, 1989.

Colhoun, E.A., 1989, Quaternary *in* Burrett, C.F. and Martin, E.L., ed., *in* Geology and mineral resources of Tasmania: Geological Society of Australia, Special Publication 15, 1989.

Corbett, K.D., and Lees, T.C., 1987, Stratigraphic and structural relationships and evidence for Cambrian deformation at the western margin of the Mount Read Volcanics, Tasmania: Australian Journal of Earth Sciences (1987) 34, p 45-67.

Corbett, K.D., and Solomon, M., 1989, Cambrian Mount Read volcanics and associated mineral deposits *in* Burrett, C.F. and Martin, E.L., ed., *in* Geology and mineral resources of Tasmania: Geological Society of Australia, Special Publication 15, 1989.

Corbett, K.D., and Turner, N.J., 1989, Early Palaeozoic deformation and tectonics *in* Burrett, C.F. and Martin, E.L., ed., *in* Geology and mineral resources of Tasmania: Geological Society of Australia, Special Publication 15, 1989.

Edwards, R., and Atkinson, K., 1986, Ore deposit geology: Chapman and Hall, London.

Einaudi, M.T., Meinert, L.D., and Newberry, R.J., 1981, Skarn deposits: Economic Geology, 75th Anniversary Volume, p. 317-391.

Elliott, C.G., Woodward, N.B., and Gray, D.R., 1993, Complex regional fault history of the Badger Head region, northern Tasmania: Australian Journal of Earth Sciences (1993) 40, p 155-168.

Gribble, C.D, and Hall, A.J., 1991, A practical Introduction to optical mineralogy: HarperCollins *Academic*, London.

Kwak, T., and Askins, P., 1981, Geology and genesis of the F-Sn-W(-Be-Zn) skarn (wrigglite) at Moina, Tasmania: Economic Geology, v. 76, p. 439-467.

Kwak, T., 1986, Fluid inclusions in skarns (carbonate replacement deposits): Journal of Metamorphic Geology, v. 4, p. 363-384.

McClay, K., 1991, The mapping of geological structures: John Wiley and Sons, England

McClay, K., 1992, ed., Trust Tectonics: Chapman and Hall, London.

364263

Megaw, P.K.M., Ruiz, J. and Titley, S.R., 1988, High-temperature, carbonate-hosted Ag-Pb-Zn(Cu) deposits of northern Mexico: Economic Geology, v. 83, p. 1865-1885.

Meinert, L D., 1983, Variability of skarn deposits - Guides to exploration, *in* Boardman, S.J., ed., Revolution in the Earth Sciences: Kendall-Hunt Publishing Co., p. 301-316.

Meinert, L.D., 1987, Skarn zonation and fluid evolution in the Groundhog Mine, Central Mining District, New Mexico: Economic Geology, v. 82, p. 523-545.

Meinert, L D., 1993, Skarns and skarn deposits, *in* Sheahan, P.A. and Cherry, M.E. eds., Ore deposit models, volume 2: Geoscience Canada, Reprint series 6, p. 117-134.

Myers, G.L, and Meinert, L.D., 1991, Alteration, mineralisation, and gold distribution in the Fortitude gold skarn, *in* Raines, G.L., Lisle, R.E., Schafer, R.W. and Wilkinson, W.H., eds., Geology and Ore Deposits of the Great Basin: Geological Survey of Nevada, Reno, v. 1, p. 407-418.

Newberry, R. J., 1982, Tungsten-bearing skarns of the Sierra Nevada. I. The Pine Creek Mine, California, Economic Geology, v. 77, p. 823-844.

Norton, D., 1982, Fluid and heat transfer phenomena typical of copper-bearing pluton environments, southeastern Arizona: *in* Titley, S.R., ed., Advances in Geology of Porphyry Copper Deposits: southwestern North America: University of Arizona Press, Tuscon, p. 59-72.

Prinz, M., Harlow, G., and Peters, J., 1991, eds., Simon and Schuster's guide to rocks and minerals: Simon and Schuster Inc., New York, 1991.

Salemink, J., and Schuiling, R.D., 1987, A two stage transient heat and mass transfer model for the granodiorite intrusion at Seriphos, Greece, and the associated formation of contact metasomatic skarn and Fe-ore deposits, *in* Helgeson, H.C., ed., Chemical transport in metasomatic processes: Department of Geology and Geophysics, University of California, Berkeley, NATO Advanced Study Institutes Series C; Mathematic and Physical Sciences 218, p. 547-575.

Shimizu, M., and Iiyama, J.T., 1982, Zinc-lead skarn deposits of the Natatatsu mine, central Japan: Economic Geology, v. 77, p. 1000-1012.

Shelton, K.L., 1983, Composition and origin of ore-forming fluids in a carbonate-hosted porphyry copper and skarn deposit: a fluid inclusion and stable isotope study of Mines Gaspé, Quebec: Economic Geology, v. 78, p. 387-421.

364264

Taylor, B.E., 1976, Origin and significance of C-O-H fluids in the formation of Ca-Fe-Si skarn, Osgood Mountains, Humboldt County, Nevada: unpublished Ph.D. thesis, Staford University, 149 p.

Turner, N.J., 1989, Precambrian *in* Burrett, C.F. and Martin, E.L., ed., Geology and mineral resources of Tasmania: Geological Society of Australia, Special Publication 15, 1989.

Twiss, R.J., and Moores, E.M., 1992, Structural geology: W.H. Freeman and Company.

Wallmach, T. and Hatton, C.J., 1989, Extreme facies of contact metamorphism developed in calc silicate xenoliths in the eastern Bushveld complex: The Canadian Mineralogist, v27, p. 509-523.

Wilcox, J.B., 1990, Gravity trends as an expression of lithospheric extension on the southern margin of Australia: Australian Journal of Earth Sciences (1990) 37, p 85-91.

Williams, E., McClenaghan, M.P., and Collins, P.L.F., 1989, Mid-Palaeozoic deformation, granitoids and ore deposits *in* Burrett, C.F. and Martin, E.L., ed., *in* Geology and mineral resources of Tasmania: Geological Society of Australia, Special Publication 15, 1989.

Woodward, N.B., Gray, D.R., and Elliott, C.G., 1993, Repeated Palaeozoic thrusting and allochthoneity of Precambrian basement, northern Tasmania: Australian Journal of Earth Sciences (1993) 40, p 297-311.

Yiming, Z., 1990, Skarn deposits in the Circum-Pacific belts: Pacific Rim 90 Congress, p. 303-311.

Yun, S., and Einaudi, M.T., 1982, Zinc-lead skarns of the Yeonhwa-Ulchin district, south Korea: Economic Geology, v. 77, p. 1013-1032.

Zharikov, V.A., 1970, Skarns: International Geology Review, v. 12, p. 541-559, 619-647, 760-775.

APPENDIX 1.

Database of field mapping

Station	Location	Lithology	Structural Element				Strike (AMG)
			Bedding	Cleavage	Fold	Extra	
MU96-1	Track into Stonehenge	Grey fine grained siltstone. Lt grey/white lenses. Minor iron leaching.	So				174
MU96-2	Cutting along track into Stonehenge	Very thin phyllites - lt grey to white.			Fa		118
					Fas		94
					Fa		47
					Fas		212
					Fa		125
MU96-3	Cutting along track into Stonehenge	Black thin shales with interbedded phyllite			Fas		146
							155
MU96-4	Track into Stonehenge	Thinly laminated slates - grey to dk grey	So				132
				Sca			114
				Scb			157
MU96-5	Cutting through old tramway	Lt grey phyllite beds with qt veining along joints. Some fine dk grey graphitic shales/slates to the north end	So				
				Sm//So			
				Sca			142
				Scb			162
						Joint	196
						Joint	116
			So				153
MU96-6	Tramway cutting	Phyllite beds		Sca			176
				Scb			115
				Scc			85
						Vein	64
			So				107
MU96-7	Tramway cutting	Thin shale/slate with folding priminant to the sthn end	So				141
			So				162
				Sm//So			
				Sca			14
				Scb			49
				Sca			84
				Scb			42
				Sca			136
				Scb			58
					Fa		84
					Fas		72
					Fa		130
					Fas		128
					Fa		91
					Fas		111
					Fa		268
					Fas		84
					Fa		77
					Fas		85
					Fa		93
					Fas		94

36426

					Fa			80
					Fas			84
					Fa			67
					Fas			72
MU96-8	Track into Stonehenge	Thin shale/slate beds - lt to dk grey. Qtz w/in compositional banding. Some fawn phyllite beds	So					163
				Sc				203
MU96-9	Track into Stonehenge	Interbeds of phyllites, shales and slates	So					166
					Fa			55
					Fas			32
MU96-10	Track into Stonehenge	Interbeds of phyllites, shales and slates	So					163
			So					153
			So					135
			So					128
MU96-11	Track into Stonehenge	Laminated shale/silt (lt-dk grey) and bands of phyllite (grey-brown)						175
MU96-12	Track into Stonehenge	Dk grey phyllites, very weathered	So					86
				Sm//So				
				Sc				65
MU96-13	Track - next to small creek running from the west	Phyllites overlying grey to black silts and shales (@ creek)	So					131
MU96-14	Track into Stonehenge	Shales - grey to black (graphitic) with phyllite beds - lt grey to white. Some brown silt layers. Possible fault zone	So					193
					Fa			107
					Fas			111
			So					215
			So					36
			So					45
			So					73
					Fa			231
					Fas			14
			So					45
			So					36
			So					203
						Fracture		137
						Fracture		78
			So					42
						Vein		42
			So					37
					Fa			143
					Fas			128
					Fa			138
					Fas			131
			So					205
			So					66
			So					49
						Fracture		116
						Fracture		36

					Fas		182
MU96-20	Down stream	Thin shale beds	So				46
						Fracture	99
						Fracture	139
MU96-21	Down stream	Black-dk grey silts and shales	So				180
				Sm//So			
				Sc			155
					Fa		110
					Fas		107
					Fa		128
					Fas		121
MU96-22	Down stream	Black-dk grey silts and shales	So				32
MU96-23	Down stream	Graphitic black shales	So				17
					Fa		97
					Fas		129
					Fa		97
					Fas		110
MU96-24	Down stream	Graphitic black shales	So				37
			So				71
					Fa		42
					Fas		39
					Fa		206
					Fas		22
					Fa		222
					Fas		52
					Fa		341
					Fas		179
					Fa		337
					Fas		160
					Fa		247
					Fas		64
					Fa		66
					Fas		47
MU96-25	Down stream	Grey shale?Phyllite?Dolomite?. slightly pyritic	So				47
			So				78
					Fa		91
					Fa		175
MU96-26	Down stream	Pyritic black/grey shales. Pyrite as fine disseminations. Sphalerite grain and fine vein	So				13
			So				33
				Sm//So			
MU96-27	Down stream	Black shale w/in predominantly grey dolomite?siliceous dolomitisation?. Pyrite specks throughout	So				23
MU96-28	Down stream	Lt grey/brown siltstone					
MU96-29	Samples collected from Colonel North workings - mineralogy						

364267

						Fa		135
						Fas		127
				So				76
				So				77
							Fault	67
					Sm//So			
					Sca			205
					Scb			89
					Sca			45
					Scb			73
					Sca			109
					Scb			169
					Sc			210
					Sca			20
					Scb			48
								12
MU96-15	SW of Colony North workings	Grey phyllite with thick quartz veining						
MU96-16	Outcrop along track - before car turn-around	Light grey quartzite or dolominte? Possible dolomitisation, overlain by phyllite (weathered light grey rock)		So				21
							Joint	98
							Joint	182
				So				187
					Sc			88
						Fa		185
						Fas		183
				So				33
MU96-17	Along creek east of track into Stonehenge - approx. 43m south turn-around. *Creek flowing SE*	Limestone? Dolomite?						
							Fracture	170
							Fracture	82
				So				188
							Fracture	13
							Fracture	134
							Fracture	98
				So				175
							Fracture	119
							Fracture	175
				So				42
				So				43
				So				47
						Fa		113
						Fas		112
				So				75
MU96-18	Down stream	Dolomite? with quartz intrusions <50cm		So				56
MU96-19	Down stream	*Grey shales with large quartz intrusions*		So				37
						Fa		182
						Fas		17
						Fa		212

					Fas		14
					Fa		191
					Fas		151
				So			17
					Fa		208
					Fas		87
				So			187
						Fracture	105
						Fracture	141
					Fa		174
					Fas		160
						Fault	160
				So			43
					Fa		164
					Fas		21
					Fa		171
					Fas		186
					Fa		369
					Fas		190
					Fa		85
					Fas		73
				So			183
MU96-36	12310E 5110N - Colonel North	Black shales		So			125
				So			140
				So			106
				So			152
				So			171
				So			66
				So			101
				So			183
					Fa		105
					Fas		109
					Fa		78
					Fas		155
					Fa		141
					Fas		138
					Fa		94
					Fas		102
					Fa		78
					Fas		93
					Fa		68
					Fas		40
				So			87
MU96-37	12310E 5100N - Colonel North	Quartzite/phyllite with shale bands. Possible silicified shales with quartz veining					75
			Sca				134
			Scc				

364268

364269

MU96-30	12330E 5000N - SSW of Colonel North	Lt grey quartzite with some quartz veining	So				18
				Sm//So			
				Sca			169
				Scb			142
				Scc			115
					Fa		187
					Fas		148
						Vein	13
						Vein	46
MU96-31	12332E 5000N - SSW of Colonel North	Lt grey quartzite with some quartz veining	So				29
				Sca			24
				Scb			181
				Scc			132
						Vein	55
MU96-32	12350E 5000N - SSW of Colonlel North	Grey to Dk grey dolomitised shale? Looks like shale but very hard - quartz veined and fawn coloured dolomite veins?. Probably phyllite					
MU96-33	12365E 5000N - sample from creek	Black shale	So				75
MU96-34	12412E 5000N	Grey quartzite					89
				Sca			151
				Scb			53
				Scc			68
						V	160
						V	190
MU96-35	Approximately 50m W of Colonel North	Grey shales grading into sandstones/quartzites to the sth	So				15
			So				86
				Sm//So			173
				Sc			22
				Sca			145
				Scb			87
				Scc			25
				Sca			107
				Scb			140
				Scc			300
					Fa		139
					Fas		245
					Fa		149
					Fas		201
					Fa		18
					Fas		362
					Fa		177
					Fas		197
					Fa		21
					Fas		149
					Fa		

MU96-38	12315E 5100N - Colonel North	Grey quartzite (dolomitised/meta shale?) - weathers to lt green shale?	So				158
					Fa		142
					Fas		138
					Fa		110
					Fas		93
					Fa		362
					Fas		367
MU96-39	Slope approximately 100m SSW Colonel North	Lt grey/white quartzite	So				66
				Sca			27
				Scb			151
MU96-40	Slope approximately 100m SSW Colonel North	Lt grey/white quartzite	So				36
MU96-41	Slope approximately 100m SSW Colonel North	Lt grey/white quartzite (outcrop or boulder?) - veining <10mm	So				61
				Sca			50
				Scb			151
						Vein	61
MU96-42	Slope approximately 100m SSW Colonel North	Lt grey/white quartzite	So				16
				Sm//So			
				Sca			184
				Scb			104
				Scc			64
MU96-43	Slope immediately NW of Grubbs	Lt grey/white quartzite	So				77
				Sm//So			
				Sca			96
				Scb			18
MU96-44	Slope immediately WSW Grubbs (~100m?)	Lt grey/white quartzite/phyllite	So				107
				Sm//So			
				Sca			129
				Scb			48
MU96-45	Slope immediately WSW Grubbs (~100m?)	Lt grey/white quartzite/phyllite	So				45
				Sm//So			
				Sca			112
				Scb			89
				Scc			149
						Vein	99
MU96-46	Slope immediately WSW Grubbs (~100m?)	Lt grey/white quartzite/phyllite			Fa		165
					Fas		132
						Vein	118
						Vein	177
						Vein	73
MU96-47	Slope immediately WSW Grubbs (~100m?)	Lt grey/white quartzite/phyllite	So				16
			So				33
			So				15
				Sm//So			
				Sca			43
				Scb			89

369270

364271

				Sca			209
				Scb			182
				Scc			91
				Sca			53
				Scb			142
				Scc			15
					Fa		304
					Fas		111
						Vein	128
						Fracture	157
						Fracture	127
MU96-48	Slope immediately WSW Grubbs (~100m?)	Lt grey/white quartzite/phyllite	So				33
MU96-49	Slope immediately WSW Grubbs (~100m?)	Lt grey/white quartzite/phyllite	So				65
MU96-50	Slope immediately WSW Grubbs (~100m?)	Lt grey/white quartzite/phyllite	So				53
			So				62
MU96-51	Slope immediately WSW Grubbs (~100m?)	Lt grey/white quartzite/phyllite	So				40
				Sc			37
MU96-52	Slope immediately WSW Grubbs (~100m?)	Lt grey/white quartzite/phyllite	So				45
					Fa		48
					Fas		45
						Vein	173
						Vein	68
MU96-53	NE Swansea (~150m?)	Lt grey/white quartzite/phyllite	So				92
				Sm//So			
				Sca			83
				Scb			189
						Vein	188
						Vein	95
MU96-54	Slightly east of Swansea	Quaternary silts and sands, lt/dk grey. Younging up	So				106
MU96-55	Top of hills sth ZS31	Lt grey/white phyllite/quartzite	So				77
				Sca			110
				Scb			163
MU96-56	Top of hills sth ZS31	Lt grey/white phyllite/quartzite	So				89
				Sca			110
				Scb			24
				Scc			163
MU96-57	Top of hills sth ZS31	Lt grey/white phyllite/quartzite	So				67
				Sca			56
MU96-58	Top of hills sth ZS31	Lt grey/white phyllite/quartzite	So				53
				Sca			63
					Fa		292
					Fas		96
MU96-59	Top of hills sth ZS31	Lt grey/white phyllite/quartzite	So				68
				Sca			57
				Scb			152

				Soc			184
MU96-60	Top of hills sth ZS31	Lt grey/white phyllite/quartzite					
MU96-61	SW along saddle from MU96-55	Lt grey/white phyllite/quartzite	So				66
						V	66
						Fracture	148
MU96-62	SW along saddle from MU96-55	Lt grey/white phyllite/quartzite	So				108
MU96-63	SW along saddle from MU96-55	Lt grey/white phyllite/quartzite	So				94
				Sca			63
				Scb			132
				Soc			176
				Sca			38
				Scb			169
					Fa		178
					Fas		175
					Fa		217
					Fas		172
			So				64
MU96-64	SW along saddle from MU96-55	Lt grey/white phyllite/quartzite	So				78
MU96-65	SW along saddle from MU96-55	Lt grey/white phyllite/quartzite	So				33
			So				80
			So				122
			So				75
			So				20
					Fa		343
					Fas		168
					Fa		157
					Fas		135
					Fa		288
					Fas		102
MU96-66	SW along saddle from MU96-55	Lt brown/grey silts - v.soft. Quartz patches	So				35
MU96-67	Old workings - 'North Swansea'. Outcropping in creek	Black shales underlying quartz and soils. Weathered to lt grey/white	So				83
						Fault	141
MU96-68	Old workings - 'North Swansea'. Outcropping in creek	Black shales	So				76
						Fracture	154
MU96-69	Old workings - 'North Swansea'. Outcropping in creek	Black shales	So				86
				Sca			44
				Scb			15
				Scc			176
MU96-70	Old workings - 'North Swansea'. Outcropping in creek	Black shales	So				77
MU96-71	Old workings - 'North Swansea'. Outcropping in creek	Black shales	So				73
MU96-72	Old workings - Swansea.	Interbedded shales and silts - lt/dk grey. Minor fine sands	So				132
			So				102
				Sca			103
				Scb			185
MU96-73	Old workings - Swansea.	Interbedded shales and silts - lt/dk grey. Minor fine sands	So				110

364272

364273

MU96-74	Old workings - Swansea.	Black shales	So				124
MU96-75	Old workings - Swansea.	Black shales with sandstone interbeds <20mm	So				135
MU96-76	Old workings - Swansea.	Siliceous black shales and sands - some gabbro?micaceous ss?cemented material	So				111
				Sc			156
MU96-77	Old workings - Swansea.	Siliceous black shales. Quartz veining and shear zones. Minor phyllites	So				168
			So				195
						Fault	47
						Fault	153
			So				64
					Fa		77
					Fas		39
					Fa		97
					Fas		18
					Fa		101
					Fas		87
					Fa		110
					Fas		93
						Fault	67
						Fault	129
MU96-78	Along Swansea track	Black shales with minor sand lenses	So				104
				Sc			126
				Sca			135
MU96-79	Along Swansea track	Cemented quartz fragments <20mm and angular silicified shales - conglomerate? - dk/lt grey when weathered					
MU96-80	Hill slopes east of Swansea Mine - approximately 250m	Quartzite beds with minor veining	So				128
				Sca			101
				Scb			65
						Vein	127
						Vein	28
MU96-81	Hill slopes east of Swansea Mine - approximately 250m	Quartzite beds with minor veining	So				106
					Fa		103
					Fas		108
					Fa		103
					Fas		128
					Fa		116
					Fas		141
MU96-82	Hill slopes ESE of Swansea Mine - approximately 280m	Quartzite beds with minor veining	So				129
				Sca			151
				Scb			54
MU96-83	Hill slopes ESE of Swansea Mine - approximately 280m	Quartzite beds with minor veining	So				132
MU96-84	Hill slopes ESE of Swansea Mine - approximately 280m	Quartzite beds with minor veining	So				152
				Sca			174
				Scb			59
				Scc			23
						Vein	162

MU96-85	Hill slopes east of Swansea Mine - approximately 270m	Quartzite beds with minor veining	So					141
MU96-86	Hill slopes east of Swansea Mine - approximately 270m	Quartzite beds with minor veining	So					138
MU96-87	Hill slopes east of Swansea Mine - approximately 270m	Quartzite beds with minor veining	So					96
MU96-88	Hill slopes east of Swansea Mine - approximately 270m	Quartzite beds with minor veining	So					118
MU96-89	Hill slopes east of Swansea Mine - approximately 270m	Quartzite beds with minor veining	So					82
MU96-90	Hill slopes east of Swansea Mine - approximately 270m	Quartzite beds with minor veining	So					98
MU96-91	Old workings (adit) in slopes along McClean Creek	Dolomite?dolomitisation?phyllites?						
MU96-92	Outcrop in McClean Creek below MU96-92	Dolomite? overlain by quartz alluvials. minor veining	So					163
MU96-93	Outcrop in McClean Creek SW of Swansea	Dolomite?						12
MU96-94	Along water race? to Swansea	Lt grey to brown phyllite	So					97
MU96-95	Outcrop along slope SW of zs31	Lt grey to brown phyllite/quartzite	So					23
MU96-96	Heading sth along ridge sth of zs31	Lt grey to brown phyllite/quartzite	So					80
MU96-97	Heading sth along ridge sth of zs31	Lt grey to brown phyllite/quartzite	So					66
			So					64
					Fa			287
					Fas			114
					Fa			230
					Fas			92
MU96-98	Heading sth along ridge sth of zs31	Lt grey to brown phyllite/quartzite	So					69
			So					54
			So					117
				Sca				99
				Scb				173
					Fa			68
					Fas			150
					Fa			302
					Fas			82
					Fa			55
					Fas			54
					Fa			30
					Fas			42
					Fa			73
					Fas			103
			So					73
MU96-99	Heading sth along ridge sth of zs31	Lt/dk grey shales with quartz veining <40mm, gen sub/bedding	So					86
MU96-100	Heading sth along ridge sth of zs31	Grey (weathered) to lt brown/fawn (fresh) phyllite/quartzite. Slight fizz	So					50
					Fa			342
					Fas			150
MU96-101	Heading sth along ridge sth of zs31	Grey (weathered) to lt brown/fawn (fresh) phyllite/quartzite. Slight fizz	So					114
				Sca				103
				Scb				34
MU96-102	Heading sth along ridge sth of zs31	Grey (weathered) to lt brown/fawn (fresh) phyllite/quartzite. Slight fizz	So					99
				Sca				104
				Scb				60
							Vein	123

364274

364275

MU96-103	Heading sth along ridge sth of zs31	Grey (weathered) to lt brown/fawn (fresh) phyllite/quartzite. Slight fizz	So				74
MU96-104	Heading sth along ridge sth of zs31	Grey (weathered) to lt brown/fawn (fresh) phyllite/quartzite. Slight fizz	So				89
			So				31
MU96-105	Heading sth along ridge sth of zs31	Grey (weathered) to lt brown/fawn (fresh) phyllite/quartzite. Slight fizz	So				65
			So				63
				Sca			113
				Scb			27
				Scc			179
MU96-106	Heading sth along ridge sth of zs31	Grey (weathered) to lt brown/fawn (fresh) phyllite/quartzite. Slight fizz	So				73
MU96-107	Adit workings at Swansea North	Grey/dk grey silts and shales	So				64
MU96-108	Track outcrop west of Swansea North (~20m)	Grey to black silts/shales - rots to dirty brown. Looks like sheared zone?	So				105
						Fracture	139
						Fracture	165
MU96-109	Track outcrop west of Swansea North (~20m)	Grey to black silts/shales - rots to dirty brown. Looks like sheared zone?	So				127
MU96-110	Track outcrop west of Swansea North (~20m)	Grey to black silts/shales - rots to dirty brown. Looks like sheared zone?	So				121
						Fracture	154
MU96-111	Track outcrop west of Swansea North (~20m)	Grey to black silts/shales - rots to dirty brown. Looks like sheared zone?	So				141
						Fracture	184
MU96-112	Track outcrop west of Swansea North (~200m)	Grey to black silts/shales - rots to dirty brown. Looks like sheared zone?	So				110
MU96-113	Track at Tasmanian	Lt grey sands within grey/dk grey shales	So				104
			So				76
			So				142
MU96-114	Track at Tasmanian	Dk grey shales	So				183
				Sc			150
MU96-115	Old workings at Tasmanian (next to shaft)	Grey to fawn phyllites	So				62
MU96-116	Track outcrop west of Tasmanian workings (~50m)	Black shales and minor sands	So				185
			So				182
				Sca			69
				Scb			124
					Fa		158
					Fas		141
MU96-117	Cutting 100m SE North Tasmanian workings	Cemented/conglomerate/sandstone? overlying silicified shale	So				99
						Joint	22
						Joint	57
MU96-118	North Tasmanian workings - shaft exposure	Dkbl grey shales/slate, very fractured, broken, crumbly	So				110
				Sca			148
				Scb			72
				Scc			15
MU96-119	TasNorth tasmanian workings - creek exposure	Dk grey shales and silts	So				88
MU96-120	Mounds rising from flat alluvial plains west of North Tasmanian	Mounds of cemented sandstone material, grey/white. Lower mounds of quartzite				Lineation	174
						Lineation	132
MU96-121	~200m NW of North Tasmanian	Grey shales weathering to grey/orange	So				98
				Sca			118
				Scb			103

				See			177
						Joint	29
						Joint	109
MU96-122	~350m NW of North Tasmanian	Grey shales weathering to grey/orange	So				91
MU96-123	~500 NW of North Tasmanian	Weathered shales to dk/lt orange, brown and pale green clay					
MU96-124	Track outcrop ~100m east of TLE	Black, brown, orange and grey clays - weathered shales? Quartz overlying	So				97
			So				186
			So				77
			So				69
MU96-125	Track outcrop north of TLE	Lt grey to brwon shales	So				143
MU96-126	Track outcrop north of TLE	Lt brown arenaceas shale	So				125
			So				62
MU96-127	Track outcrop NW of TLE	Brown to grey shales	So				170
			So				107
			So				68
					Fa		74
					Fas		85
			So				66
			So				16
			So				107
			So				132
			So				119
MU96-128	Track outcrop NW of TLE	Brown to grey shales	So				27
					Fa		250
					Fas		65
					Fa		101
					Fas		113
					Fa		88
					Fas		89
			So				149
MU96-129	Track outcrop NW of TLE	Brown to grey shales	So				105
			So				165
			So				110
					Fa		184
					Fas		182
			So				154
MU96-130	Track outcrop NW of TLE	Brown to grey shales - minor sands	So				63
MU96-131	Track outcrop NW of TLE	Brown to grey shales - minor sands					
					Fa		179
					Fas		167
					Fa		208
					Fas		37
			So				109
MU96-132	Track outcrop NW of TLE	Brown to grey shales - minor sands	So				33
MU96-133	Track outcrop NW of TLE	Brown to grey shales - minor sands	So				172
			So				86

364276

364277

					Fa		342
					Fas		153
					Fa		281
					Fas		156
					Fa		275
					Fas		133
MU96-134	Track outcrop NW of TLE	Brown to grey shales - minor sands	So				121
			So				146
					Fa		301
					Fas		131
					Fa		292
					Fas		104
MU96-135	Track junction 150m west of TLE	Weathered phyllites/sands/ shales. Conglomerate stuff? on road. Weathered shales in cutting					
MU96-136	Along track ~400m west of TLE	Orange/brown/yellow clays					
MU96-137	Along track ~600m west of TLE	Orange argillaceous rock - poss weathered siltstone. V. fine grained - orange to lt pink	So				109
			So				95
						Joint	27
						Joint	20
						Joint	164
MU96-138	Cutting along track towards Sth Comstock	Weathered black shales - argillaceous (to clays) with some rock. Silicified shales					
MU96-139	Cutting along track towards Sth Comstock	Black shales with large bands <50cm white weathered shales - v. hard. Local zones of veined silts and shales, and rotted brown clays/shales. Some fine quartz velning and faulting	So				107
						Fracture	192
						Fracture	103
						Vein	55
						Vein	110
			So				72
MU96-140	Cutting along track towards Sth Comstock	Black/dk grey shales weathering to white chalk-like outer					12
MU96-141	Cutting along track towards Sth Comstock	Slate/shale beds. Thin laminated shale beds with more massive silicified/dolomitised black shale or dolomite?	So				22
			So				191
					Fa		263
					Fas		99
MU96-142	Cutting along track towards Sth Comstock	Large beds of shale/dolomite?	So				63
MU96-143	Outcrop in small creek along gridline - near Silver Beach	Folded lt grey shales	So				109
			So				96
			So				79
			So				76
			So				103
				Sca			120
				Scb			76
				Scc			17
				Sca			142

					Scb				67
					Scc				32
						Fa			264
						Fas			79
						Fa			77
						Fas			103
						Fa			87
						Fas			98
MU96-144	~300m east of Colonel North	Grey quartzite containing pyrite and galena	So						42
MU96-145	Outcrop near track to the far east	Massive quartzite	So						185
					Sca				161
					Scb				43
					Scc				96
MU96-146	Outcrop along track to the far east	Slates and shales	So						130
MU96-147	Outcrop near track to the far east	Massive quartzite	So						20
					Sca				165
					Scb				192
					Scc				83
MU96-148	Outcrop along track to the far east	Grey to fawn coloured quartzites	So						171
MU96-149	Outcrop along track to the far east	Quartzite and shales	So						184
MU96-150	Outcrop along track to the far east	Thin quartzites	So						29
MU96-151	Outcrop along track to the far east	Thin shales and phyllites	So						*164*
			So						191
					Sc				180
					Sc				*140*
					Sca				131
MU96-152	Near Nubeena	Grey, v hard quartzite bands of silificidied black shale	So						175
			So						*149*
						Fa			153
						Fas			188
MU96-153	West along track at car turn around	Grey graphitic looking shales - thin laminae	So						37
MU96-154	West along track at car turn around	Grey shale	So						140
MU96-155	West along track at car turn around	Grey shale	So						51
MU96-156	West along track at car turn around	Grey shale	So						136
MU96-157	West along track at car turn around	Grey shale	So						132
			So						165
			So						25
								Fault	105
						Fa			120
						Fas			124
						Fa			120
						Fas			112
						Fa			112
						Fas			110
						Fa			110

364278

364279

					Fas		107
					Fa		357
					Fas		196
					Fa		342
					Fas		186
MU96-158	West along track at car turn around	Grey shale with minor sands	So				172
						Fracture	90
MU96-159	~200m SW Colonel North	Phyllites	So				38
MU96-160	~400m Sw Colonel North - near creek	Possible dolomitised limestone?					12
MU96-161	Outcrop in small creek ~400 west of Nubeena	Dk grey shale/dolomite?					12
MU96-162	Outcrop in creek ~300 NE Grubbs	Heavily cleaved phyllites with pyrite vein	So				39
						Fault	168
MU96-163	Grubb's workings						12
MU96-164	Outcrop at track cutting creek ~300m sth car turn around		So				177
				S1			152
MU96-165	Cutting ~100m east of TH17			S1			180
				S3			185
MU96-166	Cutting ~200m ESE TH17 - along track		So				79
MU96-167	Track junction SE of Victoria Zeehan	Massive quartzite/phyllite	So				171
				S1			88
			So				18
				S1			154
			So				58
				S1			177
				L3/F3			136
MU96-168	Track junction SE of Victoria Zeehan	Massive quartzite/phyllite	So				56
				S1			113
				L2/F2			125
					F1		152
MU96-169	~200m SE along track from junction	Massive quartzite/phyllite			F1a		115
MU96-170	North of Lewellan's Lode	Massive quartzite/phyllite	So				93
				S2			116
MU96-171	NE of Newallen's Lode	Massive quartzite/phyllite	So				93
				S1			130
MU96-172	~200m SW of Nebeena	Massive quartzite/phyllite	So				83
				S1			57
MU96-173	Along spur ~400m south of Nebeena	Massive quartzite/phyllite			F2/L2		92
MU96-174	Along spur ~800m south of Nebeena	Massive quartzite/phyllite	So				107
				S1			125
MU96-175	~ 150m north Grubb's	Massive quartzite/phyllite	So				76
				S1			95
MU96-176	~150m NW Grubb's	Massive quartzite/phyllite			F2a		249
MU96-177	Along ridge ~500m west Grubb's	Massive quartzite/phyllite	So				93
				S1			102
MU96-178	Along ridge ~500m west Grubb's	Massive quartzite/phyllite	So				67

MU96-179	~500m SW Colonel North	Massive quartzite/phyllite	So				43
				Sl			56
MU96-180	~150m SW Colonel North	Massive quartzite/phyllite	So				53
MU96-181	~50m SW Colonel North		So				79
				Sl			45
						Lint	65
				L3/F3			320
MU96-182	~50m SW Colonel North		So				62
						Lint	51
MU96-183	Track junction to the far east	Quartite/phyllite	So				191
			So				31
			So				62
					Fla		51
					Flas		80
					Fla		35
					Flas		71
					Fa		116
					Fas		77
					Fa		148
					Fas		98
						Fault	68
						Vein	157
			So				30
			So				78
						Vein	36
						Vein	162
MU96-184	Track junction to the far east	Quartite/phyllite	So				89
						Joint	162
MU96-185	~50m west of track junction to the far east	Quartite/phyllite	So				110
			So				87
			So				85
					Fa		93
					Fas		87
						Vein	190
MU96-186	Along ridge ~100m west track junction to the far east	Quartite/phyllite	So				91
MU96-187	Along ridge ~100m west track junction to the far east	Quartite/phyllite	So				129
MU96-188	Along ridge ~100m west track junction to the far east	Quartite/phyllite	So				144
			So				124
			So				143
MU96-189	Along ridge ~100m west track junction to the far east	Quartite/phyllite	So				136
MU96-190	Along ridge ~100m west track junction to the far east	Quartite/phyllite	So				125
MU96-191	Along ridge ~100m west track junction to the far east	Quartite/phyllite	So				107
				Sc			73
MU96-192	North along track towards Spray	Massive phyllite beds thinning and shale increasing to the north	So				107
MU96-193	North along track towards Spray	Grey phyllites	So				84

36280

364281

MU96-194	North along track towards Spray	Grey phyllites	So			102
			So			100
			So			127
			So			120
					Fa	104
					Fas	105
					Fa	236
					Fas	124
MU96-195	North along track towards Spray	Some cemented conglomerate material? - quartz fragments within phyllites	So			150
			So			103
					Fa	321
					Fas	312
MU96-196	West of track towards Spray - start of creek, possible old adit	Siltstones/weathered phyllites with quartz veining generally sub\\ to So	So			105
MU96-197	Spray shaft	Meta black shales with large folding	So			23
					Fa	207
					Fas	181
MU96-198	Spray shaft and adit running N-S	Metasediment shales with large regional folding	So			13
			So			141
			So			94
			So			132
			So			91
			So			66
					Fa	105
					Fas	104
					Fa	215
					Fas	44
MU96-199	Spray shaft and adit running N-S	Metasediment shales with large regional folding	So			114
MU96-200	Along track to east of Spray	Grey/dk grey fine grained phyllites with thin shale interbeds	So			131
MU96-201	Along track to east of Spray	Grey/dk grey fine grained phyllites with thin shale interbeds	So			99
			So			131
					Fa	137
					Fas	133
MU96-202	5000N 12500E	Lt grey/dk grey phyllite with quartz veining	So			35
				Sca		53
				Scb		158
				Scc		86
MU96-203	~400m north of Colonel North	Phyllites	So			41
				Sc		33
MU96-204	Folded outcrop in old adit ~500m east of Colonel North.	Grey to dk grey phyllites	So			23
			So			181
MU96-205	Adit at Nubeena dug at 136 deg	Grey phyllite	So			174
				Sm//So		
				Sca		146
				Scb		17

				Scc				92
MU96-206	~200m SW of Nubeena	Grey phyllite	So					63
			So					184
				Sca				52
				Scb				107
				Scc				182
				Sca				119
				Scb				42
				Scc				136
MU96-207	Outcrop in creek ~400m SW Nubeena	Grey phyllites and black shales	So					53
MU96-208	Ridge ~400m east of grubb's	Massive quartzite/phyllite	So					192
MU96-209	Ridge ~400m east of grubb's	Massive quartzite/phyllite	So					101
				Sc				82
MU96-210	Ridge ~400m east of grubb's	Massive quartzite/phyllite	So					103
				Sc				77
MU96-211	South along spur/ridge south Nubeena	Massive quartzite/phyllite	So					126
MU96-212	South along spur/ridge south Nubeena	Massive quartzite/phyllite	So					103
								77
MU96-213	South along spur/ridge south Nubeena	Massive quartzite/phyllite	So					57
					Fa			179
					Fas			133
					Fa			98
					Fas			95
					Fa			83
					Fas			80
						Vein		151
						Vein		82
MU96-214	South along spur/ridge south Nubeena	Massive quartzite/phyllite	So					96
			So					108
					Fa			41
					Fas			33
					Fa			86
					Fas			105
MU96-215	South along spur/ridge south Nubeena	Massive quartzite/phyllite	So					143
MU96-216	South along spur/ridge south Nubeena	Massive quartzite/phyllite	So					98
				Sc				87
MU96-217	South along spur/ridge south Nubeena	Massive quartzite/phyllite	So					47
				Sca				63
				Scb				117
MU96-218	South along spur/ridge south Nubeena		So					173
					Fa			80
					Fas			53
MU96-219	Grey/green siltstones - looks v sheared zone		So					140
MU96-220			So					102
MU96-221			So					132

364282

364283

MU96-222	So	182
MU96-223	So	98
MU96-224	So	125
MU96-225	So	83
MU96-226	So	11
	So	3
MU96-227	So	90
MU96-228	So	44
MU96-229	So	154
MU96-230	So	8
MU96-231	So	30
		64
MU96-232	So	10
MU96-233	So	21
MU96-234	So	151
MU96-235	So	15
MU96-236	So	63
MU96-237	So	12
MU96-238	So	34
MU96-239	So	160
MU96-240	So	1
MU96-241	So	50
MU96-242	So	13
MU96-243	So	42
MU96-244	So	125
MU96-245	So	22
MU96-246	So	123
MU96-247	So	163
MU96-248	So	129
MU96-249	So	23
MU96-250	So	161
MU96-251	So	66
MU96-252	So	20
	So	169
MU96-253	So	33
MU96-254	So	113
MU96-255	So	47
	So	88
MU96-256	So	158
MU96-257	So	156
	So	146
MU96-258	So	121
MU96-259	So	180
MU96-260	So	148
MU96-261	So	154

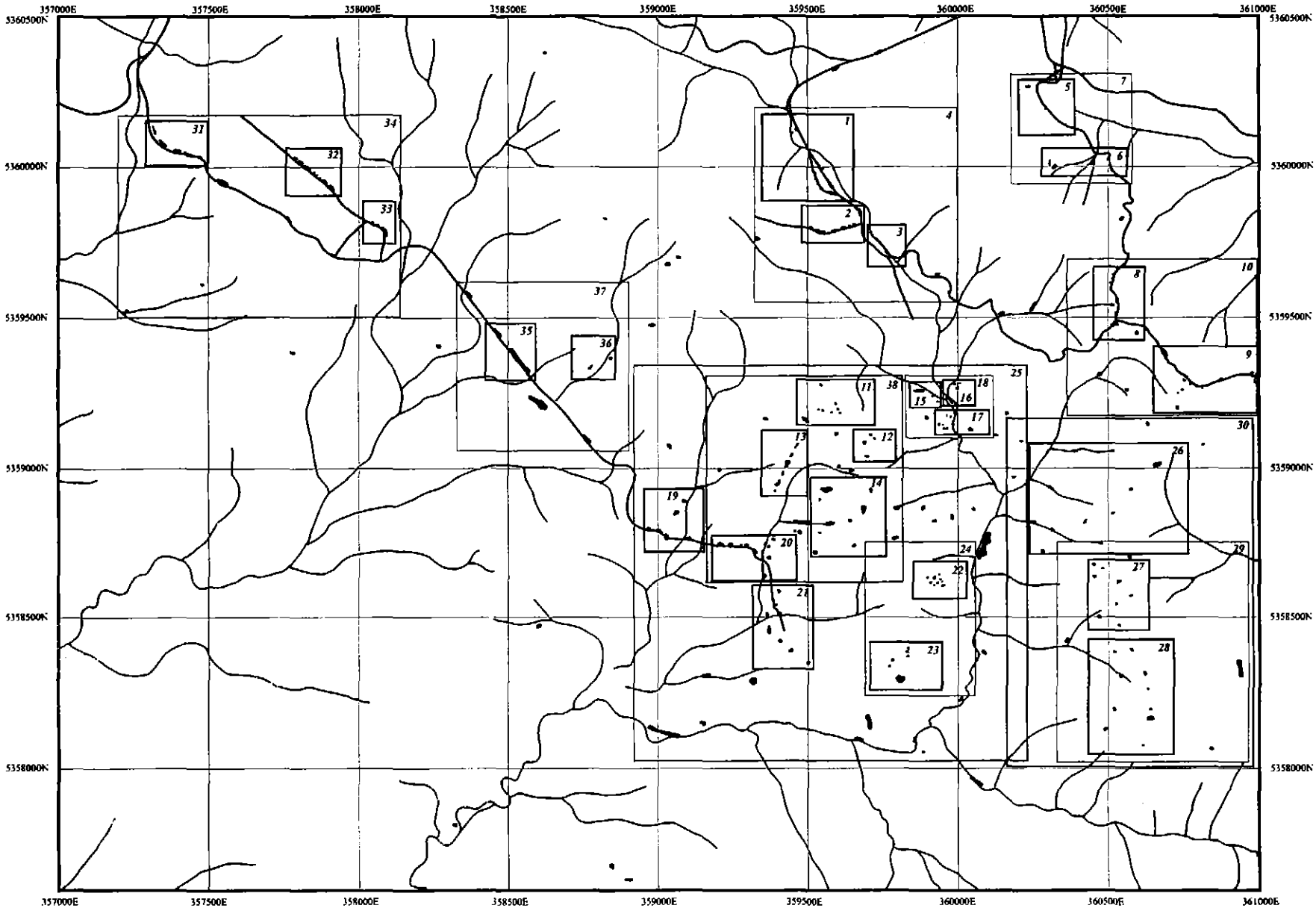
MU96-262	So	157
	So	20
	So	179
MU96-263	So	179
MU96-264	So	34
MU96-265	So	161
MU96-266	So	22
MU96-267	So	136
MU96-268	So	137
MU96-269	So	7
MU96-270	So	174
MU96-271	So	178
MU96-272		

3642841

APPENDIX 2.

Stereonet plots

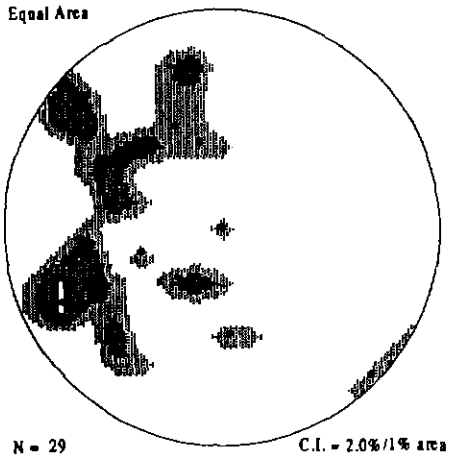
STONEHENGE STEREONET DOMAIN LOCATIONS



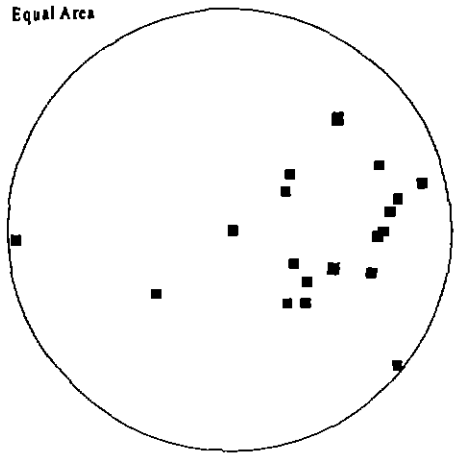
3642286

STONEHENGE DOMAIN 1 STEREONET DATA

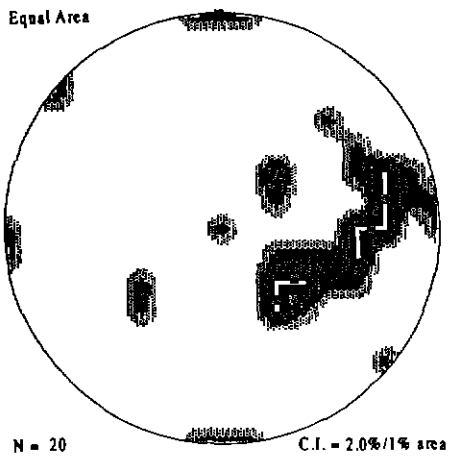
Bedding poles



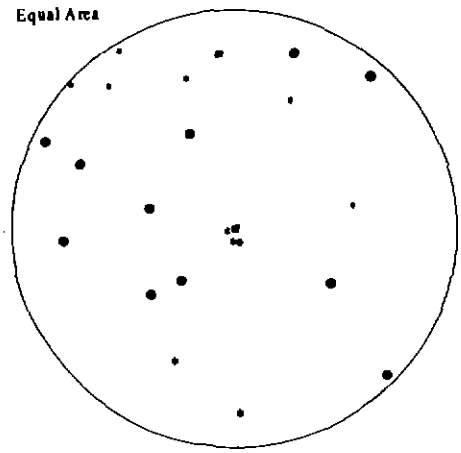
Determined and measured fold axis



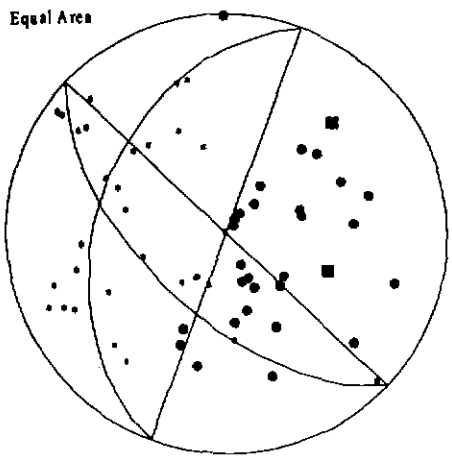
Contoured determined and measured fold axis



Cleavage 1,2 and 3 poles



Determined fold axis

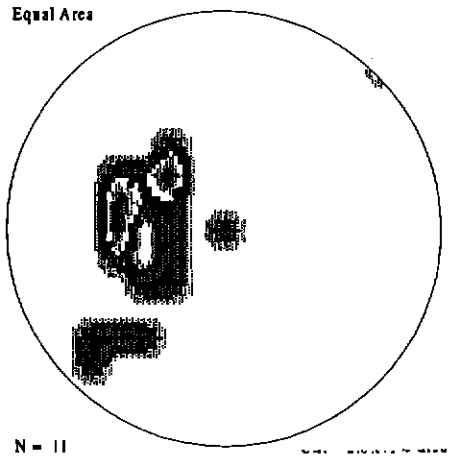


Great circle: 201/41W
Pole to great circle: 111/49

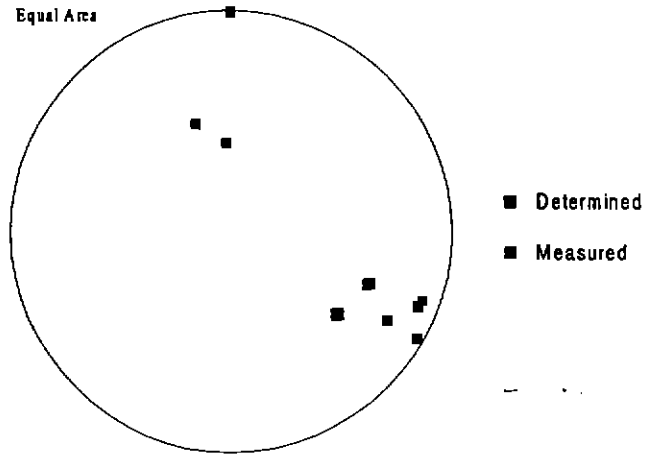
Great circle: 134/60S
Pole to great circle: 44/30

STONEHENGE DOMAIN 2 STEREONET DATA

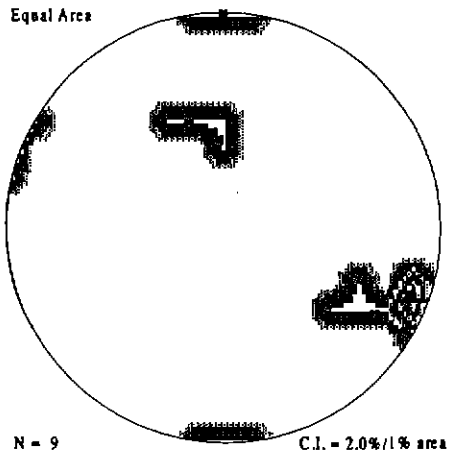
Bedding poles



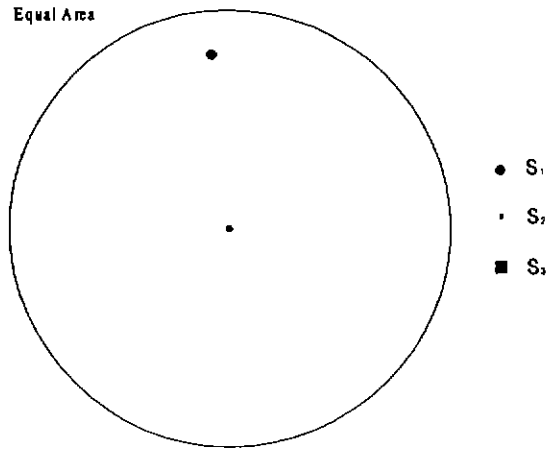
Determined and measured fold axis



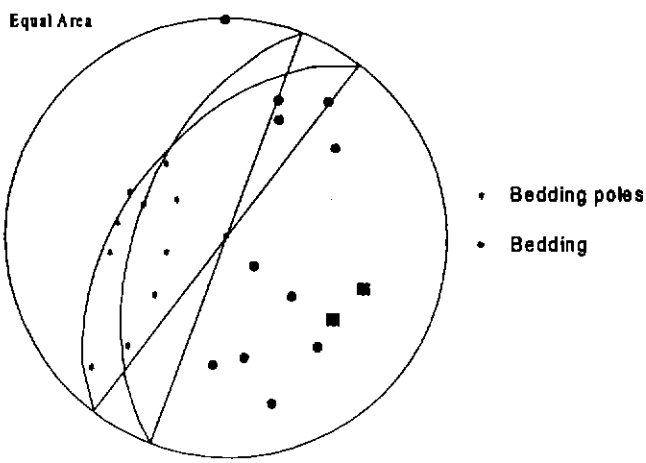
Contoured determined and measured fold axis



Cleavage 1,2 and 3 poles



Determined fold axis

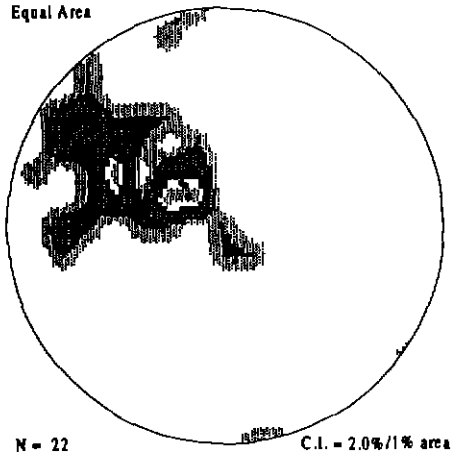


Great circle: 218/51W
Pole to great circle: 128/39

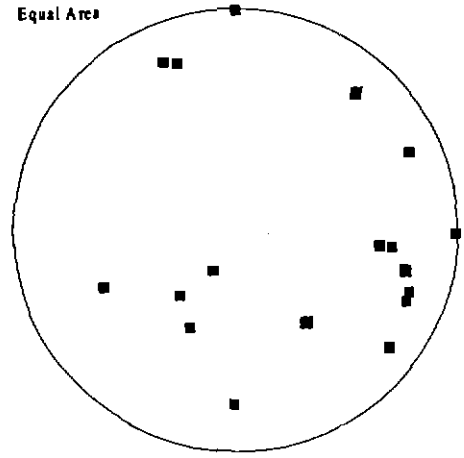
Great circle: 201/56W
Pole to great circle: 111/34

STONEHENGE DOMAIN 3 STEREONET DATA

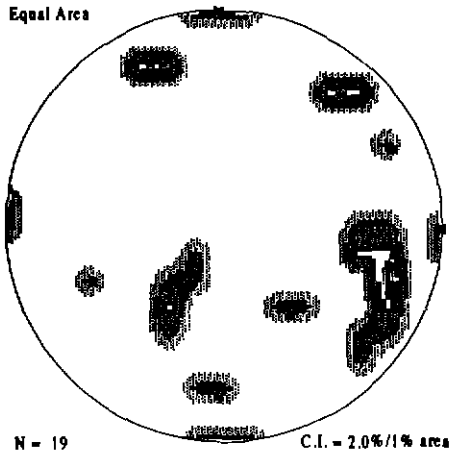
Bedding poles



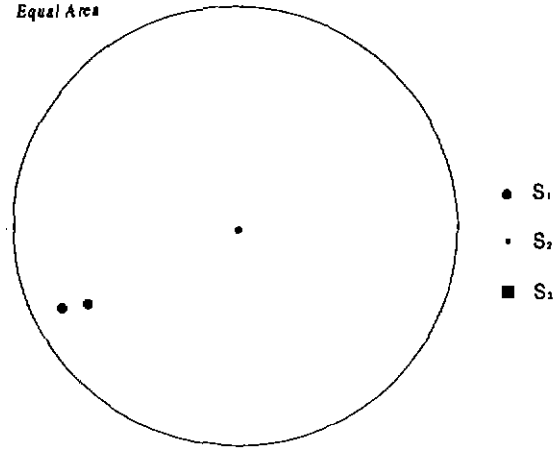
Determined and measured fold axis



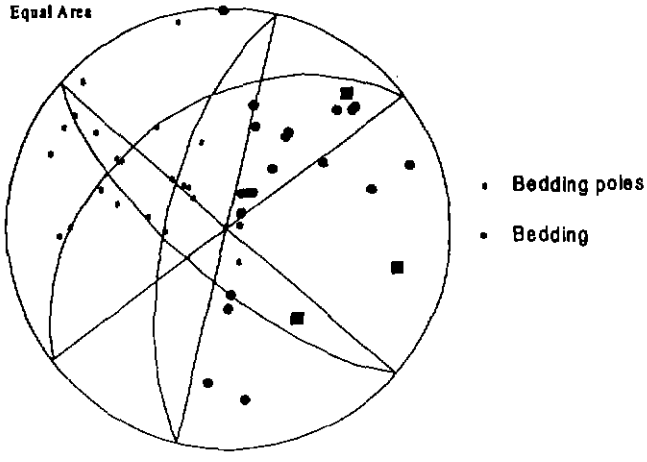
Contoured determined and measured fold axis



Cleavage 1,2 and 3 poles



Determined fold axis



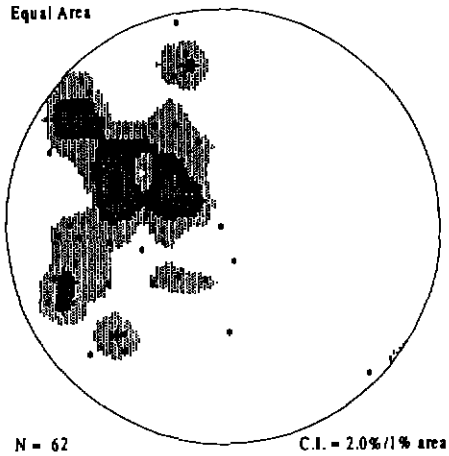
Great circle: 233/43N
Pole to great circle: 143/47

Great circle: 194/68W
Pole to great circle: 104/22

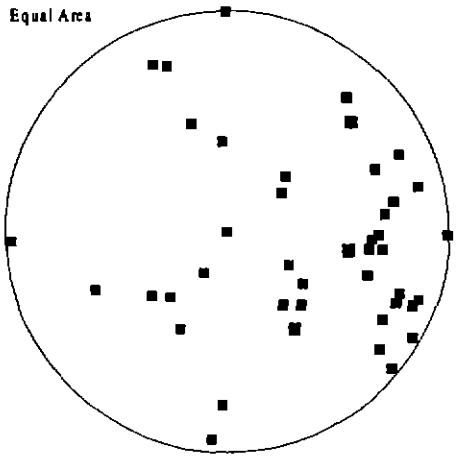
Great circle: 132/72S
Pole to great circle: 42/18

STONEHENGE DOMAIN 4 STEREONET DATA

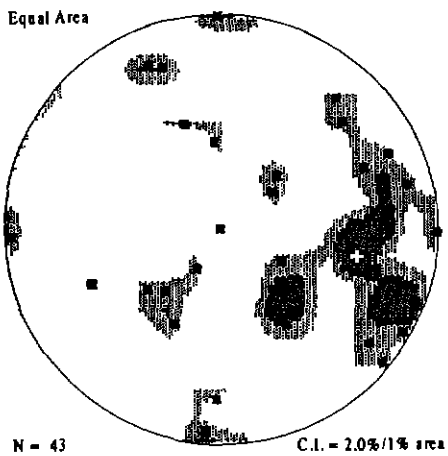
Bedding poles

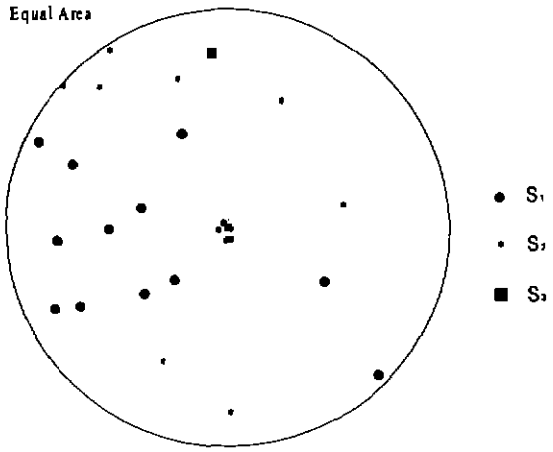


Determined and measured fold axis

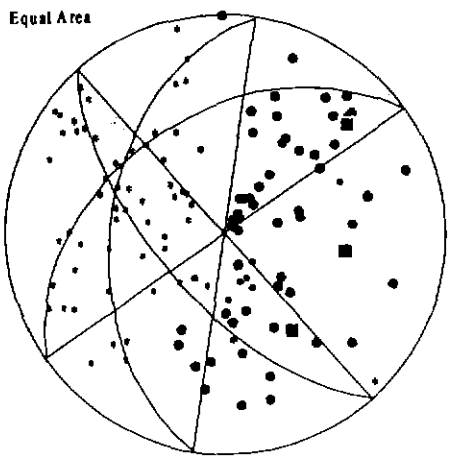


Contoured determined and measured fold axis





Determined fold axis



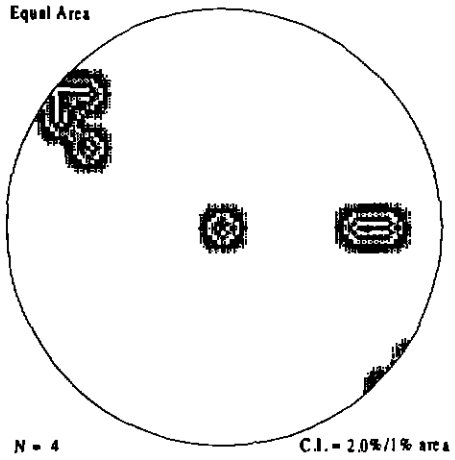
Great circle: 235/45N
Pole to great circle: 145/45

Great circle: 139/65W
Pole to great circle: 49/25

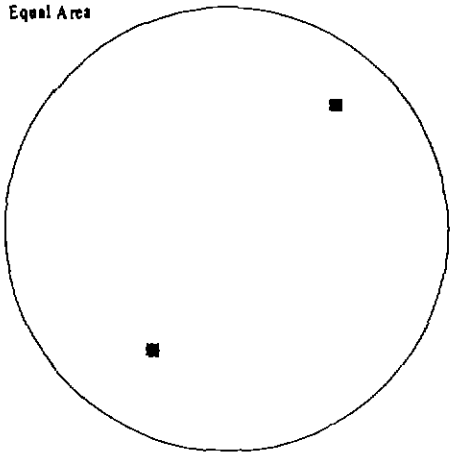
Great circle: 189/46W
Pole to great circle: 99/44

STONEHENGE DOMAIN 5 STEREONET DATA

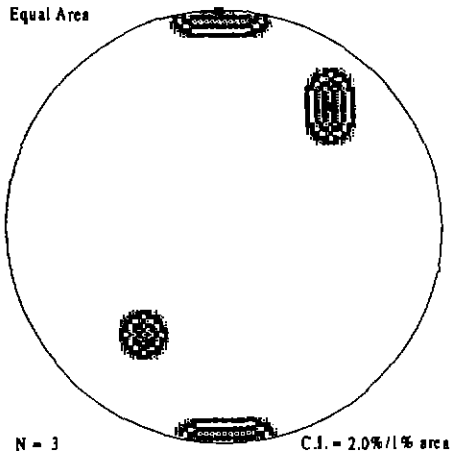
Bedding poles



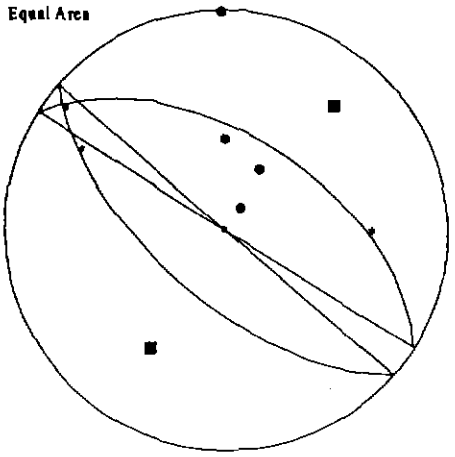
Determined and measured fold axis



Contoured determined and measured fold axis



Determined fold axis

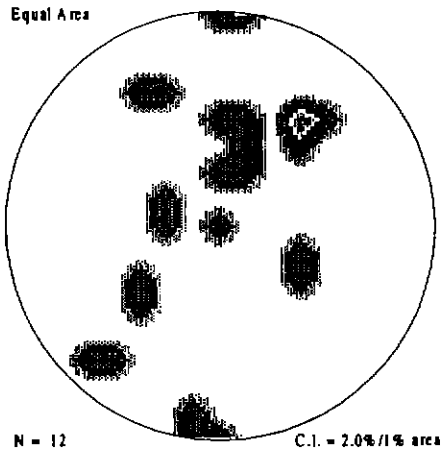


Great circle: 132/64
Pole to great circle: 42/26

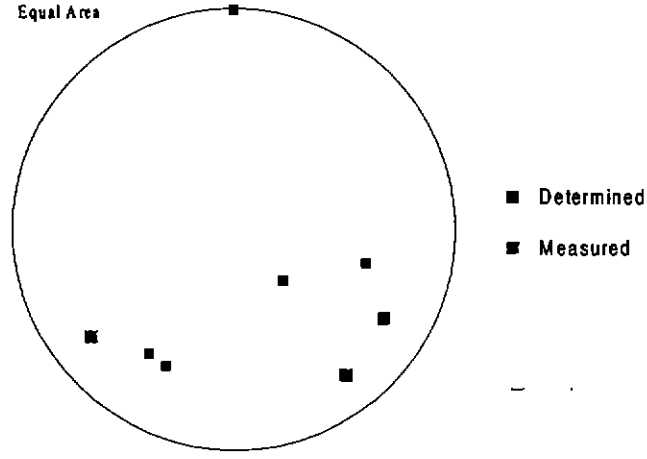
Great circle: 303/54
Pole to great circle: 213/36

STONEHENGE DOMAIN 6 STEREONET DATA

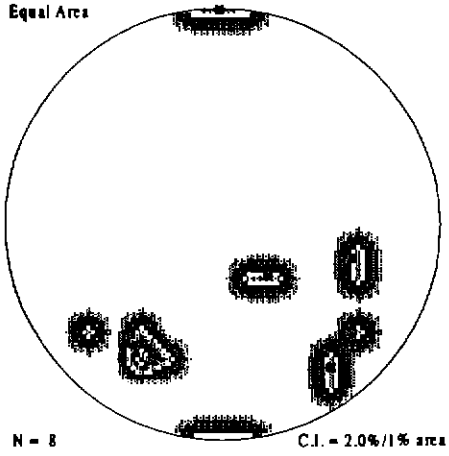
Bedding poles



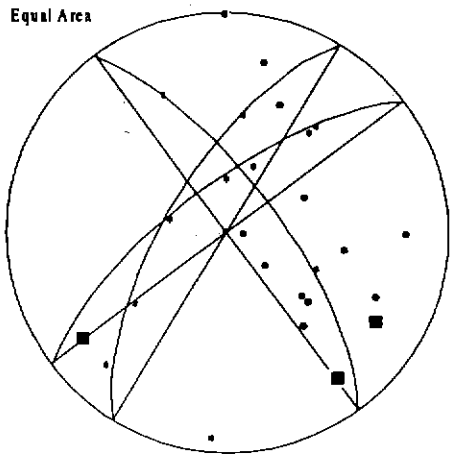
Determined and measured fold axis



Contoured determined and measured fold axis



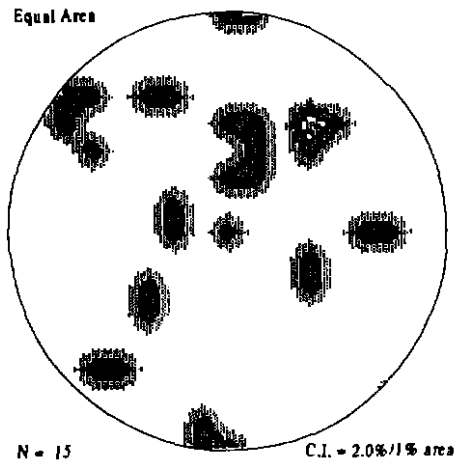
Determined fold axis



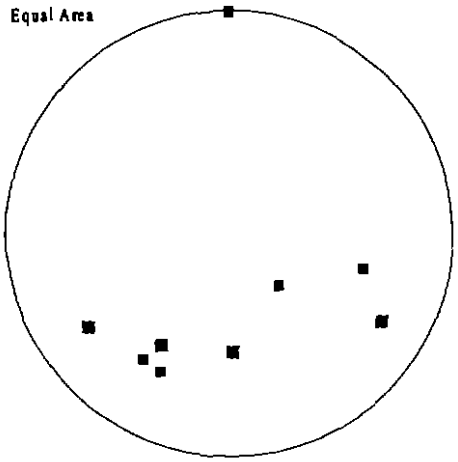
Great circle:	324/71E
Pole to great circle:	234/19
Great circle:	211/68W
Pole to great circle:	121/22
Great circle:	233/72N
Pole to great circle:	143/18

STONEHENGE DOMAIN 7 STEREONET DATA

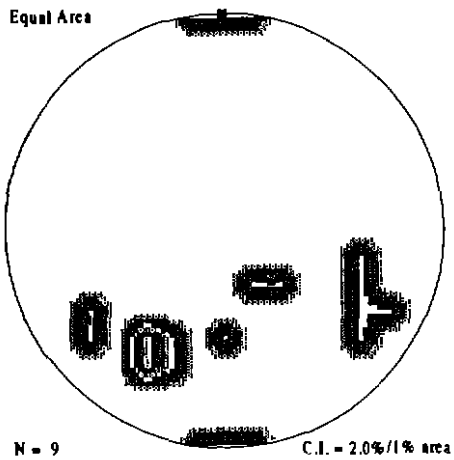
Bedding poles



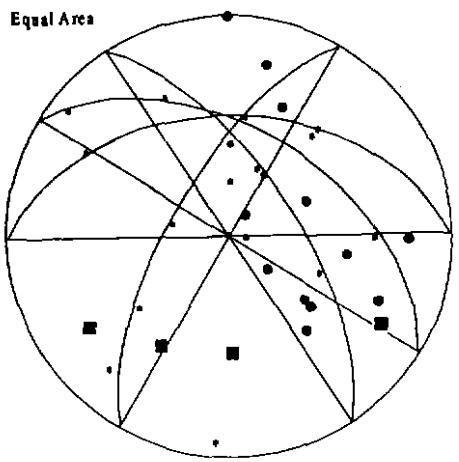
Determined and measured fold axis



Contoured determined and measured fold axis



Determined fold axis

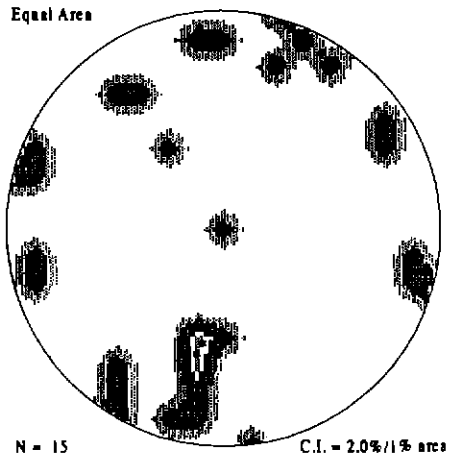


Great circle:	302/49N
Pole to great circle:	212/41
Great circle:	211/68W
Pole to great circle:	121/22
Great circle:	269/44N
Pole to great circle:	179/46
Great circle:	327/65E
Pole to great circle:	237/25

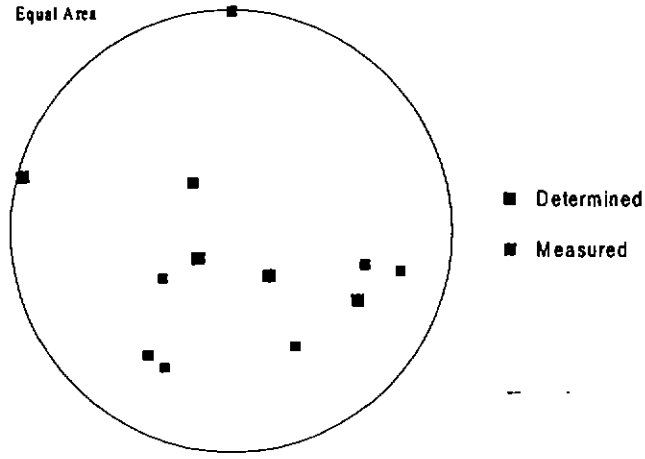
364294

STONEHENGE DOMAIN 8 STEREONET DATA

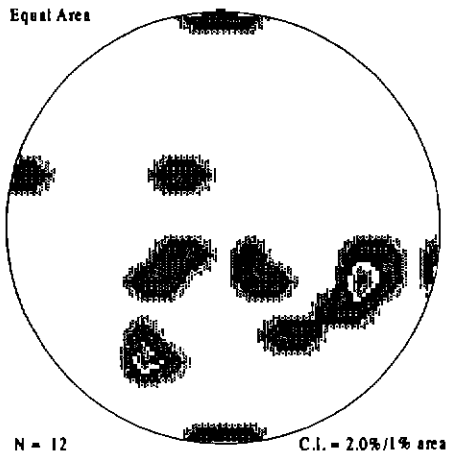
Bedding poles



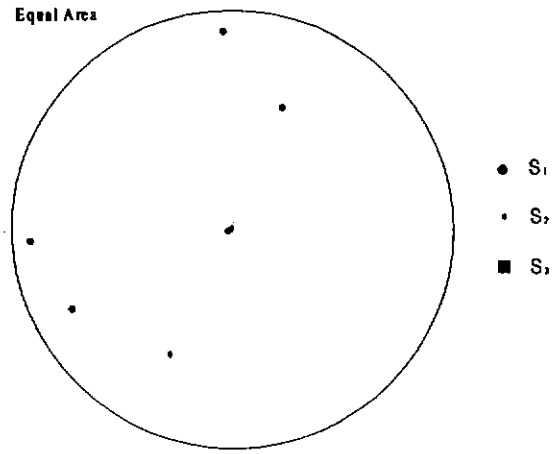
Determined and measured fold axis



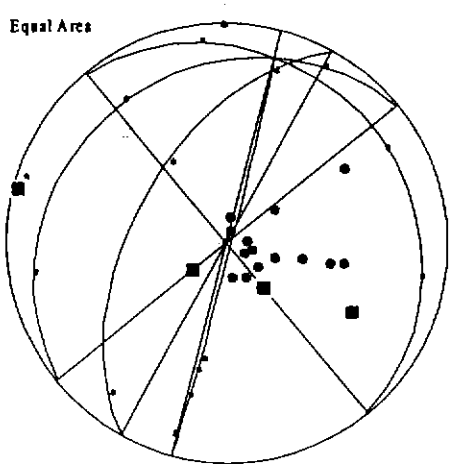
Contoured determined and measured fold axis



Cleavage 1,2 and 3 poles



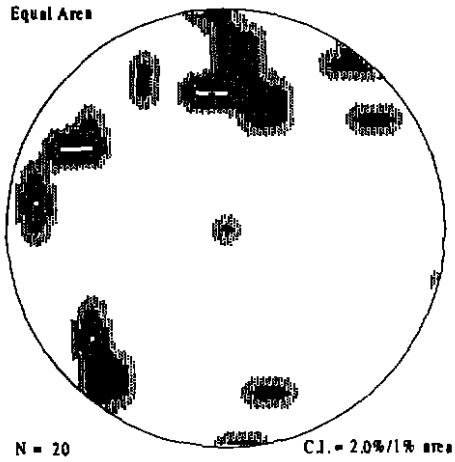
Determined fold axis



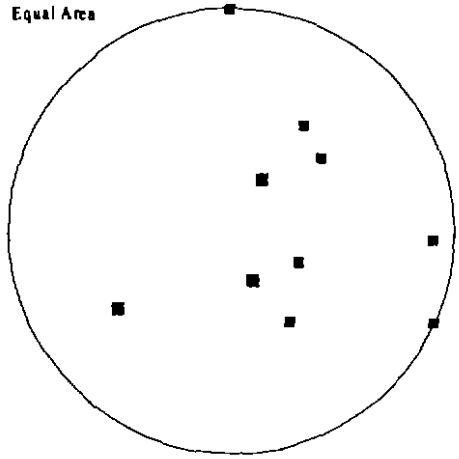
Great circle:	321/16E
Pole to great circle:	231/74
Great circle:	231/22N
Pole to great circle:	141/68
Great circle:	209/55W
Pole to great circle:	119/35
Great circle:	15/88E
Pole to great circle:	285/2

STONEHENGE DOMAIN 9 STEREONET DATA

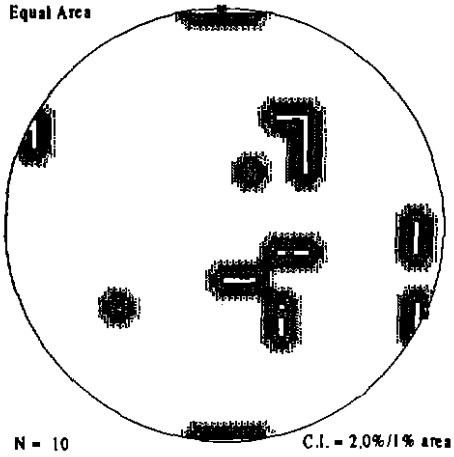
Bedding poles



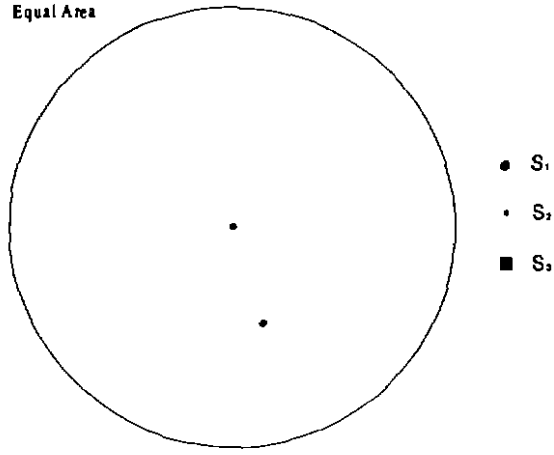
Determined and measured fold axis



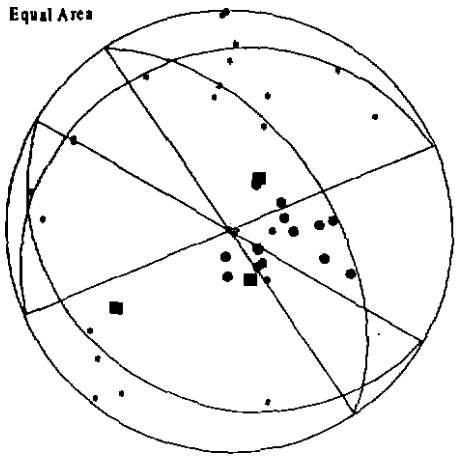
Contoured determined and measured fold axis



Cleavage 1,2 and 3 poles



Determined fold axis



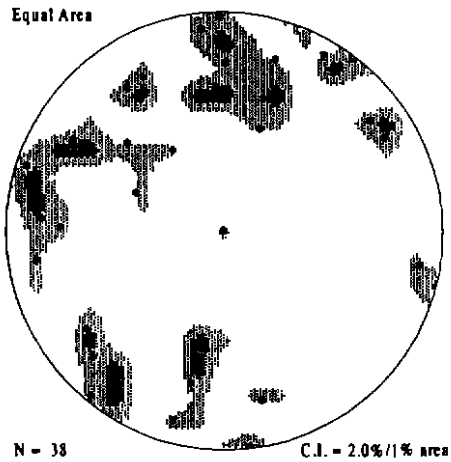
Great circle: 120/22S
Pole to great circle: 30/68

Great circle: 248/20N
Pole to great circle: 158/70

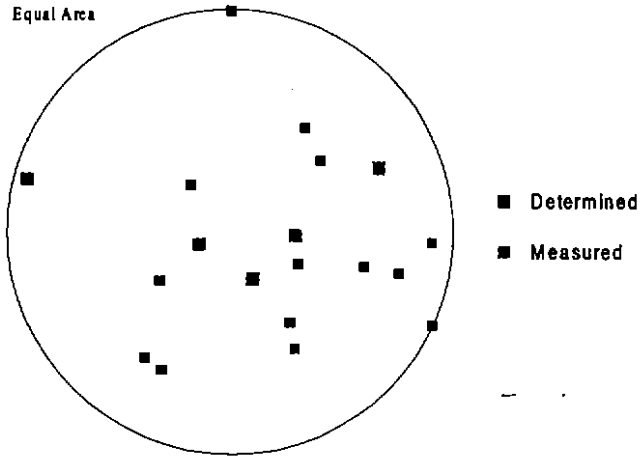
Great circle: 326/53E
Pole to great circle: 236/37

STONEHENGE DOMAIN 10 STEREONET DATA

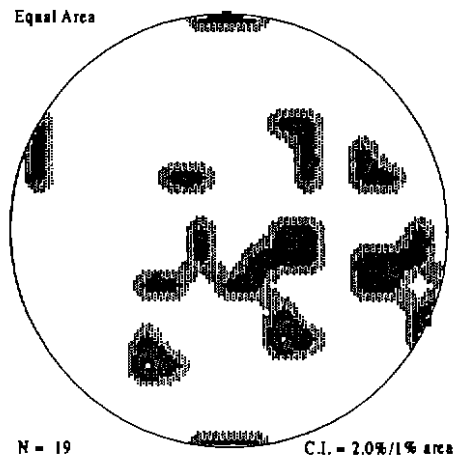
Bedding poles



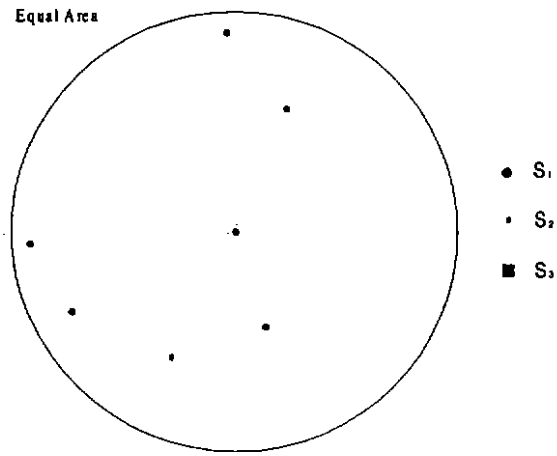
Determined and measured fold axis



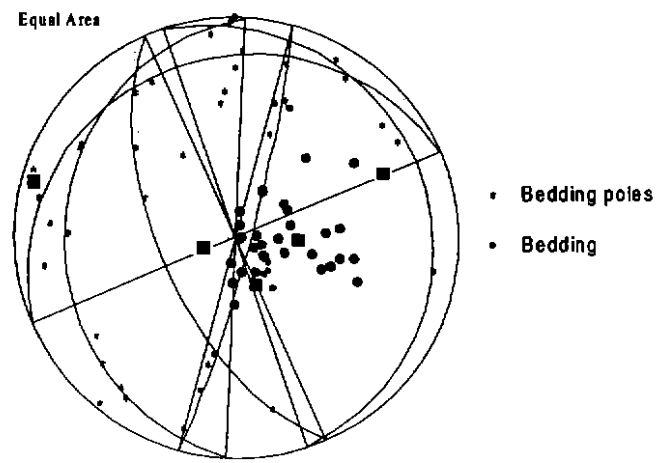
Contoured determined and measured fold axis



Cleavage 1,2 and 3 poles



Determined fold axis



Great circle: 247/19N
Pole to great circle: 157/71

Great circle: 183/23W
Pole to great circle: 93/67

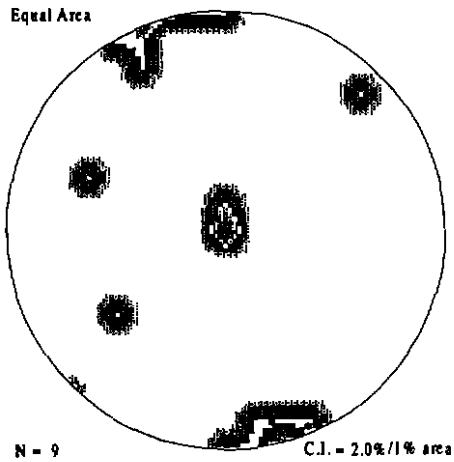
Great circle: 342/12E
Pole to great circle: 252/78

Great circle: 15/84E
Pole to great circle: 285/6

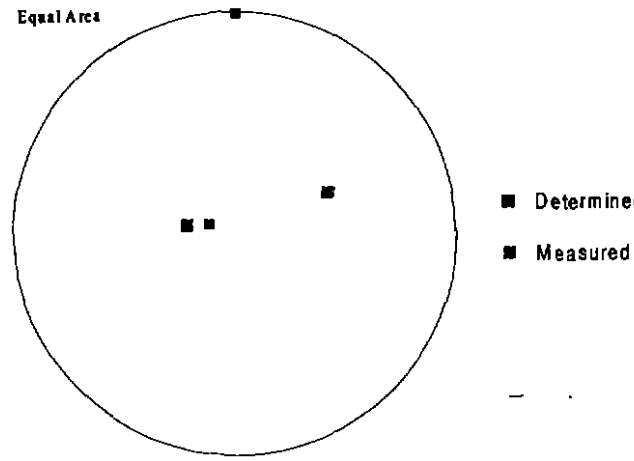
Great circle: 156/62W
Pole to great circle: 66/28

STONEHENGE DOMAIN 11 STEREONET DATA

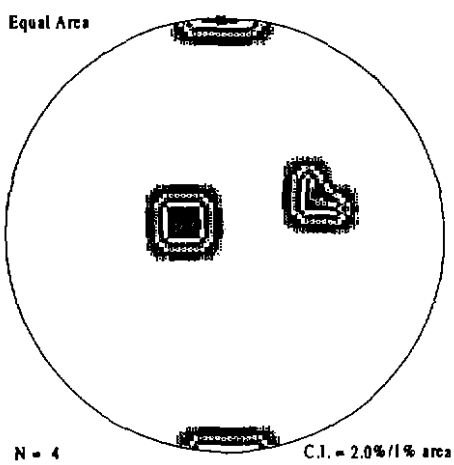
Bedding poles



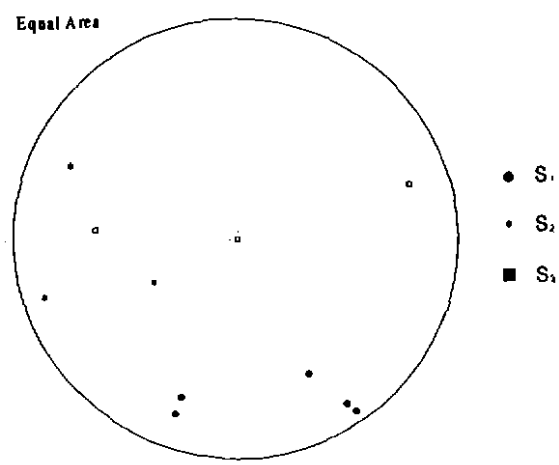
Determined and measured fold axis



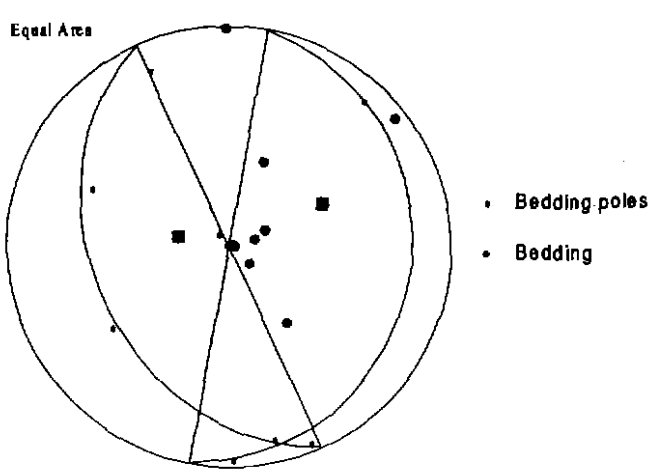
Contoured determined and measured fold axis



Cleavage 1,2 and 3 poles



Determined fold axis

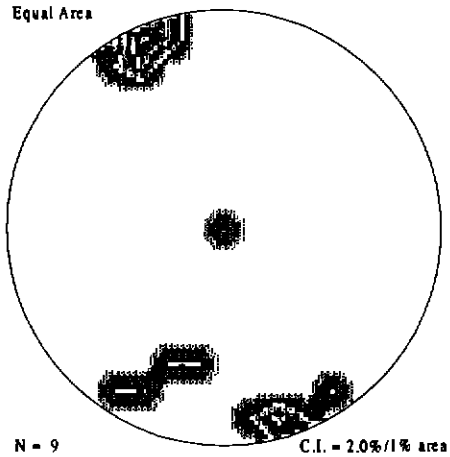


Great circle: 11/18E
Pole to great circle: 281/72

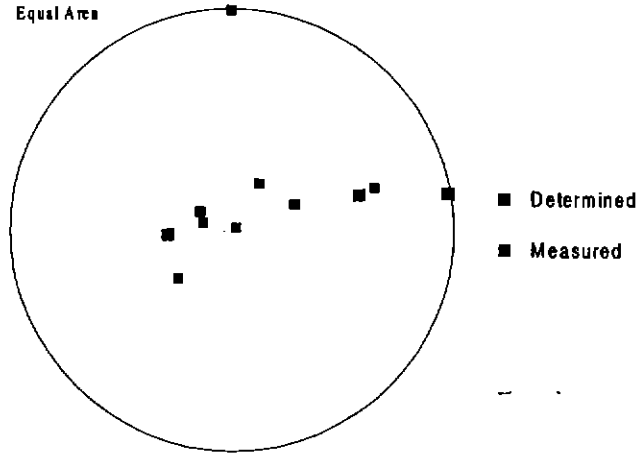
Great circle: 156/38W
Pole to great circle: 66/52

STONEHENGE DOMAIN 12 STEREONET DATA

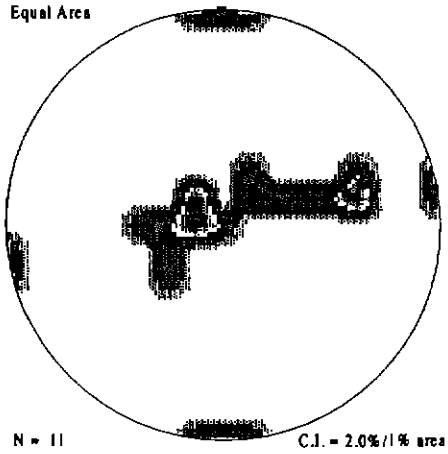
Bedding poles



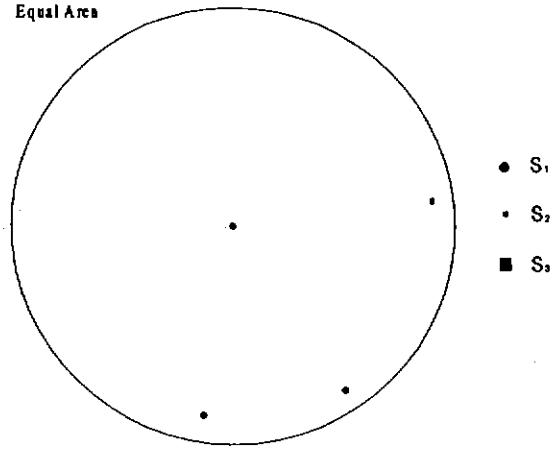
Determined and measured fold axis



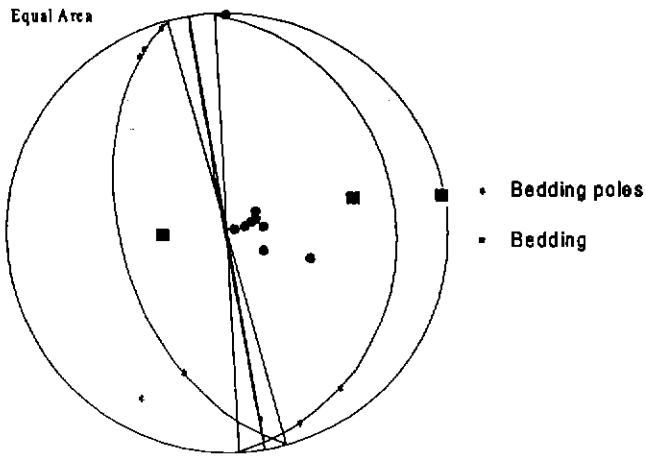
Contoured determined and measured fold axis



Cleavage 1,2 and 3 poles



Determined fold axis



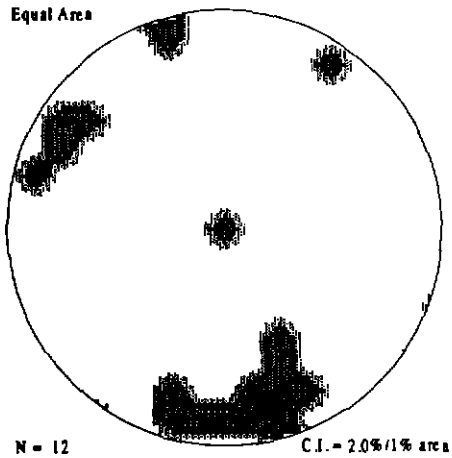
Great circle: 165/50W
Pole to great circle: 75/40

Great circle: 357/24E
Pole to great circle: 267/66

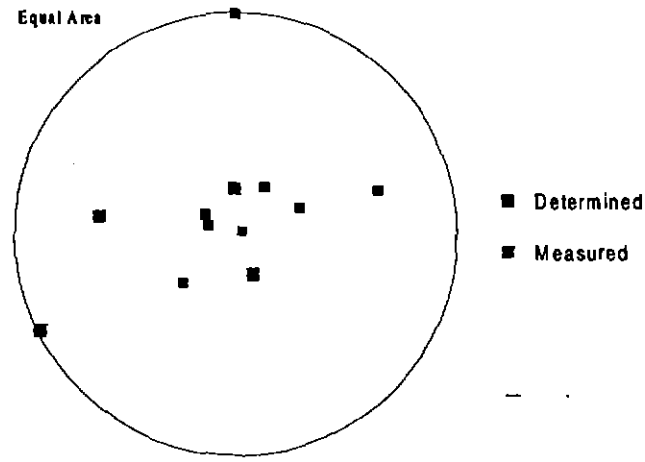
Great circle: 170/89W
Pole to great circle: 80/1

STONEHENGE DOMAIN 13 STEREONET DATA

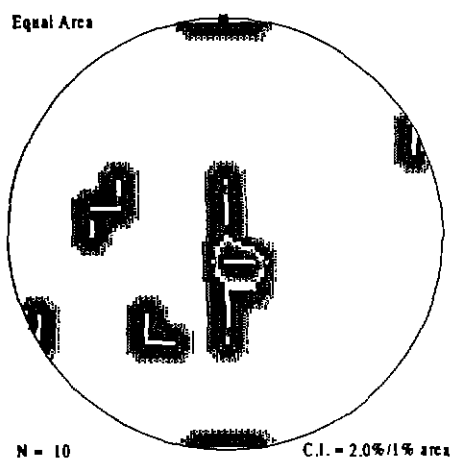
Bedding poles



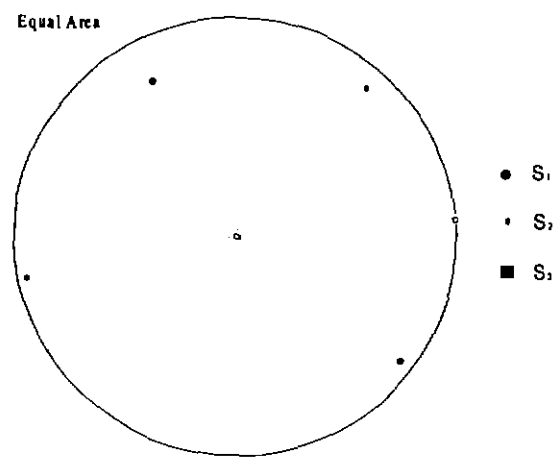
Determined and measured fold axis



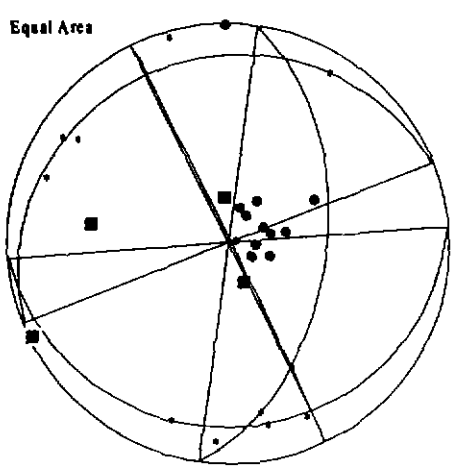
Contoured determined and measured fold axis



Cleavage 1,2 and 3 poles



Determined fold axis



Great circle: 249/16N
Pole to great circle: 159/74

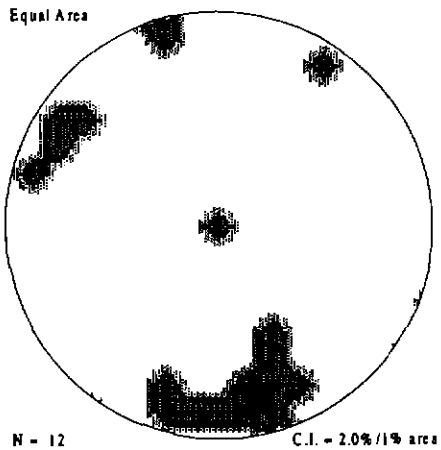
Great circle: 8/53E
Pole to great circle: 278/37

Great circle: 86/17S
Pole to great circle: 356/73

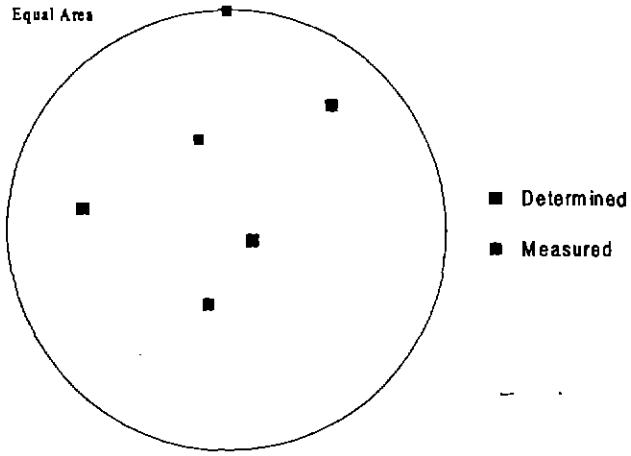
Great circle: 335/89E
Pole to great circle: 245/1

STONEHENGE DOMAIN 14 STEREONET DATA

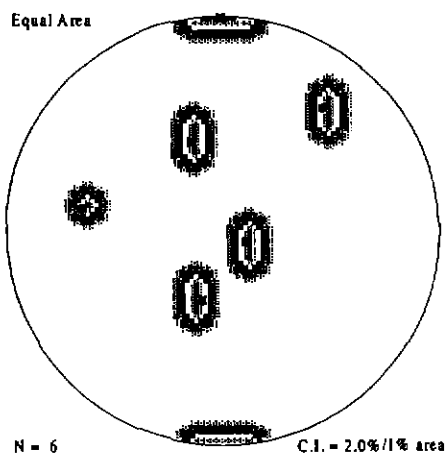
Bedding poles



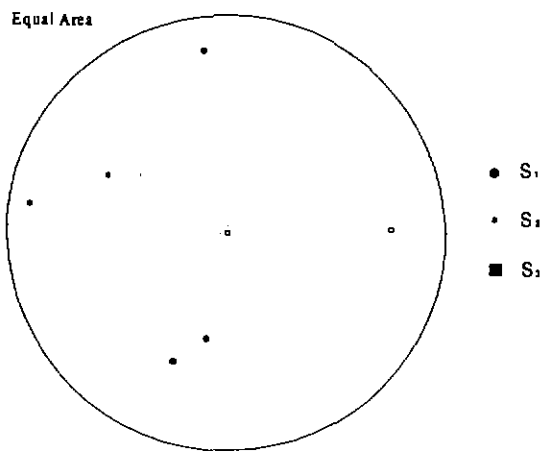
Determined and measured fold axis

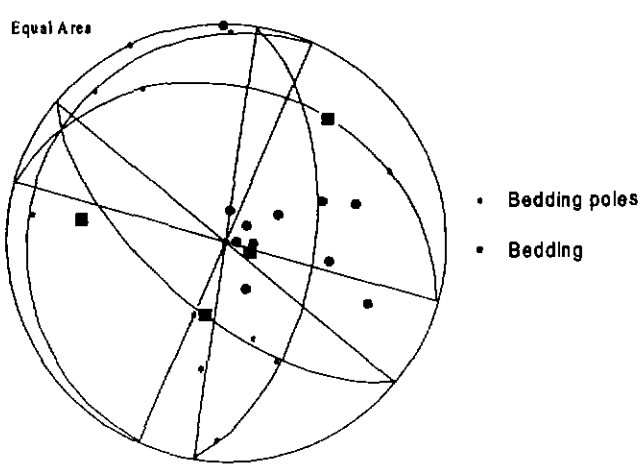


Contoured determined and measured fold axis



Cleavage 1,2 and 3 poles





Great circle: 204/10W
Pole to great circle: 114/80

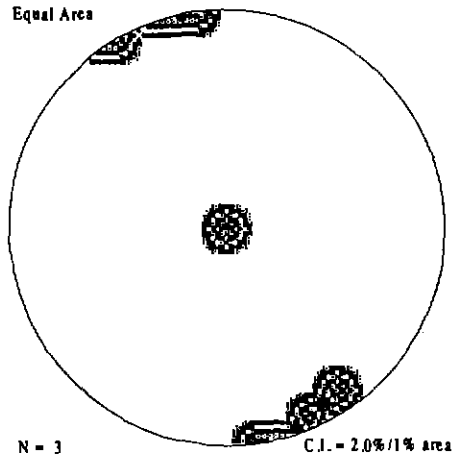
Great circle: 286/28N
Pole to great circle: 196/62

Great circle: 9/56E
Pole to great circle: 279/34

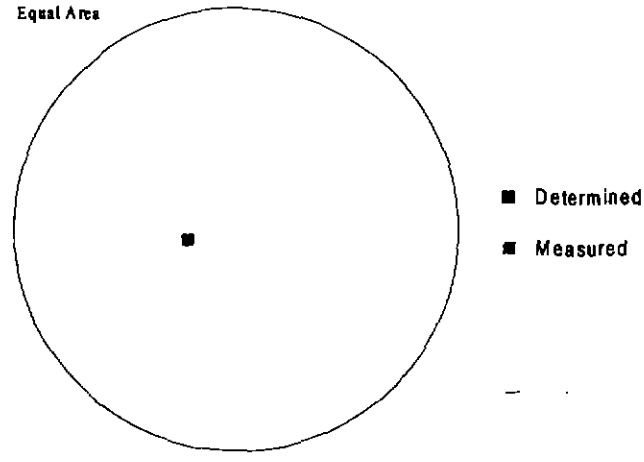
Great circle: 130/64S
Pole to great circle: 40/26

STONEHENGE DOMAIN 15 STEREONET DATA

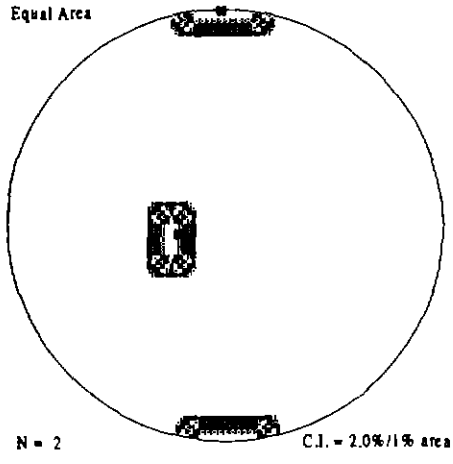
Bedding poles



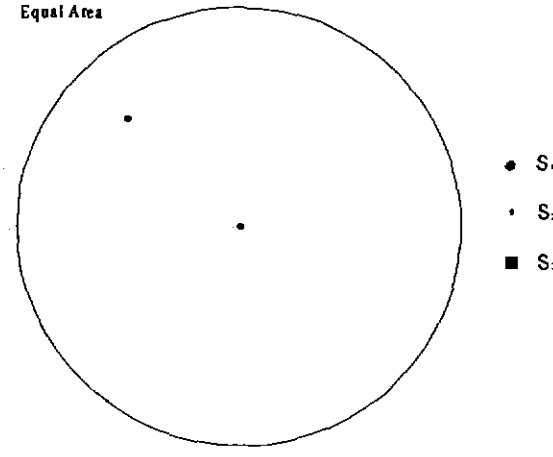
Determined and measured fold axis



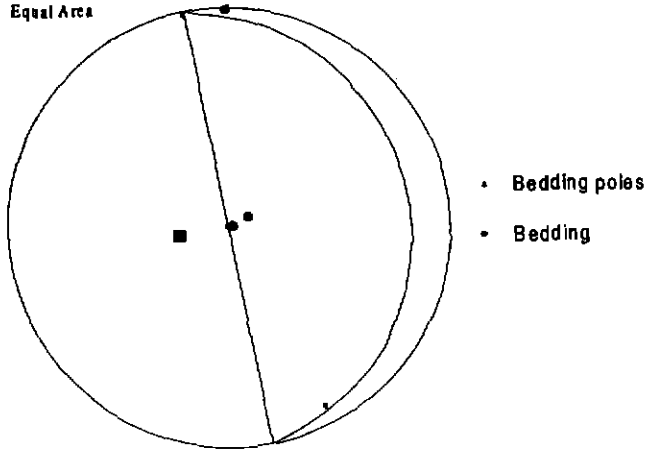
Contoured determined and measured fold axis



Cleavage 1,2 and 3 poles



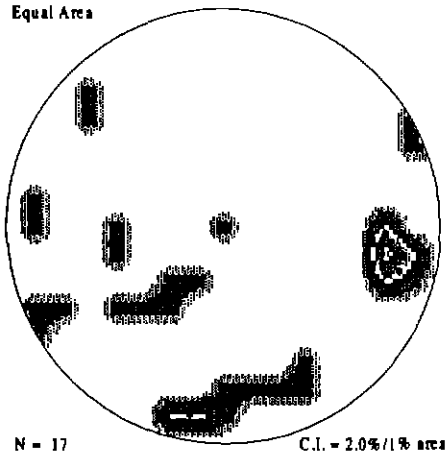
Determined fold axis



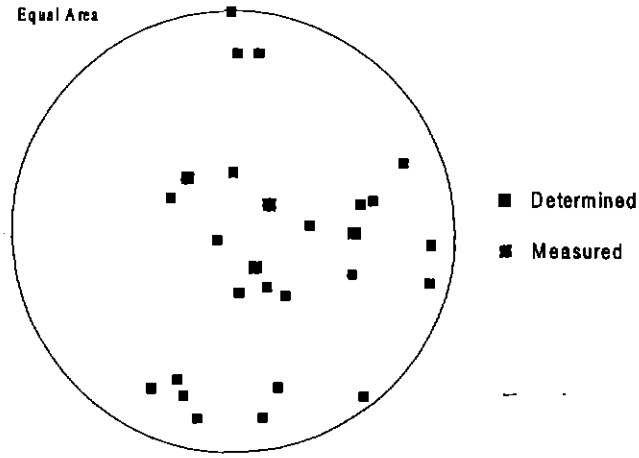
Great circle: 349/18E
Pole to great circle: 259/72

STONEHENGE DOMAIN 16 STEREONET DATA

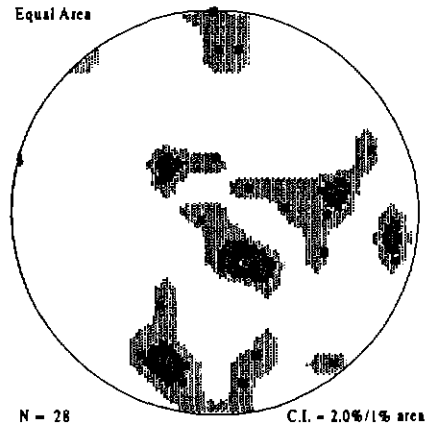
Bedding poles



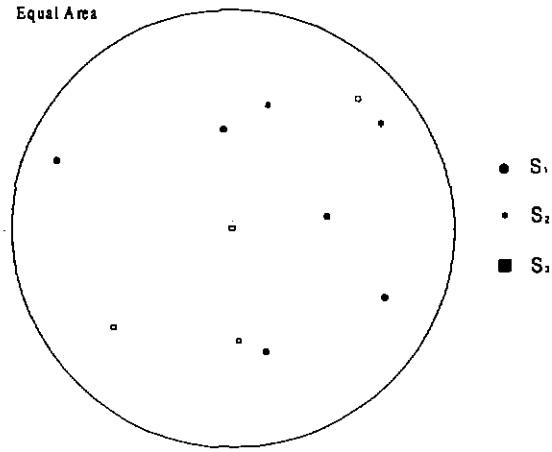
Determined and measured fold axis



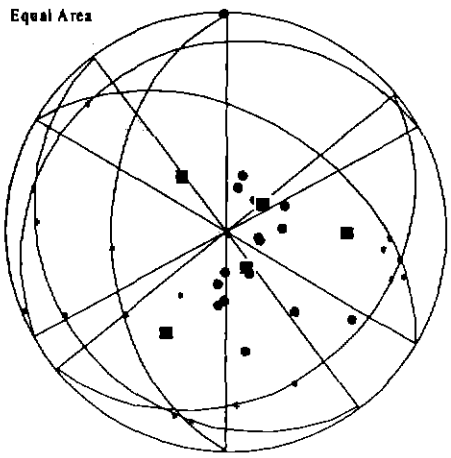
Contoured determined and measured fold axis



Cleavage 1,2 and 3 poles



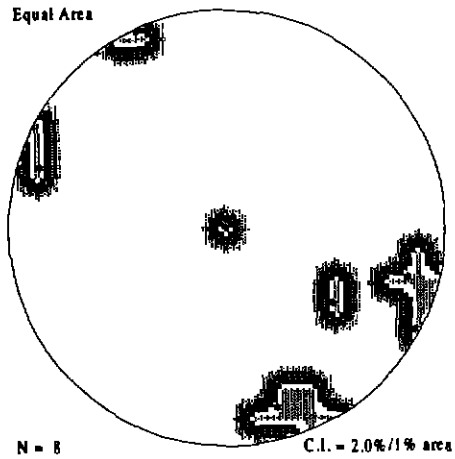
Determined fold axis



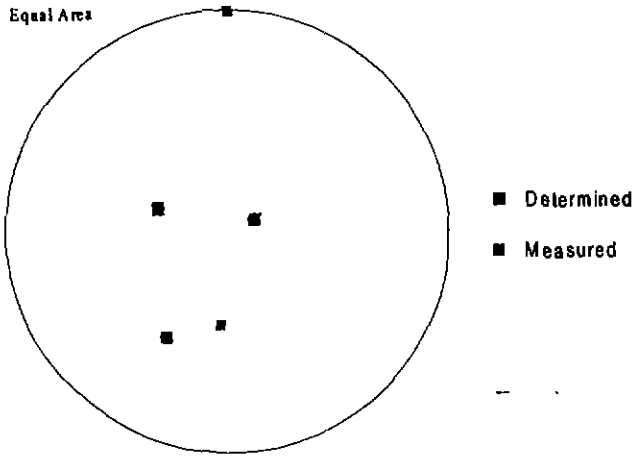
Great circle:	301/45N
Pole to great circle:	211/45
Great circle:	51/26S
Pole to great circle:	321/64
Great circle:	181/46W
Pole to great circle:	91/44
Great circle:	143/17W
Pole to great circle:	53/73
Great circle:	242/15N
Pole to great circle:	152/75

STONEHENGE DOMAIN 17 STEREONET DATA

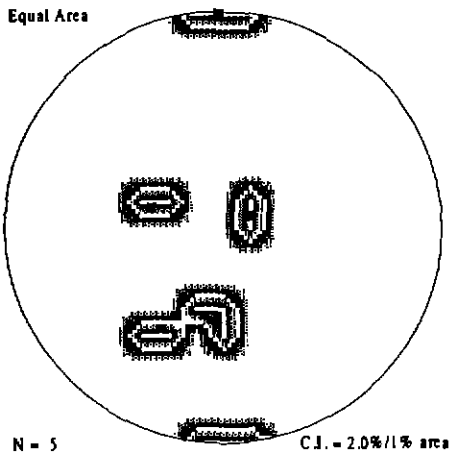
Bedding poles



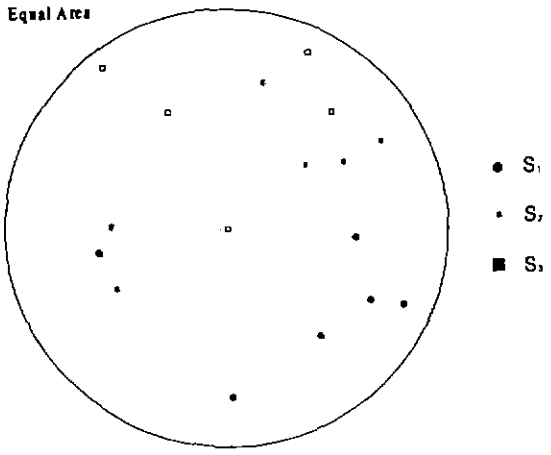
Determined and measured fold axis



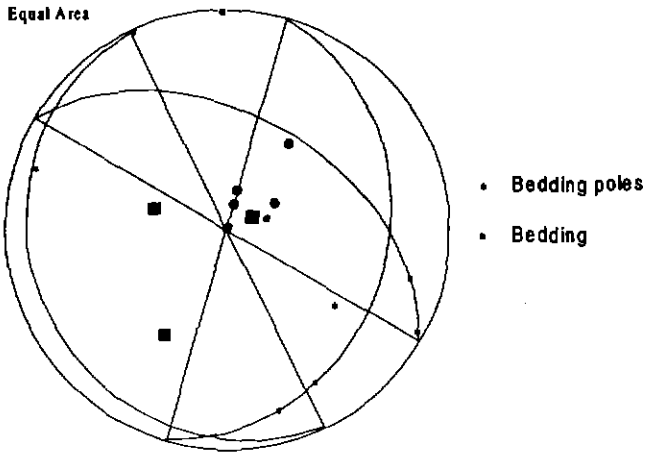
Contoured determined and measured fold axis



Cleavage 1,2 and 3 poles



Determined fold axis



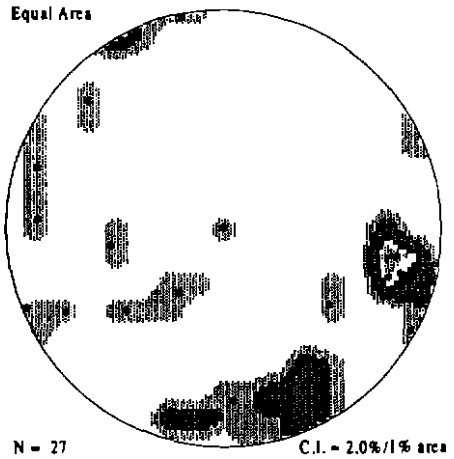
Great circle: 155/11W
Pole to great circle: 65/79

Great circle: 17/28E
Pole to great circle: 287/62

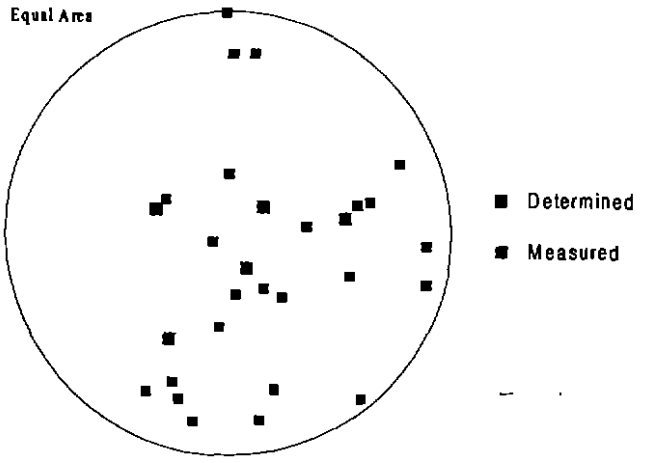
Great circle: 301/46N
Pole to great circle: 211/44

STONEHENGE DOMAIN 18 STEREONET DATA

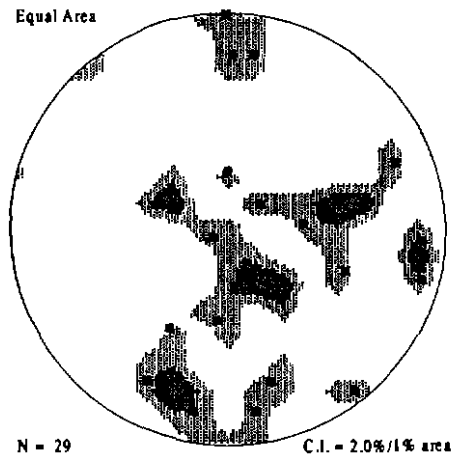
Bedding poles



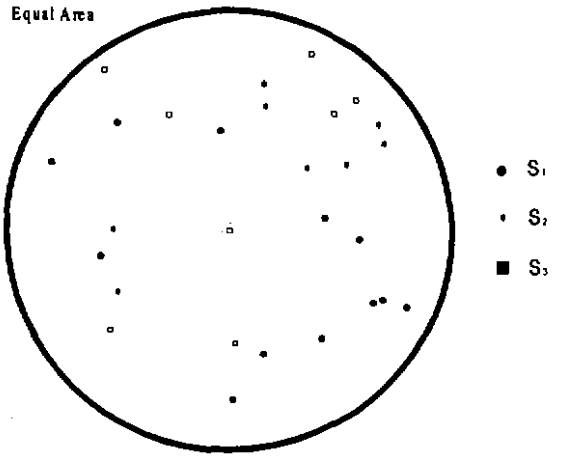
Determined and measured fold axis



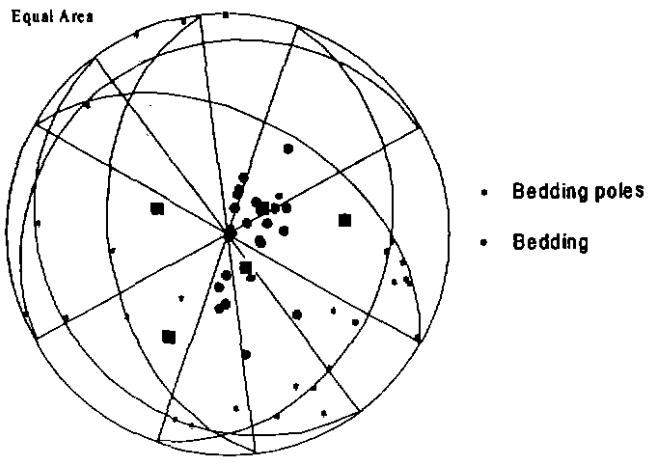
Contoured determined and measured fold axis



Cleavage 1,2 and 3 poles



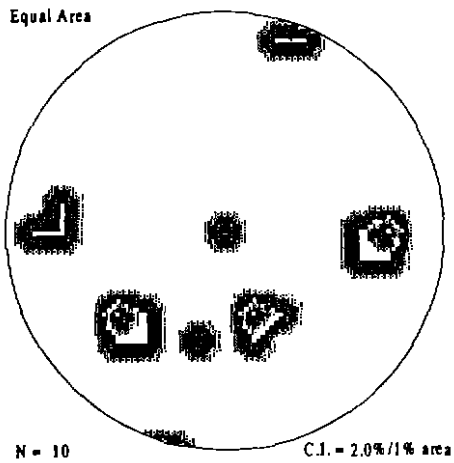
Determined fold axis



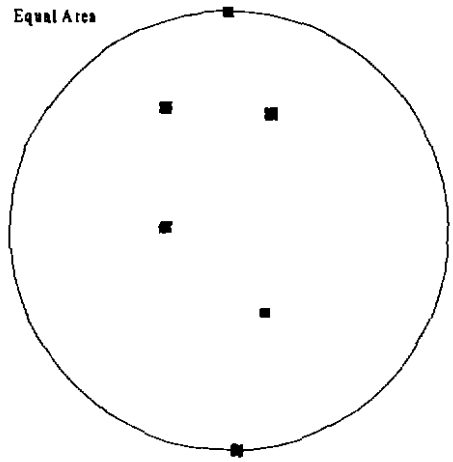
Great circle:	144/16W
Pole to great circle:	54/74
Great circle:	241/14N
Pole to great circle:	151/76
Great circle:	300/45N
Pole to great circle:	210/45
Great circle:	19/28E
Pole to great circle:	289/62
Great circle:	173/45W
Pole to great circle:	*83/45*

STONEHENGE DOMAIN 19 STEREONET DATA

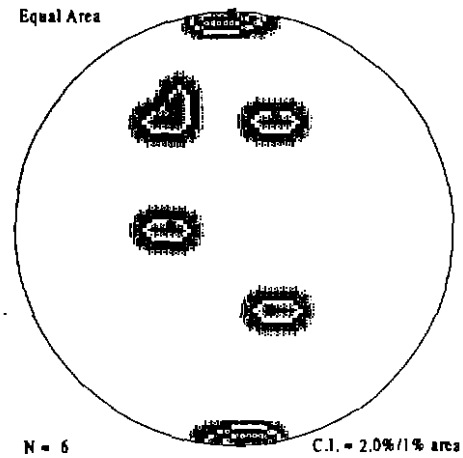
Bedding poles



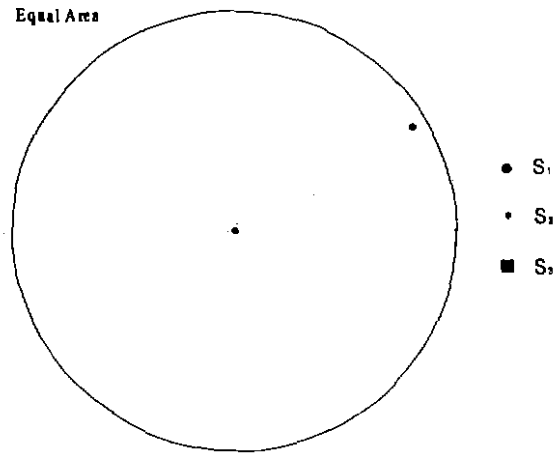
Determined and measured fold axis



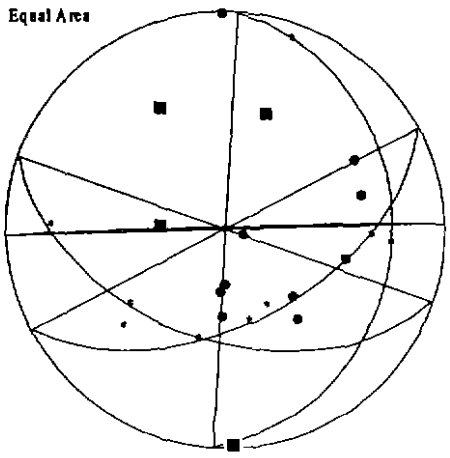
Contoured determined and measured fold axis



Cleavage 1,2 and 3 poles



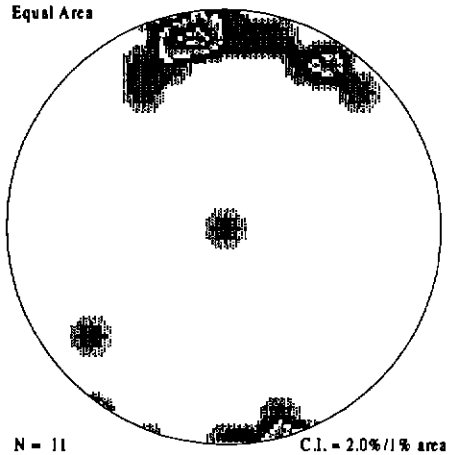
Determined fold axis



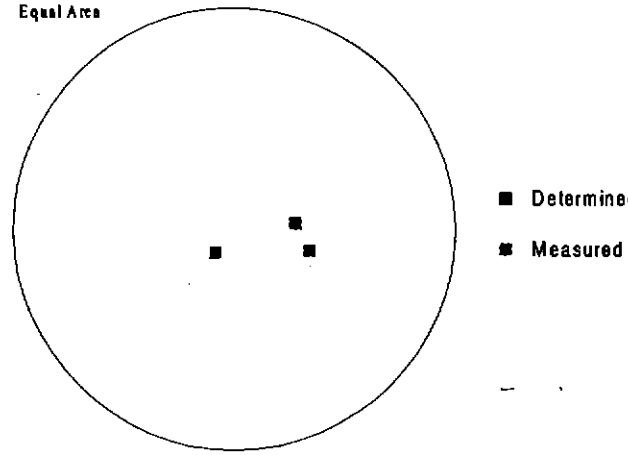
Great circle:	63/54S
Pole to great circle:	333/36
Great circle:	110/47S
Pole to great circle:	20/43
Great circle:	4/24E
Pole to great circle:	274/66
Great circle:	269/89N
Pole to great circle:	179/1

STONEHENGE DOMAIN 20 STEREONET DATA

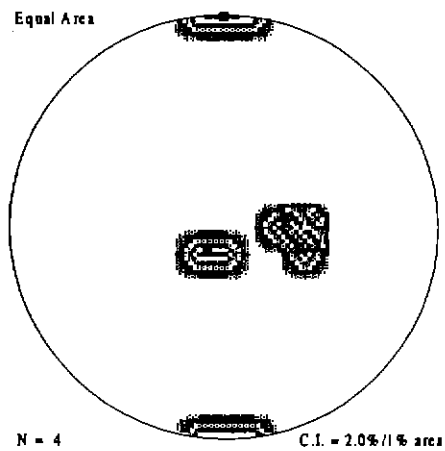
Bedding poles



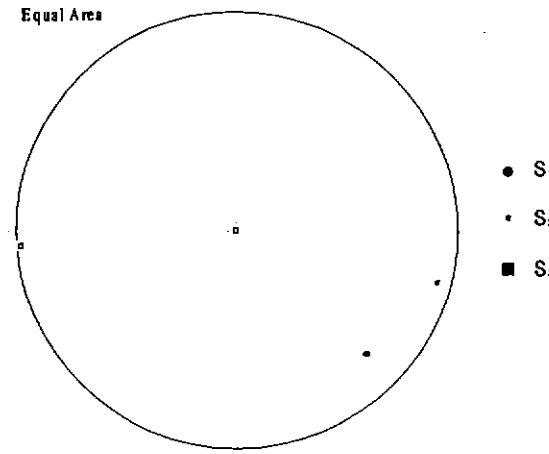
Determined and measured fold axis



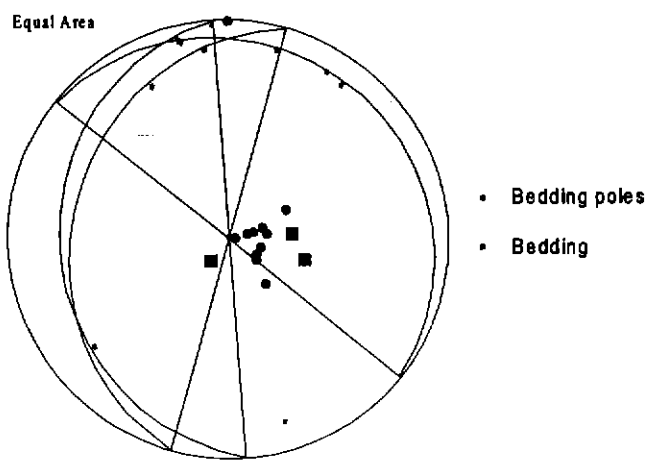
Contoured determined and measured fold axis



Cleavage 1,2 and 3 poles



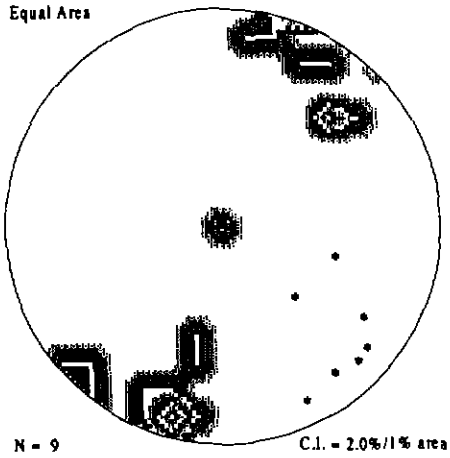
Determined fold axis



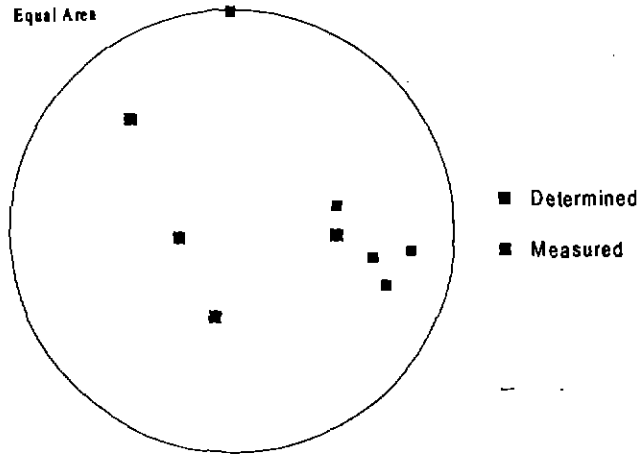
Great circle:	176/24W
Pole to great circle:	86/66
Great circle:	309/11N
Pole to great circle:	219/79
Great circle:	196/30W
Pole to great circle:	106/60

STONEHENGE DOMAIN 21 STEREONET DATA

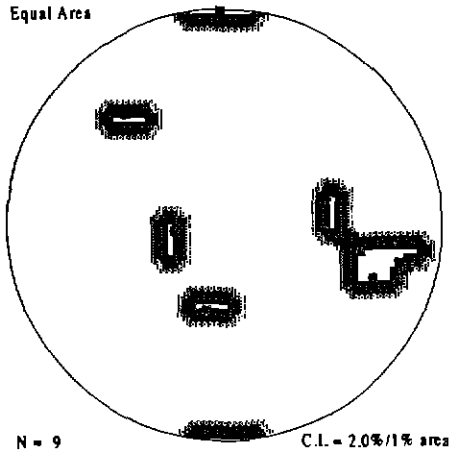
Bedding poles



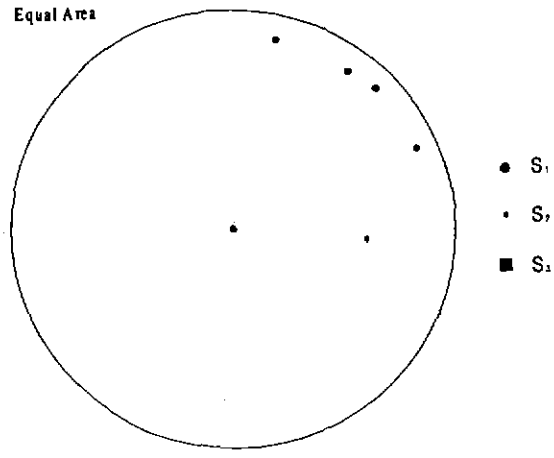
Determined and measured fold axis



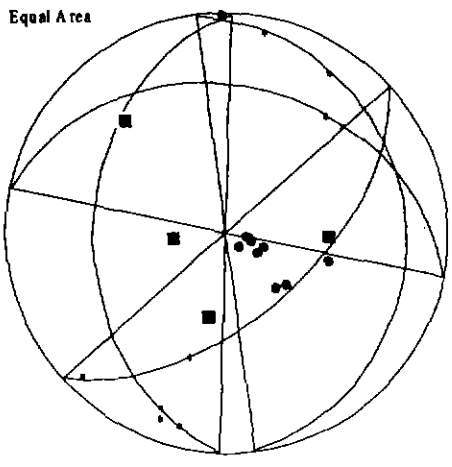
Contoured determined and measured fold axis



Cleavage 1,2 and 3 poles



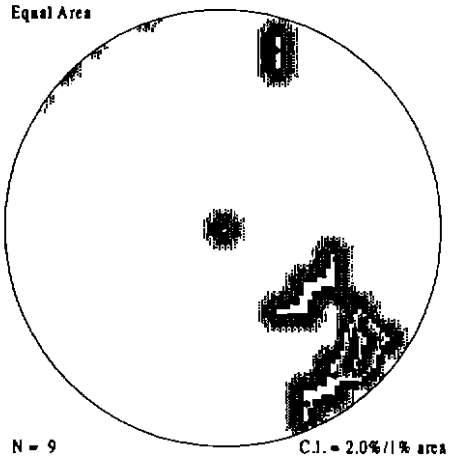
Determined fold axis



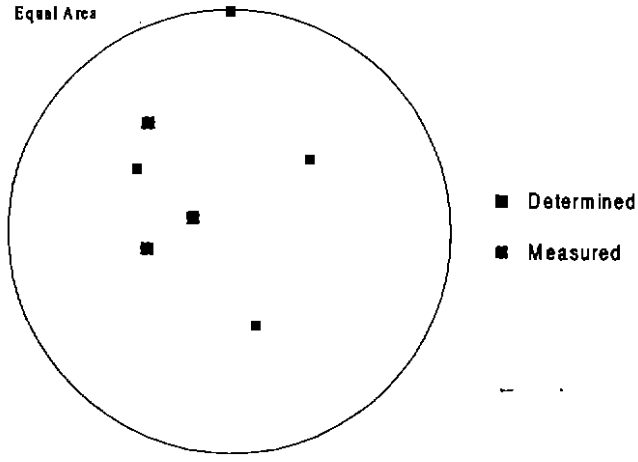
Great circle:	353/19E
Pole to great circle:	263/71
Great circle:	282/33N
Pole to great circle:	192/57
Great circle:	183/39W
Pole to great circle:	93/51
Great circle:	49/58S
Pole to great circle:	319/32

STONEHENGE DOMAIN 22 STEREONET DATA

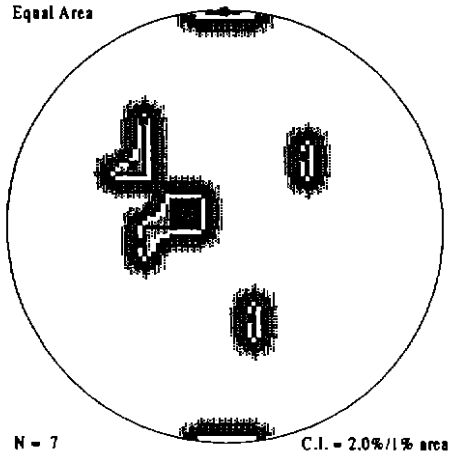
Bedding poles



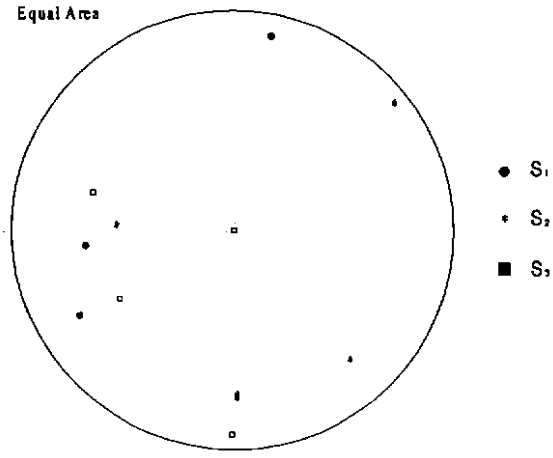
Determined and measured fold axis



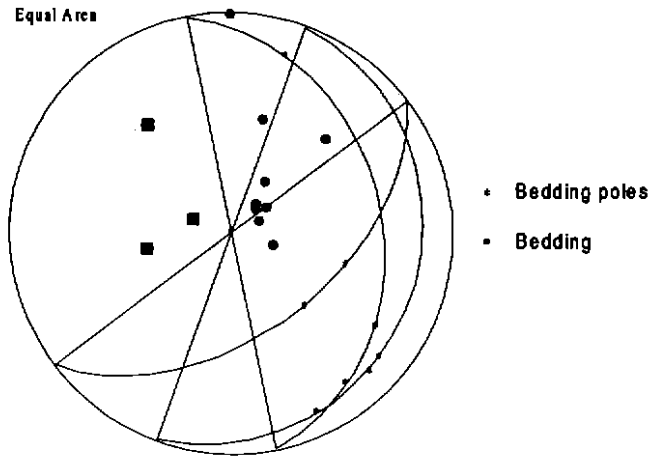
Contoured determined and measured fold axis



Cleavage 1,2 and 3 poles



Determined fold axis

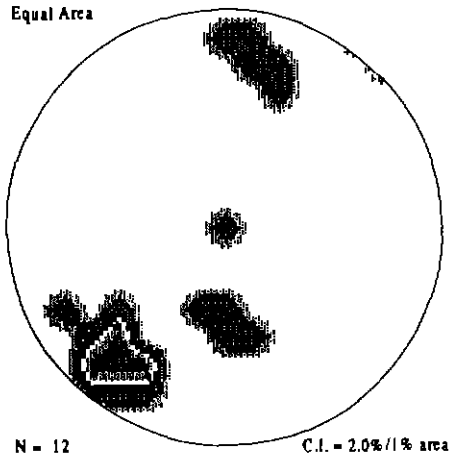


Great circle:	20/15E
Pole to great circle:	290/75
Great circle:	349/32E
Pole to great circle:	259/58
Great circle:	53/52S
Pole to great circle:	323/38

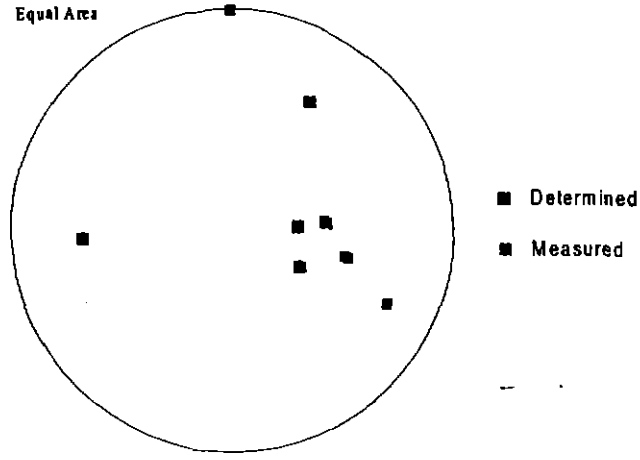
364309

STONEHENGE DOMAIN 23 STEREONET DATA

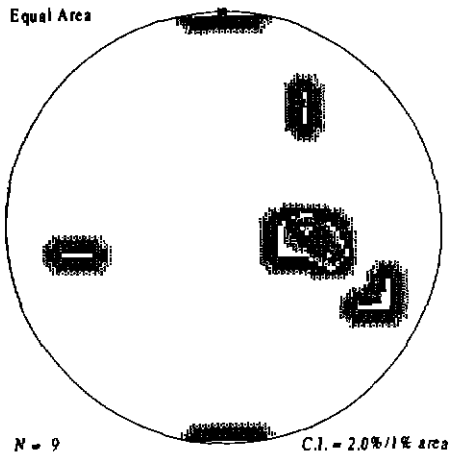
Bedding poles



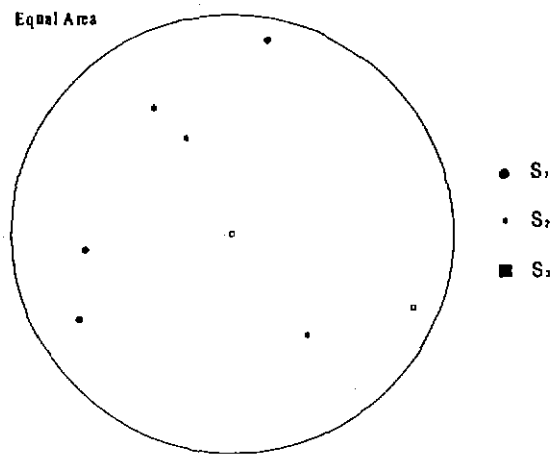
Determined and measured fold axis



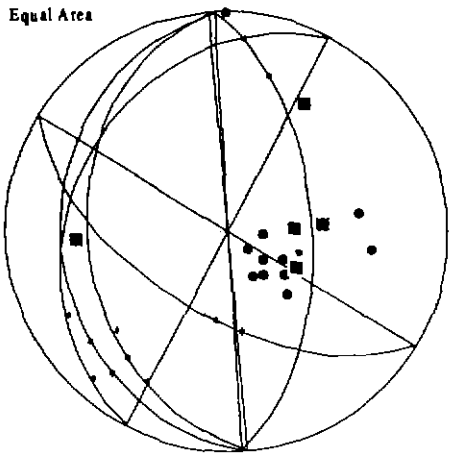
Contoured determined and measured fold axis



Cleavage 1,2 and 3 poles



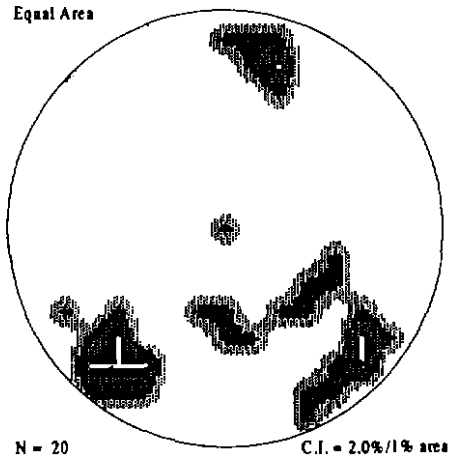
Determined fold axis



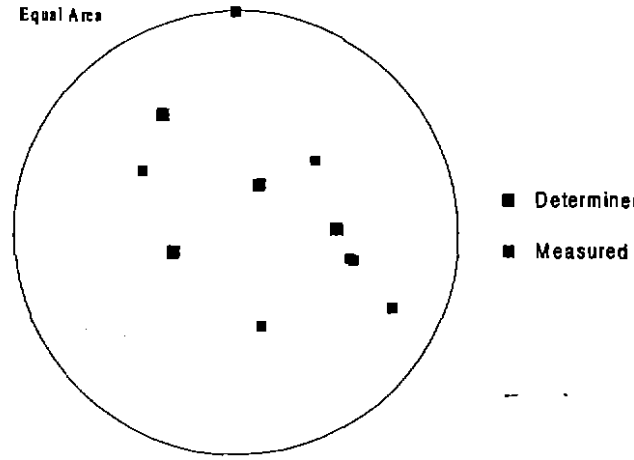
Great circle:	175/36W
Pole to great circle:	85/54
Great circle:	122/58S
Pole to great circle:	32/32
Great circle:	208/29W
Pole to great circle:	118/61
Great circle:	177/25W
Pole to great circle:	87/65
Great circle:	357/58E
Pole to great circle:	262/32

STONEHENGE DOMAIN 24 STEREONET DATA

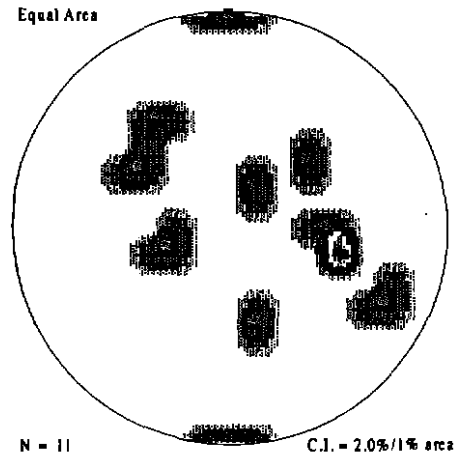
Bedding poles



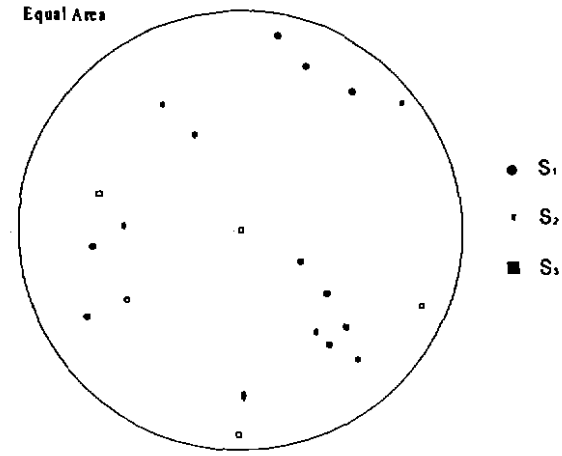
Determined and measured fold axis



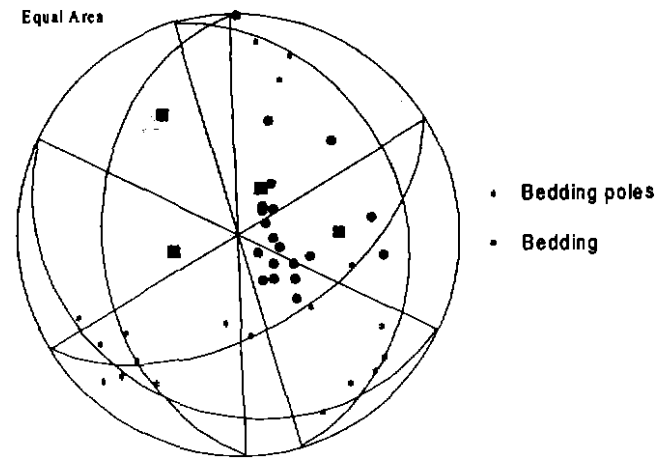
Contoured determined and measured fold axis



Cleavage 1,2 and 3 poles



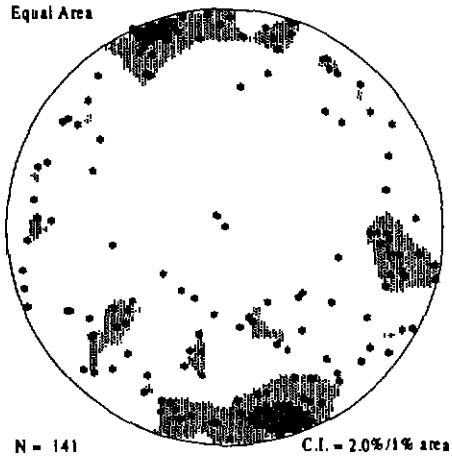
Determined fold axis



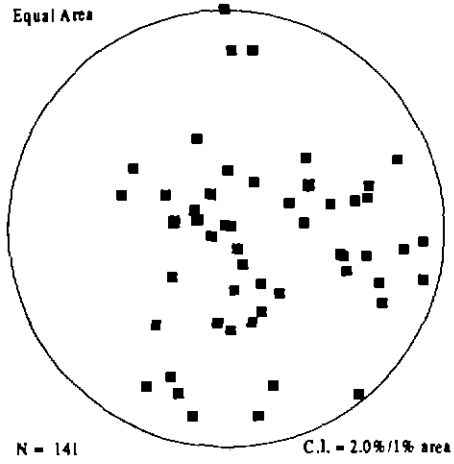
Great circle:	58/53S
Pole to great circle:	328/37
Great circle:	344/25E
Pole to great circle:	254/65
Great circle:	116/19S
Pole to great circle:	26/71
Great circle:	178/38W
Pole to great circle:	88/52

STONEHENGE DOMAIN 25 STEREONET DATA

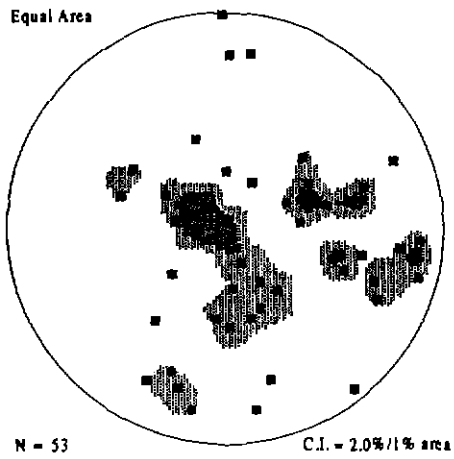
Bedding poles



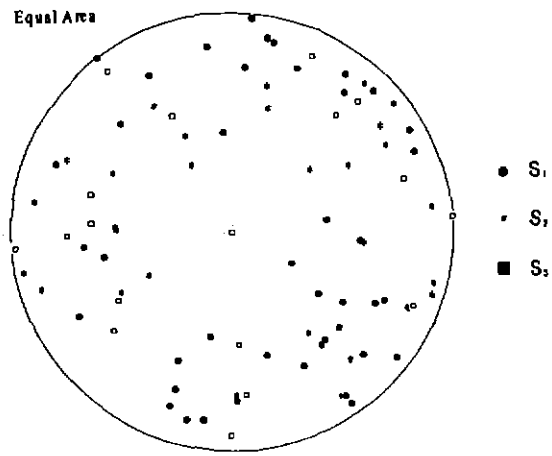
Determined and measured fold axis



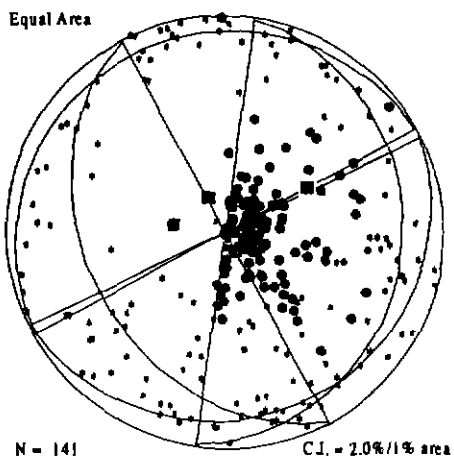
Contoured determined and measured fold axis



Cleavage 1,2 and 3 poles



Determined fold axis



Great circle: 242/8N
Pole to great circle: 152/82

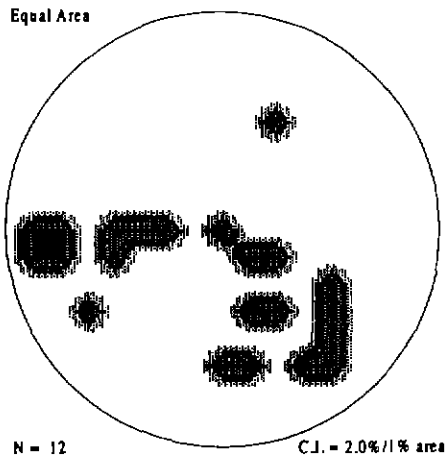
Great circle: 64/14S
Pole to great circle: 334/76

Great circle: 8/19E
Pole to great circle: 278/71

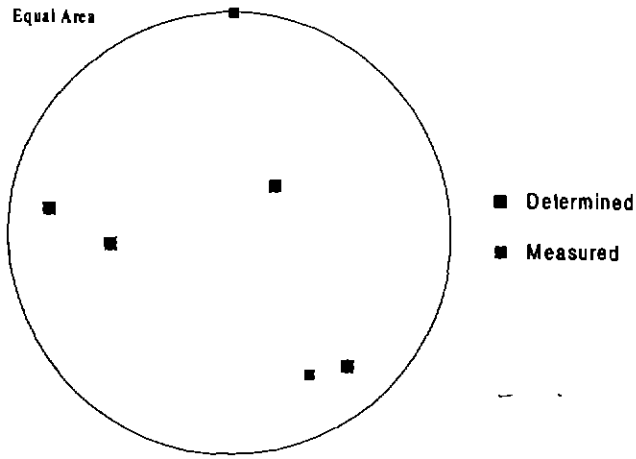
Great circle: 152/36W
Pole to great circle: 62/54

STONEHENGE DOMAIN 26 STEREONET DATA

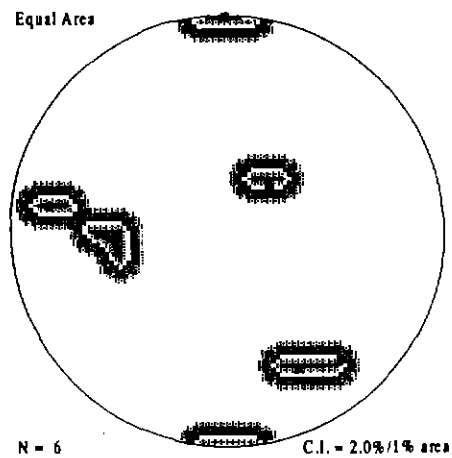
Bedding poles



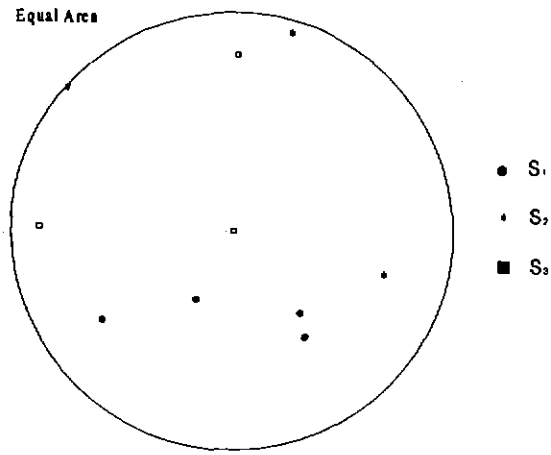
Determined and measured fold axis



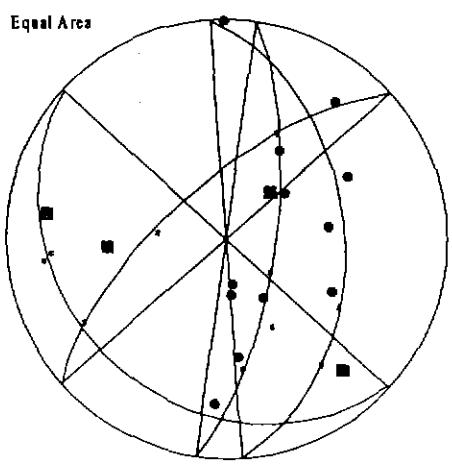
Contoured determined and measured fold axis



Cleavage 1,2 and 3 poles



Determined fold axis



Great circle: 8/72E
Pole to great circle: 278/18

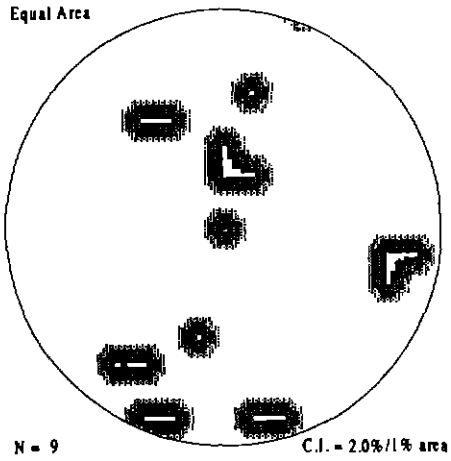
Great circle: 133/24S
Pole to great circle: 43/66

Great circle: 356/45E
Pole to great circle: 266/45

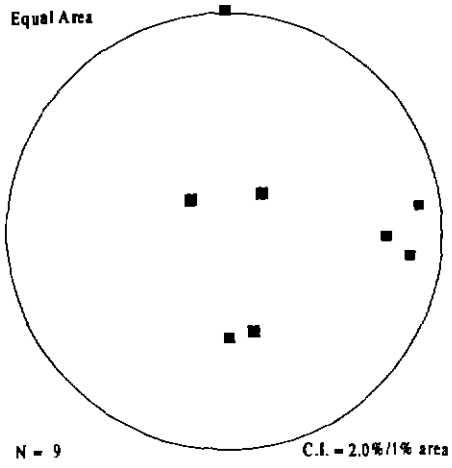
Great circle: 229/69N
Pole to great circle: 139/21

STONEHENGE DOMAIN 27 STEREONET DATA

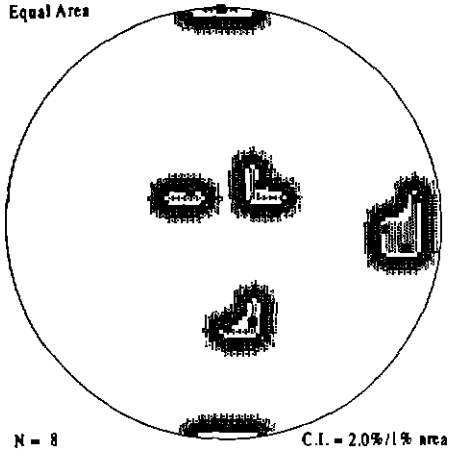
Bedding poles



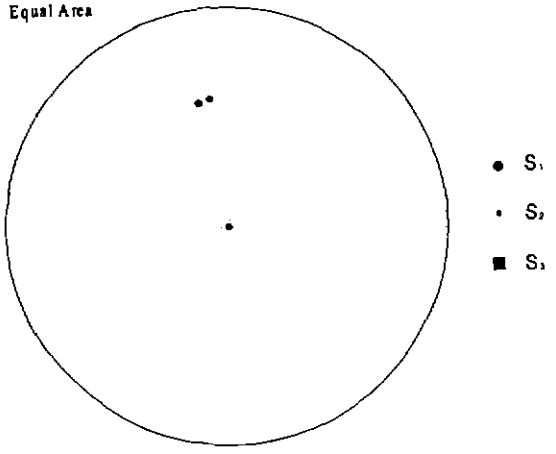
Determined and measured fold axis



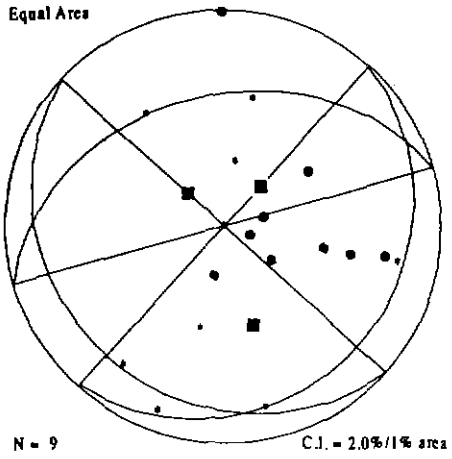
Contoured determined and measured fold axis



Cleavage 1,2 and 3 poles



Determined fold axis



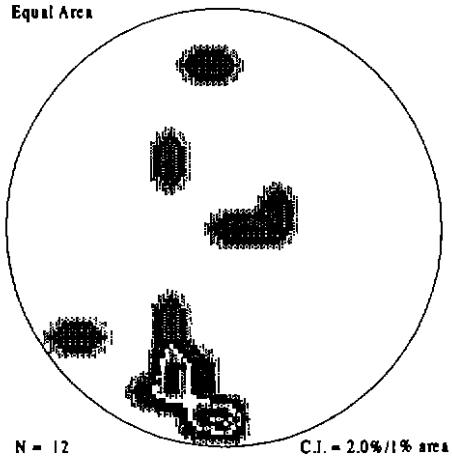
Great circle: 43/18E
Pole to great circle: 313/72

Great circle: 255/39N
Pole to great circle: 165/51

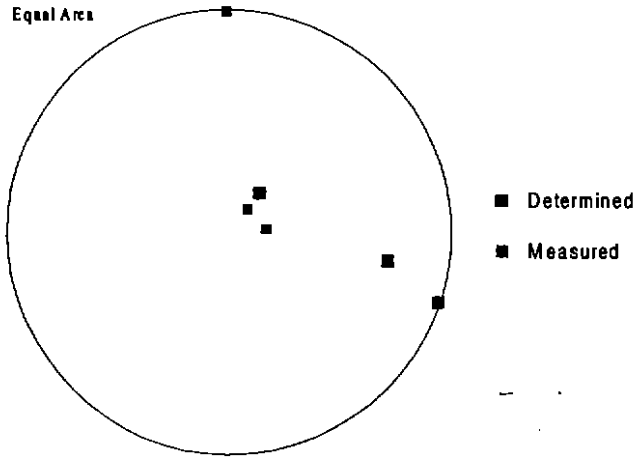
Great circle: 133/20S
Pole to great circle: 43/70

STONEHENGE DOMAIN 28 STEREONET DATA

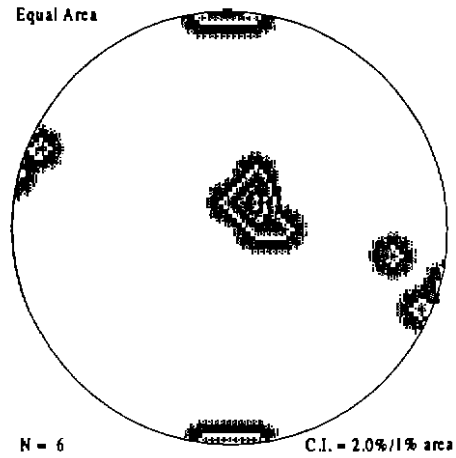
Bedding poles



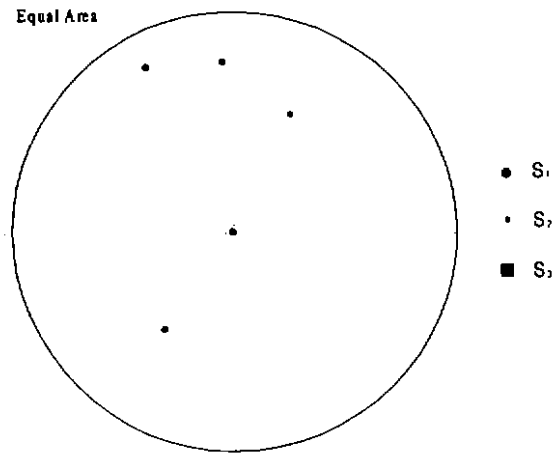
Determined and measured fold axis



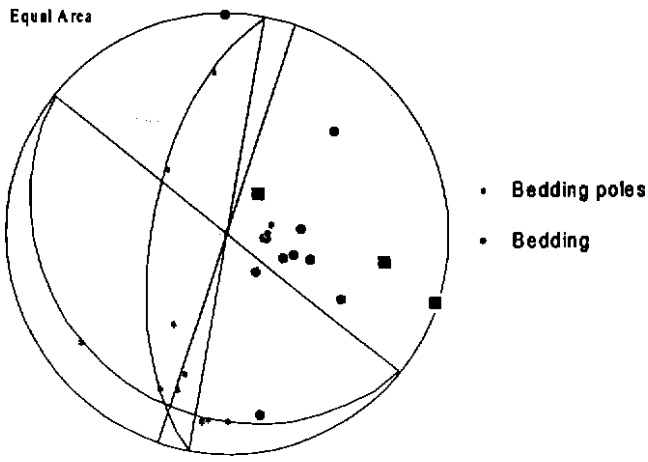
Contoured determined and measured fold axis



Cleavage 1,2 and 3 poles



Determined fold axis



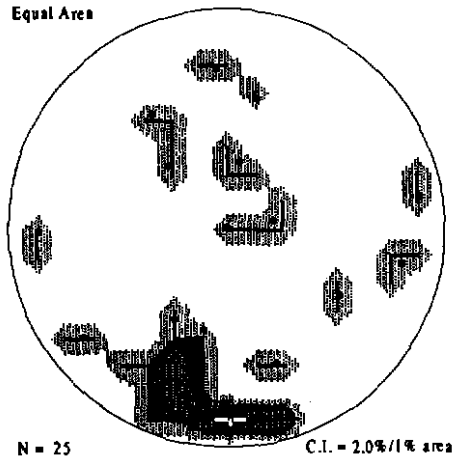
Great circle: 190/62W
Pole to great circle: 100/28

Great circle: 129/19S
Pole to great circle: 39/71

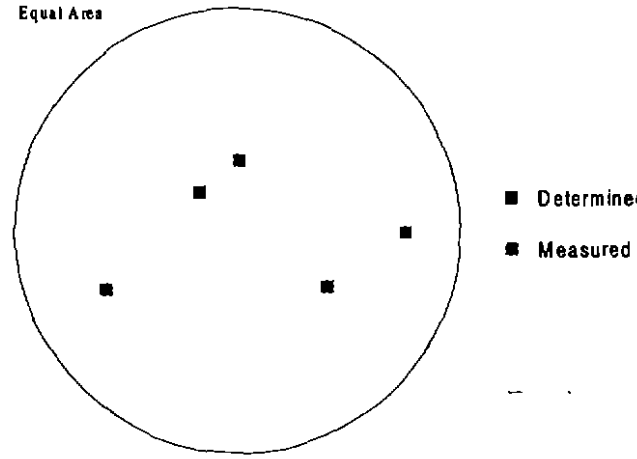
Great circle: 199/90W
Pole to great circle: 109/0

STONEHENGE DOMAIN 29 STEREONET DATA

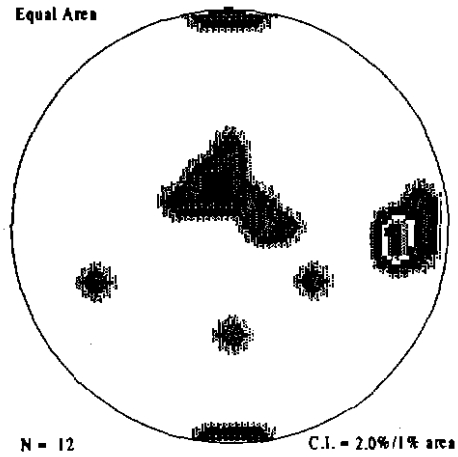
Bedding poles



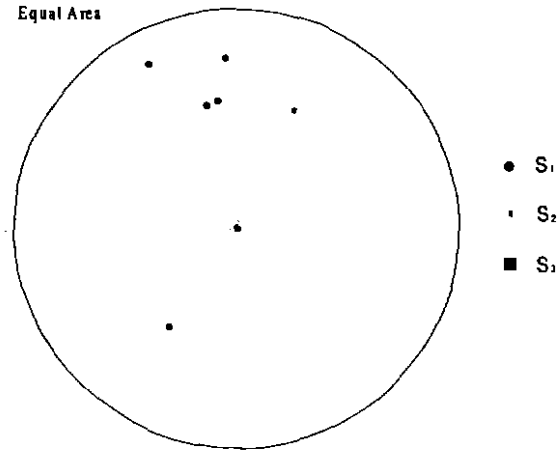
Determined and measured fold axis



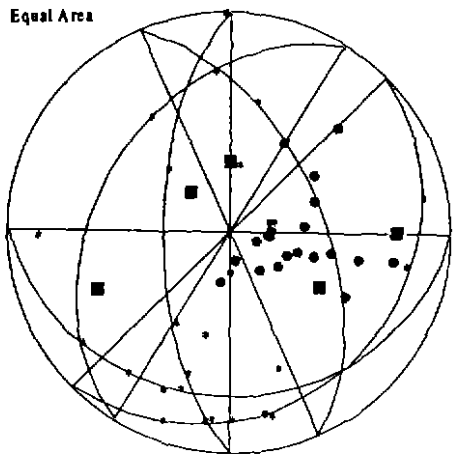
Contoured determined and measured fold axis



Cleavage 1,2 and 3 poles



Determined fold axis



Great circle: 46/20S
Pole to great circle: 316/70

Great circle: 91/26S
Pole to great circle: 1/64

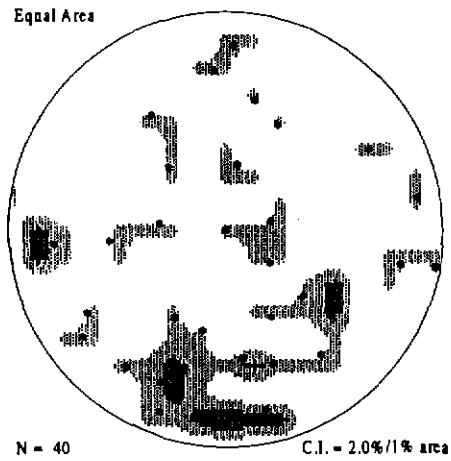
Great circle: 213/39W
Pole to great circle: 123/51

Great circle: 337/55E
Pole to great circle: 247/35

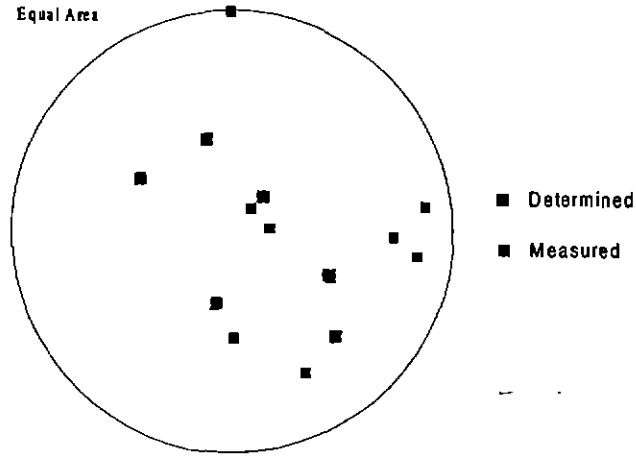
Great circle: 181/65W
Pole to great circle: 91/25

STONEHENGE DOMAIN 30 STEREONET DATA

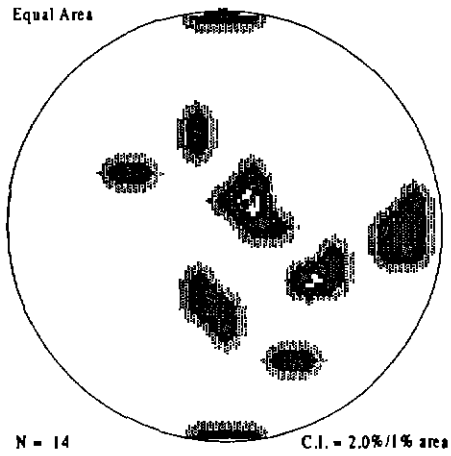
Bedding poles



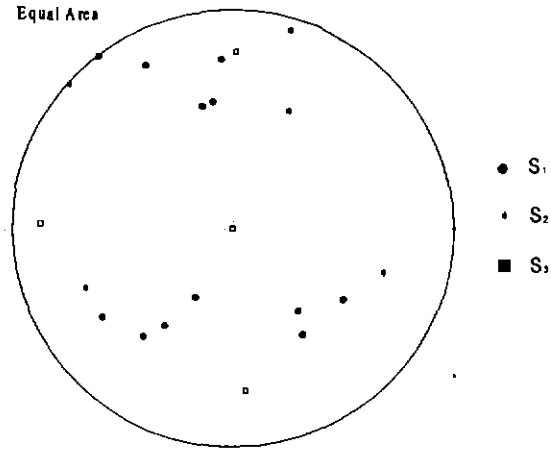
Determined and measured fold axis



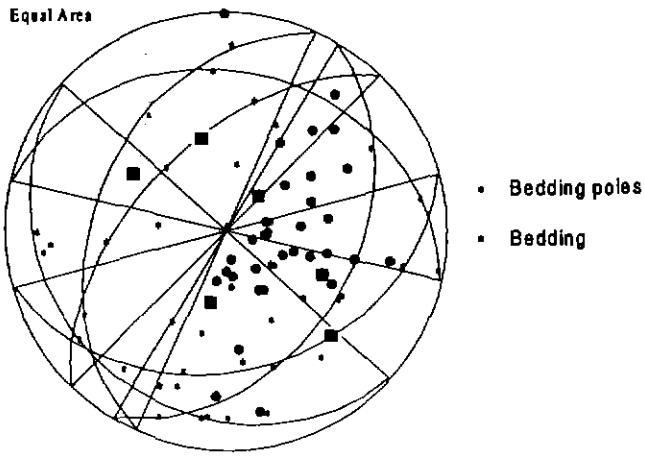
Contoured determined and measured fold axis



Cleavage 1,2 and 3 poles



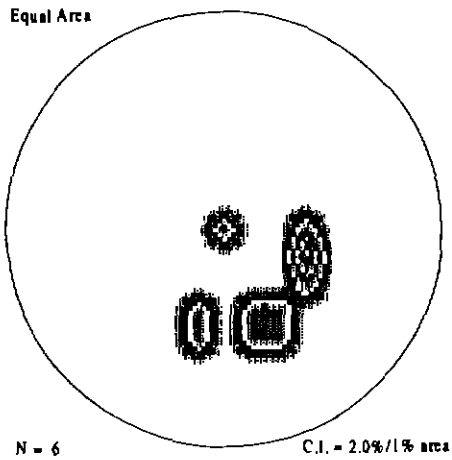
Determined fold axis



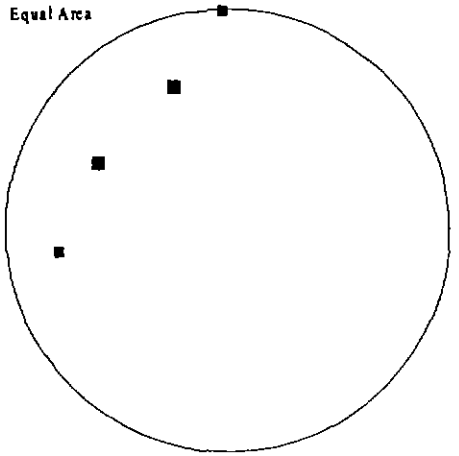
Great circle:	283/27N
Pole to great circle:	193/63
Great circle:	132/18S
Pole to great circle:	42/72
Great circle:	205/40W
Pole to great circle:	115/50
Great circle:	255/57W
Pole to great circle:	135/33
Great circle:	31/41E
Pole to great circle:	301/49
Great circle:	75/36S
Pole to great circle:	345/54

STONEHENGE DOMAIN 31 STEREONET DATA

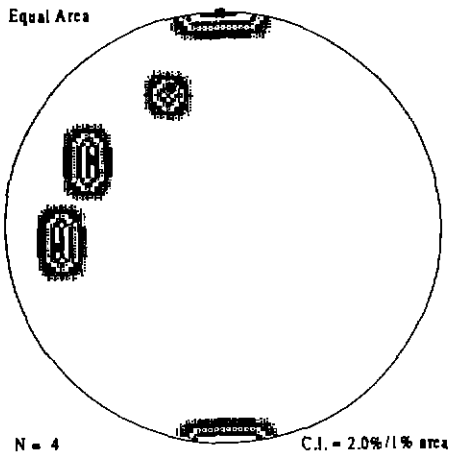
Bedding poles



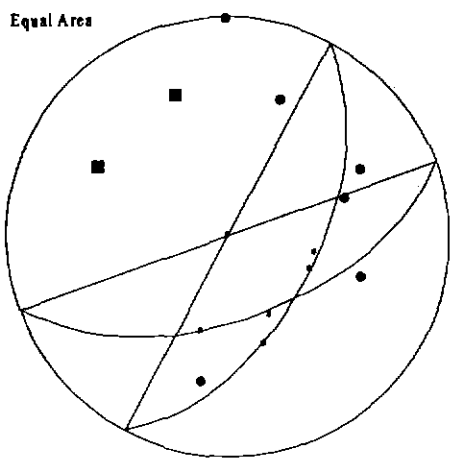
Determined and measured fold axis



Contoured determined and measured fold axis



Determined fold axis

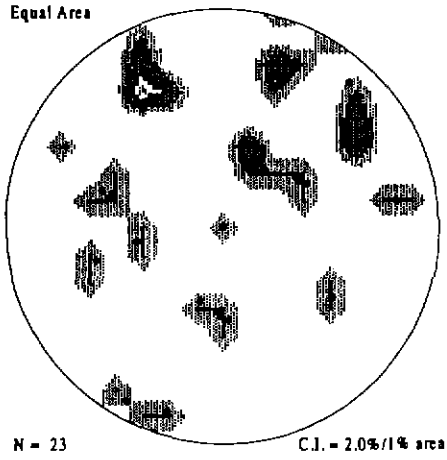


Great circle: 28/57E
Pole to great circle: 298/33

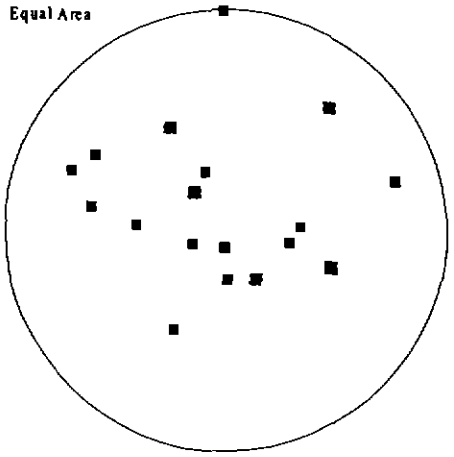
Great circle: 71/59S
Pole to great circle: 341/31

STONEHENGE DOMAIN 32 STEREONET DATA

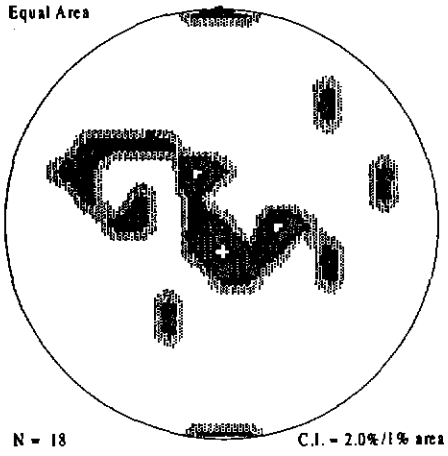
Bedding poles



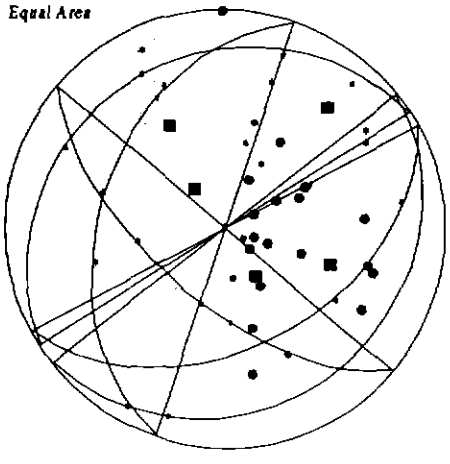
Determined and measured fold axis



Contoured determined and measured fold axis



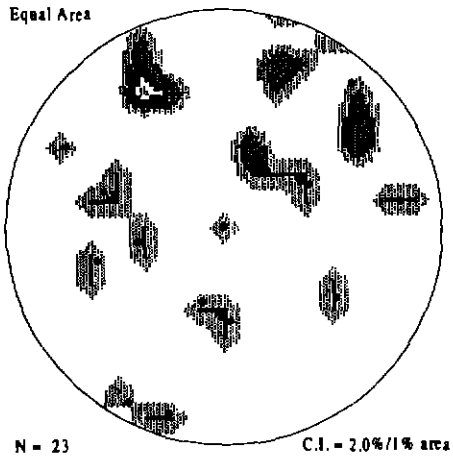
Determined fold axis



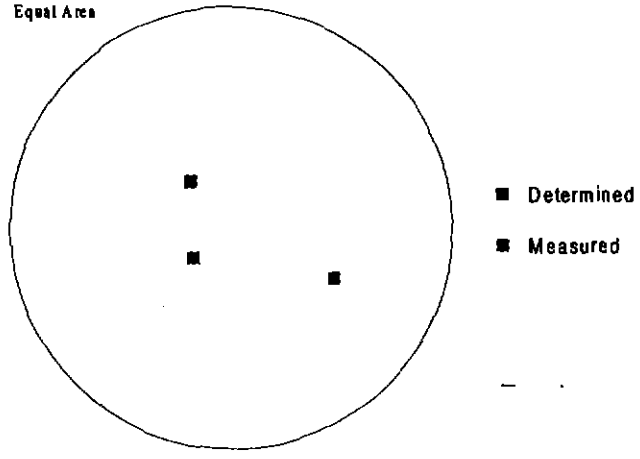
Great circle:	52/19S
Pole to great circle:	322/71
Great circle:	238/21N
Pole to great circle:	148/69
Great circle:	131/62S
Pole to great circle:	41/28
Great circle:	62/44S
Pole to great circle:	332/46
Great circle:	199/42W
Pole to great circle:	109/48

STONEHENGE DOMAIN 33 STEREONET DATA

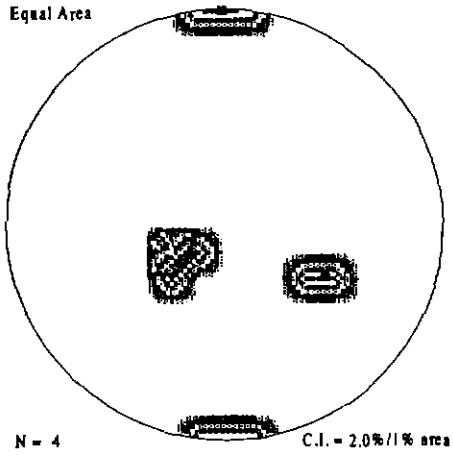
Bedding poles



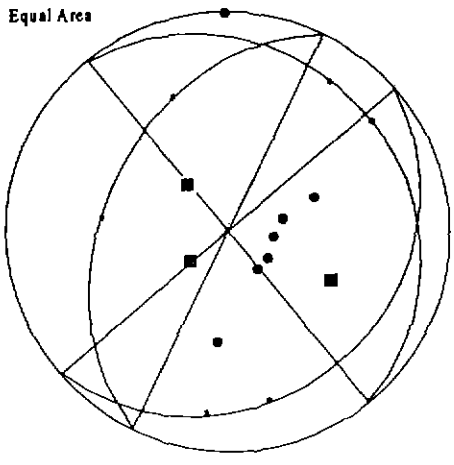
Determined and measured fold axis



Contoured determined and measured fold axis



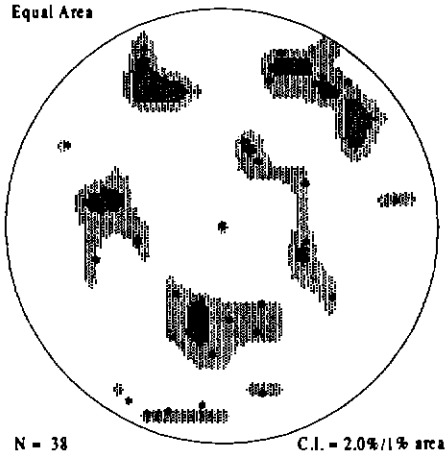
Determined fold axis



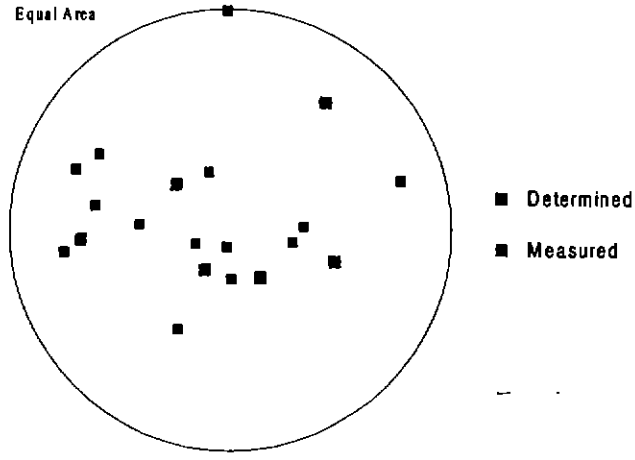
Great circle:	**321/18E**
Pole to great circle:	**231/72**
Great circle:	**206/43W**
Pole to great circle:	**116/47**
Great circle:	**50/23S**
Pole to great circle:	**230/67**

STONEHENGE DOMAIN 34 STEREONET DATA

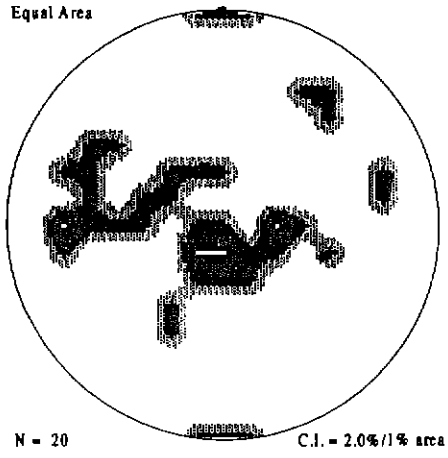
Bedding poles



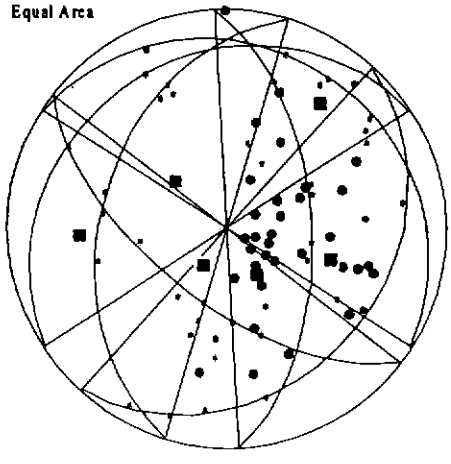
Determined and measured fold axis



Contoured determined and measured fold axis



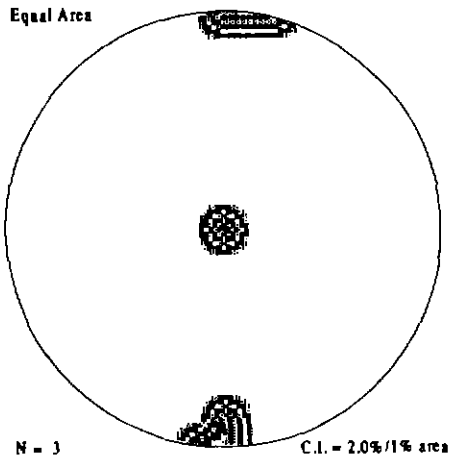
Determined fold axis



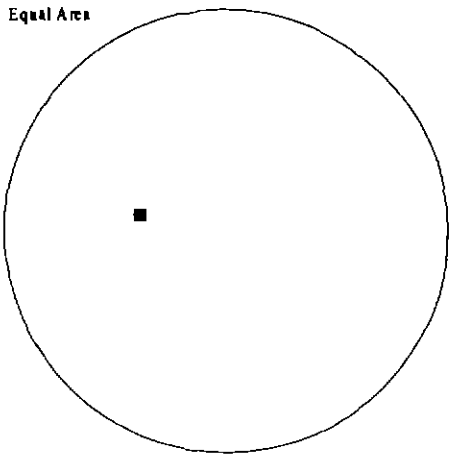
Great circle:	42/26E
Pole to great circle:	312/64
Great circle:	303/17N
Pole to great circle:	213/73
Great circle:	197/41W
Pole to great circle:	107/49
Great circle:	237/21N
Pole to great circle:	147/69
Great circle:	128/62S
Pole to great circle:	38/28
Great circle:	357/58E
Pole to great circle:	267/32

STONEHENGE DOMAIN 35 STEREONET DATA

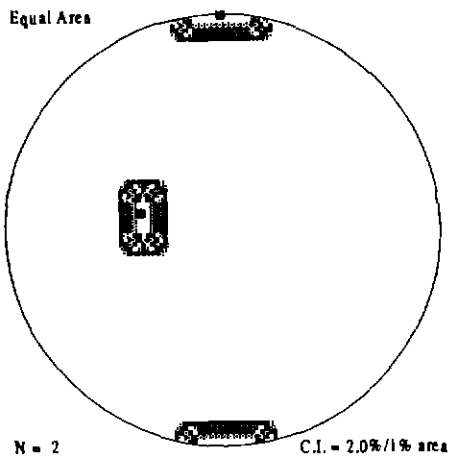
Bedding poles



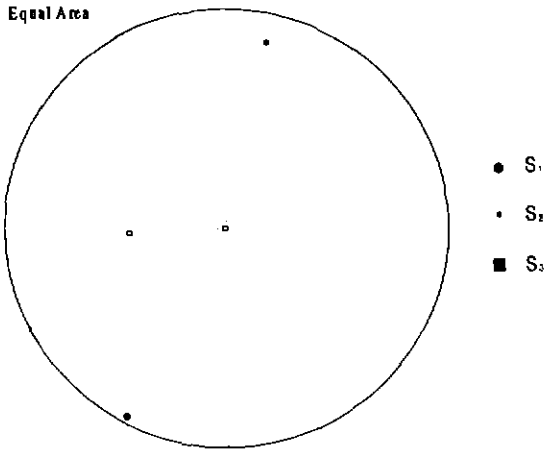
Determined and measured fold axis



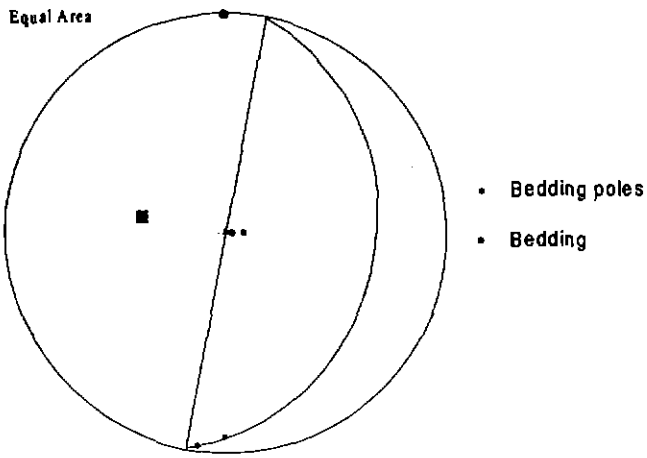
Contoured determined and measured fold axis



Cleavage 1,2 and 3 poles



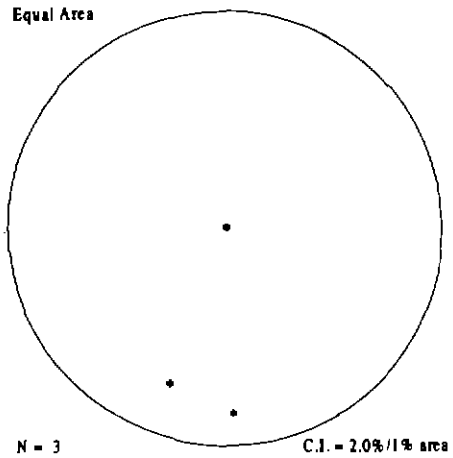
Determined fold axis



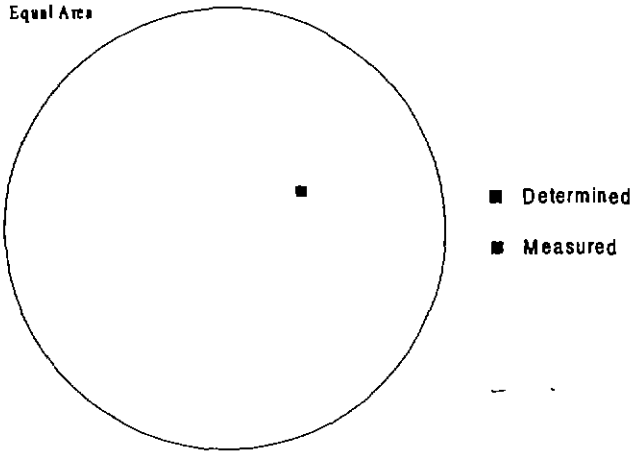
Great circle: 11/32E
Pole to great circle: 281/58

STONEHENGE DOMAIN 36 STEREONET DATA

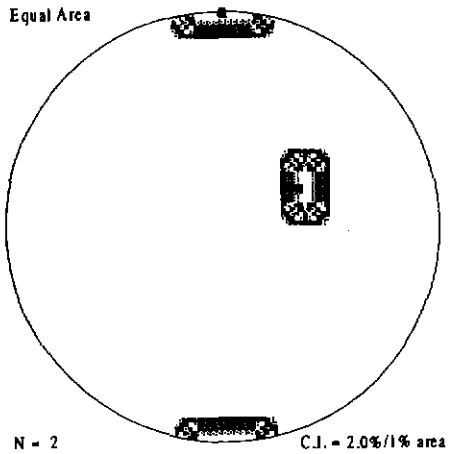
Bedding poles



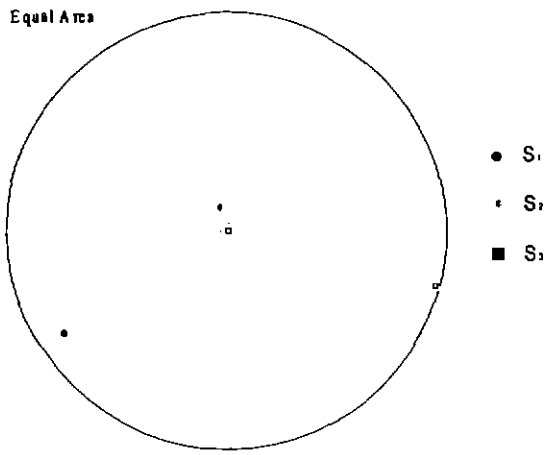
Determined and measured fold axis



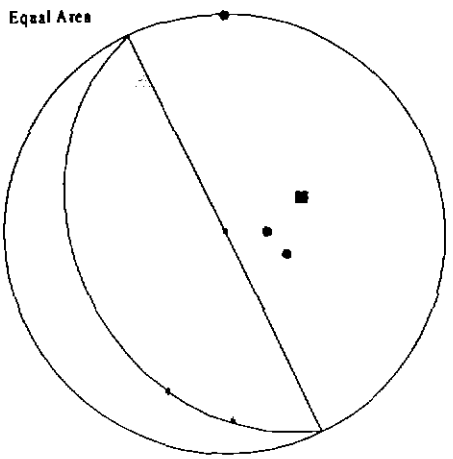
Contoured determined and measured fold axis



Cleavage 1,2 and 3 poles



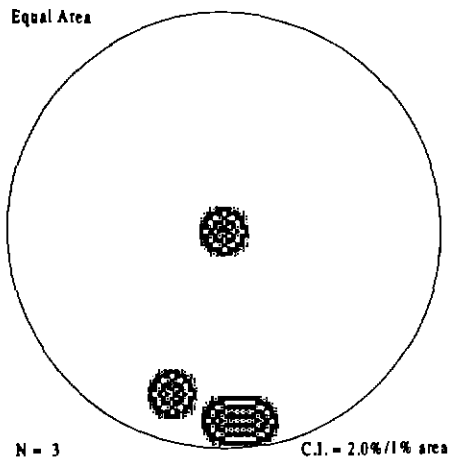
Determined fold axis



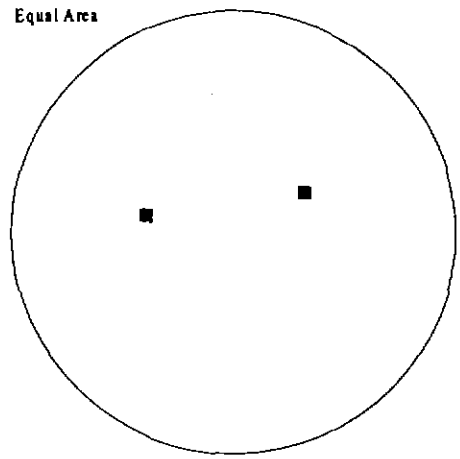
Great circle: 154/32W
Pole to great circle: 64/58

STONEHENGE DOMAIN 37 STEREONET DATA

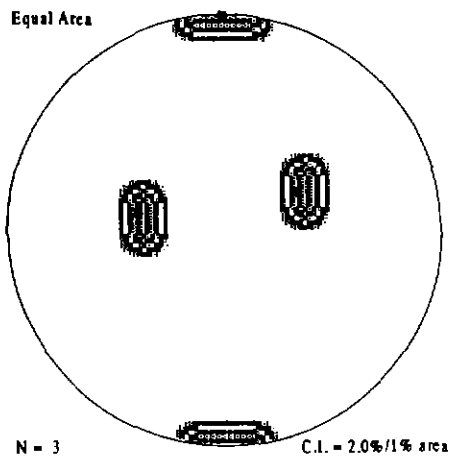
Bedding poles



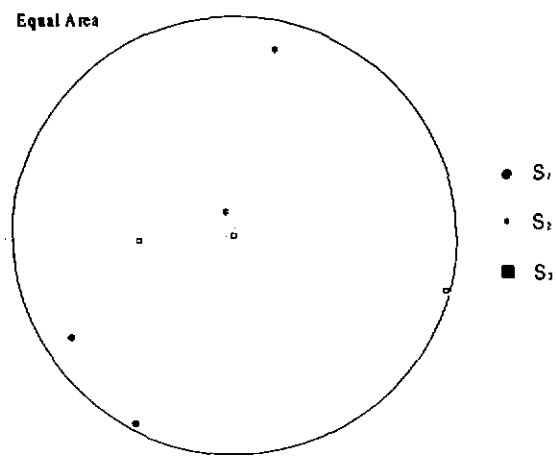
Determined and measured fold axis



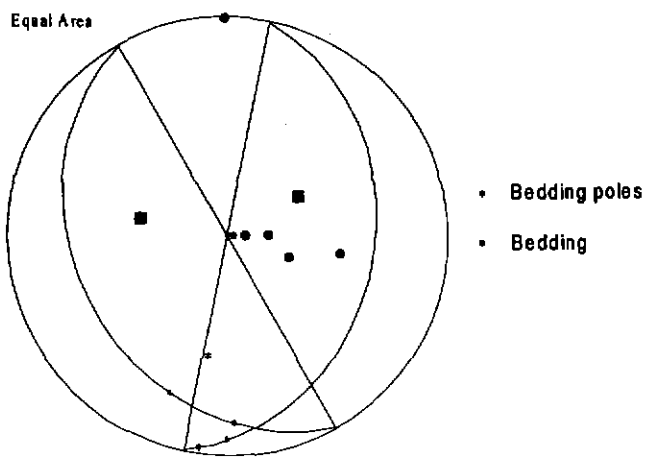
Contoured determined and measured fold axis



Cleavage 1,2 and 3 poles



Determined fold axis

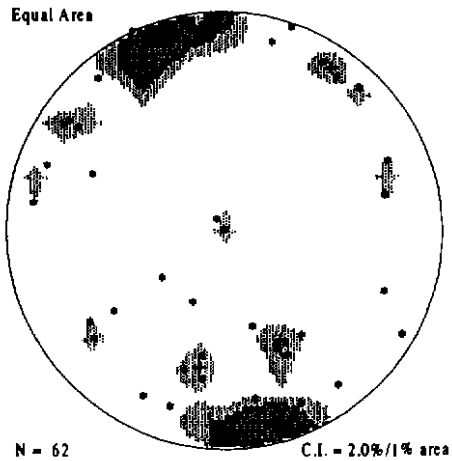


Great circle: 12/33E
Pole to great circle: 282/57

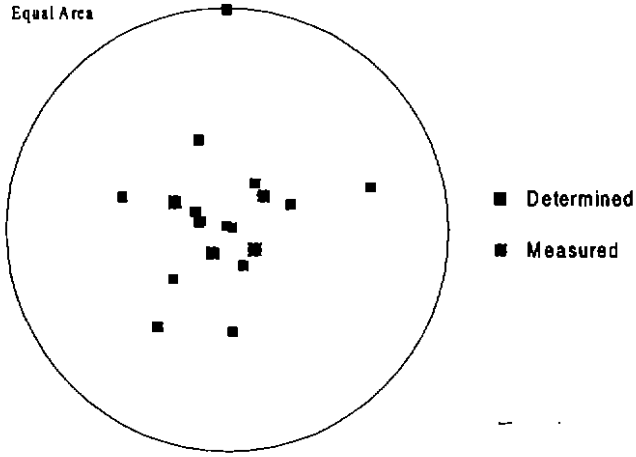
Great circle: 151/31W
Pole to great circle: 61/59

STONEHENGE DOMAIN 38 STEREONET DATA

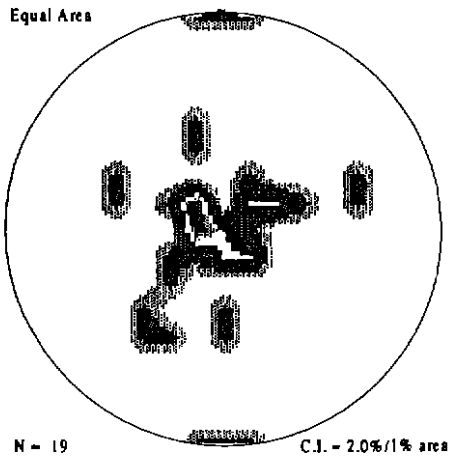
Bedding poles



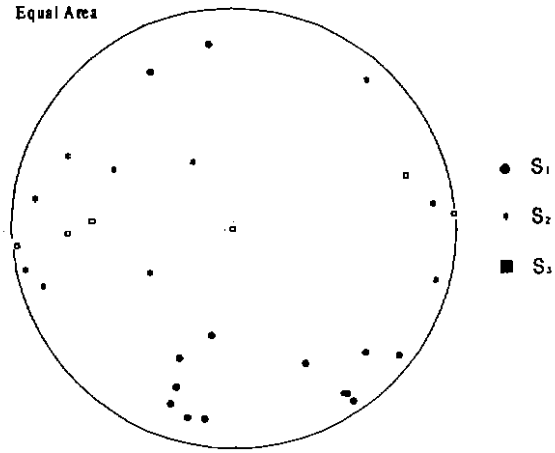
Determined and measured fold axis



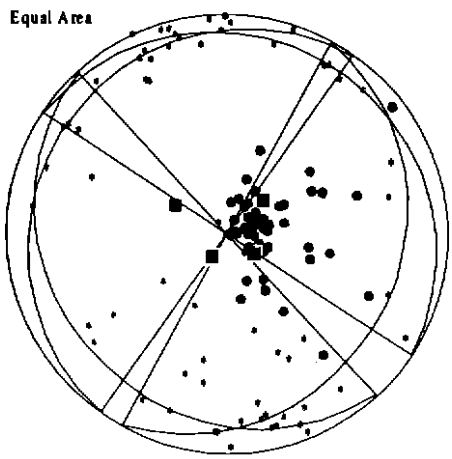
Contoured determined and measured fold axis



Cleavage 1,2 and 3 poles



Determined fold axis



Great circle: 137/18W
Pole to great circle: 47/72

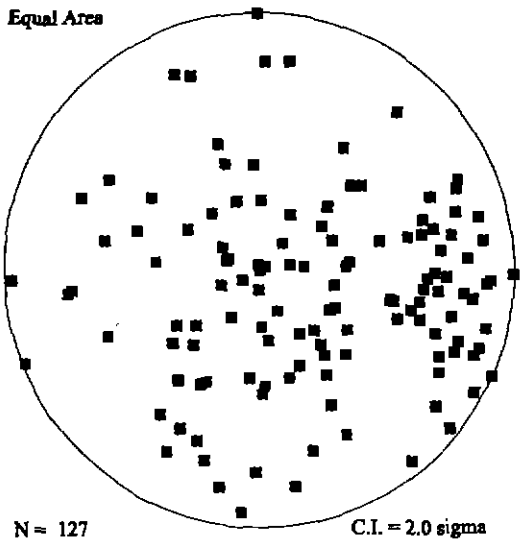
Great circle: 216/13W
Pole to great circle: 126/77

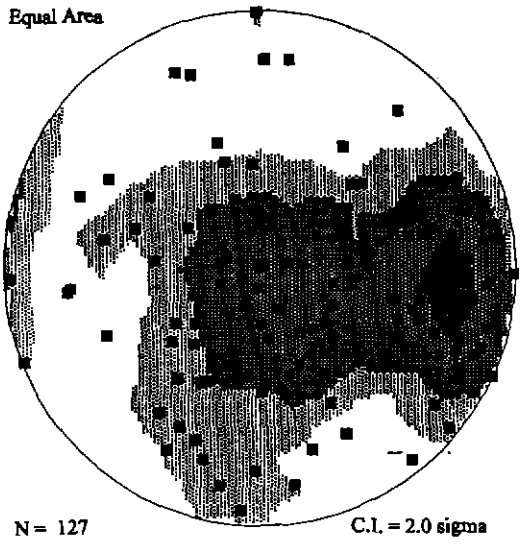
Great circle: 29/22E
Pole to great circle: 299/68

Great circle: 304/10N
Pole to great circle: 214/80

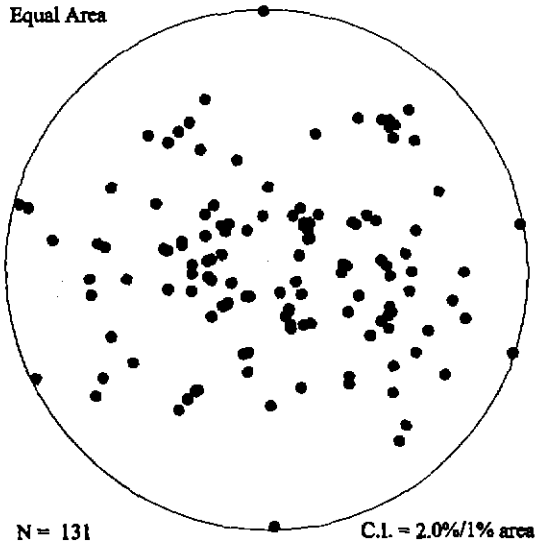
STONEHENGE COMBINED MEASURED FOLD AXIS STEREONET DATA

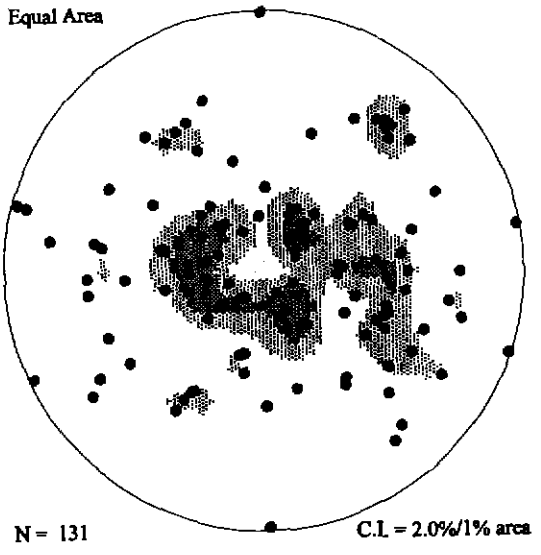
SCATTER AND CONTOUR PLOTS





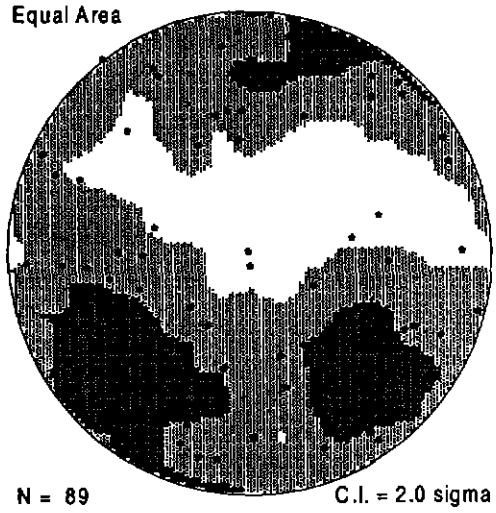
STONEHENGE COMBINED DETERMINED FOLD AXIS STEREONET DATA
SCATTER AND CONTOUR PLOTS



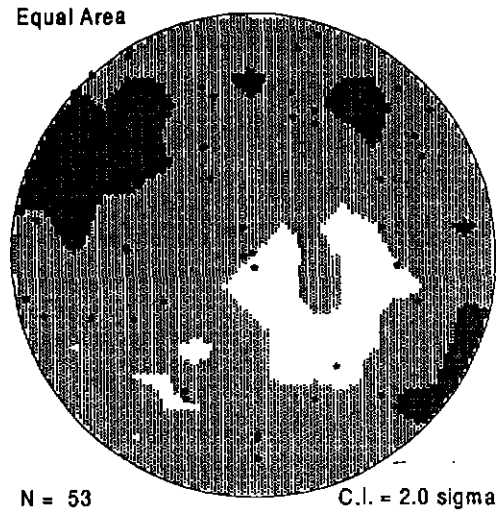


STONEHENGE COMBINED CLEAVAGE AND BEDDING POLES STEREONET DATA

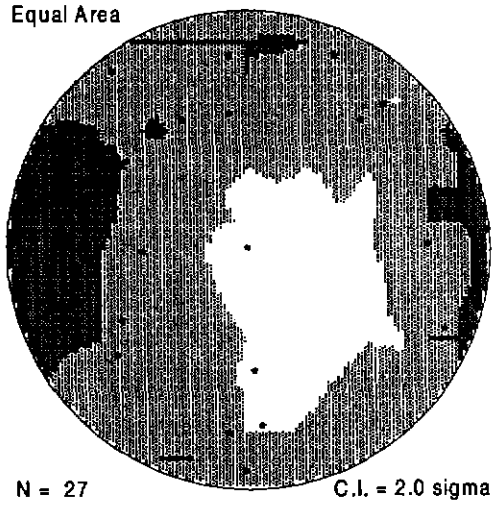
Measured cleavage 1



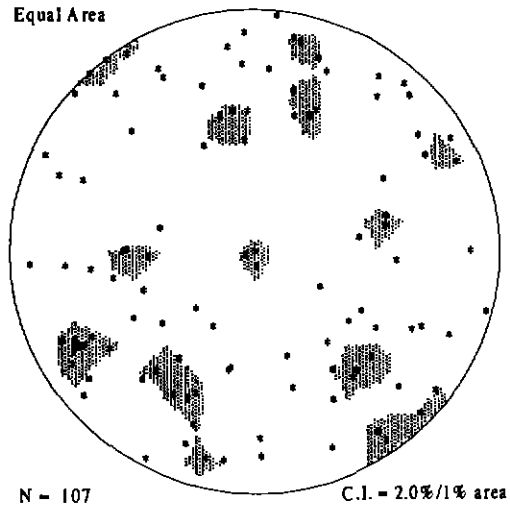
Measured cleavage 2



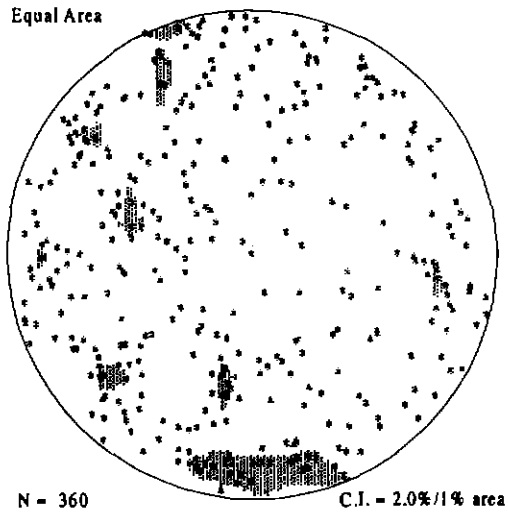
Measured cleavage 3



Combined cleavages



Bedding poles



APPENDIX 3.

Drillhole data

ZS1 DRILLCORE LOG

Hole: **ZS1, RTZ-CRA Exploration**

Prospect: **Stonehenge, Zeehan**

AMG East: **359800**

North: **5359300**

Surveys:

Depth	Azim (AMG)	Dip
0	60	-50
83	66	-51.5
166	63	-53
241	63	-52.5

Lithological Summary:

From	To	Form	Comments
0	14.3	Qha	*Overburden - no recovery*
14.3	68.1	Pos	*Quartzite, phyllite, black shales - often brecciated*
68.1	72.9	Pos	*Dolomitic limestone with thin laminated shales*
72.9	121.2	Pos	*Shales silts and sands, minor dolomitic limestone*
121.2	167	Posd	*Dolomitic limestone with shale interbeds*
167	200	Posb	*Black shales with silts, sands and minor dolomitic limestone*
200	203	Posd	*Dolomitic limestone*
203	213	Pos	*Interbedded sands and silts*
213	223.7	Posd	*Dolomitic limestone*
223.7	241.5	Posb	*Black shales*
241.5	251	Posb	*Black shales with minor sands and silts*

Mineralisation Summary:

From	To	Comments
119.2	121.35	*2.15m @ 7.78% Zn, 10.08% Pb, 191.3 ppm Ag*
143.5	162.85	*19.35m @ 1.52% Zn, 0.041% Pb, 5.7 ppm Ag*
223.8	234	*10.2m @ 1.40% Zn, 0.046% Pb, 9.8 ppm Ag*

Depth (m)		Core Description	Special Features
From	To		
14.3	30.4	Beige coloured quartzite/sandstone. Fine grained.	Bedding sub-parallel to C/A. Cleavage intersection 30deg to So
30.4	34.53	Weathered (crumbly) sandstone	
34.53	37	Broken quartz fragments	
37.4	43.8	Grey to black quartzite - rotted. Possible breccia zone	So 45deg to C/A
43.8	51	Black sandy shale, possibly rotted phyllite?	Fine disseminated pyrite throughout. Bedding 90deg to C/A. Yellow/orange veining 45 and 90deg to C/A
51	52	Breccia zone	
52	58	No recovery	
58	60	Broken shale fragments, some quartzites	
60	61.2	Grey quartzite - rotted to black	Sphalerite discolouring?
61.2	68.1	Graphitic black shales. Possible vertical breccia zone @ 62.8m. Shear zone form 65-66.3m	So 90deg to C/A. Sphalerite in small veins. Pyrite localised in disseminated groupings (very fine). Yellow/orange veining 5deg C/A - small fizz. Bedding 70deg to C/A @ 66.5m, 45deg @ 67.5m. Fractures 45deg to C/A
68.1	70	Light grey to white crumbly dolomitic limestone. Dull colouring.	Sphalerite in veins of orange to brown colour, gen 45deg to C/A. Minor quartz veining. Fractures @ 10deg to C/A.
70	70.2	Thinly laminated silts.	Quartz-calcic? veining 90deg to So. Sphalerite specks throughout. Bedding from 50-70deg to C/A
70.2	71.1	Breccia zone.	Prominent fracture 15deg to C/A
71.1	72.9	Dark to light grey dolomitic limestone. Dull colouring.	Localised disseminated pyrite throughout. Sphalerite generally within veins - parallel to C/A and offset by movement 90deg to C/A. So generally 60deg to C/A.
72.9	80	Thin laminae contact with phyllites. Black shales and light coloured quartzite/sandstone.	Sphalerite within veins as localised blobs. Fine disseminated pyrite throughout. Minor galena? Quartz/calcite veining 10deg to C/A. So 40deg to C/A @ 74.1m. Breccia zone 74.4-75.8m. Quartz vein <40mm 45deg to C/A @ 73.4m

Depth (m) From	To	Core Description	Special Features
80	90.4	Light to dark grey shale, heavily veined	So 15deg to C/A. Veins parallel and 90deg to C/A. Major vein at 87.5m, 10deg to C/A, <60mm.
90.4	102.1	Fine black shales.	Very fine disseminated pyrite, sphalerite as specks and within veins. Fawn coloured veining.
102.1	119.2	Broken core - poor recovery. Grey to black shales.	Sphalerite within veins. Veins fizz (quartz/calcite?). Major veins at 113.9-114.3, sub parallel to C/A.
119.2	120	Dolomitic limestone.	Heavily veined with large sphalerite grains and fine disseminated pyrite.
120	121.2	Strongly mineralised zone - altered to grey/red heavy ore.	Sphalerite zones and fine galena.
121.2	123.6	Dull grey dolomitic limestone.	Quartz calcite veining containing some sphalerite.
123.6	123.7	Grey quartzite.	Very fine local disseminations o f sphalerite, pyrite and galena
123.7	147.5	Light grey dolomitic limestone.	Calcite and quartz/calcite veining containing occasional clumps of fine disseminated galena, sphalerite and pyrite. Also large clusters of sphalerite within veins. Veining is generally sub-parallel to C/A. Veining @ 90deg to C/A more prominent - later.
147.5	152.2	Broken grey dolomitic limestone.	Fine local disseminations of sphalerite, pyrite and galena.
152.2	154.6	Interbeds of black shales within quartzite.	Fine sphalerite, pyrite and galena.
154.6	167	Grey dolomitic limestone.	Sphalerite predominant in veins, some pyrite and galena. Veining generally 80deg to C/A - thick quartz vein @ 166-166.5m, sub-parallel to C/A. Fault displacement sub-parallel to C/A @ 160.5m
173.8	175	Black shales.	Heavily veined and distorted.
175	179.4	Laminated black shale. Possible unconformity between shales and limestone.	So generally sub-parallel to 15deg to C/A. Quartz veining 85deg to C/A.
179.4	180	Quartz rich shale - quartzite with black shale fragments/zones.	
180	200	Laminated black shale.	So sub-parallel to C/A. Quartz veining @ 85 and 45deg to C/A. Fault movement @ 60deg to C/A (eg. @ 197.6m). Small brecciation zone.

Depth (m)		Core Description	Special Features
From	To		
200	203	Dark grey shales/dolomitic limestone.	Specks of sphalerite and galena within veins - generally 10 to 85deg to C/A.
203	213	Laminated shales (black), sands and silts.	Minor quartz veining and fault displacement.
213	221.9	Dolomitic limestone.	Fine disseminations of sphalerite and galena. Pyrite about the edge of veins, within brecciated zones, and in localised areas throughout. Fawn coloured veining - heavy beyond 217m. Breccia zones @ 215.6m and 218.4-218.6m
221.9	223.7	Grey coloured shales.	Breccia zone with moderate veining.
223.7	241.5	Black shales.	Generally fractures throughout. Fine pyrite associated with quartz grains.
241.5	251	Black shales.	Generally folded/brecciated zone. Fawn coloured veining with minor sphalerite associated.

ZS2 DRILLCORE LOG

Hole: **ZS2, RTZ-CRA Exploration**

Prospect: **Stonehenge, Zeehan**

AMG East: **359800**

North: **5359385**

Surveys:

Depth	Azim (AMG)	Dip
0	60	-45
83	64	-47
166	64.5	-50
249	66.5	-52

Lithological Summary:

From	To	Form	Comments
0	10	Qha	*Overburden - no recovery*
10	30	Pos	*Rotted dolimitic limestone with argillaceous interbeds, minor sands and shales*
30	41.7	Pos	*Calacreous sediment with sands and minor silts*
41.7	55	Pos	*Micaceous silts and shales with minor dolimitic limestone*
55	85.4	Pos	*Argillaceous silt/shale laminae, minor sands*
85.4	100.4	Pos	*Dolomitic limestone (rotted) with shale/silt beds*
100.4	103	Pos	*Sulphide zone*
103	133	Pos	*Rotted dolomitic limestone*
133	151	Posb	*Graphitic black shales*
151	165.8	Posd	*Dolomitic limestone*
165.8	170.6	Pos	*Broken core - clay*
170.6	191	Pos	*Black shales, silts, sands with minor dolomite*
191	216.7	Pos	*Dolomitic limestone (rotted and arenaceous). Sands and silts*
216.7	250	Pos	*Arenacous dolomitic limestone (rotted) with silts and shales*

Mineralogical Summary:

From	To	Comments
100.5	136	*35.5m @ 2.13% Zn, 0.56% Pb, 10.4 ppm Ag*
190.25	191	*0.75m @ 7.12% Zn, 4.48% Pb, 0.98 ppm Cu*

Depth (m)		Core Description	Special Features
From	To		
10	22.5	Generally broken black shales and silts; minor dolomitic limestone?	So generally sub parallel to C/A. Considerable veining containing sphalerite and fine disseminated pyrite.
22.5	25	No recovery.	
25	27.7	Dolomitic limestone containing some angular quartz fragments.	
27.7	30	Generally dolomitic limestone (rotted) with minor sand and silts layers.	Veining generally sub parrel to C/A.
30	41.7	Primarily grey sands and silts	So varies from 85 deg to sub parallel to C/A. Brown (siderite?) colouring of veins often 60 deg to C/A.
41.7	48.8	Silts and shales often folded.	So generally 70 deg to sub parallel to C/A. Orange brown veining (siderite?) containing fine sphalerite.
48.8	49.5	Primarily sands and silts with minor shale bands. Small bands of dolomitic limestone?	Fine locally massive disseminations of pyrite and sphalerite.
49.5	55	Sands, silts and shales.	So generally sub parallel to C/A. Quartz-calc veining 85 deg to sub parallel to C/A contains small groups of disseminated sphalerite.
55	66	Grey silts and sands with minor shale bands.	So 85 deg to C/A. Fine pyrite disseminated throughout minor veining present.
66	81	Laminated silts and shales grading into sands.	So 85 deg to C/A. Locally massive sphalerite zones (eg. 71.6 to 72m).
81	81.3	Breccia zone.	
81.3	85.4	Silts, shales and occasional sands.	So 70 deg to C/A.
85.4	91.1	Dolomitic limestone with zones of silts and shales.	So generally near 90 deg to C/A. Considerable veining often fawn/brown in colour. Fine disseminated pyrite.
91.1	100.4	Rotted dolomitic limestone? of dark grey colour.	Fawn coloured veining.
100.4	103		Heavily mineralised zone of massive sphalerite and pyrite with minor amounts of galena.

Depth (m) From	Depth (m) To	Core Description	Special Features
103	133	Generally rotted grey to black dolomitic limestone.	Quartz-calc veining containing sphalerite and pyrite disseminations, and minor galena. Mineralisation increasing with depth.
133	151	Broken and fragmented graphitic black shales.	
151	161.4	Dolomitic limestone? dark grey to black - rotted at base.	Minor orange coloured veining containing sphalerite blobs.
161.4	165.8	Breccia zone of grey to black rotted dolomitic limestone.	So sub parallel to C/A @ 161.5m Veining generally sub 90 deg to C/A containing small sphalerite blobs.
165.8	170.6	Breccia zone of grey to black rotted dolomitic limestone.	
170.6	172	Shales (black) and silts.	Moderate veining containing some fine disseminated pyrite.
172	173.7	Breccia zone of black to light grey sands, silts and shales.	Very fine local disseminations o f sphalerite, pyrite and galena
173.7	176.5	Black shales with minor sands and silts.	So generally 80 deg to C/A. Prominent veining parallel and 90 deg to So containing locally disseminated pyrite.
176.5	179.4	Fine grey sandstone or arenaceous siltstone.	Vein 45 deg to C/A @ 177.9m generally <15mm - contains brecciated fragments. Smaller fawn coloured veins contain minor disseminated pyrite.
179.4	187	Generally broken black shales containing minor silts. Black to grey in colour.	Minor pyrite present as blobs and localised disseminations.
187	187.8	Breccia zone? with considerable veining.	
187.8	190.3	Black shales with light grey rock fragments - breccia zone.	Minor pyrite within veining.
190.3	190.45		Heavily mineralisation of pyrite, sphalerite and galena.
190.45	191	Broken (rotted) zone	
191	192.7	Breccia zone of grey dolomitic limestone rock fragments.	
192.7	200.1	Grey phyllite and dolomitic limestone.	Fawn coloured veining containing very fine pyrite disseminations. Generally brecciated zone.

Depth (m)		Core Description	Special Features
From	To		
200.1	208	Rotted silts, sands and shales - grey to black in colour.	So generally 85 deg to C/A.
208	211.6	Grey quartzite? dolomitic limestone?	Prominent vein sub parallel to C/A <15mm. Smaller veining 90 deg to C/A.
211.6	215	Generally brecciated zone light to dark grey dolomitic limestone.	Large quartz vein from 211.9 to 213m
215	216.7	Grey quartzite? with black veining.	Fine pyrite and sphalerite within veining.
216.7	221	Broken/rotted black to grey shale and dolomitic limestone.	
221	222.6	Black silts and shales.	So generally parallel to 60 deg to C/A. Breccia zone also parallel to C/A.
222.6	238.8	Grey to black silts, sands and shales - often rotted.	So 60 deg to C/A @ 232.5m
238.8	245.4	Sandstone with minor shales (often rotted - black).	So 80 deg to C/A @ 239.2m Veining <10mm generally cutting So @ 80 deg.
245.4	250	Brown to grey sandstone.	

ZS3 DRILLCORE LOG

Hole: **ZS3, RTZ-CRA Exploration**

Prospect: **Stonehenge, Zeehan**

AMG East: **359625**

North: **5359450**

Surveys:

Depth	Azim (AMG)	Dip
0	200	-45
83	?	-50
166	197	-50.5
231	196	-51

Lithological Summary:

From	To	Form	Comments
0	9	Qha	*Overburden - no recovery*
9	43	Pom	*White chalky clay*
43	46	Pom	*Sands with angular quartz fragments (<5mm)*
46	52	Pom	*White chalky clay with angular quartz/rock fragments*
52	57.6	Posb	*Black graphitic shale/clay*
57.6	73	Pom	*Grey to white weathered siltstone/shale - sericitic*
73	94	Pom	*Silicified phyllite with quartz veining*
94	130	Pom	*Dark grey to black siltstone/shale*
130	137	Pos	*Interbedded sands and silts - silicified*
137	137.8	Posb	*Dolomite*
137.8	171	Pos	*Calcareous (dolomitic) sands and silts*
171	187.4	Pom	*Laminated sands, silts and shales*
187.4	205.4	Pom	*Micaceous sands, silts and shales*
205.4	231	Pom	*Semi-massive sandstone with minor silts and shales*

Lithological Summary:

From	To	Comments
64	73	*9.0m @ 0.42% Zn, 0.38% Pb*
130	133	*3.0m @ 0.9% Zn, 0.36% Pb*
159.5	160.6	*1.1m @ 3.5% Zn, 0.1% Pb*

Depth (m)		Core Description	Special Features
From	To		
9	28	Light grey to white clay.	
28	31	Orange to brown friable clay.	
31	43	Light grey to white clay - chalky. Quartz fragments @ 40m	
43	46	Loose coarse sand, non-cohesive. Angular quartz fragments <5mm.	
46	50.5	Light grey to white chalky clay containing small rock fragments <10mm. NB no recovery from 49-50.5m	
50.5	50.8	Orange/brown/grey clay containing angular rock fragments.	
50.8	52	Light grey to white fine silt with minor rock fragments and angular quartz fragments.	
52	57.6	Graphitic black shale - generally broken with some quartz fragments.	Possible So 40deg to C/A
57.6	73	Light grey to white siltstone - broken and weathered. NB 66.8-67m: orange to brown possible breccia zone with broken rock fragments.	So possibly parallel to C/A (generally), 90deg to C/A @ 66.8m.
73	94	Phyllite, generally broken with minor quartz fragments. Dolomitic zone?	Pyrite blobs within quartz-quartz/calcic veining. Veins 90deg to C/A.
94	98	Folded black shale.	So generally 40deg to C/A. Minor pyrite dissemination throughout.
98	100	No recovery.	
100	106	Generally broken grey to black shale containing minor quartz fragments.	
106	130	No recovery.	
104.8	130	Random sample (possibly 126-130m). Broken black shale containing some quartz.	Fine disseminated pyrite throughout.
130	133	Thin laminae of grey to black fine sandstone/shale.	So 70deh to C/A. Pyrite disseminated throughout and locally massive (within veins). Veining parallel to C/A.
133	135.3	No recovery.	

Depth (m)		Core Description	Special Features
From	To		
198	202	Grey phyllites.	So 70deg to C/A @ 199m and 80deg @ 200m. Quartz veining parallel to and 90deg to C/A contains minor.
202	205.4	Laminated silts and shales.	
205.4	231	Phyllites with minor silts and shales.	So varies from 45deg to 90deg to C/A. Veining generally 90deg to C/A contains sphalerite and pyrite.

Depth (m) From	To	Core Description	Special Features
135.3	137	Thinly laminated silts and sands, grey to black in colour.	So and veining 70deg to C/A. Quartz calcic veining, often with orange discolouring - dolomitisation? Fine pyrite disseminations. Brecciation zone at the base.
137	137.02	Breccia zone 75deg to C/A.	
137.02	152	Grey phyllite with zones of black shale. Dolomite from 137.02-137.8m	So 45deg to C/A @ 139m, and 10deg @138.4m. Veining 70deg and 15deg to C/A. Minor sphalerite within small veins. Fine dissemination of pyrite and galena @ 145m.
152	153	Breccia zone.	
153	159.5		Prominent veining 40-60deg to C/A. Lesser veining 90deg to major veining.
159.5	162.5	Black shales.	So 70deg to C/A @ 159.7m Faulting parallel to C/A - 18mm displacement. Veining towards the base contains pyrite along its perimeters. Sphalerite within small veins parallel to C/A - minor localised galena.
162.5	168.4	Sands and shales grading into sandstone/quartzite.	Heavily veined, generally 90deg to C/A. Sphalerite common throughout.
168.4	170.2	Sands and shales.	So 70deg to C/A. Heavily veined - containing massive sphalerite.
170.2	171	Breccia zone.	Intense shearing and faulting. Quartz/calcic veins contain minor disseminated pyrite.
171	171.2	Thinly laminated black shales.	So 80deg to C/A. Faulting parallel So. Veining parallel and 45deg to C/A.
171.2	171.5	Breccia zone.	Heavily veined.
171.5	187.4	Laminated sands, silts and shales.	So 50deg to C/A @ 173.6m, 45deg @ 177.7m, 70deg @ 176.9m and 40deg @ 191m. Minor veining parallel to C/A. Occasional pyrite within veins.
187.4	188.3		Generally quartz veined zone containing massive pyrite and fine galena locally.
188.3	198	Black shales with thinly laminated sands and silts.	So 85deg to C/A @ 188.8m, 30deg @ 190.3m, 45deg @ 194m and 50deg @ 196.8m. Orange veining common. Large quartz vein @ 195m <100mm.

ZS31 DRILLCORE LOG

Hole: **ZS31 RTZ-CRA Exploration**

Prospect: **Stonehenge, Zeehan**

AMG East: **359733**

North: **5359462**

Surveys:

Depth	Azim (AMG)	Dip
0	200	-50
50	201	-52
100	202	-49
150	201	-47.5
200	198	-47

Lithological Summary:

From	To	Form	Comments
0	2.5	Qha	Overburden - no recovery
2.5	14.7	Posb	Light brown to black clay and graphitic shale
14.7	40.5	Posb	Sheared black shales - generally mineralised zone
40.5	52.8	Pom	Buff to brown medium grained sandstone
52.8	68.35	Pos	Sandstone, laminated siltstones and dolomitic limestones
68.35	78.4	Pom	Buff sandstone and siltsone
78.4	114.8	Pos	Sanstone with silstone, shales and dolomitic limestone
114.8	147.8	Pos	Fine grained sandstones, laminated siltstones and black shales
147.8	152.95	Posd	Dolomitic limestone (rotted) with fine sandstone interbeds
152.95	158.3	Posb	Sheared siltstone and black shales with massive pyrite
158.3	171	Pos	Sandstone and silts with occasional shales and quartzite
171	241.5	Poq	Massive grey quartzites
181.5	209.5	Poq	Predominantly massive quartzite with interbedded units of laminated silts, shales and quartzites

Mineralogical Summary:

From	To	Comments
30.35	40.5	6m @ 6% Zn, Ag <119 ppm
152.95	156.2	2.51% Zn, 30 ppm Ag

Depth (m)		Core Description	Special Features
From	To		
2.5	4.5	Dark brown clay - rotted or leached from overburden.	
4.5	6.2	Light brown sandy clay containing quartz fragments.	
6.2	7.8	Soft black clay - high plasticity.	
7.8	11.9	Black shales, sheared and fractured - thinly laminated.	Fine quartz veining. So parallel to C/A.
11.9	13.1	Light grey shale.	So parallel to C/A.
13.1	14.5	Sheared black shales.	
14.5	14.7	Light grey fine grained sandstone?	
14.7	26.5	Sheared and broken black shales.	Small quartz veins and fine pyrite throughout.
26.5	28.5	Alternating light grey/black shales.	So 90deg to C/A @ 27.6m.
28.5	31.5	Sheared black shales.	Minor quartz veining. Pyrite disseminated throughout and within quartz veins (eg. @ 30.7m). Quartz showing boxworks with pyrite therein.
31.5	34.5	More argillaceous rock with black shale fragments and quartz. Minor silicification of shales.	Sphalerite sparsely disseminated throughout. Pyrite present as disseminations and bands.
34.5	34.85	Light grey fine-grained sandstone/siltstone	
34.85	35.2	Black clay - sheared black shales.	Fine grained disseminated pyrite and minor sphalerite.
35.2	37	Black clays with local silicified shales.	Massive pyrite, sphalerite and galena, with disseminations of pyrite and sphalerite. Fine quartz veins throughout.
37	37.5	Folded and fractured black shales - minor silicification.	Quartz veining. Pyrite present as small blobs.
37.5	10.1	Light to dark grey clay - fractured black shales. Quartz fragments and angular buff coloured shales beyond 39m.	Disseminated pyrite and minor sphalerite throughout.
10.1	40.5	Fractured black shales.	Quartz veining common. Disseminated pyrite within shales and fractured quartz fragments. Locally massive sphalerite and pyrite.

Depth (m)		Core Description	Special Features
From	To		
40.5	48.1	Light grey, orange and cream coloured siltstones and shales - heavily sheared, with some interbedded sandstones.	Major quartz vein at 40.5m. So parallel to C/A.
48.1	49.5	Dark grey to brown shale/fine siltstone containing small angular quartz fragments.	So 90deg to C/A?
49.5	51.5	Light grey to buff, fine-grained, sandstone unit. Generally folded throughout.	So 50deg to C/A.
51.5	52.8	Sheared sandstone with fractured angular quartz fragments. Light to dark grey and brown in colour.	
52.8	60	Light to dark grey and brown siltstone/sandstone. Locally siliceous and generally rotted to clay	Minor quartz veining and folding. So 60deg to C/A.
60	61.5	Light to dark grey thinly laminated siltstone (calcareous?). Possibly fine-grained sandstone.	Broken quartz veins throughout. Sphalerite occasional and small pyrite disseminations locally (eg. @ 60.1m).
61.5	63	Brown to dark grey sheared fine-grained sandstone.	Quartz veining common.
63	65.9	Dark grey to black sandstone - medium-grained. Very deformed and silicified.	Quartz veining (some post deformation). Dark brown sphalerite colouring and fine disseminations.
65.9	66.4	Dark grey fractured sandstone.	Quartz veining in upper regions.
66.4	67.1	Grey medium-grained sandstone.	Quartz veining with dark grey to black alteration zones. Red discolouring - siderite alteration?
67.1	67.2	Altered/decomposed sandstone - black and crumbly.	Massive sphalerite with zones of minor galena.
67.2	67.5	Strongly silicifies sandstone.	Sphalerite specks and minor galena.
67.5	68.35	Light and dark grey sandstone - altered (quartz-sericite?)	Latter vein intrusion 30-40deg to C/A.
68.35	78.4	Light brown/buff coloured sands, silts and shales. Sandstone thickly bedded. Siltstones fining upwards.	Interbedded sands, silts and shales showing sericite alteration? So generally parallel to C/A - 40deg @ 74m and 55deg @ 74.5m. Quartz vein from 74.6-75.5m.

Depth (m)		Core Description	Special Features
From	To		
78.4	91.5	Light to dark grey fine-grained sandstone/siltstone interbeds. Heavily veined and silicified.	So 30deg to C/A. Carbonaceous veining (occasional sericite alteration?). Quartz vein @ 87.4m <15mm wide, 30 deg to C/A. Latter veining period generally 30-45deg to C/A. Local zones of pyrite.
91.5	95.5	Interbedded siltstones and shales, very tightly folded. Dark grey to black with minor fine-grained sandstones.	Quartz veining - large vein @ 91.9m. Localised zones of pyrite throughout.
95.5	100.5	Grey to light grey thinly laminated sands (fine), silts and shales.	Localised pyrite zones. Quartz veining common.
100.5	100.6	Breccia zone of grey sandstone/siltstone fragments within dark grey almost silicified matrix.	
100.6	105	Predominantly fine-grained sandstone with siltstone interbeds. Sequence folded and faulted. Breccia zones (eg. 104.2m) with small sandstone/siltstone clasts.	Local pyrite clasts and specks. Dominant quartz veins 90deg to C/A, <15mm thick. Fine veining <70deg to C/A. Light blue-opaque veining possibly dolomitic?
105	107.9	Altered fine grained sandstone, light to dark grey colouring (limestone?).	Heavily veined - quartz and carbonate accounting for 50% rock.
107.9	109.3	Weakly calcareous sandstones with thin shale beds.	So (shales) <10mm, 80deg to C/A. Fault displacement of veins - prominent veining 108.5-108.8m
109.3	111	Fine grained calcarenite - dolomitisation? of light to dark grey colour.	Quartz carbonate veining generally <3mm. Initial veins parallel to C/A, second set 90deg to C/A.
111	113.5	Calcareous medium-grained limestone - calcarenite? Light yellow staining, possible dolomitisation.	Thin veins containing fine pyrite are generally parallel to <20deg to C/A.
113.5	114.8	Light grey medium-grained sandstone, grading into thinly laminated siltstone. Possible dolomitisation.	Quartz/calcite veining dominantly 90deg or <15deg to C/A. Faulting 45deg to C/A.
114.8	117	Sandstone grading into thinly laminated shales and siltstones - dark grey to black in colour.	So varies from 60-90deg to C/A - beds appear gently folded. Small joints 90deg to C/A. Quartz/calcite veining containing pyrite clasts. Thick veins @ 116.5m.
117	124	Light grey sandstone with minor siltstone/shale interbeds (dark grey to black). Quartz grains towards base. Minor silicification and possible dolomitisation throughout.	Quartz veining often discoloured to light rusty brown colour. Atleast 2 sets of veins - dominant 45deg to C/A, minor parallel to C/A. Pyrite is present as fine disseminations within veins and as small groupings in sandstone.

Depth (m) From	To	Core Description	Special Features
124	126.1	Dark grey thinly laminated siltstone.	So generally 10deg to C/A. Veining parallel to C/A - quartz/calcite towards base. Pyrite as blobs <20mm within the veins.
126.1	133.2	Interbedded fine-grained sandstone, siltstone and shale. Light grey to black in colour. Local silicification.	So generally parallel to C/A. Fine grained disseminated pyrite in masses throughout quartz-carbonate veins. Sphalerite occasionally present within veins.
133.2	140.2	Light grey, fine-grained sandstone - bioturbated. Some minor siltstone and shale interbeds.	138.5-139m - heavily veined zone showing brecciation. Large breccia zone 134.2-137.4m. Quartz-carbonate veining prominently 60deg to C/A. Pyrite with minor sphalerite and galena within veins (chalcopyrite?).
140.2	141.8	Breccia zone.	Veining (quartz-carbonate) with some disseminated pyrite, galena and sphalerite (eg. 141.3m).
141.8	146.3	Dark grey to black siltstone showing minor silicification. Beds becoming sands/silt/shale laminae.	So 80deg to C/A. Dominant veining 60deg to C/A, secondary 30deg to C/A. Veins often light orange in colour (quartz-carbonate).
146.3	147.5	Thin laminations of sandstone, siltstones and shales - light to dark grey in colour.	So varies from parallel to 90deg to C/A. Quartz-carbonate veining <3mm, generally 80deg to C/A - increased veining with depth, often containing breccia zone.
147.5	147.8	Silicified calcareous zone - fractured.	Quartz veining. "Simon says bioclastic calcarenite"
147.8	148.5	Grey to black (rotted?) zone	Breccia with quartz-carbonate veining. Galena, sphalerite and pyrite within veins and rock.
148.5	150.15	Light to dark grey limestone.	Strongly veined, generally @ 30-55deg to C/A - some discolouration (dolomitisation?).
150.15	150.9	Black rotted limestone/sandstone.	Strong quartz-carbonate veining - minor dolomitisation?
150.9	152.95	Silicified limestone? - light to dark grey in colour.	Quartz-carbonate veining 40deg to C/A, often cross-cutting. Pyrite within veins @ 152.05m - 75deg to C/A. Minor disseminated pyrite in the rock.
152.95	154.55	Black shales? sands and silts.	Sheared zone, heavily veined (quartz-carbonate). Locally massive pyrite and disseminated sphalerite and galena.

Depth (m)		Core Description	Special Features
From	To		
154.55	156.2	Black shales and fine-grained sandstones.	Quartz veining - often sheared. Massive pyrite within sandstones. Fine sphalerite disseminations throughout.
156.2	156.8	Minor argillaceous material.	Fawn coloured dolomitic vein? containing heavily disseminated/semi-massive pyrite.
156.8	157.8	Light to dark grey, medium-grained sandstone.	Fawn coloured dolomitic veins containing fine disseminated pyrite.
157.8	158.3	Sheared black shale.	So possibly 45deg to C/A.
158.3	159	Light grey fine-grained sandstone and siltstone.	Zones of semi-massive pyrite (fine) and minor sphalerite groupings.
159	162.6	Medium grained sandstone with siltstone and shale interbeds. Shales becoming more prominent with depth - flat dipping and thinly laminated.	So 75deg to C/A. Sheared quartz veining and occasional dolomitic veining generally parallel to C/A.
162.6	165.4	Quartzite/sandstone grading into dark grey graphitic shale.	Minor fine quartz and dolomitic? (fawn coloured) veining.
165.4	166.1	Dark grey shale and light grey sandstone unit.	Quartz and dolomitic veining. Veinlets contain fine pyrite. Substantial; folding throughout.
166.1	171.1	Black shales with thinly laminated siltstones interbeds.	Pyrite exists as fine lenses along bedding. More substantial pyrite at the base is associated with quartz/dolomitic veining, and in quartz veins (eg. @ 168.5m, 30deg to C/A).
171.1	181.5	Grey coloured massive quartzite.	Possible bedding of 65deg to C/A. Thick quartz vein @ 179.6m and 194.3m, 40deg to C/A. Veins often faulted. Pyrite zones associated with veining.
181.5	191.5	Predominantly grey quartzite with laminated silt/shale interbeds (fining up).	Prominent quartz veining 30deg and 90deg to C/A. Strongly sheared/brecciated/veined zone @ 188.5m contains galena and minor pyrite.
191.5	196.2	Predominantly grey quartzite with silt and shale lenses <50mm.	So 70deg to C/A. Quartz and dolomitic veining with occasional tension gashes. Veins generally 45deg to C/A.
196.2	205.7	Black shales with lenses of silts and quartzites.	Possible breccia zone beyond 205m. Considerable folding and faulting throughout. Quartz and dolomitic veining. Minor pyrite and galena within dolomitic veins.

Depth (m)		Core Description	Special Features
From	To		
205.7	206.8	Silicified grey sandstone and quartzite.	Quartz veins throughout.
206.8	209.5	Grey quartzite with dark grey shale and silt units.	Large quartz veins and reddish/brown dolomitic veins?

TH13 DRILLCORE LOG

TH13 as logged by Gold Fields Exploration Pty. Ltd.

Hole: **TH13,Gold Fields Exploration**

Prospect: **Stonehenge, Zeehan**

AMG East: **360149**

North: **5359431**

Surveys:

Depth	Azim (AMG)	Dip
0 - 431	021	-46

Lithological Summary:

From	To	Form	Comments
0	10	Pos?	*Overburden*
10	64	Pos?	*Poor recovery (weathered dolomite or fault zone)*
64	75.3	Pos?	*Mineralised breccia*
75.3	165.5	Posd	*Altered dolomite*
165.5	220.2	Pos	*Dolomitic siltstone*
220.2	272.8	Pos	*Shale*
272.8	389.4	Posd	*Dolomite*
389.4	397.7	Posb	*Black shale*
397.7	418.2	Pos	*Quartz-dolomite vein*
418.2	421	Posd	*Dolomite*

Mineralisation Summary:

From	To	Comments
64.0	75.3	*11.3m @ <0.01% Sn, 0.13% Pb, 0.43% Zn, 6 ppm Ag*
87.0	148.0	*61.0m @ <0.01% Sn, 0.90% Pb, 0.59% Zn, 29 ppm Ag*
418.0	422.0	*3.8m @ <0.01% Sn, 0.01% Pb, <0.01% Zn, <1 ppm Ag*

TH14 DRILLCORE LOG

TH14 as logged by Gold Fields Exploration Pty. Ltd.

Hole: **TH14,Gold Fields Exploration**

Prospect: **Stonehenge, Zeehan**

AMG East: **359318**

North: **5359841**

Surveys:

Depth	Azim (AMG)	Dip
0 - 170	202	-55

Lithological Summary:

From	To	Form	Comments
0	37.8	Pos?	*Overburden*
37.8	48.6	Pos	*Poor recovery (weathered dolomite or fault zone)*
48.6	55.1	Pos?	*Mineralised breccia*
55.1	58.7	Posd	*Altered dolomite*
58.7	67.35	Pos	*Dolomitic siltstone*
67.35	68.5	Pos	*Shale*
125.7	170	Posd	*Dolomite*

Mineralisation Summary:

From	To	Comments
37.8	48.5	*10.7m @ <0.01% Sn, 0.12% Pb, 0.04% Zn, 2 ppm Ag*
55.1	58.7	*3.6m @ <0.01% Sn, 0.02% Pb, 0.05% Zn, 1 ppm Ag*
143.1	147.0	*3.9m @ <0.01% Sn, 0.24% Pb, <0.01% Zn, 7 ppm Ag*

TH15 DRILLCORE LOG

TH15 as logged by Gold Fields Exploration Pty. Ltd.

Hole: **TH15,Gold Fields Exploration**

Prospect: **Stonehenge, Zeehan**

AMG East: **360249**

North: **5359695**

Surveys:

Depth	Azim (AMG)	Dip
0 - 599	201	-60

Lithological Summary:

From	To	Form	Comments
0	61.4	Poq	*Quartzite*
61.4	206	?	*Fault zone (breccia and clay)*
206	240.8	Pos	*Interbedded black shale and dolomite*
240.8	305.7	Pos	*Black shale and siltstone*
305.7	369.2	Pos	*Interebedded black shale and dolomite*
369.2	464.1	Posb	*Black shale*
464.1	487.3	Pos	*Interbedded black shale and dolomite*
487.3	508.85	Posd	*Dolomite*
508.85	518.6	Posb	*Black shale*
518.6	521.6	Pos?	*Pyritic mineralised zone*
521.6	557.8	Posd	*Dolomite*
557.8	563.75	Pos?	*Pyritic mineralised fault zone*
563.75	599	Pos	*Dolomite and minor black shale*

Mineralisation Summary:

From	To	Comments
61.4	100.5	*39.1m @ <0.01% Sn, 0.30% Pb, 0.21% Zn, 7 ppm Ag*
167.0	191.0	*324m @ <0.01% Sn, 0.27% Pb, 0.54% Zn, 1 ppm Ag*
557.8	563.75	*3.9m @ <0.01% Sn, 0.22% Pb, <0.12% Zn, 35 ppm Ag, 0.08% Cu 0.43% As, 0.05% Sb*

TH16 DRILLCORE LOG

TH16 as logged by Gold Fields Exploration Pty. Ltd.

Hole: **TH16,Gold Fields Exploration**

Prospect: **Stonehenge, Zeehan**

AMG East: **360490**

North: **5360002**

Surveys:

Depth	Azim (AMG)	Dip
0	250	-50
120	246	-51
206	248	-51.4
320	250	-48.3
400	248	-46.7

Lithological Summary:

From	To	Form	Comments
0	14.1	Pom	*Sandstone, siltstone - intraformational breccia*
14.1	26.4	Pom	*Pyritic grit, sandstone*
26.4	148.8	Pom	*Interbedded sandstone and shale*
148.8	240.9	Pom	*Quartz/carbonate veined, partially brecciated sandstone and shale*
240.9	396.7	Pom	*Interbedded sandstone and shale*
396.7	402.5	Pos	*Quartz-carbonate zone*
402.5	432.3	Pos	*Quartz-carbonate stockwork in shales*
432.3	450	Pos	*Shale and minor ?dolomitic sandstone*

Mineralisation Summary:

From	To	Comments
333	336.2	*3.2m @ 0.7% Sn, <0.02% Pb, <0.02% Zn, 0.12% Cu*
382.3	382.8	*0.5m @ 0.1% Sn, 0.16% Pb, 0.03% Zn, 0.21% Cu*

TH17 DRILLCORE LOG

TH17 as logged by Gold Fields Exploration Pty. Ltd.

Hole: **TH17, Gold Fields Exploration**

Prospect: **Stonehenge, Zeehan**

AMG East: **359690**

North: **5359619**

Surveys:

Depth	Azim (AMG)	Dip
0	290	-63.2
50.6	286	-62
128	287	-57.4
227	289	-53.4
296	292	-52.9

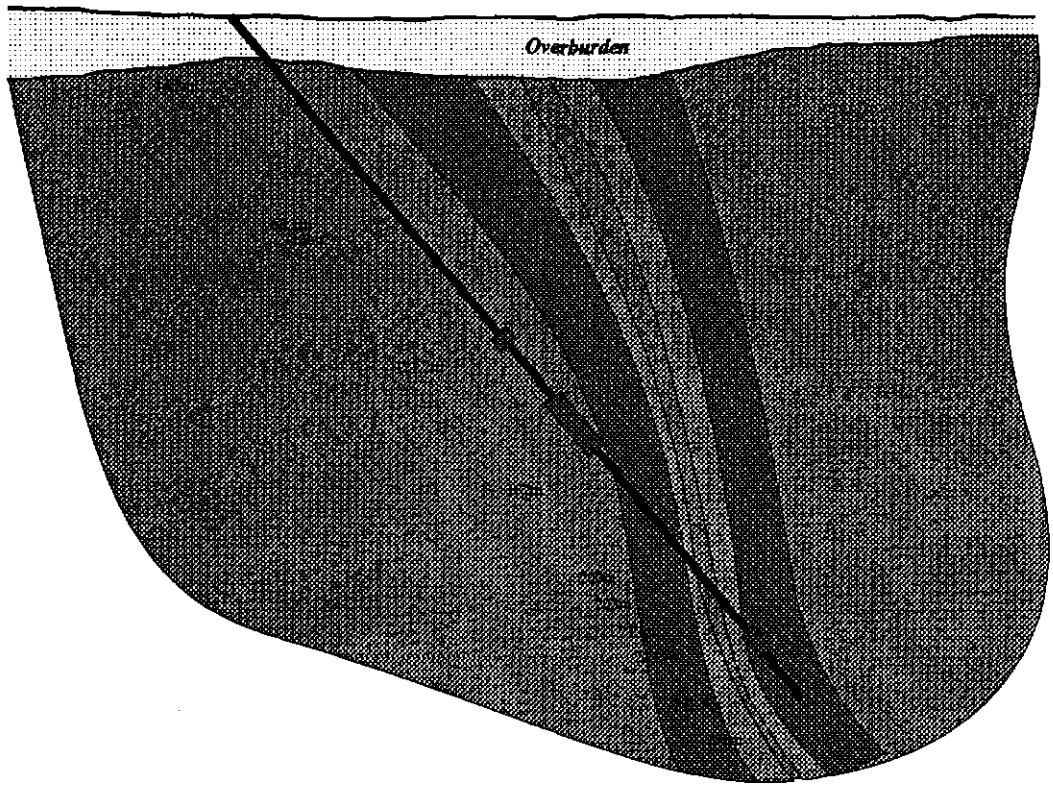
Lithological Summary:

From	To	Form	Comments
0	53.7	Pos	*Deeply weathered calcareous sediment*
53.7	197.4	Poq?	*Interbedded quartzites and shales with minor brecciation*
197.4	211.1	Pos	*?silicified, ?dolomitic quartzite and shale, partly brecciated*
211.1	239.4	Posb	*Black shale, lesser quartzite, partly brecciated*
239.4	254.2	Pos	*?silicified, ?dolomitic quartzite and shale, partly brecciated*
254.2	256.7	Pos	*Pyritic breccia*
256.7	308.3	Poq?	*Interbedded quartzites and shales, partly brecciated*

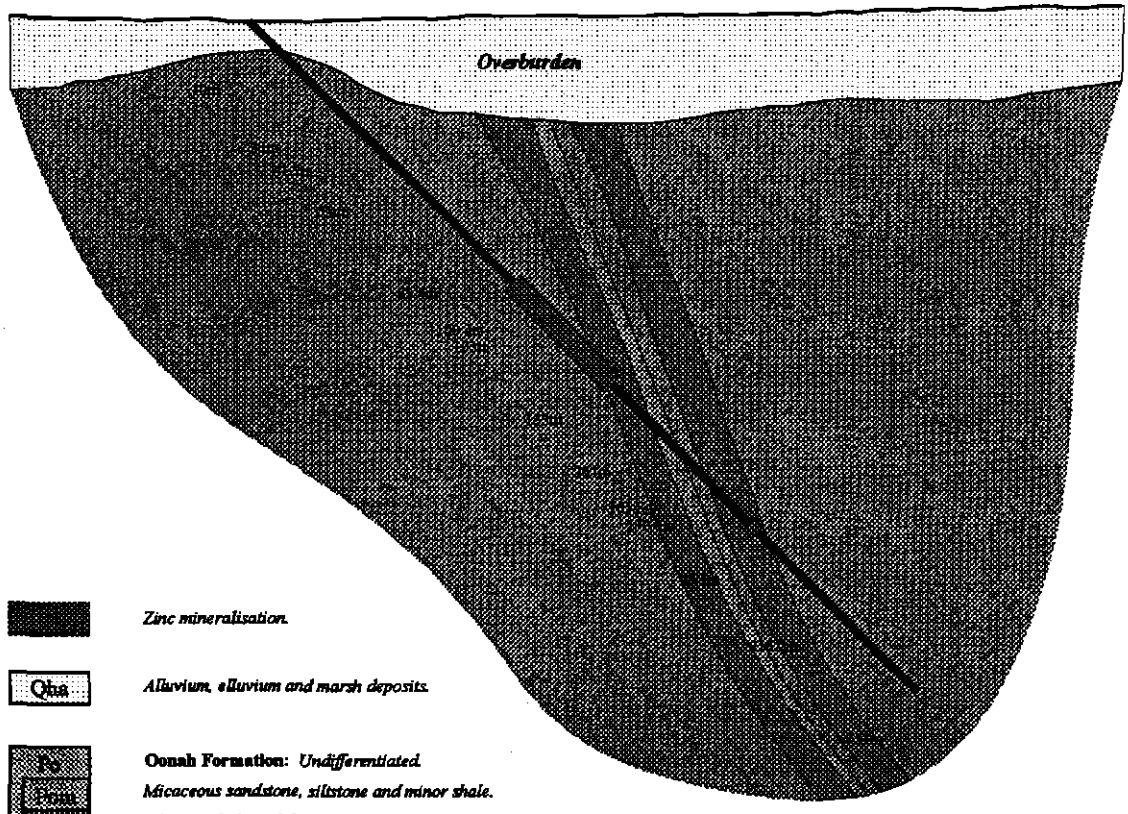
Mineralisation Summary:

From	To	Comments
58.5	59.5	*1m @ 0.02% Sn,*

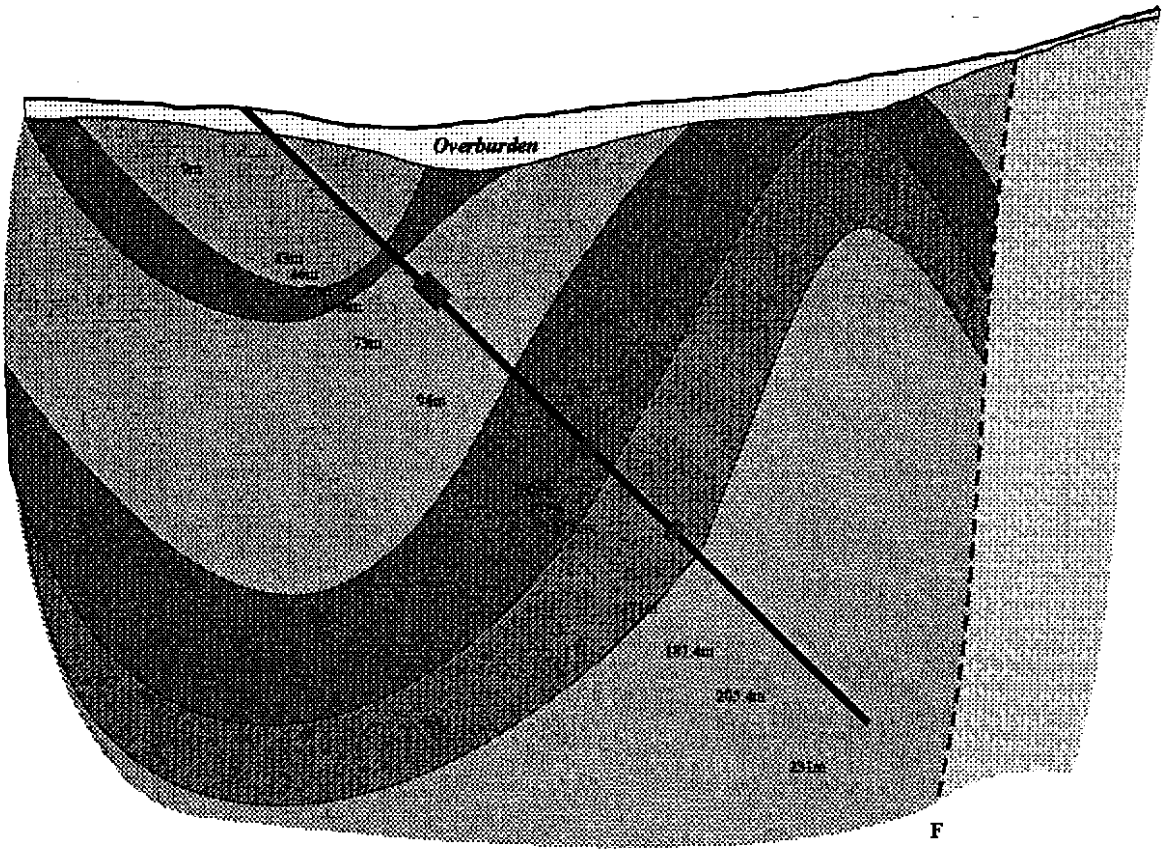
ZS1 PROFILE SHOWING ELEVATED ZINC MINERALISATION



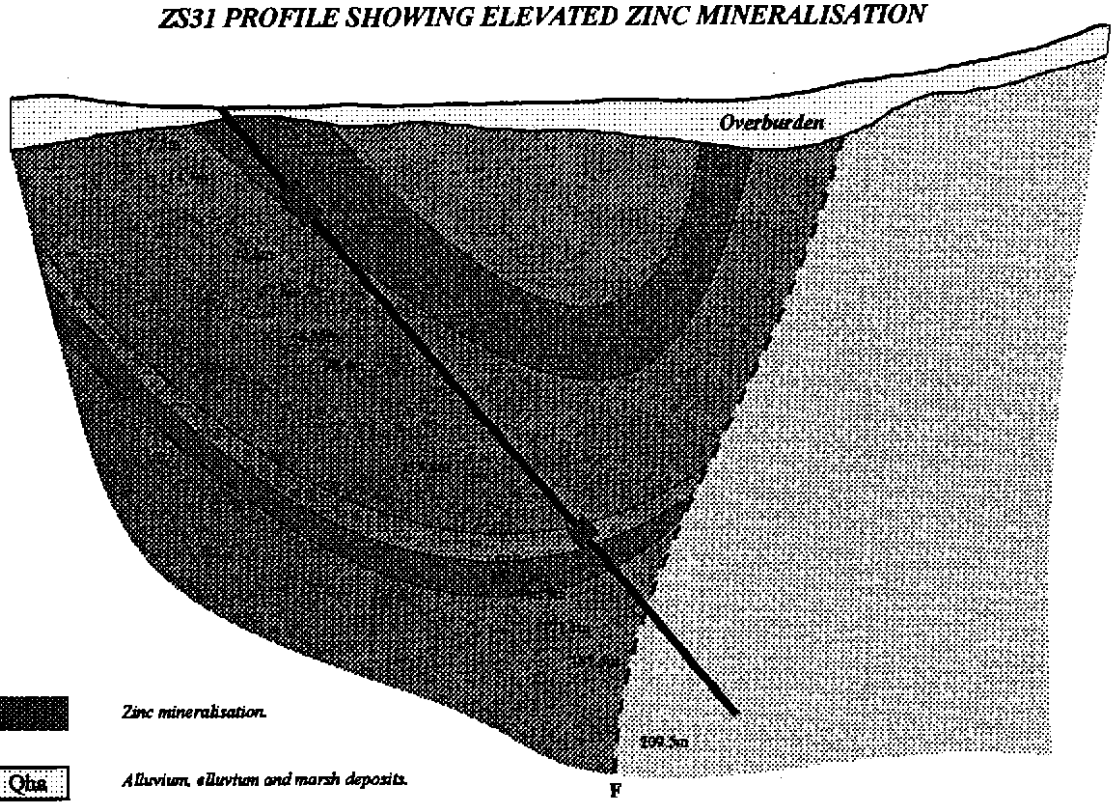
ZS2 PROFILE SHOWING ELEVATED ZINC MINERALISATION



ZS3 PROFILE SHOWING ELEVATED ZINC MINERALISATION



ZS31 PROFILE SHOWING ELEVATED ZINC MINERALISATION



Zinc mineralisation.

Qua — *Alluvium, elluvium and marsh deposits.*

Proterozoic — Quaternary

Oonah Formation: *Undifferentiated.*

Micaceous sandstone, siltstone and minor shale.

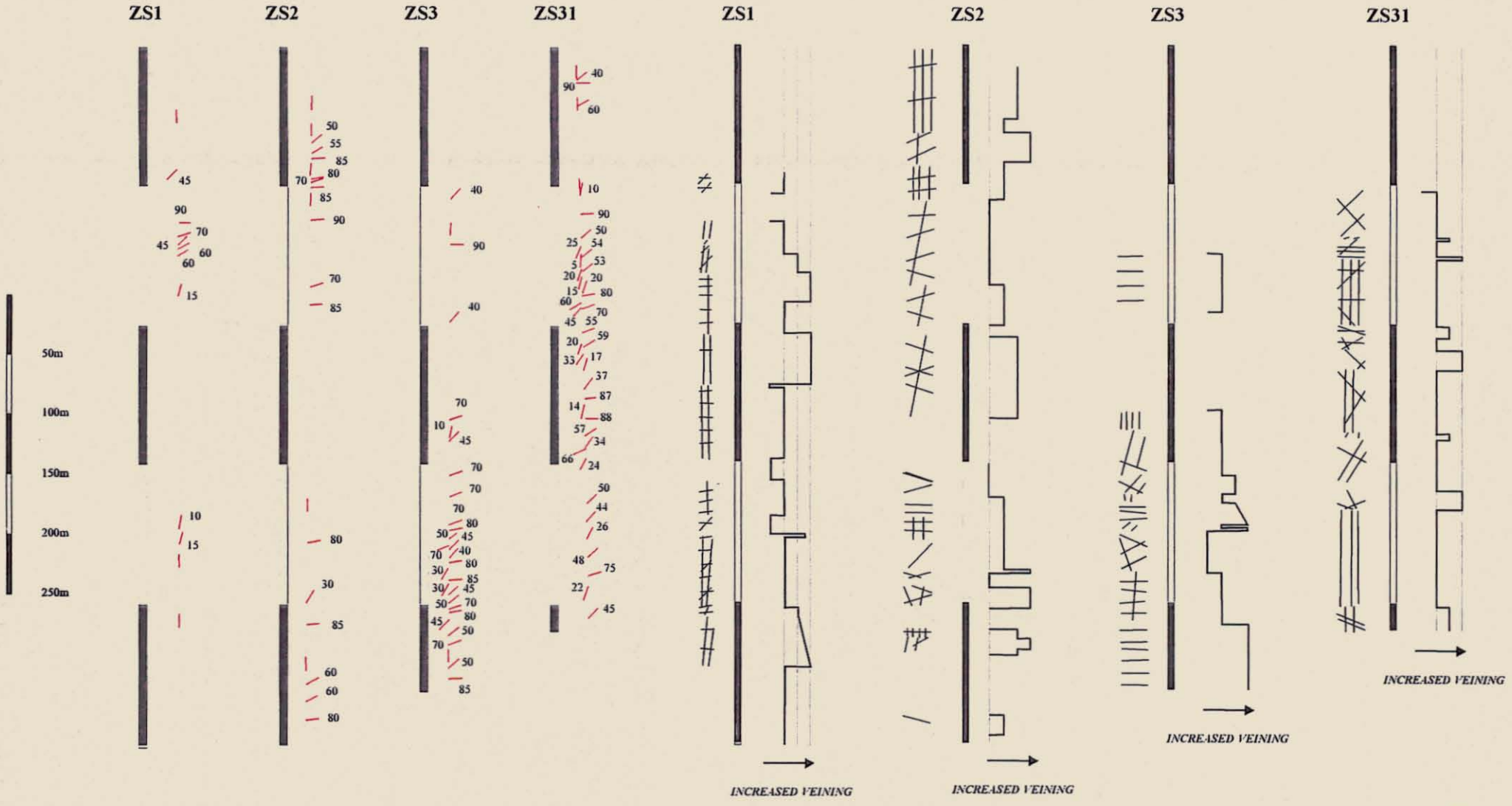
Siltsone, shale and dolomite (undifferentiated).

Graphitic black shale.

Dolomite - dolomitic limetsone dominant.

Massive quartzite.

DRILLHOLE BEDDING ORIENTATIONS AND VEIN OCCURENCE

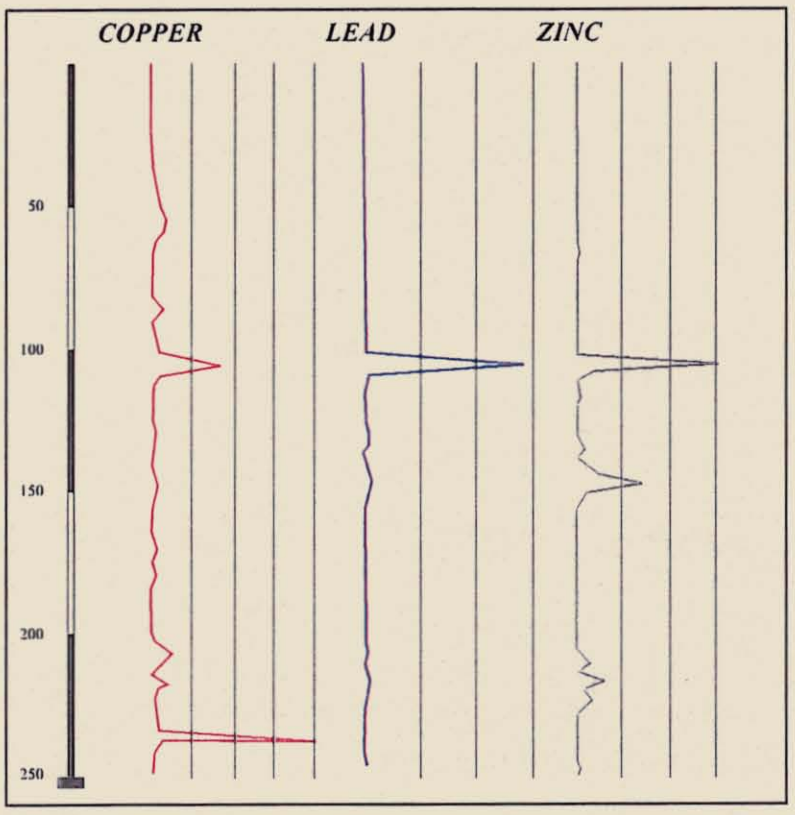


Bedding dips measured from core axis.
None of the holes have been orientated.

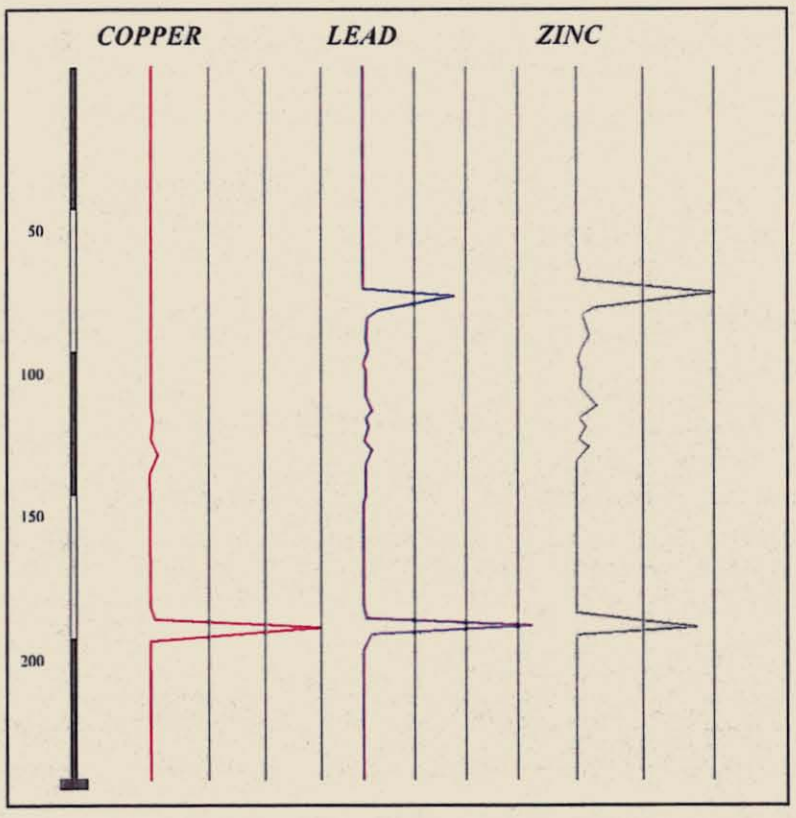
364354

ZS1 Cu, Pb, AND Zn ASSAYS

364355

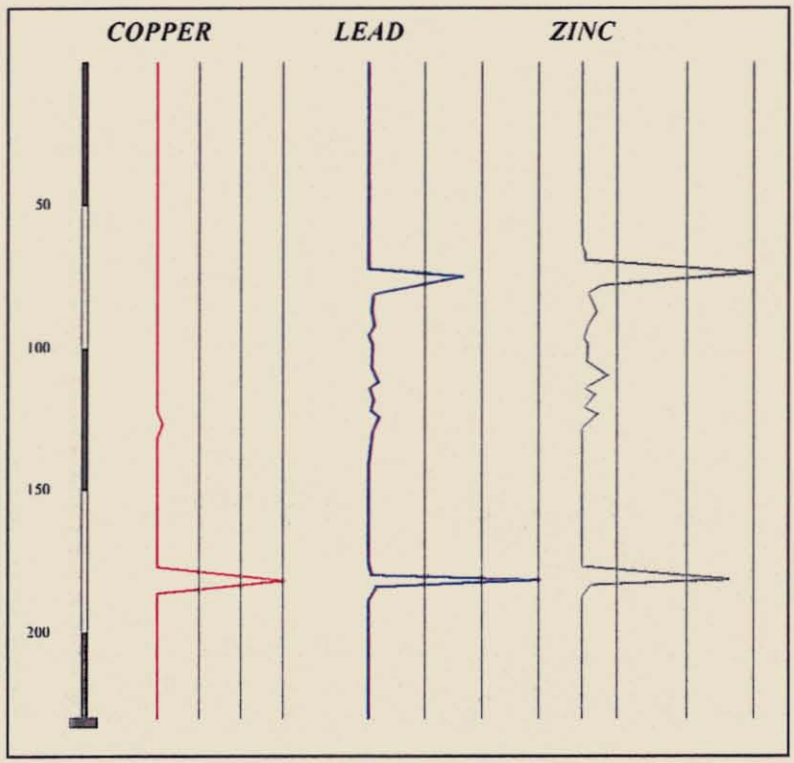


ZS2 Cu, Pb, AND Zn ASSAYS

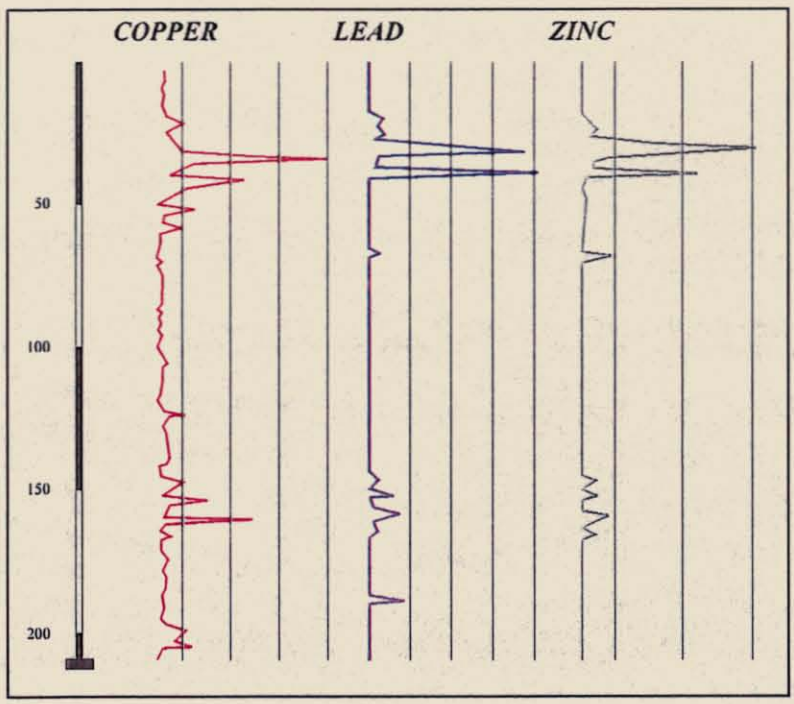


ZS3 Cu, Pb, AND Zn ASSAYS

364356



ZS31 Cu, Pb, AND Zn ASSAYS



ZS31 ASSAY RESULTS

from	to	Ag	Al	As	Au	Ba	Ca	Cu	Fe	K	Mg	Mn	Pb	Sn	Zn
9	11	-0.5	10.4	35	-0.008	555	-0.05	30	0.99	4.48	0.53	14	465	8	249
11	13.4	-0.5	10	22	-0.008	563	-0.05	33	0.71	4.41	0.52	-10	348	6	289
13.4	15.75	-0.5	9.34	49	-0.008	523	-0.05	32	1.55	3.88	0.47	28	477	10	475
15.75	18	-0.5	10.2	26	-0.008	552	-0.05	26	0.57	3.81	0.51	-10	394	6	387
18	19.5	-0.5	10.7	30	-0.008	604	-0.05	17	0.55	4.16	0.5	-10	300	4	264
19.5	20.7	-0.5	10.3	33	-0.008	571	-0.05	29	0.5	4.07	0.48	-10	107	11	295
20.7	23.6	-0.5	10.8	37	-0.008	613	-0.05	25	0.8	4.54	0.51	36	649	-3	457
23.6	25.5	-0.5	11.4	45	-0.008	679	-0.05	21	0.63	4.82	0.54	11	628	-3	405
25.5	27	-0.5	9.81	37	-0.008	586	-0.05	35	0.58	4.36	0.5	11	1020	9	776
27	28.5	-0.5	9.98	43	-0.008	615	-0.05	41	0.8	4.39	0.52	34	1340	4	1300
28.5	29.55	-0.5	9.6	49	-0.008	741	-0.05	45	0.76	4.1	0.52	38	861	9	588
29.55	30.35	9.2	9.06	255	-0.008	734	-0.05	109	2.45	3.96	0.53	40	1040	18	1620
30.35	31.5	11.7	1.89	443	0.009	264	-0.05	93	2.5	0.7	0.15	68	6750	7	9600
31.5	32.5	3	0.79	184	-0.008	91	0.05	30	1.37	0.17	0.07	36	3810	7	15100
32.5	33.5	5.2	3.05	479	0.014	214	0.05	66	2.71	1.17	0.17	55	4840	13	16800
33.5	34	11.6	2.91	628	0.009	206	0.05	71	9.32	1.18	0.18	76	8080	9	8610
34	35.2	9.7	0.5	169	-0.008	77	-0.05	71	1.77	0.11	0.06	34	2140	11	38600
35.2	35.5	26.5	1.09	303	0.01	140	-0.05	105	25.6	0.46	0.08	32	9400	12	88000
35.5	36	119	0.89	406	0.017	109	-0.05	410	12	0.31	0.06	127	49400	72	213000
36	37	108	2.69	987	0.021	198	-0.05	755	14.3	1.17	0.18	108	73000	17	108000
37	37.5	10.8	8.28	259	-0.008	519	-0.05	160	4.12	3.73	0.56	78	4260	40	31200
37.5	39	6.6	1.53	633	-0.008	194	0.06	67	4.56	0.53	0.12	74	4740	17	14600
39	40	5.1	1.46	198	-0.008	200	-0.05	50	3.35	0.57	0.12	35	2740	9	12700
40	40.5	117	1.67	674	0.01	221	-0.05	395	11.6	0.73	0.13	115	79000	57	143000
40.5	42.25	1.1	6.53	58	-0.008	442	0.1	76	1.26	3.62	1.05	41	848	8	4250
42.25	44.5	-0.5	5.36	23	-0.008	370	0.09	132	4.55	3.15	4.09	4220	70	-3	1170
44.5	46.05	-0.5	4.92	24	-0.008	314	0.14	51	7.47	2.83	5.41	7720	39	-3	1050
46.05	48.1	-0.5	5.1	18	-0.008	357	0.12	17	6.35	2.9	3.8	6890	19	-3	710
48.1	49.5	-0.5	2.77	22	-0.008	231	0.26	-5	26.4	1.4	2.99	36200	33	-3	3130
49.5	51.5	0.8	8.18	58	-0.008	575	0.25	173	14	4.88	6.74	15500	59	-3	1660
51.5	52.7	-0.5	9.01	39	-0.008	739	0.3	77	13.4	4.88	11.1	11500	24	-3	1110
52.7	54.4	-0.5	8.85	31	-0.008	703	0.3	28	15.5	4.84	9.1	11900	28	-3	853
54.4	57	0.5	3.86	22	-0.008	343	0.17	18	8.01	1.94	8.68	5440	-5	-3	282
57	58.5	1.4	4.72	28	-0.008	506	0.15	112	7.28	2.41	9	5320	20	5	337
58.5	60	-0.5	3.74	24	-0.008	529	1.78	14	9.92	1.84	4.55	8950	12	-3	412
60	61.5	-0.5	1.67	33	-0.008	383	6.8	17	15.9	0.8	4.46	16500	142	-3	2700
61.5	63	-0.5	2.78	26	-0.008	483	3.46	12	15.5	1.19	3.04	17500	32	-3	767
63	63.4	1.7	0.51	25	-0.008	120	1.11	6	22	0.22	2.71	26800	716	-3	1850
63.4	64.5	-0.5	0.07	-5	-0.008	29	10.9	-5	5.17	-0.05	7.77	6390	35	-3	104
64.5	66.2	-0.5	0.04	-5	-0.008	19	12.1	-5	9.96	-0.05	9.46	7510	22	-3	161
66.2	67.5	10.2	0.24	10	-0.008	49	1.76	23	19.8	0.1	3.94	41800	5870	-3	35100
67.5	68.35	-0.5	0.06	9	-0.008	26	9.77	-5	9.84	-0.05	9.67	5030	267	-3	1020
68.35	70.5	-0.5	3.46	9	-0.008	156	4.21	9	4.34	1.8	11.4	1990	15	5	75
70.5	72	-0.5	3.2	-5	-0.008	192	1.95	19	2.5	1.95	6.47	945	10	-3	26
72	73.5	-0.5	3.4	14	-0.008	198	2	18	2.92	2.04	8.08	1150	13	8	48
73.5	75.5	1.1	3.85	15	-0.008	248	3.08	18	3.76	2.3	8.01	1780	15	4	48
75.5	77	0.6	3.23	-5	-0.008	221	3.86	13	2.02	1.94	5.79	605	14	6	30
77	78.4	-0.5	3.15	-5	-0.008	202	3.25	21	3.92	1.94	5.79	2260	-5	-3	44
78.4	80.3	-0.5	0.04	-5	-0.008	30	14.7	6	0.47	-0.05	9.38	386	41	-3	114
80.3	82.5	-0.5	0.09	-5	-0.008	28	14.6	20	0.5	-0.05	9.4	389	23	-3	50
82.5	84	-0.5	0.06	9	-0.008	20	14.7	-5	1.02	-0.05	9.37	923	17	-3	13
84	84.5	-0.5	0.02	-5	-0.008	17	15.6	22	0.47	-0.05	10.1	365	14	-3	17
84.5	87	-0.5	0.05	-5	-0.008	18	17.1	5	0.38	-0.05	11.1	355	14	-3	10
87	88.5	-0.5	0.07	-5	-0.008	22	15.7	19	0.68	-0.05	10.2	497	29	-3	11
88.5	90	-0.5	0.09	11	-0.008	22	13.3	-5	1.76	-0.05	8.98	1150	16	-3	17
90	91.5	-0.5	0.09	-5	-0.008	21	14	22	1.15	-0.05	8.92	707	14	-3	5
91.5	93	0.8	0.11	8	-0.008	33	7.19	5	0.43	-0.05	14.9	422	50	-3	26
93	94.5	1.3	0.09	-5	-0.008	21	4.01	9	0.67	-0.05	17	750	18	-3	54
94.5	95.7	0.7	0.06	5	-0.008	21	8.44	-5	0.3	-0.05	15.5	272	19	-3	17
95.7	97.5	-0.5	0.11	-5	-0.008	30	16.9	5	1.46	-0.05	11.3	741	20	-3	7
97.5	99	-0.5	0.18	13	-0.008	28	16.1	10	1.87	0.07	9.75	1170	41	-3	12
99	100.5	0.9	0.47	15	-0.008	47	14.6	42	2.74	0.23	8.68	2180	37	-3	67

ZS31 ASSAY RESULTS

from	to	Ag	Al	As	Au	Ba	Ca	Cu	Fe	K	Mg	Mn	Pb	Sn	Zn
9	11	-0.5	10.4	35	-0.008	555	-0.05	30	0.99	4.48	0.53	14	465	8	249
11	13.4	-0.5	10	22	-0.008	563	-0.05	33	0.71	4.41	0.52	-10	348	6	289
13.4	15.75	-0.5	9.34	49	-0.008	523	-0.05	32	1.55	3.88	0.47	28	477	10	475
15.75	18	-0.5	10.2	26	-0.008	552	-0.05	26	0.57	3.81	0.51	-10	394	6	387
18	19.5	-0.5	10.7	30	-0.008	604	-0.05	17	0.55	4.16	0.5	-10	300	4	264
19.5	20.7	-0.5	10.3	33	-0.008	571	-0.05	29	0.5	4.07	0.48	-10	107	11	295
20.7	23.6	-0.5	10.8	37	-0.008	613	-0.05	25	0.8	4.54	0.51	36	649	-3	457
23.6	25.5	-0.5	11.4	45	-0.008	679	-0.05	21	0.63	4.82	0.54	11	628	-3	405
25.5	27	-0.5	9.81	37	-0.008	586	-0.05	35	0.58	4.36	0.5	11	1020	9	776
27	28.5	-0.5	9.98	43	-0.008	615	-0.05	41	0.8	4.39	0.52	34	1340	4	1300
28.5	29.55	-0.5	9.6	49	-0.008	741	-0.05	45	0.76	4.1	0.52	38	861	9	588
29.55	30.35	9.2	9.06	255	-0.008	734	-0.05	109	2.45	3.96	0.53	40	1040	18	1620
30.35	31.5	11.7	1.89	443	0.009	264	-0.05	93	2.5	0.7	0.15	68	6750	7	9600
31.5	32.5	3	0.79	184	-0.008	91	0.05	30	1.37	0.17	0.07	36	3810	7	15100
32.5	33.5	5.2	3.05	479	0.014	214	0.05	66	2.71	1.17	0.17	55	4840	13	16800
33.5	34	11.6	2.91	628	0.009	206	0.05	71	9.32	1.18	0.18	76	8080	9	8610
34	35.2	9.7	0.5	169	-0.008	77	-0.05	71	1.77	0.11	0.06	34	2140	11	38600
35.2	35.5	26.5	1.09	303	0.01	140	-0.05	105	25.6	0.46	0.08	32	9400	12	88000
35.5	36	119	0.89	406	0.017	109	-0.05	410	12	0.31	0.06	127	49400	72	213000
36	37	108	2.69	987	0.021	198	-0.05	755	14.3	1.17	0.18	108	73000	17	108000
37	37.5	10.8	8.28	259	-0.008	519	-0.05	160	4.12	3.73	0.56	78	4260	40	31200
37.5	39	6.6	1.53	633	-0.008	194	0.06	67	4.56	0.53	0.12	74	4740	17	14600
39	40	5.1	1.46	198	-0.008	200	-0.05	50	3.35	0.57	0.12	35	2740	9	12700
40	40.5	117	1.67	674	0.01	221	-0.05	395	11.6	0.73	0.13	115	79000	57	143000
40.5	42.25	1.1	6.53	58	-0.008	442	0.1	76	1.26	3.62	1.05	41	848	8	4250
42.25	44.5	-0.5	5.36	23	-0.008	370	0.09	132	4.55	3.15	4.09	4220	70	-3	1170
44.5	46.05	-0.5	4.92	24	-0.008	314	0.14	51	7.47	2.83	5.41	7720	39	-3	1050
46.05	48.1	-0.5	5.1	18	-0.008	357	0.12	17	6.35	2.9	3.8	6890	19	-3	710
48.1	49.5	-0.5	2.77	22	-0.008	231	0.26	-5	26.4	1.4	2.99	36200	33	-3	3130
49.5	51.5	0.8	8.18	58	-0.008	575	0.25	173	14	4.88	6.74	15500	59	-3	1660
51.5	52.7	-0.5	9.01	39	-0.008	739	0.3	77	13.4	4.88	11.1	11500	24	-3	1110
52.7	54.4	-0.5	8.85	31	-0.008	703	0.3	28	15.5	4.84	9.1	11900	28	-3	853
54.4	57	0.5	3.86	22	-0.008	343	0.17	18	8.01	1.94	8.68	5440	-5	-3	282
57	58.5	1.4	4.72	28	-0.008	506	0.15	112	7.28	2.41	9	5320	20	5	337
58.5	60	-0.5	3.74	24	-0.008	529	1.78	14	9.92	1.84	4.55	8950	12	-3	412
60	61.5	-0.5	1.67	33	-0.008	383	6.8	17	15.9	0.8	4.46	16500	142	-3	2700
61.5	63	-0.5	2.78	26	-0.008	483	3.46	12	15.5	1.19	3.04	17500	32	-3	767
63	63.4	1.7	0.51	25	-0.008	120	1.11	6	22	0.22	2.71	26800	716	-3	1850
63.4	64.5	-0.5	0.07	-5	-0.008	29	10.9	-5	5.17	-0.05	7.77	6390	35	-3	104
64.5	66.2	-0.5	0.04	-5	-0.008	19	12.1	-5	9.96	-0.05	9.46	7510	22	-3	161
66.2	67.5	10.2	0.24	10	-0.008	49	1.76	23	19.8	0.1	3.94	41800	5870	-3	35100
67.5	68.35	-0.5	0.06	9	-0.008	26	9.77	-5	9.84	-0.05	9.67	5030	267	-3	1020
68.35	70.5	-0.5	3.46	9	-0.008	156	4.21	9	4.34	1.8	11.4	1990	15	5	75
70.5	72	-0.5	3.2	-5	-0.008	192	1.95	19	2.5	1.95	6.47	945	10	-3	26
72	73.5	-0.5	3.4	14	-0.008	198	2	18	2.92	2.04	8.08	1150	13	8	48
73.5	75.5	1.1	3.85	15	-0.008	248	3.08	18	3.76	2.3	8.01	1780	15	4	48
75.5	77	0.6	3.23	-5	-0.008	221	3.86	13	2.02	1.94	5.79	605	14	6	30
77	78.4	-0.5	3.15	-5	-0.008	202	3.25	21	3.92	1.94	5.79	2260	-5	-3	44
78.4	80.3	-0.5	0.04	-5	-0.008	30	14.7	6	0.47	-0.05	9.38	386	41	-3	114
80.3	82.5	-0.5	0.09	-5	-0.008	28	14.6	20	0.5	-0.05	9.4	389	23	-3	50
82.5	84	-0.5	0.06	9	-0.008	20	14.7	-5	1.02	-0.05	9.37	923	17	-3	13
84	84.5	-0.5	0.02	-5	-0.008	17	15.6	22	0.47	-0.05	10.1	365	14	-3	17
84.5	87	-0.5	0.05	-5	-0.008	18	17.1	5	0.38	-0.05	11.1	355	14	-3	10
87	88.5	-0.5	0.07	-5	-0.008	22	15.7	19	0.68	-0.05	10.2	497	29	-3	11
88.5	90	-0.5	0.09	11	-0.008	22	13.3	-5	1.76	-0.05	8.98	1150	16	-3	17
90	91.5	-0.5	0.09	-5	-0.008	21	14	22	1.15	-0.05	8.92	707	14	-3	5
91.5	93	0.8	0.11	8	-0.008	33	7.19	5	0.43	-0.05	14.9	422	50	-3	26
93	94.5	1.3	0.09	-5	-0.008	21	4.01	9	0.67	-0.05	17	750	18	-3	54
94.5	95.7	0.7	0.06	5	-0.008	21	8.44	-5	0.3	-0.05	15.5	272	19	-3	17
95.7	97.5	-0.5	0.11	-5	-0.008	30	16.9	5	1.46	-0.05	11.3	741	20	-3	7
97.5	99	-0.5	0.18	13	-0.008	28	16.1	10	1.87	0.07	9.75	1170	41	-3	12
99	100.5	0.9	0.47	15	-0.008	47	14.6	42	2.74	0.23	8.68	2180	37	-3	67

APPENDIX 4.

Skarn-type lead-zinc deposits

Introduction

Zn-Pb type skarn deposits occur across all continents, within rocks of varied composition and age. The skarn deposits may form during regional or contact metamorphism, and from a variety of metasomatic processes involving fluids of magmatic, metamorphic, meteoric and/or marine origin. The spectrum of skarn formation environments include: adjacent to plutons, along faults and major shear zones, in geothermal systems at shallow crustal depths and in deeply buried metamorphic terrains. Continental settings associated with either subduction or rifting are most favourable to Zn-Pb skarn formation. In addition to a Zn-Pb-Ag metal content, zinc skarns contain a distinctive manganese- and iron-rich mineralogy.

Skarn deposits

'Skarn deposits' (Einaudi *et al.*, 1981) is a preferential term applied to ore deposits associated with skarns. Skarn deposits may be classified according to the primary rock type or composition, the mechanism of fluid movement, or the temperature and extent of magmatic involvement. Since exploration does not always enable such detailed investigation, classification is thought best to be based upon the dominant presence of economic minerals such as Fe, W, Cu, Zn-Pb, Mo and Sn (Einaudi *et al.*, 1981; Meinert, 1983; Edwards and Atkinson, 1986). Additional classification of skarn deposit is based upon the dominant calc (magnesian)-silicate mineral assemblages. Magnesian, associated with Fe, Cu, Au, Sn ,B, Be mineralisation, calcic, with Fe, Cu, W, Mo, Au, Pb, Zn , Be mineralisation and alkaline skarns occurring in U(Th) deposits are three such common skarn types. Yiming (1990) proposes a fourth category of manganoan skarns, related only to Zn-Pb-(Ag) mineralisation. Mineralogical variations and gradations within skarn deposits are a function of magma type, depth of formation, reducing capacity and composition of host rocks, distance between the carbonate horizon and magmatic source, and the degree of meteoric water involvement.

Skarn deposits tend to be Mesozoic or younger, although many important tungsten and tin deposits such as at King Island in Tasmania are Palaeozoic. Copper and lead-zinc deposits appear primarily of Tertiary age.

Deposits of this type are important suppliers of major metals throughout the world. More than half the Western Worlds tungsten is produced from skarns such as Canada Tungsten in the North American Cordilleran belt and the King Island deposit. Tin skarns may typically contain grades of 0.1 to 0.7% tin with tonnages up to 30 million tonnes. Iron skarns vary to 300 million tonnes, and zinc skarns often grade up to 12% with lower grades of lead associated. Copper associated with zinc-lead skarns is usually negligible, but silver may grade at around 250 grams/tonne. Copper skarn deposits often associate with major porphyry copper systems such as Bingham and Twin Buttes in North America (Edwards and Atkinson, 1986).

Definitions and terminologies

The term 'skarn' was originally applied to coarse-grained calc-silicate gangue associated with iron ore deposits of Sweden. Since, it has been applied to a variety of calc-silicate rocks rich in calcium, iron, magnesium, aluminium and manganese formed through replacement of originally carbonate-rich rocks. 'Skarn' is a descriptor of mineralisation regardless of economic potential. Formation processes as seen in figure 1 include (Meinert, 1993):

1. Isochemical metamorphism involving recrystallisation and change in mineral stability,
2. Reaction skarn from metamorphism of interlaid lithology's,
3. Skarnoid results from metamorphism of impure lithology's with some mass transfer by small-scale fluid movement, or
4. Fluid controlled metasomatic skarn, typically coarse-grained, loosely reflecting the composition or texture of the protolith.

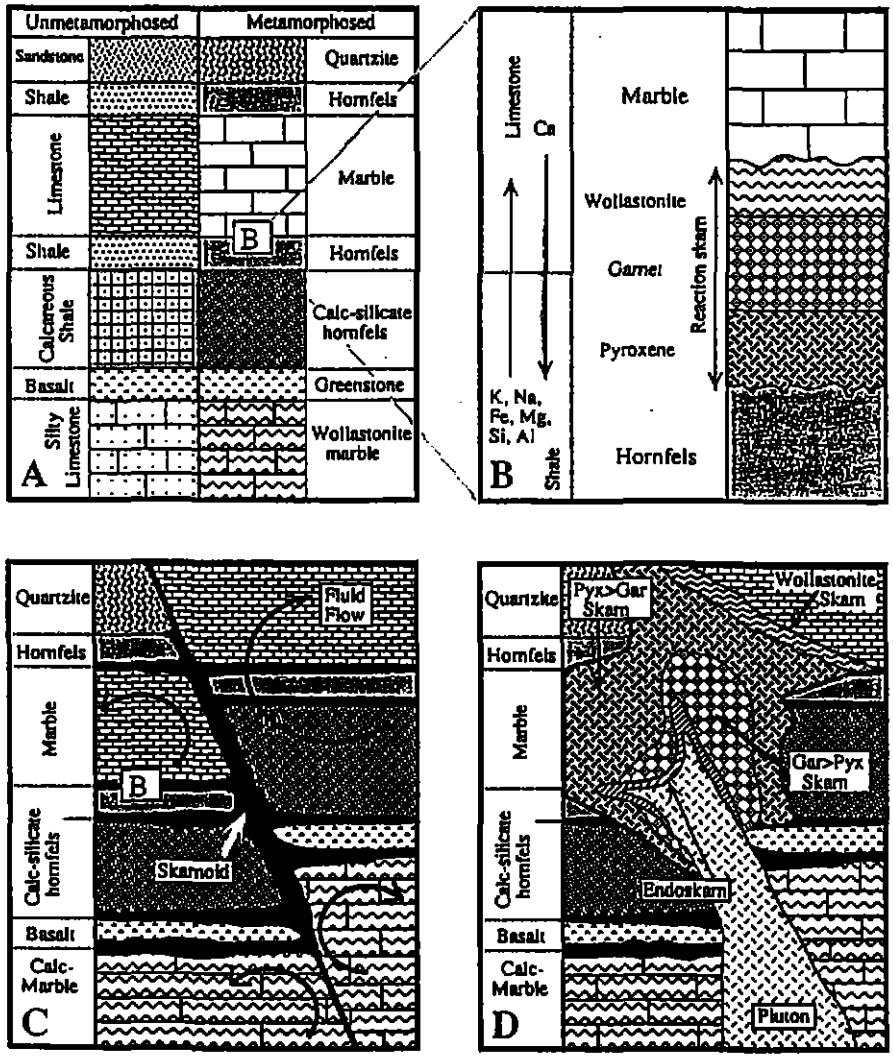


Figure 1. ***Types of skarn formation. (after Meinert, 1983)***

Classification of skarns may be done in accordance to the rock type being replaced. 'Exoskarn' and 'endoskarn' refer to replacements of carbonates and intrusive rocks respectively. This may occur within contact zones where intrusive rock was thought genetically related to the skarn-forming fluids (Einaudi and Burt, 1982). Fluid flow into the pluton or upward along its contact with carbonates is indicative of an endoskarn environment. The addition of calcium into endoskarns is reflected by mineral zoning. With reducing conditions, the sequence towards limestone is biotite-amphibole-pyroxene-(garnet). This pyroxene-plagioclase diagnostic assemblage is typical of most tungsten and some copper skarns. Most copper and lead-zinc skarns support oxidising conditions, with epidote-quartz favoured over pyroxene-plagioclase, generally containing an abundance of garnet. Exoskarns are reflective of the replaced carbonate rock composition. Evaluating the dominating calc-silicate mineral assemblage enables division into: a) magnesian skarn - replacing dolomite and consisting primarily of magnesium silicates such as forsterite and serpentine, and b) calcic skarn - replacing limestones of iron-calcium silicates such as andradite and hedenbergite. The importance of calcic exoskarns may be seen in table 1. Replacement of basalts such as at Land's End peninsula in the U.K. produce distinctive skarn mineralogy. These tin-bearing skarns are associated with a cordierite-anthophylite-biotite hornfels in an area previously worked for garnet-copper ore (Koskings, Edwards and Atkinson, 1986).

364363

Type	*Tungsten (calcic)*	*Tin (calcic)*	*Tin (magnesian)*
Metal association (minor metals)	W,Mo,Cu (Zn, Bi)	Sn,F (Be,W)	Sn,F (Be,B)
Tectonic setting	Continental margin Syn-/late orogenic	Continental margin Late to post-orogenic	
Associated intrusives	Quartz diorite/ quartz monzonite	Granite	Granite
Intrusive morphology	Large batholithic plutons	Stocks batholiths	Stocks batholiths
Intrusive alteration	Local mica, calcite, pyrite; endoskarn	Greisen	Greisen
Ore	Scheelite, molybdenite, chalcopyrite pyrrhotite, pyrite	Cassiterite, arsenopyrite, pyrrhotite, stannite	Cassiterite, minor arsenopyrite, pyrrhotite, stannite, sphalerite
Typical size (million tonnes)	0.1–2	0.1–3	1
Typical grade	0.7% WO_3	0.1–0.7% Sn	?

Copper (calcic)	*Zinc–lead (calcic)*	*Molybdenum (calcic)*	*Iron (magnesian)*	*Iron (calcic)*
Cu (Mo,W,Zn)	Zn,Pb,Ag (Cu,W)	Mo,W (Cu,Bi,Zn)	Fe (Cu, Zn)	Fe (Cu, Co, Au)
Continental margin Syn-orogenic to late orogenic		Continental margin Late orogenic	Syn-orogenic	Oceanic island arc; rifted continental margins
Granodiorite to quartz monzonite	Granodiorite to granite, diorite to syenite; plutons commonly absent	Quartz monzonite to granite	Granodiorite to granite	Gabbro to syenite mostly diorite
Stocks, dykes breccia pipes	Large stocks to dykes – if present	Stocks	Small stocks, dykes sills	Large to small stocks, dykes
Local endoskarn, K – silicate, sericitic	Extensive endoskarn?	Quartz veins K – silicate	Minor endoskarn, propylitic	Extensive endoskarn Na – silicates
Chalcopyrite, bornite, pyrite, haematite, magnetite	Sphalerite, galena, chalcopyrite arsenopyrite	Molybdenite, scheelite, bismuthinite pyrite, chalcopyrite	Magnetite, pyrite, chalcopyrite, sphalerite, pyrrhotite,	Magnetite, chalcopyrite, cobaltite, pyrrhotite,
1–100 1–2% Cu	0.2–3 9% Zn, 6% Pb, 5 oz/ton Ag	0.1–2 ?	5–100 40% Fe	5–200 40% Fe

Table 1. ***Characteristics of major skarn types. (from Einaudi et al., 1981, and Einaudi and Burt, 1982)***

Evolution of skarn deposits

Skarn deposit formation is a dynamic process requiring a transition from early/distal metamorphism producing hornfels, reaction skarn and skarnoid, to later/proximal metamorphism resulting in coarse-grained ore-bearing skarn. High temperature gradients and large fluid circulation cells produced by magma intrusion forms a complex model of isochemical recrystallisation (Norton, 1982; Salemink and Schuiling, 1987; Bowers *et al.*, 1990). Figure 2 highlights the effect of diverse fluids circulating through a carbonate protolith fracture. The vein controlled skarn mineralogy of figure 2c is actually cooler than the surrounding country rock, with the product not unlike that of prograde metamorphism. Figure 2b illustrates a similar product, whilst fig 2d involves more complex metasomatic fluids with the possible addition of magmatic components such as Fe, Si and Cu. Such early metamorphism and continued metasomatism at relatively high temperatures (>1200°C, Wallmach and Hatton, 1989) precede retrograde alteration with declining temperatures.

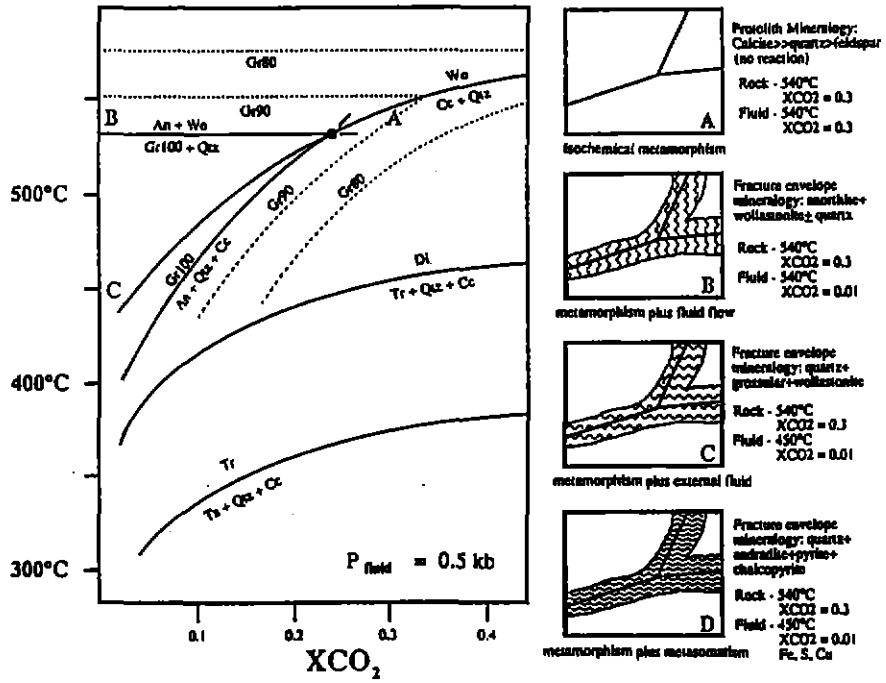


Figure 2. ***Metamorphic phase equilibria for selected reactions in the system Ca-Mg-Al-Si-H$_2$O-CO$_2$. (after Meinert, 1993)***

The development of skarns in pluton-related systems is shown in figure 3. Skarn formed at depth is likely to be of higher grade and greater expanse than that of shallow conditions (fig 3c). Conversely, shallow environments are likely proponents for retrograde alteration during cooling, with meteoric water interaction being more intense (fig 3d).

Differences in structural constraints between deep and shallow formed skarns influence skarn size and morphology.

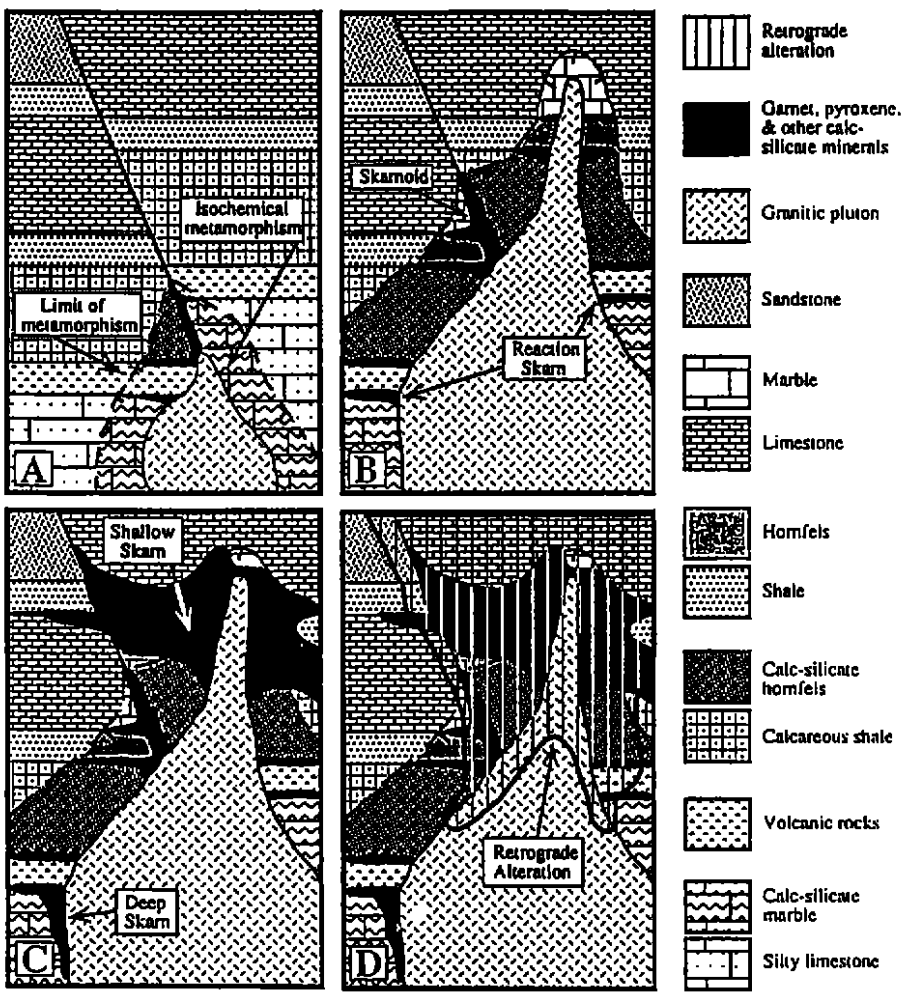


Figure 3. ***Evolutionary stages of pluton-associated skarn deposits: a) Initial intrusion causes metamorphism of sedimentary rocks; b) Metamorphic recrystallisation and phase changes reflect protolith compositions, with local bi-metasomatism and fluid circulation forming diverse calc-silicate minerals in impure lithology's and along fluid boundaries; c) Crystallisation and release of a separate aqueous phase result in fluid controlled metasomatic skarn; d) Cooling of the pluton and the possible circulation of cooler, oxygenated meteoric waters cause retrograde alteration of metamorphic and metasomatic calc-silicate assemblages. Note retrograde alteration is more extensive in shallow zones. (after Meinert, 1993)***

Genesis and controls of skarn formation

Edwards and Atkinson (1986) have recognised 3 stages in the formation of skarn deposits: emplacement of the causative pluton, producing contact metamorphism; prograde skarn growth, usually a metasomatic event; retrograde alteration. Superimposition of each produces the complex mineralogy and zoning patterns evident in most skarn deposits, the extent of each dependent upon local geological conditions.

Host rock lithology and alteration

Host rock lithology is an integral component of skarn deposit formation. It is accepted that skarns generally associate with calcareous rocks, with contact metamorphism resulting in calcium-aluminium silicates in calcareous shales, calcium-magnesium silicates in silty dolomites and wollastonite in cherty limestone.

The abundance of impure carbonates, calcareous shales and sandstones produces a large portion of metamorphic calc-silicates within the skarn deposit. These metamorphic calc-silicates are reflective of original sediment composition.

To achieve economically viable deposits, early-formed metamorphic aureole phenomena are generally overprinted by the metamorphic processes of skarn growth (Meinert, 1993). Two varieties of metasomatic skarn have been identified - reaction skarn and igneous metasomatic skarn. The former tend to form early, usually confined to moderate- to high-grade metamorphic terrains. Bulk composition is reflective of the host rocks, with ore formation not commonly associated. Igneous metasomatic skarns exhibit varied mineral associations, with a bulk composition bearing little resemblance to that of the host rocks. Produced late in the skarn forming episode, these magmatic hydrothermal systems often contain ore deposits. Sulphide deposition and retrograde alteration often occurs during a post skarn growth episode.

Depth of formation

The depth of formation has fundamental control over most skarn characteristics. Quantitative studies typically use mineral equilibria (Anovitz and Essene, 1990), fluid inclusions (Guy *et al.*, 1988) or a combination (Hames *et al.*, 1989) to establish depths of metamorphism. Qualitative methods include stratigraphic/geologic reconstructions and interpretation of igneous textures (Meinert, 1993). Field observations of chilled margins, grain size of porphyry groundmass, pluton morphology, and presence of brecciation and brittle fractures provide distinctions between shallow and deep environments.

The effect of depth upon metamorphism is primarily a function of the ambient wall rock temperature prior to, during, and after intrusion. With increased depth comes the addition of heat flux, effecting a larger rock mass for greater periods of time. In addition, high ambient temperatures could effect crystallisation, minimising the amount of retrograde alteration of skarn minerals; eg. at 12km depth, with ambient temperatures of 400°C, skarn may not cool below garnet and pyroxene stability without uplift or additional tectonic activity.

Increasing metamorphism with depth can influent host rock permeability, reducing the amount of carbonate available for reaction the metasomatic fluids. The depth of skarn formation also effects host rock mechanical properties. Rocks at depth tend to behave in a ductile manner rather than fracturing. Intrusive contacts with sedimentary rocks are generally sub-parallel to bedding (pluton intrusion along bedding planes or sedimentary rock fold or flow until alignment with the intrusive contact).

With depth beyond 5-10km, such as at Pine Creek in California (Brown *et al.*, 1985) and Osgood Mountains in Nevada (Taylor, 1976), skarn confines of narrow, but vertically extensive, zones may occur. The Pine Creek Skarn is typically less than 10 wide, but locally exceeds 1km in length and vertical extent (Newberry, 1982).

In contrast, host rocks of shallow depth deform via fracturing and faulting rather than folding. Einaudi (1982a) found shallow intrusive contacts to be sharply discordant to bedding, with skarn cuts across bedding, and massive replacement of favourable beds, often of volume (exposed) exceeding the associated pluton. Hydrofracturing generally associated with shallow intrusions increases host rock permeability, producing likely conditions for igneous-related metamorphic fluids and for later meteoric fluids (Shelton, 1983). Characteristic of shallow environment skarn formation is the meteoric water destruction of skarn minerals during retrograde alteration.

Petrogenesis and tectonic setting

Meinert's (1983) over generalised placement of skarn occurrences within a plate tectonic framework has been used to form a basis for regional exploration of specific skarn deposit types (figure 4).

Mafic igneous rocks of oceanic island-arc terrains are host almost solely to calcic magnetite skarns (figure 4a). Often of significant Cu, Co and Au, high grade zones of nickel and zinc (minus tin, tungsten and lead) may occur. The iron-rich and magnesium deficient nature is reflective of the ocean crust, the wall rocks and the plutons associated. Mid angle subduction beneath continental crust (figure 4b) typically host tungsten and base metal (Cu, Zn-Pb, Mo) sulphide skarns. Quartz monzanites and granodiorites are common plutons, often to depths of 5 to 15 kilometres. Tungsten-rich skarns are thought to have formed at greater depths, and higher temperatures than Cu and Zn-Pb skarns.

Altered and mineralised porphyry stocks and plugs of granodiorite to quartz monzanites intruded at high levels within the continental crust (figure 4c) are often host to Cu skarns. Such skarns are sulphide-rich, sought primarily for copper, copper-iron and lead-zinc. Local by-products may include molybdenum, gold and silver. Calcic lead-zinc skarns are thought to be associated with granodioritic or granitic magmatism, forming during mid- to late-orogenic stages of continental margin belts.

Tin skarns associate with ilmenite-series granites (I and S type) emplaced late in, or after, the orogenic cycle of continental magmatic ores, or within stable cratonic environments (figure 4d). Cassiterite, the most common tin source, is formed late, under relatively low temperature, retrograde alteration conditions. The amount of cassiterite is a direct function of the amount of retrograde alteration. Massive sulphide replacement bodies in dolomite, such as Renison Bell in Tasmania, are thought representative of low-temperature distal analogues of tin skarns.

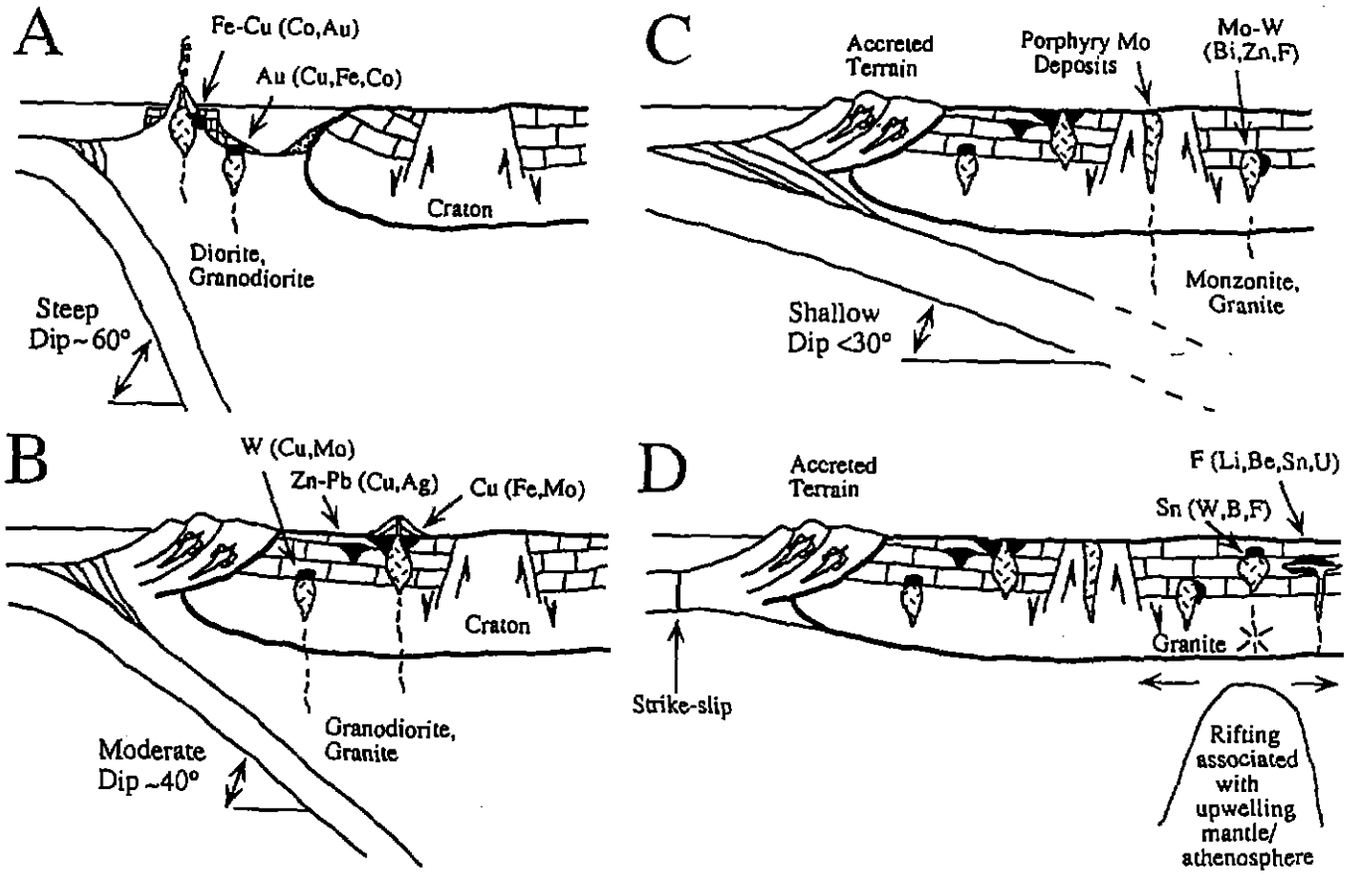


Figure 4. ***Idealised tectonic model for skarn formation: a) oceanic subduction and back arc basin environment; b) continental subduction environment with accreted oceanic terrane; c) transitional low-angle subduction environment; d) post-subduction or continental rifting environment. (from Meinert, 1983)***

Skarn mineralogy

Table 1 illustrates magnetite to be the main source of iron, scheelite of tungsten, chalcopyrite of copper, cassiterite of tin, and sphalerite and galena of zinc and lead respectively. Exoskarn gangue minerals include garnets, pyroxenes and amphibole. The minerals of figures 5 and 6 exist in all skarn types; their marked compositional variation rendering them important in classification and exploration. Garnets and pyroxenes are widely used in skarn comparisons given the ease at which their compositional variation may be illustrated (figures 5 and 6). Exoskarn compositions for main skarn types may vary in accordance to the principal mineral present.

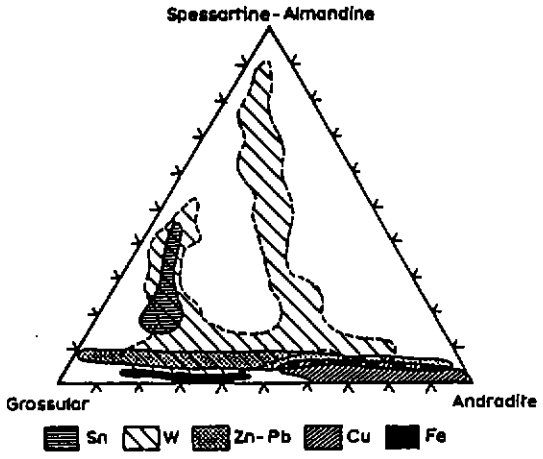


Figure 5. ***Garnet species from calcic skarn deposits. (after Einaudi and Burt, 1982)***

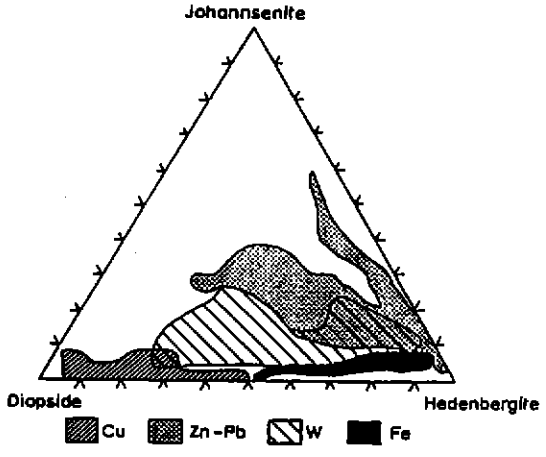


Figure 6. ***Pyroxene species from calcic skarn deposits. (after Einaudi and Burt, 1982)***

Mineralogical study enables the identification of skarn type deposits. Skarn minerals provide important information about the formation environment. As shown in table 2, minerals such as quartz and calcite exist in most skarns, whilst others such as humite, talc, serpentine, periclase and phlogopite are typically restricted to magnesian skarns. In addition, very restrictive tin, boron, beryllium and fluorine-bearing minerals act locally as important indicators of paragenesis.

Burt (1972) and Einaudi *et al.*, (1981) have modified Zharikov's (1970) earlier observations to identify a variety of deposit types and the mineralogical variations between each. Minerals such as garnet, pyroxene and amphibole, present in all skarn types, have been identified as the most useful in classification and exploration. Johannsite is an important indicator given its occurrence within zinc skarns only.

The presence of johannsite denotes skarn type, however with addition of compositional information, the mineral composition may be noted in terms of moles % of the end members; eg. Pyroxene containing 70% mole % hedenbergite, 28 mole % diopside and 2 mole % johannsite may be referred to as $Hd_{70}Di_{28}Jo_2$. Iron variations are often considered an important parameter, hence, minerals may be described in terms of their iron end member; eg. Hd_{10} or Ad_{90} (table 2) (Meinert, 1993).

General Group	End Members	Abbreviation	Composition	Series
Garnet	grossularite	Gr	$Ca_3Al_2(SiO_4)_3$	grandite
	andradite	Ad	$Ca_3Fe_2(SiO_4)_3$	
	spessartine	Sp	$Mn_3Al_2(SiO_4)_3$	sub-calcic garnet
	almandine	Al	$Fe_3Al_2(SiO_4)_3$	
	pyrope	Py	$Mg_3Al_2(SiO_4)_3$	
Pyroxene	diopside	Di	$CaMgSi_2O_6$	salite
	hedenbergite	Hd	$CaFeSi_2O_6$	
	johannsenite	Jo	$CaMnSi_2O_6$	
	fassaite	Fas	$Ca(Mg,Fe,Al)(Si,Al)_2O_6$	
Olivine	larnite	Ln	Ca_2SiO_4	monticellite
	forsterite	Fo	Mg_2SiO_4	
	fayalite	Fa	Fe_2SiO_4	knebelite
	tephroite	Tp	Mn_2SiO_4	
Pyroxenoid	ferrosilite	Fs	$FeSiO_3$	pyroxemangite
	rhodonite	Rd	$MnSiO_3$	
	wollastonite	Wo	$CaSiO_3$	bustamite
Amphibole	tremolite	Tr	$Ca_2Mg_5Si_8O_{22}(OH)_2$	actinolite
	ferroactinolite	Ft	$Ca_2Fe_5Si_8O_{22}(OH)_2$	
	manganese actinolite	Ma	$Ca_2Mn_5Si_8O_{22}(OH)_2$	
	hornblende	Hb	$Ca_2(Mg,Fe)_4Al_2Si_7O_{22}(OH)_2$	
	pargasite	Pg	$NaCa_2(Mg,Fe)_4Al_3Si_6O_{22}(OH)_2$	
	cummingtonite	Cm	$Mg_2(Mg,Fe)_5Si_8O_{22}(OH)_2$	sub-calcic amphibole
	dannemorite	Dm	$Mn_2(Fe,Mg)_5Si_8O_{22}(OH)_2$	
	grunerite	Gru	$Fe_2(Fe,Mg)_5Si_8O_{22}(OH)_2$	
Epidote	piemontite	Pm	$Ca_2(Mn,Fe,Al)_3(SiO_4)_3(OH)$	
	allanite	All	$(Ca,REE)_2(Fe,Al)_3(SiO_4)_3(OH)$	
	epidote	Ep	$Ca_2(Fe,Al)_3(SiO_4)_3(OH)$	
	clinozoisite	Cz	$Ca_2Al_3(SiO_4)_3(OH)$	
Plagioclase	anorthite	An	$CaAl_2Si_2O_8$	
Scapolite	marialite	Ml	$Na_4Al_3Si_9O_{24}(Cl,CO_3,OH,SO_4)$	
	meionite	Me	$Ca_4Al_3Si_9O_{24}(CO_3,Cl,OH,SO_4)$	
Axinite		Ax	$(Ca,Mn,Fe,Mg)_3Al_2BSi_4O_{15}(OH)$	
Other	vesuvianite (idocrase)	Vs	$Ca_{10}(Mg,Fe,Mn)_2Al_4Si_9O_{34}(OH,Cl,F)_4$	
	prehnite	Pr	$Ca_2Al_2Si_3O_{10}(OH)_2$	

Table 2. ***Skarn mineralogy. (Meinert, 1993)***

Simple triangular plots such as figure 7 illustrate variations within the compositionally complex minerals of garnet and pyroxene. Amphiboles, pertaining compositional and structural components are of greater complexity. Amphiboles in differing skarn types are characterised by variation in Fe, Mg, Mn, Ca, Al, Na and K. In Au, W and Sn skarns, amphiboles appear progressively more aluminous; in Cu, Mo and Fe skarns they are progressively more rich in the tremolite-actinolite series; and amphiboles in zinc skarns are both Mn rich and Ca deficient (Meinert 1993).

Spatial mineral zoning and temperal mineral zoning occur in skarns, superimposing to create complex patterns as seen in figure 7. Skarns in general contain a zonation pattern of proximal garnet, distal pyroxene and vesuvianite at a contact between skarn and marble. Also, individual minerals may display systematic colour or compositional variations within the larger zonation pattern.
Meinert (1987) recognised that skarn zonation patterns may be 'stretched out' for several kilometres, an important exploration consideration.

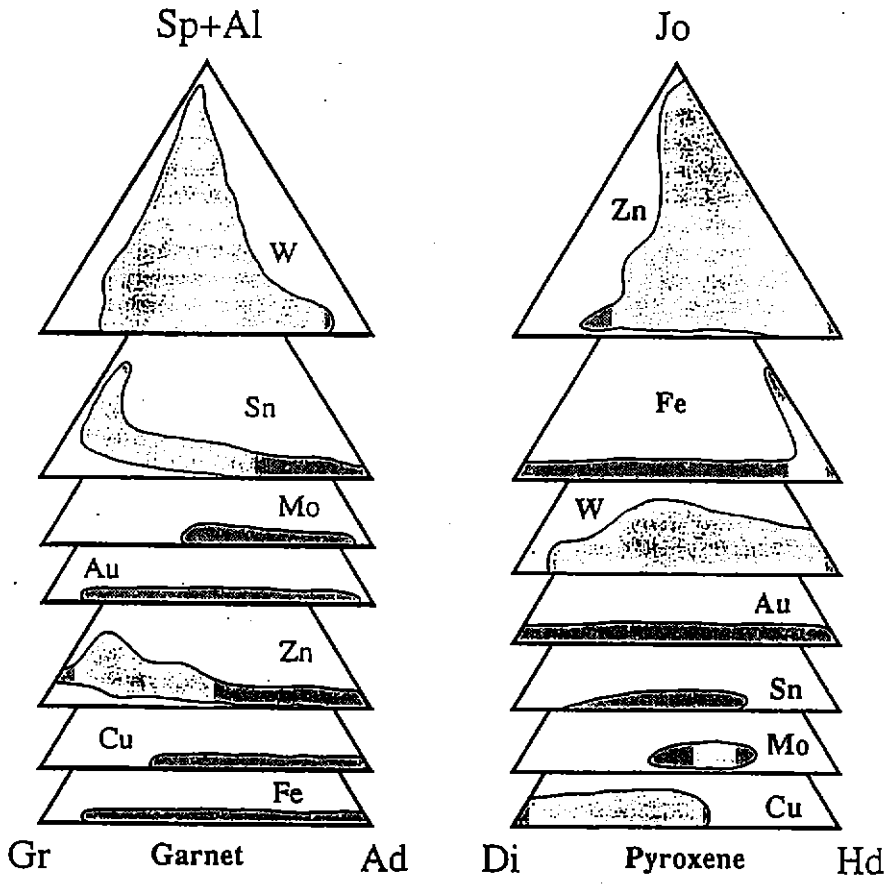


Figure 7. ***Ternary plots of garnet and pyroxene compositions from major skarn types. (after Einaudi et al., 1981, and Meinert, 1993 and 1989)***

Retrograde skarn mineralogy is generally structurally bound and overprints the pro-grade zonation sequence. General form may include epidote, amphibole, chlorite and other hydrous phases, abundant along fault, stratigraphic or intrusive contacts.

Zinc-lead Skarn mineralogy

Zinc skarns generally occur in continental environments, associated with prior subduction or rifting. Lead and silver are often associated at relatively high grades (ie. 10-20% Zn and Pb, 30-300g/t Ag). Associated intrusive bodies are varied, including quartz diorite, diabase-diorite, quartz monzonite, granodiorite, granite and quartz porphyry in the general form of stocks and dykes (representative of shallow formation environment). Geological environments include deep seated batholiths to shallow dyke-sill complexes to surface volcanic extrusions. Common to most zinc skarn ores is a distal association to the igneous rocks.

Zinc skarns may be categorised in accordance to distance from the magmatic source, temperature of formation, relative proportion of skarn and sulphide mineral and geometric relationship of the ore body. Unfortunately, most skarns form over a wide range of varying conditions, rendering such defined criteria inadequate. Megaw *et al.* (1988) noted that many zinc skarn districts, *'grade outward from intrusion-associated mineralisation to intrusion-free ores, which suggests that those districts lacking known intrusion relationships may not have been traced to their ends.'*
Meinert (1993) also recognised that most zinc skarns grade outward from skarn-rich mineralisation to skarn-poor ores, veins and massive sulphide bodies containing few, if any, skarn minerals. The presence of skarn minerals such as garnet and pyroxene indicates a distinctive and unique geochemical environment, clearly distinguishable from other ore types such as Mississippi Valley type - often containing Zn-Pb-Ag ores, but lacking skarn minerals.

Distinct mineral assemblages enable classification into calcic, magnesian and manganoan Zn-Pb skarns. Yiming's (1990) manganoan classification (unique to Zn-Pb skarns) form later than calcic skarns, often replacing them or forming within their margin. Primarily a product of fluid infiltration, Zn-Pb manganoan skarns occur along some structural or lithological contact of carbonate host rocks distal to intrusives in the form of metasomatic veins, lens or pipe (Yiming, 1990). Temperatures for manganoan skarns are thought to range from 200°C to 450°C, generally less than calcic skarns of 400°C to 650°C.

Substantial variations in skarn mineralogy may be representative of differing mineral paragenesis or stages; that is the onset of new stage deposition upon an incomplete initial deposition phase. The Ban Ban deposit in southeast Queensland, Australia, has been subjected to early stage skarn precursor replacement by a garnet-dominated assemblage, later overprinted by a sulphide phase of siderite, Fe sulphides, magnetite, various Ca (-Fe-Mn-Al-Mg)-bearing silicates, quartz and calcite, and dominated in an apparent final stage by chlorite and calcite (chlorite phase). Each stage is evident throughout all skarn lenses, changing locally in extent and mineralisation (Ashley, 1980). In addition to their Zn-Pb-Ag metal content, zinc skarns are identifiable by a distinctive manganese- and iron-rich mineralogy, by occurrence along structural and lithological contacts, and by an absence of significant metamorphic aureoles centred on the skarn.

Most zinc skarn minerals, including johannsenite (figure 8a), pyroxmangite (figure 8b), rhodonite (figure 8c), spessartine (figure 8d), garnet, pyroxene, olivine, ilvaite, actinolite, pyroxenoid, amphibole, chlorite and serpentine, may be manganese enriched.



a b b d

Figure 8. ***Skarn ore-bearing minerals: a) Johannesenite skarn, white minerals are quartz (-), x20, Dapai, Fujian; b) Pyroxmagnite skarn, (-), x20, Luoyang, Fujian; c) Sphalerite-bearing rhodonite skarn, black minerals are sphalerite, (+), x20, Baijiazi, Liaoning; d) Pyrite and sphalerite-bearing (black) spessartine skarn, (-), x20, Baijiazi, Liaoning. (Yiming, 1990)***

Zinc skarn identified within distal portions of major magmatic/hydrothermal systems may act as important exploration indicators in poorly exposed regions, regardless of the deposits expanse, by providing clues to areas not yet exposed to adequate exploration activity.

Geochemistry and geophysics

Geochemical studies of skarns generally focus upon mineral phase equilibria, fluid inclusions, isotopic investigation of fluid sources and pathways, and deformation exploration anomaly and background levels (Meinert, 1993). Phase equilibria studies enable an understanding of individual mineral reactions, and extensions thereof, to include variable compositions (eg. Bowman and Essene, 1982). Flowers and Helgeson (1983) used a thermodynamic database to model potential skarn-forming solutions. Fractionation of elements between minerals also enables estimation of skarn forming conditions.

Quartz, carbonate and fluorite are often important minerals of fluid inclusion investigation, given their possible containment of fluid inclusions, and stability over a broad T-P-X range. Continued growth and trapping of fluid from early high-temperature to later low-temperature events complicates inclusion investigation (Roedder, 1984), rendering it inadequate in providing an unambiguous measure of temperature, pressure and fluid composition. Work by Kwak (1986) supported documentation of high temperatures (>700°C) and high salinities (>50 wt.% NaCl equivalent and multiple daughter minerals) in most skarns. Copper and zinc skarns differ, yielding homogenisation temperatures of 300 to 350°C, consistent with the relatively shallow and distal geologic settings inferred.

Daughter minerals include NaCl, KCl, $CaCl_2$, $FeCl_2$, $CaCO_3$, CaF_2, C, $NaAlCO_3(OH)_2$, Fe_2O_3, Fe_3O_4, AsFeS, $CuFeS_2$ and ZnS. Magmatic fluids generally contain a KCl > $CaCl_2$ ratio, however high $CaCl_2$ fluids appear to have some interaction with more sedimentary wall rocks.

The transition from prograde to retrograde skarn event may be mapped via temperature and salinity shifts using fluid inclusions. For example, inclusion in garnet and pyroxene of iron skarns have homogenisation temperatures of 245 to 250°C and 100 to 250°C respectively with salinity less than 33 wt.% NaCl equivalent. In contrast, inclusion within scapolite, epidote and actinolite from these skarns have homogenisation temperatures of 320 to 400°C, 255-320C and 320 to 350C respectively (Meinert, 1993).

Isotopic investigations are an integral component in identifying the fluids associated with the formation of most large skarn systems. (Shimazaki, 1988). In general, stable isotope investigations support fluid inclusion and mineral equilibria analysis, demonstrating that most large skarn deposits are the product of diverse fluids, forming early, under high temperature, in saline brines, directly related to recrystallising magma systems. Meinert recognised that the highest-salinity fluids coincide with peak sulphide deposition, and that partial mixing with exchange connate or meteoric fluids is required for most deposits. The latest alteration events form primarily from dilute meteoric waters.

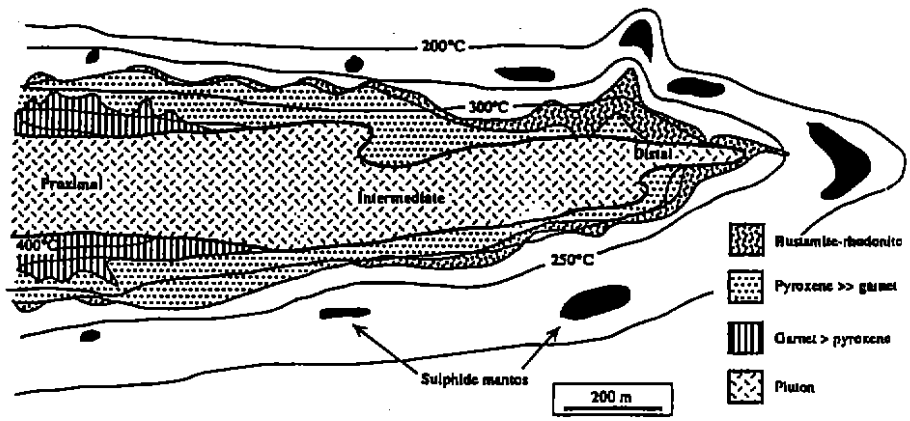
Exploration for the generally variable skarn metals may be assisted by anomalous concentrations of pathfinder elements in distal skarn zones. Metal dispersion halos have been found to form proximal Cu-Mo-Fe assemblages to distal precious metal zones and Pb-Zn-Ag veins. Meinert and Myers (1991) support thoughts that geochemical signatures among differing skarn systems produces characteristic suites of anomalous elements (background levels for a particular element of one skarn type may be highly anomalous in others). For example, Au, Te, Bi and As contents of 1, 10, 100 and 500 ppm respectively may be common for rocks and soils of gold skarn, yet may be absent for other skarn types (Meinert *et al.*, 1990; Myers and Meinert, 1991).

Skarn deposits tend to be significantly denser than surrounding rock, hence forming some gravitational anomaly or seismic discontinuity. In addition, skarns and associated plutons may form magnetic anomalies (Spector, 1972). Ishihara (1977) recognised that oxidised plutons (characteristic of Zn-Pb skarns) are likely to contain enough magnetite to form a magnetic high, whilst typical ilmenite bearing reduced plutons may form a magnetic low. Disseminated and massive sulphide minerals may produce strong IP, EM or magnetotelluric responses in skarns (Emerson and Welsh, 1988). The occurrence of carbonate rock metasomatism, and the presence of carbonaceous matter, can strongly distort electric surveys, and hence need be considered during interpretation.

Models and conclusions

Detailed mapping of the distribution of skarn mineral phases provides important information of size, characteristics and genesis of a skarn system. Several variables such as lithology, structure and timing may influence mineral development, and subsequently must be accounted for; eg. a given mineral may develop under differing P-T-X_{CO2} conditions in limestone relative to shale, or where fluid flow may be influenced by faulting or brecciation.

Models of skarn generation, such as figure 9 assist in areas of incomplete exposure or exploration. This generalised zinc model (after Meinert, 1987) combines skarn and ore mineralogy, metal ratios and geochemical data to produce a likely scenario.



Feature	Proximal	Intermediate	Distal
Garnet:pyroxene	> 1:1	1:20	No garnet
Max Jo in pyroxene	< 25%	25-50%	> 50%
Fe oxides	mt > hm	hm – mt	hm > mt
Ore sulphides	sl > gl – cp	sl > gl > cp	sl ~ gl > cp
Skarn:manto ore	> 10	1-10	< 1
Temperature	> 400°C	320° - 400°C	< 320°C
Salinity (NaCl eq. wt.%)	> 15 %	7.5-15%	< 7.5%
Zn/Cu	< 10	10-20	> 20
Zn/Pb	> 5	2-5	< 2
Pb/Cu	< 5	5-10	> 10

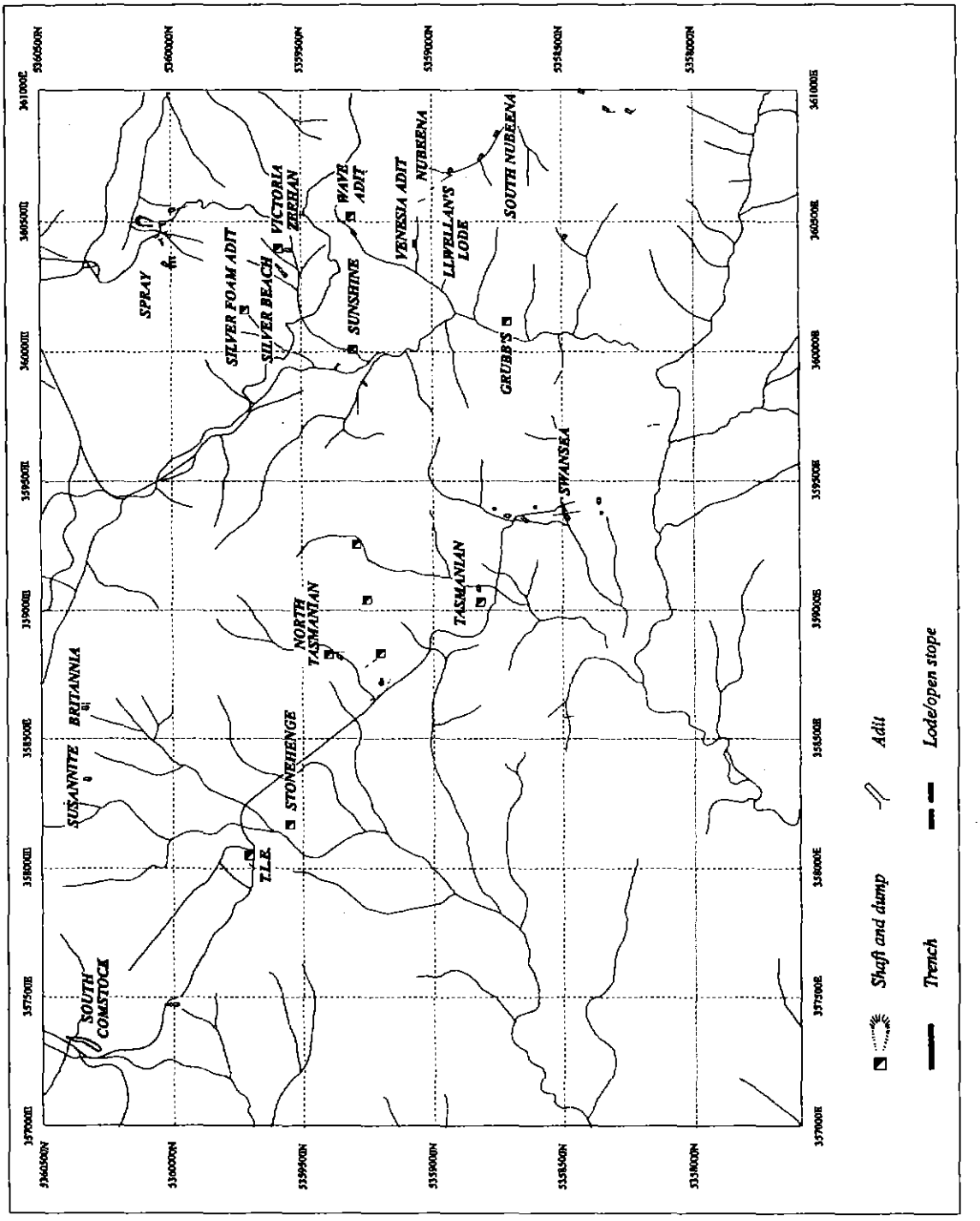
Figure 9. ***General model of zinc skarn zonation. (after Meinert, 1987)***

Distinct form many other ore deposit types, skarns are directly related to igneous intrusion, fundamentally controlling the skarn mineralogy and metal content. Alteration and mineralisation of country rock is representative of late-stage hydrothermal evolution of the pluton. The abundance of skarns within upper crust magma emplacements is a likely proponent of the reactivate of sedimentary rocks, in particular of carbonates. Although forming over a wide temperature range, it is the high-temperature spectrum that distinguishes skarns from other ore types. With high temperatures (>350C) and concentrated metasomatic fluids, distinctive skarn minerals such as garnet and pyroxene are able to stabilise (Meinert, 1993). With cooling, retrograde alteration of early skarn minerals in common.

APPENDIX 5.

Previous workings of the Stonehenge area

Blissett (1962) has investigated most (if not all) mining activities throughout the Zeehan area in some detail. Summary of his findings for those workings within the Stonehenge area (shown below) follow:



Boss

The original 80 acre lease was taken in 1888 by M.H. Oneill. In 1890 the Boss Silver Mining Co. N.L. was formed, and commenced exploring outcropping gossans in trenches, shallow adits and shafts. A lack of funds restricted activity until J. Dunn chartered the lease in 1908. During 1910 660 tons of gossan was produced for fluxing ore. The Broken Hill Proprietary Block 10 Co. Ltd. took over in 1913, exploring until 1916 - the last work to have been conducted.

Three known orebodies are hosted within Proterozoic quartzite, phyllite and slate. The main lode trends NE, containing pyrite with sphalerite and galena - reputedly to width of 16 feet. The West lode is a NW striking gossanous formation, and the East lode trends NNE comprising of a 2ft zone of sphalerite, pyrite and galena. Some 700 tons of low grade ore and flux produced 70 tons lead and 6500 ounces of silver.

Britannia

Originally leased to E.C. Mace in 1888, the Britannia ground was transferred to the Britannia Silver Mining Co. N.L. in 1890. Shallow exploration of NNE striking orebodies failed to return economic concentrate. Following several lease changes, the Mt Zeehan (Tasmania) company conducted further shallow exploration. A pyritic orebody (reported as 32ft in width) was identified, from which prospectors extracted up to 20 tons of payable ore per month from 1914 to 1917. In 1921, workings of a surficial orebody were extended, and although mineralisation proved erratic, significant galena was removed. No notable production has been recorded since 1924. The orebodies appear confined within faulted and sheared Proterozoic micaceous quartzite, siltstone and shale or phyllite, faulted against Cambrian greywacke and shale. Lodes are sporadic veins and masses of pyrite and sphalerite with impersistent bands or disseminations of pyrite.

Conclusion: Britannia orebodies are small and generally of low grade.

Colonel North Mines

The Colonel North Mines and Railway Co. N.L. incorporated several workings - primarily to the south of the Spray mine, and north of the Swansea mine. Major workings include Grubb's, Colonel North, Victoria-Zeehan, Silver Foam, Silver Wave and Silver Beach. First leased in 1888 by W.C. Grubb, the Grubb's Silver Mining Co. N.L. was established in 1890, and a shaft sunk soon after (Grubb's workings). The Colonel North Mines and Railway Co. N.L. formed in 1903.

The Victoria-Zeehan Silver-Lead Mining Co. N.L. formed in 1906. Working transferred grounds from the Colonel North company (NE of Colonel North), a shaft was sunk to 310 feet, however by 1910, inadequate water pumps forced closure. Colonel North and tribute parties continued several workings until 1911. Little mining/exploration has been conducted since.

Folded Oonah Quartzite and Slate host fissure veins of galena with sphalerite in gangue of siderite, pyrite and quartz. Primarily trending NW-NNW, the lodes are less than 8ft thick, with sulphides as masses or disseminations throughout the gangue. Barite in quartz has been recorded from the Grubb's Main shaft (Twelvetrees and Ward, 1910), and galena and jamesonite from the Silver Foam adit (Waller, 1904).

Workings:

Victoria-Zeehan: Situated NE of the Colonel North shaft with the view of intersecting predicted extensions of the Spray lodes. A shaft to 310ft was dug, with a crosscut driven east from the 300ft level. At 184ft the drive intersected a lode formation up to 6ft wide, containing minor galena in a gangue of siderite and quartz.

Silver Foam Adit: The Silver Foam Tributing Co. held tribute land from Colonel North Co prior to take over by the Victoria-Zeehan company. A NE adit extending some 600ft was cut in 1901-1902. The lode intersected contained zones of galena and jamesonite. A shaft sunk to 100ft revealed only traces of galena. The Victoria-Zeehan company later followed a minor vein of jamesonite and galena.

Colonel North Shaft: The Colonel North company sunk a shaft to 200ft, from which a crosscut was driven to the NE to an eventual length of 450ft. Two lodes of siderite and quartz were intersected.

Silver Beach ("Office") Adit: SE of the Colonel North shaft, the adit extended some 600ft NE, intersecting several siliceous gossanous formations within decomposed slate. No significant mineralisation was located.

Grubb's Shaft: To a depth of 330ft, four major drives were cut:

- No.1 (130ft) level: driven north, the orebody maintained a 3ft width, with high grade galena for 70ft, thinning into 50ft of galena and sphalerite 1ft in width. A south drive extending beyond 300ft intersected several small galena and sphalerite lenses.
- No.2 (200ft) level: A 200ft NW drive followed a lode formation of two galena and sphalerite veins. The orebody stoped out to the No.1 level and down to the No.3 level. A second drive extended 240ft to the SE.
- No.3 (270ft?) Level: The main lode channel extending north for 235ft recovered only minor galena. A south drive of 330ft cut sphalerite masses.
- No.4 (320ft) level: A small sphalerite vein of no economic value was the only intersection of a north drive, bounded by an east striking fault. Also fault bound, a drive to the south produced minor working of galena ore shoots.

Recorded Production - Colonel North Mines

	Ore (Tons)	Silver (OZ)	Lead (Tons)
Grubbs and Colonel North	2379	127225	1534
Victoria-Zeehan	43	850	15
Total	2422	128075	1549

Conclusions: Although orebodies in Colonel North leases may be southern continuations of the spray mine mineralised belt, it is difficult to correlate with specific Spray lodes given dislocation during post mineralised faulting.

Galena and sphalerite appear in bands and shoots within siderite and pyrite gangue. The main shoot in upper levels of the Grubb's workings plunges south (Twelvetrees, 1901). Siderite and galena seemingly increase in lower levels, with a possible re-occurrence of galena bands or lenses at depth. Small amounts of galena may be obtained from shallow workings within the mineralised zone north of the Colonel North shaft and south of the Spray mine - although thoroughly prospected.

Comstock and South Comstock

In 1888, lease was taken by W. Barlow, and soon after was transferred to the Comstock Mining Co. N.L. High concentrations of sphalerite were initially regarded as economic, and led to the subsequent extraction of galena. Shallow workings revealed disappointing results with little exploration extending beyond 1895. Upon acquisition of a consolidated lease in 1947, M.C. Howard, R.M. Waller and E. Tomkins re-opened workings. The electrolytic Zinc Co. of Australasia Ltd gained lease in 1948, and with tributors produced minor lead and zinc until 1952.

A total of 80 acres pegged by W.H. Foley in 1888 was transferred to the South Comstock Silver Mining Co. N.L. in 1889. A drive as continuation of the Comstock main lode was ceased prior to 1890. In 1896 F. O'Neil and W. Flaherty gained lease and mined the main lode as an open-cut before take over by Zeehan South Comstock Ltd in 1901. Primary activities continued until 1916, with only significant extraction thereafter being that of argentiferous galena between 1926 and 1937 (J. Dunkley and party)

Host rocks primarily consist of successive disturbed and contorted mica-schist, phyllite and slate with quartzite and sub-greywacke. Locally, dark grey limestone and calcareous siltstone exist near the Comstock Creek.

Fissure vein lodes contain sphalerite, galena and minor chalcopyrite in gangue of pyrite, siderite and quartz. The four lodes worked trend NNW and dip steeply east:

- No.1 (Main) lode: up to 50ft, consisting of irregular masses of sphalerite with pyrite and galena within decomposed limestone and shale.
- West lode: pyritic formation containing minor sphalerite and galena.
- No.2 lode: pyritic orebody with bands of galena and sphalerite.
- East (Allison's) lode: massive sphalerite mixed with small quantities of pyrite and galena.

Combined production estimates for Comstock and South Comstock include 4021 tons galena ore and 3245 tons zinc ore.

Nubeena

Located upon Nubeena Hill, the original lease was taken by E. Mace in 1889, and was transferred to Nubeena Silver Mining Co. N.L. in 1893. Exploration of three orebodies from 1891 to 1895 produced a few tons of galena, primarily from near surface workings. Following numerous lease transfers, the Venezia tribute party successfully worked several adits for A Shillington from 1906 to 1913. In 1928 the perry brothers produced ore containing 32 tons lead and 1535 ounces silver. During 1936, Higginson extracted minor quantities of ore.

Folded shale, slate and pale grey saccharoidal quartzite of the Oonah Quartzite and Slate host fissure lodes of irregular veins and aggregates of galena, pyrite and minor traces of tetrahedrite within a siderite and quartz gangue. Although generally trending NNW, the 'old Nubeena lode' (western) strikes NNE. Galena has assayed up to 100 ounces silver per ton and 70% lead.
Some 500 tons of concentrate has been removed, containing 325 tons lead and 42000 ounces silver.

Conclusions: Country rocks are highly fissured and faulted, with galena scattered throughout ore channels. Post-mineralisation faults may have dislocated the lodes. Workable ore is concentrated in small irregular masses or bands whose behaviour is unpredictable - doubtful economic interest.

South Nubeena

First leased to J. Duncan in 1888, little work was conducted until acquisition in 1903 by G.E. Butler. A shattered and faulted zone hosted an orebody in which only fine galena veins - although assaying at 70% lead and 100 ounces silver per ton. Between 1906 and 1913 some 77 tons ore containing 50 tons lead and 7000 ounces silver was sold.

Spray

Separate leases claimed in 1887 were transferred to E.J. Freeman in 1888. Established the following year, the Silver Spray Silver Mining Co. N.L. cut an adit of 265ft with little success. The same year, leases were obtained by the Mount Zeehan (Tasmania) Silver0Lead Mines Ltd, whose attention was captured at the Spray section by the discovery of antimonal silver-lead ore (jasmesonite) assaying up to 2000 ounces silver per ton (Twelvetrees, 1901). By 1908 several adits and shafts were sunk.
A drillhole completed in 1932 intersected the orebody, but consisted only of siderite and pyrite with jamesonite traces.

Zeehan Explorations commenced drilling of the Main lode in 1949, however the hole with stopped with mineralisation restricted to stringers of siderite or quartz with minor pyrite and jamesonite.
Striking NNW, the fissure lode orebodies dip steeply within the Oonah Quartzite and Slate.

Austral Creek to the north flows near the boundary with Cambrian greywacke, dolomitic siltstone and shale though apart of the Crimson Creek Formation. East of the workings, Cambrian beds overlie the Proterozoic quartzite and slate with no evidence of an angular unconformity. The Balstrup Fault lies to the north and NW. Waller (1904) reports that although the lodes were only productive within the quartzite, the Main lodes extends north into the Cambrian rocks - workings here are shallow and the orebody oxidised. The contain shoots of galena and jamesonite (up to 16ft wide) within a gangue of pyrite, siderite and quartz.`

For the quarter ending December 31, 1900, 652 tons concentrate produced by the Mount Zeehan (Tasmania) company, primarily from the Spray mine, yielded 443 tons lead and 65232 ounces silver. The first quarter of 1901 produced 1047 tons concentrate containing 656 tons lead and 107104 ounces silver.. Mount Zeehan Tasmania0 company produced from the Spray mine until 1909. Between 1933 and 1934, prospectors removed 28 tons lead and 3000 ounces silver concentrate.

Stonehenge

Leased to W.E Brooks in 1888 and transferred to the Stonehenge Silver Mining Co. N.L. in 1893, a single NNE trending lode was unsuccessfully worked until 1894. During 1907 C. Brumby and A. Nicholas extended an existing shaft to 60ft. Twelvetrees described the orebody as near vertical but of variable dip, containing pyrite and sphalerite with minor chalcopyrite in which galena appears as blobs. Gangue is of quartz and siderite. Drives to the north and south from the 30ft level intersected small ore shoots. South of the shaft, a galena ore shoot 10 inches wide was located, extending for only a few feet.

Susannite

Originally claimed by J. Spencer 1888, the lease changed numerous times until acquisition by J.J. Walsh in 1919. Between 1919 and 1923, pyrite assaying at 42% sulphur was mined and shipped to the Mt Lyell company plant in Yarraville, Victoria.

Two NW trending orebodies were exploited:

- Western lode: containing up to 18ft of pyrite with galena and cerussite. Waller (1903) reported two types of galena; the first a dense fine grained variety, assaying 50 ounces silver per ton, the second a cubical ore exceeding 100 ounces silver per ton.
- Eastern lode: cut 100 below a gossan outcrop contains a broad band of loose pyrite and 12ft of gossan containing cerussite and campylite (Twelvetrees and ward, 1910) assaying 116 ounces silver per ton.

Up to 40 tons of silver-bearing ore has been extracted with a metal content of 3500 ounces silver and 20 tons lead.

Swansea

SE of the Tasmanian mine, R.B. Montgomery was first to obtain lease in 1899. Several changes (including the Swansea Mining Co. N.L.) led to L. Murphy gaining lease in 1908. Twelvetrees and Ward (1910) noted an adit had been driven for 200ft SE of a galena and sphalerite orebody dipping slightly to the NE. No output was reported - lease relinquished. By 1922 the Swansea Prospecting Syndicate N.L. had sunk a shaft to 130ft, however lack of capital impeded further development.

Country rocks include contorted hard black shale or slate, pale fine to coarse quartzite (quartz veined) and pale conglomerate bands. Apart of the upper Proterozoic Oonah Quartzite and Slate or Lower Cambrian Crimson Creek Formation, the beds have been subjected to intense faulting. Primarily, post-ore faulting through Jurassic/Tertiary periods dislocated the orebodies.

Fissure lodes contain galena and coarse sphalerite, with chalcopyrite and minor tetrahedrite in gangue of siderite and quartz. Mineralisation exists as ore shoots up to 110ft long, cutting a clearly defined lode channel striking NW.

Production - Swansea mine

	Galena Ore (Tons)	Zinc Ore (Tons)	Lead Content (Tons)	Silver Content (Ozs)	Zinc Content (Tons)	Cadmium Content (Tons)
to 1925	2000	1000	1200	32000	470	40
1926	200	220	107	3300	100	
1929	20		12	330		
Total	2220	1220	1319	35630	570	40

Sylvester Skarn

Transferred to the Sylvester company by R. Ritchie and A.N. Alison in 1891, two parties were let work the galena/mixed pyrite orebody. From 1895, little interest was shown until 1899 when the Tasmanian Smelting Co. chartered lease and commenced driving long deep trenches, revealing nothing of economic value. Ore and gossan material was extracted from the Main lode - a large NNE trending formation of pyrite with galena and sphalerite, again of little economic proportion. Latter workings conducted by W.C. Robinson and E.A. Tomkins from 1958 to 1961 included shallow trenches and pits cut into shale, quartzite and greywacke of the Oonah Quartzite and Slate west of the Main lode. Veins of quartz with pyrite, galena and sphalerite were intersected.

Post-mineralisation brecciation and movement evident throughout the area.

Production - Sylvester Mine

	Ore (Tons)	Lead (Tons)	Silver (Ozs)
to 1893	38	17	2888
1898	207	66	4630
1899	192		
1904	36		
1906	516	190	19000
1907	150		
1908	50		
1950	3	1	42
Total	1192	274	16560

Tasmanian

An original lease taken by L. Susman in 1888 was transferred to the Tasmanian Silver Mining Co. Ltd in 1890. Mineralisation projecting NNW from the Swansea mine was explored by adit, and a shaft sunk to 72ft. An orebody up to 4ft in thickness was cut containing galena masses and less common sphalerite throughout.

Deepening of the shaft in 1895 discovered no further mineralisation.

J. Hill conducted further exploration from 1941. Trenches, shallow adits and prospecting shafts identified small galena orebodies, with minor ore production continuing until 1961. Northern workings are within sheared and shattered Proterozoic quartzite, siltstone and shale, faulted against Cambrian chert-conglomerate and siltstone. Permian tillites overlie.

North Tasmanian

First claimed in 1888 by J.J. Martin, the North Tasmanian workings were held by the Tasmanian Silver Mining Co. Ltd in 1890. Two parallel lodes were located and exploited in shallow workings and a shaft dug in No.1 Lode.

Fissure veins of galena and sphalerite within a pyrite, quartz and siderite gangue trend NNW through Oonah Quartzite and Slate. These contorted and shattered units are faulted to the southeast (of Main shaft) against Cambrian greywacke, grit and shale.

- No.1 (North Tasmanian) lode: the Main shaft was to 190ft. Shoots of galena and sphalerite were extracted.
- No.2 lode: some 200ft SW of the main shaft, No.2 lode was worked as an adit and shallow stopes parallel to the No.1 lode. Twelvetrees (1901) suggests that given the NW dip is shallower than that of the No.1 lode, the two may meet at depth.
- Horton's No.1 adit: 180ft long, driven east from 400ft east of the main shaft - nothing of economic significance.
- Horton's No.2 adit: 430ft westerly from 500ft north of the main shaft - no reward
- Riley's Workings (No.3 lode): non-viable lode intersected.

Boreholes sunk by the Tasmanian Department of Mines in 1957 intersected a few veinlets of galena, sphalerite and pyritised argillite, all displaced during post-ore faulting.

Production - Tasmanian/North Tasmanian Mines

	Ore (Tons)	Lead (Tons)	Silver (Ozs)	Zinc (Tons)
to 1893	957	575	28700	
1933	5	3	282	
1934	20	13.2	1106	
1935	11.8	8.2	823.9	
1936	37.4	27.1	2592	
1937	24.5	17.7	1749.8	
1938	17.4	9.2	859.5	
1940	31.4	21.3	1731.8	
1947	20.3	9.1	625.6	4.8
1948	34.4	24.1	2085.2	
1950	4.5	3.1	250.6	
1951	14.6	5.1	236.2	3
1953	5.7	3.9	256.5	
Total	1184	720	41299.1	7.8

T.L.E.

The workings were first held by V. Ellis in 1888, and later by the Tasmanian Land Exploration Co. Ltd inn 1891. Three lodes have been worked:

- Main (No.1) lode: the NNE striking orebody was initially worked as adit, with a shaft later sunk to 110ft. A crosscut was driven 15ft to the east. A drive 200ft north of the shaft produced milling ore high in silver content.
- No.2 (Hughes') lode: 220ft east and parallel to the main lode, this was initially worked as an adit and later through shaft. A 200ft drive along the orebody enabled extraction of silver rich ore (no sphalerite).
- No.3 (Thurston's) lode: worked by the Thurston tribute party (1908), the orebody is west of No.1 lode and strikes NNW.

Greywacke-conglomerate, grit, greywacke and shale thought part of the Cambrian Crimson Creek Formation comprise the country rock unit. Slightly north, the Tenth Legion Fault separates these beds with the Oonah Quartzite and Slate. Lodes are fissure veins of galena and sphalerite assaying up to 80% lead and 130 ounces silver per ton.

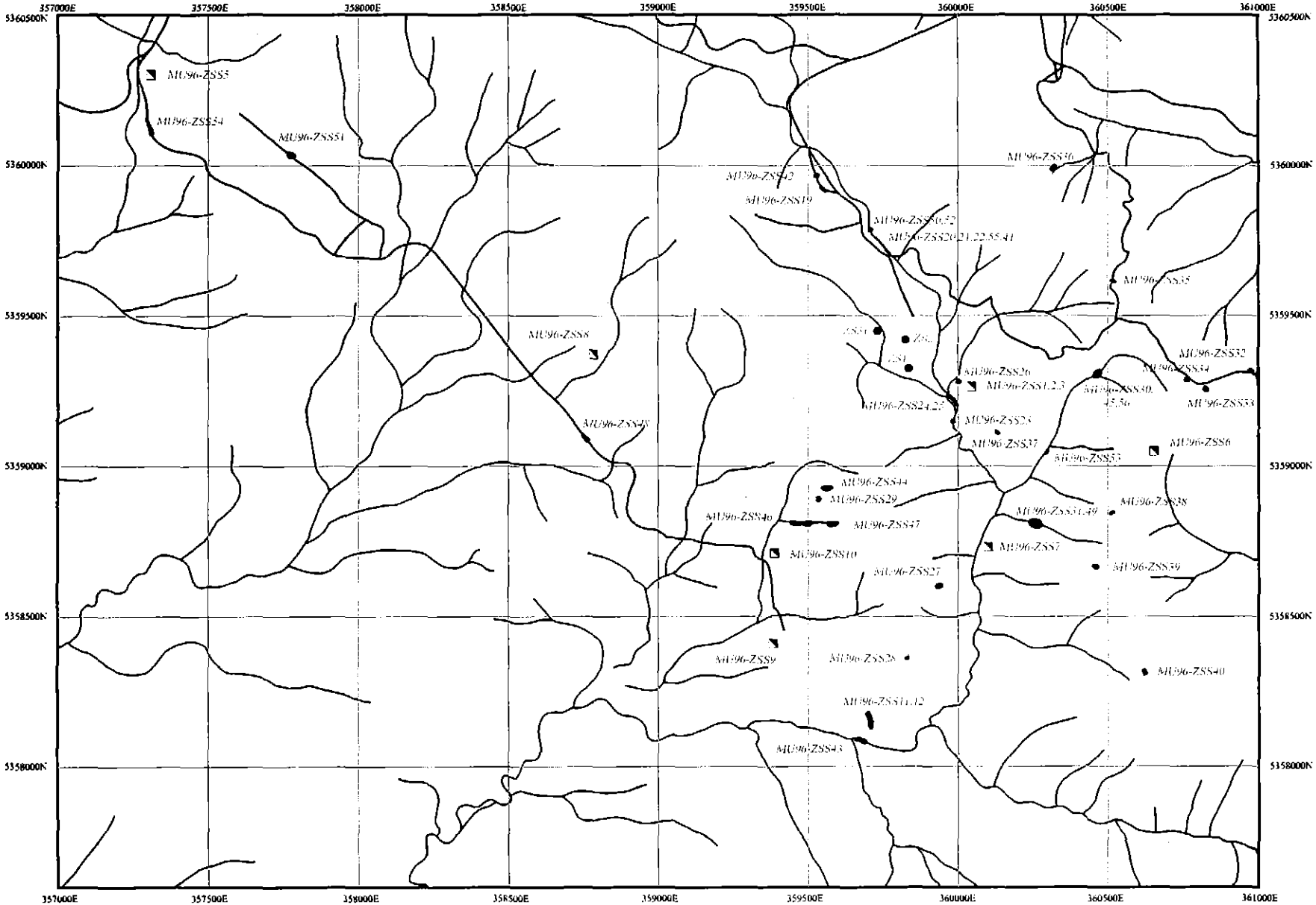
Until 1911, workings had extracted 300 tons of galena containing 200 tons lead and 30000 ounces silver. In 1954 a further 5.43 tons were removed, containing 2.8 tons lead, 0.74 tons zinc and 31 ounces silver.

364386

APPENDIX 6.

Thin section locations

STONEHENGE THIN SECTION/POLISHED SECTION LOCATIONS



Mine Workings

ZSS1 - Colonel North
ZSS2 - Colonel North
ZSS3 - Colonel North
ZSS4 - Oceana
ZSS5 - South Comstock
ZSS6 - Nubeena
ZSS7 - Grubb's
ZSS8 - North Tasmania
ZSS9 - Swansea
ZSS10 - Swansea North

CRA Diamond Drillholes

ZSS13 - ZS1 @ 120m
ZSS14 - ZS1 @ 158.3m
ZSS15 - ZS2 @ 101m
ZSS16 - ZS31 @ 129.9m
ZSS17 - ZS31 @ 154.6m
ZSS18 - ZS31 @ 188.5m

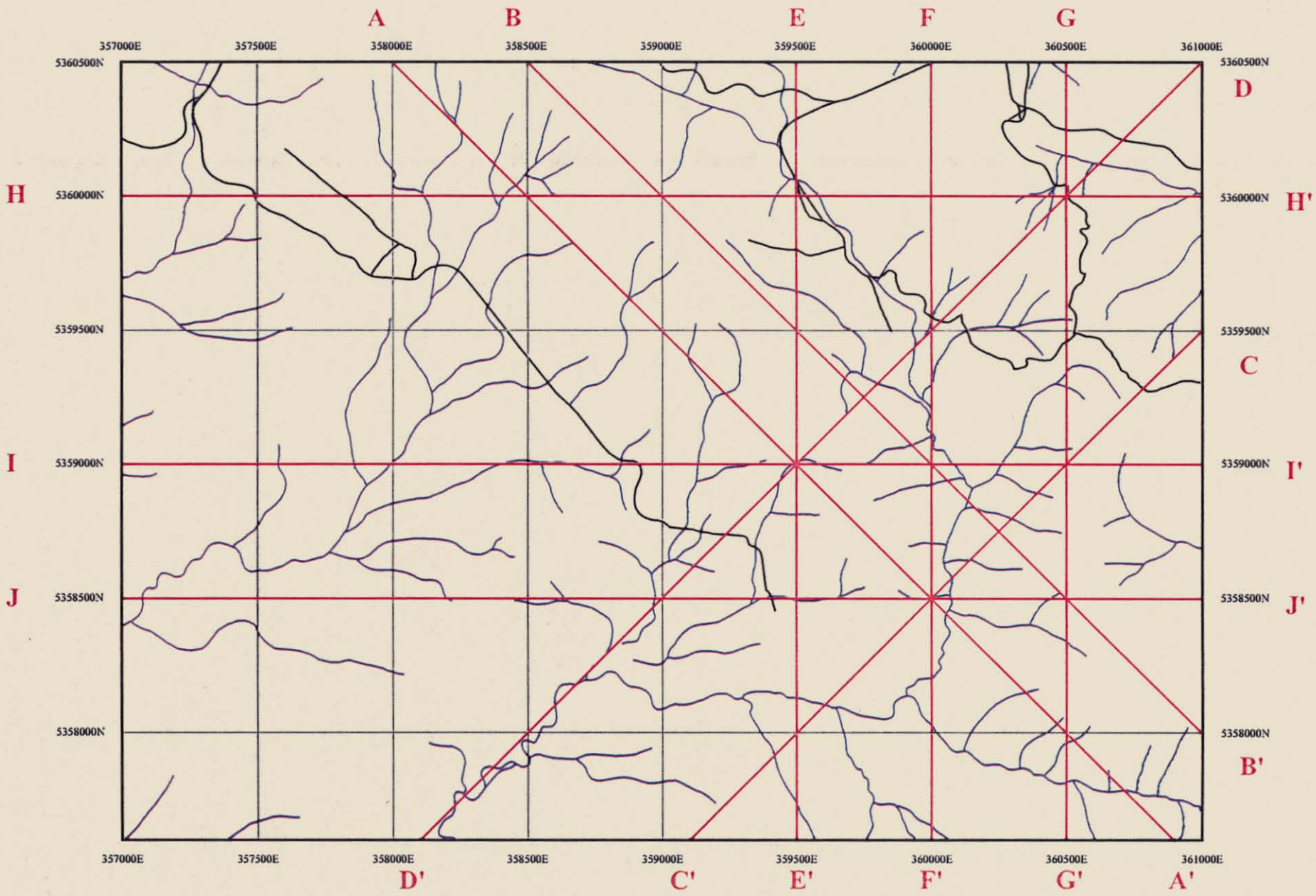
3948187

ZSS1	-	Colonel North	mine workings	mineralogical
ZSS2	-	Colonel North		
ZSS3	-	Colonel North		
ZSS4	-	Oceana		
ZSS5	-	Comstock		
ZSS6	-	Nubeena		
ZSS7	-	Grubb's		
ZSS8	-	North Tasmania		
ZSS9	-	Swansea		
ZSS10	-	Swansea North		
ZSS11	-	location MU96-91		
ZSS12	-	location MU96-91		
ZSS13	-	ZS1, 120m	diamond drillholes	
ZSS14	-	ZS1, 158.3m		
ZSS15	-	ZS2, 101m		
ZSS16	-	ZS31, 129.9m		
ZSS17	-	ZS31, 154.6m		
ZSS18	-	ZS31, 188.5m		
ZSS19	-	location MU96-13	orientated samples	structural
ZSS20	-	location MU96-22		
ZSS21	-	location MU96-23		
ZSS22	-	location MU96-24		
ZSS23	-	location MU96-33		
ZSS24	-	location MU96-35(E)		
ZSS25	-	location MU96-35(G)		
ZSS26	-	location MU96-38		
ZSS27	-	location MU96-47		
ZSS28	-	location MU96-84		
ZSS29	-	location MU96-101		
ZSS30	-	location MU96-144		
ZSS31	-	location MU96-162		
ZSS32	-	location MU96-183		
ZSS33	-	location MU96-186		
ZSS34	-	location MU96-189		
ZSS35	-	location MU96-193		
ZSS36	-	location MU96-198		
ZSS37	-	location MU96-202		
ZSS38	-	location MU96-206		
ZSS39	-	location MU96-210		
ZSS40	-	location MU96-215		
ZSS41	-	location MU96-27		
ZSS42	-	location MU96-11		
ZSS43	-	location MU96-92		
ZSS44	-	location MU96-100		
ZSS45	-	location MU96-144		
ZSS46	-	location MU96-102		
ZSS47	-	location MU96-103		
ZSS48	-	location MU96-117		
ZSS49	-	location MU96-162		
ZSS50	-	location MU96-17		
ZSS51	-	location MU96-134		
ZSS52	-	location MU96-17(C)		
ZSS53	-	location MU96-160		
ZSS54	-	location MU96-142		
ZSS55	-	location MU96-25		
ZSS56	-	location MU96-144		

APPENDIX 7.

Profile lines

PROFILE LINES ACROSS THE STONEHENGE AREA



364390

Stonehenge Structure

Zeehan, Tasmania

364391

97-3958

ANNUAL REPORT ZEEHAN NO 1
EL 28/88 - P.E. NOV 1996 - CRA
S TEAR/R RUSSELL- VOL 3 OF 3

357000E 357500E 358000E 358500E 359000E 359500E 360000E 360500E 361000E

5360500N 5360000N 5359500N 5359000N 5358500N 5358000N

Balstrup Fault

Tenth Legion Fault

SWANSEA SYNCLINE

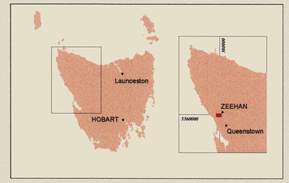
- *Strike and dip of bedding (So)*
- *Direction and plunge of fold axis - antiform*
- *Direction and plunge of fold axis - synform*
- *Strike and dip of cleavage (S_1, S_2, S_3)*
- *Geological boundary possibly including faults*
- *Thrust fault with teeth on upper plate*
- *Undifferentiated fault*
- *Bedding trace*
- *Outcrop trace from air photo interpretation*
- MU96-171 *Sample location stations*
- ZS1 *CRAE diamond drillhole locations*
- TH14 *Gold Fields Exploration diamond drillhole locations*
- ZS4 *Air core locations*
- *Air core gridlines*
- *Local grid line*
- *Creeks*
- *Roads/Tracks*
- *Shaft and dump*
- *Trench*
- *Adit*
- *Lode/open stope*

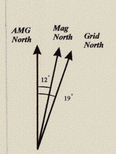
5 cm

SCALE 1:5 000

100 0 100 200 300 400 500 metres

LOCATION MAP





Field Stations

Zeehan, Tasmania

97-3958

ANNUAL REPORT ZEEHAN NO 1
EL 28/88 e P.E. NOV 1996 e CRA
S TEAR/R RUSSELL- VOL 3 OF 3

364392

- Strike and dip of bedding (So)
- Direction and plunge of fold axis - antiform
- Direction and plunge of fold axis - synform
- Strike and dip of cleavage (S_1, S_2, S_3)
- Geological boundary possibly including faults
- Thrust fault with teeth on upper plate
- Undifferentiated fault
- Bedding trace
- Outcrop trace from air photo interpretation

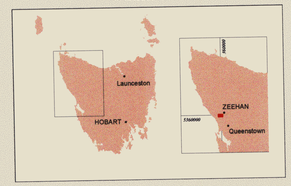
- MU96-171 — Sample location stations
- ZS1 — CRAE diamond drillhole locations
- TH14 — Gold Fields Exploration diamond drillhole locations
- ZS4 — Air core locations
- Air core gridlines
- Local grid line
- Creeks
- Roads/Tracks
- Shaft and dump
- Trench
- Adit
- Lode/open stope

5 cm

SCALE 1:5 000

100 0 100 200 300 400 500 metres

LOCATION MAP



AMG North — Mag North — Grid North

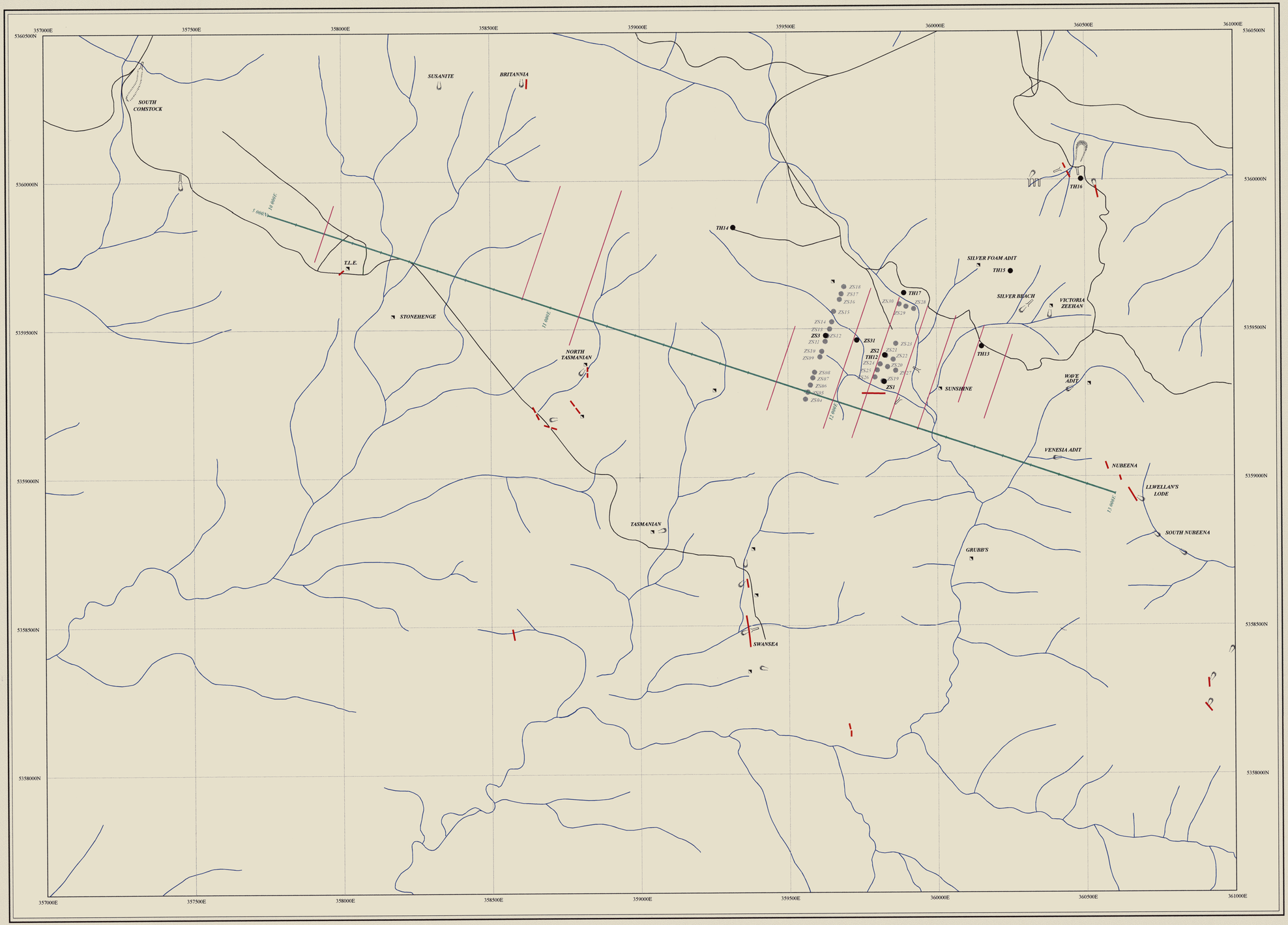
12 19°

Drillhole Locations

Zeehan, Tasmania

97-3958

ANNUAL REPORT ZEEHAN NO 1
EL 28/88 - P.E. NOV 1996 - CRA
S TEAR/R RUSSELL- VOL 3 OF 3



364393

- Strike and dip of bedding (So)
- Direction and plunge of fold axis - antiform
- Direction and plunge of fold axis - synform
- Strike and dip of cleavage (S_1, S_2, S_3)
- Geological boundary possibly including faults
- Thrust fault with teeth on upper plate
- Undifferentiated fault
- Bedding trace
- Outcrop trace from air photo interpretation
- MI96-171 — Sample location stations
- ZS1 — CRAE diamond drillhole locations
- TH14 — Gold Fields Exploration diamond drillhole locations
- ZS4 — Air core locations
- Air core gridlines
- Local grid line
- Creeks
- Roads/Tracks
- Shaft and dump
- Trench
- Adit
- Lode/open stope

5 cm

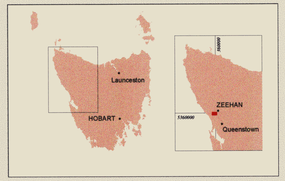
SCALE 1:5 000

100 0 100 200 300 400 500 metres

AMG North — Mag North — Grid North

12° 19°

LOCATION MAP



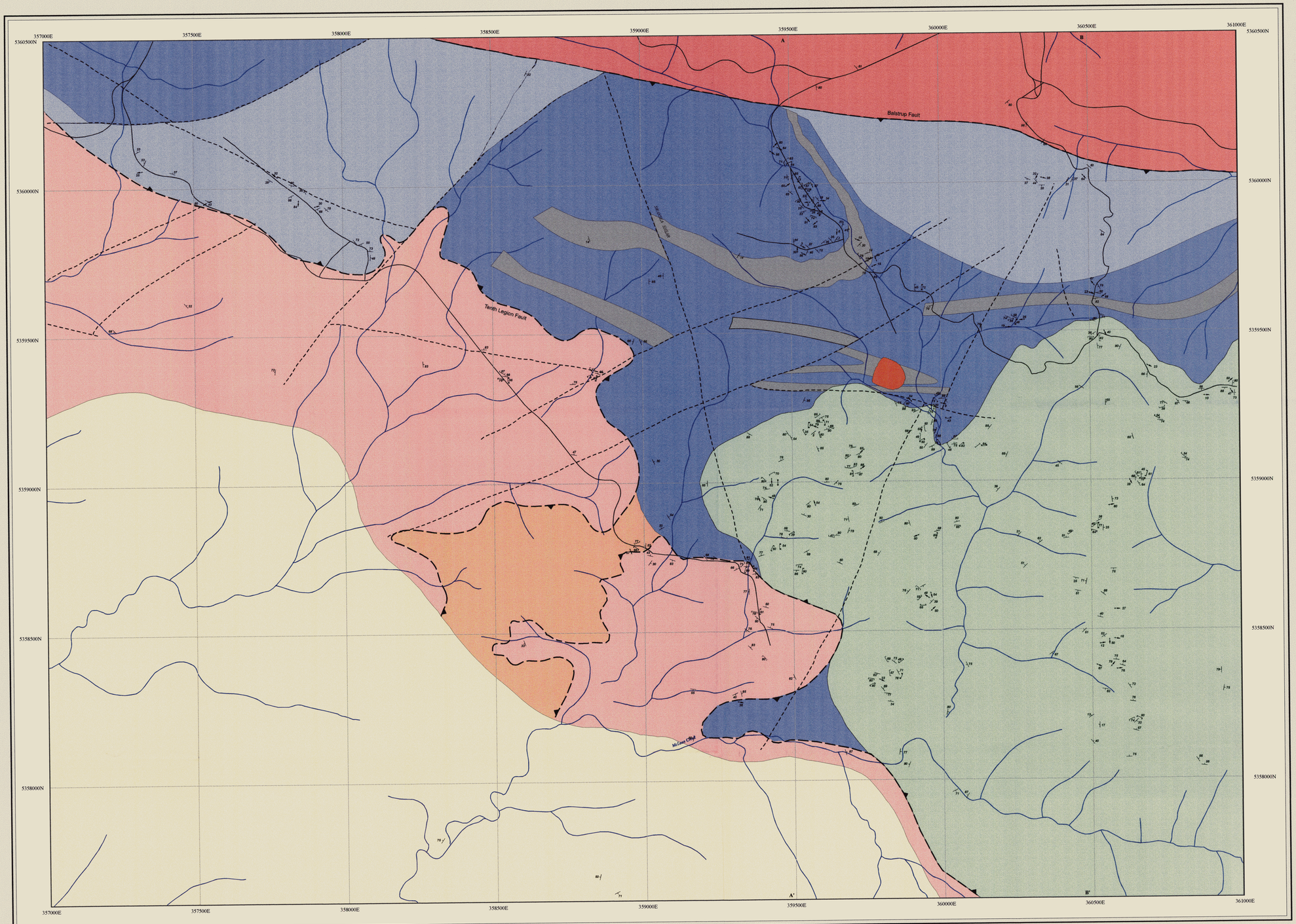
Stonehenge Geology

Zeehan, Tasmania

364394

97-3958

ANNUAL REPORT ZEEHAN NO 1
EL 28/88 - PE. NOV 1996 - CRA
S TEAR/R RUSSELL- **VOL3 OF 3**



PROTEROZOIC
- Qha — *Alluvium, elluvium and marsh deposits.*
- T — *Surficial massive ironstone (gossan?).*
- €d — **Dundas Group:** *Undifferentiated chert conglomerates, gritty sandstone, siltstone and light green basalt.*
- €c — **Crimson Creek Formation:** *Interbedded dark green basalt, reddish-orange volcaniclastics, khaki mudstone and dark grey shale.*
- Po — **Oonah Formation:** *Undifferentiated.*
- Pom — *Micaceous sandstone, siltstone and minor shale.*
- Pos — *Siltsone, shale and dolomite (undifferentiated).*
- Posb — *Graphitic black shale.*
- Posd — *Dolomite - dolomitic limetsone dominant.*
- Poq — *Massive quartzite.*

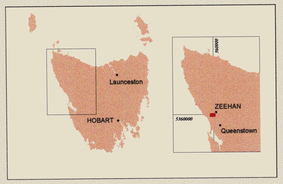
ZEEHAN REGION STRATIGRAPHIC COLUMN

5 cm

SCALE 1:5 000

100 0 100 200 300 400 500 metres

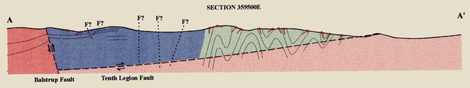
LOCATION MAP



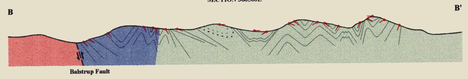
- Strike and dip of bedding (So)
- Direction and plunge of fold axis - antiform
- Direction and plunge of fold axis - synform
- Strike and dip of cleavage (S_1, S_2, S_3)
- Geological boundary possibly including faults
- Thrust fault with teeth on upper plate
- Undifferentiated fault
- Bedding trace
- Outcrop trace from air photo interpretation
- MU96-171 — *Sample location stations*
- ZS1 — *CRAE diamond drillhole locations*
- TH14 — *Gold Fields Exploration diamond drillhole locations*
- ZS4 — *Air core locations*
- *Air core gridlines*
- *Local grid line*
- *Creeks*
- *Roads/Tracks*
- *Shaft and dump*
- *Trench*
- *Adit*
- *Lode/open stope*

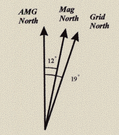
Bedding trends at surface.
Interpretated bedding form.

SECTION 359500E



SECTION 360500E





Appendix XI

Additional Assays for DD95ZS31: Stonehenge

[redacted] Stone [redacted] DD9 [redacted] Assa [redacted]

Borehole	From	To	Width	Ag ppm	Al %	As ppm	Au ppm	Ba ppm	Ca %	Cu ppm	Fe %	K %	Mg %	Mn ppm	P ppm	Pb ppm	Sn ppm	Zn ppm	S %
DD95ZS31	9	11	2	-0.5	10.4	35	-0.008	555	-0.05	30	0.99	4.48	0.53	14	160	465	8	249	
DD95ZS31	11	13.4	2.4	-0.5	10	22	-0.008	563	-0.05	33	0.71	4.41	0.52	-10	145	348	6	289	
DD95ZS31	13.4	15.75	2.35	-0.5	9.34	49	-0.008	523	-0.05	32	1.55	3.88	0.47	28	140	477	10	475	
DD95ZS31	15.75	18	2.25	-0.5	10.2	26	-0.008	552	-0.05	26	0.57	3.81	0.51	-10	120	394	6	387	
DD95ZS31	18	19.5	1.5	-0.5	10.7	30	-0.008	604	-0.05	17	0.55	4.16	0.5	-10	145	300	4	264	
DD95ZS31	19.5	20.7	1.2	-0.5	10.3	33	-0.008	571	-0.05	29	0.5	4.07	0.48	-10	120	107	11	295	
DD95ZS31	20.7	23.6	2.9	-0.5	10.8	37	-0.008	613	-0.05	25	0.8	4.54	0.51	36	125	649	-3	457	
DD95ZS31	23.6	25.5	1.9	-0.5	11.4	45	-0.008	679	-0.05	21	0.63	4.82	0.54	11	130	628	-3	405	
DD95ZS31	25.5	27	1.5	-0.5	9.81	37	-0.008	586	-0.05	35	0.58	4.36	0.5	11	110	1020	9	776	
DD95ZS31	27	28.5	1.5	-0.5	9.98	43	-0.008	615	-0.05	41	0.8	4.39	0.52	34	110	1340	4	1300	
DD95ZS31	28.5	29.55	1.05	-0.5	9.6	49	-0.008	741	-0.05	45	0.76	4.1	0.52	38	215	861	9	588	
DD95ZS31	29.55	30.35	0.8	9.2	9.06	255	-0.008	734	-0.05	109	2.45	3.96	0.53	40	195	1040	18	1620	
DD95ZS31	30.35	31.5	1.15	11.7	1.89	443	0.009	264	-0.05	93	2.5	0.7	0.15	68	80	6750	7	9600	2.82
DD95ZS31	31.5	32.5	1	3	0.79	184	-0.008	91	0.05	30	1.37	0.17	0.07	36	60	3810	7	15100	1.99
DD95ZS31	32.5	33.5	1	5.2	3.05	479	0.014	214	0.05	66	2.71	1.17	0.17	55	70	4840	13	16800	3.22
DD95ZS31	33.5	34	0.5	11.6	2.91	628	0.009	206	0.05	71	9.32	1.18	0.18	76	65	8080	9	8610	9.42
DD95ZS31	34	35.2	1.2	9.7	0.5	169	-0.008	77	-0.05	71	1.77	0.11	0.06	34	-50	2140	11	38600	3.24
DD95ZS31	35.2	35.5	0.3	26.5	1.09	303	0.01	140	-0.05	105	25.6	0.46	0.08	32	-50	9400	12	88000	32.9
DD95ZS31	35.5	36	0.5	119	0.89	406	0.017	109	-0.05	410	12	0.31	0.06	127	-50	49400	72	213000	23.5
DD95ZS31	36	37	1	108	2.69	987	0.021	198	-0.05	755	14.3	1.17	0.18	108	65	73000	17	108000	21.8
DD95ZS31	37	37.5	0.5	10.8	8.28	259	-0.008	519	-0.05	160	4.12	3.73	0.56	78	215	4260	40	31200	5
DD95ZS31	37.5	39	1.5	6.6	1.53	633	-0.008	194	0.06	67	4.56	0.53	0.12	74	70	4740	17	14600	4.84
DD95ZS31	39	40	1	5.1	1.46	198	-0.008	200	-0.05	50	3.35	0.57	0.12	35	55	2740	9	12700	3.27
DD95ZS31	40	40.5	0.5	117	1.67	674	0.01	221	-0.05	395	11.6	0.73	0.13	115	50	79000	57	143000	19.6
DD95ZS31	40.5	42.25	1.75	1.1	6.53	58	-0.008	442	0.1	76	1.26	3.62	1.05	41	390	848	8	4250	
DD95ZS31	42.25	44.5	2.25	-0.5	5.36	23	-0.008	370	0.09	132	4.55	3.15	4.09	4220	265	70	-3	1170	
DD95ZS31	44.5	46.05	1.55	-0.5	4.92	24	-0.008	314	0.14	51	7.47	2.83	5.41	7720	235	39	-3	1050	
DD95ZS31	46.05	48.1	2.05	-0.5	5.1	18	-0.008	357	0.12	17	6.35	2.9	3.8	6890	285	19	-3	710	
DD95ZS31	48.1	49.5	1.4	-0.5	2.77	22	-0.008	231	0.26	-5	26.4	1.4	2.99	36200	380	33	-3	3130	
DD95ZS31	49.5	51.5	2	0.8	8.18	58	-0.008	575	0.25	173	14	4.88	6.74	15500	235	59	-3	1660	
DD95ZS31	51.5	52.7	1.2	-0.5	9.01	39	-0.008	739	0.3	77	13.4	4.88	11.1	11500	415	24	-3	1110	
DD95ZS31	52.7	54.4	1.7	-0.5	8.85	31	-0.008	703	0.3	28	15.5	4.84	9.1	11900	365	28	-3	853	
DD95ZS31	54.4	57	2.6	0.5	3.86	22	-0.008	343	0.17	18	8.01	1.94	8.68	5440	400	-5	-3	282	
DD95ZS31	57	58.5	1.5	1.4	4.72	28	-0.008	506	0.15	112	7.28	2.41	9	5320	420	20	5	337	
DD95ZS31	58.5	60	1.5	-0.5	3.74	24	-0.008	529	1.78	14	9.92	1.84	4.55	8950	390	12	-3	412	
DD95ZS31	60	61.5	1.5	-0.5	1.67	33	-0.008	383	6.8	17	15.9	0.8	4.46	16500	240	142	-3	2700	
DD95ZS31	61.5	63	1.5	-0.5	2.78	26	-0.008	483	3.46	12	15.5	1.19	3.04	17500	410	32	-3	767	
DD95ZS31	63	63.4	0.4	1.7	0.51	25	-0.008	120	1.11	6	22	0.22	2.71	26800	155	716	-3	1850	
DD95ZS31	63.4	64.5	1.1	-0.5	0.07	-5	-0.008	29	10.9	-5	5.17	-0.05	7.77	6390	175	35	-3	104	
DD95ZS31	64.5	66.2	1.7	-0.5	0.04	-5	-0.008	19	12.1	-5	9.96	-0.05	9.46	7510	200	22	-3	161	
DD95ZS31	66.2	67.5	1.3	10.2	0.24	10	-0.008	49	1.76	23	19.8	0.1	3.94	41800	140	5870	-3	35100	1.96
DD95ZS31	67.5	68.35	0.85	-0.5	0.06	9	-0.008	26	9.77	-5	9.84	-0.05	9.67	5030	155	267	-3	1020	
DD95ZS31	68.35	70.5	2.15	-0.5	3.46	9	-0.008	156	4.21	9	4.34	1.8	11.4	1990	365	15	5	75	
DD95ZS31	70.5	72	1.5	-0.5	3.2	-5	-0.008	192	1.95	19	2.5	1.95	6.47	945	260	10	-3	26	
DD95ZS31	72	73.5	1.5	-0.5	3.4	14	-0.008	198	2	18	2.92	2.04	8.08	1150	270	13	8	48	
DD95ZS31	73.5	75.5	2	1.1	3.85	15	-0.008	248	3.08	18	3.76	2.3	8.01	1780	235	15	4	48	
DD95ZS31	75.5	77	1.5	0.6	3.23	-5	-0.008	221	3.86	13	2.02	1.94	5.79	605	225	14	6	30	
DD95ZS31	77	78.4	1.4	-0.5	3.15	-5	-0.008	202	3.25	21	3.92	1.94	5.79	2260	295	-5	-3	44	
DD95ZS31	78.4	80.3	1.9	-0.5	0.04	-5	-0.008	30	14.7	6	0.47	-0.05	9.38	386	175	41	-3	114	
DD95ZS31	80.3	82.5	2.2	-0.5	0.09	-5	-0.008	28	14.6	20	0.5	-0.05	9.4	389	180	23	-3	50	
DD95ZS31	82.5	84	1.5	-0.5	0.06	9	-0.008	20	14.7	-5	1.02	-0.05	9.37	923	185	17	-3	13	
DD95ZS31	84	84.5	0.5	-0.5	0.02	-5	-0.008	17	15.6	22	0.47	-0.05	10.1	365	215	14	-3	17	
DD95ZS31	84.5	87	2.5	-0.5	0.05	-5	-0.008	18	17.1	5	0.38	-0.05	11.1	355	255	14	-3	10	
DD95ZS31	87	88.5	1.5	-0.5	0.07	-5	-0.008	22	15.7	19	0.68	-0.05	10.2	497	205	29	-3	11	
DD95ZS31	88.5	90	1.5	-0.5	0.09	11	-0.008	22	13.3	-5	1.76	-0.05	8.98	1150	165	16	-3	17	

364396

[redacted] Stone [redacted] DD9[redacted] Assa[redacted]

Borehole	From	To	Width	Ag ppm	Al %	As ppm	Au ppm	Ba ppm	Ca %	Cu ppm	Fe %	K %	Mg %	Mn ppm	P ppm	Pb ppm	Sn ppm	Zn ppm	S %
DD95ZS31	90	91.5	1.5	-0.5	0.09	-5	-0.008	21	14	22	1.15	-0.05	8.92	707	310	14	-3	5	
DD95ZS31	91.5	93	1.5	0.8	0.11	8	-0.008	33	7.19	5	0.43	-0.05	14.9	422	170	50	-3	26	
DD95ZS31	93	94.5	1.5	1.3	0.09	-5	-0.008	21	4.01	9	0.67	-0.05	17	750	190	18	-3	54	
DD95ZS31	94.5	95.7	1.2	0.7	0.06	5	-0.008	21	8.44	-5	0.3	-0.05	15.5	272	210	19	-3	17	
DD95ZS31	95.7	97.5	1.8	-0.5	0.11	-5	-0.008	30	16.9	5	1.46	-0.05	11.3	741	350	20	-3	7	
DD95ZS31	97.5	99	1.5	-0.5	0.18	13	-0.008	28	16.1	10	1.87	0.07	9.75	1170	255	41	-3	12	
DD95ZS31	99	100.5	1.5	0.9	0.47	15	-0.008	47	14.6	42	2.74	0.23	8.68	2180	255	37	-3	67	
DD95ZS31	100.5	102	1.5	-0.5	1.61	16	-0.008	86	13.1	22	2.71	0.88	7.69	1550	375	196	-3	25	
DD95ZS31	102	103.5	1.5	-0.5	1.86	22	-0.008	269	15.1	18	2.54	1.06	9.15	1330	385	132	4	27	
DD95ZS31	103.5	104.7	1.2	0.8	4.16	30	-0.008	524	9.29	29	2.71	2.42	5.88	873	305	91	-3	54	
DD95ZS31	104.7	106.3	1.6	-0.5	1.35	17	-0.008	142	14.6	8	3.52	0.75	8.95	3570	290	206	-3	570	
DD95ZS31	106.3	107.9	1.6	0.6	0.93	-5	-0.008	75	18.5	15	2.48	0.51	11.3	2020	375	129	-3	374	
DD95ZS31	107.9	109.25	1.35	-0.5	2.15	21	-0.008	122	15.5	9	2.18	1.15	9.42	1340	600	267	-3	96	
DD95ZS31	109.25	111	1.75	-0.5	0.24	13	-0.008	26	20.5	13	1.07	0.1	12.6	1470	330	157	-3	557	
DD95ZS31	111	113.6	2.6	-0.5	0.13	47	-0.008	31	19.6	-5	1.39	0.06	12.3	2610	360	62	-3	188	
DD95ZS31	113.6	114.73	1.13	-0.5	0.95	9	-0.008	72	17.1	16	2.28	0.55	10.1	1240	370	71	-3	169	
DD95ZS31	114.73	117.1	2.37	1.1	1.81	-5	-0.008	255	11.9	24	2.6	1.1	7.41	1550	690	99	-3	61	
DD95ZS31	117.1	118.2	1.1	6.7	0.7	14	-0.008	73	14.3	123	4.31	0.38	9.19	3670	615	119	-3	143	
DD95ZS31	118.2	120	1.8	3.6	1.4	35	-0.008	250	11.3	48	4.43	0.79	7.56	3430	470	700	-3	228	
DD95ZS31	120	121.5	1.5	2.5	1.52	11	-0.008	334	13.9	26	1.91	0.95	8.5	1100	470	575	-3	115	
DD95ZS31	121.5	124	2.5	1.3	1.4	6	-0.008	361	21.5	23	2.52	0.85	13.2	1480	390	155	-3	76	
DD95ZS31	124	126	2	2.3	4.44	114	-0.008	793	3.77	36	7.81	2.8	4.47	4470	450	444	-3	149	
DD95ZS31	126	127.2	1.2	1.6	2.38	714	0.027	254	8.66	23	7.16	1.33	6.61	5820	400	241	-3	250	
DD95ZS31	127.2	128.3	1.1	2.8	2.22	2180	0.054	147	1.95	30	16.5	1.11	4.52	12500	375	279	-3	154	
DD95ZS31	128.3	130	1.7	3.9	4.76	66	-0.008	524	0.85	31	7.64	2.75	2.37	5980	580	745	5	405	
DD95ZS31	130	132	2	5.7	3.67	680	0.025	446	0.69	36	9.47	2.12	1.92	16500	510	1420	-3	1520	
DD95ZS31	132	133.15	1.15	5.3	2.45	75	-0.008	425	7.7	60	2.12	1.6	4.88	1150	935	386	-3	295	
DD95ZS31	133.15	135	1.85	1.8	0.28	8	0.01	64	14.2	47	1.45	0.14	8.72	1200	350	34	-3	84	
DD95ZS31	135	136.5	1.5	-0.5	0.13	25	-0.008	42	16.2	7	3.05	0.06	10.6	3390	235	39	-3	55	
DD95ZS31	136.5	137.9	1.4	-0.5	0.12	7	-0.008	47	17.8	18	1.29	0.05	11.2	982	340	45	-3	22	
DD95ZS31	137.9	140.1	2.2	1	0.18	-5	-0.008	44	13.8	7	1.62	0.08	8.6	1200	260	51	-3	67	
DD95ZS31	140.1	141.7	1.6	5.6	0.17	18	-0.008	48	14.5	116	2.22	0.07	8.73	2160	220	1270	-3	716	
DD95ZS31	141.7	143.6	1.9	11.9	0.32	166	-0.008	34	4.45	43	11.5	0.18	3.82	38500	295	4770	25	15200	1.49
DD95ZS31	143.6	145.3	1.7	4.4	0.31	32	0.016	45	9.67	27	4.08	0.19	5.8	9710	250	1050	-3	970	
DD95ZS31	145.3	147.65	2.35	-0.5	0.43	12	-0.008	58	12.3	14	1.72	0.25	7.04	1580	325	290	-3	83	
DD95ZS31	147.65	148.5	0.85	17.5	0.39	59	-0.008	95	3.42	220	8.32	0.21	2.37	20400	465	11100	10	17000	1.48
DD95ZS31	148.5	150.15	1.65	0.6	0.22	19	-0.008	46	12.8	53	2.4	0.15	6.77	3100	600	127	-3	256	
DD95ZS31	150.15	152.1	1.95	3.8	0.38	113	-0.008	54	12.6	39	2.95	0.23	6.42	4540	390	808	-3	1870	
DD95ZS31	152.1	152.95	0.85	3.4	2.62	94	-0.008	357	9.48	24	2.86	1.41	4.86	3550	550	1580	4	734	
DD95ZS31	152.95	154.5	1.55	49.3	2.59	9550	0.269	218	2.05	428	16.7	1.32	1.64	14700	540	14900	6	32100	15.2
DD95ZS31	154.5	156.2	1.7	11.4	0.75	2300	0.03	117	0.18	32	32.4	0.38	0.38	6580	100	2630	-3	18800	37.4
DD95ZS31	156.2	157.87	1.67	4.1	1.11	264	0.009	132	0.37	6	23.5	0.59	5.66	22100	180	1300	-3	2950	
DD95ZS31	157.87	158.31	0.44	13	8.99	218	-0.008	467	0.2	59	7.19	4.48	0.79	2050	520	2580	17	489	
DD95ZS31	158.31	159	0.69	11.3	0.44	293	0.014	45	0.41	15	19.3	0.22	3.65	37000	140	4560	-3	15700	5
DD95ZS31	159	160	1	1.7	6.77	102	-0.008	646	0.25	20	4.97	3.52	0.92	3810	340	418	9	585	
DD95ZS31	160	161.5	1.5	0.6	8.57	35	-0.008	806	0.11	15	3.5	4.35	0.81	1110	290	78	5	133	
DD95ZS31	161.5	162.8	1.3	0.7	7.11	54	-0.008	567	0.1	29	3.77	3.72	1.17	1490	330	55	5	74	
DD95ZS31	162.8	165.5	2.7	1.6	6.25	20	-0.008	440	0.09	51	3.17	3.3	1.01	1710	310	82	4	67	
DD95ZS31	165.5	167.5	2	-0.5	8.27	41	-0.008	595	0.11	26	3.58	4.11	0.83	613	320	38	-3	153	
DD95ZS31	167.5	169	1.5	-0.5	8.56	29	-0.008	651	0.11	20	3.8	4.22	1.08	715	330	37	8	40	
DD95ZS31	169	171.1	2.1	1.3	8.43	60	-0.008	598	0.12	24	4.51	4.18	0.96	1110	365	270	11	105	
DD95ZS31	171.1	174	2.9	-0.5	3.44	17	-0.008	244	-0.05	40	2.31	1.87	0.64	545	165	15	-3	39	
DD95ZS31	174	177	3	-0.5	4.49	8	-0.008	296	0.13	24	3.14	2.36	0.79	1630	530	74	-3	246	
DD95ZS31	177	180	3	1.2	4.64	24	-0.008	306	0.07	36	3.11	2.45	0.74	2480	215	313	6	1970	
DD95ZS31	180	182	2	-0.5	5.4	13	-0.008	355	0.09	21	2.91	2.83	0.83	804	330	15	4	32	

364397

[redacted] Ston[redacted] DD9[redacted] Assa[redacted]

Borehole	From	To	Width	Ag ppm	Al %	As ppm	Au ppm	Ba ppm	Ca %	Cu ppm	Fe %	K %	Mg %	Mn ppm	P ppm	Pb ppm	Sn ppm	Zn ppm	S %
DD95ZS31	182	184.65	2.65	-0.5	4.93	17	-0.008	318	0.09	21	3.35	2.6	0.85	1330	300	37	5	43	
DD95ZS31	184.65	187.5	2.85	1	5.3	30	-0.008	307	0.07	21	3.5	2.9	0.91	3030	195	213	4	45	
DD95ZS31	187.5	189	1.5	39.4	6.34	33	-0.008	412	0.13	31	3.33	3.48	0.8	3800	430	16300	-3	121	
DD95ZS31	189	190.5	1.5	1	5.21	20	-0.008	352	0.07	22	3.1	2.84	0.64	3510	205	200	6	99	
DD95ZS31	190.5	193.5	3	-0.5	4.01	10	-0.008	273	-0.05	14	2.71	2.22	0.69	1280	155	65	6	43	
DD95ZS31	193.5	196.2	2.7	-0.5	2.86	6	-0.008	182	-0.05	58	2.79	1.59	0.71	736	165	16	-3	16	
DD95ZS31	196.2	198.7	2.5	1.3	5.06	56	-0.008	321	0.1	30	3.94	2.6	0.57	5110	300	288	5	46	
DD95ZS31	198.7	200.4	1.7	2.8	6.24	32	-0.008	328	0.09	125	3.64	3.26	0.64	5110	230	604	12	42	
DD95ZS31	200.4	202	1.6	6.1	6.53	54	-0.008	428	0.1	93	4.85	3.56	0.69	5980	220	396	8	48	
DD95ZS31	202	204	2	4.2	5.28	30	-0.008	291	0.08	68	4.08	2.69	0.6	4740	210	309	8	20	
DD95ZS31	204	205.7	1.7	5.2	6.69	35	-0.008	370	0.09	155	4.15	3.34	0.67	5240	260	310	7	60	
DD95ZS31	205.7	206.5	0.8	1.6	5.84	36	-0.008	385	0.07	19	3.37	3.14	0.59	4840	270	406	8	43	
DD95ZS31	206.5	208	1.5	2.7	7.48	39	-0.008	504	0.09	25	2.95	4.16	0.72	2770	335	322	6	62	
DD95ZS31	208	209.5	1.5	1.3	3.25	8	-0.008	160	0.07	11	4.44	1.73	0.66	8010	200	167	5	54	

364398

364399

Appendix XII

Zinc Mineralisation in the Gordon Limestone

Zinc Mineralisation in the Gordon Limestone

CRAE's exploration and research activities directed at locating carbonate-hosted Zn-Pb mineralisation within Gordon Limestone at Zeehan have led to a number of mineralisation styles being recognised. The following discussion is a synthesis of CRAE's current level of knowledge, grained from work throughout the Zeehan area.

CRAE's exploration activities in the Zeehan area have indicated that Zn-Pb mineralisation within the Gordon Limestone may be pre-Devonian in age, and therefore unrelated to the Tabberabberan Orogeny. On this basis, it is possible that carbonate-hosted Zn-Pb mineralisation may be more widespread than that presently under evaluation at Zeehan.

The Gordon Limestone originally occupied a large area, deposited at the close of a major period of tectonic activity that produced the metal-rich Mount Read Volcanics. During and immediately before carbonate deposition the tectonic regime was still unstable, evidenced by rapid changes in stratigraphic thickness of Ordovician strata. Hydrothermal systems may have continued to emit metals into this system, focused by basement irregularities and syn-sedimentary faults.

The present Gordon Limestone exposure is a vestige of Devonian deformation. Ordovician mineralisation may have a distribution totally independent of the well-documented Devonian systems.

Five targets are recognised for the carbonate-hosted Zn mineralisation in Gordon Limestone at Zeehan, subdivided by the stratigraphic interval in which they are hosted (Figure):-

- stratabound at the lower limestone-sandstone contact
- stratabound at the upper limestone-quartzite contact
- stratabound within a sub-unit in the middle of the limestone sequence
- structurally controlled discordant mineralisation
- surficial "clay-hosted" accumulations developed above primary mineralisation.

Stratabround at the lower limestone-sandstone contact
Mineralisation at Grieves and Mariposa falls into this category. Alteration located at Blackjacks, Pyramid and Professor Range may also belong to this deposit type.

This position is characterised by carbonaceous and/or ferruginous clays resting on the Moina Sandstone, in turn overlain by a massive siderite zone. The siderite zones passes stratigraphically upward either gradationally or abruptly into unaltered and unmineralised limestone. The clay layer may be up to 50m thick and the siderite zone up to 25m thick. Both may contain Zn mineralisation up to several percent. The clay and siderite zone are laterally quite uniform and it may be that the mineralisation is actually stratiform.

Mineralisation of this style has an alteration halo that is both visually and geochemically distinct. This halo, characterised by vughy, broken or massive recrystallised Fe-carbonate and Fe-rich clays, may extend laterally hundreds of metres beyond the main Zn mineralisation, and thus present a considerably larger target than the mineralised core. Lateral alteration geochemistry is reflected by Fe-Mn-As-Zn. Stratigraphy above the mineralised core is a weaker halo of elevated Zn ($\pm$ As).

Ore mineralogy, based on work at Grieves, is complex with a mixture of zincian siderite and minor sphalerite in the siderite zone, and a Zn-clay with minor to moderate amounts of sphalerite in the siderite zone, and a Zn-clay with minor to moderate amounts of sphalerite in the clay zone. It is not known whether this is a regional characteristic of this position.

The stratiform character, replacive style of alteration/mineralisation, intense Fe-Mn alteration, and reasonably predictable geometry suggest similarities to Navan or Reocin.

Stratabound at the upper limestone-quartzite contact
Low-grade but widely anomalous zones from Firewood Siding, Grieves, Professor Range, Sunny Corner, and Mariposa are examples of this type.

Upper zone mineralisation occurs near the contact between the limestone and overlying Crotty Quartzite. Mineralisation is not closely bound to the upper quartzite contact, but may "wander" up to 100m stratigraphically below the contact.

Mineralisation appears characterised by widespread but low-level Zn in the 0.1% to 2% Zn range. None of the prospects tested has revealed a higher-grade core, although given the limited drilling it is entirely possible high-grade cores may exist. Limited mineralogy suggests all Zn to be as sphalerite.

Air-core drilling shows the mineralised zones to be comprised of clays and decomposed carbonate. Rare fresher material is usually a granular recrystallised dolomite, and can be ferroan. Intense siderite alteration is absent. A detailed geochemical study of the alteration has not been completed.

The upper zone style may be occurring within karstic structures formed by Ordovician weathering before deposition of the Crotty Quartzite. This setting is analogous to Bleiberg or Cracow-Silesia.

Stratabround in a middle sub-unit of the limestone sequence
Currently two occurrences fall into this grouping, Grieves middle zone, and Oceana. Apart from their stratigraphic concurrence, these two deposits may not share many other similarities.

The mineralised middle sub-unit is equidistant from the upper and lower contacts, although facies variations may affect the location at other prospects. Mineralisation is breccia hosted, and in the case of Grieves has a linear aspect. For Grieves there is very little indication of proximity to mineralisation as there is virtually no alteration outside the breccia zone itself.

Mineralogy at Grieves is a mixture of zincian siderite and sphalerite. Oceana is dominated by galena with subordinate (?) sphalerite. There is also intense siderite alteration at Oceana, presumably containing Zn?

Zinc grades at both prospects are high, locally forming massive sulphide.

There has been insufficient work completed at Grieves middle zone to suggest any controlling mechanisms.

Structurally controlled discordant mineralisation
Most mineralisation in the Zeehan area is structurally controlled. Mineralisation at the historic Mariposa mine, and at Myrtle belong to this type. Possibly some of the mineralisation at Oceana is also structurally controlled.

Structurally controlled mineralisation may occur at any stratigraphic level. It appears to be late-stage filling of brittle fractures. Alteration of wall-rocks is absent, and the gangue to mineralisation may be pure calcite. Mineralisation within the structures is patchily distributed. Ore minerals are coarse-grained sulphides.

Devonian deformation is the likely cause of the fracturing and mineralisation. Potential deposit size is small, although the presence of discordant mineralisation may indicate a nearby stratabound source. Late-stage structurally controlled deposits *per se* are not currently considered a valid CRAE target.

Surficial clay-hosted accumulations developed above primary mineralisation
Surficial Zn accumulations within decomposed carbonate was CRAE's original target for carbonate exploration in Zeehan. All currently tested prospects were selected due to the presence of known surficial mineralisation.

It has now been conclusively demonstrated that the surficial mineralisation occupies the surface trace of underlying stratabound mineralisation. Geometry of the surficial deposits are therefore dependent on the shape and extent of this underlying mineralisation. Depth extent of the Zn-rich clays and decomposed carbonates averages 10m to 20m, but have been reported to be over 100m at Oceana.

A thin layer of decomposed carbonate exists over large areas of limestone, but this layer only thickens and becomes substantially Zn-rich as "basement" mineralisation is approached. Areas of +0.1% Zn in the clay layer are regionally extensive, indicating substantial dispersions from the primary zone. Clay thickness and Zn grade may be useful vectors toward primary zones. Geochemically inert peat and gravels up to 5m thick obscure the clays and limestone over virtually the entire trace of the Gordon Limestone.

Zinc ore mineralogy is dominantly to exclusively sphalerite.

Because of their restriction to the surface zone, the potential size of the surficial deposit is somewhat limited. They are probably unlikely to be a CRA target in themselves. Their main attraction is their usefulness as an indicator of the underlying primary mineralisation. If a large primary deposit suitable to CRAE's requirements can be identified, then the surficial deposits would possible be an easy way to generate short-term cash-flow whilst the major deposit was being developed.

Zinc-rich clay deposits overlying primary carbonate mineralisation have been described at Tynagh and Silvermines.

R.G. Parkinson (1994)